frontiers | Research Topics

Recent advances in Campylobacter research

Edited by
Stuart A. Thompson, Ozan Gundogdu and Nicolae Corcionivoschi

Published in
Frontiers in Microbiology

ISSN 1664-8714
ISBN 978-2-8325-6633-6
DOI 10.3389/978-2-8325-6633-6

Generative AI statement
Any alternative text (Alt text) provided alongside figures in the articles in this ebook has been generated by Frontiers with the support of artificial intelligence and reasonable efforts have been made to ensure accuracy, including review by the authors wherever possible. If you identify any issues, please contact us.

About Frontiers

Frontiers is more than just an open access publisher of scholarly articles: it is a pioneering approach to the world of academia, radically improving the way scholarly research is managed. The grand vision of Frontiers is a world where all people have an equal opportunity to seek, share and generate knowledge. Frontiers provides immediate and permanent online open access to all its publications, but this alone is not enough to realize our grand goals.

Frontiers journal series

The Frontiers journal series is a multi-tier and interdisciplinary set of open-access, online journals, promising a paradigm shift from the current review, selection and dissemination processes in academic publishing. All Frontiers journals are driven by researchers for researchers; therefore, they constitute a service to the scholarly community. At the same time, the *Frontiers journal series* operates on a revolutionary invention, the tiered publishing system, initially addressing specific communities of scholars, and gradually climbing up to broader public understanding, thus serving the interests of the lay society, too.

Dedication to quality

Each Frontiers article is a landmark of the highest quality, thanks to genuinely collaborative interactions between authors and review editors, who include some of the world's best academicians. Research must be certified by peers before entering a stream of knowledge that may eventually reach the public - and shape society; therefore, Frontiers only applies the most rigorous and unbiased reviews. Frontiers revolutionizes research publishing by freely delivering the most outstanding research, evaluated with no bias from both the academic and social point of view. By applying the most advanced information technologies, Frontiers is catapulting scholarly publishing into a new generation.

What are Frontiers Research Topics?

Frontiers Research Topics are very popular trademarks of the *Frontiers journals series*: they are collections of at least ten articles, all centered on a particular subject. With their unique mix of varied contributions from Original Research to Review Articles, Frontiers Research Topics unify the most influential researchers, the latest key findings and historical advances in a hot research area.

Find out more on how to host your own Frontiers Research Topic or contribute to one as an author by contacting the Frontiers editorial office: frontiersin.org/about/contact

Recent advances in Campylobacter research

Topic editors
Stuart A. Thompson — Augusta University, United States
Ozan Gundogdu — University of London, United Kingdom
Nicolae Corcionivoschi — Agri-Food and Biosciences Institute, United Kingdom

Citation
Thompson, S. A., Gundogdu, O., Corcionivoschi, N., eds. (2025). *Recent advances in Campylobacter research*. Lausanne: Frontiers Media SA.
doi: 10.3389/978-2-8325-6633-6

Table of contents

frontiers | Frontiers in Microbiology

TYPE Editorial
PUBLISHED 08 July 2025
DOI 10.3389/fmicb.2025.1646828

OPEN ACCESS

EDITED AND REVIEWED BY
Axel Cloeckaert,
Institut National de recherche pour l'agriculture, l'alimentation et l'environnement (INRAE), France

*CORRESPONDENCE
Stuart A. Thompson
✉ stthomps@augusta.edu

RECEIVED 14 June 2025
ACCEPTED 17 June 2025
PUBLISHED 08 July 2025

CITATION
Thompson SA, Corcionivoschi N, Tresse O and Gundogdu O (2025) Editorial: Recent advances in *Campylobacter* research. *Front. Microbiol.* 16:1646828. doi: 10.3389/fmicb.2025.1646828

Editorial: Recent advances in *Campylobacter* research

Stuart A. Thompson[1]*, Nicolae Corcionivoschi[2], Odile Tresse[3] and Ozan Gundogdu[4]

[1]Department of Medicine, Division of Infectious Diseases, Augusta University, Augusta, GA, United States, [2]Bacteriology Branch, Veterinary Sciences Division, Agri-Food and Biosciences Institute, Belfast, United Kingdom, [3]Nantes Université/INRAE, UMR 1280, PhAN, Nantes, France, [4]Faculty of Infectious and Tropical Diseases, London School of Hygiene and Tropical Medicine, London, United Kingdom

KEYWORDS

biofilm, *Campylobacter jejuni*, *Campylobacter* coli, *Campylobacter* concisus, *Campylobacter* fetus, Antibiotic resistance (ABR), microbiota

Editorial on the Research Topic
Recent advances in *Campylobacter* research

Campylobacter spp. are responsible for more than 100 million cases of human disease each year. While the majority of cases result from infection with *C. jejuni* and *C. coli*, other *Campylobacter* species such as *C. concisus* are increasingly recognized as being responsible for disease pathogenesis. Additionally, species such as *C. fetus* are important veterinary pathogens. As with many pathogens, antibiotic resistance in *Campylobacter* is becoming increasingly problematic, leading to these bacteria being classified as high-level threats by the U.S. Centers for Disease Control (CDC) and the World Health Organization (WHO). However, despite decades of study, the mechanisms by which these bacteria cause illness are not fully understood, and no effective control strategies for animal reservoirs exist. In this Special Topic in Frontiers in Microbiology, "*Recent Advances in Campylobacter research*," features 10 manuscripts that explore various aspects of *Campylobacter* antibiotic resistance, host colonization, and pathogenesis.

Cho et al. used RNA-Seq to evaluate the responses of *C. jejuni* to antibiotic tolerance induced by ciprofloxacin and tetracycline. The transcriptional response was surprisingly broad, and encompassed changes in numerous genes of various functional categories that presumably promote survival upon exposure to antibiotics. In particular, mutational studies showed that protein chaperones facilitate cellular survival by managing protein disaggregation.

García-Fernández et al. performed a study on a collection of Italian isolates of *C. jejuni* and *C. coli*, using Whole-Genome Sequence (WGS) and Multilocus Sequence Typing (MLST) to evaluate the prevalence of antibiotic resistance and virulence determinants. The authors found widespread antibiotic resistance in both species. Furthermore, virulence determinants were more highly represented in specific MLST types, suggesting the potential of WGS to identify strains of greater clinical significance.

A study by Deforet et al. explored *Campylobacter* antibiotic resistance. Aminopenicillin resistance is associated with a point mutation in the promoter for the chromosomal β-lactamase gene bla_{OXA61}; however, this can generally be overcome by combination treatment with clavulanic acid. While resistance to amoxicillin-clavulanic acid is rare, the authors identified three *C. coli* strains with amoxicillin-clavulanic acid resistance. A combination of WGS and mass spectrometry (MS) was used to identify the mechanism of this resistance as a second promoter mutation that results in increased bla_{OXA61} expression.

Concerning therapeutics against *Campylobacter*, Deblais et al. targeted the twin-arginine translocation (Tat) system, which is responsible for *C. jejuni* formate utilization but is not present in mammals and chickens. Inhibition of this system, therefore, may prevent *C. jejuni* colonization. Because the Tat system also mediates $CuSO_4$ resistance by *C. jejuni*, the authors identified small-molecule inhibitors of the Tat pathway by selecting for increased susceptibility to $CuSO_4$. The identified small-molecule inhibitors were non-toxic to Caco-2 cells and reduced *Campylobacter* colonization in chicks, suggesting their utility as a control strategy.

One major impediment to a better understanding of *C. jejuni* pathogenesis is the lack of effective mammalian colonization models, due in part to the inhibitory effect of the intestinal microbiota of mouse strains on *Campylobacter* colonization. To gain a greater understanding of this issue, Shayya et al. used a targeted metabolomics approach to define characteristics associated with colonization resistance. The microbiota of mice with colonization resistance contained greater abundances of lactobacilli and Mouse Intestinal Bacteroides, and lower abundances of enterobacteria, enterococci, and *Clostridium coccoides* group. This microbial community structure was accompanied by elevated levels of antimicrobial bile acids and fatty acids, and a reduced abundance of amino acids that are essential for *C. jejuni* growth, thus providing an explanation for colonization resistance.

To further develop mouse models and to study therapeutic interventions against *C. jejuni* infection, Mousavi et al. used human microbiota-associated IL-$10^{-/-}$ mice, which developed symptoms of acute campylobacteriosis. Administration of carvacrol (alone or in combination with deferoxamine, deoxycholate, and 2-fucosyllactose) resulted in a reduced ileal load of *C. jejuni*, along with a decrease in diarrhea and histopathological/inflammatory responses. These compounds may therefore represent a promising therapeutic approach as opposed to antibiotic therapy.

To examine the interactions between *C. jejuni* and other bacteria, Dreyer et al. used a data-independent acquisition mass spectrometry (DIA-MS) approach to determine changes in the whole-cell proteome of *C. jejuni* upon co-colonization with three Gram-positive *bacterial species*, and exposure to the bile acid deoxycholate (DCA). All three co-incubation scenarios induced large-scale changes to the *C. jejuni* proteome and allowed the identification of a core set of 54 proteins that comprised a common co-incubation response. Although the response to DCA was substantially larger, the co-incubation and DCA responses partially overlapped, and data suggested a synergistic response to the different stimuli.

In contrast to its fastidious nature in laboratory culture and its sensitivity to atmospheric oxygen, *C. jejuni* can survive in a number of challenging environments. One aspect of its biology that allows it to do so is its ability to form protective biofilms, which are cells encased in an Extracellular Matrix (ECM). Pavlinjek et al. described the physical and chemical methods for isolating this ECM. The isolated ECM varied greatly using the different methods, but was rich in protein, polysaccharides, and extracellular DNA. These methods can be used to select the appropriate ones for downstream analytical experiments.

Luk et al. examined the gastric pathogenicity of *C. concisus*, using cultured gastric epithelial AGS cells. Exposure to *C. concisus* induced several changes in AGS cells, including the induction of IL-8, actin polymerization, and caspase 3/7. Significantly, *C. concisus* also elicited an increase in *CYP1A1* gene expression; increased *CYP1A1* expression is associated with poorer survival in gastric cancer patients. Together, these data suggest that *C. concisus* may induce gastric inflammation and could affect gastric cancer prognosis.

Finally, Ong et al. used WGS to gain further insight into the veterinary pathogen *C. fetus* subsp. *fetus* (four genomes) and *C. fetus* subsp. *venerealis* (five genomes). Despite host differences between the two subspecies, they have been difficult to distinguish from each other. While the genomes of the two subspecies were remarkably similar in this study, within this conserved framework were several single-nucleotide polymorphisms that can be used to distinguish the two subspecies.

Together, the manuscripts published in this Research Topic represent important advances in various areas of *Campylobacter* research.

Author contributions

ST: Writing – review & editing, Writing – original draft. NC: Writing – review & editing. OT: Writing – review & editing. OG: Writing – review & editing.

Funding

The author(s) declare that financial support was received for the research and/or publication of this article. ST was funded by grant AI164078 from the U.S. National Institutes of Health.

Conflict of interest

The authors declare that the research was conducted in the absence of any commercial or financial relationships that could be construed as a potential conflict of interest.

The author(s) declared that they were an editorial board member of Frontiers, at the time of submission. This had no impact on the peer review process and the final decision.

Generative AI statement

The authors declare that no Gen AI was used in the creation of this manuscript.

Publisher's note

frontiers | Frontiers in Microbiology

TYPE Original Research
PUBLISHED 09 November 2023
DOI 10.3389/fmicb.2023.1285236

OPEN ACCESS

EDITED BY
Ozan Gundogdu,
University of London, United Kingdom

REVIEWED BY
Marja-Liisa Hänninen,
University of Helsinki, Finland
Mohamed K. Fakhr,
University of Tulsa, United States

*CORRESPONDENCE
Philippe Lehours
philippe.lehours@u-bordeaux.fr

RECEIVED 29 August 2023
ACCEPTED 25 October 2023
PUBLISHED 09 November 2023

CITATION
Deforet F, Jehanne Q, Bénéjat L, Aptel J, Prat R, Desbiolles C, Ducournau A, Jauvain M, Bonnet R, Vandenesch F, Lemoine J and Lehours P (2023) Combined genomic-proteomic approach in the identification of *Campylobacter coli* amoxicillin-clavulanic acid resistance mechanism in clinical isolates. *Front. Microbiol.* 14:1285236. doi: 10.3389/fmicb.2023.1285236

Combined genomic-proteomic approach in the identification of *Campylobacter coli* amoxicillin-clavulanic acid resistance mechanism in clinical isolates

Francis Deforet[1], Quentin Jehanne[2], Lucie Bénéjat[2], Johanna Aptel[2], Roxane Prat[3], Chloé Desbiolles[3], Astrid Ducournau[2], Marine Jauvain[2,4], Richard Bonnet[5], François Vandenesch[3], Jérôme Lemoine[1] and Philippe Lehours[2,4]*

[1]Institut des Sciences Analytiques, Université Claude Bernard Lyon 1, Lyon, France, [2]Bacteriology Department, CHU de Bordeaux, National Reference Center for Campylobacters and Helicobacters, Bordeaux, France, [3]Institut des Agents Infectieux, Hospices Civils de Lyon, Lyon, France, [4]Bordeaux Institute of Oncology, BRIC U1312, INSERM, Université de Bordeaux, Bordeaux, France, [5]Laboratoire Associé CNR de la Résistance aux Antibiotiques, CHU de Clermont-Ferrand, Clermont-Ferrand, France

Introduction: Aminopenicillins resistance among *Campylobacter jejuni* and *Campylobacter coli* strains is associated with a single mutation in the promoting region of a chromosomal beta-lactamase bla_{OXA61}, allowing its expression. Clavulanic acid is used to restore aminopenicillins activity in case of bla_{OXA61} expression and has also an inherent antimicrobial activity over *Campylobacter* spp. Resistance to amoxicillin-clavulanic acid is therefore extremely rare among these species: only 0.1% of all *Campylobacter* spp. analyzed in the French National Reference Center these last years (2017–2022).

Material and methods: Whole genome sequencing with bioinformatic resistance identification combined with mass spectrometry (MS) was used to identify amoxicillin-acid clavulanic resistance mechanism in Campylobacters.

Results: A G57T mutation in bla_{OXA61} promoting region was identified in all *C. jejuni* and *C. coli* ampicillin resistant isolates and no mutation in ampicillin susceptible isolates. Interestingly, three *C. coli* resistant to both ampicillin and amoxicillin-clavulanic acid displayed a supplemental deletion in the promoting region of bla_{OXA61} beta-lactamase, at position A69. Using MS, a significant difference in the expression of Bla_{OXA61} was observed between these three isolates and amoxicillin-clavulanic acid susceptible *C. coli*.

Conclusion: A combined genomics/proteomics approach allowed here to identify a rare putative resistance mechanism associated with amoxicillin-clavulanic acid resistance for *C. coli*.

KEYWORDS

AMR, amoxicillin-clavulanic acid, *Campylobacter*, beta-lactamase, gene expression

Introduction

Campylobacter jejuni and *Campylobacter coli* are the most common cause of bacterial gastro-enteritis worldwide, before *Salmonella* (Chlebicz and Śliżewska, 2018). They are foodborne pathogens transmitted via the consumption of contaminated products, especially meat (mainly chicken, beef and pork). In Europe in 2021, campylobacteriosis accounted for more than 120,000 cases of illness (The European Union One Health, 2021) while in the USA, the number of *Campylobacter* infections is estimated at 1.5 million illnesses each year (Delahoy et al., 2023). Campylobacteriosis can cause symptoms such as abdominal pains, fever and diarrhea, which are significant risks of complications at the extreme ages of life (Fernández-Cruz et al., 2010). Antimicrobial therapy is considered in case of serious infections, but resistance to commonly used antimicrobials is of concern.

In 2022, 6,772 *C. jejuni* and 1,138 *C. coli* clinical isolates were tested at the French National Reference Center for Campylobacters and Helicobacters (Lehours et al., 2023) (NRCCH) showing 63.1 and 64% resistance to ciprofloxacin, 46.9 and 79.4% resistance to tetracycline as well as 33.5 and 29.1% resistance for ampicillin, respectively. However, resistance to macrolides and aminoglycosides remained very low, even though *C. coli* showed a concerning increase in erythromycin resistance through the emergence of new mechanisms (Jehanne et al., 2021). In France, 0.3% of *C. jejuni* and 7% of *C. coli* isolates are resistant to erythromycin and 0.4% of *C. jejuni* and 2.4% of *C. coli* isolates are resistant to gentamicin. In addition, less than 0.1% of both *C. jejuni* and *C. coli* are resistant to amoxicillin-clavulanic acid, a phenomena which is more common for *Campylobacter* closely related species, for instance *Aliarcobacter butzleri* (Zacharow et al., 2015).

Due to the excessive use of antimicrobials, especially in animal, specific genetic mechanisms of resistance have been selected among *C. jejuni* and *C. coli* (Griggs et al., 2005; Ladely et al., 2009; Qin et al., 2014; Florez-Cuadrado et al., 2017; Chen et al., 2018; Fabre et al., 2018; Elhadidy et al., 2019; Anampa et al., 2020; Greninger et al., 2020; Hormeño et al., 2020; Wallace et al., 2020; Jehanne et al., 2021). The G57T mutation in the promoting region of bla_{OXA61} (Zeng et al., 2014) is, in particular, associated with ampicillin resistance. However, no amoxicillin-clavulanic acid resistance mechanism has yet been described. Amoxicillin-clavulanic acid can therefore be an antimicrobial of choice against campylobacteriosis, especially in case of bacteremia (Abay et al., 2014; Schiaffino et al., 2019; Tinévez et al., 2022). However, high levels of resistance can be found in some clinical isolates with minimum inhibitory concentration (MIC) reaching 256 mg/L or above. In the present study, 30 clinical isolates from the collection of the NRCCH were analyzed. Amoxicillin-clavulanic acid and ampicillin resistant and susceptible *C. jejuni* and *C. coli* were selected (i) to perform whole-genome sequencing (WGS), (ii) to quantify the expression of Bla_{OXA61} using mass spectrometry (MS) in order to (iii) identify the genetic mechanism associated with amoxicillin-clavulanic acid resistance. It allowed us to link Bla_{OXA61} expression levels to the sequence of its promoting region and especially amoxicillin-clavulanic acid resistance to the presence of a supplemental deletion at position A69 in *C. coli*.

Materials and methods

Isolates selection

A total of 30 isolates (12 *C. coli* and 18 *C. jejuni*), listed in Table 1 with their corresponding ENA accession number, were analyzed in the present study as well as two references (*C. jejuni* CCUG 11284 and *C. coli* CCUG 11283). The mean age and sex ratio (m/f) of the dataset were 38.4 years and 1.7, respectively. It is composed of clinical strains that have been isolated between 2017 and 2020 from stools and send to the French National Reference Center for Campylobacters and Helicobacters (NRCCH) (Bordeaux, France) by clinical laboratories participating to its surveillance network. Among the *C. jejuni* isolates, nine were ampicillin (AMP)-susceptible (S), and nine were AMP-resistant (R). They were all amoxicillin-clavulanic acid (AMC)-susceptible. Four of the 12 *C. coli* were AMP-S and eight were AMP-R. Three AMP-R *C. coli*, from 2017, 2018 and 2020, were resistant to amoxicillin-clavulanic acid (AMC). Species were identified by matrix-assisted laser desorption ionization-time of flight-mass spectrometry as already described (Bessède et al., 2011). Antimicrobial susceptibility to ampicillin, amoxicillin-clavulanic acid, ciprofloxacin, erythromycin, tetracycline, and gentamicin were performed by diffusion using EUCAST guidelines.[1] Ampicillin and amoxicillin-clavulanic acid MICs were determined using Etest (bioMérieux, Marcy l'Etoile, France) and interpreted according to the cut-off values proposed by the CASFM: S ≤ 4 mg/L, R > 16 mg/L.[2]

Whole genome sequencing and genomes analyses

Each clinical isolate was grown on Columbia blood agar (CBA) plate with 5% sheep's blood (Thermo Fisher Scientific, MA) and incubated at 37°C in a jar. An Anoxomat microprocessor (Mart Microbiology BV, Lichtenvoorde, The Netherlands) created an microaerobic atmosphere of 79.7% N_2, 7.1% CO_2, and 7.1% H_2 and 6% O_2. DNA was then extracted from pure bacterial colonies using the MagNA Pure 6 DNA and viral NA SV kit, and DNA purification was performed by bacterial lysis on a MagNA Pure 96 system (Roche Applied Science, Manheim, Germany). Whole genome sequencing (WGS) was performed either on Illumina ISeq 100 (locally at the NRCCH) or Nova Seq 6000 sequencer (Integragen, Evry, France). Sequencing data was analyzed using an in-house pipeline. Specifically, raw reads were cleaned using Sickle v1.33 (Joshi and Fass, 2011) and genomes were assembled using SPAdes v3.15.5 (Bankevich et al., 2012). Generated contigs were filtered depending on their depth (minimum five) and length (minimum 200). Bacterial species were confirmed from *in vitro* Average Nucleotide Identity method using FastANI v1.1 (Jain et al., 2018) and potential sources of contamination were identified using STRUCTURE tool v2.3.4 (Pritchard et al., 2000) combined with host-segregating genomic markers for *C. jejuni* (Thépault et al., 2017) and *C. coli* (Jehanne et al., 2020). Finally,

1 http://www.eucast.org

2 https://www.sfm-microbiologie.org/boutique/comite-de-lantibiograme-de-la-sfm-casfm/

TABLE 1 *C. coli* and *C. jejuni* French clinical isolates from 2017 to 2020 analyzed in the present study.

											Molecular resistance identification[f]			
Isolates	Species	ANI score[a]	Patient age	Patient sex	Source	Sample date	AMP MIC (mg/L)[b]	AMC MIC (mg/L)[c]	*blaOXA61* promoter[d]	ENA assembly accession[e]	CIP	ERY	TET	GEN
2017-1086H	*Campylobacter coli*	98.67	80	Female	Stools	Dec 2017	**>256 (R)**	**12 (R)**	G57T + ΔA69	GCA_958296275	GyrA D90N	23S A2075G	*tet(O)*	–
2018-0030H	*Campylobacter coli*	98.73	3	Male	Stools	Jan 2018	**>256 (R)**	**12 (R)**	G57T + ΔA69	GCA_958296255	GyrA D90N	23S A2075G	*tet(O)*	–
2020-0472	*Campylobacter coli*	98.71	69	Female	Stools	May 2020	**>256 (R)**	**256 (R)**	G57T + ΔA69	GCA_958295195	GyrA T86I	23S A2075G	*tet(O)*	–
2018-2008	*Campylobacter coli*	98.76	2	Male	Stools	Sep 2018	**128 (R)**	2 (S)	G57T	GCA_958296215	GyrA T86I	23S A2075G	*tet(O)*	–
2019-0242H	*Campylobacter coli*	99.06	16	Female	Stools	May 2019	**64 (R)**	1.5 (S)	G57T	GCA_958296265	GyrA T86I	23S A2075G	*tet(O-M-O)*	*APH(2″)-IIIa*
2019-0409	*Campylobacter coli*	98.72	34	Female	Stools	Mar 2019	**>256 (R)**	1.5 (S)	G57T	GCA_958296375	GyrA T86I	–	–	–
2020-0014H	*Campylobacter coli*	98.70	17	Male	Stools	Jan 2020	**>256 (R)**	3 (S)	G57T	GCA_958295415	GyrA T86I	–	*tet(O)*	–
2020-0548	*Campylobacter coli*	98.78	7	Female	Stools	May 2020	**96 (R)**	2 (S)	G57T	GCA_958296355	GyrA T86I	–	*tet(O)*	–
2018-1149	*Campylobacter coli*	99.02	43	Male	Stools	Jun 2018	4 (S)	1 (S)	*wt*	GCA_958296365	GyrA T86I	*erm(B)*	*tet(O)*	–
2019-2217	*Campylobacter coli*	98.92	1	Male	Stools	Sep 2019	2 (S)	1 (S)	*wt*	GCA_958295225	–	–	–	–
2020-0368	*Campylobacter coli*	98.76	89	Male	Stools	Apr 2020	4 (S)	1 (S)	*wt*	GCA_958295175	GyrA T86I	–	*tet(O)*	–
2020-0448H	*Campylobacter coli*	98.69	68	Female	Stools	Jul 2020	3 (S)	1 (S)	*wt*	GCA_958295215	–	23S A2074G	*tet(O)*	–
2018-0007	*Campylobacter jejuni*	97.67	29	Female	Stools	Jan 2018	**32 (R)**	<0.016 (S)	G57T	GCA_958295635	–	–	–	–
2018-0008	*Campylobacter jejuni*	97.68	8	Male	Stools	Jan 2018	**24 (R)**	<0.016 (S)	G57T	GCA_958295325	GyrA T86I	–	*tet(O)*	–
2018-0013	*Campylobacter jejuni*	97.53	52	Female	Stools	Jan 2018	**32 (R)**	<0.016 (S)	G57T	GCA_958295375	GyrA T86I	–	*tet(O)*	–
2018-0015	*Campylobacter jejuni*	97.38	48	Male	Stools	Jan 2018	**64 (R)**	<0.016 (S)	G57T	GCA_958295345	GyrA T86I	–	*tet(O)*	–
2018-0024H	*Campylobacter jejuni*	97.65	3	Male	Stools	Jan 2018	**64 (R)**	<0.016 (S)	G57T	GCA_958295235	GyrA T86I	–	*tet(O-32-O)*	–
2018-1793	*Campylobacter jejuni*	97.53	74	Female	Stools	Aug 2018	**32 (R)**	<0.016 (S)	G57T	GCA_958295365	GyrA T86I	23S A2075G	*tet(O-M-O)*	–
2019-0006H	*Campylobacter jejuni*	97.58	21	Male	Stools	Jan 2019	**64 (R)**	<0.016 (S)	G57T	GCA_958295285	GyrA T86I	–	*tet(O)*	–
2019-0008	*Campylobacter jejuni*	97.66	4	Male	Stools	Jan 2019	**24 (R)**	<0.016 (S)	G57T	GCA_958295355	GyrA T86I	–	–	–
2019-1193	*Campylobacter jejuni*	97.53	45	Male	Stools	Jun 2019	**32 (R)**	0.016 (S)	G57T	GCA_958295305	GyrA T86I	23S A2074C	*tet(O-32-O)*	–
2018-0009H	*Campylobacter jejuni*	97.63	66	Female	Stools	Jan 2018	3 (S)	<0.016 (S)	*wt*	GCA_958295385	GyrA T86I	–	–	–
2018-0014	*Campylobacter jejuni*	97.55	21	Male	Stools	Jan 2018	1.5 (S)	<0.016 (S)	*wt*	GCA_958295275	GyrA T86I	–	–	–
2018-0023H	*Campylobacter jejuni*	97.60	16	Male	Stools	Jan 2018	1.5 (S)	<0.016 (S)	*wt*	GCA_958295585	GyrA T86I	–	–	–
2018-0069H	*Campylobacter jejuni*	97.65	87	Male	Stools	Feb 2018	1 (S)	<0.016 (S)	*wt*	GCA_958295295	–	–	*tet(O)*	–
2018-0082H	*Campylobacter jejuni*	97.49	100	Male	Stools	Feb 2018	2 (S)	<0.016 (S)	*wt*	GCA_958295205	–	–	–	–
2018-0116	*Campylobacter jejuni*	97.72	67	Male	Stools	Jan 2018	2 (S)	<0.016 (S)	*wt*	GCA_958295245	GyrA T86I	23S A2075G	*tet(O)*	–
2019-0011	*Campylobacter jejuni*	97.68	22	Female	Stools	Jan 2019	2 (S)	<0.016 (S)	*wt*	GCA_958295255	GyrA T86I	–	*tet(O)*	–
2019-0026	*Campylobacter jejuni*	97.52	2	Male	Stools	Jan 2019	2 (S)	<0.016 (S)	*wt*	GCA_958295335	GyrA T86I	–	*tet(O)*	–
2019-0207	*Campylobacter jejuni*	97.14	58	Male	Stools	Feb 2019	2 (S)	<0.016 (S)	*wt*	GCA_958295265	GyrA T86I	23S A2074T	*tet(O)*	–

Genomes were assembled using SPAdes and species were confirmed using ANI with a threshold ≥95% [a]. Values and corresponding phenotypes (R: resistant; S: susceptible) of ampicillin (AMP [b]) and amoxicillin-clavulanic acid (AMC [c]) are displayed as MICs in mg/L from Etest analyses. Genotypes of interest in the bla_{OXA61} promoting sequence are shown using their corresponding positions [d] (wt: wild type). Genomes in fasta format are available within the ENA database using listed accession numbers [e]. Mutations and genes expression associated to ciprofloxacin (CIP), erythromycin (ERY), tetracycline (TET) and gentamicin (GEN) resistances are also indicated [f]. Bold values correspond to resistant isolates.

10.3389/fmicb.2023.1285236

resistance markers (genes and mutations) were isolated from each assembled genomes using Nucleotide-Nucleotide/Protein–Protein BLAST 2.12.0+ (Altschul et al., 1997) command line tool combined with multiple databases: ncbi, card, resfinder, plasmidfinder and an in-house database for *Campylobacter* sp. based on various previous publications (Griggs et al., 2005; Ladely et al., 2009; Qin et al., 2014; Zeng et al., 2014; Fabre et al., 2018; Hormeño et al., 2020; Jehanne et al., 2021).

Sample preparation for LC–MS/MS analysis

Primary cultures of *C. coli* and *C. jejuni* strains were performed in triplicates on Columbia agar +5% sheep blood plates (bioMérieux, Marcy L'étoile, France) at 37°C for 48 h in microaerobic atmosphere. Sub-cultures were performed under the same conditions and bacterial suspensions were prepared in LC–MS grade water to reach a minimum density of four McFarland. Two hundred microliters of bacterial suspension were transferred into 1.5 mL tubes containing approximately 70 mg of 150–212 µm glass beads (Sigma-Aldrich) and 50 µL of 1 mg/ml recombinant trypsin (Roche) in 150 mM NH_4HCO_3 (Sigma-Aldrich) were added to each tube. Bacterial lysis and protein digestion were performed in a thermostated (50°C) Bioruptor ultrasonicator (Diagenode, Lièges, Belgium) for 10 min with ultrasounds being applied for 30 s every minute. Trypsin digestion was stopped by adding 5 µL of formic acid (Sigma-Aldrich). Tubes were then centrifuged at 9600 × *g* for 5 min and 100 µL of supernatant were transferred to a final 2 mL glass vial for LC–MS/MS analysis.

LC–MS/MS analysis

Samples were analyzed with an Agilent 1290 Infinity liquid chromatography coupled to a SCIEX QTRAP6500+ Triple-quadrupole mass spectrometer equipped with an ESI Turbo V ion source. Ten microliters of samples were injected on the system. Mobile phases were H_2O + 0.1% formic acid (Buffer A) and ACN + 0.1% formic acid (Buffer B). LC separation was carried out on a Waters Xbridge Peptide BEH C18 (1 mm × 100 mm, particle size 3.5 µm) column heated at 60°C. The analytical gradient was set as follow: 2 to 10% B from 0 to 0.1 min, 10 to 30.5% B from 0.1 to 13.1 min, and 30.5 to 50% B from 13.1 to 15.95 min. Flow rate was set at 100 µL/min. The mass spectrometer ion source temperature was 550°C and the ion spray voltage set at 5500 V. Curtain gas, nebulizer gas (GS1) and heating gas (GS2) were, respectively, set at 50, 70, and 60 psi.

MRM assay development

The amino-acid sequence of Bla_{OXA61} beta-lactamase was digested *in silico* with trypsin using Skyline software (version 22.2.0.351) to generate every potential surrogate peptide. An initial MRM method was built monitoring three y ion-type fragments for each doubly and triply charged putative peptides to identify the ones detectable in strains known to express high amounts of Bla_{OXA61}. All peptides selected during the first screening step were included in a second MRM method to monitor every y and b ions of the most intense charge state. Signal specificity was confirmed when at least eight transitions were detected at the same retention time in strains known to express *bla*$_{OXA61}$ and when no signal was observed for strains known to have intrinsic repression of the beta-lactamase expression. A final MRM assay was built with the three most intense fragment ions of each Bla_{OXA61} peptide as well as three y ions for five peptides derived from *Campylobacter* ribosomal proteins (Supplementary Table 1).

Peak detection and relative quantification

Raw chromatograms were analyzed using Skyline software. For each peptide, peak integration was manually checked and curated when necessary to ensure correct quantification. Label-free quantification strategies have now been widely applied and demonstrated their robustness for quantification of proteins in biological samples (Cecchini et al., 2018; Fournier et al., 2021; Pivard et al., 2023). Those approaches rely on the assumption that signal of the most intense transitions of the best flying peptide correlate with protein abundance and can therefore be used as an indicator of protein amounts (Ludwig et al., 2012). Here, the area of the three transitions of three Bla_{OXA61} peptides (EQAILLFR, YLDELVK and IDTFWLDNSLK) were summed to compensate for potential slight variations in fragmentation and trypsin digestion repeatability across runs. Moreover, to take into account bacterial load variations across samples, the sum of Bla_{OXA61} peptides is expressed relative to signals of five housekeeping peptides derived from ribosomal proteins used as indicators of bacterial density due to their quantotypic properties (Cecchini et al., 2018; Pivard et al., 2023). In other words, quantification values are obtained using Equation 1:

$$Quantification = \frac{\sum of\ the\ 3\ transitions\ of\ 3\ BlaOXA61\ peptides}{\sum of\ the\ 3\ transitions\ of\ 5\ ribosomal\ peptides} \quad (1)$$

Results

Genomic analyses

C. jejuni and *C. coli* genomes were properly assembled and species were confirmed with average scores of 97.57% (±0.14) and 98.79% (±0.13) for *C. jejuni* and *C. coli* isolates, respectively (Table 1). The average genomes size was 1.72 Mbp (±67 kbp) with an average contigs number of 80 (±196; isolate fasta "2018–0015" is comprised of more than 1000 contigs which significantly increases the data) and an average contig length of 42 kbp (±15.8 kbp). Moreover, genomes GC % was about 32% (±2.2%) and the average number of coding sequences (CDS) was 1,766 (±66), in accordance with previously published data (Pearson et al., 2013; He et al., 2020). Additionally, most of the selected clinical isolates were attributed to the chicken reservoir using source attribution models (*data not shown*), which represents 63.3% of the dataset. Genomic antimicrobial resistance (AMR) analysis allowed to display the G57T mutation in the *bla*$_{OXA61}$ promoting region among every AMP-R *C. jejuni* and *C. coli* isolates, highlighting the importance of this marker in ampicillin resistance for Campylobacters (Zeng et al., 2014). A supplemental

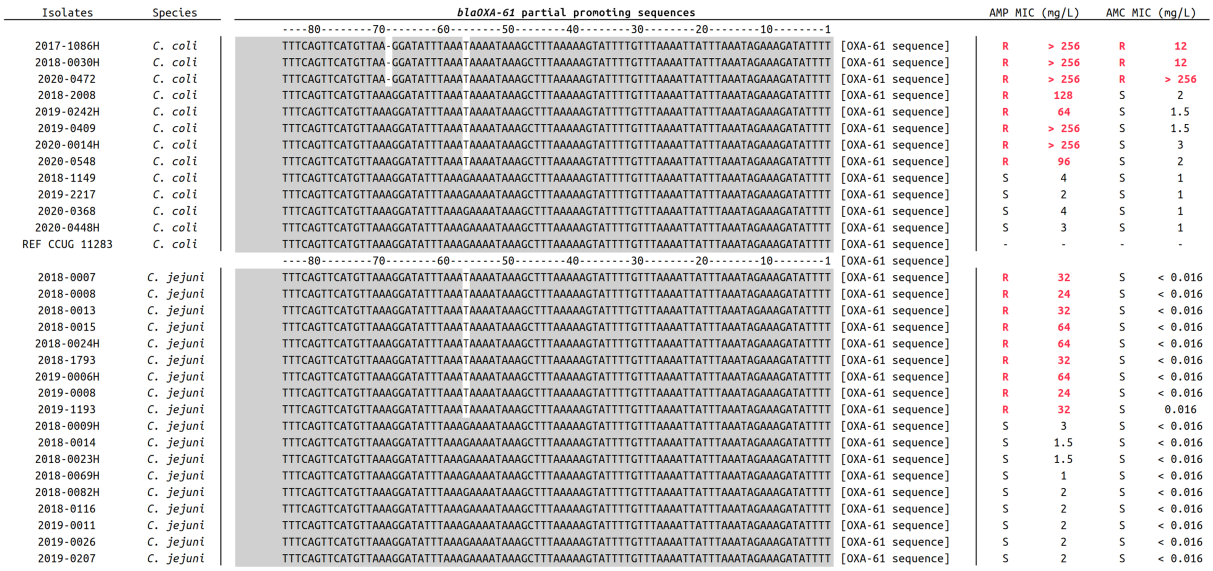

Isolates	Species	*blaOXA-61* partial promoting sequences		AMP MIC (mg/L)		AMC MIC (mg/L)	
		----80--------70--------60--------50--------40--------30--------20--------10--------1					
2017-1086H	*C. coli*	TTTCAGTTCATGTTAA-GGATATTTAAATAAAATAAAGCTTTAAAAAGTATTTTGTTTAAAATTATTTAAATAGAAAGATATTTT	[OXA-61 sequence]	R	> 256	R	12
2018-0030H	*C. coli*	TTTCAGTTCATGTTAA-GGATATTTAAATAAAATAAAGCTTTAAAAAGTATTTTGTTTAAAATTATTTAAATAGAAAGATATTTT	[OXA-61 sequence]	R	> 256	R	12
2020-0472	*C. coli*	TTTCAGTTCATGTTAA-GGATATTTAAATAAAATAAAGCTTTAAAAAGTATTTTGTTTAAAATTATTTAAATAGAAAGATATTTT	[OXA-61 sequence]	R	> 256	R	> 256
2018-2008	*C. coli*	TTTCAGTTCATGTTAAAGGATATTTAAATAAAATAAAGCTTTAAAAAGTATTTTGTTTAAAATTATTTAAATAGAAAGATATTTT	[OXA-61 sequence]	R	128	S	2
2019-0242H	*C. coli*	TTTCAGTTCATGTTAAAGGATATTTAAATAAAATAAAGCTTTAAAAAGTATTTTGTTTAAAATTATTTAAATAGAAAGATATTTT	[OXA-61 sequence]	R	64	S	1.5
2019-0409	*C. coli*	TTTCAGTTCATGTTAAAGGATATTTAAATAAAATAAAGCTTTAAAAAGTATTTTGTTTAAAATTATTTAAATAGAAAGATATTTT	[OXA-61 sequence]	R	> 256	S	1.5
2020-0014H	*C. coli*	TTTCAGTTCATGTTAAAGGATATTTAAATAAAATAAAGCTTTAAAAAGTATTTTGTTTAAAATTATTTAAATAGAAAGATATTTT	[OXA-61 sequence]	R	> 256	S	3
2020-0548	*C. coli*	TTTCAGTTCATGTTAAAGGATATTTAAATAAAATAAAGCTTTAAAAAGTATTTTGTTTAAAATTATTTAAATAGAAAGATATTTT	[OXA-61 sequence]	R	96	S	2
2018-1149	*C. coli*	TTTCAGTTCATGTTAAAGGATATTTAAAGAAAATAAAGCTTTAAAAAGTATTTTGTTTAAAATTATTTAAATAGAAAGATATTTT	[OXA-61 sequence]	S	4	S	1
2019-2217	*C. coli*	TTTCAGTTCATGTTAAAGGATATTTAAAGAAAATAAAGCTTTAAAAAGTATTTTGTTTAAAATTATTTAAATAGAAAGATATTTT	[OXA-61 sequence]	S	2	S	1
2020-0368	*C. coli*	TTTCAGTTCATGTTAAAGGATATTTAAAGAAAATAAAGCTTTAAAAAGTATTTTGTTTAAAATTATTTAAATAGAAAGATATTTT	[OXA-61 sequence]	S	4	S	1
2020-0448H	*C. coli*	TTTCAGTTCATGTTAAAGGATATTTAAAGAAAATAAAGCTTTAAAAAGTATTTTGTTTAAAATTATTTAAATAGAAAGATATTTT	[OXA-61 sequence]	S	3	S	1
REF CCUG 11283	*C. coli*	TTTCAGTTCATGTTAAAGGATATTTAAAGAAAATAAAGCTTTAAAAAGTATTTTGTTTAAAATTATTTAAATAGAAAGATATTTT	[OXA-61 sequence]	-	-	-	-
		----80--------70--------60--------50--------40--------30--------20--------10--------1	[OXA-61 sequence]				
2018-0007	*C. jejuni*	TTTCAGTTCATGTTAAAGGATATTTAAATAAAATAAAGCTTTAAAAAGTATTTTGTTTAAAATTATTTAAATAGAAAGATATTTT	[OXA-61 sequence]	R	32	S	< 0.016
2018-0008	*C. jejuni*	TTTCAGTTCATGTTAAAGGATATTTAAATAAAATAAAGCTTTAAAAAGTATTTTGTTTAAAATTATTTAAATAGAAAGATATTTT	[OXA-61 sequence]	R	24	S	< 0.016
2018-0013	*C. jejuni*	TTTCAGTTCATGTTAAAGGATATTTAAATAAAATAAAGCTTTAAAAAGTATTTTGTTTAAAATTATTTAAATAGAAAGATATTTT	[OXA-61 sequence]	R	32	S	< 0.016
2018-0015	*C. jejuni*	TTTCAGTTCATGTTAAAGGATATTTAAATAAAATAAAGCTTTAAAAAGTATTTTGTTTAAAATTATTTAAATAGAAAGATATTTT	[OXA-61 sequence]	R	64	S	< 0.016
2018-0024H	*C. jejuni*	TTTCAGTTCATGTTAAAGGATATTTAAATAAAATAAAGCTTTAAAAAGTATTTTGTTTAAAATTATTTAAATAGAAAGATATTTT	[OXA-61 sequence]	R	64	S	< 0.016
2018-1793	*C. jejuni*	TTTCAGTTCATGTTAAAGGATATTTAAATAAAATAAAGCTTTAAAAAGTATTTTGTTTAAAATTATTTAAATAGAAAGATATTTT	[OXA-61 sequence]	R	32	S	< 0.016
2019-0006H	*C. jejuni*	TTTCAGTTCATGTTAAAGGATATTTAAATAAAATAAAGCTTTAAAAAGTATTTTGTTTAAAATTATTTAAATAGAAAGATATTTT	[OXA-61 sequence]	R	64	S	< 0.016
2019-0008	*C. jejuni*	TTTCAGTTCATGTTAAAGGATATTTAAATAAAATAAAGCTTTAAAAAGTATTTTGTTTAAAATTATTTAAATAGAAAGATATTTT	[OXA-61 sequence]	R	24	S	< 0.016
2019-1193	*C. jejuni*	TTTCAGTTCATGTTAAAGGATATTTAAATAAAATAAAGCTTTAAAAAGTATTTTGTTTAAAATTATTTAAATAGAAAGATATTTT	[OXA-61 sequence]	R	32	S	0.016
2018-0009H	*C. jejuni*	TTTCAGTTCATGTTAAAGGATATTTAAAGAAAATAAAGCTTTAAAAAGTATTTTGTTTAAAATTATTTAAATAGAAAGATATTTT	[OXA-61 sequence]	S	3	S	< 0.016
2018-0014	*C. jejuni*	TTTCAGTTCATGTTAAAGGATATTTAAAGAAAATAAAGCTTTAAAAAGTATTTTGTTTAAAATTATTTAAATAGAAAGATATTTT	[OXA-61 sequence]	S	1.5	S	< 0.016
2018-0023H	*C. jejuni*	TTTCAGTTCATGTTAAAGGATATTTAAAGAAAATAAAGCTTTAAAAAGTATTTTGTTTAAAATTATTTAAATAGAAAGATATTTT	[OXA-61 sequence]	S	1.5	S	< 0.016
2018-0069H	*C. jejuni*	TTTCAGTTCATGTTAAAGGATATTTAAAGAAAATAAAGCTTTAAAAAGTATTTTGTTTAAAATTATTTAAATAGAAAGATATTTT	[OXA-61 sequence]	S	1	S	< 0.016
2018-0082H	*C. jejuni*	TTTCAGTTCATGTTAAAGGATATTTAAAGAAAATAAAGCTTTAAAAAGTATTTTGTTTAAAATTATTTAAATAGAAAGATATTTT	[OXA-61 sequence]	S	2	S	< 0.016
2018-0116	*C. jejuni*	TTTCAGTTCATGTTAAAGGATATTTAAAGAAAATAAAGCTTTAAAAAGTATTTTGTTTAAAATTATTTAAATAGAAAGATATTTT	[OXA-61 sequence]	S	2	S	< 0.016
2019-0011	*C. jejuni*	TTTCAGTTCATGTTAAAGGATATTTAAAGAAAATAAAGCTTTAAAAAGTATTTTGTTTAAAATTATTTAAATAGAAAGATATTTT	[OXA-61 sequence]	S	2	S	< 0.016
2019-0026	*C. jejuni*	TTTCAGTTCATGTTAAAGGATATTTAAAGAAAATAAAGCTTTAAAAAGTATTTTGTTTAAAATTATTTAAATAGAAAGATATTTT	[OXA-61 sequence]	S	2	S	< 0.016
2019-0207	*C. jejuni*	TTTCAGTTCATGTTAAAGGATATTTAAAGAAAATAAAGCTTTAAAAAGTATTTTGTTTAAAATTATTTAAATAGAAAGATATTTT	[OXA-61 sequence]	S	2	S	< 0.016

FIGURE 1
Alignment of *bla*$_{OXA61}$ promoting sequences in 18 *C. jejuni* and 12 *C. coli* included in the present study. For each isolate, ampicillin and amoxicillin-clavulanic acid MICs are indicated. Promoting regions were extracted from every assembled genome using Nucleotide-Nucleotide BLAST 2.12.0+ (Altschul et al., 1997), and sequences were aligned using Muscle v3.8.1551 (Edgar, 2004). Relevant genotypes are here highlighted in white at positions −57 and −69.

deletion in position A69 of that promoting sequence was also exclusively identified among all three AMC-R *C. coli* isolates (two from chicken and one from pig according to the source attribution markers), as shown in Figure 1. The use of mass-spectrometry was used to estimate the impact of such deletion on the expression of Bla$_{OXA61}$.

MRM analyses

To quantitatively assess the expression levels of Bla$_{OXA61}$, each strain was grown in triplicates and trypsin-digested bacterial lysates were analyzed by targeted mass spectrometry for the detection of Bla$_{OXA61}$. Due to variations observed in the relative intensities of ribosomal peptides (used as housekeeping standards for cell number and expression level normalization, as described in material and methods) between *C. jejuni* and *C. coli*, Bla$_{OXA61}$ expression levels were only compared within the same species.

In comparison to the wild type promoter, the addition of the G57T mutation in *bla*$_{OXA61}$ promoting region leads to an increase of the beta-lactamase expression and confers resistance to ampicillin for both *Campylobacter* species (Figures 2A, 3A). Relative quantification revealed a significant 15-fold and 16-fold increase in overexpression of Bla$_{OXA61}$ compared to the ampicillin susceptible (wild type promoter) in *C. jejuni* and *C. coli* isolates, respectively (Figures 2B, 3B).

The combination of the G57T mutation with a supplemental deletion in position A69 was associated with a significant overexpression of Bla$_{OXA61}$ and resistance to amoxicillin-clavulanic acid in the three *C. coli* strains included in the present study. Indeed, a significant 54 and 16-fold increase was observed compared with strains harboring a WT or a G57T *bla*$_{OXA61}$ promoter (Figure 3B), respectively.

Data availability

Corresponding genome accession numbers of each clinical isolates are available in Table 1 and under ENA Study number PRJEB63218. MRM raw data and transition list are available via PASSEL with the accession number PASS05834.[3]

Discussion

Campylobacter resistance to antimicrobials is concerning (Wieczorek and Osek, 2013). However, resistance to amoxicillin combined to clavulanic acid beta lactamase-inhibitor among human *Campylobacter* isolates remains sparse (Deckert et al., 2013; Post et al., 2017; Wallace et al., 2021), even though ampicillin resistance rates in poultry reservoirs are high (Casagrande Proietti et al., 2020; Béjaoui et al., 2022; Gharbi et al., 2023) (up to 73%). This current study proposes a combined genomic and proteomic approach to characterize the mechanism responsible for amoxicillin-clavulanic acid (AMC) resistance in *Campylobacter* clinical isolates, specifically *C. coli*. This experimental strategy used both molecular and mass spectrometry analyzes and highlighted a deletion at position A69 in the *bla*$_{OXA61}$ promoting region contributing to a significant increase of the beta-lactamase expression, which is associated with amoxicillin-clavulanic acid resistance.

The existence of beta-lactamases among *C. jejuni* and *C. coli* isolates is now well described, such as *bla*$_{OXA61}$, *bla*$_{OXA489}$ or *bla*$_{OXA193}$, with *bla*$_{OXA61}$ being the most frequently observed

3 https://db.systemsbiology.net/sbeams/cgi/PeptideAtlas/PASS_View

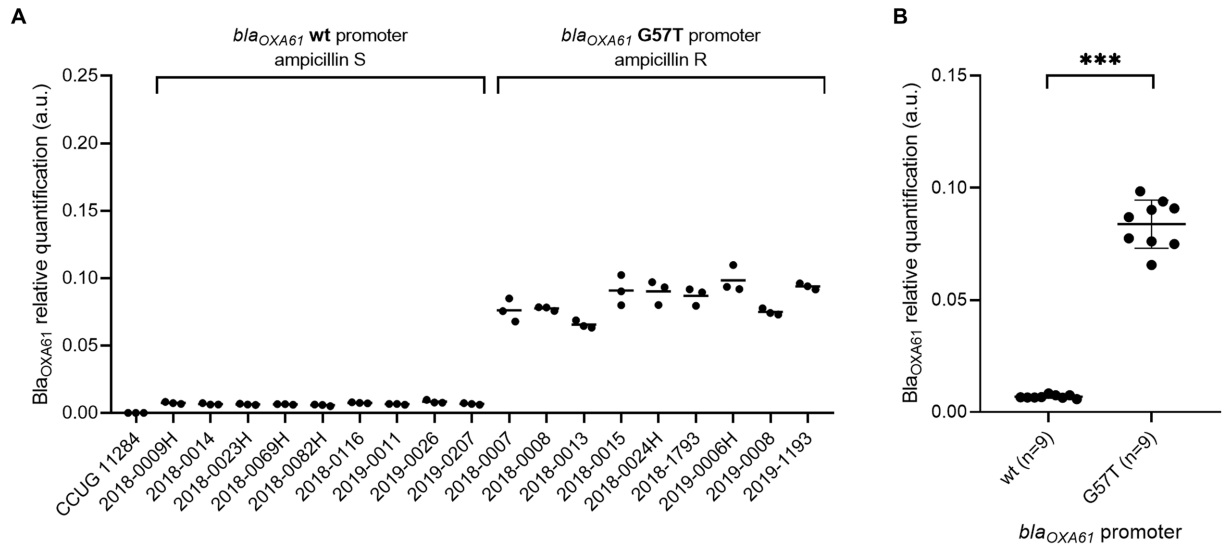

FIGURE 2
Bla_{OXA61} relative quantification in ampicillin-susceptible and resistant *C. jejuni* isolates. **(A)** Each strain individually. **(B)** Strains grouped according to the bla_{OXA61}-promoting sequences. Data are expressed in arbitrary units. In panel **(B)**, the mean of triplicates was used to perform a Mann–Whitney *U* test. ***p value <0.001. wt, wild type; S, susceptible; R, resistant. No signal was observed for *C. jejuni* reference CCUG 11284.

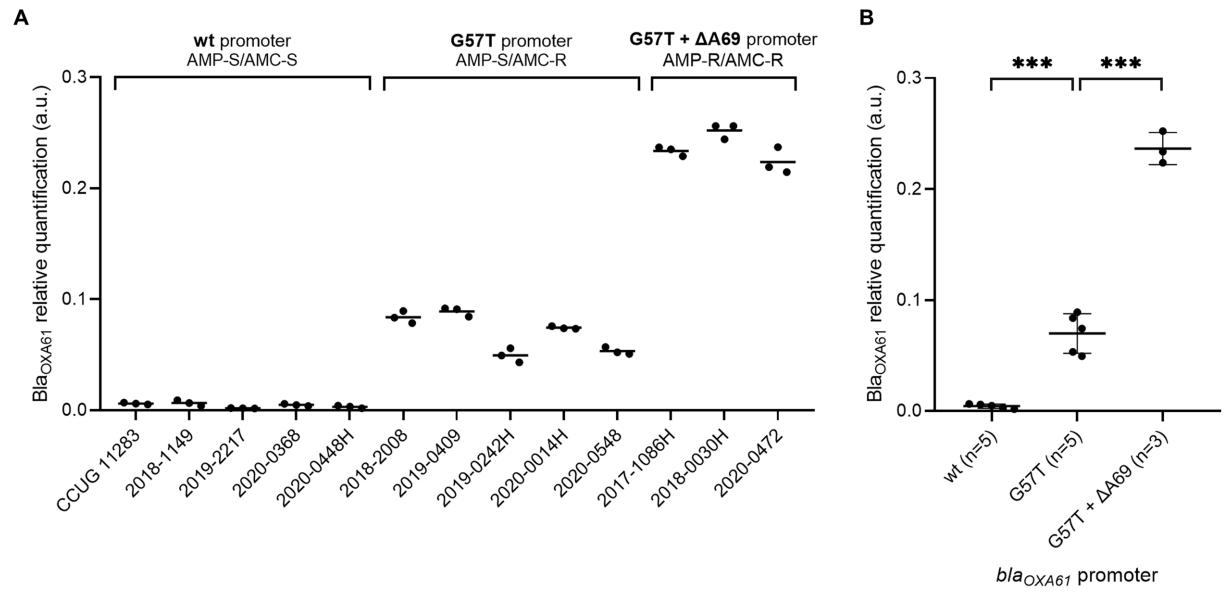

FIGURE 3
Expression levels of Bla_{OXA61} in *C. coli* isolates with wild type, G57T or G57T + ΔA69 promoters. **(A)** Each strain individually. **(B)** Strains grouped according to the bla_{OXA61}-promoting sequences. Data are expressed in arbitrary units. In panel **(B)**, the mean of triplicates was used to perform one-way ANOVA. ***p-value <0.001. wt, wild type; AMP, ampicillin; AMC, amoxicillin + clavulanic acid; S, susceptible; R, resistant.

(Cobo-Díaz et al., 2021). Even though their expression has been widely associated with aminopenicillin resistance, many previous studies are based uniquely on the presence or absence of beta-lactamase genes without taking into account the importance of the promoting region (Gharbi et al., 2023). As a matter of fact, a single nucleotide at position 57 (G → T) in this specific sequence is associated with ampicillin resistance (Zeng et al., 2014). Activity of beta-lactamase inhibitors such as clavulanic acid used in combination to amoxicillin may be significantly impaired in case of bla_{OXA61} overexpression, as shown in a previous study using PCR and qPCR amplification (Casagrande Proietti et al., 2020).

In the present study, LC–MS/MS allowed to confirm that the G57T mutation in the *bla*$_{OXA61}$ promoting region is responsible for an increased expression of the beta-lactamase, thus conferring ampicillin resistance. However, every *C. jejuni* and *C. coli* clinical isolates which only displayed that single mutation remain highly susceptible to the amoxicillin-clavulanic acid activity. Nevertheless, we showed that three AMC-resistant *C. coli* isolates displayed a supplemental A69 deletion responsible for an overexpression of Bla$_{OXA61}$. Those high levels of Bla$_{OXA61}$ production seems to fully encounter clavulanic acid inhibitor activity. Additional *C. coli* isolates with both G57T + ΔA69 genotypes but also isolates showing ΔA69 only would need to be collected to ensure more robust statistical analysis and therefore better assess the correlation between their resistance phenotype and the expression level of Bla$_{OXA61}$.

According to Tajada et al. (1996) the great activity of clavulanic acid in *C. jejuni* and *C. coli* is due to its ability to bind Penicillin Binding Proteins with lower MICs in *C. jejuni* compared to *C. coli*. It is therefore maybe not surprising to observe amoxicillin-clavulanic acid resistance only in *C. coli*. Amoxicillin-clavulanic acid resistance remains however very rare among *C. jejuni* and *C. coli* clinical isolates. Nevertheless, such broadened resistance spectrum conferred by overexpression of a beta-lactamases due to point mutations in the promoter region is not unusual, as it has been well described in other species especially *E. coli* (Corvec et al., 2002; Tracz et al., 2005; Singh et al., 2019). Site-directed mutagenesis to induce changes in the *bla*$_{OXA61}$ promoting sequence of amoxicillin-clavulanic acid and ampicillin susceptible isolates could however be performed in order to fully observe the impact on the gene expression.

In conclusion, combined genomic-proteomic approach here allowed us to identify a new *bla*$_{OXA61}$ promoting region displaying both G57T mutation and an uncharacterized A69 deletion which leads to a significative overexpression of this beta-lactamase and may be responsible for amoxicillin-clavulanic acid resistance. These results are even more valuable as we lack consensus data on such phenotypes. Indeed, *C. jejuni* and *C. coli* breakpoints for amoxicillin-clavulanic acid today are based on that for other species, such as the use of EUCAST *Enterobacteriaceae* recommendations. Although this mechanism is rare among *C. coli* clinical isolates, it needs to be seriously considered since *C. coli* species isolates can easily adapt to their environment.

Data availability statement

The datasets presented in this study can be found in online repositories. The names of the repository/repositories and accession number(s) can be found in the article/Supplementary material.

Ethics statement

Ethical review and approval was not required for the study in accordance with the local legislation and institutional requirements. Written informed consent for participation was not required for this study in accordance with the national legislation and the institutional requirements. Written informed consent was not obtained from the individual(s) for the publication of any potentially identifiable images or data included in this article.

Author contributions

FD: Formal analysis, Methodology, Validation, Writing – original draft, Writing – review & editing. QJ: Formal analysis, Writing review & editing, Software. LB: Methodology, Writing – review & editing. JA: Methodology, Writing – review & editing. RP: Methodology, Writing – review & editing. CD: Methodology, Writing – review & editing. AD: Methodology, Writing – review & editing. MJ: Writing – review & editing. RB: Writing – review & editing, Methodology. FV: Writing – review & editing. JL: Writing – review & editing. PL: Writing – review & editing, Data curation, Formal analysis, Funding acquisition, Methodology, Project administration, Supervision, Validation, Writing – original draft.

Funding

The author(s) declare financial support was received for the research, authorship, and/or publication of this article. Open access funding provided by the French National Reference Center for Campylobacters and Helicobacters, Bordeaux, France. Financially supported by Santé Publique France (www.santepubliquefrance.fr).

Acknowledgments

The authors want to thank all the laboratories that sent Campylobacter isolates to our reference center, particularly the Centre Hospitalier de Cannes (Cannes, France) and the laboratory SYNLAB Beaumont (Beaumont, France), which sent the 3 amoxicillin-clavulanic-acid-resistant *C. coli* isolates included in the present study. The current manuscript was edited for proper English language using American Journal Experts services (verification code 4A53-3591-EE3 C-F0A7-37A0).

Conflict of interest

The authors declare that the research was conducted in the absence of any commercial or financial relationships that could be construed as a potential conflict of interest.

Publisher's note

Supplementary material

The Supplementary material for this article can be found online at: https://www.frontiersin.org/articles/10.3389/fmicb.2023.1285236/full#supplementary-material

References

Abay, S., Kayman, T., Otlu, B., Hizlisoy, H., Aydin, F., and Ertas, N. (2014). Genetic diversity and antibiotic resistance profiles of *Campylobacter jejuni* isolates from poultry and humans in Turkey. *Int. J. Food Microbiol.* 178, 29–38. doi: 10.1016/j.ijfoodmicro.2014.03.003

Altschul, S. F., Madden, T. L., Schäffer, A. A., Zhang, J., Zhang, Z., Miller, W., et al. (1997). Gapped BLAST and PSI-BLAST: a new generation of protein database search programs. *Nucleic Acids Res.* 25, 3389–3402. doi: 10.1093/nar/25.17.3389

Anampa, D., Benites, C., Lázaro, C., Espinoza, J., Angulo, P., Díaz, D., et al. (2020). Detection of the *ermB* gene associated with macrolide resistance in *Campylobacter* strains isolated from chickens marketed in Lima, Peru. *Rev. Panam. Salud Publica Pan Am. J. Public Health* 44:e60. doi: 10.26633/rpsp.2020.60

Bankevich, A., Nurk, S., Antipov, D., Gurevich, A. A., Dvorkin, M., Kulikov, A. S., et al. (2012). SPAdes: a new genome assembly algorithm and its applications to single-cell sequencing. *J. Comput. Biol.* 19, 455–477. doi: 10.1089/cmb.2012.0021

Béjaoui, A., Gharbi, M., Bitri, S., Nasraoui, D., Ben Aziza, W., Ghedira, K., et al. (2022). Virulence profiling, multidrug resistance and molecular mechanisms of *Campylobacter* strains from chicken carcasses in Tunisia. *Antibiotics* 11:830. doi: 10.3390/antibiotics11070830

Bessède, E., Solecki, O., Sifré, E., Labadi, L., and Mégraud, F. (2011). Identification of *Campylobacter* species and related organisms by matrix assisted laser desorption ionization-time of flight (MALDI-TOF) mass spectrometry. *Clin. Microbiol. Infect. Off. Publ. Eur. Soc. Clin. Microbiol. Infect. Dis.* 17, 1735–1739. doi: 10.1111/j.1469-0691.2011.03468.x

Casagrande Proietti, P., Guelfi, G., Bellucci, S., de Luca, S., di Gregorio, S., Pieramati, C., et al. (2020). Beta-lactam resistance in *Campylobacter coli* and *Campylobacter jejuni* chicken isolates and the association between *blaOXA-61* gene expression and the action of β-lactamase inhibitors. *Vet. Microbiol.* 241:108553. doi: 10.1016/j.vetmic.2019.108553

Cecchini, T., Yoon, E. J., Charretier, Y., Bardet, C., Beaulieu, C., Lacoux, X., et al. (2018). Deciphering multifactorial resistance phenotypes in *Acinetobacter baumannii* by genomics and targeted label-free proteomics. *Mol. Cell. Proteomics* 17, 442–456. doi: 10.1074/mcp.RA117.000107

Chen, J. C., Tagg, K. A., Joung, Y. J., Bennett, C., Francois Watkins, L., Eikmeier, D., et al. (2018). Report of *erm(B)+ Campylobacter jejuni* in the United States. *Antimicrob. Agents Chemother.* 62:e02615-17. doi: 10.1128/AAC.02615-17

Chlebicz, A., and Śliżewska, K. (2018). Campylobacteriosis, salmonellosis, yersiniosis, and listeriosis as zoonotic foodborne diseases: a review. *Int. J. Environ. Res. Public Health* 15:863. doi: 10.3390/ijerph15050863

Cobo-Díaz, J. F., González del Río, P., and Álvarez-Ordóñez, A. (2021). Whole resistome analysis in *Campylobacter jejuni* and *C. coli* genomes available in public repositories. *Front. Microbiol.* 12:662144. doi: 10.3389/fmicb.2021.662144

Corvec, S., Caroff, N., Espaze, E., Marraillac, J., and Reynaud, A. (2002). −11 mutation in the ampC promoter increasing resistance to β-lactams in a clinical *Escherichia coli* strain. *Antimicrob. Agents Chemother.* 46, 3265–3267. doi: 10.1128/AAC.46.10.3265-3267.2002

Deckert, A. E., Reid-Smith, R. J., Tamblyn, S. E., Morrell, L., Seliske, P., Jamieson, F. B., et al. (2013). Antimicrobial resistance and antimicrobial use associated with laboratory-confirmed cases of *Campylobacter* infection in two health units in Ontario. *Can. J. Infect. Dis. Med. Microbiol.* 24:e16–21. doi: 10.1155/2013/176494

Delahoy, M. J., Shah, H. J., Weller, D. L., Ray, L. C., Smith, K., McGuire, S., et al. (2023). Preliminary incidence and trends of infections caused by pathogens transmitted commonly through food — foodborne diseases active surveillance network, 10 U.S. Sites, 2022. *MMWR Morb. Mortal. Wkly Rep.* 72, 701–706. doi: 10.15585/mmwr.mm7226a1

Edgar, R. C. (2004). MUSCLE: multiple sequence alignment with high accuracy and high throughput. *Nucleic Acids Res.* 32, 1792–1797. doi: 10.1093/nar/gkh340

Elhadidy, M., Miller, W. G., Arguello, H., Álvarez-Ordóñez, A., Dierick, K., and Botteldoorn, N. (2019). Molecular epidemiology and antimicrobial resistance mechanisms of *Campylobacter coli* from diarrhoeal patients and broiler carcasses in Belgium. *Transbound. Emerg. Dis.* 66, 463–475. doi: 10.1111/tbed.13046

Fabre, A., Oleastro, M., Nunes, A., Santos, A., Sifré, E., Ducournau, A., et al. (2018). Whole-genome sequence analysis of multidrug-resistant *Campylobacter* isolates: a focus on aminoglycoside resistance determinants. *J. Clin. Microbiol.* 56:e00390-18. doi: 10.1128/JCM.00390-18

Fernández-Cruz, A., Muñoz, P., Mohedano, R., Valerio, M., Marín, M., Alcalá, L., et al. (2010). *Campylobacter* bacteremia: clinical characteristics, incidence, and outcome over 23 years. *Medicine* 89, 319–330. doi: 10.1097/MD.0b013e3181f2638d

Florez-Cuadrado, D., Ugarte-Ruiz, M., Meric, G., Quesada, A., Porrero, M. C., Pascoe, B., et al. (2017). Genome comparison of erythromycin resistant *Campylobacter* from turkeys identifies hosts and pathways for horizontal spread of *erm*(B) genes. *Front. Microbiol.* 8:2240. doi: 10.3389/fmicb.2017.02240

Fournier, D., Carrière, R., Bour, M., Grisot, E., Triponney, P., Muller, C., et al. (2021). Mechanisms of resistance to ceftolozane/tazobactam in *Pseudomonas aeruginosa*: results of the GERPA multicenter study. *Antimicrob. Agents Chemother.* 65:e01117-20. doi: 10.1128/AAC.01117-20

Gharbi, M., Béjaoui, A., Hamrouni, S., Arfaoui, A., and Maaroufi, A. (2023). Persistence of *Campylobacter spp.* in poultry flocks after disinfection, virulence, and antimicrobial resistance traits of recovered isolates. *Antibiot. Basel Switz.* 12:890. doi: 10.3390/antibiotics12050890

Greninger, A. L., Addetia, A., Starr, K., Cybulski, R. J., Stewart, M. K., Salipante, S. J., et al. (2020). International spread of multidrug-resistant *Campylobacter coli* in men who have sex with men in Washington state and Québec, 2015–2018. *Clin. Infect. Dis.* 71, 1896–1904. doi: 10.1093/cid/ciz1060

Griggs, D. J., Johnson, M. M., Frost, J. A., Humphrey, T., Jørgensen, F., and Piddock, L. J. V. (2005). Incidence and mechanism of ciprofloxacin resistance in *Campylobacter spp*. isolated from commercial poultry flocks in the United Kingdom before, during, and after fluoroquinolone treatment. *Antimicrob. Agents Chemother.* 49, 699–707. doi: 10.1128/AAC.49.2.699-707.2005

He, Y., Reed, S., and Strobaugh, T. P. (2020). Complete genome sequence and annotation of *Campylobacter jejuni* YH003, isolated from retail chicken. *Microbiol. Resour. Announc.* 9:e01307-19. doi: 10.1128/MRA.01307-19

Hormeño, L., Campos, M. J., Vadillo, S., and Quesada, A. (2020). Occurrence of *tet(O/M/O)* mosaic gene in tetracycline-resistant *Campylobacter*. *Microorganisms* 8:1710. doi: 10.3390/microorganisms8111710

Jain, C., Rodriguez-R, L. M., Phillippy, A. M., Konstantinidis, K. T., and Aluru, S. (2018). High throughput ANI analysis of 90K prokaryotic genomes reveals clear species boundaries. *Nat. Commun.* 9:5114. doi: 10.1038/s41467-018-07641-9

Jehanne, Q., Bénéjat, L., Ducournau, A., Domingues-Martins, C., Cousinou, T., Bessède, E., et al. (2021). Emergence of erythromycin resistance methyltransferases in *Campylobacter coli* strains in France. *Antimicrob. Agents Chemother.* 65:e0112421. doi: 10.1128/AAC.01124-21

Jehanne, Q., Pascoe, B., Bénéjat, L., Ducournau, A., Buissonnière, A., Mourkas, E., et al. (2020). Genome-wide identification of host-segregating single-nucleotide polymorphisms for source attribution of clinical *Campylobacter coli* isolates. *Appl. Environ. Microbiol.* 86:e01787-20. doi: 10.1128/AEM.01787-20

Joshi, N., and Fass, J. *Sickle: a sliding-window, adaptive, quality-based trimming tool for FastQ files (Version 1.33) [software]*. (2011).

Ladely, S. R., Meinersmann, R. J., Englen, M. D., Fedorka-Cray, P. J., and Harrison, M. A. (2009). *23S rRNA* gene mutations contributing to macrolide resistance in *Campylobacter jejuni* and *Campylobacter coli*. *Foodborne Pathog. Dis.* 6, 91–98. doi: 10.1089/fpd.2008.0098

Lehours, P, Bessède, E., Jauvain, M., Bénéjat, L., Jehanne, Q., Ducournau, A., et al. French National Reference Center for Campylobacters & Helicobacters (Bordeaux Hospital University Center). 2022 campylobacters surveillance report. French National Reference Center for Campylobacters & Helicobacters, Bordeaux, France. (2023).

Ludwig, C., Claassen, M., Schmidt, A., and Aebersold, R. (2012). Estimation of absolute protein quantities of unlabeled samples by selected reaction monitoring mass spectrometry. *Mol. Cell. Proteomics* 11:M111.013987. doi: 10.1074/mcp.M111.013987

Pearson, B. M., Rokney, A., Crossman, L. C., Miller, W. G., Wain, J., and van Vliet, A. H. M. (2013). Complete genome sequence of the *Campylobacter coli* clinical isolate 15-537360. *Genome Announc.* 1:e01056-13. doi: 10.1128/genomeA.01056-13

Pivard, M., Bastien, S., Macavei, I., Mouton, N., Rasigade, J. P., Couzon, F., et al. (2023). Targeted proteomics links virulence factor expression with clinical severity in staphylococcal pneumonia. *Front. Cell. Infect. Microbiol.* 13:1162617. doi: 10.3389/fcimb.2023.1162617

Post, A., Martiny, D., van Waterschoot, N., Hallin, M., Maniewski, U., Bottieau, E., et al. (2017). Antibiotic susceptibility profiles among *Campylobacter* isolates obtained from international travelers between 2007 and 2014. *Eur. J. Clin. Microbiol. Infect. Dis.* 36, 2101–2107. doi: 10.1007/s10096-017-3032-6

Pritchard, J. K., Stephens, M., and Donnelly, P. (2000). Inference of population structure using multilocus genotype data. *Genetics* 155, 945–959. doi: 10.1093/genetics/155.2.945

Qin, S., Wang, Y., Zhang, Q., Zhang, M., Deng, F., Shen, Z., et al. (2014). Report of ribosomal RNA methylase gene *erm*(B) in multidrug-resistant *Campylobacter coli*. *J. Antimicrob. Chemother.* 69, 964–968. doi: 10.1093/jac/dkt492

Schiaffino, F., Colston, J. M., Paredes-Olortegui, M., François, R., Pisanic, N., Burga, R., et al. (2019). Antibiotic resistance of *Campylobacter* species in a pediatric cohort study. *Antimicrob. Agents Chemother.* 63:e01911-18. doi: 10.1128/aac.01911-18

Singh, T., Singh, P. K., das, S., Wani, S., Jawed, A., and Dar, S. A. (2019). Transcriptome analysis of beta-lactamase genes in diarrheagenic *Escherichia coli*. *Sci. Rep.* 9:3626. doi: 10.1038/s41598-019-40279-1

Tajada, P., Gomez-Graces, J. L., Alós, J. I., Balas, D., and Cogollos, R. (1996). Antimicrobial susceptibilities of *Campylobacter jejuni* and *Campylobacter coli* to 12 beta-lactam agents and combinations with beta-lactamase inhibitors. *Antimicrob. Agents Chemother.* 40, 1924–1925. doi: 10.1128/AAC.40.8.1924

The European Union One Health (2021) Zoonoses Report | EFSA. Available at: https://www.efsa.europa.eu/en/efsajournal/pub/7666 (2022).

Thépault, A., Méric, G., Rivoal, K., Pascoe, B., Mageiros, L., Touzain, F., et al. (2017). Genome-wide identification of host-segregating epidemiological markers for source attribution in *Campylobacter jejuni*. *Appl. Environ. Microbiol.* 83:e03085-16. doi: 10.1128/AEM.03085-16

Tinévez, C., Velardo, F., Ranc, A. G., Dubois, D., Pailhoriès, H., Codde, C., et al. (2022). Retrospective multicentric study on *Campylobacter* spp. bacteremia in France: the campylobacteremia study. *Rev. Infect. Dis.* 75, 702–709. doi: 10.1093/cid/ciab983

Tracz, D. M., Boyd, D. A., Bryden, L., Hizon, R., Giercke, S., van Caeseele, P., et al. (2005). Increase in ampC promoter strength due to mutations and deletion of the attenuator in a clinical isolate of cefoxitin-resistant *Escherichia coli* as determined by RT–PCR. *J. Antimicrob. Chemother.* 55, 768–772. doi: 10.1093/jac/dki074

Wallace, R., Bulach, D., McLure, A., Varrone, L., Jennison, A. V., Valcanis, M., et al. (2021). Antimicrobial resistance of *Campylobacter spp.* causing human infection in Australia: an international comparison. *Microb. Drug Resist.* 27, 518–528. doi: 10.1089/mdr.2020.0082

Wallace, R. L., Bulach, D., Valcanis, M., Polkinghorne, B. G., Pingault, N., Stylianopoulos, A., et al. (2020). Identification of the first *erm*(B)-positive *Campylobacter jejuni* and *Campylobacter coli* associated with novel multidrug resistance genomic islands in Australia. *J. Glob. Antimicrob. Resist.* 23, 311–314. doi: 10.1016/j.jgar.2020.09.009

Wieczorek, K., and Osek, J. (2013). Antimicrobial resistance mechanisms among *Campylobacter*. *Biomed. Res. Int.* 2013:340605. doi: 10.1155/2013/340605

Zacharow, I., Bystroń, J., Wałecka-Zacharska, E., Podkowik, M., and Bania, J. (2015). Prevalence and antimicrobial resistance of *Arcobacter butzleri* and *Arcobacter cryaerophilus* isolates from retail meat in lower Silesia region, Poland. *Pol. J. Vet. Sci.* 18, 63–69. doi: 10.1515/pjvs-2015-0008

Zeng, X., Brown, S., Gillespie, B., and Lin, J. (2014). A single nucleotide in the promoter region modulates the expression of the β-lactamase *OXA-61* in *Campylobacter jejuni*. *J. Antimicrob. Chemother.* 69, 1215–1223. doi: 10.1093/jac/dkt515

frontiers | Frontiers in Microbiology

TYPE Original Research
PUBLISHED 09 November 2023
DOI 10.3389/fmicb.2023.1247211

OPEN ACCESS

EDITED BY
Odile Tresse,
INRA Centre Angers-Nantes Pays de la Loire, France

REVIEWED BY
Vathsala Mohan,
Commonwealth Scientific and Industrial Research Organisation (CSIRO), Australia
Stuart A. Thompson,
Augusta University, United States

*CORRESPONDENCE
Andreas Erich Zautner
azautne@gwdg.de

†These authors have contributed equally to this work

RECEIVED 28 June 2023
ACCEPTED 24 October 2023
PUBLISHED 09 November 2023

CITATION
Dreyer A, Lenz C, Groß U, Bohne W and Zautner AE (2023) Characterization of *Campylobacter jejuni* proteome profiles in co-incubation scenarios.
Front. Microbiol. 14:1247211.
doi: 10.3389/fmicb.2023.1247211

Characterization of *Campylobacter jejuni* proteome profiles in co-incubation scenarios

Annika Dreyer[1], Christof Lenz[2,3], Uwe Groß[1], Wolfgang Bohne[1†] and Andreas Erich Zautner[1,4,5*†]

[1]Institute for Medical Microbiology and Virology, University Medical Center Göttingen, Göttingen, Germany, [2]Bioanalytical Mass Spectrometry Group, Max Planck Institute for Multidisciplinary Sciences, Göttingen, Germany, [3]Department of Clinical Chemistry, University Medical Center Göttingen, Göttingen, Germany, [4]Institute of Medical Microbiology and Hospital Hygiene, Medical Faculty, Otto-von-Guericke University Magdeburg, Magdeburg, Germany, [5]Center for Health and Medical Prevention (CHaMP), Otto-von-Guericke University Magdeburg, Magdeburg, Germany

In dynamic microbial ecosystems, bacterial communication is a relevant mechanism for interactions between different microbial species. When *C. jejuni* resides in the intestine of either avian or human hosts, it is exposed to diverse bacteria from the microbiome. This study aimed to reveal the influence of co-incubation with *Enterococcus faecalis*, *Enterococcus faecium*, or *Staphylococcus aureus* on the proteome of *C. jejuni* 81–176 using data-independent-acquisition mass spectrometry (DIA-MS). We compared the proteome profiles during co-incubation with the proteome profile in response to the bile acid deoxycholate (DCA) and investigated the impact of DCA on proteomic changes during co-incubation, as *C. jejuni* is exposed to both factors during colonization. We identified 1,375 proteins by DIA-MS, which is notably high, approaching the theoretical maximum of 1,645 proteins. *S. aureus* had the highest impact on the proteome of *C. jejuni* with 215 up-regulated and 230 down-regulated proteins. However, these numbers are still markedly lower than the 526 up-regulated and 516 down-regulated proteins during DCA exposure. We identified a subset of 54 significantly differentially expressed proteins that are shared after co-incubation with all three microbial species. These proteins were indicative of a common co-incubation response of *C. jejuni*. This common proteomic response partly overlapped with the DCA response; however, several proteins were specific to the co-incubation response. In the co-incubation experiment, we identified three membrane-interactive proteins among the top 20 up-regulated proteins. This finding suggests that the presence of other bacteria may contribute to increased adherence, e.g., to other bacteria but eventually also epithelial cells or abiotic surfaces. Furthermore, a conjugative transfer regulon protein was typically up-expressed during co-incubation. Exposure to both, co-incubation and DCA, demonstrated that the two stressors influenced each other, resulting in a unique synergistic proteomic response that differed from the response to each stimulus alone. Data are available via ProteomeXchange with identifier PXD046477.

KEYWORDS

***Campylobacter jejuni*, co-incubation, *Enterococcus faecalis*, *Enterococcus faecium*, *Staphylococcus aureus*, bile acids, proteomics**

1. Introduction

Campylobacter jejuni belongs to the most frequently diagnosed bacterial gastrointestinal pathogens in humans worldwide (Acheson and Allos, 2001). In the developed world, foodborne infections most commonly occur after consumption of cross-contaminated food, prepared in parallel with poultry meat., whereas *Campylobacter* spp. belong to the natural commensal microbiome in poultry (Skirrow, 1991). Additional sources for infections are water, raw milk or other livestock animals (Blaser et al., 1980, 1983; Szewzyk et al., 2000). Symptoms of campylobacteriosis include severe bloody diarrhea, fever, abdominal cramps and nausea. Furthermore, *Campylobacter* infections are associated with severe follow-up diseases, for example the Guillain-Barré syndrome, a neural disease that can lead to paralyzes and damage of the nervous system (Rees and Hughes, 1995; Sejvar et al., 2011).

The ideal growth temperature for the Gram-negative, helical-shaped and microaerophilic bacterium lies between 37°C and 42°C. Due to its broad spectrum of virulence-associated factors that enable the survival in varying environmental conditions, *C. jejuni* can successfully colonize the gut of avian and mammal hosts. One of these virulence-associated factors is the ability to survive high concentrations of bile acid in the human or animal gut. Among the diverse functions of bile is the solubilization and emulsification of fat, which makes it an important biological detergent (Begley et al., 2005; Chiang, 2017). Under the exposition of bile acids, the composition of fatty acids and phospholipids of the bacterial cell membranes are altered, which leads to instabilities in the cell's surface and consequently to the disruption of the cell (Taranto et al., 2003). Furthermore, DNA damages might be induced by the presence of bile acid in different bacteria, such as *E. coli* (Kandell and Bernstein, 1991; Begley et al., 2005). To overcome this stress, bacterial gut inhabitants have developed several mechanisms to cope with bile acid and are able to tolerate varying concentrations of bile.

Co-incubation can have several important positive or negative effects on the growth of different bacteria. In presence of other microbes, some pathogenic bacteria show an increase in in their virulence (Stacy et al., 2016; Fast et al., 2018). However, proteomic studies on co-incubation remain rare. A proteomic study by García-Pérez and coworkers has shown that co-incubation can reduce the number of extracellular proteins in microbial communities in wounds (García-Pérez et al., 2018). In addition, co-incubation of different bacteria with yeasts, such as *C. albicans,* has shown positive effects on the growth of both species, probably due to the release of nutrients into the medium or beneficial changes in pH (Ellepola et al., 2019). During co-incubation with other bacteria, *C. jejuni* has been shown to interact with a variety of other bacteria, for instance *Bifidobacterium longum* which prevents the adherence of *C. jejuni* to intestinal tract cells (Quinn et al., 2020a,b). A combination of different bacteria that include *E. faecium* can lead to a decrease of *C. jejuni* in the gastro-intestinal tract of poultry (Neveling and Dicks, 2021). Anis and colleagues showed that studying the co-incubation of *C. jejuni* with other bacteria might be an interesting topic, as the bacterial interaction might enhance *C. jejuni* survival when exposed to external stresses, such as the presence of oxygen (Anis et al., 2022). Further studies about co-cultivation of *C. jejuni* with *E. coli* and *L. monocytogenes,* showed that the adhesion potential of *C. jejuni* to all tested surfaces was significantly increased. In summary, this study suggests that the presence of other (foodborne) bacteria may increase the adhesion of *C. jejuni*, and thus, co-incubation might contribute to its pathogenicity (Klančnik et al., 2020). The only co-cultivation study that investigated transcriptomics or proteomics in *C. jejuni* during co-cultivation involved eukaryotic cells, specifically human INT 407 and Caco-2 epithelial cells (Negretti et al., 2019). Thus, our study aiming the proteomic adaptations of *C. jejuni* to bacterial co-cultivation is novel and covers a so far unexplored subject.

To our knowledge. Proteomic or transcriptomic studies of *C. jejuni* with other bacteria do not exist so far. The only co-cultivation studies that investigated transcriptomics or proteomics in *C. jejuni* during co-cultivation include eukaryotic cells, such as human INT 407 and Caco-2 epithelial cells (Negretti et al., 2019). Thus, our study aiming the proteomic adaptations of *C. jejuni* to bacterial co-cultivation is novel and covers a so far unexplored subject.

In this study, we aimed to observe the impact of co-incubation on the *C. jejuni* proteome and the possible effects of co-incubation on the bile acid response of the bacterium. Therefore, we analyzed the proteome of *C. jejuni* in co-incubation and under deoxycholate (DCA = deoxycholic acid) stress. DCA is a secondary bile acid, which is a product of dehydroxylation by gut microbiota and has been shown to have inhibiting effects on the growth of *C. jejuni* and other bacteria at a certain concentration (Lertpiriyapong et al., 2012; Vidal et al., 2021) and furthermore substantial effects on the proteome (Masanta et al., 2019). The three bacterial species chosen for co-incubation were less resistant toward DCA than *C. jejuni.*

One of the bacterial species chosen for the co-incubation study was *E. faecalis,* a Gram-positive, facultative anaerobic coccal opportunistic pathogen that belongs to the human commensal microbiome, but can also be found in environmental samples (Lebreton et al., 2014; Van Tyne and Gilmore, 2014; Fiore et al., 2019). Furthermore, we tested a close relative of *E. faecalis, E. faecium,* which is also an opportunistic pathogen of global importance due to its high antibiotic resistance potential (Lopes et al., 2006; Gorrie et al., 2019). The third bacterium used in this study was *Staphylococcus aureus,* another Gram-positive pathogen of high clinical relevance due to the high number of severe infections caused by multidrug resistant *S. aureus* (Klevens et al., 2007; Rasigade et al., 2014; Cheung et al., 2021).

This study aims to provide a deeper look at the co-incubation proteome of the pathogen *C. jejuni* with other bacteria that are usually present in the human body and the respective proteomic changes in presence of DCA. We used data-independent acquisition mass spectrometry (DIA-MS) to systematically compare the proteomic changes in co-incubation of the different bacteria with *C. jejuni* as well as the proteomic response to bile acid (DCA). This technique enables the quantitative analysis of every detectable compound in a sample of proteins and thus provides high reliability in the quantitative results (Huang et al., 2015). To our knowledge, this is the first proteomic co-incubation study on *C. jejuni.*

2. Materials and methods

2.1. Bacterial strains and growth conditions

Campylobacter jejuni 81–176 (purchased from the American Type Culture Collection: ATCC-BAA-2151) was used for all described

experiments. *C. jejuni* was grown overnight on CAM-agar plates from Biomérieux (Marcy-l'Étoile, France) at 42°C. Mueller-Hinton (MH) broth served as liquid medium at 37°C. To generate a microaerophilic environment, the Gas Pak™ EZ Campy Container System by BD (Franklin Lakes, NJ, USA) and an anaerobic jar for incubation were used.

Enterococcus faecalis ATCC 700802 (V583; purchased from the American Type Culture Collection), *Enterococcus faecium* TX0016 (also purchased from the American Type Culture Collection: ATCC BAA-472) and *Staphylococcus aureus* NCTC 8325 (PS 47, purchased from the BCCM/LMG: LMG 21764) were used for co-incubation experiments and grown overnight on Columbia agar plates supplemented with sheep blood purchased from Biomérieux (Marcy-l'Étoile, France).

2.2. Co-incubation

For co-incubation experiments, the optical density at 600 nm (OD_{600}) of *C. jejuni* was set to 0.5 and the OD_{600} of the respective other bacterium was set to 0.1. Incubation was performed in phosphate buffered saline (PBS) to avoid effects of the medium on the bile acid resistance. DCA was added to the medium at a concentration of 0.1% for *E. faecalis* and *E. faecium* and 0.075 for *S. aureus*. These concentrations are lethal to these Gram-positive bacteria when cultured individually. Incubation was carried out for 3 h at 37°C and shaking at 150 rpm. After three hours, a spot assay on Mueller-Hinton agar plates was done to show the survival of the bacteria after 3 h in a dilution series. Subsequently, protein extraction was done.

The three Gram-positive bacterial species without presence of *C. jejuni* served as positive control while the approaches of the Gram-positive bacteria with the respective amount of DCA served as negative control. All samples were prepared in biological triplicates.

2.3. Protein extraction from pellet

Cultures were centrifuged at 4,000 rpm for 10 min at 4°C. For protein-extraction from the pellet, the supernatant was discarded. For samples containing *C. jejuni,* pellets were resuspended in 2 mL 0.9% saline and kept on ice over the procedure. Subsequently, the Gram-negative cells were disrupted via sonification using a Branson sonifier 250 from Branson ultrasonics (Brookfield, Connecticut, USA) with the following settings: output control = 3, duty cycler = 30%. The sonification process was performed five times for 30 s followed by 30 s of cooling to avoid overheating of the proteins. Afterwards, the Gram-positive cells were disrupted using 0.75 g of 4 mm glass beads that were added to the samples and were subsequently treated in a "Fast prep 96 Homogenizer" (MP Biomedicals Germany GmbH, Eschwege, Germany) for 2 × 20 s, followed by centrifugation at 5,500 g for one minute. The supernatant was then removed and samples were centrifuged at 13,500 xg for 10 min at 4°C in a tabletop centrifuge. Finally, the supernatant was used for a Pierce assay, that was performed to determine the protein concentration of all samples. After this, the concentrations were adjusted to 1 µg/µL for DIA-MS analysis. For all samples, biological triplicates were prepared.

2.4. Data-independent-acquisition mass spectrometry (DIA-MS)

Protein samples were loaded onto a 4–12% NuPAGE Novex Bis-Tris Minigels (Invitrogen) and run into the gel for 1.5 cm. Following Coomassie staining, the protein areas were cut out, diced, and subjected to reduction with dithiothreitol, alkylation with iodoacetamide and finally overnight digestion with trypsin was performed. Tryptic peptides were extracted from the gel, the solution dried in a Speedvac and kept at −20°C for further analysis.

Protein digests were analyzed on a nanoflow chromatography system (nanoElute) hyphenated to a hybrid timed ion mobilityquadrupole-time of flight mass spectrometer (timsTOF Pro, all Bruker Daltonics GmbH & Co. KG, Bremen, Germany). In brief, 250 ng equivalents of peptides were dissolved in loading buffer (2% acetonitrile, 0.1% trifluoroacetic acid in water), enriched on a reversed-phase C18 trapping column (0.3 cm × 300 µm, Thermo Fisher Scientific) and separated on a reversed phase C18 column with an integrated CaptiveSpray Emitter (Aurora 25 cm × 75 µm, IonOpticks) using a 50 min linear gradient of 5–35% acetonitrile / 0.1% formic acid (v:v) at 250 nL min^{-1}, and a column temperature of 50°C. For identification, representative samples were analyzed in PASEF acquisition mode using default manufacturer's settings [n = 12] (Meier et al., 2018). For identification and quantification samples were analyzed in diaPASEF mode using a customized 16×2 window acquisition scheme (Skowronek et al., 2022). For each biological replicate, three technical replicates were performed in diaPASEF mode for quantitation.

2.5. Data processing and statistics

The data processing was performed using the Spectronaut v16.0.220606.53000 software package (Biognosys AG, Schlieren, Switzerland). Identification of proteins as well as hybrid spectral library generation from 12×2 DDA acquisitions and 12×2 DIA acquisitions experiments were done using the Pulsar search engine against UniProtKB *C. jejuni* 81–176, *E. faecalis* ATCC 700802, *E. faecium* TX0016 and *S. aureus* NCTC 8325 proteomes using the default parameters. The False Discovery Rate (FDR) was set to 1% on the spectral, peptide and protein group levels for all samples. DIA quantification was performed with up to 6 fragments per peptide and up to 10 peptides per protein. A dynamic retention time alignment was done, as well as dynamic mass recalibration and quartile normalization, for the 1% FDR. Imputation of global data was executed for the final results table.

Perseus v1.6.2.2 was used for the statistical analysis and for generation of volcano plots to compare the different samples (Storey and Tibshirani, 2003; Tyanova et al., 2016). As significant regulation level, two-fold up- or down-expression was chosen. Proteins present in 80% of the samples were considered for further analysis. For volcano-plot generation in Perseus, a t-test was chosen with a number of randomizations = 250 and a FDR of 0.05 (Storey and Tibshirani, 2003). All proteins that are described in the following as up- or down-expressed were significantly regulated, if not otherwise stated.

Clusters of orthologous genes (COG)-categories were assigned to the proteins using the online-tool eggNOGmapper v 2.18 (Huerta-Cepas et al., 2017, 2019; Cantalapiedra et al., 2021). To identify

commonly expressed proteins, Venn diagrams were generated utilizing InteractiVenn (Heberle et al., 2015). All Plots were generated using matplotlib in python3 (Van Rossum and Drake, 2009).

3. Results and discussion

3.1. Identification of *Campylobacter jejuni* proteins that are commonly regulated during co-incubation with different Gram-positive bacteria

The interbacterial communication between *C. jejuni* and other bacterial species remains poorly explored to date, lacking comprehensive investigation. Our research is aimed to investigate mechanisms of this cross-talk and its potential implications in various ecological and pathogenic contexts.

We hypothesized that co-incubation of *C. jejuni* with other bacterial species triggers a proteomic response in *C. jejuni*. Three different Gram-positive species were chosen for co-incubation with *C. jejuni*, namely *E. faecalis*, *E. faecium* and *S. aureus*, which are all putative inhabitants of the intestinal host microbiome. The bacteria were incubated for three hours at 37°C in PBS, without nutrient supply since we were not interested in responses due to different degrees of nutrient competition (see scheme of the workflow in Figure 1). Instead, we aimed to target responses resulting from direct bacterial contact or from interactions with secreted molecules. Using volcano-plots generated from DIA-MS data, we compared the proteome of *C. jejuni* in monoculture with each of the three bacteria with *C. jejuni* in co-incubations.

Co-incubation resulted in all cases in an altered proteomic profile, whose dimension depends on the species used for co-incubation. With *S. aureus,* the changes in the proteomic profile exhibited the highest intensity with 445 differentially expressed proteins.

It is well known that *S. aureus* produces several toxins and hemolysins that might act against other bacteria (Shinefield, 1963; Otto, 2014). Conversely, *S. aureus* can also secrete beneficial substances for other microorganisms and co-exist in polymicrobial communities, which can be advantageous for infections (Nguyen and Oglesby-Sherrouse, 2016; García-Pérez et al., 2018; Karki et al., 2021). These characteristics of *S. aureus* might contribute to the increased number of differentially expressed proteins in the co-incubation with *C. jejuni*.

In the co-incubation assay with *E. faecium*, 405 proteins were differentially expressed and in the assay with *E. faecalis*, 241 proteins were differentially expressed. The ratio of up-expressed and down-expressed proteins also varied specifically.

Among the differential expressed proteins, 54 were commonly up-expressed in all three co-incubation approaches and 100 proteins were commonly down-expressed (Figure 2). The distribution of COG-categories differs between commonly up-expressed and down-expressed proteins (Figure 3). Down-expressed proteins are characterized by a higher proportion of the categories C (energy production and conversion), E (amino acid metabolism and transport), F (nucleotide metabolism and transport), I (lipid metabolism) and G (carbohydrate metabolism and transport). In contrast, up-expressed proteins are characterized by a higher proportion of the categories J (translation), L (replication and repair), M (cell wall / membrane / envelope biogenesis) and T (signal transduction).

The differentially expressed proteins in all approaches were sorted according to their difference expression level. We compared the top 20 up- and down-expressed proteins of each co-incubation proteome (see Supplementary Excel file), in order to identify commonly regulated proteins with a high degree of regulation. Four commonly up-expressed proteins were found in the top 20 up-expressed proteins: hemolysin A (A0A0H3PEK7_CAMJJ), a DNA/RNA non-specific endonuclease (A0A0H3PJE6_CAMJJ), a putative lipoprotein (A0A0H3PA71_CAMJJ), and a putative membrane protein (A0A0H3PDB2_CAMJJ). Hemolysin A is associated with the lysis of cells via disruption of the cell membrane. This phenomenon is particularly observed for red blood cells (erythrocytes), as certain pathogens have the ability to cause lysis of these cells to access an iron source (Skals et al., 2010; Wiles and Mulvey, 2013). Therefore hemolysis is considered as an important virulence factor (Elliott et al., 1998; Kielian et al., 2001; Vandenesch et al., 2012). The putative lipoprotein can be associated with cell–cell contact with host epithelial cells, but probably also with other bacteria (Speare et al., 2022). Putative lipoproteins can be considered as virulence factors, as well. Many outer membrane proteins in pathogenic bacteria are virulence factors that enable or facilitate bacterial attachment to host cell surfaces (Gao et al., 2021). The exact function of the putative membrane protein remains unknown. However, this membrane associated protein might also play a role in intercellular communication. Lipoproteins are a diverse group of membrane proteins that play crucial roles in various biological processes, including cellular physiology, cell division, and virulence. They have significant

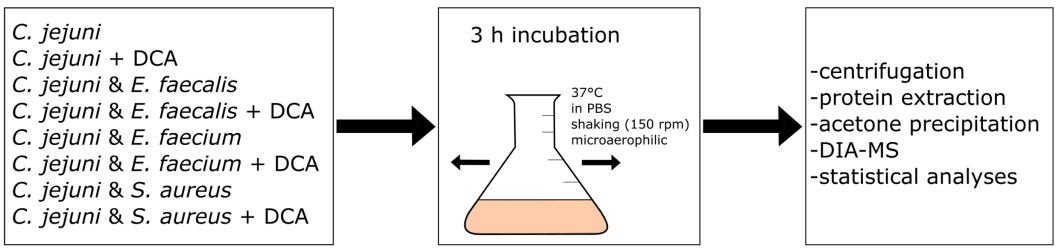

FIGURE 1
Workflow scheme: eight different approaches of mono- or co-incubation were prepared and incubated at 150 rpm and 37°C for three hours. After incubation, the approaches were centrifuged and the proteins were extracted and precipitated with acetone. Data-Independent Acquisition Mass Spectrometry (DIA-MS) was performed, followed by data analysis and statistical analysis.

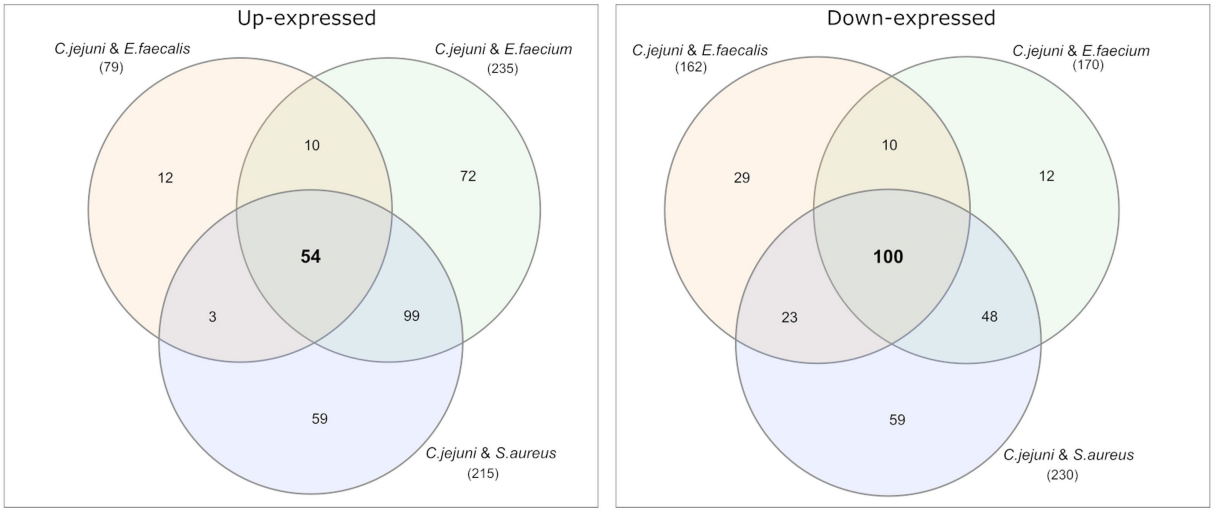

FIGURE 2
Venn diagrams were used to show the commonly up- and down-expressed proteins in *C. jejuni* during co-incubation with *E. faecalis*, *E. faecium*, and *S. aureus* in the pellet. The analysis revealed that 54 proteins were commonly up-expressed in all three co-incubation approaches, while 100 proteins were commonly down-expressed.

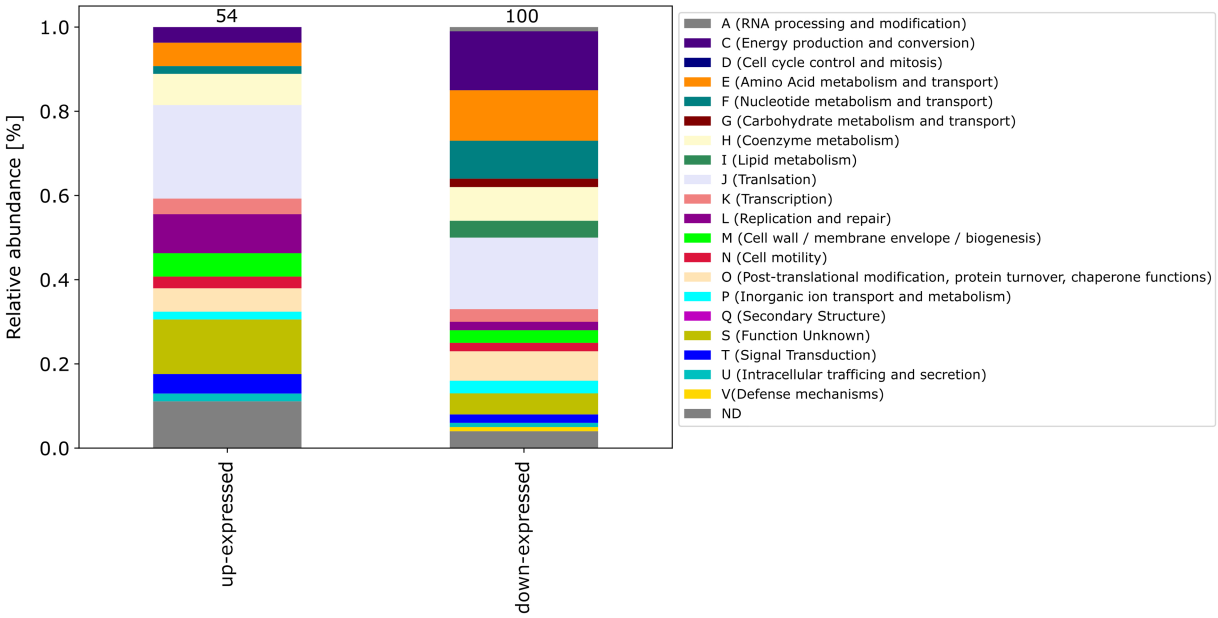

FIGURE 3
This figure shows the COG-categories of the 54 proteins commonly up-expressed and 100 proteins commonly down-expressed in all three co-incubation approaches. The samples were normalized before analysis. The stacked bar plot displays the percentage distribution of the COG-categories, with different colors representing different categories.

importance and impact on these phenomena (Kovacs-Simon et al., 2011).

Among the top 20 up-expressed proteins in co-incubation were three membrane-interactive proteins, which might indicate an increased adherence to other bacteria through contact with other bacterial species. Enhanced adherence is only one possible reason for the high expression of membrane associated proteins in co-incubation. Whether these effects are due to co-incubation remains unclear. Our study employed *in vitro* co-incubation experiments to investigate proteomic changes. While these experiments allow for controlled conditions and precise analysis, they may not fully replicate the complex interactions that occur within host environments. A genomic assessment could validate this hypothesis. Nevertheless, it is known that in presence of other commensal microbes, some (pathogenic) bacteria can enhance their virulence (Stacy et al., 2016; Fast et al., 2018).

Moreover, four commonly down-expressed proteins were found in the top 20 down-expressed proteins, namely the translation initiation factor IF-3 (IF3_CAMJJ), a DNA-directed RNA polymerase subunit omega (RPOZ_CAMJJ), an ATP synthase subunit beta

(ATPB_CAMJJ) and a 6,7-dimethyl-8-ribityllumazine synthase (RISB_CAMJJ).

Some *Campylobacter* strains possess the capability to employ a type 6 secretion system (T6SS), which can be used for communication with their surrounding environment including other bacteria (Chen et al., 2015; Gallique et al., 2017). However, *C. jejuni* 81–176 does not harbor a type 6 secretion system (Liaw et al., 2019), which implies the utilization of alternative mechanisms for bacterial communication. However, other *C. jejuni* strains, for example the strains *C. jejuni* 488, 43,431 or RC039 utilize a type 6 secretion system (Liaw et al., 2019), indicating that cross-talk via a type 6 secretion system-dependent protein secretion would be possible in some *C. jejuni* strains.

3.2. The co-incubation response and the bile acid stress response partly overlap

In order to identify proteins that are specifically regulated during co-incubation, we compared the changes in the proteomic profile after co-incubation with the stress response during incubation with bile acids, which was previously shown to trigger a strong proteomic stress response in *C. jejuni* (Masanta et al., 2019). After 3 h incubation with 0.1% DCA, a substantial proportion of *C. jejuni* proteins were differentially expressed. A total of 526 proteins were identified among the up-expressed proteins, which is ~10-fold more than the 54 up-expressed proteins during co-incubation with Gram-positve bacteria. Likewise, 516 proteins were down-expressed after DCA incubation, which is ~5-fold more than the number during co-incubation with Gram-positve bacteria. This leads to the assumption that the exposure to DCA provokes a significantly more pronounced proteomic response compared to the co-incubation scenarios.

Venn diagrams show the overlapping proteins between both approaches (Figure 4 and Supplementary Figures S2, S3). Out of the 54 commonly up-expressed proteins during co-incubation, 36 proteins were also found in *C. jejuni* monoculture with DCA. This indicates that only the 18 remaining proteins are specific for co-incubation (see Supplementary Table S1). Moreover, from the 516 down-expressed proteins in *C. jejuni* in presence of DCA, 78 were shared with the 100 down-expressed proteins in the co-incubation approach (Figure 4), indicating that the 22 remaining proteins are specifically down-expressed in co-incubation (see Supplementary Table S6). In total, 343 proteins were commonly up-expressed and 277 proteins were commonly down-expressed in presence of DCA and co-incubation (Figure 5).

The pattern of the COG categories of differentially proteins in the monoculture approach with DCA differs from commonly expressed proteins in co-incubation (Figures 6, 7). The percentage of up-expressed proteins assigned to the categories J (translation), L (replication and repair) and T (signal transduction) is higher in the co-incubation proteome, while categories C (energy production and conversion), G (carbohydrate metabolism and transport), M (cell wall / membrane / envelope / biogenesis) and V (defense mechanisms) are more present in the monoculture of *C. jejuni* and DCA. Categories C, E, F and J are more down-expressed in the co-incubation approach.

In *C. jejuni* the most relevant mechanism to survive bile acid stress is the CmeABC multidrug efflux pump, that belongs to the resistance nodulation-division (RND) type multidrug efflux systems (Lin et al., 2003). CmeABC consists of a three-gene operon encoding for a membrane fusion protein - CmeA, the efflux pump membrane transporter - CmeB and CmeC, which is the outer membrane lipoprotein (Lin et al., 2002). Knockout mutants of these genes led to significant loss of bile acid resistance (Lin et al., 2003). In a proteomic study, Masanta et al. showed that the proteins belonging to the CmeABC multidrug efflux pump were up-expressed under bile acid stress exposure (Masanta et al., 2019). Furthermore, Malik-Kale et al. found CmeABC and other virulence genes up-regulated under DCA stress in a microarray study (Malik-Kale et al., 2008).

Both publications explored the response of *C. jejuni* to bile acids, but they differ in their methods and focus. Malik-Kale et al. investigated the effect of DCA on the virulence gene expression of *C. jejuni* such as *ciaB, cmeABC*, *dccR*, and *tlyA* using microarray analyses, while Masanta et al. used label-free mass spectrometry to analyze the proteome of *C. jejuni* in response to sublethal concentrations of DCA. However, both studies focused on the response of *C. jejuni* to bile acids and suggest that bile acids can alter the behavior of *C. jejuni*. In contrast to Malik-Kale and colleagues, who focused on the kinetics of cell invasion, Masanta et al. focused on the downregulation of basic biosynthetic pathways and the transcription machinery.

As in Masanta et al.'s study, we used data independent mass spectrometry to obtain the data. However, the focus of our study was the proteome during co-incobation under bile acid stress. Due to the findings in previous work on the reaction of *C. jejuni* to DCA, the presence of CmeA, B or C in all our samples with DCA served as indicator that the proteome under bile acid stress is detected and depicted. In the co-incubation approach without DCA, none of the the CmeABC proteins was detected (Supplementary Table S2).

Among the 22 specifically down-expressed proteins during co-incubation were mostly general metabolic proteins. In the 18 commonly up-expressed proteins during co-incubation, we found proteins that might play a role in the interaction between *C. jejuni* with other bacteria. For example, a conjugative transfer regulon protein (Q9KIR9_CAMJJ) was detected among the up-expressed proteins in all three samples. The presence of this protein indicates that horizontal gene transfer may be occurring between these bacteria, whereby genetic material can be exchanged between different species (Llosa et al., 2002). This mechanism of genetic exchange could allow for the acquisition of novel genetic traits, such as antibiotic resistance or other beneficial genes and indicates a potential for cross-communication between bacteria.

Additionally, the chaperone protein DnaJ was found among these proteins (DNAJ_CAMJJ), indicating an active response toward stress. DnaJ and related Hsp proteins are highly conserved among species and play a role in diverse processes such as folding and unfolding of proteins, translation and ATPase activity of specific chaperones (Qiu et al., 2006). This indicates that the bacteria might be stressed by either the presence of other bacteria or the absence of nutrients.

3.3. Co-incubation of *Campylobacter jejuni* with Gram-positive bacteria in the presence of bile acids triggers a unique proteomic response different from the single stimuli

We also studied the proteomic response in the presence of both triggers, DCA plus co-incubation with Gram-positive bacteria. This should reveal the relative influence of the individual triggers on the common response. Among the 18 up-expressed proteins that were

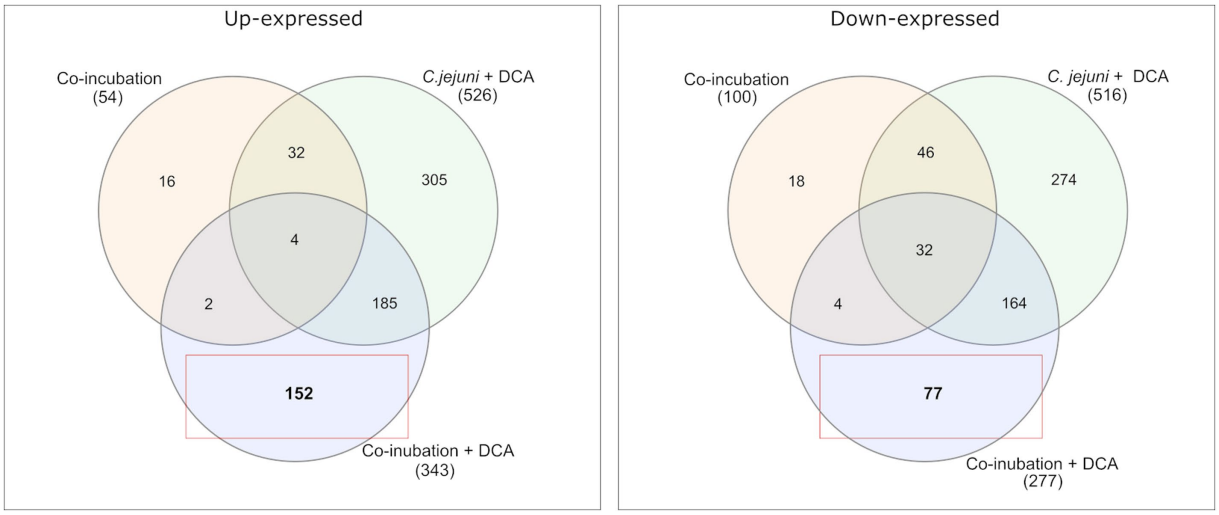

FIGURE 4
A Venn diagram is presented to compare the commonly up-expressed proteins (left) of *C. jejuni* in co-incubation with *E. faecalis*, *E. faecium*, and *S. aureus* with and without DCA, and the up-expressed proteins of *C. jejuni* with DCA in monoculture. A total of 152 proteins were specifically detected in co-incubation with DCA and not in the other approaches. The down-expressed proteins are shown on the right. The red boxes highlight proteins that are uniquely and specifically expressed in the co-incubation with DCA approach.

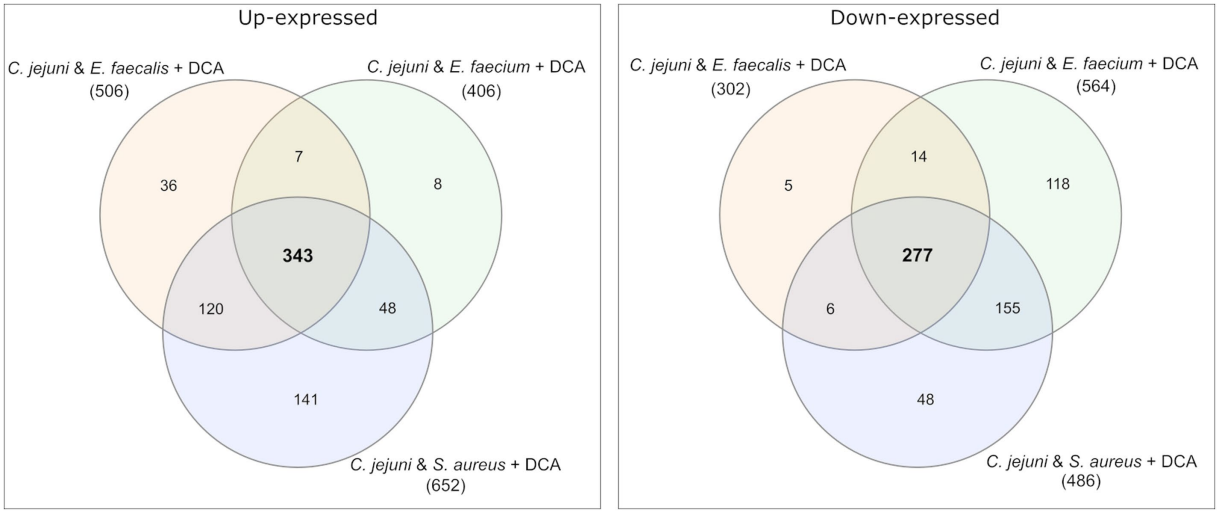

FIGURE 5
Venn diagrams were used to illustrate the commonly up- and down-expressed proteins of *C. jejuni* in co-incubation with *E. faecalis*, *E. faecium*, and *S. aureus* in the pellet after the addition of DCA. The analysis revealed that 343 proteins were commonly up-expressed in all three co-incubation approaches, while 277 proteins were commonly down-expressed.

specific to co-incubation, only two were up-expressed in the approach of co-incubation with DCA (Figure 4). These proteins were a Histidine kinase (A0A0H3PE96_CAMJJ) and a tRNA modification GTPase MnmE (MNME_CAMJJ) (Supplementary Table S1). Furthermore, of 22 down-expressed proteins that were specific for co-incubation, only four proteins remained down-expressed when DCA was added. The limited number of commonly regulated proteins in co-incubation with and without DCA indicates that DCA seems to suppress the specific co-incubation response to a large extent.

Comparing the co-incubation plus DCA approach to the monoculture of *C. jejuni* with DCA, 185 proteins occurred commonly among the up-expressed candidates, which corresponded to ~37.8% of the 490 proteins that were up-expressed in the monoculture with DCA, excluding the 36 proteins, that also occurred in co-incubation without DCA (Figures 4, 5). This led to the assumption that the additional trigger of co-incubation might also inhibit the expression of a certain amount of the DCA response specific proteins in *C. jejuni*. Moreover, 77 proteins were uniquely down-expressed in the approach of co-incubation plus DCA (Figure 4), while 196 of the 277 down-expressed proteins in this approach were shared with the *C. jejuni* monoculture with DCA.

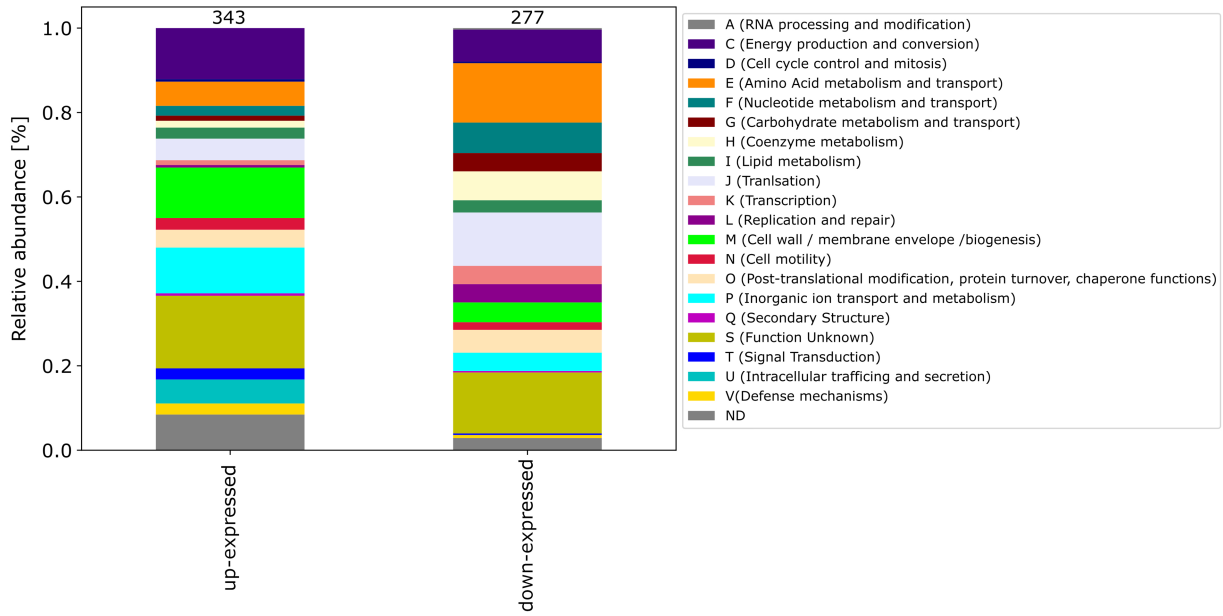

FIGURE 6
Stacked bar plots were generated to visualize the up- and down-expressed proteins of *C. jejuni* during co-incubation with DCA. A total of 343 up-expressed and 277 down-expressed proteins were assigned to their respective COG categories. The stacked bar plot displays the percentage distribution of COG categories in different colors.

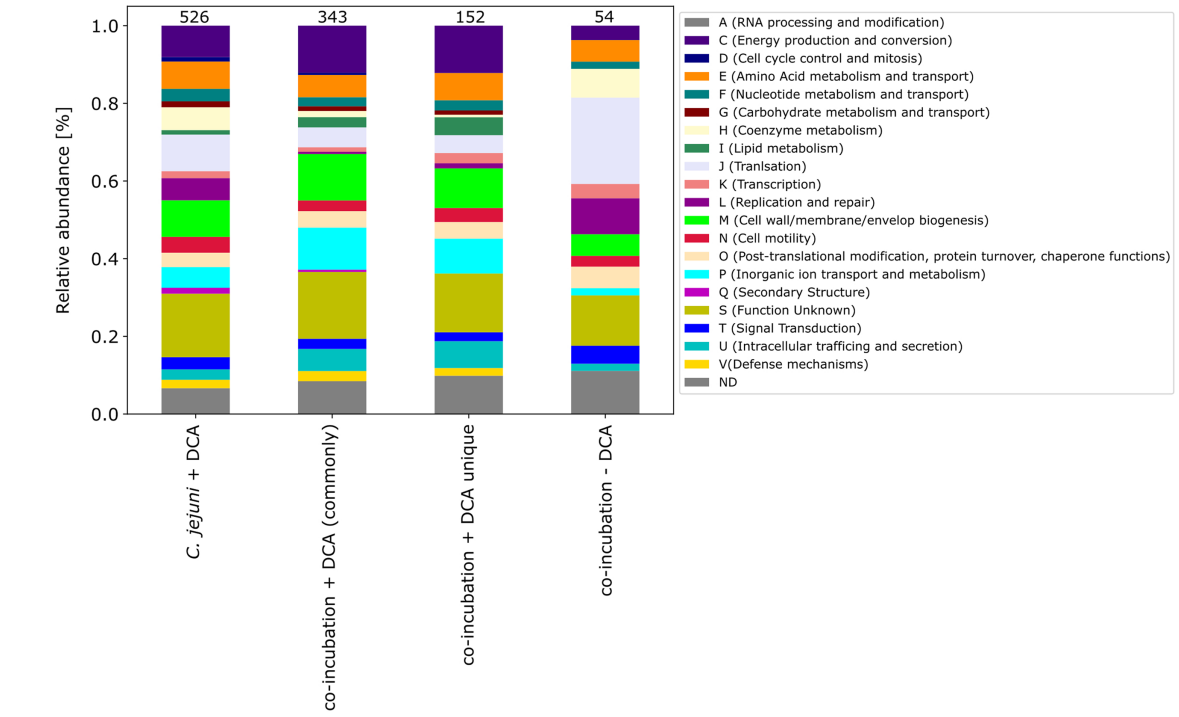

FIGURE 7
The COG categories of the proteins that were up-expressed in the *C. jejuni* mono-culture approach with DCA, the proteins that were commonly expressed in co-incubation with DCA, and the unique up-expressed proteins of the co-cultivation approach are shown. For comparison, the approach of the 54 up-expressed proteins in co-incubation without DCA is also depicted on the right.

The proteomes in co-incubation with and without DCA exhibit significant dissimilarities. In total, 152 proteins were found to be specifically up-expressed when both triggers, co-incubation plus DCA, are present. Due to the fact that these 152 proteins occurred only in the approach co-incubation plus DCA, and were not a combination of both triggers, it can be assumed, that the proteomic response in presence of both, DCA and another bacterium possesses a unique character (Figure 4).

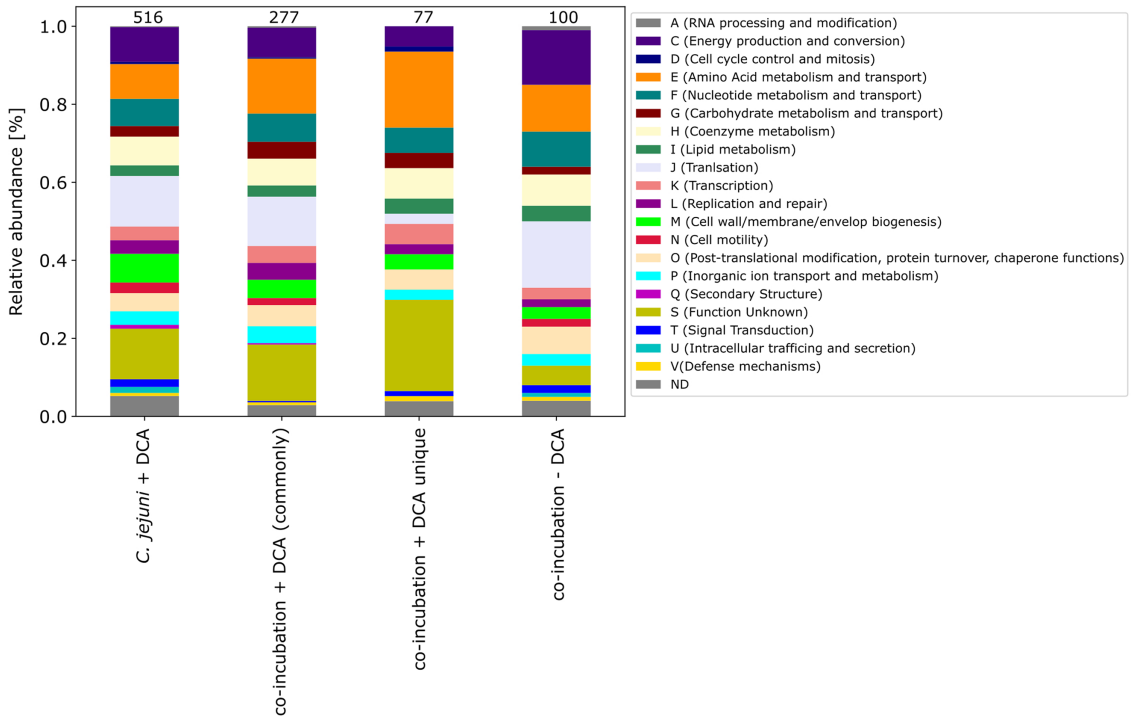

FIGURE 8
The COG categories of proteins that were down-expressed in the *C. jejuni* mono-culture approach with DCA, as well as the commonly expressed proteins in co-incubation with DCA and the unique up-expressed proteins of the co-cultivation approach are depicted. For comparison, the approach of the 100 down-expressed proteins in co-incubation without DCA is shown on the right.

Moreover, the respective COG-categories were assigned to these 152 proteins (Figure 7). Compared to the monoculture proteome with DCA, the categories M (cell wall / membrane envelope / biogenesis), P (inorganic ion transport and metabolism) and U (intracellular trafficking) were increased in co-incubation with DCA. A detailed analysis of these 152 proteins revealed a high number of ABC-transporter associated proteins, proteins related to antibiotic resistance, efflux and transport proteins and general membrane proteins (Supplementary Table S5).

Furthermore, the COG categories of the 77 proteins commonly exclusively down-expressed in the approach of co-incubation with DCA were determined. When compared to the 516 down-expressed proteins in *C. jejuni* with DCA and the 277 commonly down-expressed proteins in co-incubation with DCA, the pattern of the 77 proteins shows similarities but also differences (Figure 8). An increase of proteins belonging to the category E (amino acid metabolism and transport) was observed and a decrease of proteins belonging to the category J (translation) was observed when compared to the other samples.

3.4. Conclusion

In summary, our investigation highlights the proteomic response of *C. jejuni* to co-incubation as well as bile acid stress. We cover a high percentage of the total proteome of *C. jejuni* in our DIA-MS analysis, which demonstrates a small but distinct interaction potential between *C. jejuni* and the other bacteria via membrane-interactive proteins, indicating that the other bacteria contribute to an increased virulence in the environment.

We also report a remarkable overlap between the proteomic response of *C. jejuni* in co-incubation in presence of DCA and the approach of *C. jejuni* monoculture with bile acid.

However, we were able to identify a unique response when both triggers (co-incubation and DCA) are present. This distinct response highlights the complexity of cellular interactions and shows the potential role of *C. jejuni* in proteomic response pathways under these specific conditions and enables future research in the field of proteomic analyses under different influences.

3.5. Limitations of the study

One limitation of this study is the labor-intensive nature of DIA MS analysis, which makes it difficult to undertake additional research in this experimental setup. Furthermore, the findings may not be generalizable to other *Campylobacter* strains since only a single strain (*C. jejuni* 81–176) was included. Although the study primarily focused on the *C. jejuni* proteome, there is a lack of comprehensive analysis regarding the proteomic responses of the other bacteria involved in the co-incubation. To provide a more holistic understanding of the interactions and proteomic dynamics within the complex co-incubation system, future research should aim to explore this aspect. We acknowledge that our study primarily focused on proteomic changes in *C. jejuni* during co-incubation with other bacteria. While our results provide valuable insights into proteomic alterations, we did not perform a genomic assessment of *C. jejuni*. Therefore, we are unable to definitively conclude that the observed effects in communication and potential virulence enhancement are solely due to co-incubation.

Data availability statement

The mass spectrometry proteomics data have been deposited to the ProteomeXchange Consortium via the PRIDE [1] partner repository with the dataset identifier PXD046477.

Author contributions

CL, WB, UG, and AZ: conceptualization. CL, WB, and AZ: methodology. CL and AD: software. AD, WB, and CL: validation. AD and CL: formal analysis and investigation. AD performed growth curve analysis and prepared bacterial samples. CL performed mass-spectrometric analysis and resources. UG and AZ: data curation. AD and CL: writing—original draft preparation. AD: writing—review and editing. AD, CL, UG, WB, and AZ: visualization. AD prepared all figures. WB and AZ: supervison. AZ: project administration. AZ and UG: funding acqusition. All authors have read and agreed to the published version of the manuscript.

Funding

This work was funded by the Deutsche Forschungsgemeinschaft (DFG) (grant number ZA 697/6–1). The APC of the paper was funded by the Open Access support program of the Deutsche Forschungsgemeinschaft and the publication fund of the Georg August Universität Göttingen.

Acknowledgments

We thank Lisa Neuenroth and Fabio Trebini (UMG) for the implementation of DIA-MS. This publication is part of AD's doctoral study. This publication is part of Annika Dreyer's doctoral study "Proteomic Profiles of Campylobacter jejuni and Enterococci during Co-incubation and under Bile Acid Stress" (2023).

Conflict of interest

The authors declare that the research was conducted in the absence of any commercial or financial relationships that could be construed as a potential conflict of interest.

Publisher's note

All claims expressed in this article are solely those of the authors and do not necessarily represent those of their affiliated organizations, or those of the publisher, the editors and the reviewers. Any product that may be evaluated in this article, or claim that may be made by its manufacturer, is not guaranteed or endorsed by the publisher.

Supplementary material

The Supplementary material for this article can be found online at: https://www.frontiersin.org/articles/10.3389/fmicb.2023.1247211/full#supplementary-material

References

Acheson, D., and Allos, B. M. (2001). *Campylobacter jejuni infections*: update on emerging issues and trends. *Clin. Infect. Dis.* 32, 1201–1206. doi: 10.1086/319760

Anis, N., Bonifait, L., Quesne, S., Baugé, L., Yassine, W., Guyard-Nicodème, M., et al. (2022). Survival of *Campylobacter jejuni* co-cultured with *Salmonella* spp. in aerobic conditions. *Pathogens* 11:812. doi: 10.3390/pathogens11070812

Begley, M., Gahan, C. G. M., and Hill, C. (2005). The interaction between bacteria and bile. *FEMS Microbiol. Rev.* 29, 625–651. doi: 10.1016/j.femsre.2004.09.003

Blaser, M. J., LaForce, F. M., Wilson, N. A., and Wang, W. L. L. (1980). Reservoirs for human Campylobacteriosis. *J. Infect. Dis.* 141, 665–669. doi: 10.1093/infdis/141.5.665

Blaser, M. J., Taylor, D. N., and Feldman, R. A. (1983). Epidemiology of *Campylobacter jejuni* infections. *Epidemiol. Rev.* 5, 157–176. doi: 10.1093/oxfordjournals.epirev.a036256

Cantalapiedra, C. P., Hernández-Plaza, A., Letunic, I., Bork, P., and Huerta-Cepas, J. (2021). eggNOG-mapper v2: functional annotation, orthology assignments, and domain prediction at the metagenomic scale. *Mol. Biol. Evol.* 38, 5825–5829. doi: 10.1093/molbev/msab293

Chen, L., Zou, Y., She, P., and Wu, Y. (2015). Composition, function, and regulation of T6SS in *Pseudomonas aeruginosa*. *Microbiol. Res.* 172, 19–25. doi: 10.1016/j.micres.2015.01.004

Cheung, G. Y. C., Bae, J. S., and Otto, M. (2021). Pathogenicity and virulence of *Staphylococcus aureus*. *Virulence* 12, 547–569. doi: 10.1080/21505594.2021.1878688

Chiang, J. Y. (2017). Recent advances in understanding bile acid homeostasis. *F1000Res* 6:2029. doi: 10.12688/f1000research.12449.1

Ellepola, K., Truong, T., Liu, Y., Lin, Q., Lim, T. K., Lee, Y. M., et al. (2019). Multi-omics analyses reveal synergistic carbohydrate metabolism in *Streptococcus mutans-Candida albicans* mixed-species biofilms. *Infect. Immun.* 87, e00339–e00319. doi: 10.1128/IAI.00339-19

Elliott, S. J., Srinivas, S., Albert, M. J., Alam, K., Robins-Browne, R. M., Gunzburg, S. T., et al. (1998). Characterization of the roles of Hemolysin and other toxins in enteropathy caused by alpha-hemolytic *Escherichia coli* linked to human diarrhea. *Infect. Immun.* 66, 2040–2051. doi: 10.1128/IAI.66.5.2040-2051.1998

Fast, D., Kostiuk, B., Foley, E., and Pukatzki, S. (2018). Commensal pathogen competition impacts host viability. *Proc. Natl. Acad. Sci. U. S. A.* 115, 7099–7104. doi: 10.1073/pnas.1802165115

Fiore, E., Van Tyne, D., and Gilmore, M. S. (2019). Pathogenicity of Enterococci. *Microbiol. Spectr.* 7. doi: 10.1128/microbiolspec.GPP3-0053-2018

Gallique, M., Bouteiller, M., and Merieau, A. (2017). The type VI secretion system: a dynamic system for bacterial communication? *Front. Microbiol.* 8:1454. doi: 10.3389/fmicb.2017.01454

Gao, Q., Lu, S., Wang, M., Jia, R., Chen, S., Zhu, D., et al. (2021). Putative *Riemerella anatipestifer* outer membrane protein H affects virulence. *Front. Microbiol.* 12:708225. doi: 10.3389/fmicb.2021.708225

García-Pérez, A. N., de Jong, A., Junker, S., Becher, D., Chlebowicz, M. A., Duipmans, J. C., et al. (2018). From the wound to the bench: exoproteome interplay between wound-colonizing *Staphylococcus aureus* strains and co-existing bacteria. *Virulence* 9, 363–378. doi: 10.1080/21505594.2017.1395129

Gorrie, C., Higgs, C., Carter, G., Stinear, T. P., and Howden, B. (2019). Genomics of vancomycin-resistant Enterococcus faecium. *Microb. Genomics* 5:e000283. doi: 10.1099/mgen.0.000283

Heberle, H., Meirelles, G. V., da Silva, F. R., Telles, G. P., and Minghim, R. (2015). InteractiVenn: a web-based tool for the analysis of sets through Venn diagrams. *BMC Bioinformatics* 16:169. doi: 10.1186/s12859-015-0611-3

Huang, Q., Yang, L., Luo, J., Guo, L., Wang, Z., Yang, X., et al. (2015). SWATH enables precise label-free quantification on proteome scale. *Proteomics* 15, 1215–1223. doi: 10.1002/pmic.201400270

Huerta-Cepas, J., Forslund, K., Coelho, L. P., Szklarczyk, D., Jensen, L. J., von Mering, C., et al. (2017). Fast genome-wide functional annotation through orthology assignment by eggNOG-mapper. *Mol. Biol. Evol.* 34, 2115–2122. doi: 10.1093/molbev/msx148

Huerta-Cepas, J., Szklarczyk, D., Heller, D., Hernández-Plaza, A., Forslund, S. K., Cook, H., et al. (2019). eggNOG5.0: a hierarchical, functionally and phylogenetically

annotated orthology resource based on 5090 organisms and 2502 viruses. *Nucleic Acids Res.* 47, D309–D314. doi: 10.1093/nar/gky1085

Kandell, R. L., and Bernstein, C. (1991). Bile salt/acid induction of DNA damage in bacterial and mammalian cells: implications for colon cancer. *Nutr. Cancer* 16, 227–238. doi: 10.1080/01635589109514161

Karki, A. B., Ballard, K., Harper, C., Sheaff, R. J., and Fakhr, M. K. (2021). *Staphylococcus aureus* enhances biofilm formation, aerotolerance, and survival of *Campylobacter* strains isolated from retail meats. *Sci. Rep.* 11:13837. doi: 10.1038/s41598-021-91743-w

Kielian, T., Cheung, A., and Hickey, W. F. (2001). Diminished virulence of an alpha-toxin mutant of *Staphylococcus aureus* in experimental brain abscesses. *Infect. Immun.* 69, 6902–6911. doi: 10.1128/IAI.69.11.6902-6911.2001

Klančnik, A., Gobin, I., Jeršek, B., Smole Možina, S., Vučković, D., Tušek Žnidarič, M., et al. (2020). Adhesion of *Campylobacter jejuni* is increased in association with foodborne Bacteria. *Microorganisms* 8:201. doi: 10.3390/microorganisms8020201

Klevens, R. M., Morrison, M. A., Nadle, J., Petit, S., Gershman, K., Ray, S., et al. (2007). Invasive methicillin-resistant *Staphylococcus aureus* infections in the United States. *Jama* 298, 1763–1771. doi: 10.1001/jama.298.15.1763

Kovacs-Simon, A., Titball, R. W., and Michell, S. L. (2011). Lipoproteins of bacterial pathogens. *Infect. Immun.* 79, 548–561. doi: 10.1128/IAI.00682-10

Lebreton, F., Willems, R. J. L., and Gilmore, M. S. (2014). "*Enterococcus* Diversity, Origins in Nature, and Gut Coloni-zation", in *Enterococci: From Commensals to Leading Causes of Drug Resistant Infection*, eds. M. S. Gilmore, D. B. Clewell, Y. Ike and N. Shankar (Boston: Massachusetts Eye and Ear Infirmary). Available at: http://www.ncbi.nlm.nih.gov/books/NBK190427/ (Accessed October 28, 2023).

Lertpiriyapong, K., Gamazon, E. R., Feng, Y., Park, D. S., Pang, J., Botka, G., et al. (2012). *Campylobacter jejuni* type VI secretion system: roles in adaptation to Deoxycholic acid, host cell adherence, invasion, and *in vivo* colonization. *PLoS One* 7:e42842. doi: 10.1371/journal.pone.0042842

Liaw, J., Hong, G., Davies, C., Elmi, A., Sima, F., Stratakos, A., et al. (2019). The *Campylobacter jejuni* type VI secretion system enhances the oxidative stress response and host colonization. *Front. Microbiol.* 10:2864. doi: 10.3389/fmicb.2019.02864

Lin, J., Michel, L. O., and Zhang, Q. (2002). CmeABC functions as a multidrug efflux system in *Campylobacter jejuni*. *Antimicrob. Agents Chemother.* 46, 2124–2131. doi: 10.1128/AAC.46.7.2124-2131.2002

Lin, J., Sahin, O., Michel, L. O., and Zhang, Q. (2003). Critical role of multidrug efflux pump CmeABC in bile resistance and *in vivo* colonization of *Campylobacter jejuni*. *Infect. Immun.* 71, 4250–4259. doi: 10.1128/IAI.71.8.4250-4259.2003

Llosa, M., Gomis-Ruth, F. X., Coll, M., and Cruz, F. D. L. (2002). Bacterial conjugation: a two-step mechanism for DNA transport. *Mol. Microbiol.* 45, 1–8. doi: 10.1046/j.1365-2958.2002.03014.x

Lopes, M. de F. S., Simões, A. P., Tenreiro, R., Marques, J. J. F., and Crespo, M. T. B. (2006). Activity and expression of a virulence factor, gelatinase, in dairy enterococci. *Int. J. Food Microbiol.* 112, 208–214. doi: 10.1016/j.ij-foodmicro.2006.09.004

Malik-Kale, P., Parker, C. T., and Konkel, M. E. (2008). Culture of *Campylobacter jejuni* with sodium Deoxycholate induces virulence gene expression. *J. Bacteriol.* 190, 2286–2297. doi: 10.1128/JB.01736-07

Masanta, W. O., Zautner, A. E., Lugert, R., Bohne, W., Gross, U., Leha, A., et al. (2019). Proteome profiling by label-free mass spectrometry reveals differentiated response of *Campylobacter jejuni* 81–176 to sublethal concentrations of bile acids. *Prot. Clin. Appl.* 13:e1800083. doi: 10.1002/prca.201800083

Meier, F., Brunner, A.-D., Koch, S., Koch, H., Lubeck, M., Krause, M., et al. (2018). Online parallel accumulation–serial fragmentation (PASEF) with a novel trapped ion mobility mass spectrometer. *Mol. Cell. Proteomics* 17, 2534–2545. doi: 10.1074/mcp.TIR118.000900

Negretti, N. M., Clair, G., Talukdar, P. K., Gourley, C. R., Huynh, S., Adkins, J. N., et al. (2019). *Campylobacter jejuni* demonstrates conserved proteomic and transcriptomic responses when co-cultured with human INT 407 and Caco-2 epithelial cells. *Front. Microbiol.* 10:755. doi: 10.3389/fmicb.2019.00755

Neveling, D. P., and Dicks, L. M. T. (2021). Probiotics: an antibiotic replacement strategy for healthy broilers and productive rearing. *Probiotics & Antimicro. Prot.* 13, 1–11. doi: 10.1007/s12602-020-09640-z

Nguyen, A. T., and Oglesby-Sherrouse, A. G. (2016). Interactions between *Pseudomonas aeruginosa* and *Staphylococcus aureus* during co-cultivations and polymicrobial infections. *Appl. Microbiol. Biotechnol.* 100, 6141–6148. doi: 10.1007/s00253-016-7596-3

Otto, M. (2014). *Staphylococcus aureus* toxins. *Curr. Opin. Microbiol.* 17, 32–37. doi: 10.1016/j.mib.2013.11.004

Qiu, X.-B., Shao, Y.-M., Miao, S., and Wang, L. (2006). The diversity of the DnaJ/Hsp40 family, the crucial partners for Hsp70 chaperones. *Cell. Mol. Life Sci.* 63, 2560–2570. doi: 10.1007/s00018-006-6192-6

Quinn, E. M., Kilcoyne, M., Walsh, D., Joshi, L., and Hickey, R. M. (2020a). A whey fraction rich in immunoglobulin G combined with *Bifidobacterium longum* subsp. *infantis* ATCC 15697 exhibits synergistic effects against *Campylobacter jejuni*. *IJMS* 21:4632. doi: 10.3390/ijms21134632

Quinn, E. M., Slattery, H., Walsh, D., Joshi, L., and Hickey, R. M. (2020b). *Bifidobacterium longum* subsp. *infantis* ATCC 15697 and goat Milk oligosaccharides show synergism *in vitro* as anti-Infectives against *Campylobacter jejuni*. *Foods* 9:348. doi: 10.3390/foods9030348

Rasigade, J.-P., Dumitrescu, O., and Lina, G. (2014). New epidemiology of *Staphylococcus aureus* infections. *Clin. Microbiol. Infect.* 20, 587–588. doi: 10.1111/1469-0691.12718

Rees, J. H., and Hughes, R. A. C. (1995). *Campylobacter jejuni* infection and Guillain–Barré syndrome. *N. Engl. J. Med.* 333, 1374–1379. doi: 10.1056/NEJM199511233332102

Sejvar, J. J., Baughman, A. L., Wise, M., and Morgan, O. W. (2011). Population incidence of Guillain-Barré syndrome: a systematic review and Meta-analysis. *Neuroepidemiology* 36, 123–133. doi: 10.1159/000324710

Shinefield, H. R. (1963). V. An analysis and interpretation. *Arch. Pediatr. Adolesc. Med.* 105:683. doi: 10.1001/archpedi.1963.02080040685019

Skals, M., Jensen, U. B., Ousingsawat, J., Kunzelmann, K., Leipziger, J., and Praetorius, H. A. (2010). *Escherichia coli* α-Hemolysin triggers shrinkage of erythrocytes via KCa3.1 and TMEM16A channels with subsequent phosphatidylserine exposure. *J. Biol. Chem.* 285, 15557–15565. doi: 10.1074/jbc.M109.082578

Skirrow, M. B. (1991). Epidemiology of Campylobacter enteritis. *Int. J. Food Microbiol.* 12, 9–16. doi: 10.1016/0168-1605(91)90044-P

Skowronek, P., Thielert, M., Voytik, E., Tanzer, M. C., Hansen, F. M., Willems, S., et al. (2022). Rapid and in-depth coverage of the (Phospho-)proteome with deep libraries and optimal window design for dia-PASEF. *Mol. Cell. Proteomics* 21:100279. doi: 10.1016/j.mcpro.2022.100279

Speare, L., Woo, M., Dunn, A. K., and Septer, A. N. (2022). A putative lipoprotein mediates cell-cell contact for type VI secretion system-dependent killing of specific competitors. *MBio* 13:e0308521. doi: 10.1128/mbio.03085-21

Stacy, A., Fleming, D., Lamont, R. J., Rumbaugh, K. P., and Whiteley, M. (2016). A commensal bacterium promotes virulence of an opportunistic pathogen via cross-respiration. *MBio* 7, e00782–e00716. doi: 10.1128/mBio.00782-16

Storey, J. D., and Tibshirani, R. (2003). Statistical significance for genomewide studies. *Proc. Natl. Acad. Sci. U. S. A.* 100, 9440–9445. doi: 10.1073/pnas.1530509100

Szewzyk, U., Szewzyk, R., Manz, W., and Schleifer, K.-H. (2000). Microbiological safety of drinking water. *Annu. Rev. Microbiol.* 54, 81–127. doi: 10.1146/annurev.micro.54.1.81

Taranto, M. P., Fernandez Murga, M. L., Lorca, G., and Valdez, G. F. (2003). Bile salts and cholesterol induce changes in the lipid cell membrane of *Lactobacillus reuteri*. *J. Appl. Microbiol.* 95, 86–91. doi: 10.1046/j.1365-2672.2003.01962.x

Tyanova, S., Temu, T., Sinitcyn, P., Carlson, A., Hein, M. Y., Geiger, T., et al. (2016). The Perseus computational platform for comprehensive analysis of (prote)omics data. *Nat. Methods* 13, 731–740. doi: 10.1038/nmeth.3901

Vandenesch, F., Lina, G., and Henry, T. (2012). *Staphylococcus aureus* Hemolysins, bi-component Leukocidins, and Cytolytic peptides: a redundant arsenal of membrane-damaging virulence factors? *Front. Cell. Inf. Microbio.* 2:12. doi: 10.3389/fcimb.2012.00012

Van Rossum, G., and Drake, F. L. (2009). *Python 3 Reference Manual*. Scotts Valley, CA: CreateSpace.

Van Tyne, D., and Gilmore, M. S. (2014). Friend turned foe: evolution of enterococcal virulence and antibiotic resistance. *Annu. Rev. Microbiol.* 68, 337–356. doi: 10.1146/annurev-micro-091213-113003

Vidal, J. E., Wier, M. N., Angulo-Zamudio, U. A., McDevitt, E., Vidal, A. G. J., Alibayov, B., et al. (2021). Prophylactic inhibition of colonization by *Streptococcus pneumoniae* with the secondary bile acid metabolite Deoxycholic acid. *Infect. Immun.* 89:e0046321. doi: 10.1128/IAI.00463-21

Wiles, T. J., and Mulvey, M. A. (2013). The RTX pore-forming toxin α-hemolysin of uropathogenic *Escherichia coli*: progress and perspectives. *Future Microbiol.* 8, 73–84. doi: 10.2217/fmb.12.131

frontiers | Frontiers in Microbiology

TYPE Original Research
PUBLISHED 18 December 2023
DOI 10.3389/fmicb.2023.1331114

OPEN ACCESS

EDITED BY
Stuart A. Thompson,
Augusta University, United States

REVIEWED BY
Bassam A. Elgamoudi,
Griffith University, Australia
Orhan Sahin,
Iowa State University, United States
Marja-Liisa Hänninen,
University of Helsinki, Finland

*CORRESPONDENCE
Markus M. Heimesaat
markus.heimesaat@charite.de

†These authors share senior authorship

RECEIVED 31 October 2023
ACCEPTED 24 November 2023
PUBLISHED 18 December 2023

CITATION
Shayya NW, Bandick R, Busmann LV, Mousavi S, Bereswill S and Heimesaat MM (2023) Metabolomic signatures of intestinal colonization resistance against *Campylobacter jejuni* in mice.
Front. Microbiol. 14:1331114.
doi: 10.3389/fmicb.2023.1331114

Metabolomic signatures of intestinal colonization resistance against *Campylobacter jejuni* in mice

Nizar W. Shayya, Rasmus Bandick, Lia V. Busmann, Soraya Mousavi, Stefan Bereswill† and Markus M. Heimesaat*†

Gastrointestinal Microbiology Research Group, Institute of Microbiology, Infectious Diseases and Immunology, Charité - University Medicine Berlin, Berlin, Germany

Introduction: *Campylobacter jejuni* stands out as one of the leading causes of bacterial enteritis. In contrast to humans, specific pathogen-free (SPF) laboratory mice display strict intestinal colonization resistance (CR) against *C. jejuni*, orchestrated by the specific murine intestinal microbiota, as shown by fecal microbiota transplantation (FMT) earlier.

Methods: Murine infection models, comprising SPF, SAB, hma, and mma mice were employed. FMT and microbiota depletion were confirmed by culture and culture-independent analyses. Targeted metabolome analyses of fecal samples provided insights into the associated metabolomic signatures.

Results: In comparison to hma mice, the murine intestinal microbiota of mma and SPF mice (with CR against *C. jejuni*) contained significantly elevated numbers of lactobacilli, and Mouse Intestinal Bacteroides, whereas numbers of enterobacteria, enterococci, and *Clostridium coccoides* group were reduced. Targeted metabolome analysis revealed that fecal samples from mice with CR contained increased levels of secondary bile acids and fatty acids with known antimicrobial activities, but reduced concentrations of amino acids essential for *C. jejuni* growth as compared to control animals without CR.

Discussion: The findings highlight the role of microbiota-mediated nutrient competition and antibacterial activities of intestinal metabolites in driving murine CR against *C. jejuni*. The study underscores the complex dynamics of host-microbiota-pathogen interactions and sets the stage for further investigations into the mechanisms driving CR against enteric infections.

KEYWORDS

***Campylobacter jejuni*, colonization resistance, gut microbiota, metabolome, bile acids, amino acids, fatty acids, host-pathogen interactions**

1 Introduction

In humans, the Gram-negative spirally curved *Campylobacter jejuni* is one of the common causative agents of bacterial enteritis (Igwaran and Okoh, 2019). Campylobacteriosis is initially characterized by severe enteritis with diarrhea and lower gastrointestinal tract hemorrhage. Less frequently, other non-gastrointestinal aftermaths are associated with campylobacteriosis such as systemic manifestations, which include infectious complications like bacteremia, and

post-infectious immune disorders, like reactive arthritis or Guillain-Barré syndrome (Peterson, 1994; Heimesaat et al., 2021).

In the course of zoonotic infections *C. jejuni* is transmitted to humans via the oral route by consuming contaminated raw or undercooked meat, unpasteurized milk, in addition to uncooked cross-contaminated food, whereas human transmission is possible via the fecal-oral route (Kaakoush et al., 2015). To establish infection, *C. jejuni* colonizes the intestinal lumen, penetrates the mucus layer, adheres to epithelial cells, and invades subepithelial tissues. This is achieved via flagella, adhesins, and invasins (Heimesaat et al., 2014; Schmidt et al., 2019; Tegtmeyer et al., 2021). In the subepithelial tissues *C. jejuni* induces an inflammatory response by innate immune system activation via its surface endotoxin, the lipo-oligosaccharide (LOS) (Mousavi et al., 2020). The majority of strains causing disease lack conventional exotoxins, but cytolethal distending toxin or cholera-like toxins have been detected in some pathogenic strains and may increase symptom severity (Lara-Tejero and Galán, 2000).

The human host is highly susceptible to *C. jejuni* infection as emphasized by a low infection dosage (Igwaran and Okoh, 2019). In contrast to humans, conventional specific pathogen-free (SPF) laboratory mice are completely resistant to *C. jejuni* infection (Bereswill et al., 2011; Mousavi et al., 2021). Research in murine laboratory models revealed that the resistance to infection is caused by the inability of *C. jejuni* to multiply and to establish stable colonization in the presence of the specific intestinal microbiota present in conventional mice (Bereswill et al., 2011; Mousavi et al., 2021). This protective shield against bacterial infection is termed colonization resistance (CR) and is in general attributed to diverse antagonistic mechanisms including antimicrobial metabolites, nutrient depletion and/or bacteriophages (Lawley and Walker, 2013; Herzog et al., 2023). Notably, CR has gained considerable attention in research exploring the protective effects of intestinal microbiota against *Salmonella enterica* (Wotzka et al., 2019), *Escherichia coli* (Mundy et al., 2006), *Listeria monocytogenes* (Becattini et al., 2017), and *Clostridioides difficile* (Chen et al., 2008). Results from earlier studies demonstrated that CR against *C. jejuni* is caused by the specific murine microbiota (Bereswill et al., 2011). In contrast to SPF mice, secondary abiotic (SAB) mice in which the intestinal microbiota was completely depleted by antibiotic treatment display no CR and are highly susceptible to *C. jejuni* colonization (Bereswill et al., 2011; Mousavi et al., 2021; Heimesaat et al., 2022). Most importantly, CR was reconstituted in SAB mice upon recolonization with a murine intestinal microbiota, while SAB mice recolonized with a human intestinal microbiota lacked CR and were highly susceptible to *C. jejuni* colonization (Bereswill et al., 2011). Moreover, CR against *C. jejuni* was absent in mice with reduced species diversity of the intestinal microbiota, as both, antibiotics treated mice (O'Loughlin et al., 2015; Iizumi et al., 2016) and infant mice harboring a limited gut microbiota were proven liable to *C. jejuni* infection (Chang and Miller, 2006; Haag et al., 2012a; Stahl et al., 2014). Moreover, inflammation-induced dysbiosis shifts in the enteric microbiota composition toward elevated *E. coli* levels disrupted CR against *C. jejuni* as was observed independently in mice with *Toxoplasma gondii*-induced acute ileitis as well as in IL-10 deficient mice suffering from chronic colitis. Interestingly, intestinal *E. coli* loads were elevated in susceptible infant mice and CR against *C. jejuni* was abrogated by feeding of SPF mice with *E. coli* via the drinking water (Haag et al., 2012a,b).

However, molecular mechanisms involved in CR against *C. jejuni* have not been unraveled so far, but the causative role of the murine microbiota in CR indicates that nutrient competition and bactericidal killing by gut bacteria might play important roles therein. Unlike other enteric pathogens, *C. jejuni* generally lacks the ability to utilize carbohydrates as carbon sources and relies on organic acids and amino acids as primary nutrient sources (Hofreuter, 2014). Nevertheless, despite the restricted carbohydrate utilization, some fucose—catabolizing strains have been described such as *C. jejuni* NTC 11168 (Muraoka and Zhang, 2011).

Thus, amino acids are essentially required for *C. jejuni* multiplication and stable colonization in the gut (Hofreuter, 2014). Results from earlier investigations demonstrate that serine, aspartate, asparagine, and glutamate, and after that proline are used by the pathogen in a sequential manner (Wright et al., 2009). This rather limited array of substrates to fuel the central metabolism suggests that *C. jejuni* may effectively be outcompeted by other gut bacteria with similar substrate preferences. Additionally, the intestinal microbiota might provide CR by production of antimicrobials such as short-chain fatty acids (SCFAs), secondary bile acids or bacteriocins (Ducarmon et al., 2019). The role of SCFAs and bile acids in intestinal lifestyle of *C. jejuni* is evidenced by the fact that both substance groups are sensed by *C. jejuni* and regulate expression of factors involved in virulence and colonization (Ducarmon et al., 2019). Furthermore, *C. jejuni* is highly susceptible to killing by bile acids and has therefore, developed resistance mechanisms such as multidrug efflux pumps (Lin et al., 2003; Sun et al., 2018).

It seems feasible that the mechanisms involved in causing CR are key to eradicate enteric pathogens such as *C. jejuni* from the gut. Thus, better understanding the metabolic composition of the intestinal milieu in mice with and without CR will help to unravel the mechanisms underlying CR, and this might pave the way for developing novel drugs for prevention and treatment of campylobacteriosis.

To address these challenges and gain a comprehensive understanding of the mechanisms underlying murine CR against *C. jejuni*, we utilized a targeted metabolomics approach to characterize distinct metabolite patterns associated with CR in our well-established murine models of *C. jejuni* infection with known CR against the pathogen, namely, SPF mice, microbiota-depleted SAB mice, and SAB mice in which murine or human intestinal microbiota was reintroduced by fecal microbiota transplantation (FMT) via the oral route. In particular, the murine microbiota (mma) and human microbiota associated (hma) mice, both containing a complete intestinal microbiota of different composition, were used as study groups, whereas SAB and SPF mice served as controls.

2 Materials and methods

2.1 Mice

C57BL/6J mice were maintained in the facilities of the "Forschunginstitute fur Experimentelle Medizin" (FEM, Charite

– Universitätsmedizin, Berlin, Germany), under SPF conditions. Age and sex matched mice aged between 10 and 12 weeks were used.

2.2 Generation of SAB mice

To eradicate the commensal gut microbiota, mice were transferred to sterile cages and were subjected to an ampicillin plus sulbactam antibiotic regimen (2 g/L plus 1 g/L, respectively; purchased from Dr. Friedrich Ebert Arzneimittel, Ursensollen, Germany) as a drinking solution for a period of 8 weeks. These mice were kept and handled under strict aseptic conditions. Microbiota depletion was confirmed using cultural and molecular analyses of fecal samples, as described earlier (Heimesaat et al., 2022).

2.3 Fecal microbiota transplantation

Fresh fecal samples were collected from five individual healthy human volunteers and murine animals, respectively, after screening to ensure their exclusion of enteropathogenic bacteria, parasites, and viruses. Fecal samples were pooled separately for humans and mice and dissolved in an equal volume of sterile phosphate-buffered saline (PBS, Thermo Fischer Scientific, Waltham, MA, United States). Pooled samples were aliquoted and stored at −80°C until further use. Prior to gavage experiments, aliquots of the pooled fecal samples were thawed, and bacterial communities were analyzed using both culture-dependent and culture-independent methods with 16S rRNA gene sequencing. Quantification of total bacterial load and identification of individual bacterial groups were also done using cultural and culture-independent analyses. Starting a week prior to infection (i.e., on days −7, −6, and − 5), mice were gavaged with 300 µL of the respective fecal suspension as described in details earlier (Bereswill et al., 2011; Shayya et al., 2023), to study the effects of bacterial communities on host physiology and housed under SPF conditions with *ad libitum* access to food and water.

2.4 Gut microbiota analysis

Cultural analysis, biochemical identification, and molecular detection of luminal bacterial communities from stomach, duodenum, ileum, and colon were performed as previously described (Weschka et al., 2021; Shayya et al., 2023). In brief, DNA extracts and plasmids were quantified using Quat-iT PicoGreen reagent (Invitrogen, Paisley, UK) and adjusted to a concentration of 1 ng per µL. Abundance of the major bacterial groups within the gut microbiota was assessed using quantitative real time polymerase chain reaction (qRT-PCR) with group-specific primers targeting the 16S rRNA gene (Tib MolBiol, Berlin, Germany). The number of 16S rRNA gene copies per µg of DNA in each sample was determined, and the frequencies of the respective bacterial groups were computed relative to the eubacterial (V3) amplicon.

2.5 *Campylobacter jejuni* infection

For infection experiments, we utilized the *C. jejuni* strain 81-176, which was derived from frozen stocks and inoculated on karmali agar plates (Oxoid, Wesel, Germany). The bacteria were grown under microaerophilic conditions at 37°C in a closed container containing gas packs (CampyGen, Oxoid, Wesel, Germany) for 48 h to obtain optimal growth conditions. To establish an infection model, we infected SPF, SAB, mma, and hma mice with 10^9 viable *C. jejuni* bacterial cells via oral gavage in a total volume of 300 µL of PBS on two consecutive days (days 0 and 1).

2.6 Sampling procedures

Mice were sacrificed by CO_2 asphyxiation on day 21 post infection. Luminal samples from the gastrointestinal tract (stomach, duodenum, ileum, colon) of each mouse were harvested for a set of post-experimental analyses, including cultural and molecular analyses. Respective samples were homogenized in sterile PBS (Thermo Fisher Scientific, Waltham, MA, United States) and serial dilutions were plated onto karmali agar (Oxoid, Wesel, Germany) and incubated under microaerophilic conditions for 48 h at 37°C as described earlier in details (Heimesaat et al., 2022).

2.7 Metabolomic analysis

Targeted metabolomic analysis of fecal samples from d0 was performed by Biocrates Lifesciences AG (Innsbruck, Austria) using their McP Quant 500 platform. Fecal samples were collected from each subject and immediately frozen at −80°C until further analysis. Samples were shipped on dry ice to Biocrates for metabolomic analysis. Biocrates' MxP® Quant 500 product uses mass spectrometry (MS) to quantify over 500 metabolites in a single run, including amino acids, biogenic amines, organic acids, and lipids. The quality of the samples was assessed using internal standards, and data were preprocessed to remove contaminants, drift, and other systematic errors. Lipids and hexoses were analyzed using flow injection analysis-tandem mass spectrometry (FIA-MS/MS) on a SCIEX 5500 QTRAP® instrument (AB SCIEX, Darmstadt, Germany) with an electrospray ionization (ESI) source. Small molecules were analyzed using liquid chromatography–tandem mass spectrometry (LC–MS/MS) on a Xevo® TQ-XS instrument (Waters, Milford, MA, United States). To prepare the samples for analysis, a 96-well based sample preparation device was used, which contained inserts impregnated with internal standards. A predefined amount of the sample was added to the inserts, followed by the addition of a phenyl isothiocyanate (PITC) solution to derivatize some of the analytes (e.g., amino acids). After the derivatization was completed, the target analytes were extracted using an organic solvent, followed by a dilution step. The extracted metabolites were then analyzed by FIA-MS/MS and LC–MS/MS using multiple reaction monitoring (MRM) to detect the analytes. Concentrations of the metabolites were calculated using an appropriate mass

spectrometry software (Sciex Analyst® and Waters MassLynx™) and imported into Biocrates' MetIDQ™ software for further analysis. The metabolite concentrations were then determined in each sample by normalizing to the weight and dilution factor from the original metabolome extraction protocol, then provided in "µM," which were subsequently exported as an excel file. Individual metabolites were grouped by classes and visualized using GraphPad Prism (V9; San Diego, CA, United States).

2.8 Minimum inhibitory concentration determinations

The minimum inhibitory concentration (MIC) values for deoxycholic acid (Sigma-Aldrich, St. Louis, Missouri, United States; 30,960) were determined using the broth microdilution method in BactoTM Brain Heart Infusion (BHI) (BD Biosciences, Heidelberg, Germany) broth supplemented with 5% fetal bovine serum (FBS) (Biochrom, Berlin, Germany). The bacterial inoculum of *C. jejuni* 81-176 was prepared from overnight growth on karmali agar plates (Oxoid, Wesel, Germany) and suspended in 5 mL of BHI broth supplemented with 5% FBS to an optical density at 600 nm (OD600) of 0.1. Two-fold serial dilutions of the test compounds were prepared in 96-well plates in the range of 1–2,048 mg/L to a final volume of 200 µL per well, and 10 µL of the bacterial suspension was added to the respective wells. The plates were incubated for 48 h under microaerophilic conditions at 37°C, and then the OD was measured at 600 nm using a microplate reader (Infinite M Flex, Tecan, Switzerland). The MIC was defined as the lowest concentration of the compound that completely inhibited bacterial growth.

2.9 Statistical analysis

We conducted statistical analyses to evaluate the significance of observed differences between groups. Prior to analysis, we first assessed the normality of the data using the Anderson-Darling test. Medians and significance levels were then calculated using GraphPad Prism (V9; San Diego, CA, United States). For pairwise comparisons of the groups, we employed the Student's *t*-test for normally distributed data and the Mann–Whitney test for non-normally distributed data. Moreover, to account for the possibility of errors resulting from multiple comparisons, we utilized the one-sided ANOVA with Tukey's post correction for normally distributed data, and the Kruskal-Wallis test with Dunn's post correction for non-normally distributed data. A two-sided probability (p) value of ≤ 0.05 was considered statistically significant.

2.10 Ethics statement

The animal studies were conducted in adherence to the European animal welfare guidelines (2010/64/EU) after receiving authorization from the local commission for animal experiments ("Landesamt für Gesundheit und Soziales." LaGeSo, Berlin; under registration number G0172/16). Clinical conditions of mice after infection were surveyed daily.

3 Results

3.1 Survey of pathogen loads following *Campylobacter jejuni* infection

To establish CR against *C. jejuni* in SAB mice, and to confirm the role of the specific murine or human gut microbiota therein, we introduced human or murine gut microbiota to SAB mice by FMT via gavage. One week after reconstitution, these mice were perorally infected with 10^9 viable *C. jejuni* on day (d) 0 and d1 along with conventional SPF mice and SAB mice as controls with and without CR, respectively. This setting enabled us to analyze CR by assessing the kinetics of pathogen shedding in fecal samples and in distinct gastrointestinal compartments.

Cultural analysis of fecal samples from SPF mice exhibited effective clearance of the pathogen within a few days of infection, indicative for a strong CR against *C. jejuni* given a complete absence of colonization (Figure 1A). In contrast, CR was abrogated in SAB mice which revealed a robust and persistent colonization of the colon by *C. jejuni*, with pathogen densities ranging from 10^8 to 10^9 colony-forming units per gram (CFU/g) during the experimental period (Figure 1B). Conversely, SAB mice reconstituted with murine gut microbiota mma showed a protective CR with sporadic colonization occurring in only a few individuals (Figure 1C). On the other hand, hma mice displayed absence of CR as indicated by susceptibility to *C. jejuni* intestinal colonization, maintaining high median pathogen loads between 10^7 and 10^9 CFU/g of feces throughout the experiment (Figure 1D).

Furthermore, we investigated pathogen numbers along the gastrointestinal tract in the distinct mouse cohorts. As anticipated, CR against *C. jejuni* observed in SPF and mma mice extended throughout the gut, as demonstrated by significantly higher *C. jejuni* loads in the stomach, duodenum, ileum, and colon of SAB mice compared to SPF and mma mice, and in hma mice compared to mma mice ($p < 0.01$–0.001) (Figures 2A–D).

Hence, these results demonstrate that the two mice groups - with and without CR each – were excellently suited to investigate the metabolite patterns in the intestinal milieu associated with presence and absence of murine CR against *C. jejuni*.

3.2 Microbiota composition in mice with and without CR

To further ensure the quality of our mice models with and without CR, we quantified the major microbial groups in the gut microbiota by qRT-PCR based on 16S rRNA analysis before infection. Our objective was to elucidate the differences in microbial communities between mice harboring human or murine gut microbiota known from earlier studies (Bereswill et al., 2011; Mrazek et al., 2019) to ensure that the different microbiota transplants had successfully engrafted in the mouse intestines. Our analysis revealed that hma mice harbored higher total eubacterial loads compared to SPF mice ($p < 0.05$), while no significant differences in the gene numbers were observed between SPF and mma, and between hma and mma mice (Figure 3A). Moreover, significantly higher enterobacterial loads were observed in hma mice (~10^3 gene numbers/ng DNA) prior to infection compared to SPF and mma

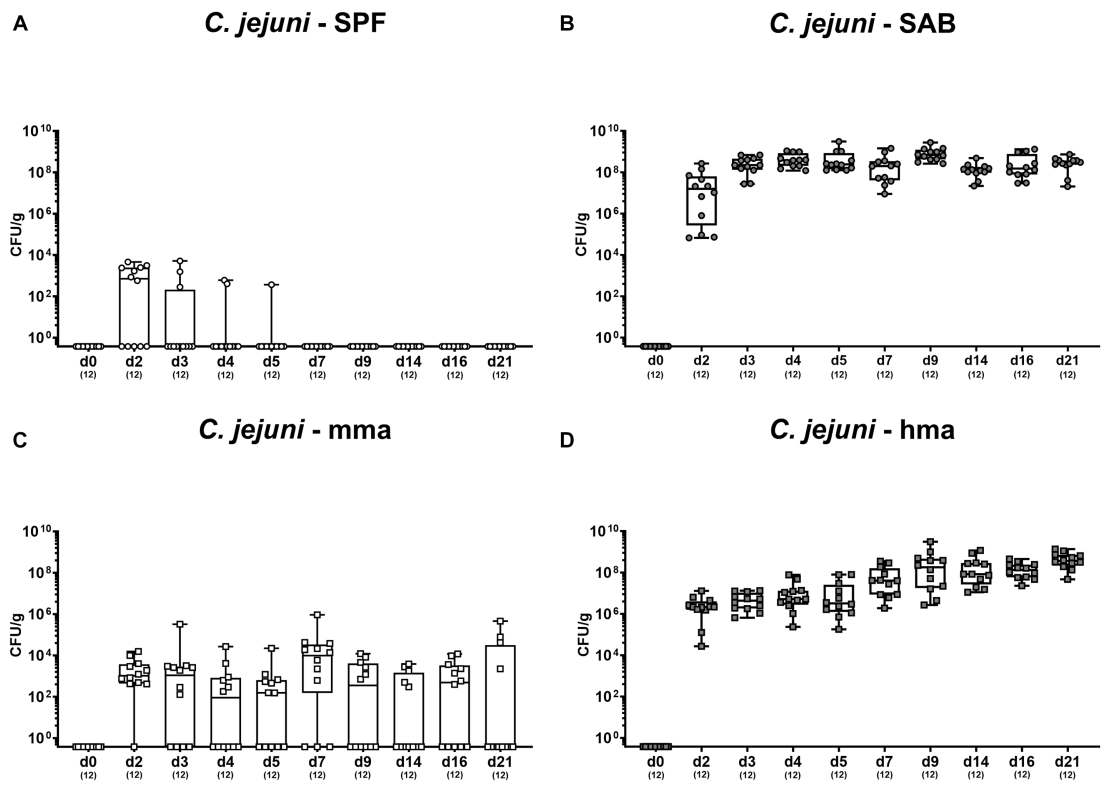

FIGURE 1
Survey of fecal pathogen loads over time post *C. jejuni* infection. Following peroral infection with *C. jejuni* strain 81-176 on day (d) 0 and d1, intestinal pathogen loads were surveyed in fecal samples over time post-infection from **(A)** conventional but specific pathogen-free (SPF), **(B)** secondary abiotic (SAB), **(C)** murine microbiota-associated (mma), and **(D)** human microbiota-associated (hma) mice using cultural analysis and expressed as colony forming units per gram of feces (CFU/g). Box plots indicate the 25th and 75th percentiles of the median (black bar inside the box). Each dot corresponds to an individual mouse. Numbers (in parentheses) specify the number of mice included.

mice (~10 gene numbers/ng DNA) ($p < 0.001$) (Figure 3B). Differences in enterococci fecal loads were evident, with hma mice exhibiting significantly higher loads (~10^2 gene numbers/ng DNA) than both murine models (~10^{-2} gene numbers/ng DNA) ($p < 0.001$) (Figure 3C). Similarly, in line with the distinctive species composition of the gut microbiota, hma mice harbored significantly lower fecal loads of lactobacilli (~10^{-2} gene numbers/ng DNA) compared to the resistant models, SPF and mma mice (~10^5 gene numbers/ng DNA) ($p < 0.01$–0.001) (Figure 3D). Interestingly, mma mice displayed higher bifidobacterial loads (~10^4 gene numbers/ng DNA) ($p < 0.01$–0.001) compared to both SPF and hma mice (~10^3 and 10^4 gene numbers/ng DNA, respectively) (Figure 3E). Furthermore, the levels of *Bacteroides*/*Prevotella* species were significantly elevated in hma mice (~10^6 gene numbers/ng DNA) compared to SPF and mma mice (~10^4 gene numbers/ng DNA) ($p < 0.001$) (Figure 3F). Similarly, hma mice also exhibited significantly higher loads (~10^5 gene numbers/ng DNA) of the *Clostridium coccoides* group than SPF and mma mice (~10^4 gene numbers/ng DNA) ($p < 0.001$) (Figure 3G). On the other hand, both hma and mma mice displayed higher fecal loads (~10^5 gene numbers/ng DNA) of the *Clostridium leptum* group compared to SPF mice (~10^4 gene numbers/ng DNA) ($p < 0.01$–0.001) (Figure 3H). Lastly, SPF and mma mice exhibited significantly higher loads (~10^6 gene numbers/ng DNA) ($p < 0.001$) of Mouse Intestinal Bacteroides compared to hma mice, where these bacteria were nearly absent (Figure 3I). Hence, murine CR against *C. jejuni* is associated with higher loads of lactobacilli and Mouse Intestinal Bacteroides, but with lower loads of enterobacteria, enterococci, *Bacteroides*/*Prevotella* species, and *Clostridium coccoides* group. The fact that these results were comparable to observations in earlier studies confirm the successful establishment of the murine and human microbiota in the intestines of mice following oral FMT, and that CR was associated with a specific murine microbiota composition. Finally, species-specific differences in the microbiota compositions associated with presence and absence of CR are further used as a basis for the interpretation of results obtained from metabolomic analyses.

3.3 Metabolomic profiling of amino acid concentrations

In consideration of *C. jejuni* relying on amino acids as a primary nutrient and energy source within the gut (Wright et al., 2009), we conducted a comprehensive analysis of the amino acid concentrations in fecal samples of mice with and without CR prior to infection. The resulting metabolomics assessment revealed notable variations in the composition of amino acids among the different cohorts (Figure 4). As could be expected due to the absence

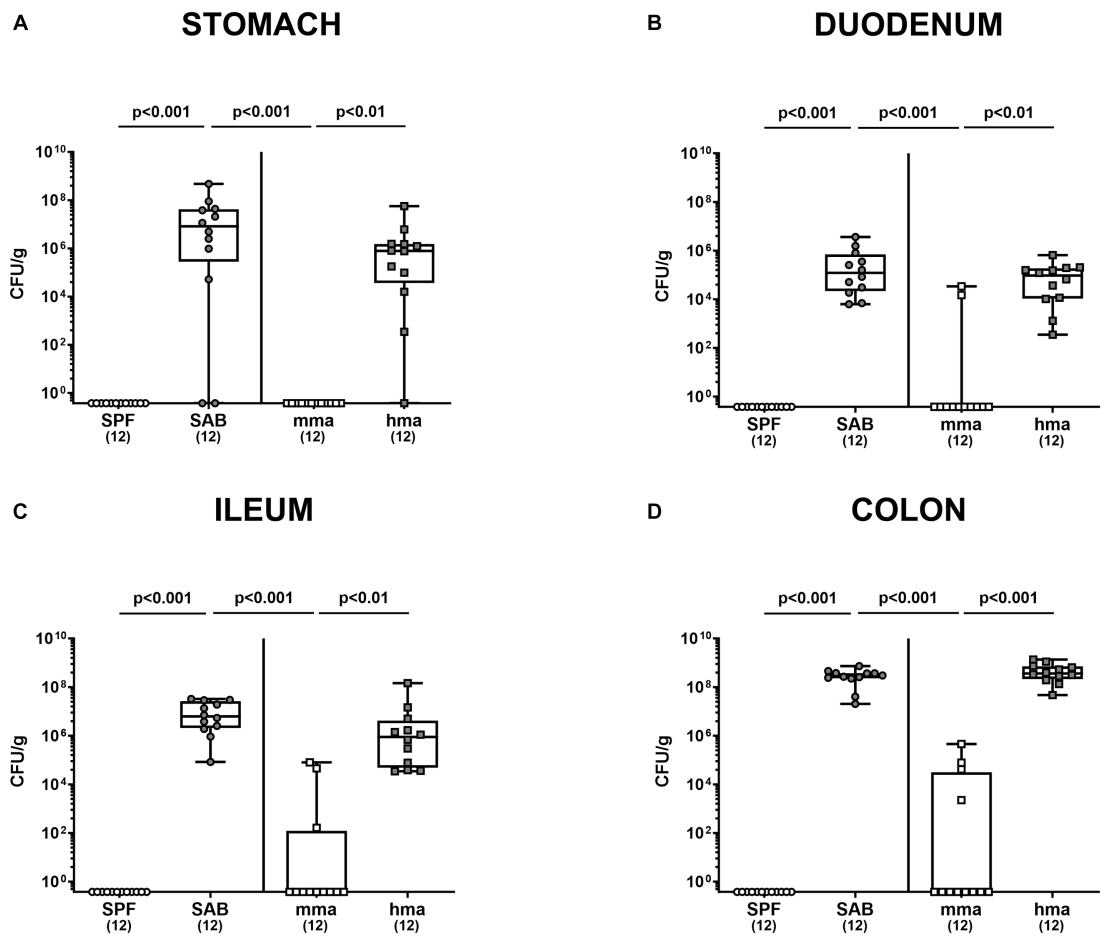

FIGURE 2
Gastrointestinal pathogen loads following *C. jejuni* infection in SPF, SAB, mma, and hma mice. Conventional but specific pathogen-free (SPF; white circles), secondary abiotic (SAB; gray circles), murine microbiota-associated (mma; white squares), and human microbiota-associated (hma; gray squares) mice were perorally infected with *C. jejuni* strain 81-176 on days 0 and 1. Cultural analysis for **(A)** stomach, **(B)** duodenum, **(C)** ileum, and **(D)** colon contents at the end of the experiment on day 21 were expressed as CFU/g of feces. Box plots indicate the 25th and 75th percentiles of the median (indicated by a black bar inside the box), as well as the range. Significance levels (*p* values) were determined by the Kruskal-Wallis test with Dunn's post correction. Numbers (in parentheses) specify the number of mice included.

of intestinal bacteria, the SAB mice exhibited significantly higher total concentrations of free amino acids compared to the other mice groups ($p < 0.05$–0.001) (Supplementary Figure S1). Concerning individual amino acids, we focused first on the amino acids essential for *C. jejuni* growth. Most importantly, levels of cysteine which is required for *C. jejuni* growth in the absence of serine, were significantly reduced in SPF mice and in mma as compared to hma and to SAB mice ($p < 0.05$–0.001) (Figure 4H). Notably, this was the only amino acid that was significantly reduced in mma mice in comparison to hma mice. Furthermore, the abundance of other amino acids essential for fueling *C. jejuni* metabolism including serine, glutamine, asparagine, threonine, and proline, was markedly lower in SPF, mma, and hma mice compared to SAB mice ($p < 0.01$–0.001) (Figures 4A–E). On the other hand, aspartic acid concentrations were lower in SPF and mma mice compared to SAB mice ($p < 0.05$), and glutamic acid levels were lower only in mma mice compared to SAB ($p < 0.05$), nevertheless a trend toward lower concentrations of both amino acids in mma mice compared to hma mice was observed (Figures 4F,G). Similarly, this pattern extended to arginine with significantly lower concentrations in SPF mice compared to SAB mice and in mma mice compared to hma and to SAB mice ($p < 0.05$–0.001) (Supplementary Figure S2A).

Moreover, SPF mice exhibited substantially lower concentrations of other amino acids, including leucine, isoleucine, lysine, histidine, phenylalanine, tryptophan, tyrosine, and valine, as compared to SAB mice, with a trend observed toward lower concentrations in mma mice compared to hma mice ($p < 0.05$–0.001) (Supplementary Figures S2B–I). Noteworthy, the levels of these amino acids were also significantly lower in both hma and mma mice compared to SAB mice ($p < 0.05$–0.001) (Supplementary Figures S2B–I). Additionally, glycine concentrations were significantly lower in SPF and mma mice compared to SAB mice, with a trend observed toward lower levels in mma mice compared to hma mice ($p < 0.05$–0.01) (Supplementary Figure S2J). Similarly, methionine levels were significantly lower in SPF mice compared to SAB mice, and a trend toward lower concentrations in mma compared to hma mice was observed ($p < 0.05$) (Supplementary Figure S2K). On the other hand, no significant differences were detected for alanine levels between the different mouse cohorts, yet a trend toward lower concentrations in

10.3389/fmicb.2023.1331114

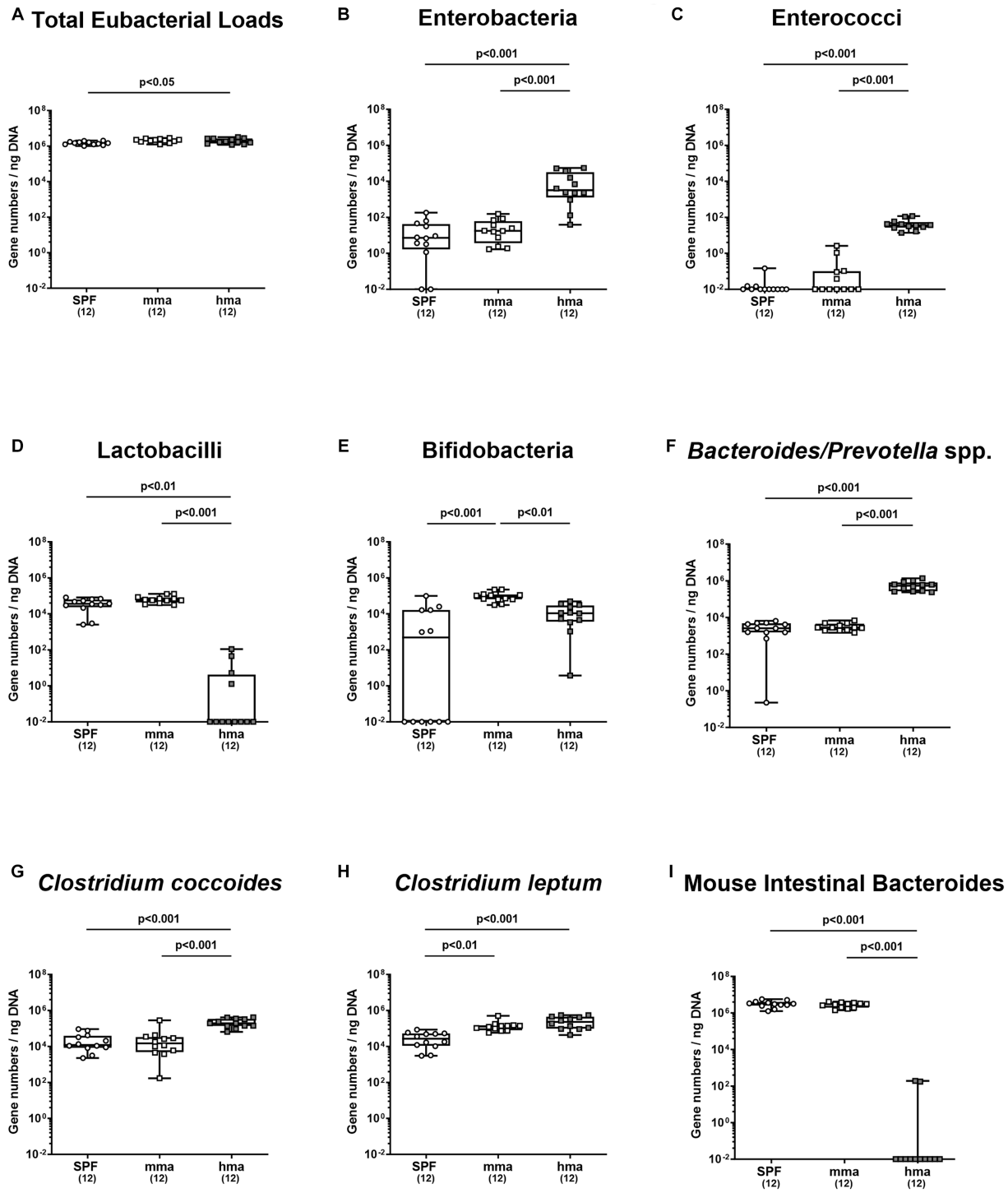

FIGURE 3
Fecal microbiota composition before and after *C. jejuni* infection. Mice were infected perorally with *C. jejuni* strain 81-176 on days 0 and 1. Gut microbiota composition was determined immediately before infection (day 0) for **(A)** total eubacterial loads, **(B)** enterobacteria, **(C)** enterococci, **(D)** lactobacilli, **(E)** bifidobacteria, **(F)** *Bacteroides/Prevotella* species, **(G)** *Clostridium coccoides* group, **(H)** *Clostridium leptum* group, and **(I)** Mouse Intestinal Bacteroides, using culture-independent, molecular methods (expressed as gene copies per ng DNA). Box plots indicate the 25th and 75th percentiles of the median (black bar inside the box). Each dot corresponds to an individual mouse. Significance levels (*p* values) are determined by the Mann–Whitney test with Tukey's post correction or Kruskal-Wallis test with Dunn's post correction. Numbers (in parentheses) show the number of mice included.

SPF mice compared to SAB mice and in mma mice compared to hma mice was observed (Supplementary Figure S2L). Furthermore, the amino acid-related metabolites sarcosine and phenylalanine betaine were also evaluated and revealed a distinct pattern. Sarcosine levels were significantly higher in SPF and mma mice compared to SAB and hma mice, respectively ($p < 0.001$ and $p < 0.05$, respectively)

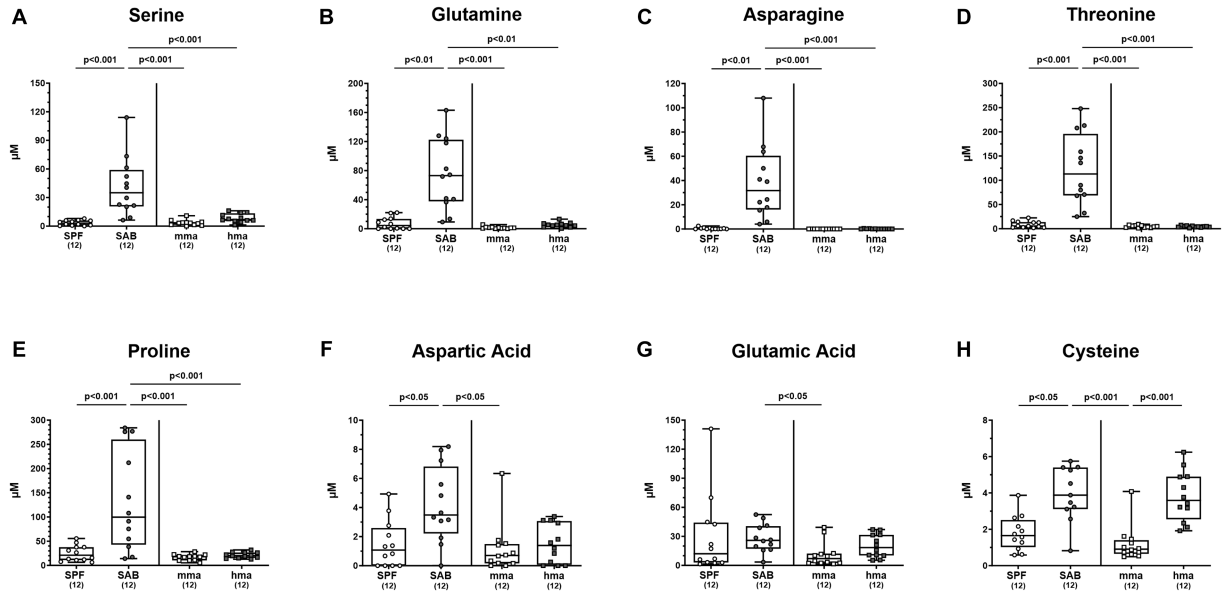

FIGURE 4
Fecal concentrations of amino acids essential for *C. jejuni* growth, in mice with and without CR. Fecal samples from conventional but specific pathogen-free (SPF) mice ($n = 12$), secondary abiotic (SAB) mice ($n = 12$), murine microbiota-associated (mma) mice ($n = 12$), and human microbiota-associated (mma) mice ($n = 12$) were harvested on day 0 before infection. Fecal levels of the amino acids **(A)** serine, **(B)** glutamine, **(C)** asparagine, **(D)** threonine, **(E)** proline, **(F)** aspartic acid, **(G)** glutamic acid and **(H)** cysteine were analyzed by LC–MS/MS, before *C. jejuni* infection. Metabolite concentration was expressed by µM. Box plots indicate the 25th and 75th percentiles of the median (black bar inside the box), as well as the total range. Significance levels (*p* values) were determined by the Mann–Whitney test with Tukey's post correction or Kruskal-Wallis test with Dunn's post correction, and numbers (in parentheses) indicate the number of mice included.

(Supplementary Figure S3A). Similarly, phenylalanine betaine levels were significantly elevated in SPF mice compared to SAB mice ($p < 0.001$), while mma mice exhibited higher levels compared to hma mice ($p < 0.001$) (Supplementary Figure S3B). Of note, mma mice also exhibited significantly lower levels of these metabolites compared to SAB mice ($p < 0.01$–0.001) (Supplementary Figures S3A,B). Hence, comparisons of metabolomic signatures among our mice cohorts revealed that murine CR against *C. jejuni* is significantly associated with a shortage in amino acids creating an unfavorable environment for *C. jejuni*.

3.4 Metabolomic profiling of bile acid concentrations

A comprehensive targeted metabolomic analysis of the bile acid composition in fecal samples of mice on d0 prior to *C. jejuni* 81-176 infection revealed significant differences between the distinct mouse cohorts. The mice with CR, namely SPF and mma mice, exhibited a bile acid profile characterized by a predominant secondary bile acid pool compared to the mice without CR, the SAB and hma mice, respectively. This was evident by a significantly lower ratio of primary to total bile acids in SPF mice compared to SAB mice, and in mma mice compared to hma and SAB mice ($p < 0.001$) (Figure 5A), as well as the significantly higher ratio of secondary to total bile acids in SPF mice compared to SAB mice, and in mma mice compared to hma and SAB mice ($p < 0.01$–0.001) (Figure 5B). Additionally, the ratio of secondary bile acids to primary bile acids, an indicator of secondary bile acid synthesis, was found to be significantly upregulated in the SPF mice compared to SAB mice ($p < 0.001$), and in mma mice compared to hma and to SAB mice ($p < 0.01$ and $p < 0.001$, respectively) (Figure 5C).

It is of note that the secondary bile acid deoxycholic acid, which is highly toxic to *C. jejuni* was significantly associated with CR in the mice groups. It was elevated in SPF mice compared to SAB mice, as well as in mma mice compared to hma and SAB mice ($p < 0.05$–0.001) (Figure 6E).

Moreover, it was reported that tauroconjugation of cholic acid is associated with a higher bacterial 7-α-dehydroxylation into deoxycholic acid (Eldere et al., 1996). Taurine-conjugated bile acids were predominant in the bile acid pool of SAB mice and hma mice, leaving SPF mice with significantly lower levels compared to SAB mice, and mma mice with lower levels compared to hma and SAB mice ($p < 0.05$–0.001) (Figure 6A). In particular, significantly lower concentrations of taurocholic acid and tauromuricholic acids were observed in SPF and mma mice compared to SAB mice, and in mma mice compared to hma mice for taurocholic acid ($p < 0.01$–0.001) (Figures 6B,C), with a trend toward lower concentrations for tauromuricholic acids (Figure 6C). Remarkably, the primary bile acid cholic acid exhibited a distinct pattern, with SPF mice harboring significantly higher concentrations compared to SAB mice, and mma mice harboring significantly lower concentrations than hma mice ($p < 0.05$–0.01) (Figure 6D). Moreover, the cholic acid concentrations were significantly lower in SAB mice compared to mma and hma mice ($p < 0.05$ and $p < 0.001$, respectively) (Figure 6D).

Hence, the results from bile acid profiling highlight distinct metabolomic signatures associated with CR against *C. jejuni* which is characterized by a predominance of secondary bile acids.

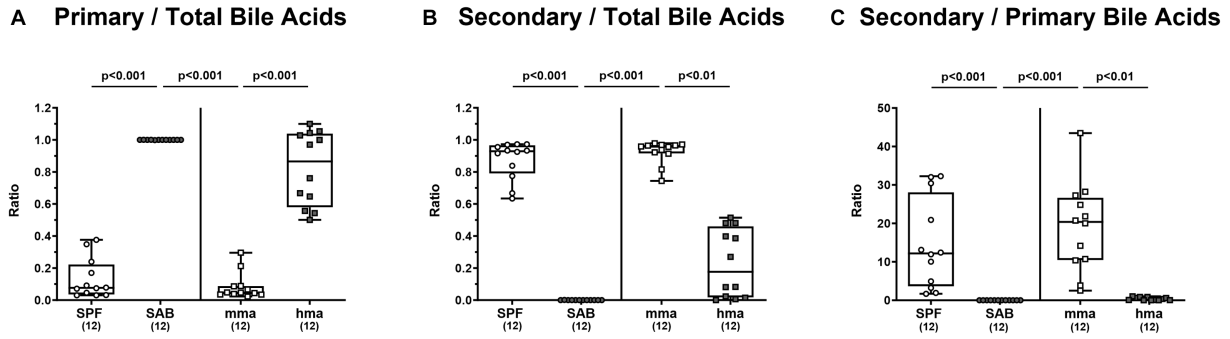

FIGURE 5
Fecal bile acid profile of mice resistant and susceptible to *C. jejuni* 81-176 infection. Fecal samples from conventional but specific pathogen-free (SPF), secondary abiotic (SAB), murine microbiota-associated (mma), and human microbiota-associated (hma) mice were harvested on day 0, and LC–MS/MS analysis was employed. The ratios of **(A)** primary bile acids concentrations as well as **(B)** secondary bile acids concentrations, to total bile acids concentrations were computed. Secondary bile acid synthesis **(C)**, defined as ratio of cytotoxic secondary bile acids to primary bile acids was also calculated. Box plots indicate the 25th and 75th percentiles of the median (black bar inside the box), as well as the total range. Significance levels (*p* values) are determined by the Kruskal-Wallis test with Dunn's post correction. Numbers (in parentheses) show the number of mice included.

3.5 Metabolomic profiling of fatty acids concentrations

In light of the pivotal antimicrobial roles of fatty acids and their potential impact on the composition of the gut microbiota, we conducted an in-depth investigation into the fatty acid profiles present in the colonic milieu of our distinct mouse models on day 0 before infection. Through comprehensive metabolomic analysis, we unraveled distinct patterns of fatty acid concentrations that distinguished between mouse groups exhibiting CR or susceptibility to *C. jejuni* colonization. Remarkably, our findings revealed that SPF mice exhibited significantly higher concentrations of free fatty acids in the colon compared to SAB mice ($p < 0.001$, Figure 7A). A similar trend was observed for mma mice, demonstrating significantly elevated levels of free fatty acids compared to hma and to SAB mice ($p < 0.001$, Figure 7A). Moreover, when examining the sum of monounsaturated and polyunsaturated fatty acids, SPF mice displayed significantly higher concentrations of both types of fatty acids compared to SAB mice ($p < 0.001$), while mma mice had significantly higher concentrations compared to hma and SAB mice ($p < 0.001$) (Figures 7B,C). Notably, monounsaturated fatty acid concentrations were found to be significantly higher ($p < 0.001$) in hma mice compared to SAB mice (Figure 7B).

Further delving into the differentially expressed fatty acids, particularly within the monounsaturated fatty acid class, we observed significant differences in octadecenoic acid and eicosenoic acid. Octadecenoic acid levels were significantly elevated in SPF and in mma mice compared to SAB and hma mice, respectively ($p < 0.001$) (Figure 8A). Additionally, hma mice displayed higher concentrations of octadecenoic acid compared to SAB mice ($p < 0.001$) (Figure 8A). A similar pattern emerged for eicosenoic acid, with SPF and mma mice exhibiting substantially elevated levels of this fatty acid compared to SAB and hma mice, respectively ($p < 0.01$–0.001) (Figure 8B), whereas no statistically significant difference was observed between the two susceptible groups (Figure 8B).

Interestingly, the distinctive patterns observed between resistant and susceptible groups extended to specific polyunsaturated fatty acids, although not all fatty acids followed these patterns. Octadecadienoate, eicosadienoic acid, and eicosatrienoic acid exhibited different patterns, with SPF mice harboring higher fecal concentrations of these fatty acids compared to susceptible models SAB mice, and mma mice harboring higher concentrations compared to hma and SAB mice ($p < 0.05$–0.001) (Figures 8C–E). On the other hand, although SPF and mma mice exhibited significantly higher fecal concentrations of arachidonic acid compared to SAB mice ($p < 0.001$ and $p < 0.05$, respectively), a trend toward higher concentrations in mma mice compared to hma mice was still observed (Figure 8F). Furthermore, SPF, mma, and hma mice displayed higher colonic concentrations of docosahexaenoic acid and eicosapentaenoic acid compared to SAB mice ($p < 0.05$–0.001) (Figures 8G,H). Nevertheless, no significant differences were observed in colonic levels of the latter fatty acids between mma and hma mice (Figures 8G,H). Hence, these results indicate that elevated free fatty acids represent another metabolomic signature significantly associated with murine CR against *C. jejuni*.

3.6 Other metabolites

In addition to investigating the role of bile acids, amino acids, and fatty acids, we explored the metabolomic landscape of other classes of metabolites present in the colon of our mouse models before infection. Specifically, we delved into the analysis of phosphatidylcholines and diglycerides, which hold potential relevance to host-microbe interactions, in addition to the crucial components of nucleic acids, namely purines. Our investigation into purine metabolites revealed distinct profiles that distinguished between mice cohorts with and without CR (Figure 9A). Mma mice exhibited significantly higher levels of purine metabolites compared to hma mice ($p < 0.001$) (Figure 9A). Interestingly, although no significant differences were observed between SAB and the resistant cohorts, a trend was still observed, and SAB mice displayed higher concentrations of purines compared to hma mice ($p < 0.05$) (Figure 9A). In particular,

10.3389/fmicb.2023.1331114

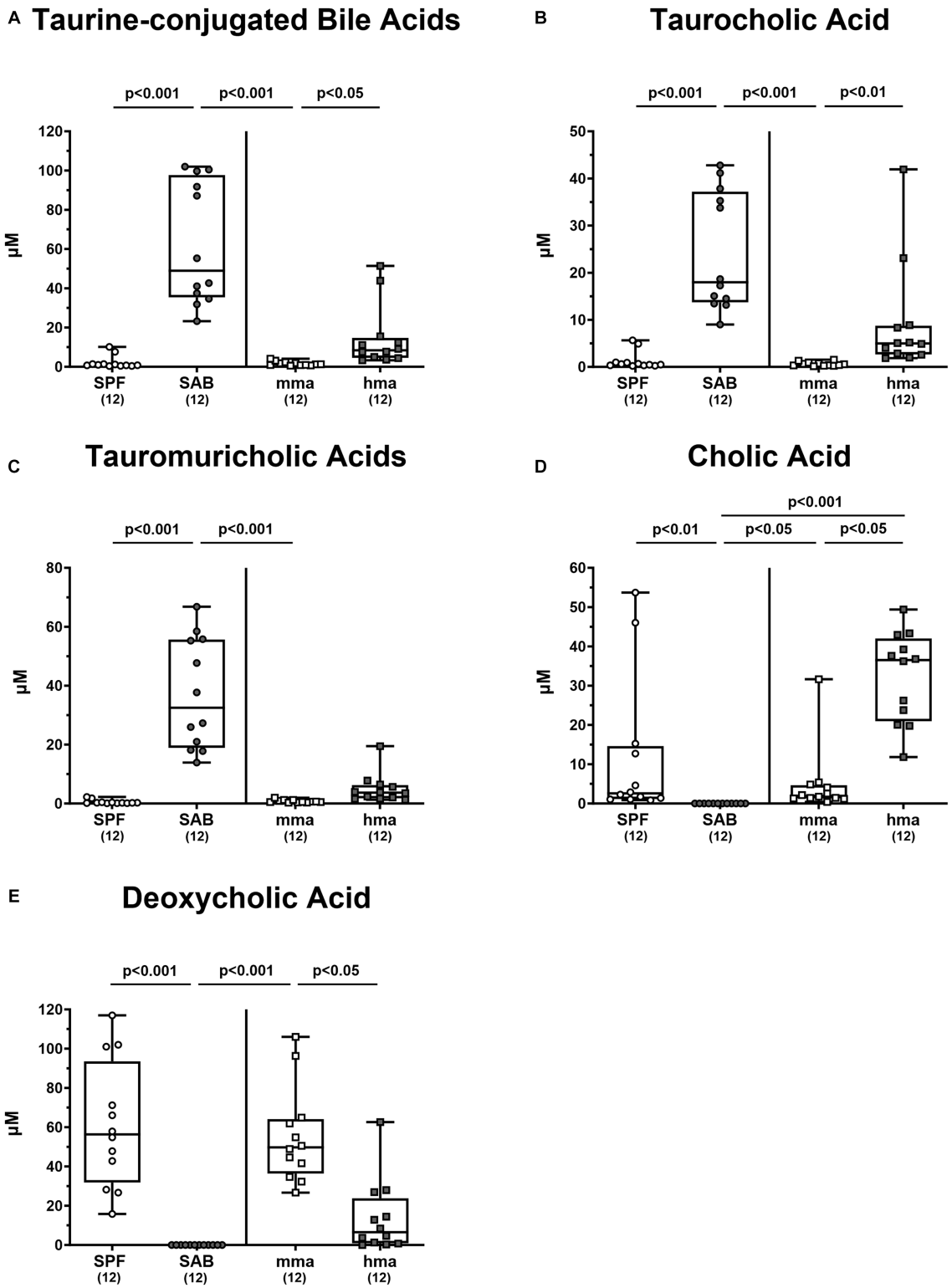

FIGURE 6
Primary and secondary bile acids in the feces of mice with and without CR. **(A)** The sum of taurine conjugated bile acids were computed. Fecal concentrations of **(B)** tauromuricholic acids, **(C)** taurocholic acid, **(D)** cholic acid, and **(E)** deoxycholic acid were measured using LC–MS/MS, from 4 mouse cohorts, SAB, SPF, hma, and mma mice on day 0 prior to infection. Metabolite concentrations are expressed in µM. Box plots reveal the 25th and 75th percentiles of the median (black bar inside the box), as well as the total range were assigned. Significance levels (*p* values) were determined by the Kruskal-Wallis test with Dunn's post correction, and numbers (in parentheses) indicate the number of mice included.

xanthine concentrations in SPF, mma, and SAB mice were significantly higher compared to hma mice ($p < 0.01$–0.001) (Supplementary Figure S4A). On the other hand, hypoxanthine displayed a different pattern, as SPF mice harbored significantly higher levels compared to SAB mice, and this was also the case for mma mice compared to hma and SAB mice ($p < 0.01$–0.001)

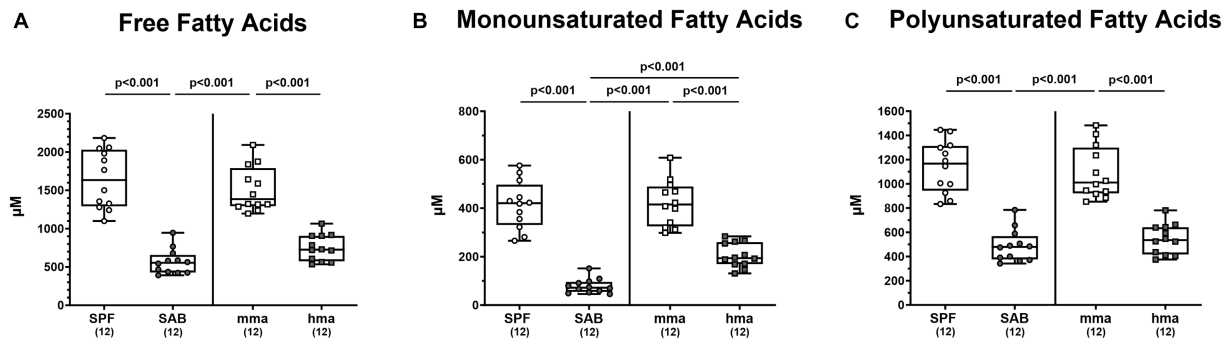

FIGURE 7
Fatty acid composition in the feces mice resistant and susceptible to *C. jejuni* infection. Fecal samples were analyzed by LC–MS/MS, from secondary abiotic (SAB) mice ($n = 12$), conventional but specific pathogen-free (SPF) mice ($n = 12$), human microbiota-associated (hma) mice ($n = 12$), and murine microbiota-associated (mma) mice ($n = 12$), to characterize the fatty acid composition in the colon of the distinct mouse cohorts on day 0 prior to infection. Sums of **(A)** free fatty acids, **(B)** monounsaturated fatty acids, and **(C)** polyunsaturated fatty acids were computed. Metabolite concentrations were expressed in µM. Box plots indicate the 25th and 75th percentiles of the median (black bar inside the box), as well as the total range. Significance levels (p values) were determined by one-sided ANOVA with Tukey's post correction. The number of mice included are indicated by numbers (in parentheses).

(Supplementary Figure S4B). Notably, SAB mice exhibited a higher xanthine synthesis computed by the ratio of xanthine to hypoxanthine compared to both SPF and mma mice ($p < 0.001$) (Supplementary Figure S4C).

Moreover, these distinct patterns extended to phosphatidylcholines, diglycerides, and triglycerides. SPF and mma mice exhibited significantly higher concentrations of all three classes of the metabolites compared to SAB mice ($p < 0.05$–0.001) (Figures 9B–D). Nevertheless, compared to hma mice, only diglycerides were measured at significantly higher concentrations in mma mice ($p < 0.05$), albeit a trend toward higher levels of phosphatidylcholines and triglycerides in mma mice compared to hma mice could still be observed (Figures 9B–D).

4 Discussion

Murine models have proven invaluable in uncovering the complex interplay between host, microbiota, and intestinal pathogens. The intricate role of the gut microbiota in murine CR against *C. jejuni* represents a pivotal step in disease initiation, progression, and pathogenesis of campylobacteriosis. Comparing SPF and microbiota-depleted (i.e., SAB) mice reveals metabolomic signatures associated with the presence or absence of the gut microbiota. Additionally, contrasting hma mice with mma or SPF counterparts unveils species-specific metabolic profiles. In order to identify metabolites of potential benefit for prevention and treatment of *C. jejuni* infection, we employed a comprehensive metabolomics profiling approach to shed light on the metabolome signatures and distinct metabolites associated with CR against the gut pathogen.

Our findings demonstrate robust CR against *C. jejuni* 81-176 in the colon of SPF mice which is abrogated by antibiotic treatment in SAB mice, confirming the crucial role of the gut microbiota in CR and in preventing pathogen growth as shown earlier (Bereswill et al., 2011) and confirmed here (Figures 1, 2). In addition, the restoration of CR in mma mice but not in hma mice nicely proved that the characteristic species-specific microbiota was established by FMT of SAB mice in mma as well as hma mice and reproduce again our data concerning the specific host's endogenous gut microbiota composition in previous studies (Bereswill et al., 2011; Ducarmon et al., 2019; Mousavi et al., 2021; Herzog et al., 2023; Shayya et al., 2023). Notably, our findings suggest that lactobacilli are associated with CR against *C. jejuni*, as supported by the notable increase in lactobacilli levels observed in SPF and mma mice with CR, as compared to the hma mice without CR (Figure 3), which was also true for Mouse Intestinal Bacteroides. These results align with previous studies demonstrating the beneficial effects of lactobacilli in inhibiting various other enteric pathogens, including *Salmonella* (Bernet-Camard et al., 1997), *E. coli* (Mangell et al., 2002), and *Listeria monocytogenes* (de Waard et al., 2002). Importantly, some studies have also reported a protective effect of lactobacilli in preventing *Campylobacter* infections (Morishita et al., 1997; Willis and Reid, 2008; Wagner et al., 2009). However, monocolonization with a single *Lactobacillus johnsonii* strain isolated from our mice was not able to protect SAB mice from *C. jejuni* infection, indicating that the role of individual *Lactobacillus* species in CR is complex and needs to be analyzed in more detail in ongoing studies (Bereswill et al., 2017).

Interestingly, treating human intestinal epithelial cells with *Lactobacillus helveticus* R0052 reduced *C. jejuni* invasion into these cells, suggesting a contribution of competitive exclusion by adherent bacteria (Wine et al., 2009). Another study also reported the capacity of other *Lactobacillus* strains to prevent *C. jejuni* adhesion and invasion to intestinal cells (Wang et al., 2014). Finally, the lactobacilli dominating in the murine intestinal tract might inhibit *C. jejuni* growth by lowering the pH and by production of bacteriocins as shown earlier (Robyn et al., 2012; Zommiti et al., 2016; Kobierecka et al., 2017).

In addition, nutrient competition is a key factor in driving CR against bacterial pathogens (Maltby et al., 2013). Thus, the antimicrobial effects of lactobacilli mentioned above might be further supported by consumption of amino acids leading to out-competition of *C. jejuni*. In contrast to other gut bacteria, the lactobacilli colonize the entire gastrointestinal tract including upper parts like the forestomach and small

10.3389/fmicb.2023.1331114

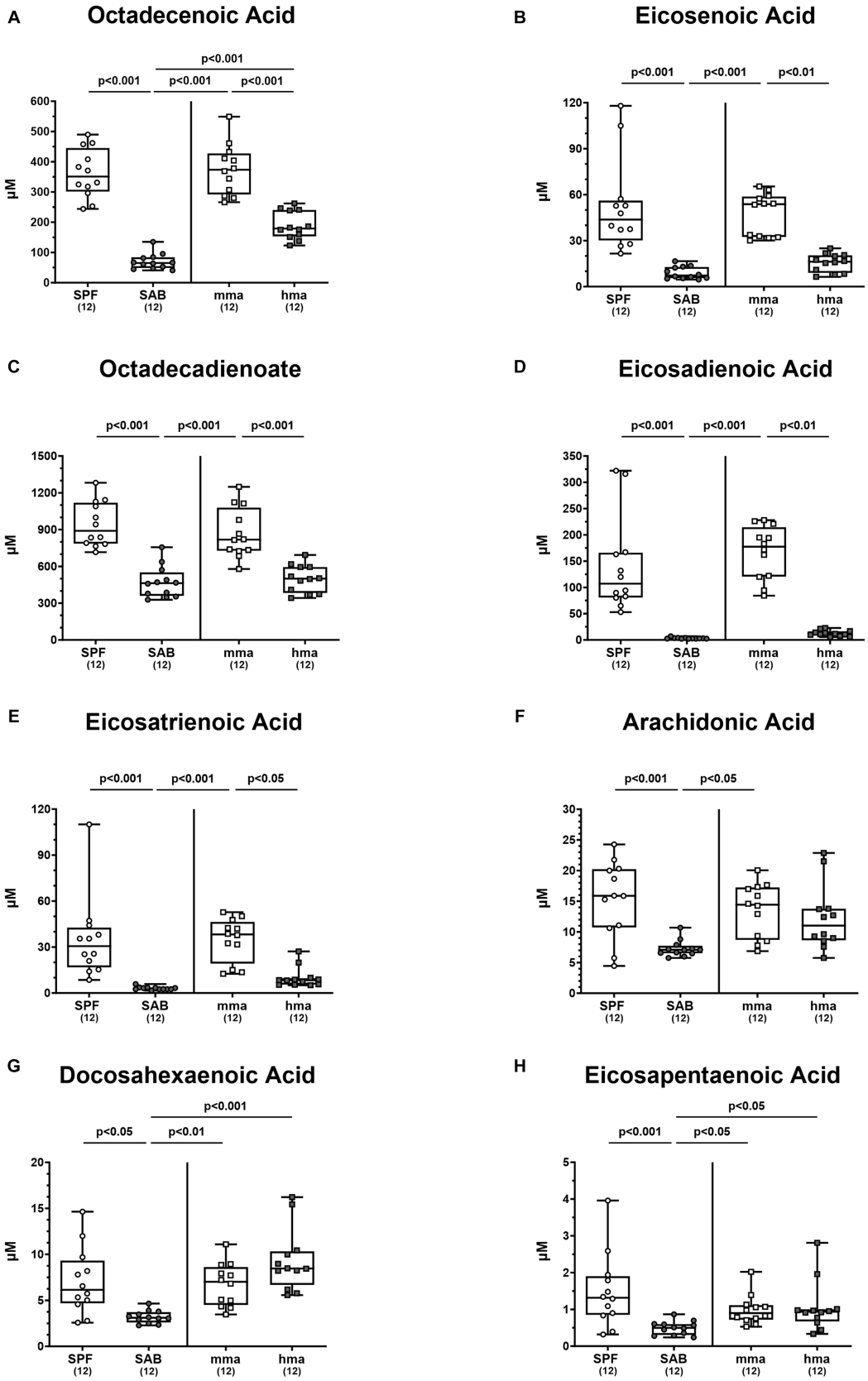

FIGURE 8
Monounsaturated and polyunsaturated fatty acids in mice with and without CR. Fecal samples were analyzed by LC–MS/MS, from conventional but specific pathogen-free (SPF), secondary abiotic (SAB), murine microbiota-associated (mma), and human microbiota-associated (mma) mice on day 0 prior to infection. The monounsaturated fatty acids **(A)** octadecenoic acid and **(B)** eicosenoic acid, as well as the polyunsaturated fatty acids

(Continued)

FIGURE 8 (Continued)

(C) octadecadienoate, **(D)** eicosadienoic acid, **(E)** eicosatrienoic acid, **(F)** arachidonic acid, **(G)** docosahexaenoic acid, and **(H)** eicosapentaenoic acid were shown. Metabolite concentrations were expressed in μM. Box plots indicate the 25th and 75th percentiles of the median (black bar inside the box), as well as the total range. Significance levels (*p* values) were determined by one-sided ANOVA with Tukey's post correction or the Kruskal-Wallis test with Dunn's correction. The number of mice included are indicated by numbers (in parentheses).

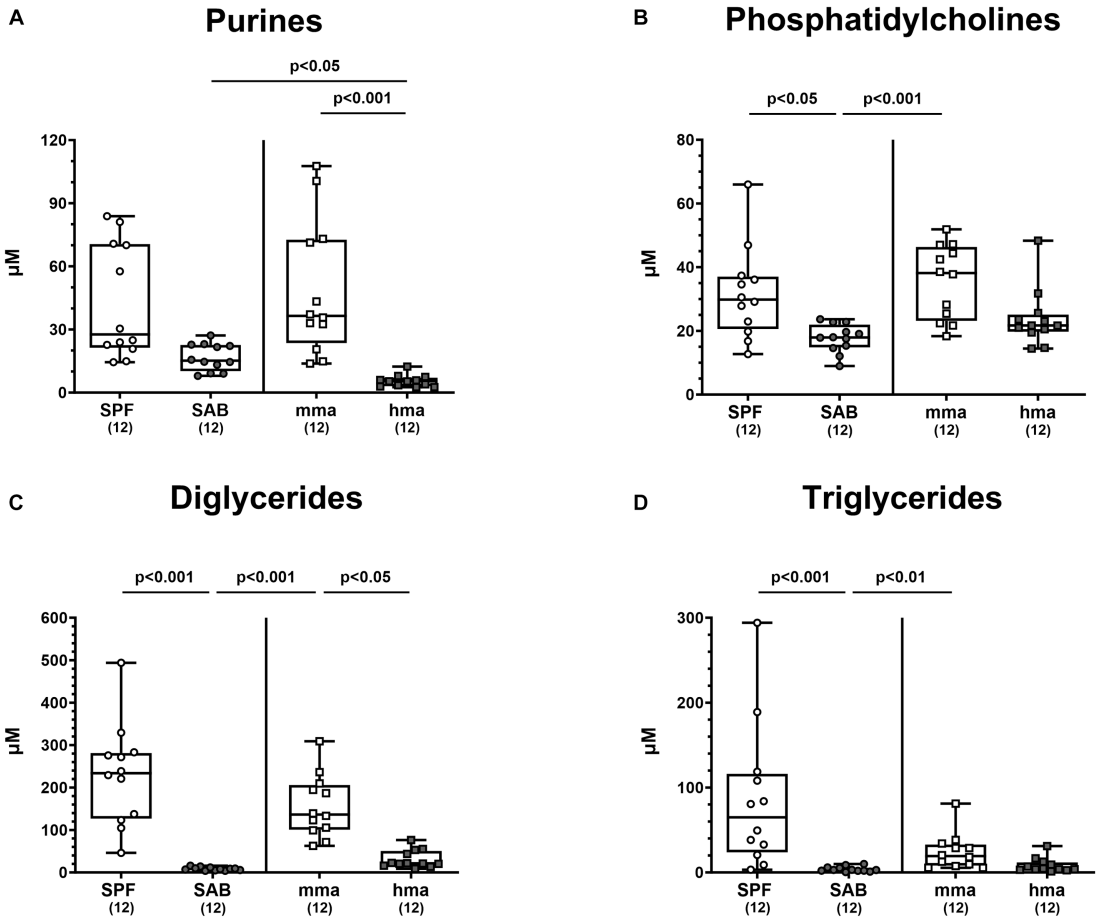

FIGURE 9

Other classes of metabolites differentially expressed between mice cohorts resistant and susceptible to *C. jejuni* infection. Fecal samples analyzed by LC–MS/MS, derived from the mice cohorts (conventional but specific pathogen-free (SPF), secondary abiotic (SAB), murine microbiota-associated (mma), and human microbiota-associated (mma) mice) on day 0 prior to infection. The sum **(A)** of purines, **(B)** phosphatidylcholines, **(C)** diglycerides, and **(D)** triglycerides were shown. Metabolite concentrations were expressed in μM. Box plots indicate the 25th and 75th percentiles of the median (black bar inside the box), as well as the total range. Significance levels (*p* values) were determined by the Kruskal-Wallis test with Dunn's post correction. The number of mice included are indicated by numbers (in parentheses).

intestine at high numbers. In consequence, consumption by lactobacilli might add substantially to the scarcity of essential amino acids for *C. jejuni* established in mice with CR. This is supported by significantly higher levels of free amino acids detected in SAB mice as compared to the other mouse cohorts (Supplementary Figure S1) which can be attributed to the absence of a complex gut microbiota that typically metabolize and utilize these nutrients. Without microbial nutrient competition, these amino acids are utilized by *C. jejuni* for the multiplication required for gut colonization. *C. jejuni* utilize transporters and other uptake systems to acquire essential amino acids, including cysteine, serine, aspartate, asparagine, glutamate, glutamine, threonine, and proline (Velayudhan et al., 2004; Hofreuter et al., 2006; Leon-Kempis Mdel et al., 2006; Heimesaat et al., 2023). Most importantly, cysteine has been shown to be essential for *C. jejuni* 81-176 growth *in vitro* (Vorwerk et al., 2014; Hitchcock et al., 2022). To overcome this limitation, *C. jejuni* utilize free cysteine and cysteine-containing peptides to fuel respiration as a sulfur source. Unlike other enteropathogenic bacteria, *C. jejuni* cannot obtain cysteine from sulfur (Vegge et al., 2009; Man et al., 2020) and thus, cysteine acts as a chemoattractant for *C. jejuni*, and is required for the vitality of this pathogen. Our data clearly highlight significantly elevated levels of free cysteine available in the colonic environment of mice without CR, namely SAB and hma mice (Figure 4), indicating that the scarcity of cysteine in SPF and mma mice might support the CR in these murine infection models. In this context it is noteworthy that some *Lactobacillus* species depend on cysteine uptake from the environment (Bloom et al., 2022). Thus, lactobacilli might compete for cysteine with *C. jejuni*.

Interestingly, elevated levels of the other essential amino acids were observed in SAB mice (Figure 4). This, however, was not observed in hma mice, which displayed different patterns in amino acid levels.

Our metabolome analyses revealed that concentrations of bactericidal molecules including bile acids and fatty acids were elevated in fecal samples derived from mice with CR as compared to mice without CR. This points toward a direct killing of *C. jejuni* in the colonic milieu of SPF and mma mice with a murine gut microbiota. Both molecular classes may represent key drivers of CR against the pathogen. Bile acids are synthesized in the liver and secreted into the intestinal tract to aid in digesting dietary lipids. Conjugation with glycine or taurine increases their solubility and this conjugation can be modified by gut bacteria (Hofmann, 1999). Consistent with our findings, SAB mice, which lack microbial bile acid transformations, exhibited an exclusive composition of liver-derived tauro-conjugated primary bile acids (Figure 6). On that note, tauroconjugated cholic acid enhances bacterial 7-α-dehydroxylation into deoxycholic acid, essentially by providing a sulfur source for the anabolic pathways involved in dihydroxylation (Eldere et al., 1996). Interestingly, our findings indicate a depletion of tauroconjugated bile acids in the colonic environment of mice with CR as compared to the susceptible cohorts (Figure 6), suggesting their potential transformation to secondary bile acids, which were elevated in the resistant mice compared to the susceptible ones (Figure 5). The majority of conjugated bile acids are reabsorbed in the distal ileum, while the remaining undergo bacterial metabolism in the colon, particularly through 7α-dehydroxylation carried out by a few bacteria, primarily belonging to the *Clostridium* species, resulting in the production of secondary bile acids such as deoxycholic acid which exerts a strong antimicrobial activity (Hirano et al., 1981). Importantly, bacterial deconjugation of conjugated bile acids by bile salt hydrolase (BSH), which is highly expressed in lactobacilli, represents a key regulator in bile acid metabolism into secondary bile acids (Jia et al., 2019). This is well in line with the elevated loads of lactobacilli in SPF and mma mice with CR as compared to the susceptible hma mice (Figure 3D). Additionally, BSH activity profoundly influences host lipid metabolism, linking it to fecal fatty acids levels in our murine models (Joyce et al., 2014). We suggest that the robust BSH activity in SPF mice, and similarly in mma mice, indicated by diminished taurine-conjugated bile acids, leads to a reduction in fatty acid resorption, increasing the fecal fatty acid content. Conversely, SAB mice exhibit elevated taurocholic acids, which increases fatty acid resorption, thus depleting fecal fatty acids. On the other hand, hma mice exhibit an intermediate phenotype, with moderate BSH activity leading to a moderate fatty acid resorption. Deoxycholic acid has been shown to exhibit potent bactericidal effects against *C. jejuni* (Kurdi et al., 2006; Sannasiddappa et al., 2017; Thanissery et al., 2017). Previous studies have highlighted the critical role of the CmeABC efflux pump in *C. jejuni*'s resistance to bile acids and subsequent intestinal colonization (Lin et al., 2003). Moreover, it has been shown that *C. jejuni* accommodates a well-developed chemotaxis system that repels the pathogen from bile constituents in particular secondary bile acids (Hugdahl et al., 1988; Vegge et al., 2009). The MIC and MIC50 values of deoxycholic acid against *C. jejuni* strain 81-176 (determined in our laboratories as described in methods) were 256 mg/L and 128 mg/L, respectively. Therefore, it is not surprising that deoxycholic acid effectively reduced *C. jejuni* 81-176 colonization of the intestinal tract of broiler chickens (Alrubaye et al., 2019). The concentration of deoxycholic acid measured by targeted metabolomics in murine fecal matter was 94 mg/L, high enough to exert antimicrobial effects against *C. jejuni*. However, treatment of *C. jejuni* 81-176 infection of germ-free IL-10$^{-/-}$ mice with deoxycholic acid below the MIC did not decrease densities but ameliorated some disease manifestations (Sun et al., 2018).

In addition, fecal samples of mice with CR contained elevated levels of fatty acids including medium-chain fatty acids (MCFAs) such as octadecenoic acid, an isomer of oleic acid, as compared to mice without CR (Figure 8). Long-chain fatty acids exerting potent antimicrobial properties play a crucial role in modulating the microbiota composition by selecting for resistant gut bacterial species (Alcock and Lin, 2015). It has been demonstrated that oleic acid effectively eradicates *Campylobacter* on chicken skins (Hinton and Ingram, 2000), and *in vitro* analyses revealed a potent bactericidal effect of MCFAs and long-chain fatty acids against *C. jejuni* (Sprong et al., 2001). Further studies reported that feeding broiler chicks with different concentrations of MCFAs diet led to less distinct pathogen colonization along the gastrointestinal tract (Van Deun et al., 2008; de los Santos et al., 2009, 2010; Metcalf et al., 2011). In addition, our results clearly indicate that high concentrations of diglycerides and triglycerides are associated with CR against *C. jejuni* in mice (Figures 9C,D). Diglycerides derived from fatty acids display potent antimicrobial activities. Even though triglycerides were not described to have potent antimicrobial activities, nevertheless, upon hydrolysis, these lipids release free fatty acids and monoglycerides, which in turn possess potent antimicrobial properties (Churchward et al., 2018; Yoon et al., 2018; Fischer, 2020).

Another metabolite of interest is hypoxanthine, which was found to be significantly associated with CR in our mice models. While there is no cumulative evidence to suggest that hypoxanthine itself possesses direct antibacterial properties, it can be metabolized into other compounds such as xanthine and uric acid, that have been shown to exhibit antimicrobial features (Martin et al., 2004). According to our data, CR mice displayed higher levels of xanthine compared to hma mice (Supplementary Figure S4), although SAB mice also harbored high xanthine concentrations.

Finally, these findings highlight the fact that murine CR against *C. jejuni* is characterized by complex interactions between the gut microbiota, amino acids, bile acids, and lipids. It is noteworthy that the congruence between the metabolite concentrations in our hma mice and those reported in human fecal samples, utilizing the same analytical kit (Erben et al., 2021), underscores the translational relevance of our findings. This further validates the hma mouse model as a representation of human metabolomic profiles. It is clear that CR against *C. jejuni* cannot be solely attributed to a single metabolite. Thus, the precise role of the metabolites identified here in *C. jejuni* clearance has yet to be determined. Nevertheless, based on the results presented, it is plausible that antimicrobial activities act together with substrate competition to support murine CR against *C. jejuni*.

5 Conclusion

Investigations into murine CR against *C. jejuni* using a comprehensive metabolomic profiling approach shed light on the dynamic gut microbiota interactions of *C. jejuni* and uncover distinct metabolome signatures associated with CR against this enteropathogen. The findings that concentrations of bactericidal molecules including

secondary bile acids, fatty acids, and di-glycerides were elevated in mice with CR as compared to mice without CR points toward a growth inhibition or direct killing of *C. jejuni* in SPF and mma mice, indicating that respective metabolites may represent key drivers of CR against the pathogen. Notably, the scarcity of amino acids, which are essential for fueling *C. jejuni* growth, in mice with CR provide evidence that antimicrobial effects might be supported by out-competition mediated by lactobacilli or other gut bacterial species via similar substrate requirements. Importantly, these murine models provide valuable insights into the dynamic relationship between the vertebrate host, microbiota, and pathogen, offering a deeper understanding of metabolite-driven processes underlying CR. In addition to its implications in understanding colonization resistance against *C. jejuni*, the alignment between the hma mouse model and human metabolites enhances our comprehension of host-microbiota interaction and positions the hma mice as a versatile model for investigating a spectrum of microbiota-related metabolic phenomena (Erben et al., 2021). However, the complexity of the gut microbiota and the multitude of metabolic interactions therein necessitate further studies to decipher the specific mechanisms by which distinct metabolites and metabolic pathways influence different physiological functions, and particularly colonization resistance against *C. jejuni* in the intestinal milieu. Additionally, we employed a targeted approach for the metabolomics and microbiota composition analyses. For that, using untargeted approaches could offer a more comprehensive view of gut microbiota composition and of the metabolites, thus extending our understanding of host-microbiota interplay. Respective findings will pave the way for the broader goal of using mechanisms of CR for developing novel therapeutic approaches to combat and prevent campylobacteriosis and possibly other enteric infections.

Data availability statement

The raw data supporting the conclusions of this article will be made available by the authors, without undue reservation.

Ethics statement

The animal study was approved by Landesamt für Gesundheit und Soziales, Berlin. The study was conducted in accordance with the local legislation and institutional requirements.

Author contributions

NS: Investigation, Formal analysis, Visualization, Writing – original draft. RB: Investigation, Writing – review & editing. LB: Investigation, Writing – review & editing. SM: Investigation, Writing – review & editing. SB: Writing – review & editing, Conceptualization, Funding acquisition, Supervision, Validation. MH: Conceptualization, Funding acquisition, Supervision, Validation, Writing – review & editing, Investigation.

Funding

The author(s) declare financial support was received for the research, authorship, and/or publication of this article. This project received funding from the Open Access Publication Fund of Charité – Universitätsmedizin Berlin, the German Research Foundation (DFG) and the European Union's Horizon 2020 research and innovation programme (under the Marie Sklodowska-Curie grant agreement No. 956279; COL_RES project).

Acknowledgments

The authors would like to thank the technical support provided by Alexandra Bittroff-Leben, Ulrike Fiebiger, Sumaya Abdul-Rahman, Ines Puschendorf, Gernot Reifenberger, and the staff of the animal research facility at FEM of Charité – Universitätsmedizin Berlin.

Conflict of interest

The authors declare that the research was conducted in the absence of any commercial or financial relationships that could be construed as a potential conflict of interest.

The author(s) declared that they were an editorial board member of Frontiers, at the time of submission. This had no impact on the peer review process and the final decision.

Publisher's note

Supplementary material

The Supplementary material for this article can be found online at: https://www.frontiersin.org/articles/10.3389/fmicb.2023.1331114/full#supplementary-material

References

Alcock, J., and Lin, H. C. (2015). Fatty acids from diet and microbiota regulate energy metabolism. *F1000Res* 4:738. doi: 10.12688/f1000research.6078.1

Alrubaye, B., Abraha, M., Almansour, A., Bansal, M., Wang, H., Kwon, Y. M., et al. (2019). Microbial metabolite deoxycholic acid shapes microbiota against *Campylobacter jejuni* chicken colonization. *PLoS One* 14:e0214705. doi: 10.1371/journal.pone.0214705

Becattini, S., Littmann, E. R., Carter, R. A., Kim, S. G., Morjaria, S. M., Ling, L., et al. (2017). Commensal microbes provide first line defense against *Listeria monocytogenes* infection. *J. Exp. Med.* 214, 1973–1989. doi: 10.1084/jem.20170495

Bereswill, S., Ekmekciu, I., Escher, U., Fiebiger, U., Stingl, K., and Heimesaat, M. M. (2017). *Lactobacillus johnsonii* ameliorates intestinal, extra-intestinal and systemic pro-

inflammatory immune responses following murine *Campylobacter jejuni* infection. *Sci. Rep.* 7:2138. doi: 10.1038/s41598-017-02436-2

Bereswill, S., Fischer, A., Plickert, R., Haag, L. M., Otto, B., Kühl, A. A., et al. (2011). Novel murine infection models provide deep insights into the "ménage à trois" of *Campylobacter jejuni*, microbiota and host innate immunity. *PLoS One* 6:e20953. doi: 10.1371/journal.pone.0020953

Bernet-Camard, M. F., Liévin, V., Brassart, D., Neeser, J. R., Servin, A. L., and Hudault, S. (1997). The human *Lactobacillus acidophilus* strain LA1 secretes a nonbacteriocin antibacterial substance(s) active *in vitro* and *in vivo*. *Appl. Environ. Microbiol.* 63, 2747–2753. doi: 10.1128/aem.63.7.2747-2753.1997

Bloom, S. M., Mafunda, N. A., Woolston, B. M., Hayward, M. R., Frempong, J. F., Abai, A. B., et al. (2022). Cysteine dependence of *Lactobacillus iners* is a potential therapeutic target for vaginal microbiota modulation. *Nat. Microbiol.* 7, 434–450. doi: 10.1038/s41564-022-01070-7

Chang, C., and Miller, J. F. (2006). *Campylobacter jejuni* colonization of mice with limited enteric flora. *Infect. Immun.* 74, 5261–5271. doi: 10.1128/iai.01094-05

Chen, X., Katchar, K., Goldsmith, J. D., Nanthakumar, N., Cheknis, A., Gerding, D. N., et al. (2008). A mouse model of *Clostridium difficile*-associated disease. *Gastroenterology* 135, 1984–1992. doi: 10.1053/j.gastro.2008.09.002

Churchward, C. P., Alany, R. G., and Snyder, L. A. S. (2018). Alternative antimicrobials: the properties of fatty acids and monoglycerides. *Crit. Rev. Microbiol.* 44, 561–570. doi: 10.1080/1040841X.2018.1467875

de los Santos, F. S., Donoghue, A. M., Venkitanarayanan, K., Metcalf, J. H., Reyes-Herrera, I., Dirain, M. L., et al. (2009). The natural feed additive caprylic acid decreases *Campylobacter jejuni* colonization in market-aged broiler chickens. *Poult. Sci.* 88, 61–64. doi: 10.3382/ps.2008-00228

de los Santos, F. S., Hume, M., Venkitanarayanan, K., Donoghue, A. M., Hanning, I., Slavik, M. F., et al. (2010). Caprylic acid reduces enteric campylobacter colonization in market-aged broiler chickens but does not appear to alter cecal microbial populations. *J. Food Prot.* 73, 251–257. doi: 10.4315/0362-028x-73.2.251

de Waard, R., Garssen, J., Bokken, G. C., and Vos, J. G. (2002). Antagonistic activity of *Lactobacillus casei* strain shirota against gastrointestinal *Listeria monocytogenes* infection in rats. *Int. J. Food Microbiol.* 73, 93–100. doi: 10.1016/s0168-1605(01)00699-7

Ducarmon, Q. R., Zwittink, R. D., Hornung, B. V. H., van Schaik, W., Young, V. B., and Kuijper, E. J. (2019). Gut microbiota and colonization resistance against bacterial enteric infection. *Microbiol. Mol. Biol. Rev.* 83:e00007-19. doi: 10.1128/mmbr.00007-19

Eldere, J. V., Celis, P., Pauw, G. D., Lesaffre, E., and Eyssen, H. (1996). Tauroconjugation of cholic acid stimulates 7 alpha-dehydroxylation by fecal bacteria. *Appl. Environ. Microbiol.* 62, 656–661. doi: 10.1128/aem.62.2.656-661.1996

Erben, V., Poschet, G., Schrotz-King, P., and Brenner, H. (2021). Evaluation of different stool extraction methods for metabolomics measurements in human faecal samples. *BMJ Nutr. Prev. Health* 4, 374–384. doi: 10.1136/bmjnph-2020-000202

Fischer, C. L. (2020). Antimicrobial activity of host-derived lipids. *Antibiotics (Basel)* 9:75. doi: 10.3390/antibiotics9020075

Haag, L. M., Fischer, A., Otto, B., Grundmann, U., Kühl, A. A., Göbel, U. B., et al. (2012a). *Campylobacter jejuni* infection of infant mice: acute enterocolitis is followed by asymptomatic intestinal and extra-intestinal immune responses. *Eur. J. Microbiol. Immunol. (Bp)* 2, 2–11. doi: 10.1556/EuJMI.2.2012.1.2

Haag, L. M., Fischer, A., Otto, B., Plickert, R., Kühl, A. A., Göbel, U. B., et al. (2012b). Intestinal microbiota shifts towards elevated commensal *Escherichia coli* loads abrogate colonization resistance against *Campylobacter jejuni* in mice. *PLoS One* 7:e35988. doi: 10.1371/journal.pone.0035988

Heimesaat, M. M., Backert, S., Alter, T., and Bereswill, S. (2021). Human Campylobacteriosis-a serious infectious threat in a one health perspective. *Curr. Top. Microbiol. Immunol.* 431, 1–23. doi: 10.1007/978-3-030-65481-8_1

Heimesaat, M. M., Backert, S., Alter, T., and Bereswill, S. (2023). Molecular targets in Campylobacter infections. *Biomol. Ther.* 13:409. doi: 10.3390/biom13030409

Heimesaat, M. M., Lugert, R., Fischer, A., Alutis, M., Kühl, A. A., Zautner, A. E., et al. (2014). Impact of *Campylobacter jejuni* cj0268c knockout mutation on intestinal colonization, translocation, and induction of immunopathology in gnotobiotic IL-10 deficient mice. *PLoS One* 9:e90148. doi: 10.1371/journal.pone.0090148

Heimesaat, M. M., Mousavi, S., Bandick, R., and Bereswill, S. (2022). *Campylobacter jejuni* infection induces acute enterocolitis in IL-10−/− mice pretreated with ampicillin plus sulbactam. *Eur. J. Microbiol. Immunol.* 12, 73–83. doi: 10.1556/1886.2022.00014

Herzog, M. K., Cazzaniga, M., Peters, A., Shayya, N., Beldi, L., Hapfelmeier, S., et al. (2023). Mouse models for bacterial enteropathogen infections: insights into the role of colonization resistance. *Gut Microbes* 15:2172667. doi: 10.1080/19490976.2023.2172667

Hinton, A. Jr., and Ingram, K. D. (2000). Use of oleic acid to reduce the population of the bacterial flora of poultry skin. *J. Food Prot.* 63, 1282–1286. doi: 10.4315/0362-028x-63.9.1282

Hirano, S., Nakama, R., Tamaki, M., Masuda, N., and Oda, H. (1981). Isolation and characterization of thirteen intestinal microorganisms capable of 7 alpha-dehydroxylating bile acids. *Appl. Environ. Microbiol.* 41, 737–745. doi: 10.1128/aem.41.3.737-745.1981

Hitchcock, N., Kelly, D. J., Hitchcock, A., and Taylor, A. J. (2022). Cysteine biosynthesis in *Campylobacter jejuni*: substrate specificity of CysM and the dualism of sulfide. *Biomol. Ther.* 13:86. doi: 10.3390/biom13010086

Hofmann, A. F. (1999). The continuing importance of bile acids in liver and intestinal disease. *Arch. Intern. Med.* 159, 2647–2658. doi: 10.1001/archinte.159.22.2647

Hofreuter, D. (2014). Defining the metabolic requirements for the growth and colonization capacity of *Campylobacter jejuni*. *Front. Cell. Infect. Microbiol.* 4:137. doi: 10.3389/fcimb.2014.00137

Hofreuter, D., Tsai, J., Watson, R. O., Novik, V., Altman, B., Benitez, M., et al. (2006). Unique features of a highly pathogenic *Campylobacter jejuni* strain. *Infect. Immun.* 74, 4694–4707. doi: 10.1128/iai.00210-06

Hugdahl, M. B., Beery, J. T., and Doyle, M. P. (1988). Chemotactic behavior of *Campylobacter jejuni*. *Infect. Immun.* 56, 1560–1566. doi: 10.1128/iai.56.6.1560-1566.1988

Igwaran, A., and Okoh, A. I. (2019). Human campylobacteriosis: a public health concern of global importance. *Heliyon* 5:e02814. doi: 10.1016/j.heliyon.2019.e02814

Iizumi, T., Taniguchi, T., Yamazaki, W., Vilmen, G., Alekseyenko, A. V., Gao, Z., et al. (2016). Effect of antibiotic pre-treatment and pathogen challenge on the intestinal microbiota in mice. *Gut Pathog.* 8:60. doi: 10.1186/s13099-016-0143-z

Jia, E. T., Liu, Z. Y., Pan, M., Lu, J. F., and Ge, Q. Y. (2019). Regulation of bile acid metabolism-related signaling pathways by gut microbiota in diseases. *J Zhejiang Univ Sci B* 20, 781–792. doi: 10.1631/jzus.B1900073

Joyce, S. A., MacSharry, J., Casey, P. G., Kinsella, M., Murphy, E. F., Shanahan, F., et al. (2014). Regulation of host weight gain and lipid metabolism by bacterial bile acid modification in the gut. *Proc. Natl. Acad. Sci. U. S. A.* 111, 7421–7426. doi: 10.1073/pnas.1323599111

Kaakoush, N. O., Castaño-Rodríguez, N., Mitchell, H. M., and Man, S. M. (2015). Global epidemiology of Campylobacter infection. *Clin. Microbiol. Rev.* 28, 687–720. doi: 10.1128/cmr.00006-15

Kobierecka, P. A., Wyszyńska, A. K., Aleksandrzak-Piekarczyk, T., Kuczkowski, M., Tuzimek, A., Piotrowska, W., et al. (2017). *In vitro* characteristics of Lactobacillus spp. strains isolated from the chicken digestive tract and their role in the inhibition of Campylobacter colonization. *Microbiology* 6:e00512. doi: 10.1002/mbo3.512

Kurdi, P., Kawanishi, K., Mizutani, K., and Yokota, A. (2006). Mechanism of growth inhibition by free bile acids in lactobacilli and bifidobacteria. *J. Bacteriol.* 188, 1979–1986. doi: 10.1128/jb.188.5.1979-1986.2006

Lara-Tejero, M., and Galán, J. E. (2000). A bacterial toxin that controls cell cycle progression as a deoxyribonuclease I-like protein. *Science* 290, 354–357. doi: 10.1126/science.290.5490.354

Lawley, T. D., and Walker, A. W. (2013). Intestinal colonization resistance. *Immunology* 138, 1–11. doi: 10.1111/j.1365-2567.2012.03616.x

Leon-Kempis Mdel, R., Guccione, E., Mulholland, F., Williamson, M. P., and Kelly, D. J. (2006). The *Campylobacter jejuni* PEB1a adhesin is an aspartate/glutamate-binding protein of an ABC transporter essential for microaerobic growth on dicarboxylic amino acids. *Mol. Microbiol.* 60, 1262–1275. doi: 10.1111/j.1365-2958.2006.05168.x

Lin, J., Sahin, O., Michel, L. O., and Zhang, Q. (2003). Critical role of multidrug efflux pump CmeABC in bile resistance and *in vivo* colonization of *Campylobacter jejuni*. *Infect. Immun.* 71, 4250–4259. doi: 10.1128/iai.71.8.4250-4259.2003

Maltby, R., Leatham-Jensen, M. P., Gibson, T., Cohen, P. S., and Conway, T. (2013). Nutritional basis for colonization resistance by human commensal *Escherichia coli* strains HS and Nissle 1917 against *E. coli* O157:H7 in the mouse intestine. *PLoS One* 8:e53957. doi: 10.1371/journal.pone.0053957

Man, L., Dale, A. L., Klare, W. P., Cain, J. A., Sumer-Bayraktar, Z., Niewold, P., et al. (2020). Proteomics of *Campylobacter jejuni* growth in Deoxycholate reveals Cj0025c as a Cystine transport protein required for wild-type human infection phenotypes. *Mol. Cell. Proteomics* 19, 1263–1280. doi: 10.1074/mcp.RA120.002029

Mangell, P., Nejdfors, P., Wang, M., Ahrné, S., Weström, B., Thorlacius, H., et al. (2002). *Lactobacillus plantarum* 299v inhibits *Escherichia coli*-induced intestinal permeability. *Dig. Dis. Sci.* 47, 511–516. doi: 10.1023/A:1017947531536

Martin, H. M., Hancock, J. T., Salisbury, V., and Harrison, R. (2004). Role of xanthine oxidoreductase as an antimicrobial agent. *Infect. Immun.* 72, 4933–4939. doi: 10.1128/iai.72.9.4933-4939.2004

Metcalf, J. H., Donoghue, A. M., Venkitanarayanan, K., Reyes-Herrera, I., Aguiar, V. F., Blore, P. J., et al. (2011). Water administration of the medium-chain fatty acid caprylic acid produced variable efficacy against enteric Campylobacter colonization in broilers. *Poult. Sci.* 90, 494–497. doi: 10.3382/ps.2010-00891

Morishita, T. Y., Aye, P. P., Harr, B. S., Cobb, C. W., and Clifford, J. R. (1997). Evaluation of an avian-specific probiotic to reduce the colonization and shedding of *Campylobacter jejuni* in broilers. *Avian Dis.* 41, 850–855. doi: 10.2307/1592338

Mousavi, S., Bereswill, S., and Heimesaat, M. M. (2020). Novel clinical *Campylobacter jejuni* infection models based on sensitization of mice to Lipooligosaccharide, a major bacterial factor triggering innate immune responses in human Campylobacteriosis. *Microorganisms* 8:482. doi: 10.3390/microorganisms8040482

Mousavi, S., Bereswill, S., and Heimesaat, M. M. (2021). Murine models for the investigation of colonization resistance and innate immune responses in *Campylobacter Jejuni* infections. *Curr. Top. Microbiol. Immunol.* 431, 233–263. doi: 10.1007/978-3-030-65481-8_9

Mrazek, K., Bereswill, S., and Heimesaat, M. M. (2019). Fecal microbiota transplantation decreases intestinal loads of multi-drug resistant *Pseudomonas*

aeruginosa in murine carriers. *Eur J Microbiol Immunol (Bp)* 9, 14–22. doi: 10.1556/1886.2019.00002

Mundy, R., Girard, F., FitzGerald, A. J., and Frankel, G. (2006). Comparison of colonization dynamics and pathology of mice infected with enteropathogenic *Escherichia coli*, enterohaemorrhagic E. Coli and *Citrobacter rodentium*. *FEMS Microbiol. Lett.* 265, 126–132. doi: 10.1111/j.1574-6968.2006.00481.x

Muraoka, W. T., and Zhang, Q. (2011). Phenotypic and genotypic evidence for L-Fucose utilization by *Campylobacter jejuni*. *J. Bacteriol.* 193, 1065–1075. doi: 10.1128/jb.01252-10

O'Loughlin, J. L., Samuelson, D. R., Braundmeier-Fleming, A. G., White, B. A., Haldorson, G. J., Stone, J. B., et al. (2015). The intestinal microbiota influences *Campylobacter jejuni* colonization and Extraintestinal dissemination in mice. *Appl. Environ. Microbiol.* 81, 4642–4650. doi: 10.1128/aem.00281-15

Peterson, M. C. (1994). Clinical aspects of *Campylobacter jejuni* infections in adults. *West. J. Med.* 161, 148–152.

Robyn, J., Rasschaert, G., Messens, W., Pasmans, F., and Heyndrickx, M. (2012). Screening for lactic acid bacteria capable of inhibiting *Campylobacter jejuni* in *in vitro* simulations of the broiler chicken caecal environment. *Benef. Microbes* 3, 299–308. doi: 10.3920/bm2012.0021

Sannasiddappa, T. H., Lund, P. A., and Clarke, S. R. (2017). *In vitro* antibacterial activity of unconjugated and conjugated bile salts on *Staphylococcus aureus*. *Front. Microbiol.* 8:1581. doi: 10.3389/fmicb.2017.01581

Schmidt, A. M., Escher, U., Mousavi, S., Tegtmeyer, N., Boehm, M., Backert, S., et al. (2019). Immunopathological properties of the *Campylobacter jejuni* flagellins and the adhesin CadF as assessed in a clinical murine infection model. *Gut Pathog.* 11:24. doi: 10.1186/s13099-019-0306-9

Shayya, N. W., Foote, M. S., Langfeld, L. Q., Du, K., Bandick, R., Mousavi, S., et al. (2023). Human microbiota associated IL-10−/− mice: a valuable enterocolitis model to dissect the interactions of *Campylobacter jejuni* with host immunity and gut microbiota. *Eur. J. Microbiol. Immunol. (Bp)* 12, 107–122. doi: 10.1556/1886.2022.00024

Sprong, R. C., Hulstein, M. F. E., and van der Meer, R. (2001). Bactericidal activities of Milk lipids. *Antimicrob. Agents Chemother.* 45, 1298–1301. doi: 10.1128/aac.45.4.1298-1301.2001

Stahl, M., Ries, J., Vermeulen, J., Yang, H., Sham, H. P., Crowley, S. M., et al. (2014). A novel mouse model of *Campylobacter jejuni* gastroenteritis reveals key pro-inflammatory and tissue protective roles for toll-like receptor signaling during infection. *PLoS Pathog.* 10:e1004264. doi: 10.1371/journal.ppat.1004264

Sun, X., Winglee, K., Gharaibeh, R. Z., Gauthier, J., He, Z., Tripathi, P., et al. (2018). Microbiota-derived metabolic factors reduce Campylobacteriosis in mice. *Gastroenterology* 154, 1751–1763.e2. doi: 10.1053/j.gastro.2018.01.042

Tegtmeyer, N., Sharafutdinov, I., Harrer, A., Soltan Esmaeili, D., Linz, B., and Backert, S. (2021). Campylobacter virulence factors and molecular host-pathogen interactions. *Curr. Top. Microbiol. Immunol.* 431, 169–202. doi: 10.1007/978-3-030-65481-8_7

Thanissery, R., Winston, J. A., and Theriot, C. M. (2017). Inhibition of spore germination, growth, and toxin activity of clinically relevant *C. difficile* strains by gut microbiota derived secondary bile acids. *Anaerobe* 45, 86–100. doi: 10.1016/j.anaerobe.2017.03.004

Van Deun, K., Haesebrouck, F., Van Immerseel, F., Ducatelle, R., and Pasmans, F. (2008). Short-chain fatty acids and L-lactate as feed additives to control *Campylobacter jejuni* infections in broilers. *Avian Pathol.* 37, 379–383. doi: 10.1080/03079450802216603

Vegge, C. S., Brøndsted, L., Li, Y. P., Bang, D. D., and Ingmer, H. (2009). Energy taxis drives *Campylobacter jejuni* toward the most favorable conditions for growth. *Appl. Environ. Microbiol.* 75, 5308–5314. doi: 10.1128/aem.00287-09

Velayudhan, J., Jones, M. A., Barrow, P. A., and Kelly, D. J. (2004). L-serine catabolism via an oxygen-labile L-serine dehydratase is essential for colonization of the avian gut by *Campylobacter jejuni*. *Infect. Immun.* 72, 260–268. doi: 10.1128/iai.72.1.260-268.2004

Vorwerk, H., Mohr, J., Huber, C., Wensel, O., Schmidt-Hohagen, K., Gripp, E., et al. (2014). Utilization of host-derived cysteine-containing peptides overcomes the restricted Sulphur metabolism of *Campylobacter jejuni*. *Mol. Microbiol.* 93, 1224–1245. doi: 10.1111/mmi.12732

Wagner, R. D., Johnson, S. J., and Kurniasih Rubin, D. (2009). Probiotic bacteria are antagonistic to Salmonella enterica and Campylobacter jejuni and influence host lymphocyte responses in human microbiota-associated immunodeficient and immunocompetent mice. *Mol. Nutr. Food Res.* 53, 377–388. doi: 10.1002/mnfr.200800101

Wang, G., Zhao, Y., Tian, F., Jin, X., Chen, H., Liu, X., et al. (2014). Screening of adhesive lactobacilli with antagonistic activity against *Campylobacter jejuni*. *Food Control* 44, 49–57. doi: 10.1016/j.foodcont.2014.03.042

Weschka, D., Mousavi, S., Biesemeier, N., Bereswill, S., and Heimesaat, M. M. (2021). Survey of pathogen-lowering and Immuno-modulatory effects upon treatment of *Campylobacter coli*-infected secondary abiotic IL-10(−/−) mice with the probiotic formulation Aviguard(®). *Microorganisms* 9:1127. doi: 10.3390/microorganisms9061127

Willis, W. L., and Reid, L. (2008). Investigating the effects of dietary probiotic feeding regimens on broiler chicken production and *Campylobacter jejuni* Presence1. *Poult. Sci.* 87, 606–611. doi: 10.3382/ps.2006-00458

Wine, E., Gareau, M. G., Johnson-Henry, K., and Sherman, P. M. (2009). Strain-specific probiotic (*Lactobacillus helveticus*) inhibition of *Campylobacter jejuni* invasion of human intestinal epithelial cells. *FEMS Microbiol. Lett.* 300, 146–152. doi: 10.1111/j.1574-6968.2009.01781.x

Wotzka, S. Y., Kreuzer, M., Maier, L., Arnoldini, M., Nguyen, B. D., Brachmann, A. O., et al. (2019). *Escherichia coli* limits *Salmonella Typhimurium* infections after diet shifts and fat-mediated microbiota perturbation in mice. *Nat. Microbiol.* 4, 2164–2174. doi: 10.1038/s41564-019-0568-5

Wright, J. A., Grant, A. J., Hurd, D., Harrison, M., Guccione, E. J., Kelly, D. J., et al. (2009). Metabolite and transcriptome analysis of *Campylobacter jejuni in vitro* growth reveals a stationary-phase physiological switch. *Microbiology (Reading)* 155, 80–94. doi: 10.1099/mic.0.021790-0

Yoon, B. K., Jackman, J. A., Valle-González, E. R., and Cho, N. J. (2018). Antibacterial free fatty acids and Monoglycerides: biological activities, experimental testing, and therapeutic applications. *Int. J. Mol. Sci.* 19:1114. doi: 10.3390/ijms19041114

Zommiti, M., Almohammed, H., and Ferchichi, M. (2016). Purification and characterization of a novel anti-Campylobacter Bacteriocin produced by *Lactobacillus curvatus* DN317. *Probiotics Antimicrob. Proteins* 8, 191–201. doi: 10.1007/s12602-016-9237-7

frontiers | Frontiers in Microbiology

TYPE Original Research
PUBLISHED 08 January 2024
DOI 10.3389/fmicb.2023.1293666

OPEN ACCESS

EDITED BY
Stuart A. Thompson,
Augusta University, United States

REVIEWED BY
Jörg Linde,
Friedrich Loeffler Institut, Germany
Anand Bahadur Karki,
University of Tulsa, United States
Eman Khalifa,
Alexandria University Branch (Matrouh University), Egypt
Shimaa Tawfeeq Omara,
National Research Centre, Egypt

*CORRESPONDENCE
Aurora Garcia-Fernandez
✉ aurora.garciafernandez@iss.it
Anna Janowicz
✉ a.janowicz@izs.it

RECEIVED 13 September 2023
ACCEPTED 07 December 2023
PUBLISHED 08 January 2024

CITATION
Garcia-Fernandez A, Janowicz A, Marotta F, Napoleoni M, Arena S, Primavilla S, Pitti M, Romantini R, Tomei F, Garofolo G and Villa L (2024) Antibiotic resistance, plasmids, and virulence-associated markers in human strains of *Campylobacter jejuni* and *Campylobacter coli* isolated in Italy. *Front. Microbiol.* 14:1293666. doi: 10.3389/fmicb.2023.1293666

Antibiotic resistance, plasmids, and virulence-associated markers in human strains of *Campylobacter jejuni* and *Campylobacter coli* isolated in Italy

Aurora Garcia-Fernandez[1]*, Anna Janowicz[2]*, Francesca Marotta[2], Maira Napoleoni[3], Sergio Arena[1], Sara Primavilla[3], Monica Pitti[4], Romina Romantini[2], Fiorella Tomei[5], Giuliano Garofolo[2] and Laura Villa[1]

[1]Department of Infectious Diseases, Istituto Superiore di Sanità, Rome, Italy, [2]National Reference Laboratory for Campylobacter, Istituto Zooprofilattico Sperimentale dell'Abruzzo e del Molise "G. Caporale", Teramo, Italy, [3]Centro di Riferimento Regionale Patogeni Enterici, CRRPE, Istituto Zooprofilattico Sperimentale dell'Umbria e delle Marche "T. Rosati", Perugia, Italy, [4]Centro di Riferimento per la Tipizzazione delle Salmonelle, CeRTiS, Istituto Zooprofilattico Sperimentale del Piemonte Liguria e Valle d'Aosta, Turin, Italy, [5]BIOS Laboratory, Rome, Italy

Campylobacteriosis, a prevalent foodborne gastrointestinal infection in Europe, is primarily caused by *Campylobacter jejuni* and *Campylobacter coli*, with rising global concerns over antimicrobial resistance in these species. This study comprehensively investigates 133 human-origin *Campylobacter* spp. strains (102 *C. jejuni* and 31 *C. coli*) collected in Italy from 2013 to 2021. The predominant Multilocus Sequence Typing Clonal complexes (CCs) were ST-21 CC and ST-206 CC in *C. jejuni* and ST-828 CC in *C. coli*. Ciprofloxacin and tetracycline resistance, mainly attributed to GyrA (T86I) mutation and *tet*(O) presence, were prevalent, while erythromycin resistance was associated with 23S rRNA gene mutation (A2075G), particularly in *C. coli* exhibiting multidrug-resistant pattern CipTE. Notable disparities in virulence factors among strains were observed, with *C. jejuni* exhibiting a higher abundance compared to *C. coli*. Notably, specific *C. jejuni* sequence types, including ST-21, ST-5018, and ST-1263, demonstrated significantly elevated counts of virulence genes. This finding underscores the significance of considering both the species and strain-level variations in virulence factor profiles, shedding light on potential differences in the pathogenicity and clinical outcomes associated with distinct *C. jejuni* lineages. *Campylobacter* spp. plasmids were classified into three groups comprising pVir-like and pTet-like plasmids families, exhibiting diversity among *Campylobacter* spp. The study underscores the importance of early detection through Whole Genome Sequencing to identify potential emergent virulence, resistance/virulence plasmids, and new antimicrobial resistance markers. This approach provides actionable public health data, supporting the development of robust surveillance programs in Italy.

KEYWORDS

***Campylobacter*, cgMLST, virulence, pTet, pVir, tet(O), antibiotic resistance, GyrA**

1 Introduction

Campylobacteriosis has been the most frequently reported foodborne gastrointestinal infection in humans in the European Union (EU) since 2007. In 2021, the total number of confirmed human cases in the EU was 127,840, and *Campylobacter* spp. was the fourth most common cause of foodborne outbreaks reported by 17 Member States (MSs) and three non-MSs at EU level (EFSA and ECDC, 2022). The main *Campylobacter* species reported in EU was *Campylobacter jejuni* (88.4%), followed by *Campylobacter coli* (10.1%) (EFSA and ECDC, 2021). The incidence of campylobacteriosis varies globally between countries, and its true incidence remains uncertain due to underreporting of *Campylobacter* spp. infection cases, disparities in reporting systems, diagnosis challenges, and differences in outbreak surveillance (Hansson et al., 2018). Notifications of campylobacteriosis cases in Italy are gathered by the Enter-Net Italia surveillance and reported annually to the European Center for Disease Prevention and Control (ECDC). This surveillance was non-mandatory until 2022, leading to underestimating the annual number of reported cases. The iceberg effect is well known, and a population-based serological study indicated Italy as a country with a low reporting rate in 2009–2013 (Cassini et al., 2018). Despite the parsimonious collection of strains in Italy, it remains crucial to determine the main characteristics of the circulating strains through their complete characterization. *Campylobacter* spp. is primarily found in the digestive tract of poultry and poultry meat, as well as other animals and food matrices thereof such as cattle and swine (Wysok et al., 2015). Contact with dogs and cats can also be a risk factor for human campylobacteriosis (Andrzejewska et al., 2013).

Campylobacteriosis is typically self-limiting and usually resolves within a week from the onset of symptoms (Blaser and Engberg, 2008). Antimicrobial treatment should be reserved for cases of severe gastroenteritis, extraintestinal infections, or immunocompromised patients. Nonetheless, the rising antibiotic resistance (AMR) of *Campylobacter* spp. has emerged as a global issue (Skirrow, 1994; Dai et al., 2020). According to the European data, very high to extremely high levels of resistance to ciprofloxacin in *C. jejuni* and *C. coli* and high and very high levels of tetracycline resistance, respectively, in *C. jejuni* and *C. coli* were reported in humans (EFSA and ECDC, 2023). While, erythromycin resistance for *C. jejuni* was either absent or detected at very low levels, *C. coli* exhibited higher resistance levels. Low levels of gentamicin resistance were observed in *C. coli*. Combined resistance to ciprofloxacin and erythromycin, critical antimicrobials for the campylobacteriosis treatment, was generally uncommon in *C. jejuni* and moderately common in *C. coli* (EFSA and ECDC, 2023).

The main mechanism causing quinolone and fluoroquinolone resistance in *Campylobacter* spp. is the C257T point mutation in *gyrA* that yields a Thr-86-Ile amino acid change. Mutations in the 23S rRNA genes, amino acid changes in L4/L22 ribosomal proteins, and the presence of the ribosomal methylase encoded by *ermB* gene confer resistance to macrolides. The *tet*(O) gene encoding a ribosomal protection protein is mainly responsible for tetracycline resistance (Connell et al., 2003; Vacher et al., 2005; Iovine, 2013; Panzenhagen et al., 2021; Bunduruș et al., 2023).

Multilocus sequence typing (MLST) is a gold standard informative tool to analyze the molecular epidemiology of *Campylobacter* spp. allowing the characterization of the population structure of *Campylobacter* spp. and the identification of lineages such as sequence types (STs) and clonal complexes (CCs) (Dingle et al., 2001). Previous MLST studies on *C. jejuni* demonstrated that its population is genetically diverse and weakly clonal, consisting of large CCs representing epidemiologically relevant units for investigating *C. jejuni* epidemiology (Manning et al., 2003; Mouftah et al., 2021). Additionally, a higher level of discrimination is given by comparing the genomic sequences through the core genome multilocus sequence typing (cgMLST), which provides high-resolution data across related but not identical strains (Maiden et al., 2013; Cody et al., 2017; Hsu et al., 2020).

Specific *Campylobacter* spp. virulence genes encompassing its virulome represent relevant public health risks due to their capacity to strengthen the bacterium against the immunological response mounted by the host (Bunduruș et al., 2023). Most of the studies about the *Campylobacter* spp. virulome have been performed in *C. jejuni*, with fewer focused on *C. coli* (Fiedoruk et al., 2019; Bravo et al., 2021; Panzenhagen et al., 2021; Deblais et al., 2023; El-Adawy et al., 2023). Several *Campylobacter* spp. virulence factors have been linked to pathogenesis, severe illness and post-infection issues (Lapierre et al., 2016; Wieczorek et al., 2018). Utilizing flagella for motility, these bacteria navigate the mucus layer to reach and adhere to intestinal epithelial cells, a pivotal step in initiating infection. The ability to invade these cells, coupled with the production of toxins such as the cytolethal distending toxin (CDT), enhances the pathogenicity of the bacteria by inducing cell cycle arrest and apoptosis. Certain strains exhibit increased virulence through the presence of a protective polysaccharide capsule, while the microaerophilic nature of *Campylobacter* spp. enables them to thrive in the low-oxygen environment of the intestinal tract (Bunduruș et al., 2023; Kemper and Hensel, 2023). This intricate combination of virulence factors underscores the complexity of *Campylobacter* spp. pathogenesis, necessitating a comprehensive understanding of the development of effective preventive and therapeutic strategies.

Plasmids in *Campylobacter* spp., play a crucial role in shaping the pathogenicity and adaptability of these foodborne pathogens. Studies have identified various plasmid families, including pVir-like and pTet-like, each with particular replicon types or relaxases and potential implications for bacterial virulence and survival (van Vliet et al., 2021; Hull et al., 2023). Additionally, plasmids facilitate horizontal gene transfer, rapidly disseminating genetic material and traits, further enhancing the adaptability of *Campylobacter* spp. populations. The presence of plasmids carrying virulence factors underscores their significance in the pathogenic potential of these bacteria.

Understanding the mechanisms underlaying *Campylobacter* spp's ability to acquire AMR, identifying virulence factors involved in the pathogenesis of campylobacteriosis, and studying plasmids carrying both genetic determinants are crucial in comprehending the infection mechanisms and the bacterium's response to host immunity defense and antibiotic treatments.

This study employed whole genome sequencing (WGS) to comprehensively investigate the genetic diversity, antibiotic resistance, virulence content, and plasmid distribution in 133 *Campylobacter* spp. strains (102 *C. jejuni* and 31 *C. coli*) of human origin, collected in Italy from 2013 to 2021. This investigation integrated both resistome analysis and phenotypic approaches to assess antibiotic resistance, providing a comprehensive understanding of the genomic and phenotypic characteristics of these pathogens.

2 Materials and methods

2.1 Settings and bacterial strains

Surveillance for *Campylobacter* spp. in human strains in Italy is based on a systematic voluntary network (Enter-Net Italia) coordinated by the Infectious Disease Department of the *Istituto Superiore di Sanità* (ISS). The selection criteria in this study involved choosing epidemiologically unrelated viable strains from 2013 to 2021. Epidemiologically unrelated strains were defined as those isolated from patients without any known epidemiological link. This approach aimed to avoid possible submerged clonal events and assess the extent of clonal diversity during the chosen period in our country. One-hundred-thirty-three strains belonging to the two main notified species were selected: 102 *C. jejuni* and 31 *C. coli* (Supplementary Table S1), which were isolated from feces (128) and blood (5). These strains were received in swabs with already isolated and identified *C. jejuni* and *C. coli* strains. Subsequently, they were inoculated onto modified charcoal cefoperazone deoxycholate agar (mCCD Agar; Biolife Italiana srl, Milan, Italy) and Columbia Blood Agar Horse plates (Biolife Italiana srl, Milan, Italy). The plates were all incubated at 41.5°C ± 1°C for 48 ± 2 h in a microaerobic atmosphere and then screened for antibiotic susceptibility and DNA extraction.

2.2 Antibiotic susceptibility testing

Susceptibility was determined by the reference broth microdilution method and the Kirby-Bauer disk diffusion susceptibility test, following the international guideline recommendations of the European Committee on Antimicrobial Susceptibility Testing (EUCAST; www.eucast.org). Four antibiotics (Becton Dickinson, MD 21152–0999, United States) were tested by disk diffusion method, and the antibiotic concentrations were as follows: ciprofloxacin (Cip, 5 μg), tetracycline (T, 30 μg), erythromycin (E, 15 μg), and gentamicin (Gm, 10 μg). The control strain for antibiotics susceptibility testing was *C. jejuni* strain ATCC 33560. The susceptibility results were interpreted using the EUCAST guidelines.[1] Broth microdilution method using Sensititre automated system (TREK Diagnostic Systems, Venice, Italy) was used to determine the antibiotic susceptibility of *Campylobacter* spp. strains. Cip, T, E, and Gm were tested according to previously reported methods (Marotta et al., 2020).

The strains were classified as resistant and susceptible according to minimum inhibitory concentration (MIC) breakpoints using Swin v3.3 Software (Thermo Fisher Scientific) following the epidemiological cutoff values (ECOFFs) as defined by EUCAST.[2] MIC breakpoints of resistance applied were > 0.5 μg/mL for Cip (*C. jejuni* and *C. coli*), > 4 μg/mL for E (*C. jejuni*) and > 8 μg/mL (*C. coli*), > 2 μg/mL for Gm (*C. jejuni* and *C. coli*), and > 1 μg/mL for T (*C. jejuni*) and > 2 μg/mL (*C. coli*). *Campylobacter jejuni* strain NCTC11351 was used as a control. Multidrug resistance (MDR) was defined as the resistance to three or more classes of antibiotics.

2.3 Whole genome sequencing

All the strains were sequenced by next-generation sequencing. Genomic DNAs were purified using the Macherey-Nagel NucleoSpin Tissue kit (Fisher Scientific Italia, Segrate, Italy). DNA libraries were created using Nextera XT Library Preparation Kit (Illumina, Inc., San Diego, CA, United States) and sequenced with Illumina NextSeq 500 sequencer, producing 150 bp paired-end reads.

Multiple online web-based bioinformatics tools (accessed September–December 2022) were used for pathogen characterization. Basic metrics and quality check of FASTQ-formatted sequencing reads were determined with FastQC Read Quality Reports v.0.72 (https://www.bioinformatics.babraham.ac.uk/projects/fastqc/; Galaxy-ARIES; Afgan et al., 2018; Knijn et al., 2020). The obtained raw reads were screened for contamination and reidentification of the species using Quality control species-identification pipelines KmerFinder v.3.2 for bacteria organisms (Center for Genomic Epidemiology, CGE; https://www.genomicepidemiology.org/; Hasman et al., 2014; Larsen et al., 2014; Clausen et al., 2018) and RefSeq Masher Matches v.0.1.2 (Galaxy-ARIES, https://w3.iss.it/site/aries/; Ondov et al., 2016; Knijn et al., 2020).

Quality trimming was performed by Trimmomatic v.0.38.1 to remove low-quality and adapter sequences for paired-end reads, filtering for a minimum read length of 50 and trimming low-quality 3′ ends of reads. Nucleotide positions in the reads with a quality score lower than Q20 were removed (Parameters: LEADING: 3; TRAILING: 3; SLIDINGWINDOW: 4:20; MINLEN:50) (Galaxy-ARIES; Bolger et al., 2014). *De novo* assembly of Illumina reads was performed using the SPAdes v.3.14.1 (Parameters: single-cell, with error correction and automatically k-mer values and coverage cuttoff) (Galaxy-ARIES; Bankevich et al., 2012; Afgan et al., 2018; Knijn et al., 2020). With the Staramr v.0.9.1 tool (Galaxy Europe, http://usegalaxy.eu/; Bharat et al., 2022), the genomes have been checked for genome sizes between the 1.6–1.9 Mbp range and the number of assembled contigs (Afgan et al., 2018; Bharat et al., 2022).

2.4 MLST and cgMLST analysis

Multilocus sequence typing scheme for *C. jejuni* and *C. coli* based on seven loci (a*spA, glnA, gltA, glyA, pgm, tkt, and uncA*) was performed by mlst 2.22.0 (Galaxy Europe; Bharat et al., 2022). Where STs were not defined, allele sequences were submitted to the *Campylobacter* spp. public database for molecular typing and microbial genome diversity.[3] Based on their STs, strains were assigned to CCs using the *Campylobacter jejuni/coli* PubMLST.org database (Jolley et al., 2018).

Analysis by cgMLST assignment based on the 1,343 core loci using the *Campylobacter jejuni/coli* PubMLST.org database was conducted (Jolley et al., 2018). The cgMLST scheme used was described in Cody et al. (2017). The percentage of called targets ranged from 80.0 to 95.7% with an average of 92.5% of alleles called.

A dendrogram was generated based on cgMLST allelic differences, selecting the "Campylobacter (PubMLST) species" parameter.

1 http://www.eucast.org/clinical_breakpoints/v.11.0

2 www.eucast.org

3 https://pubmlst.org/organisms/campylobacter-jejunicoli/

We used the Newick matrix created by the cgMLST Finder 1.2 v.1.0.1 method version 3.69 (CGE) to generate Neighbor-Joining tree (Clausen et al., 2018; Jolley et al., 2018). The tree was annotated using iTOL version 6 (Letunic and Bork, 2007). A minimum spanning tree was generated using the MSTree V2 algorithm in the stand-alone GrapeTree visualization program.

2.5 Resistome analysis

Resistance genes and point mutation content were obtained using two different tools: Amrfinder v.3.1.1b, developed by NCBI selecting *Campylobacter* species parameter (Galaxy-ARIES; Feldgarden et al., 2019), and Staramr v.0.9.1 tool, enabling the scanning for point mutations for *Campylobacter* species (Galaxy Europe; Bharat et al., 2022).

2.6 Virulome analysis

Bacterial virulome identification was performed using the Virulence Factor of Pathogenic Bacteria server (VFDB, http://www.mgc.ac.cn/VFs/; Chen et al., 2005, 2012, 2016; Yang et al., 2008; Liu et al., 2018). Additionally, the presence of genes involved in "capsule biosynthesis and transport" and genes categorized as "immune evasion-LOS" was verified using a custom-built database, using *C. jejuni* NCTC 11168 (AL111168.1) as the reference genome. The custom database was built using ABRicate version 1.0.1 (Seemann T, Abricate, GitHub, https://github.com/tseemann/abricate). All genomes were queried against the databases with ABRicate using coverage and identity cutoff of 80%.

The results obtained from VFDB and ABRicate were used to generate a gene presence/absence matrix (Supplementary Table S2). Where two or more copies of the same gene were identified, they were treated as a single hit. The matrix was used to create concatenated sequences for all the samples, which were combined to obtain a binary alignment. A dendrogram was constructed using IQtree version 1.6.9 (Nguyen et al., 2015) using the obtained binary alignment as an input and using default settings. GTR2 + FO + R3 model was selected using ModelFinder feature in IQTree (Kalyaanamoorthy et al., 2017). The tree was annotated with iTOL version 6 (Letunic and Bork, 2007). The genes belonging to the T6SS system present in the genomes were analyzed using the web-based resource Type VI Secretion System Resource (SecReT6) version 3.0. (https://bioinfo-mml.sjtu.edu.cn/SecReT6/t6ss_prediction.php; Supplementary Table S3; Zhang J. et al., 2023).

2.7 Plasmid content analysis

The MOB-Recon v.3.0.3 tool predicted sequences' origin (plasmid or chromosome) (Galaxy Europe; Robertson and Nash, 2018). MOB-Recon differentiated and reconstructed individual plasmid sequences from draft genome assemblies using the plasmid reference databases, detecting circular contigs. The screening was performed with a minimum sequence identity and coverage of 80%. Contigs under 1,000 bp were not considered. Only the plasmids described as circular by this tool were selected and annotated by the Bakta server (http://bakta.computational.bio/, accessed in March 2023; Schwengers et al., 2021).

Plasmids bigger than 10 kb were also subjected to a Pangenome analysis by the Genomic Context View (GView) server (https://server.gview.ca/; Petkau et al., 2010). The BLAST parameters used were *e*-value (<1*e*−10), alignment length cutoff 100%, and identity cutoff value 80%. The pangenome was constructed by iteratively appending unique regions onto an initial seed sequence.

A MAFFT multiple alignment of the plasmid nucleotide sequences, using the default parameters, was performed by the online server MAFFT v. 7 (https://mafft.cbrc.jp/alignment/server/; Katoh and Standley, 2013). This tool performed a sequence alignment using Fast Fourier Transforms. The Neighbor-Joining (NJ) method and the Juke-Cantor model were used to perform a phylogenetic tree by Phylo.io 1.0.0 (Robinson et al., 2016). Only plasmids bigger than 10 kb were selected for MAFFT analysis. These two analyses also included a selection of 11 plasmids, called reference plasmids in this study, based on the MOB and Rep type and the Mash nearest neighbors obtained with the MOB-recon analysis.

3 Results

3.1 MLST and cgMLST analysis

The WGSs of 133 human non-epidemiologically related *Campylobacter* spp. strains were analyzed and showed a draft genome size between 1.59 and 1.96 Mb with a median N50 of assemblies of 229 kb (IQR = 58–1,000 kb). The number of assembled contigs was between 7 and 99, and the median number of contigs recovered per sample was 32 (Supplementary Table S1). The Kmer-based approach identification and the RefSeq masher confirmed the species of 102 *C. jejuni* and 31 *C. coli* and the absence of contaminated sequences.

Analysis of the 133 *Campylobacter* spp. genomes identified 61 previously described STs and four novel STs (ST-11200, ST-12068, ST-12069, and ST-12070). Seventeen and two different CCs were observed in *C. jejuni* and *C. coli*, respectively. Among *C. jejuni* strains, the main CCs observed were the ST-21 CC, representing 21.24% of the strains, followed by the ST-206 CC (15.53%), the ST-353 CC (9.71%), the ST-354 CC (8.74%), and the ST-658 CC (5.83%). The main STs observed were ST-50, ST-19, and ST-21, inside the ST-21 CC, ST-122 and ST-3335, inside the ST-206 CC and the ST-2116, inside the ST-353 CC. Overall, the predominant CC observed in *C. coli* was the ST-828 CC detected in 80.65% of strains, while only one strain was assigned to ST-1150 CC. The most prevalent *C. coli* STs were ST-7159 and ST-832, members of ST 828 CC (Supplementary Table S1).

A total of 106 cgMLST profiles were observed through *Campylobacter* spp. strains. The most frequent cgMLST types (cgSTs) in *C. jejuni* were the cgST-3020, assigned to six strains and the cgST-11062, assigned to five. In *C. coli,* the most frequent cgSTs were the cgST-35299 (four strains), the cgST-13890 (three strains), and the cgST-20838 (three strains). *Campylobacter jejuni* and *C. coli* did not present common cgMLST. For 19 strains, the exact cgMLST profile was not assigned, as more than one closely matching profile was identified by the Oxford pubMLST (Supplementary Table S1). These strains contained 1–738 mismatches, observing from 99.9 to 80.7% allele match in *C. jejuni* and 98.8 to 45% in *C. coli* (data not shown).

3.2 Cluster analysis of human *Campylobacter* spp. strains

The dendrogram constructed using cgMLST divided the strains of *C. jejuni* from *C. coli*. Most of the genomes were genetically distant from one another, forming distinct long branches in the tree topology. In particular, the lineage of *C. coli* was split into two branches. The first one contained only one genome assigned to ST-1150 CC, and the second was split further, forming a large clade composed of strains of ST-828 CC or with no CC assigned yet. In general, for *C. coli,* we did not detect clusters of related strains, and only one pair of identical strains was identified within ST-7159 (Figure 1).

For *C. jejuni* strains, instead, we detected several clusters of genomically highly similar strains that included three clusters containing five or more genomes. The biggest one was composed of ST-3335 and contained strains isolated between 2016 and 2020. The pairwise allele distance between genomes in this cluster ranged from one to 35 differing alleles, generally corresponding to the differences in the date or the place of the strain isolation (data not shown). Other two clusters comprised strains assigned to ST-2116 or ST-2863. The allelic differences in the genomes in the ST-2116 cluster ranged between 0 and 23, and for ST-2863, the pairwise distance ranged between zero and 17 alleles. The strains from both clusters were isolated between 2015 and 2021. We also identified several smaller clusters of identical or genetically very similar strains, for instance, within ST-19 or ST-1039. Our dataset's most populated clonal complex, ST-21 CC, was split between two large clades. The first included ST-21, ST-5018, and ST-1943, and the second comprised ST-19, ST-50, and ST-822. While most strains assigned to this CC were not genetically closely related, two small clusters of similar genomes were noted, one belonging to ST-19 and the other to ST-21 (Figure 1).

3.3 Antibiotic susceptibility and genotype analysis

Susceptibility to all antibiotics tested, Cip, E, Gm, and T, was observed in 17.64% (18/102) and 6.45% (2/31) of *C. jejuni* and *C. coli* strains, respectively. All the strains but two (*C. jejuni*) were susceptible to Gm (98.50%). A total of 30.39% (31/102) of *C. jejuni* and 9.68% (3/31) of *C. coli* were only resistant to Cip. A higher number of *C. jejuni* (42.16%; 43/102) and *C. coli* (41.94%; 13/31) were resistant to CipT. 38.71% (12/31) of *C. coli* was characterized by the MDR pattern CipTE; however, a low number (2.94%; 3/102) of CipTE-resistant *C. jejuni* was observed (Supplementary Table S1).

Each interpretation (resistance or susceptible) for an antibiotic susceptibility test result was compared to the presence or absence of a corresponding known resistance gene(s) and/or specific mutations.

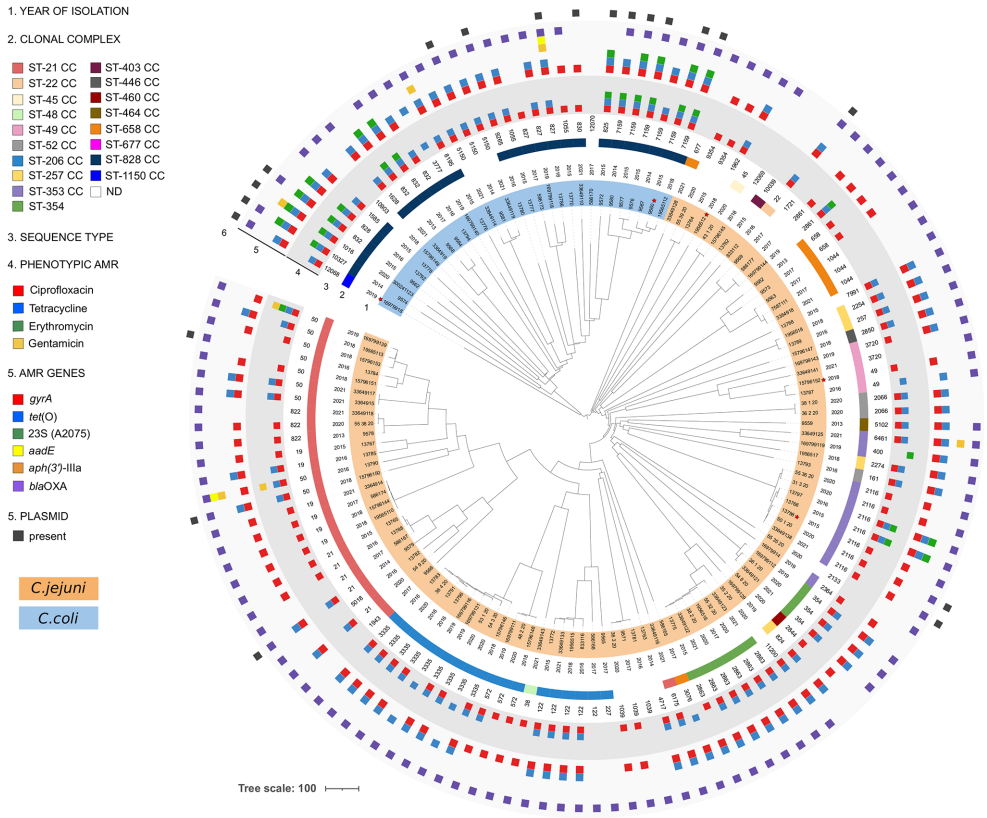

FIGURE 1
Dendrogram of *Campylobacter jejuni* and *Campylobacter coli* isolated from human samples in Italy between 2013 and 2021. A total of 133 strains were analyzed using cgMLST using a template composed of 1,343 loci. The dendrogram was generated by pairwise comparison of the target core genes and midpoint rooted. Strains marked with red stars were isolated from blood, while the others were isolated from feces. *C. jejuni* and *C. coli* strains are highlighted in orange and blue, respectively.

The *in silico* analysis of the 133 sequenced *Campylobacter* spp. strains revealed the presence of the GyrA (T86I) mutation in 77.45% (79/102) of *C. jejuni* and 83.87% (26/31) of *C. coli*, conferring Cip resistance in all strains except one. The GyrA (T86V) was also present in one Cip-resistant *C. jejuni*, and the double GyrA mutation (T86I, D90N) was present in one Cip-resistant *C. coli*. One *C. jejuni* presented the GyrA mutation (T86A), not conferring Cip resistance. A 20.59% (21/102) *C. jejuni* and a 12.90% (4/31) *C. coli* did not present any GyrA mutation responsible for Cip resistance, being all but one susceptible to this antibiotic (Supplementary Table S1). For the genotype–phenotype correlation, there is no linkage in 1.85% (2/108) of *Campylobacter* strains presenting fluoroquinolone resistance or mutation.

Fifty percent (51/102) of *C. jejuni* and 16.13% (5/31) of *C. coli* did not present any *tet* gene responsible for tetracycline resistance. The *tet*(O) gene was present in 30.39% (31/102) of *C. jejuni* and 67.74% (21/31) of *C. coli*; additionally, 19.60% (20/102) of *C. jejuni* and 12.90% (4/31) of *C. coli* presented the mosaic gene *tet*(O/32/O). The *tet*(W) was present in only one *C. coli* (3.23%; 1/31) (Supplementary Table S1). Two of the *C. jejuni* presenting the *tet*(O) and one of the *C. jejuni* presenting the *tet*(O/32/O) gene were susceptible to T, and four *C. jejuni* resistant to T did not present any *tet* gene. There is no match in the genotype and phenotype correlation in 6.64% (7/81) of *Campylobacter* strains presenting tetracycline resistance or gene.

All but four E-resistant strains presented the 23S RNA mutation A2075G. The transferable *erm*(B) gene was absent. For the genotype and phenotype correlation, there is no match in 2.35% (4/17) of *Campylobacter* strains presenting erythromycin resistance or mutation. Other resistance genes present in this collection were *aadE* [also called *ant(6)-Ia*], *aph(2″)-Ii* (*aadE-Cc*), and *aph(3′)-IIIa* (Supplementary Table S1). Only one of the two strains presenting *aph(3′)-IIIa* gene was resistant to Gm; the other presented a partial *aph(3′)-IIIa*. Instead, one of the two Gm-resistant strains did not present any known mechanism conferring this resistance.

Although the ampicillin resistance was not tested phenotypically in this study, the presence of the bla_{OXA} gene and its variants were studied. The bla_{OXA} gene was present in a 93.14% (95/102) *C. jejuni* and 80.65% (25/31) *C. coli*. The main bla_{OXA} present in *C. jejuni* were $bla_{OXA\text{-}193}$ 67.65% (69/102) and $bla_{OXA\text{-}466}$ 7.84% (8/102). *Campylobacter coli* mainly presented $bla_{OXA\text{-}193}$ 29.03% (9/31) and $bla_{OXA\text{-}489}$ 19.35% (6/31). A 6.86% (7/102) of *C. jejuni* and a 19.35% (6/31) of *C. coli* did not present bla_{OXA} genes (Supplementary Table S1). The 50S rRNA L22 A103V mutation in 15 *C. jejuni* and seven *C. coli* did not confer any resistant pattern to the strains. Considering the four tested antibiotics, only nine strains (6.7%) did not present a correlated pheno-genotype (Supplementary Table S1). The presence of specific antibiotic resistance genes generally corresponded with the cgMLST dendrogram, and strains placed closer together were resistant to the same antibiotics. Some exceptions were noted, however, including two multidrug-resistant strains in the ST-2116 cluster (Figure 1).

3.4 Distribution of virulence genes

The *Campylobacter* spp. collection presented a virulome composed of 158 identified genes out of the 32,827 virulence factor-related genes settled in the virulence finder database VFDB. Out of 158 virulence genes identified, 134 *Campylobacter* spp. specific genes were used to generate a dendrogram based on the binary gene presence/absence matrix. We observed significant differences in the number of virulence genes detected in the individual genomes, with a minimum of 78 genes and a maximum of 125 (Supplementary Tables S2, S3). Fewer virulence genes were found in *C. coli* strains than in *C. jejuni*. The strains with the most detected virulence genes belonged to ST-21 and ST-5018 (ST-21 CC). Of these 134 *Campylobacter* spp. specific genes, 68 virulence genes were conserved in 99% of analyzed strains, and five genes were detected in one strain of *C. jejuni* only. The remaining 61 genes belonged to five separate categories: Capsule biosynthesis and transport (CBT), Glycosylation system, Immune system evasion (lipooligosaccharides—LOS), Motility, and export system and Toxins (Supplementary Table S2; Figure 2). The most significant difference between the strains was observed in the presence or absence of CBT and LOS genes.

The dendrogram grouped the dataset into specific clusters based on the similarity of virulomes, and the individual clusters generally corresponded to *Campylobacter* species and specific CCs, but with some exceptions (Figure 2). ST-21 CC was divided into two clusters, the first grouping ST-21 and ST-5018 and the second composed mainly of ST-50 and ST-19 strains. Strains from both clusters differed from the others in the dataset by the presence of nine genes in the LOS cassette (*Cj1136–Cj1144c*; Figure 2); however, the first cluster contained additional nine genes in the CBT cassette. Moreover, while most *C. coli* genomes were grouped, three strains were found among *C. jejuni* strains, suggesting a possible gene exchange between the two species.

The VFDB analysis showed that 75 out of 133 strains (48 *C. jejuni* and 27 *C. coli*) carried virulence genes associated with bacterial species different from *Campylobacter* spp. (Supplementary Table S3). Thirty *C. jejuni* and two *C. coli* strains carried three virulence genes associated with ACE Type VI secretion system (T6SS) of *Escherichia coli*, T6SS of *Aeromonas* spp., and virulence-associated secretion (VAS) effector protein of *Vibrio* spp. Six of these 30 *C. jejuni* strains belonged to ST-354 CC and nine to ST-353 CC (Supplementary Table S3). Twenty out of 133 strains (9 *C. jejuni* and 11 *C. coli*) carried a virulence gene linked to the Lvh type IVA secretion system (*Legionella* spp. *vir* homologs). Among the *C. jejuni* strains, six were classified as ST-353 CC. Likewise, among the *C. coli* strains, nine were classified as ST-828 CC. Twenty-three *Campylobacter* spp. strains (12 *C. jejuni* and 11 *C. coli*) showed a gene coding for Phytotoxin phaseolotoxin (*Pseudomonas* spp.), and no clear correlation with any CCs was observed (Supplementary Table S3). Eight out of the 31 strains of *C. coli* belonging to ST-828 CC presented virulence genes associated with serum resistance and immune evasion, anti-phagocytosis, and other functions classified by the VFDB tool as lipopolysaccharide (LPS) gene of *Francisella* spp., capsule of *Klebsiella* spp., and O-antigen of *Yersinia* spp., respectively (Supplementary Table S3).

3.5 Plasmid analysis

MOB-recon analysis classified the contigs of all the strains in chromosomal or plasmidic, assigning plasmidic contigs as circular or incomplete (Supplementary Table S4). This tool identified plasmid-derived contigs in all 102 *C. jejuni* strains and only 18 *C. coli* (Supplementary Table S4). Additionally, 19 out of 133 *Campylobacter* spp. strains presented one plasmid classified as circular, while one

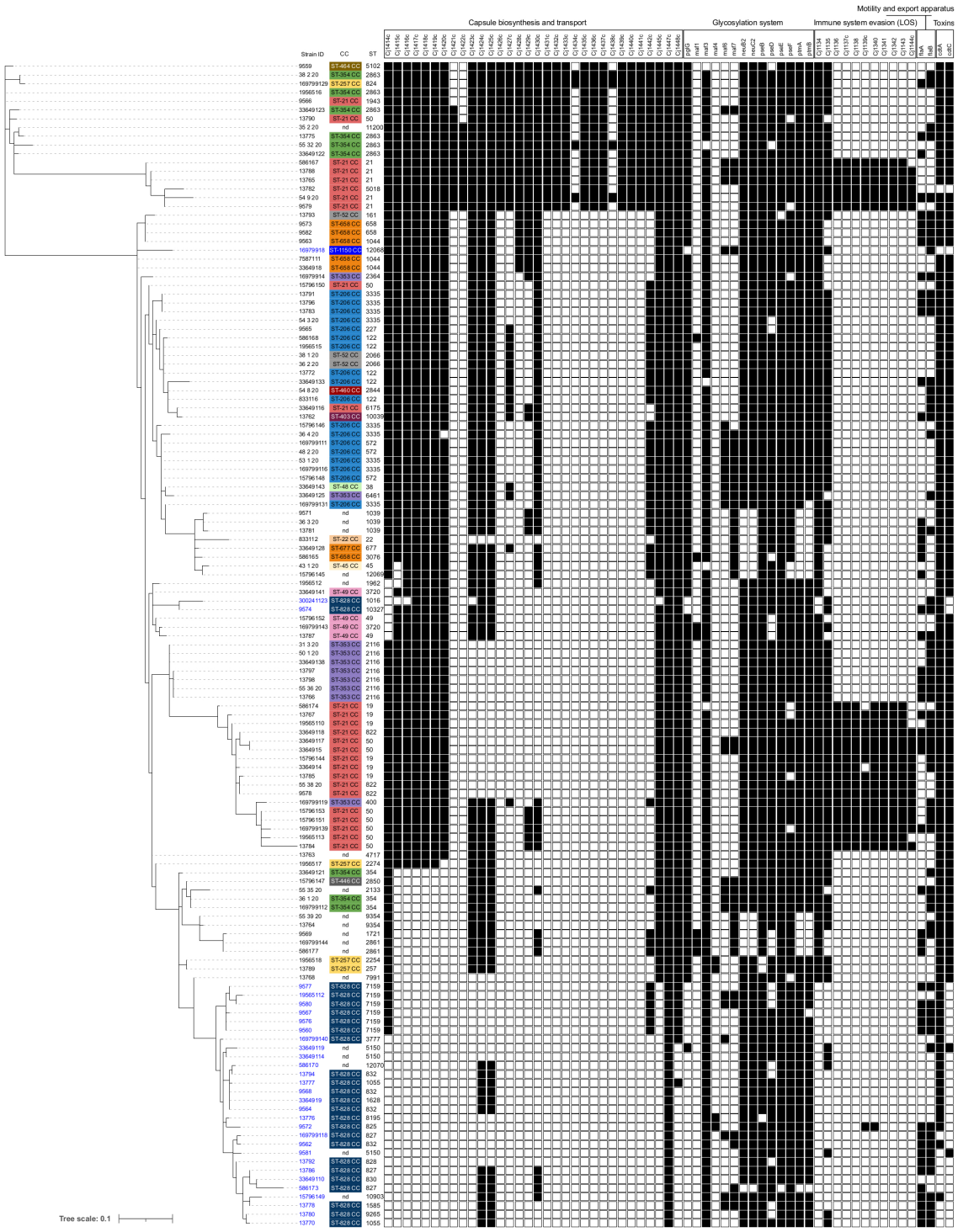

FIGURE 2
Presence and absence of virulence genes divided by category, in 133 genomes of *Campylobacter jejuni* and *Campylobacter coli* isolated from humans. The dendrogram was constructed using a binary presence/absence matrix of 134 *Campylobacter*-specific virulence genes. Genes detected in >1% and < 99% of genomes are shown (black boxes). IDs are colored according to species: *C. jejuni* are shown in black and *C. coli* in blue. Clonal complexes (CC) are color-coded, and individual Sequence Type (ST) are shown.

strain (833,112 strain) presented three circularized plasmids (Table 1; Supplementary Table S1). Six *C. jejuni* and 14 *C. coli* presented circularized plasmids (Table 1). All circularized plasmids exhibited homology with previously characterized *Campylobacter* spp. plasmids (Table 1). Plasmid sizes varied between 2,427 and 49,853 bp (Table 1). Four circularized plasmids <10 kb were defined as cryptic. The distribution of strains containing circularized plasmids was observed across the cgMLST dendrogram except for *C. coli* ST-7159 strains. Five out of six ST-7159 strains contained a plasmid (Figure 1). Four out of the 20 plasmids presented the *tet*(O) gene (Table 1).

TABLE 1 MOB-recon *Campylobacter* spp. circularized plasmids results and antimicrobial resistance genes.

Plasmid name	Plasmid acc. n.	Strain	Resistance gene	Plasmid size (bp)	GC%	CDS[a]	*rep* type	*rep* acc. n.[b]	Relaxase type	Relaxase acc. n.[b]	Mash nearest neighbor[b]
p9574	OQ553938	*C. coli* 9574	-	2,427	26	3	-	-	-	-	CP007185
p300241123	OQ553956	*C. coli* 300241123	-	2,908	30	4	rep_cluster_840	NC_004997	-	-	AY256846
p9562	OQ553936	*C. coli* 9562	-	3,267	32	4	rep_cluster_950	CP017855	-	-	MH634988
p833112_4kb	OQ553947	*C. jejuni* 833112	-	4,367	31	7	rep_cluster_795	NC_008052	MOBP	NC_008051	MH634989
p9581	OQ553943	*C. coli* 9581	-	24,869	29	30	-	-	MOBP	CP017870	**CP017870**
p9576	OQ553939	*C. coli* 9576	-	25,341	29	31	-	-	MOBP	CP017870	CP017870
p9577	OQ553940	*C. coli* 9577	-	25,341	29	31	-	-	MOBP	CP017870	CP017870
p833112_26kb	OQ553949	*C. jejuni* 833112	-	26,724	29	45	-	-	MOBP	CP006703	**CP017231**
p19565112	OQ553953	*C. coli* 19565112	-	27,225	29	35	-	-	MOBP	CP006703	CP006703
p9560	OQ553935	*C. coli* 9560	-	27,235	29	36	-	-	MOBP	CP006703	CP006703
p33649110	OQ553954	*C. coli* 33649110	-	27,538	30	33	-	-	MOBP	CP006703	**CP045792**
p9580	OQ553942	*C. coli* 9580	-	27,544	30	33	-	-	MOBP	CP006703	CP045792
p16979918	OQ553952	*C. coli* 16979918	-	30,346	28	38	-	-	MOBP	CP006703	CP017231
p50_1_20	OQ553934	*C. jejuni* 50_1_20	-	30,346	28	38	-	-	MOBP	CP006703	CP017231
p33649138	OQ553955	*C. jejuni* 33649138	-	30,348	28	38	-	-	MOBP	CP006703	CP017231
p13780	OQ553944	*C. coli* 13780	-	30,631	29	39	-	-	MOBP	CP006703	**CP006703**
p13784	OQ553945	*C. coli* 13784	-	35,326	26	47	rep_cluster_1502	**CP013734**	MOBP	**NZ_ AZNS01000034**	CP014746
p9572	OQ553937	*C. coli* 9572	-	39,389	28	45	-	-	MOBP	**NC_022355**	**CP043764**
p833112_43kb	OQ722348	*C. jejuni* 833112	*tet*(O)	43,681	28	47	-	-	MOBP	NC_022355	**CP022471**
p15796150	OQ553951	*C. jejuni* 15796150	*tet*(O)	44,310	28	50	-	-	MOBP	NC_022355	CP022471
p9579	OQ553941	*C. jejuni* 9579	*tet*(O)	44,469	30	49	rep_cluster_475	**KX686749**	MOBP	NC_022355	**CP011017**
p13786	OQ553946	*C. coli* 13786	*tet*(O), *aph(2″)-Ii*, *aph(3′)-IIIa*Δ	49,853	29	57	-	-	MOBP	NC_022355	CP043764

[a]Bakta v.1.7.0 predicted reading frames; [b]In bold, reference plasmids selected for the Gview and MAFFT_NJ plasmid analysis; Δ: partial gene.

10.3389/fmicb.2023.1293666

MOB-recon analysis confirmed the presence of replicase (*rep*) and *mob* relaxase genes. Rep proteins were present in three circularized cryptic plasmids, presenting high homologies to three previously described cryptic plasmids (Table 1). The Bakta server identified a replication initiation protein Rep_3 (RepB family) in the fourth cryptic p9574; this protein was misidentified by the MOB-recon tool.

In 11 strains without circularized plasmids, MOB-recon identified 12 non-circularized plasmid contigs that encoded MOB relaxases (and one also encoded a Rep protein). Four non-circularized plasmid contigs also presented the *tet*(O) gene (Supplementary Tables S1, S4).

The GView pangenome analysis, of 18 circularized plasmid sequences larger than 10 kb and 11 reference plasmids added for comparative purposes (Table 1; Figure 3), revealed a comprehensive overview through a circular map displaying the pangenome BLAST atlas of all sequences (Figure 3). The GView analysis grouped the plasmids into three main groups (A–C). This grouping was further supported by the NJ-phylogenetic tree generated through MAFFT analysis (Figure 4), reinforcing the consistency of the results obtained from both methodologies. Within these groups, distinct clades of pTet-like, pCC42-like, and pVir-like plasmids emerged, aligning with their respective reference plasmids.

The *tet*(O)-carrying plasmids plus the p9572 were classified into group A as pTet-like plasmids, alongside the five reference plasmids previously described as pTet (Table 1; Figure 3). The 39 kb-p9572 did not present the *tet*(O) gene but maintained most of the pTet-plasmid backbone. This strain presented the *tet*(O) gene in a 173 kb-contig classified as chromosomal by MOB-recon (Supplementary Table S4) and presented a 97% of coverage and 99.91% of identity with the *C. coli* strain meC0467 chromosome (CP027638). The p13786 classified as group A (pTet-like) presented a partial *aph(3′)-IIIa* gene, intact in the Tx40 plasmid and pN29710-1 reference plasmids. p1378 also presented the *aph(2″)-Ii* gene. These four pTet-like plasmids were observed in one ST-828 CC *C. coli* and three *C. jejuni* of ST-21 CC and ST-22 CC (Supplementary Table S1).

Group B, or pCC42-like, was the biggest one (70.58% of the total of circularized plasmids), with 17 plasmids ranging from 25 to 30 kb (four reference plasmids and 12 circularized plasmids); their plasmid backbone was mainly constituted by a significant coding region for the Tra/Vir type IV secretion system (T4SS). Seventy-five per cent (9/12) of these plasmids were associated with *C. coli*. Among these *C. coli*-associated plasmids, a subset of 55.5% (5/9) was identified in ST-7159 (ST-828 CC) strains isolated in different years; nevertheless, plasmids grouped in two closely related subclades (Figure 4). The remaining plasmids, which formed a third sub-clade, were found in three strains of *C. jejuni* and one strain of *C. coli*. Interestingly, the *C. coli* strain

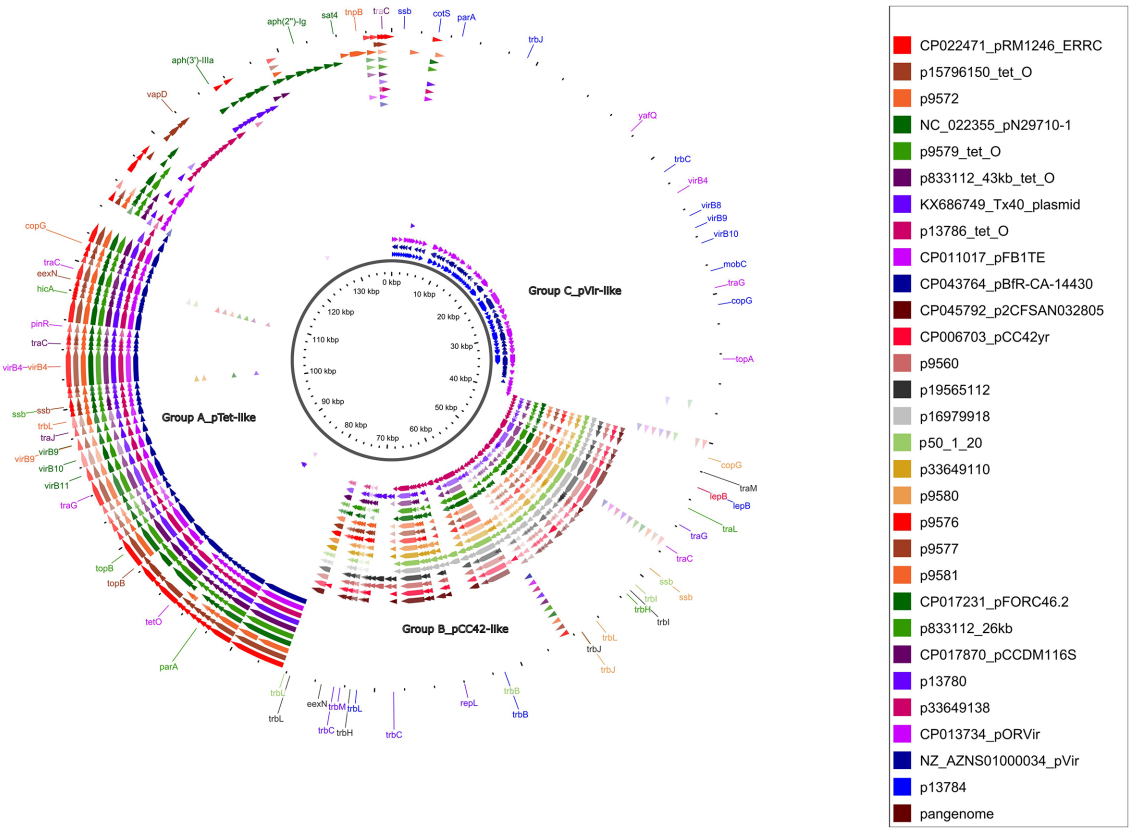

FIGURE 3
Pangenome analysis of circularized *Campylobacter* spp. plasmids bigger than 10 kb. GView server showed a circular figure with 18 circularized plasmid sequences plus 11 reference plasmids. Individual colored slots (circles) in the figure represent one plasmid sequence. Circles showed regions with BLAST hits between the constructed pangenome and the other uploaded sequences. The significant gaps showed regions missing from the pangenome but found in one of the other sequences. The dark brown circle showed the constructed pangenome using all the uploaded concatenated plasmid sequences. Individual arrows represent the CDS.

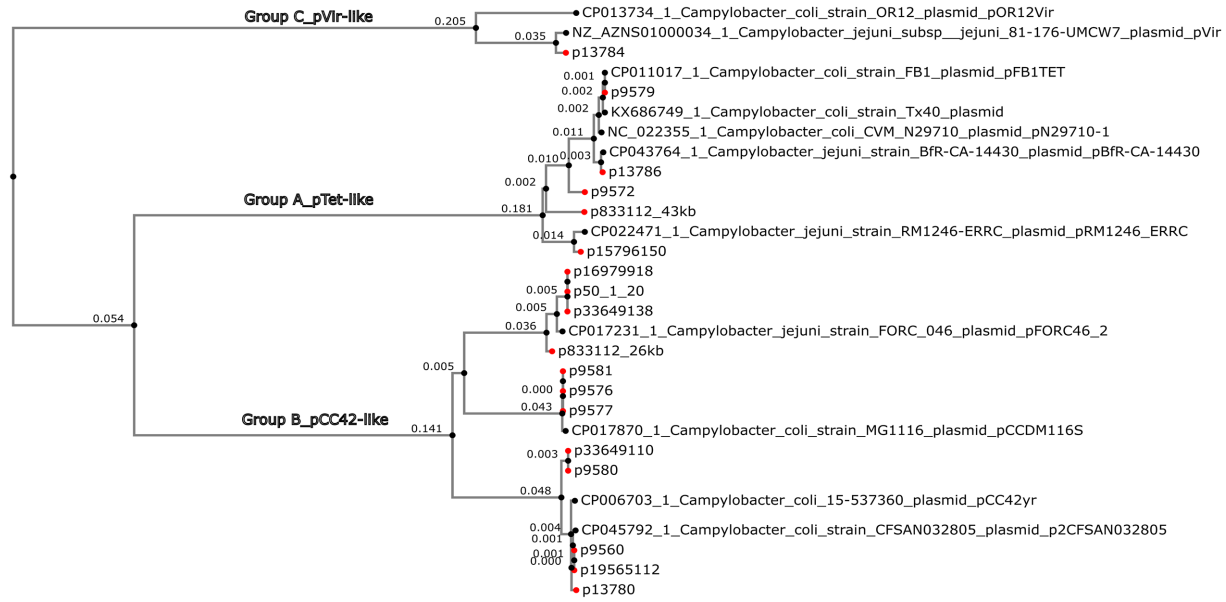

FIGURE 4
Phylogeny of *Campylobacter jejuni* and *Campylobacter coli* circularized plasmids bigger than 10 kb. A MAFFT multiple alignment of the plasmid nucleotides was performed. The Neighbor-Joining method and Juke-Cantor model were used to perform a phylogenetic tree by Phylo.io 1.0.0. Eighteen circularized plasmids (red dots) plus 11 reference plasmids are represented.

identified in this sub-clade did not belong to the ST-828 CC but was classified as ST-12068 (ST-1150 CC).

Group C, or pVir-like, was constituted by the p13784 and two reference plasmids, pOR12Vir and pVir, previously described as *Campylobacter* spp. virulence plasmids (Figure 3). The pVir-like p13874 presented 97% of coverage and 97.99% of identity with pVir and 95% of coverage and 97.84% of identity with pOR12Vir. The plasmids of this group were characterized to present seven genes encoding homologs of type IV secretion proteins and are clustered in a region spanning 8.9 kb. One of these genes was previously identified by VFDB analysis as Lvh type IVA secretion system (*Legionella* spp. *vir* homologs).

4 Discussion

Campylobacteriosis cases have increased worldwide (Whiley et al., 2013; Gibbons et al., 2014; EFSA and ECDC, 2021, 2022). Nevertheless, this infection is frequently underdiagnosed and underreported (Gibbons et al., 2014). Genetic characterization and comparison of *Campylobacter* spp. play a crucial role in advancing our knowledge of the dynamics and characteristics of circulating lineage clusters. A high genetic diversity of *C. jejuni* strains has been extensively documented worldwide and possesses a notable capacity for genetic exchange, enhancing its adaptability (Golz et al., 2020; Bravo et al., 2021; Harrison et al., 2021; Ocejo et al., 2021; Prendergast et al., 2022; Zhong et al., 2022; Hull et al., 2023). Notably, extensive introgression (transfer of genetic material between different species), predominantly from *C. jejuni* to *C. coli,* has been observed, resulting in the replacement of approximately 10 and 23% of the *C. coli* core genome with *C. jejuni* DNA in ST-828 and ST-1150 CCs, respectively (Sheppard et al., 2008; Tanoeiro et al., 2022).

In this study, genome analysis showed a significant genetic divergence in the selected collection. The assignment to different STs and CCs demonstrated that 41% of the *C. jejuni* strains were grouped into two main CCs, ST-21 CC and ST-206 CC, defined as host generalists (capable of infecting wide range of host species) (Baumler and Fang, 2013; Thépault et al., 2017; Bravo et al., 2021; Mouftah et al., 2021; Dessouky et al., 2022; Ghielmetti et al., 2023).

Our results agree with several studies, demonstrating that ST-21 CC is prevalent in the *C. jejuni* population in humans in Italy (Manfreda et al., 2016; Di Giannatale et al., 2019; Ocejo et al., 2021; Conesa et al., 2022; Iannino et al., 2022). ST-21 CC is also among the most reported CC in poultry and is often associated with cattle, wild birds, sheep, dogs, dairy products, and water (Kwan et al., 2008; Cuevas-Ferrando et al., 2020; Conesa et al., 2022; Deblais et al., 2023). ST-206 CC has also been found frequently in humans in Germany, chicken meat, dogs in Italy, chickens in Poland, and sheep in Spain (Rosner et al., 2017; Wieczorek et al., 2017; Di Giannatale et al., 2019; Ocejo et al., 2021; Iannino et al., 2022). ST-353 CC, detected in 9.8% (10/102) of the strains, has been classified as a chicken specialist due to its prevalence in this host (Cobo-Díaz et al., 2021). *Campylobacter coli* showed a low CC heterogeneity, as all the strains except one were classified as ST-828 (Mouftah et al., 2021).

Many studies have suggested approaches to overcome the limited discriminatory power of the conventional seven loci MLST by exploiting WGS data (Cody et al., 2017). Our collection presented a high variability of cgMLST profiles, aligning with our objective of choosing non-epidemiologically linked strains for this study. The cgMLST dendrogram highlighted that most strains analyzed were not genetically related. This was particularly evident for *C. coli*, where clusters of similar genomes remained undetected. The high variability of cgSTs circulating in our country suggests that human infections in Italy are usually sporadic, likely associated with improper handling of

food products, which mirrors the epidemiology of campylobacteriosis in EU (EFSA and ECDC, 2022; Liu et al., 2022).

Only a few small groups of strains were classified as the same cgST, mainly associated with the ST-2116, ST-2863, and ST-3335. These strains were isolated in different years, suggesting they did not originate from an outbreak but were potentially acquired from a common source. Recent studies have indicated that ST-2116 and ST-2863 are the most prevalent STs isolated from broilers in Italy, exhibiting genetic homogeneity (Di Giannatale et al., 2019; Marotta et al., 2023). This suggests that human infections caused by these clones, which are extensively circulating in Italy, are likely linked to broilers and the consumption of contaminated poultry meat and related food products. Conversely, infections involving ST-3335 have been attributed to cattle and sheep, indicating a probable connection with ruminant reservoirs (Arning et al., 2021). Therefore, it is crucial to conduct further research utilizing more precise attribution models to examine the sources of infection.

The analysis of the *Campylobacter* spp. collection revealed a diverse virulome among individual genomes. Notably, *C. jejuni* strains carried more virulence genes than *C. coli* strains (Bravo et al., 2021; Hull et al., 2023). The virulome of *Campylobacter* spp. has mainly been studied in *C. jejuni*, and most of the commonly used virulence factor databases have been constructed based on the reference genome of this species. The low number of virulence factors detected in *C. coli* may be attributed to either the absence of *C. coli*-specific genes in the database queried or a sequence identity below the VFDB tool's threshold between the *C. coli* virulence genes and those in the *C. jejuni* reference genomes.

The dendrogram, generated from a binary matrix indicating the presence or absence of virulence genes, provided insights into the clustering of strains based on their virulomes. The identified clusters corresponded to specific *Campylobacter* species and CCs. Specific virulence genes were associated with particular STs, such as ST-21 and ST-5018 (ST-21 CC), highlighting the potential role of these genes on the pathogenicity of *Campylobacter* spp. (Zhang D. et al., 2023). However, few exceptions were observed, including two distinct clusters within the ST-21 CC, suggesting genetic differences within this complex. A nine-gene LOS cassette also distinguished the strains in these clusters, with one cluster carrying additional genes in the CBT cassette. We did not detect any significant difference between the strains isolated from blood and fecal samples, which could suggest that the cases of bacteraemia were not associated with the changes in the strain's virulence but rather with the host-specific factors. Interestingly, the presence of *C. coli* strains among *C. jejuni* strains suggested the possibility of gene exchange between these two species.

A recent study on the genomic diversity and virulence profile of the genus *Campylobacter* demonstrated that the number of genes has undergone expansion or contraction during the evolution of different *Campylobacter* species (Zhong et al., 2022). VFDB analysis revealed that many strains (75 out of 131) carried virulence genes associated with bacterial species other than *Campylobacter* spp., suggesting potential gene transfer events between different bacterial species. *Campylobacter jejuni* strains, particularly those belonging to ST-354 CC and ST-353 CC, both ranking among the top four most frequent STs in our collection, carried virulence genes associated with *E. coli*, *Aeromonas* spp., and *Vibrio* spp. This highlights a wide variety of virulence factors within specific clonal complexes. This study suggests that the T6SS virulence genes of *E. coli*, and *Aeromonas* spp. are probably acquired from other bacterial species upon multiple and independent genetic uptakes. The identification of these virulence genes in two *C. coli* strains suggests a more comprehensive bioinformatic analysis of T6SS and the determination of associated effectors in *C. coli* is still needed.

The presence of virulence genes associated with other species in *C. coli*, such as LPS gene of *Francisella* spp., capsule of *Klebsiella* spp., and O-antigen of *Yersinia* spp., underscores their importance for the bacterium's survival during colonization and infection of host tissues (Lehmann et al., 2006). It has been demonstrated that *C. jejuni* bind to a diverse range of host glycans that are potentially crucial for the initial attachment to and continued colonization of the host (Morrow et al., 2005; Day et al., 2009); a better comprehension of the factors involved in glycan expression and recognition by *C. coli* and the host may elucidate the mechanisms involved in *C. coli* commensal colonization and pathogenic infection.

Antibiotic resistance surveillance in *Campylobacter* spp. has become a challenge in recent years. Our study showed high levels of resistance to Cip and T and low levels of resistance to macrolides and aminoglycosides, as described previously (EFSA and ECDC, 2022). Despite a generally high concordance between antibiotic resistance genotypes and phenotypes, tetracycline exhibited the lowest correlation between the presence of the *tet* gene and susceptibility patterns. The absence of complete matching is widely described worldwide due to a misdetection of some AMR mechanisms (Engberg et al., 2001; Luo et al., 2003; Painset et al., 2020; Rokney et al., 2020; Mouftah et al., 2021; Dessouky et al., 2022). Without a precise mechanism, erythromycin and/or tetracycline resistance could be present due to mutations in CmeABC operon, its transcriptional regulator CmeR or in its promoter (Aksomaitiene et al., 2018; García-Fernández et al., 2018; Oncel et al., 2023). CmeABC efflux pump can also synergise with the GyrA and 23S rRNA mutations in maintaining high levels of resistance to fluoroquinolones and macrolides (Payot et al., 2006). Using an automated annotation pipeline to detect antibiotic resistance mechanisms could mislead some mechanisms. The presence or absence of efflux pumps, membrane permeability, frameshift mutations, and the existence of mosaic or new resistance genes could impact the phenotypic resistance pattern (Hormeño et al., 2020). Technical issues such as poor-quality sequences, assembly errors, and incorrect analysis may also contribute to discrepancies in antibiotic resistance patterns (Bortolaia et al., 2020; Elhadidy et al., 2020). Addressing these complexities is crucial for accurate and comprehensive antibiotic resistance surveillance in *Campylobacter* spp.

Consistent with global observations, this study identified the GyrA (T86I) mutation and the *tet*(O) gene as the primary mechanisms responsible for quinolone and tetracycline resistance, respectively (Luo et al., 2003; García-Fernández et al., 2018; Ocejo et al., 2021). A lack of a clear association between increased virulence genes and antibiotic resistance profiles in *C. jejuni* or *C. coli* was observed. *Campylobacter coli*, despite having fewer virulence genes, exhibited higher resistance, including MDR. The contrasting situation with *C. jejuni* ST-21 CC, being the most virulent CC and presenting a high percentage of strains resistant to CipT. Moreover, susceptible strains were distributed along the presence/absence virulence gene dendrogram without a clear correlation, demonstrating that the susceptibility of *Campylobacter* spp. strains may not be directly linked with the degree of virulence the strains exhibit.

The presence of plasmids in *Campylobacter* spp. collections isolated from humans have not been extensively studied, and few studies have been conducted on this topic (Lee et al., 1994). Nevertheless, with the increasingly widespread adoption of WGS, recent studies have revealed a notable occurrence of plasmids in *Campylobacter* spp. strains (Marasini and Fakhr, 2017; Deblais et al., 2023; Ghielmetti et al., 2023; Hull et al., 2023). Fifteen percent of strains of our collection presented plasmids; nevertheless, many linear contigs were classified by the MOB-recon tool as plasmidic, suggesting a potentially higher prevalence of plasmids beyond those directly identified as circular (Hull et al., 2023).

The *tet*(O) genes were mainly found on the bacterial chromosome, with only a small percentage found in circularized plasmids, aligning with previous findings (Ghielmetti et al., 2023). One of the plasmids carrying *tet*(O), the pTet-like p13786, also showed the *aph(3′)-IIIa* and a partial *aph(2″)-Ii* genes, which did not confer resistance to Gm. The presence of the pTet family in *C. jejuni*, containing multiple resistance genes, suggested a potential role in enhancing multidrug resistance, promoting bacterial survival, and contributing to virulence. These plasmids also presented genes coding type II toxin-antitoxin system HicA-HicB, the CagA pathogenicity island protein, the VapD virulence-associated protein and several genes encoding predicted type IV secretion/conjugal transfer proteins with homology to T4SS. These findings suggested a complex interplay between plasmids and the expression of virulence and resistance factors in *Campylobacter* spp. (Batchelor et al., 2004; Wallden et al., 2010; Bunduruş et al., 2023; Gabbert et al., 2023; Morita et al., 2023) The p13876, next to the *tet*(O) gene, presented two Type II CRISPR-associated endonucleases coding genes, *cas1* and *cas2,* described in the *Campylobacter* spp. chromosome rather than in plasmids. Together with CRISPR, these proteins could provide acquired genetic immunity against the entry of mobile genetic elements after infection by a phage expressing a Cas4-like protein (Hooton and Connerton, 2014; van Vliet et al., 2021). This CRISPR-mediated autoimmunity could, therefore, profoundly direct the shape of evolution in these species (Lee et al., 1994; Marasini and Fakhr, 2017; Deblais et al., 2023).

Cryptic plasmids have been identified in several *Campylobacter* species encoding for replication proteins (Alfredson and Korolik, 2003; Hiett et al., 2013). The cryptic plasmids found in our study presented genes encoding for replication proteins and shared homology with previously described cryptic plasmids deposited in the GenBank database. The precise role of these small plasmids remains unclear. Some studies suggest that those may act as modifiable vectors for genetic innovation in other species, such as *Aeromonas salmonicida* (Attéré et al., 2017).

Gview analysis and the Phylogenetic NJ-tree classified plasmids found in this study into three groups or clades (A–C), preserving well-determined lineages. These phylogenetic tree clades supported the categorization obtained with the pangenomic analysis, revealing sub-braches indicative of evolutionary divergence within each clade.

Group A comprised pTet-like plasmids, which presented essential genes responsible for conjugation, virulence (including the Type IV secretion system), and were associated with carrying MDR genes (Bacon et al., 2002; Marasini and Fakhr, 2016; Hull et al., 2023; Morita et al., 2023).

Group B, previously known as pCC42-like plasmids, was formed by plasmids coding for conjugative transfer genes (*trb*/*tra*) with type IV secretion system genes (*virB3/B4*) (Bacon et al., 2002; van Vliet et al., 2021; Ghielmetti et al., 2023). This plasmid class was prevalently associated with ST-7159 *C. coli* strains isolated in different years, emphasizing the persistence of this plasmid-associated sequence type over time.

Group C, or pVir-like, included p13784, presenting significant homology with pVir. It encoded genes homologous to the type IV secretion system in *Helicobacter pylori*. This system was involved in invading *C. jejuni* strain 81–176, which demonstrated virulence in human volunteer studies (Bacon et al., 2002; Ghielmetti et al., 2023).

It is noteworthy that pVir-like plasmids are less prevalent than pTet-like plasmids in *Campylobacter* spp. strains (Marasini et al., 2018). A previous study conducted with *Campylobacter* spp. strains isolated from retail meat corroborated our classification groups, including an additional fourth group of plasmids <10 kb called in our study as cryptic plasmids (Marasini et al., 2018).

This genomic approach provides an interesting understanding of plasmid diversity, facilitating the identification of distinct groups and highlighting the evolutionary relationships among the plasmids, thereby contributing to our comprehension of *Campylobacter* spp. plasmid dynamics (Marasini et al., 2018). A more in-depth exploration of the plasmids present in our *Campylobacter* spp. collection, using long-read sequencing technologies, could substantially contribute to providing a more accurate assessment of the proper frequency of plasmid presence within our *Campylobacter* spp. collection.

Our study demonstrated a large genomic diversity within a population of *Campylobacter* spp. associated with human infections in Italy. While some of the detected MLST clusters were previously linked to the consumption or handling of poultry meat, others seem to be associated with different animal sources, including cattle and sheep or domestic pets.

Therefore, it is important to implement surveillance and control measures for *Campylobacter* spp. in broiler farms and dairy production to reduce the carriage of *Campylobacter* spp. and, consequently, decrease the risk of carcass and food contamination during the primary phases of the production chain. Moreover, good safety and hygiene practices must be applied when handling raw meat and, importantly, when preparing artisanal dairy and food products based on unpasteurised milk (Dai et al., 2020; Emanowicz et al., 2021; Al Hakeem et al., 2022).

In addition, considering the consistently high level of antibiotic resistance to fluoroquinolones and tetracycline in Italian strains of *C. jejuni* and *C. coli*, continuous effort must be maintained in limiting the use of antibiotics in the food-producing animals to avoid further spread of the resistant strains (Mouftah et al., 2021; EFSA and ECDC, 2023; Fonseca et al., 2023).

Whole genome sequencing emerges as a valuable tool for developing new strategies to address antibiotic resistance. Accurate whole-genome characterization, and the prediction of antibiotic resistance improves current surveillance programs' accuracy and effectiveness (Ocejo et al., 2021; Ghielmetti et al., 2023). WGS also gives high resolution typing methods allowing precise differentiation among *Campylobacter* strains. This approach not only facilitates comprehensive "One Health" epidemiological investigations, but also enables the thorough examination of foodborne disease outbreaks related to *Campylobacter* spp. and the tracking of transmission sources (Cody et al., 2019; Zhang D. et al., 2023). The accurate understanding of the source of *Campylobacter*, whether it originates from specific food, environmental reservoirs, or specific animal hosts, is crucial for target intervention and preventive measures.

Data availability statement

Genome sequences were deposited in GenBank (https://www.ncbi.nlm.nih.gov) under BioProject ID PRJNA913772. Strains were stored under the consecutive BioSample accession numbers: SAMN32306040–SAMN32306055 and SAMN32306053–SAMN32306173. Plasmids were submitted and consecutively assigned to NCBI accession numbers from OQ553934–OQ553947, OQ553949, OQ553951–OQ553956, and OQ722348 (Table 1). Strain-specific details for bacteria can be found in Table 1 and Supplementary Table S1. The presence of genes involved in "capsule biosynthesis and transport" and genes categorized as "immune evasion-LOS" was verified using a custom-built database, using *C. jejuni* NCTC 11168 (AL111168.1) as the reference genome. The custom database was built using ABRicate version 1.0.1 (Seemann T, Abricate, GitHub https://github.com/tseemann/abricate). The results obtained from VFDB and ABRicate were used to generate a gene presence/absence matrix (Supplementary Table S2). The authors confirm all supporting data, code and protocols have been provided within the article or through Supplementary material.

Author contributions

AG-F: Conceptualization, Data curation, Formal analysis, Investigation, Methodology, Project administration, Software, Supervision, Validation, Visualization, Writing – original draft, Writing – review & editing. AJ: Software, Writing – original draft, Writing – review & editing, Data curation, Validation. FM: Methodology, Writing – review & editing, Data curation. MN: Data curation, Writing – original draft, Writing – review & editing, Methodology. SA: Methodology, Writing – review & editing. SP: Data curation, Methodology, Writing – review & editing. MP: Data curation, Methodology, Writing – review & editing. RR: Methodology, Writing – review & editing. FT: Methodology, Writing – review & editing. GG: Conceptualization, Data curation, Supervision, Writing – review & editing. LV: Conceptualization, Funding acquisition, Investigation, Project administration, Resources, Supervision, Writing – original draft, Writing – review & editing.

Funding

The author(s) declare financial support was received for the research, authorship, and/or publication of this article. This research was supported by the Italian Ministry of Health-National Center for Disease Prevention and Control (CCM 2022, fasc. Fasc. 7S20) "Genomic analysis of *Salmonella* spp. and *Campylobacter* spp. isolates in humans."

Acknowledgments

We gratefully acknowledge the contribution of Ida Luzzi as a point of reference and promoter of the Enter-Net Italia surveillance. We thank her efforts to create the valuable *Campylobacter* spp. Biobank and her support.

Conflict of interest

The authors declare that the research was conducted in the absence of any commercial or financial relationships that could be construed as a potential conflict of interest.

Publisher's note

Supplementary material

The Supplementary material for this article can be found online at: https://www.frontiersin.org/articles/10.3389/fmicb.2023.1293666/full#supplementary-material

References

Afgan, E., Baker, D., Batut, B., Van Den Beek, M., Bouvier, D., Ech, M., et al. (2018). The galaxy platform for accessible, reproducible and collaborative biomedical analyses: 2018 update. *Nucleic Acids Res.* 46, W537–W544. doi: 10.1093/NAR/GKY379

Aksomaitiene, J., Ramonaite, S., Olsen, J. E., and Malakauskas, M. (2018). Prevalence of genetic determinants and phenotypic resistance to ciprofloxacin in *Campylobacter jejuni* from Lithuania. *Front. Microbiol.* 9:203. doi: 10.3389/fmicb.2018.00203

Al Hakeem, W. G., Fathima, S., Shanmugasundaram, R., and Selvaraj, R. K. (2022). *Campylobacter jejuni* in poultry: pathogenesis and control strategies. *Microorganisms* 10:2134. doi: 10.3390/microorganisms10112134

Alfredson, D. A., and Korolik, V. (2003). Sequence analysis of a cryptic plasmid pCJ419 from *Campylobacter jejuni* and construction of an *Escherichia coli-Campylobacter* shuttle vector. *Plasmid* 50, 152–160. doi: 10.1016/S0147-619X(03)00060-X

Andrzejewska, M., Szczepańska, B., Klawe, J. J., Śpica, D., and Chudzińska, M. (2013). Prevalence of *Campylobacter jejuni* and *campylobacter coli* species in cats and dogs from Bydgoszcz (Poland). *Region* 16, 115–120. doi: 10.2478/PJVS-2013-0016

Arning, N., Sheppard, S. K., Bayliss, S., Clifton, D. A., and Wilson, D. J. (2021). Machine learning to predict the source of campylobacteriosis using whole genome data. *PLoS Genet.* 17:e1009436. doi: 10.1371/journal.pgen.1009436

Attéré, S. A., Vincent, A. T., Paccaud, M., Frenette, M., and Charette, S. J. (2017). The role for the small cryptic plasmids as moldable vectors for genetic innovation in *Aeromonas salmonicida* subsp. *salmonicida*. *Front. Genet.* 8:211. doi: 10.3389/fgene.2017.00211

Bacon, D. J., Alm, R. A., Hu, L., Hickey, T. E., Ewing, C. P., Batchelor, R. A., et al. (2002). DNA sequence and mutational analyses of the pVir plasmid of *Campylobacter jejuni* 81-176. *Infect. Immun.* 70, 6242–6250. doi: 10.1128/IAI.70.11.6242-6250.2002

Bankevich, A., Nurk, S., Antipov, D., Gurevich, A. A., Dvorkin, M., Kulikov, A. S., et al. (2012). SPAdes: a new genome assembly algorithm and its applications to single-cell sequencing. *J. Comput. Biol.* 19, 455–477. doi: 10.1089/CMB.2012.0021

Batchelor, R. A., Pearson, B. M., Friis, L. M., Guerry, P., and Wells, J. M. (2004). Nucleotide sequences and comparison of two large conjugative plasmids from different *Campylobacter* species. *Microbiology* 150, 3507–3517. doi: 10.1099/mic.0.27112-0

Baumler, A., and Fang, F. C. (2013). Host specificity of bacterial pathogens. *Cold Spring Harb. Perspect. Med.* 3:a010041. doi: 10.1101/CSHPERSPECT.A010041

Bharat, A., Petkau, A., Avery, B. P., Chen, J., Folster, J., Carson, C. A., et al. (2022). Correlation between phenotypic and in silico detection of antimicrobial resistance in *Salmonella enterica* in Canada using staramr. *Microorganisms* 10:292. doi: 10.3390/microorganisms10020292

Blaser, M. J., and Engberg, J. (2008). "Clinical Aspects of *Campylobacter jejuni* and *Campylobacter coli* Infections," in *Campylobacter*. Eds. I. Nachamkin, C. M. Szymanski and M. J. Blaser, 3rd Edn, (Washington: ASM Press), 99–121.

Bolger, A. M., Lohse, M., and Usadel, B. (2014). Trimmomatic: A flexible trimmer for illumina sequence data. *Bioinformatics* 30, 2114–2120. doi: 10.1093/bioinformatics/btu170

Bortolaia, V., Kaas, R. S., Ruppe, E., Roberts, M. C., Schwarz, S., Cattoir, V., et al. (2020). ResFinder 4.0 for predictions of phenotypes from genotypes. *J. Antimicrob. Chemother.* 75, 3491–3500. doi: 10.1093/jac/dkaa345

Bravo, V., Katz, A., Porte, L., Weitzel, T., Varela, C., Gonzalez-Escalona, N., et al. (2021). Genomic analysis of the diversity, antimicrobial resistance and virulence potential of clinical Campylobacter jejuni and *Campylobacter coli* strains from Chile. *PLoS Negl. Trop. Dis.* 15:e0009207. doi: 10.1371/journal.pntd.0009207

Bunduruș, I. A., Balta, I., Ștef, L., Ahmadi, M., Peț, I., McCleery, D., et al. (2023). Overview of virulence and antibiotic resistance in *Campylobacter* spp. livestock isolates. *Antibiotics* 12:402. doi: 10.3390/antibiotics12020402

Cassini, A., Colzani, E., Pini, A., Mangen, M. J., Plass, D., McDonald, S. A., et al. (2018). Impact of infectious diseases on population health using incidence-based disability-adjusted life years (DALYs): results from the burden of communicable diseases in Europe study, European Union and european economic area countries, 2009 to 2013. *Euro Surveill.* 23:454. doi: 10.2807/1560-7917.ES.2018.23.16.17-00454

Chen, L., Xiong, Z., Sun, L., Yang, J., and Jin, Q. (2012). VFDB 2012 update: Toward the genetic diversity and molecular evolution of bacterial virulence factors. *Nucleic Acids Res.* 40, D641–D645. doi: 10.1093/nar/gkr989

Chen, L., Yang, J., Yu, J., Yao, Z., Sun, L., Shen, Y., et al. (2005). VFDB: A reference database for bacterial virulence factors. *Nucleic Acids Res.* 33, D325–D328. doi: 10.1093/nar/gki008

Chen, L., Zheng, D., Liu, B., Yang, J., and Jin, Q. (2016). VFDB 2016: hierarchical and refined dataset for big data analysis-10 years on. *Nucleic Acids Res.* 44, D694–D697. doi: 10.1093/nar/gkv1239

Clausen, P. T. L. C., Aarestrup, F. M., and Lund, O. (2018). Rapid and precise alignment of raw reads against redundant databases with KMA. *BMC Bioinformatics* 19, 1–8. doi: 10.1186/S12859-018-2336-6/TABLES/2

Cobo-Díaz, J. F., González del Río, P., and Álvarez-Ordóñez, A. (2021). Whole resistome analysis in *Campylobacter jejuni* and *C. coli* genomes available in public repositories. *Front. Microbiol.* 12:662144. doi: 10.3389/fmicb.2021.662144

Cody, A. J., Bray, J. E., Jolley, K. A., McCarthy, N. D., and Maidena, M. C. J. (2017). Core genome multilocus sequence typing scheme for stable, comparative analyses of Campylobacter jejuni and C. coli human disease isolates. *J. Clin. Microbiol.* 55, 2086–2097. doi: 10.1128/JCM.00080-17

Cody, A. J., Maiden, M. C., Strachan, N. J., and McCarthy, N. D. (2019). A systematic review of source attribution of human campylobacteriosis using multilocus sequence typing. *Euro Surveill.* 24:1800696. doi: 10.2807/1560-7917.ES.2019.24.43.1800696

Conesa, A., Garofolo, G., Di Pasquale, A., and Cammà, C. (2022). Monitoring AMR in *Campylobacter jejuni* from Italy in the last 10 years (2011–2021). *EFSA J.* 20:e200406. doi: 10.2903/J.EFSA.2022.E200406

Connell, S. R., Trieber, C. A., Dinos, G. P., Einfeldt, E., Taylor, D. E., and Nierhaus, K. H. (2003). Mechanism of tet(O)-mediated tetracycline resistance. *EMBO J.* 22, 945–953. doi: 10.1093/EMBOJ/CDG093

Cuevas-Ferrando, E., Guirado, P., Miró, E., Iglesias-Torrens, Y., Navarro, F., Alioto, T. S., et al. (2020). Tetracycline resistance transmission in *Campylobacter* is promoted at temperatures resembling the avian reservoir. *Vet. Microbiol.* 244:108652. doi: 10.1016/J.VETMIC.2020.108652

Dai, L., Sahin, O., Grover, M., and Zhang, Q. (2020). New and alternative strategies for the prevention, control, and treatment of antibiotic-resistant *Campylobacter*. *Transl. Res.* 223, 76–88. doi: 10.1016/j.trsl.2020.04.009

Day, C. J., Tiralongo, J., Hartnell, R. D., Logue, C. A., Wilson, J. C., von Itzstein, M., et al. (2009). Differential carbohydrate recognition by *Campylobacter jejuni* strain 11168: influences of temperature and growth conditions. *PLoS One* 4:e4927. doi: 10.1371/JOURNAL.PONE.0004927

Deblais, L., Jang, H., Kauffman, M., Gangiredla, J., Sawyer, M., Basa, S., et al. (2023). Whole genome characterization of thermophilic *Campylobacter* species isolated from dairy manure in small specialty crop farms of Northeast Ohio. *Front. Microbiol.* 14:1074548. doi: 10.3389/fmicb.2023.1074548

Dessouky, Y. E., Elsayed, S. W., Abdelsalam, N. A., Saif, N. A., Álvarez-Ordóñez, A., and Elhadidy, M. (2022). Genomic insights into zoonotic transmission and antimicrobial resistance in *Campylobacter jejuni* from farm to fork: a one health perspective. *Gut Pathog.* 14, 44–11. doi: 10.1186/s13099-022-00517-w

Di Giannatale, E., Calistri, P., Di Donato, G., Decastelli, L., Goffredo, E., Adriano, D., et al. (2019). Thermotolerant *Campylobacter* spp. in chicken and bovine meat in Italy: prevalence, level of contamination and molecular characterization of isolates. *PLoS One* 14:e0225957. doi: 10.1371/JOURNAL.PONE.0225957

Dingle, K. E., Colles, F. M., Wareing, D. R. A., Ure, R., Fox, A. J., Bolton, F. E., et al. (2001). Multilocus sequence typing system for Campylobacter jejuni. *J. Clin. Microbiol.* 39, 14–23. doi: 10.1128/JCM.39.1.14-23.2001

EFSA and ECDC (2021). The European Union one health 2020 zoonoses report. *Sci. Rep.* 19:e06971. doi: 10.2903/J.EFSA.2021.6971

EFSA and ECDC (2022). The European Union one health 2021 zoonoses report. *Sci. Rep.* 20:e07666. doi: 10.2903/J.EFSA.2022.7666

EFSA and ECDC (2023). The European Union summary report on antimicrobial resistance in zoonotic and indicator bacteria from humans, animals and food in 2020/2021. *Sci. Rep.* 21:e07867. doi: 10.2903/J.EFSA.2023.7867

El-Adawy, H., Hotzel, H., García-Soto, S., Tomaso, H., Hafez, H. M., Schwarz, S., et al. (2023). Genomic insight into Campylobacter jejuni isolated from commercial turkey flocks in Germany using whole-genome sequencing analysis. *Front. Vet. Sci.* 10:1092179. doi: 10.3389/fvets.2023.1092179

Elhadidy, M., Ali, M. M., El-Shibiny, A., Miller, W. G., Elkhatib, W. F., Botteldoorn, N., et al. (2020). Antimicrobial resistance patterns and molecular resistance markers of *Campylobacter jejuni* isolates from human diarrheal cases. *PLoS One* 15:e0227833. doi: 10.1371/journal.pone.0227833

Emanowicz, M., Meade, J., Bolton, D., Golden, O., Gutierrez, M., Byrne, W., et al. (2021). The impact of key processing stages and flock variables on the prevalence and levels of Campylobacter on broiler carcasses. *Food Microbiol.* 95:103688. doi: 10.1016/j.fm.2020.103688

Engberg, J., Aarestrup, F. M., Taylor, D. E., Gerner-Smidt, P., and Nachamkin, I. (2001). Quinolone and macrolide resistance in *Campylobacter jejuni* and *C. coli*: Resistance mechanisms and trends in human isolates. *Emerg. Infect. Dis.* 7, 24–34. doi: 10.3201/eid0701.700024

Feldgarden, M., Brover, V., Haft, D. H., Prasad, A. B., Slotta, D. J., Tolstoy, I., et al. (2019). Using the NCBI AMRFinder tool to determine antimicrobial resistance genotype-phenotype correlations within a collection of NARMS isolates. bioRxiv [Preprint]. doi: 10.1101/550707v1

Fiedoruk, K., Daniluk, T., Rozkiewicz, D., Oldak, E., Prasad, S., and Swiecicka, I. (2019). Whole-genome comparative analysis of Campylobacter jejuni strains isolated from patients with diarrhea in northeastern Poland. *Gut Pathog.* 11:32. doi: 10.1186/s13099-019-0313-x

Fonseca, M., Heider, L. C., Stryhn, H., McClure, J. T., Léger, D., Rizzo, D., et al. (2023). Antimicrobial use and its association with the isolation of and antimicrobial resistance in *Campylobacter* spp. recovered from fecal samples from Canadian dairy herds: a cross-sectional study. *Prev. Vet. Med.* 215:105925. doi: 10.1016/j.prevetmed.2023.105925

Gabbert, A. D., Mydosh, J. L., Talukdar, P. K., Gloss, L. M., McDermott, J. E., Cooper, K. K., et al. (2023). The missing pieces: The role of secretion systems in *Campylobacter jejuni* virulence. *Biomol. Ther.* 13:135. doi: 10.3390/BIOM13010135

García-Fernández, A., Dionisi, A. M., Arena, S., Iglesias-Torrens, Y., Carattoli, A., and Luzzi, I. (2018). Human Campylobacteriosis in Italy: emergence of multi-drug resistance to ciprofloxacin, tetracycline, and erythromycin. *Front. Microbiol.* 9:1906. doi: 10.3389/fmicb.2018.01906

Ghielmetti, G., Seth-Smith, H. M. B., Roloff, T., Cernela, N., Biggel, M., Stephan, R., et al. (2023). Whole-genome-based characterization of *Campylobacter jejuni* from human patients with gastroenteritis collected over an 18 year period reveals increasing prevalence of antimicrobial resistance. *Microb. Genom.* 9:mgen000941. doi: 10.1099/mgen.0.000941

Gibbons, C. L., Mangen, M. J. J., Plass, D., Havelaar, A. H., Brooke, R. J., Kramarz, P., et al. (2014). Measuring underreporting and under-ascertainment in infectious disease datasets: a comparison of methods. *BMC Public Health* 14:147. doi: 10.1186/1471-2458-14-147

Golz, J. C., Epping, L., Knüver, M. T., Borowiak, M., Hartkopf, F., Deneke, C., et al. (2020). Whole genome sequencing reveals extended natural transformation in Campylobacter impacting diagnostics and the pathogens adaptive potential. *Sci. Rep.* 10:3686. doi: 10.1038/s41598-020-60320-y

Hansson, I., Sandberg, M., Habib, I., Lowman, R., and Engvall, E. O. (2018). Knowledge gaps in control of *Campylobacter* for prevention of campylobacteriosis. *Transbound. Emerg. Dis.* 65, 30–48. doi: 10.1111/tbed.12870

Harrison, L., Mukherjee, S., Hsu, C. H., Young, S., Strain, E., Zhang, Q., et al. (2021). Core genome MLST for source attribution of Campylobacter coli. *Front. Microbiol.* 12:703890. doi: 10.3389/fmicb.2021.703890

Hasman, H., Saputra, D., Sicheritz-Ponten, T., Lund, O., Svendsen, C. A., Frimodt-Moller, N., et al. (2014). Rapid whole-genome sequencing for detection and characterization of microorganisms directly from clinical samples. *J. Clin. Microbiol.* 52, 139–146. doi: 10.1128/JCM.02452-13

Hiett, K. L., Rothrock, M. J. B., and Seal, B. S. (2013). Characterization of the *Campylobacter jejuni* cryptic plasmid pTIW94 recovered from wild birds in the southeastern United States. *Plasmid* 70, 268–271. doi: 10.1016/j.plasmid.2013.04.004

Hooton, S. P. T., and Connerton, I. F. (2014). *Campylobacter jejuni* acquire new host-derived CRISPR spacers when in association with bacteriophages harboring a CRISPR-like Cas4 protein. *Front. Microbiol.* 5:744. doi: 10.3389/fmicb.2014.00744

Hormeño, L., Campos, M. J., Vadillo, S., and Quesada, A. (2020). Occurrence of *tet*(O/M/O) mosaic gene in tetracycline-resistant *Campy*lobacter. *Microorganisms* 8:1710. doi: 10.3390/microorganisms8111710

Hsu, C., Harrison, L., Mukherjee, S., Strain, E., Mcdermott, P., Zhang, Q., et al. (2020). Core genome multilocus sequence typing for food animal source attribution of human *Campylobacter jejuni* infections. *Pathogens* 9:532. doi: 10.3390/pathogens9070532

Hull, D. M., Harrel, E., Harden, L., and Thakur, S. (2023). Detection of resistance and virulence plasmids in *Campylobacter coli* and *Campylobacter jejuni* isolated from North Carolina food animal production, 2018-2019. *Food Microbiol.* 116:104348. doi: 10.1016/j.fm.2023.104348

Iannino, F., Di Donato, G., Salucci, S., Ruggieri, E., Vincifori, G., Danzetta, M. L., et al. (2022). Campylobacter and risk factors associated with dog ownership: A retrospective study in household and in shelter dogs. *Vet. Ital.* 58, 59–66. doi: 10.12834/VETIT.2299.15789.1

Iovine, N. M. (2013). Resistance mechanisms in *Campylobacter jejuni*. *Virulence* 4, 230–240. doi: 10.4161/viru.23753

Jolley, K. A., Bray, J. E., and Maiden, M. C. J. (2018). Open-access bacterial population genomics: BIGSdb software, the PubMLST.org website and their applications. *Wellcome Open Res.* 3:124. doi: 10.12688/wellcomeopenres.14826.1

Kalyaanamoorthy, S., Minh, B. Q., Wong, T. K. F., Von Haeseler, A., and Jermiin, L. S. (2017). ModelFinder: fast model selection for accurate phylogenetic estimates. *Nat. Methods* 14, 587–589. doi: 10.1038/NMETH.4285

Katoh, K., and Standley, D. M. (2013). MAFFT multiple sequence alignment software version 7: improvements in performance and usability. *Mol. Biol. Evol.* 30, 772–780. doi: 10.1093/molbev/mst010

Kemper, L., and Hensel, A. (2023). *Campylobacter jejuni*: targeting host cells, adhesion, invasion, and survival. *Appl. Microbiol. Biotechnol.* 107, 2725–2754. doi: 10.1007/s00253-023-12456-w

Knijn, A., Michelacci, V., Orsini, M., and Morabito, S. (2020). Advanced research infrastructure for experimentation in genomic (ARIES): A lustrum of galaxy experience. bioRxiv [Preprint]. doi: 10.1101/2020.05.14.095901

Kwan, P. S. L., Barrigas, M., Bolton, F. J., French, N. P., Gowland, P., Kemp, R., et al. (2008). Molecular epidemiology of *Campylobacter jejuni* populations in dairy cattle, wildlife, and the environment in a farmland area. *Appl. Environ. Microbiol.* 74, 5130–5138. doi: 10.1128/AEM.02198-07

Lapierre, L., Gatica, M. A., Riquelme, V., Vergara, C., Yañez, J. M., San Martín, B., et al. (2016). Characterization of antimicrobial susceptibility and its association with virulence genes related to adherence, invasion, and cytotoxicity in *Campylobacter jejuni* and *Campylobacter coli* isolates from animals, meat, and humans. *Microb. Drug Resist.* 22, 432–444. doi: 10.1089/mdr.2015.0055

Larsen, M. V., Cosentino, S., Lukjancenko, O., Saputra, D., Rasmussen, S., Hasman, H., et al. (2014). Benchmarking of methods for genomic taxonomy. *J. Clin. Microbiol.* 52, 1529–1539. doi: 10.1128/JCM.02981-13

Lee, C. Y., Tai, C. L., Lin, S. C., and Chen, Y. T. (1994). Occurrence of plasmids and tetracycline resistance among Campylobacter jejuni and Campylobacter coli isolated from whole market chickens and clinical samples. *Int. J. Food Microbiol.* 24, 161–170. doi: 10.1016/0168-1605(94)90115-5

Lehmann, F., Tiralongo, E., and Tiralongo, J. (2006). Sialic acid-specific lectins: occurrence, specificity and function. *Cell. Mol. Life Sci.* 63, 1331–1354. doi: 10.1007/s00018-005-5589-y

Letunic, I., and Bork, P. (2007). Interactive tree of life (iTOL): an online tool for phylogenetic tree display and annotation. *Bioinformatics* 23, 127–128. doi: 10.1093/BIOINFORMATICS/BTL529

Liu, F., Lee, S. A., Xue, J., Riordan, S. M., and Zhang, L. (2022). Global epidemiology of campylobacteriosis and the impact of COVID-19. *Front. Cell. Infect. Microbiol.* 12:979055. doi: 10.3389/fcimb.2022.979055/bibtex

Liu, B., Zheng, D., Jin, Q., Chen, L., and Yang, J. (2018). VFDB 2019: A comparative pathogenomic platform with an interactive web interface. *Nucleic Acids Res.* 47, D687–D692. doi: 10.1093/nar/gky1080

Luo, N., Sahin, O., Lin, J., Michel, L. O., and Zhang, Q. (2003). In vivo selection of Ccampylobacter isolates with high levels of fluoroquinolone resistance associated with gyrA mutations and the function of the CmeABC efflux pump. *Antimicrob. Agents Chemother.* 47, 390–394. doi: 10.1128/AAC.47.1.390-394.2003

Maiden, M. C. J., Van Rensburg, M. J. J., Bray, J. E., Earle, S. G., Ford, S. A., Jolley, K. A., et al. (2013). MLST revisited: the gene-by-gene approach to bacterial genomics. *Nat. Rev. Microbiol.* 11, 728–736. doi: 10.1038/NRMICRO3093

Manfreda, G., Parisi, A., De Cesare, A., Mion, D., Piva, S., and Zanoni, R. G. (2016). Typing of *Campylobacter jejuni* isolated from turkey by genotypic methods, antimicrobial susceptibility, and virulence gene patterns: A retrospective study. *Foodborne Pathog. Dis.* 13, 93–100. doi: 10.1089/fpd.2015.2048

Manning, G., Dowson, C. G., Bagnall, M. C., Ahmed, I. H., West, M., and Newell, D. G. (2003). Multilocus sequence typing for comparison of veterinary and human isolates of *Campylobacter jejuni*. *Appl. Environ. Microbiol.* 69, 6370–6379. doi: 10.1128/AEM.69.11.6370-6379.2003

Marasini, D., and Fakhr, M. K. (2016). Whole-genome sequencing of a *Campylobacter jejuni* Strain isolated from retail chicken meat reveals the presence of a Megaplasmid with mu-like prophage and multidrug resistance genes. *Genome Announc.* 4, 460–476. doi: 10.1128/genomeA.00460-16

Marasini, D., and Fakhr, M. K. (2017). Complete genome sequences of plasmid-bearing Campylobacter coli and Campylobacter jejuni strains isolated from retail chicken liver. *Genome Announc.* 5, e01350–e01367. doi: 10.1128/GENOMEA.01350-17/FORMAT/EPUB

Marasini, D., Karki, A. B., Buchheim, M. A., and Fakhr, M. K. (2018). Phylogenetic relatedness among plasmids harbored by Campylobacter jejuni and Campylobacter coli isolated from retail meats. *Front. Microbiol.* 9:2167. doi: 10.3389/fmicb.2018.02167

Marotta, F., Janowicz, A., Marcantonio, L. D., Ercole, C., Donato, G. D., Garofolo, G., et al. (2020). Molecular characterization and antimicrobial susceptibility of C. jejuni isolates from Italian wild bird populations. *Pathogens* 9:304. doi: 10.3390/PATHOGENS9040304

Marotta, F., Janowicz, A., Romantini, R., Di Marcantonio, L., Di Timoteo, F., Romualdi, T., et al. (2023). Genomic and antimicrobial surveillance of *Campylobacter* population in Italian poultry. *Foods* 12:2919. doi: 10.3390/foods12152919

Morita, D., Arai, H., Isobe, J., Maenishi, E., Kumagai, T., Maruyama, F., et al. (2023). Whole-genome and plasmid comparative analysis of *Campylobacter jejuni* from human patients in Toyama, Japan, from 2015 to 2019. *Microbiol. Spectr.* 11:e0265922. doi: 10.1128/spectrum.02659-22

Morrow, A. L., Ruiz-Palacios, G., Jiang, X., and Newburg, D. S. (2005). Human-milk glycans that inhibit pathogen binding protect breast-feeding infants against infectious diarrhea. *J. Nutr.* 135, 1304–1307. doi: 10.1093/JN/135.5.1304

Mouftah, S. F., Cobo-Díaz, J. F., Álvarez-Ordóñez, A., Elserafy, M., Saif, N. A., Sadat, A., et al. (2021). High-throughput sequencing reveals genetic determinants associated with antibiotic resistance in Campylobacter spp. from farm-to-fork. *PLoS One* 16:e0253797. doi: 10.1371/journal.pone.0253797

Nguyen, L., Schmidt, H. A., von Haeseler, A., and Minh, B. Q. (2015). IQ-TREE: A fast and effective stochastic algorithm for estimating maximum-likelihood phylogenies. *Mol. Biol. Evol.* 32, 268–274. doi: 10.1093/molbev/msu300

Ocejo, M., Oporto, B., Lavín, J. L., and Hurtado, A. (2021). Whole genome-based characterisation of antimicrobial resistance and genetic diversity in Campylobacter jejuni and *Campylobacter coli* from ruminants. *Sci. Rep.* 11:8998. doi: 10.1038/S41598-021-88318-0

Oncel, B., Hasdemir, U., Aksu, B., and Pournaras, S. (2023). Antibiotic resistance in Campylobacter jejuni and Campylobacter coli: significant contribution of an RND type efflux pump in erythromycin resistance. *J. Chemother.* 13, 1–9. doi: 10.1080/1120009X.2023.2267895

Ondov, B. D., Treangen, T. J., Melsted, P., Mallonee, A. B., Bergman, N. H., Koren, S., et al. (2016). Mash: fast genome and metagenome distance estimation using MinHash. *Genome Biol.* 17, 1–14. doi: 10.1186/S13059-016-0997-X/FIGURES/5

Painset, A., Day, M., Doumith, M., Rigby, J., Jenkins, C., Grant, K., et al. (2020). Comparison of phenotypic and WGS-derived antimicrobial resistance profiles of *Campylobacter jejuni* and *Campylobacter coli* isolated from cases of diarrhoeal disease in England and Wales, 2015–16. *J. Antimicrob. Chemother.* 75, 883–889. doi: 10.1093/JAC/DKZ539

Panzenhagen, P., Portes, A. B., Dos Santos, A. M. P., Duque, S. D. S., and Conte Junior, C. A. (2021). The distribution of *Campylobacter jejuni* virulence genes in genomes worldwide derived from the NCBI pathogen detection database. *Gene* 12:1538. doi: 10.3390/GENES12101538

Payot, S., Bolla, J. M., Corcoran, D., Fanning, S., Mégraud, F., and Zhang, Q. (2006). Mechanisms of fluoroquinolone and macrolide resistance in *Campylobacter* spp. *Microb. Infect.* 8, 1967–1971. doi: 10.1016/J.MICINF.2005.12.032

Petkau, A., Stuart-Edwards, M., Stothard, P., and van Domselaar, G. (2010). Interactive microbial genome visualization with GView. *Bioinformatics* 26, 3125–3126. doi: 10.1093/BIOINFORMATICS/BTQ588

Prendergast, D. M., Lynch, H., Whyte, P., Golden, O., Murphy, D., Gutierrez, M., et al. (2022). Genomic diversity, virulence and source of *Campylobacter jejuni* contamination in Irish poultry slaughterhouses by whole genome sequencing. *J. Appl. Microbiol.* 133, 3150–3160. doi: 10.1111/JAM.15753

Robertson, J., and Nash, J. H. E. (2018). MOB-suite: software tools for clustering, reconstruction and typing of plasmids from draft assemblies. *Microb. Genom.* 4:e000206. doi: 10.1099/mgen.0.000206

Robinson, O., Dylus, D., and Dessimoz, C. (2016). Phylo.io: interactive viewing and comparison of large phylogenetic trees on the web. *Mol. Biol. Evol.* 33, 2163–2166. doi: 10.1093/molbev/msw080

Rokney, A., Valinsky, L., Vranckx, K., Feldman, N., Agmon, V., Moran-Gilad, J., et al. (2020). WGS-based prediction and analysis of antimicrobial resistance in *Campylobacter jejuni* isolates from Israel. *Front. Cell. Infect. Microbiol.* 10:365. doi: 10.3389/fcimb.2020.00365

Rosner, B. M., Schielke, A., Didelot, X., Kops, F., Breidenbach, J., Willrich, N., et al. (2017). A combined case-control and molecular source attribution study of human *Campylobacter* infections in Germany, 2011–2014. *Sci. Rep.* 7, 1–12. doi: 10.1038/s41598-017-05227-x

Schwengers, O., Jelonek, L., Dieckmann, M. A., Beyvers, S., Blom, J., and Goesmann, A. (2021). Bakta: rapid and standardized annotation of bacterial genomes via alignment-free sequence identification. *Microb. Genom.* 7:685. doi: 10.1099/mgen.0.000685

Sheppard, S. K., McCarthy, N. D., Falush, D., and Maiden, M. C. J. (2008). Convergence of Campylobacter species: Implications for bacterial evolution. *Science* 320, 237–239. doi: 10.1126/SCIENCE.1155532

Skirrow, M. B. (1994). Diseases due to *Campylobacter*, *Helicobacter* and related bacteria. *J. Comp. Pathol.* 111, 113–149. doi: 10.1016/S0021-9975(05)80046-5

Tanoeiro, L., Oleastro, M., Nunes, A., Marques, A. T., Duarte, S. V., Gomes, J. P., et al. (2022). Cryptic prophages contribution for Campylobacter jejuni and Campylobacter coli introgression. *Microorganisms* 10:516. doi: 10.3390/MICROORGANISMS10030516/S1

Thépault, A., Méric, G., Rivoal, K., Pascoe, B., Mageiros, L., Touzain, F., et al. (2017). Genome-wide identification of host-segregating epidemiological markers for source attribution in *Campylobacter jejuni*. *Appl. Environ. Microbiol.* 83:e03085-16. doi: 10.1128/AEM.03085-16

Vacher, S., Menard, A., Bernard, E., Santos, A., and Megraud, F. (2005). Detection of mutations associated with macrolide resistance in thermophilic *Campylobacter* spp. by real-time PCR. *Microb. Drug Resist.* 11, 40–47. doi: 10.1089/mdr.2005.11.40

van Vliet, A. H. M., Charity, O. J., and Reuter, M. (2021). A Campylobacter integrative and conjugative element with a CRISPR-Cas9 system targeting competing plasmids: A history of plasmid warfare? *Microb. Genom.* 7:000729. doi: 10.1099/mgen.0.000729

Wallden, K., Rivera-Calzada, A., and Waksman, G. (2010). Type IV secretion systems: versatility and diversity in function. *Cell. Microbiol.* 12, 1203–1212. doi: 10.1111/j.1462-5822.2010.01499.x

Whiley, H., van den Akker, B., Giglio, S., and Bentham, R. (2013). The role of environmental reservoirs in human campylobacteriosis. *Int. J. Environ. Res. Public Health* 10, 5886–5907. doi: 10.3390/ijerph10115886

Wieczorek, K., Denis, E., Lachtara, B., and Osek, J. (2017). Distribution of *Campylobacter jejuni* multilocus sequence types isolated from chickens in Poland. *Poult. Sci.* 96, 703–709. doi: 10.3382/PS/PEW343

Wieczorek, K., Wołkowicz, T., and Osek, J. (2018). Antimicrobial resistance and virulence-associated traits of *Campylobacter jejuni* isolated from poultry food chain and humans with diarrhea. *Front. Microbiol.* 9:1508. doi: 10.3389/fmicb.2018.01508

Wysok, B., Uradziński, J., and Wojtacka, J. (2015). Determination of the cytotoxic activity of Campylobacter strains isolated from bovine and swine carcasses in north-eastern Poland. *Pol. J. Vet. Sci.* 18, 579–586. doi: 10.1515/PJVS-2015-0075

Yang, J., Chen, L., Sun, L., Yu, J., and Jin, Q. (2008). VFDB 2008 release: an enhanced web-based resource for comparative pathogenomics. *Nucleic Acids Res.* 36, D539–D542. doi: 10.1093/nar/gkm951

Zhang, J., Guan, J., Wang, M., Li, G., Djordjevic, M., Tai, C., et al. (2023). SecReT6 update: a comprehensive resource of bacterial type VI secretion systems. *Sci. China Life Sci.* 66, 626–634. doi: 10.1007/S11427-022-2172-X

Zhang, D., Zhang, X., Lyu, B., Tian, Y., Huang, Y., Lin, C., et al. (2023). Genomic analysis and antimicrobial resistance of *Campylobacter jejuni* isolated from diarrheal patients—Beijing municipality, China, 2019-2021. *China CDC Wkly.* 5, 424–433. doi: 10.46234/ccdcw2023.080

Zhong, C., Qu, B., Hu, G., and Ning, K. (2022). Pan-genome analysis of Campylobacter: Insights on the genomic diversity and virulence profile. *Microbiol. Spectr.* 10:e0102922. doi: 10.1128/SPECTRUM.01029-22

10.3389/fmicb.2023.1293666

Glossary

MLST	Multilocus sequence typing
CCs	Clonal complexes
EU	European Union
MSs	Member States
ECDC	European Center for Disease Prevention and Control
STs	Sequence types
cgMLST	Core genome multilocus sequence typing
cgST	cgMLST type
ISS	Istituto Superiore di Sanità
mCCD Agar	Modified charcoal cefoperazone deoxycholate agar
EUCAST	European Committee on Antimicrobial Susceptibility Testing
Cip	Ciprofloxacin
T	Tetracycline
E	Erythromycin
Gm	Gentamicin
ECOFFs	Epidemiological cutoff values
WGS	Whole genome sequencing
CGE	Center for genomic epidemiology
VFDB	Virulence factor of pathogenic bacteria server
GView	Genomic Context View
NJ	Neighbor-joining
CBT	Capsule biosynthesis and transport
LOS	Lipooligosaccharides
T6SS	Type VI secretion system
VAS	Virulence-associated secretion
LPS	Lipopolysaccharide
T4SS	Type IV secretion system

frontiers | Frontiers in Microbiology

TYPE Original Research
PUBLISHED 11 January 2024
DOI 10.3389/fmicb.2023.1289549

OPEN ACCESS

EDITED BY
Stuart A. Thompson,
Augusta University, United States

REVIEWED BY
Sankarasubramanian Jagadesan,
University of Nebraska Medical Center, United States
Mohsina Huq,
Qassim University, Saudi Arabia

*CORRESPONDENCE
Li Zhang
✉ L.Zhang@unsw.edu.au
Liang Wang
✉ wangliang@gdph.org.cn

RECEIVED 06 September 2023
ACCEPTED 19 December 2023
PUBLISHED 11 January 2024

CITATION
Luk CYM, Lee SA, Naidovski N, Liu F, Tay ACY, Wang L, Riordan S and Zhang L (2024) Investigation of *Campylobacter concisus* gastric epithelial pathogenicity using AGS cells.
Front. Microbiol. 14:1289549.
doi: 10.3389/fmicb.2023.1289549

Investigation of *Campylobacter concisus* gastric epithelial pathogenicity using AGS cells

Christopher Yau Man Luk[1], Seul A. Lee[1], Nicholas Naidovski[1], Fang Liu[1], Alfred Chin Yen Tay[2], Liang Wang[3,4,5]*, Stephen Riordan[6] and Li Zhang[1]*

[1]School of Biotechnology and Biomolecular Sciences, University of New South Wales, Sydney, NSW, Australia, [2]Helicobacter Research Laboratory, School of Pathology and Laboratory Medicine, Marshall Centre for Infectious Diseases Research and Training, University of Western Australia, Perth, WA, Australia, [3]Laboratory Medicine, Guangdong Provincial People's Hospital (Guangdong Academy of Medical Sciences), Southern Medical University, Guangzhou, Guangdong, China, [4]The Center for Precision Health, School of Medical and Health Sciences, Edith Cowan University, Perth, WA, Australia, [5]Department of Medical Informatics, School of Medical Informatics and Engineering, Xuzhou Medical University, Xuzhou, Jiangsu, China, [6]Gastrointestinal and Liver Unit, Prince of Wales Hospital, University of New South Wales, Sydney, NSW, Australia

Campylobacter concisus is an oral bacterium. Recent studies suggest that *C. concisus* may be involved in human gastric diseases. The mechanisms, however, by which *C. concisus* causes human gastric diseases have not been investigated. Here we examined the gastric epithelial pathogenicity of *C. concisus* using a cell culture model. Six *C. concisus* strains and the human gastric epithelial cell line AGS cells were used. IL-8 produced by AGS cells after incubation with *C. concisus* was measured using enzyme-linked immunosorbent assay (ELISA), and AGS cell apoptosis was determined by caspase 3/7 activities. The effects of *C. concisus* on actin arrangement in AGS cells was determined using fluorescence staining. The effects of *C. concisus* on global gene expression in AGS cells was determined by transcriptomic analysis and quantitative real-time PCR (qRT-PCR). The role of the upregulated *CYP1A1* gene in gastric cancer survival was assessed using the Kaplan-Meier method. *C. concisus* induced production of IL-8 by AGS cells with strain variation. Significantly increased caspase 3/7 activities were observed in AGS cells incubated with *C. concisus* strains when compared to AGS cells without bacteria. *C. concisus* induced actin re-arrangement in AGS cells. *C. concisus* upregulated 30 genes in AGS cells and the upregulation of *CYP1A1* gene was confirmed by qRT-PCR. The Kaplan-Meier analysis showed that upregulation of *CYP1A1* gene is associated with worse survival in gastric cancer patients. Our findings suggest that *C. concisus* may play a role in gastric inflammation and the progression of gastric cancer. Further investigation in clinical studies is warranted.

KEYWORDS

***Campylobacter concisus*, *Campylobacter*, gastritis, oral *Campylobacter*, CYP1A1**

Introduction

Campylobacter concisus is a gram-negative bacterium that is motile, with a curved or spiral shape. The bacterium can grow under both anaerobic and microaerophilic conditions, with hydrogen gas being crucial for its growth (Lee et al., 2014). *C. concisus* is further classified into two genomospecies (GS): GS1 and GS2, distinguished by the core-genome, 23 rRNA gene, and GS-specific genes (Miller et al., 2012; Chung et al., 2016; Huq et al., 2017; Liu et al., 2018; Aagaard et al., 2021; Cornelius et al., 2021). Previous studies have reported that *C. concisus* GS2 strains exhibit better adaptation in the gastrointestinal tract (Wang et al., 2017) and a better ability to invade intestinal epithelial cells compared to GS1 strains (Kalischuk and Inglis, 2011; Ismail et al., 2012; Mahendran et al., 2015). These findings align with the observation that GS2 strains are more frequently detected in mucosal biopsy samples and fecal samples from patients with gastrointestinal diseases (Kirk et al., 2018). Virulence factors of *C. concisus*, such as zonula occludens toxin, phospholipase A, as well as the functional protein BisA, have been characterized (Istivan et al., 2004; Mahendran et al., 2016; Benoit and Maier, 2023).

While commonly present in the human oral cavity as a commensal bacterium (Zhang et al., 2010), *C. concisus* is associated with inflammatory conditions of extraoral diseases such as inflammatory bowel disease (IBD), including Crohn's disease (CD) and ulcerative colitis (UC) (Zhang L. et al., 2009; Man et al., 2010; Mukhopadhya et al., 2011), microscopic colitis, and Barrett's esophagus (Macfarlane et al., 2007; Yang et al., 2009; Nielsen et al., 2020). Previous studies have also investigated the pathogenic mechanisms by which *C. concisus* may contribute to the development of the associated intestinal and esophageal diseases, including the induction of proinflammatory cytokines such as interleukin 8 (IL-8) and tumor necrosis factor alpha (TNF-α), epithelial cell death, immunmodulators MD-2 and programmed death-ligand 1 (PD-L1), as well as enhancing the responses of epithelial cells and macrophages to commensal bacterial species (Lee et al., 2021).

Recent studies suggest that *C. concisus* may also be involved in human gastric diseases. A study by Ferreira et al. (2022) examined the cultivation of *Helicobacter pylori* and *C. concisus* from 2,191 gastric biopsies. They reported that *C. concisus* was cultured from 50 gastric biopsies (50/2191, 2.3%) and *H. pylori* cultured from 168 gastric biopsies (168/2191, 7.7%). In twenty-eight cases with concurrent histology, *C. concisus* was found to be *H. pylori* immunoreactive positive (Ferreira et al., 2022). A study by Cui et al. (2019) examined the tongue coating microbiome of 78 patients with gastritis and 50 healthy controls. This study found that the abundance of *C. concisus* in tongue coating microbiome was associated with the gastric precancerous cascade. They also detected *C. concisus* in gastric fluids of patients with gastritis (Cui et al., 2019).

Despite being suggested to play a role in human gastric diseases, no studies have examined the mechanisms by which *C. concisus* may contribute to the pathogenesis of gastric diseases. Considering that gastric epithelial cells are the first line of human cells to encounter pathogens in the stomach, this study aimed to examine the pathogenic effects of *C. concisus* strains on human gastric epithelial cells using a cell culture model. Our data provide novel insights into understanding *C. concisus* gastric pathogenicity.

Materials and methods

Bacterial strains used in this study

For this study, we randomly selected six oral *C. concisus* strains with complete genomes sequenced from *C. concisus* strains we previously isolated from human saliva samples (Liu et al., 2020). P10CDO-S2, P3UCO1, and H1O1 are GS1 strains and P2CDO4, P15UCO-S2, and H16O-S1 are GS2 strains. The details of the six *C. concisus* strains were provided in **Supplementary Table 1**. The *C. concisus* strains were cultured on horse blood agar (HBA) plates, using blood agar base No. 2 (Thermo Fisher Scientific, CA, USA), supplemented with 6% defibrinated horse blood. The cultures were incubated at 37^{o}C under anaerobic conditions with 5% hydrogen for 48 h, as previously described (Lee et al., 2014).

H. pylori strain 26695, a human gastric pathogen, was used as a positive control in this study (Ashktorab et al., 2008; Fazeli et al., 2016). *H. pylori* strain 26695 was cultured on HBA plates at 37^{o}C under microaerobic conditions generated using CampyGen 2.5L Atmosphere Generation System (Thermo Fisher Scientific) for 48 h before being used in experiments.

Maintenance of AGS cells

The human gastric adenocarcinoma cell line AGS (ATCC No. CRL-1739) was used as a model for human gastric epithelium. AGS cells were maintained in F-12K medium (Thermo Fisher Scientific) supplemented with 10% fetal bovine serum (FBS) (Cytiva, MA, USA), 100 U/mL penicillin, and 100 μg/mL streptomycin (Thermo Fisher Scientific), which was referred to as F-12K/FBS/Antibiotics medium in this study. The AGS cells were incubated in a humidified incubator at 37°C with 5% CO_2, following recommended maintenance procedures by ATCC.

Measurement of IL-8 by enzyme-linked immunosorbent assay (ELISA)

Enzyme-linked immunosorbent assay was used to measure IL-8 production by AGS cells in response to *C. concisus*. AGS cells were seeded on a 96-well plate at a concentration of 1×10^5 cells/well in F-12K/FBS/Antibiotics medium. Following 24 h incubation, the cell culture medium was replaced with F-12K medium supplemented with FBS but without penicillin and streptomycin, which was referred to as F-12K/FBS medium. The AGS cells were then incubated with the six *C. concisus* strains (in triplicates) described above at a multiplicity of infection (MOI) of 100 for 24 h. As *C. concisus* at MOI 100 induced the production of IL-8 by other epithelial cells of the gastrointestinal tract in a previous study, this condition was therefore used in the current study (Lee et al., 2021). AGS cells without bacterial infection served as the negative control. *H. pylori* strain 26695 was also introduced at MOI 10 and 100,

which served as a positive control (O'Hara et al., 2006; Zhang Y. et al., 2009). To investigate the combined effects of *C. concisus* and *H. pylori* on IL-8 production by AGS cells, AGS cells were incubated with *C. concisus* strains P2CDO4 and P3UCO1 at MOI 100 along with *H. pylori* strain 26695 at MOI 10 and 100 for 24 h, respectively. The AGS cell culture supernatants were then collected to measure the concentration of IL-8 using commercially available ELISA kits (Invitrogen, CA, USA) in triplicates, following the manufacturer's instructions.

Caspase 3/7 assay

Measurement of caspase 3/7 activity was used to assess apoptotic activity in AGS cells induced by *C. concisus*, as described previously (Lee et al., 2021). In brief, AGS cells were seeded on a black-walled 96-well plate with transparent bottoms at a concentration of 1×10^5 cells/well in F-12K/FBS/Antibiotics medium. After 24 h incubation, the cell culture medium was replaced with F-12K/FBS medium. The AGS cells were then incubated with the six *C. concisus* strains described above at MOI 100 for 24 h, with untreated AGS cells serving as the negative control. *H. pylori* strain 26695 was included at MOI 10 and 100 as the bacterial control. To examine the combined effects of *C. concisus* and *H. pylori* on the apoptotic activity of AGS cells, AGS cells were incubated with *C. concisus* strains P2CDO4 and P3UCO1 at MOI 100 along with *H. pylori* strain 26695 at MOI 10 and 100 for 24 h, respectively. AGS cells were washed three times with Dulbecco's phosphate-buffered saline (DPBS) before being stained with CellEvent Caspase-3/7 Green ReadyProbes reagent (Invitrogen), following manufacturer's instructions. The fluorescence readings of caspase 3/7 activity were measured in triplicates and expressed in fold change relative to the untreated control.

Examination of the effects of *C. concisus* on F-actin arrangement in AGS cells by fluorescence staining

AGS cells were seeded on coverslips in a 24-well plate at a concentration of 1×10^6 cells/well in F-12K/FBS/Antibiotics medium. After 24 h incubation, the cell culture medium was replaced with F-12K/FBS medium. AGS cells were then incubated with *C. concisus* strains P2CDO4, P3UCO1, or *H. pylori* strain 26695 at MOI 100 for 24 h, with untreated AGS cells serving as the negative control. The AGS cells were fixed with 3.6% paraformaldehyde for 15 min, permeabilized with 0.1% triton for 10 min, and blocked with 1% bovine serum albumin (BSA) for 1 h. The filamentous actin (F-actin) and nuclei were then stained with Alexa Fluor 488 phalloidin (8878S, Cell Signaling Technology, MA, USA) and Hoechst 33342 (Invitrogen) respectively. The cells were mounted onto glass slides with 50% glycerol in water and examined using a fluorescent microscope (Olympus BX61; Olympus, Tokyo, Japan) with FITC (Excitation wavelength: 480 nm; Emission wavelength: 520 nm) and DAPI (Excitation wavelength: 365 nm; Emission wavelength: 430 nm) filters under the 100X objective. AGS cells without bacteria served as the negative control, and AGS cells incubated with *H. pylori* served as the positive control (Chang et al., 2016).

Examination of the global gene responses induced by *C. concisus* in AGS cells by transcriptomic analysis

AGS cells were seeded in triplicates on 6-well cell culture plates at a concentration of 2×10^6 cells/well in F-12K/FBS/Antibiotics medium. After 24 h incubation, the medium was replaced with F-12K/FBS medium. The AGS cells were then incubated with *C. concisus* strain P2CDO4, which was randomly selected.

Supernatants from AGS cells incubated with *C. concisus* strain P2CDO4 at MOI 50 for 4 h and without bacterial infection were collected for IL-8 measurement, as described above. The AGS cells were then washed three times with DPBS before being collected for RNA extraction. The total RNA of AGS cells was extracted using the ISOLATE II RNA Mini Kit (cat. no. BIO-52072; Bioline, NSW, Australia), following the manufacturer's instructions. The purity and concentration of the extracted total RNA were measured using a NanoDrop spectrophotometer. The extracted total RNA was then submitted to the Ramaciotti Centre for Genomics, University of New South Wales, for RNA sequencing. The library preparation was conducted as previously described (Lee et al., 2023).

For RNA-seq data analysis, the raw RNA-seq reads were first checked for quality using FastQC (version 0.11.8). Adapters and low-quality reads were then trimmed using Trimmomatic (version 0.38) with the leading and trailing filters set to a minimum of Phred score 3 and a sliding window of 4:15, filtered reads with length less than 30 bp were also removed (Bolger et al., 2014). The trimmed reads were mapped against the human reference genome GRCh38.p14 using HISAT2 (version 2.1.0) under default settings (Kim et al., 2019). The mapped read counts SAM files generated from HISAT2 were then converted into BAM files using SAMtools (version 1.11) (Danecek et al., 2021). The mapped read counts were then quantified using featureCounts under the Subread package (version 2.0.1) for DEG analysis (Liao et al., 2014). Significantly differentially expressed genes between AGS cells with and without *C. concisus* infection were identified using the BioConductor package DESeq2 (version 1.36.0) in the R programming environment under default normalization methods, with adjusted $P < 0.05$ and $\log_2$ fold change < -1 and > 1 being considered significant (Love et al., 2014).

Gene ontology (GO) enrichment analysis

The list of differentially expressed genes (DEG) was uploaded to Metascape for GO enrichment analysis under default settings (Zhou et al., 2019). Enriched clusters of cellular biological processes were sorted according to *P*-value.

Quantitative real-time PCR (qRT-pCR)

A literature search in the PubMed database was conducted to examine whether the upregulated genes in AGS cells, as

revealed by transcriptomic analysis, were associated with the development of gastric cancer, using the gene name and gastric cancer as keywords. The upregulation of the gastric cancer-associated gene, *CYP1A1*, was further confirmed using qRT-PCR. For qRT-PCR, the total RNA (2 μg/sample) extracted from AGS cells with or without *C. concisus* infection was subjected to cDNA synthesis using the Tetro cDNA Synthesis kit (Bioline, NSW, Australia), following manufacturer's instructions. SensiFAST SYBR No-ROX Mix (Bioline, NSW, Australia) was used for quantifying the synthesized cDNA in qRT-PCR in triplicates. The mRNA expression levels were normalized to the levels of the housekeeping gene glyceraldehyde 3-phosphate dehydrogenase (GAPDH) and expressed as fold changes relative to untreated cells, using the comparative threshold cycle CT ($2^{-\Delta\Delta CT}$) method (Livak and Schmittgen, 2001). The sequences of PCR primers for quantification of CYP1A1 and qRT-PCR conditions are in **Supplementary Table 2**.

Analysis of the role of CYP1A1 in gastric cancer patient survival

The gene encoding CYP1A1 was subjected to survival analysis in gastric cancer patients using the Kaplan–Meier Plotter website (Lánczky and Győrffy, 2021). The survival plot was generated using JetSet best probe set for the submitted genes, with a database of 631 gastric cancer patients which are classified as low or high expression cohorts. The overall survival differences between low and high expression cohorts were analyzed using the Kaplan-Meier method and log-rank test, $P < 0.05$ was considered as significant and other options remained default.

Summary of experimental workflow

The experimental workflow of this study is summarized in **Figure 1**, outlining the key experiments conducted. These include the examination of *C. concisus* pathogenicity to AGS cells, transcriptomic analysis of gene expression changes, and the subsequent validation of *CYP1A1* gene expression through qRT-PCR.

Statistical analysis

P-values for different samples in ELISA and caspase 3/7 assay were calculated using one-way analysis of variance (ANOVA) with Dunnett's test, while *P*-value for samples in qRT-PCR were

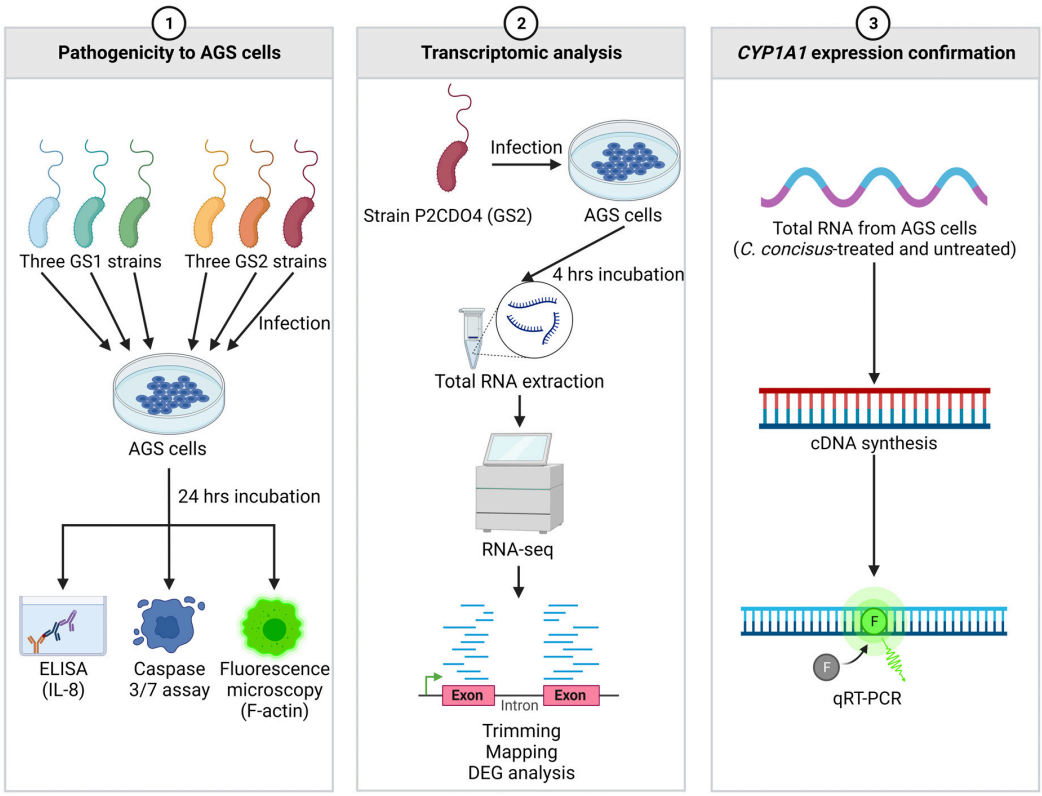

FIGURE 1
Summary of experimental workflow of this study. Experiments conducted in this study were classified into three categories. The first category involved examining the pathogenicity of *C. concisus* in AGS cells using ELISA, caspase 3/7 assay, and fluorescence microscopy. The second category focused on transcriptomic analysis of global gene response in AGS cells incubated with *C. concisus* through RNA-seq. The third category aimed to validate the gene expression level of *CYP1A1* using qRT-PCR. Figure created with BioRender.com.

10.3389/fmicb.2023.1289549

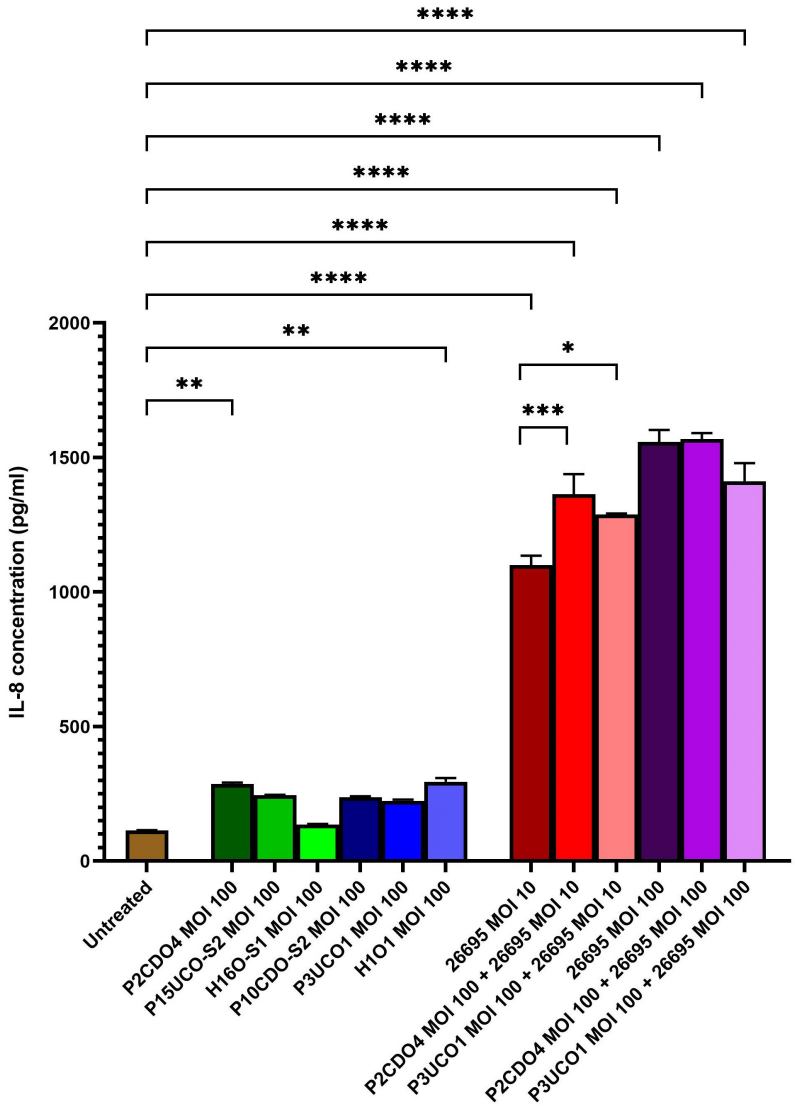

FIGURE 2
IL-8 production by AGS cells induced by *C. concisus* strains and *H. pylori* strain 26695 after 24 h incubation. IL-8 concentrations were measured by ELISA using supernatants of AGS cells after incubating with *C. concisus* strains and *H. pylori* strain 26695 for 24 h. *C. concisus* strains P2CDO4 and H1O1 at MOI 100 induced significantly higher IL-8 productions in AGS cells as compared to the untreated control ($P < 0.01$). *H. pylori* strain 26695 at both MOI 10 and 100 induced significantly higher IL-8 productions as compared to *C. concisus* at MOI 100. Co-incubation of *H. pylori* at MOI 10 with *C. concisus* strains (P2CDO4 and P3UCO1) induced significantly higher levels of IL-8 production as compared to that incubated by *H. pylori* alone ($P < 0.001$ and $P < 0.05$ respectively), however this increase was not observed when *H. pylori* was incubated at MOI 100. One-way analysis of variance (ANOVA) with Dunnett's test was performed to test for statistical significance between untreated and infected AGS cells. Graph columns represent averages of triplicate experiments ± standard error (****$P < 0.0001$, ***$P < 0.001$, **$P < 0.01$, *$P < 0.05$; MOI, multiplicity of infection).

calculated using two-tailed unpaired *t*-test. $P < 0.05$ was considered statistically significant. All statistical analyses were conducted using GraphPad Prism (version 9.5.1).

Results

C. concisus induced IL-8 production in AGS cells

All six *C. concisus* strains examined at MOI 100 induced the production of IL-8 by AGS cells after a 24-h incubation period. Notably, the levels of IL-8 production in AGS cells incubated with *C. concisus* strains P2CDO4 and H1O1 were 286.64 ± 4.75 and 295.29 ± 11.5 pg/ml, respectively ($P < 0.01$). These values were statistically significant, indicating a higher induction of IL-8 production compared to AGS cells without bacterial infection (114.63 ± 0.68 pg/ml) (Figure 2). IL-8 production by AGS cells incubated with *C. concisus* strains P15UCO-S2, H16O-S1, P10CDO-S2, and P3UCO1 were 244.9 ± 1.22, 135.19 ± 2.41, 237.2 ± 3.12, and 224.54 ± 3.92 pg/ml, respectively. While these values were higher than the untreated sample, they were not considered statistically significant ($P > 0.05$) (Figure 2). Furthermore, *H. pylori* strain 26695 induced higher IL-8 production in AGS cells compared to *C. concisus* strains. The

10.3389/fmicb.2023.1289549

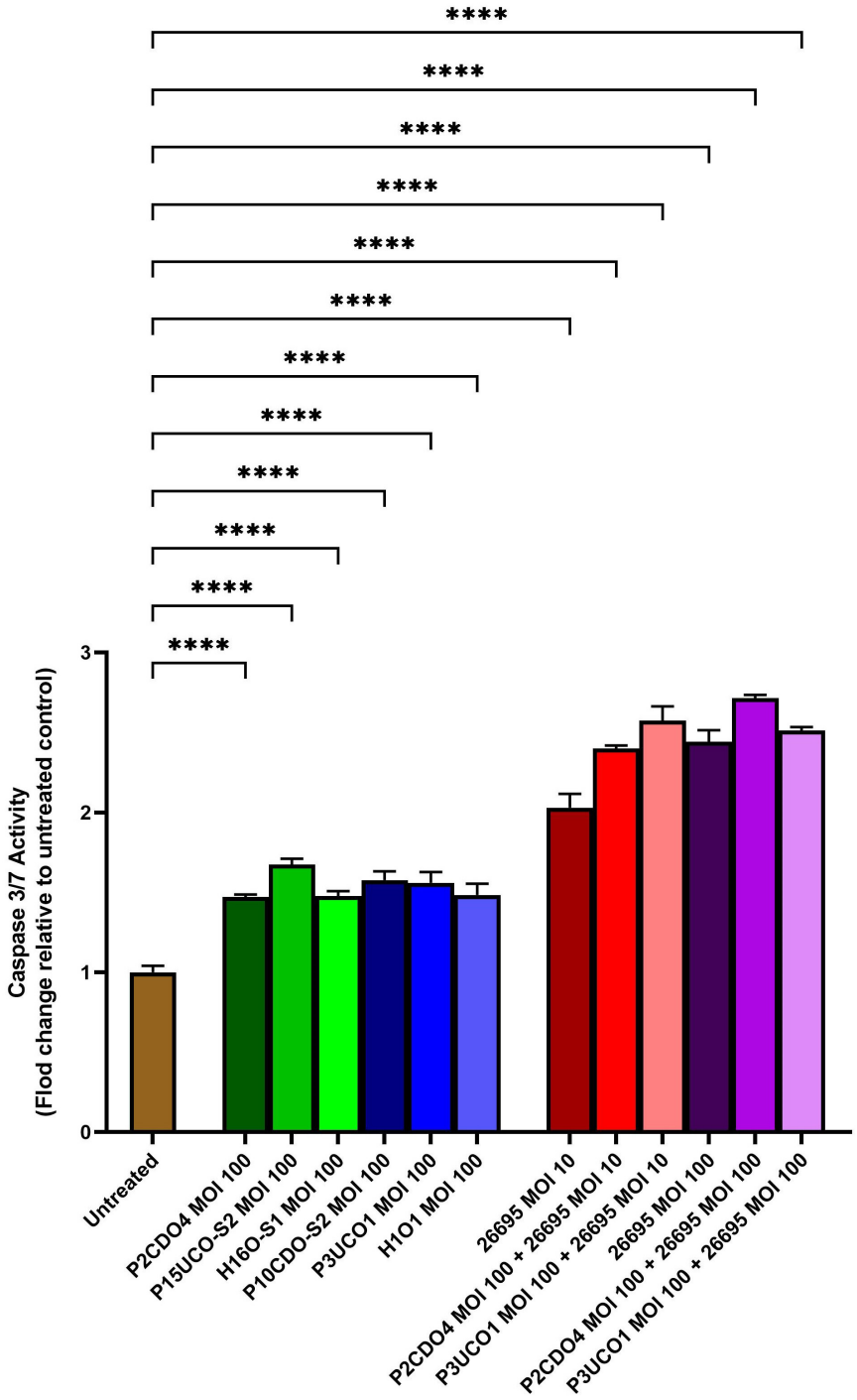

FIGURE 3
Caspase 3/7 activity of AGS cells infected with *C. concisus* strains and *H. pylori* strain 26695 after 24 h. Caspase 3/7 activity was measured using CellEvent caspase 3/7 green detection reagent. All six *C. concisus* strains at MOI 100, as well as *H. pylori* strain 26695 at both MOI 10 and 100, induced significantly higher levels of caspase 3/7 activity as compared to the untreated control ($P < 0.0001$). Co-incubation of *C. concisus* with *H. pylori* did not induce higher levels of caspase 3/7 activity as compared to that incubated with *H. pylori* alone. One-way analysis of variance (ANOVA) with Dunnett's test was performed to test for statistical significance between untreated and infected AGS cells. Graph columns represent averages of triplicate experiments ± standard error (****$P < 0.0001$; MOI, multiplicity of infection).

levels of IL-8 production by AGS cells incubated with *H. pylori* strain 26695 at MOI 10 and 100 were 1099.58 ± 29.18 and 1557.94 ± 36.05 pg/ml, respectively, which were significantly higher than the IL-8 production induced by the *C. concisus* strains ($P < 0.0001$) (Figure 2).

In AGS cells incubated with *H. pylori* strain 26695 at MOI 10, the presence of *C. concisus* increased the production of IL-8. Co-incubation of *H. pylori* strain 26695 with P2CDO4 and P3UCO1 resulted in significantly higher levels of IL-8 compared to AGS cell incubated with *H. pylori* alone, with concentrations

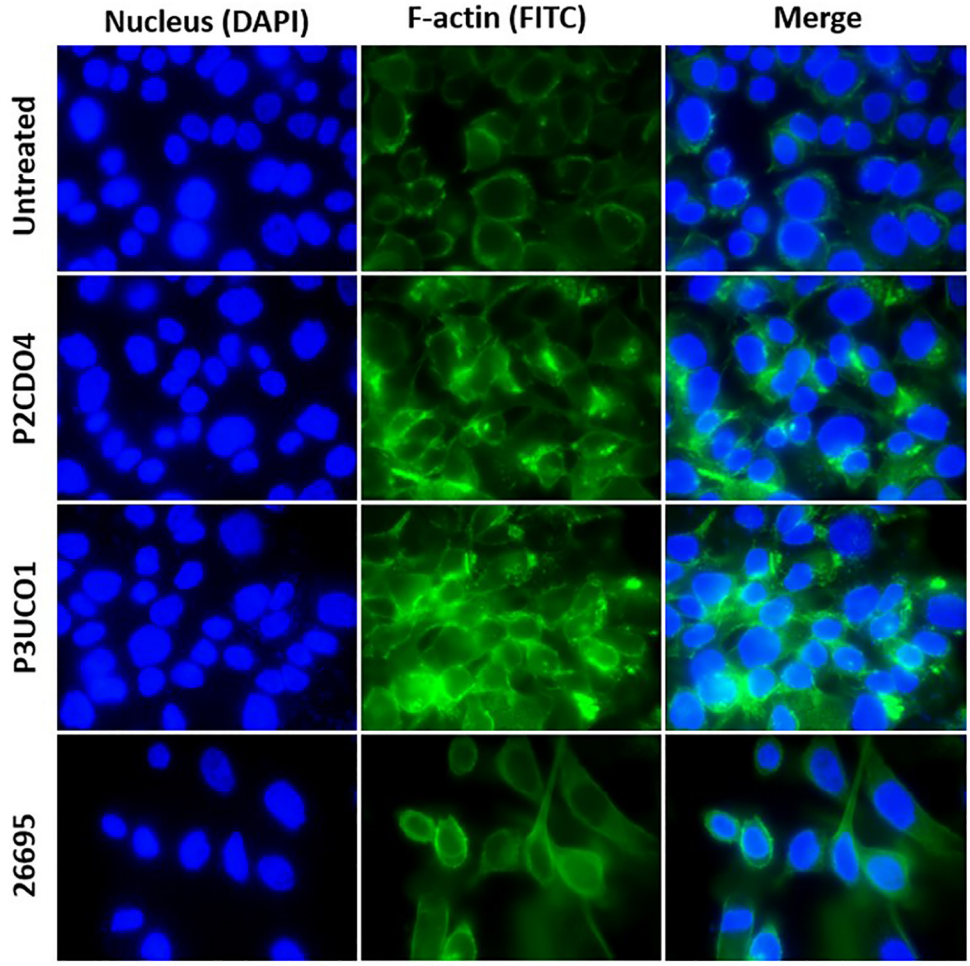

FIGURE 4
F-actin arrangement in AGS cells incubated with *C. concisus* strain P2CDO4, P3UCO1, and *H. pylori* strain 26695 for 24 h. Cell nucleus and F-actin were stained with Hoechst 33342 and Alexa Fluor 488 phalloidin and visualized using DAPI and FITC filters, respectively. Infection of AGS cells with the *C. concisus* strains P2CDO4 and P3UCO1 showed F-actin aggregation. *H. pylori* infection caused an elongated cell phenotype of AGS cells.

of 1363.63 ± 60.97 ($P < 0.001$) and 1287.99 ± 3.47 pg/ml ($P < 0.05$), respectively (Figure 2). However, in AGS cells incubated with *H. pylori* strain 26695 at MOI 100, co-incubation with *C. concisus* strains P2CDO4 and P3UCO1 induced IL-8 production at 1568.5 ± 18.48 and 1412.19 ± 55 pg/ml, respectively, which was not significantly different from that induced by *H. pylori* alone ($P > 0.05$) (Figure 2).

C. concisus induced apoptosis in AGS cells

C. concisus induced apoptosis in AGS cells when incubated with *C. concisus* strains at MOI 100 for 24 h, as indicated by increased caspase 3/7 activity. The levels of caspase 3/7 activity (expressed as fold change relative to the untreated AGS cells) in AGS cells incubated with *C. concisus* strains P2CDO4, P15UCO-S2, H16O-S1, P10CDO-S2, P3UCO1, and H1O1 at MOI 100 were 1.47 ± 0.01, 1.67 ± 0.03, 1.48 ± 0.02, 1.58 ± 0.04, 1.56 ± 0.06, and 1.48 ± 0.06 fold, respectively ($P < 0.0001$) (Figure 3). These values were all significantly higher than that of the untreated AGS cells. The caspase 3/7 activity in AGS cells incubated with *H. pylori* strain 26695 at MOI 10 and 100 for 24 h was 2.03 ± 0.07 and 2.44 ± 0.06 fold, respectively ($P < 0.0001$), indicating a higher apoptotic activity compared to that induced by *C. concisus* strains. Moreover, AGS cells incubated with *C. concisus* strain P2CDO4 at MOI 100, and P3UCO1 at MOI 100 along with *H. pylori* strain 26695 at MOI 10 and 100 respectively, also exhibited significantly higher apoptotic activity at 2.4 ± 0.02, 2.57 ± 0.07, 2.71 ± 0.02, and 2.51 ± 0.02 fold, respectively ($P < 0.0001$).

C. concisus induced F-actin aggregation in AGS cells

Both *C. concisus* strains examined caused F-actin aggregation in comparison to AGS cells without bacterial infection (Figure 4). AGS cells incubated with *H. pylori* strain 26695 showed sign of elongation, indicative of the hummingbird phenotype caused by the protein encoded by cytotoxin-associated gene A (CagA) in *H. pylori* (Moese et al., 2004; Chang et al., 2016).

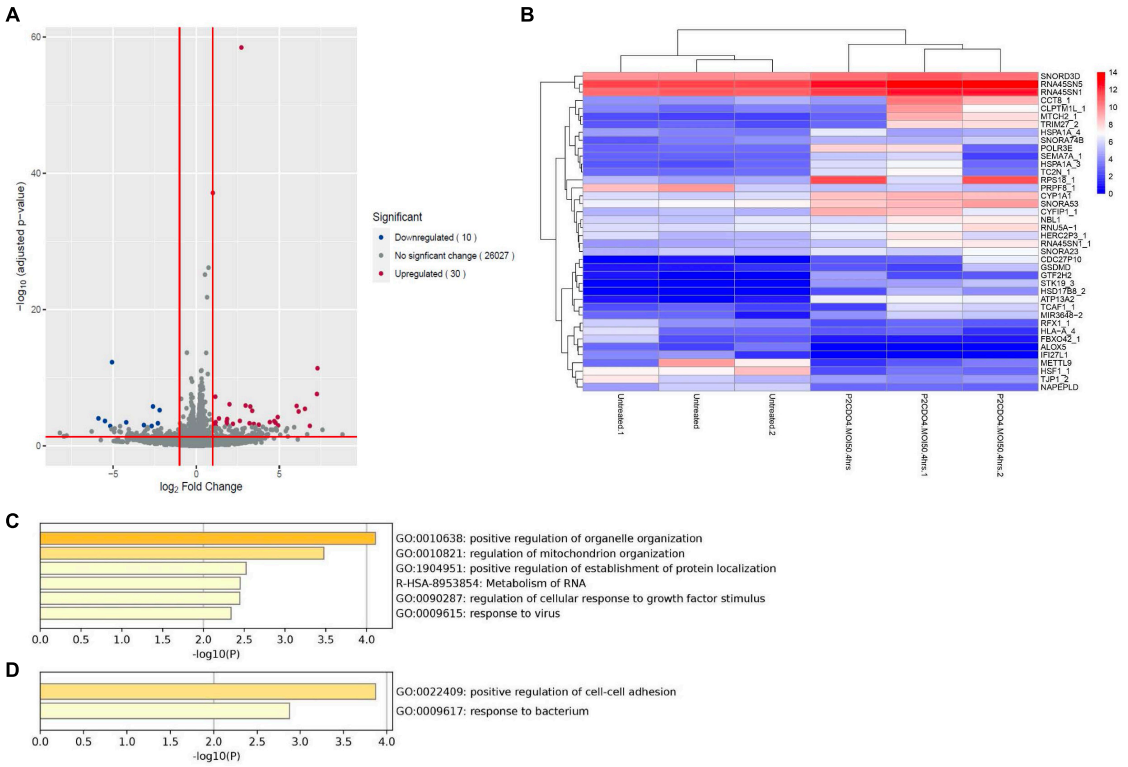

FIGURE 5
Transcriptomic analysis on global gene expression in AGS cells induced by *C. concisus* strain P2CDO4 after 4 h incubation. **(A)** The volcano plot illustrates a total of 26,067 transcripts from RNA-seq reads, with 30 transcripts significantly upregulated (red) and 10 transcripts significantly downregulated (blue). Genes with adjusted *P*-value < 0.05 and $\log_2$ fold change < -1 and >1 were considered statistically significant. Volcano plot generated using the EnhancedVolcano package on the R platform. **(B)** The heatmap shows the 40 differentially expressed genes based on $\log_2$ gene counts. Heatmap generated using the pheatmap package on the R platform. **(C)** The Gene ontology (GO) enrichment analysis revealed that upregulated genes mainly affect the regulation of organelle and mitochondria organization. **(D)** The GO enrichment analysis revealed that downregulated genes mainly affect the regulation of cell-cell adhesion.

C. concisus upregulated the expression of gastric cancer associated CYP1A1 gene in AGS cells

Analysis of RNA-seq data revealed notable alterations in global gene response in AGS cells incubated with *C. concisus* strain P2CDO4 for 4 h, compared to untreated AGS cells (**Supplementary Figure 1**). From the global gene response, 40 genes were considered significantly altered in expression (adjusted *P*-value < 0.05, $\log_2$ fold change < -1 and >1), of which 30 genes were upregulated and 10 genes downregulated (**Figures 5A, B** and **Supplementary Table 3**). The upregulated genes are predicted to predominately affect organelle and mitochondrion organization, and the down regulated genes mainly affect the regulation of cell-cell adhesion (**Figures 5C, D**). Of the 30 upregulated genes by *C. concisus*, four genes were reported to be associated with gastric cancer including *HSD17B8_2*, *TRIM27_2*, *TC2N_1*, and *CYP1A1*. However, three of these genes had an underscore following their gene names, showing that they are on alternate reference locus (Bruford et al., 2020). We therefore decided to further characterize only *CYP1A1* gene using qRT-PCR.

Transcriptomic analysis revealed that the expression of the upregulated gene *CYPIA1* was 6.57 fold in AGS cells incubated with *C. concisus* P2CDO4 at MOI 50 for 4 h, with a read count of 342.7 ± 35.38, compared to 62.3 ± 5.17 reads in untreated AGS cells (**Figure 6A**). This was confirmed using by qRT-PCR, which showed a 4.2 ± 0.64 fold increase relative to AGS cells without *C. concisus* infection (**Figure 6B**). According to the Kaplan-Meier Plotter survival analysis, a higher level expression of *CYP1A1* is associated with poor prognosis in gastric cancer patients, with a hazard ration of 1.86 and median survival period of 20.4 months as opposed to 56.9 months in low expression cohort (**Figure 6C**).

The IL-8 level was 199.96 ± 1.58 pg/ml in the supernatant of AGS cells incubated with *C. concisus* strain P2CDO4 for 4 h, and 179.83 ± 6.02 pg/ml in the supernatant of untreated AGS cells ($P < 0.005$).

The RNA-seq data have been deposited in NCBI's Gene Expression Omnibus and are accessible through GEO Series accession number GSE242316.[1]

Discussion

This study aimed to investigate the pathogenic effects of *C. concisus* strains on human gastric epithelial cells using AGS cells as a model for gastric epithelium.

1 https://www.ncbi.nlm.nih.gov/geo/query/acc.cgi?acc=GSE242316

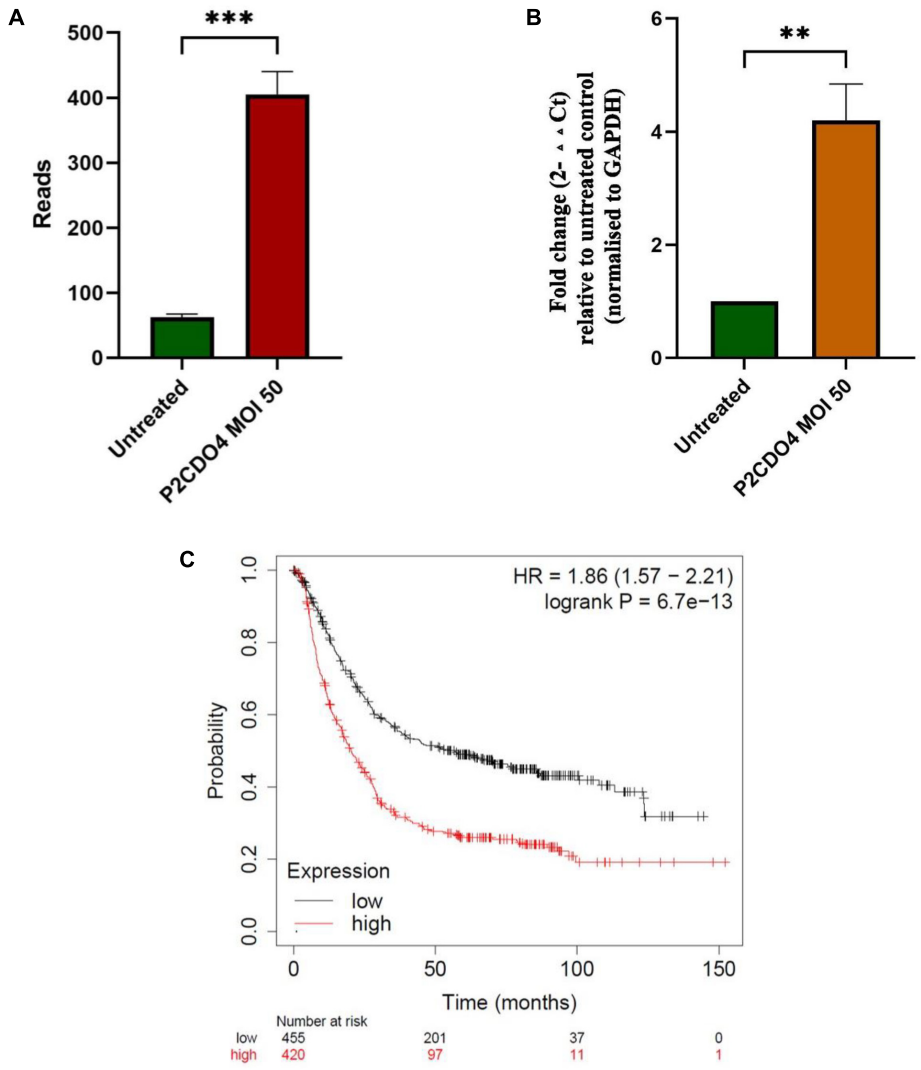

FIGURE 6
C. concisus strain P2CDO4 upregulated expression of gastric cancer associated *CYP1A1* gene in AGS cells. **(A)** The upregulation of the *CYP1A1* gene induced *by C. concisus* P2CDO4 was shown by gene reads from RNA-seq (***$P < 0.001$). **(B)** The upregulation of the *CYP1A1* gene was confirmed by qRT-PCR, with the experimental samples being AGS cells incubated with *C. concisus* strain P2CDO4 at MOI 50 for 4 h, and the untreated AGS cells as negative control. Fold change is calculated using the comparative threshold cycle CT ($2^{-\Delta\Delta CT}$) method. Target gene fold change is relative to the untreated control, normalized to housekeeping gene GAPDH. Graph columns represent averages of triplicate experiments ± standard error (**$P < 0.01$; MOI, multiplicity of infection). **(C)** The survival plot shows that a higher level expression of CYP1A1 is associated with poor prognosis in gastric cancer patients, with a hazard ratio (HR) of 1.86 and median survival period of 20.4 months as opposed to 56.9 months in low expression cohort.

C. concisus strains were found to induce the production of proinflammatory cytokine IL-8 in AGS cells following 24 h of incubation. IL-8, a chemokine known for inducing chemotaxis of neutrophils and other immune cells (Harada et al., 1994). In our study, all *C. concisus* strains induced the production of IL-8 in AGS cells, suggesting that *C. concisus* has the potential to induce gastric inflammation. The significant genomic diversity observed among *C. concisus* strains aligns with their varying capacities to induce IL-8 (**Figure 2**; Gemmell et al., 2018; Aagaard et al., 2021). *C. concisus* strains induced much less gastric epithelial production of IL-8, as compared to *H. pylori* strain 26695 (**Figure 2**). This finding suggests that *C. concisus* bacteria are more inclined to cause mild gastric inflammation in comparison to the more robust inflammatory response triggered by *H. pylori*.

In a study by Ma et al. (2015) it was observed that 4 out of 20 *C. concisus* strains were able to survive a 30-min exposure to low pH in a test tube. This suggests that certain *C. concisus* bacteria may endure the gastric environment for a limited period, potentially allowing them to relocate to a safer zone (Ma et al., 2015). In the human stomach, the mucus layer proximal to the epithelial cells maintains a higher pH. Given the motility and spiral to curved shape of *C. concisus* bacteria, it is conceivable that they could swim toward a more secure region closer to the gastric epithelium, similar to *H. pylori*. This ability to survive in the gastric environment aligns with findings by Ferreira et al. (2022)

who cultured *C. concisus* from gastric biopsies, providing further evidence for the potential colonization of the human stomach by *C. concisus* bacteria. However, as *C. concisus* does not possess urease, their ability in resisting gastric acid would be lower than *H. pylori*.

Interestingly, we found that co-infection of *C. concisus* and *H. pylori* increased the production of IL-8 in AGS cells, suggesting a potential synergistic effect between these bacteria in inducing inflammation. This could have implications for individuals with gastric *H. pylori* colonization, where the presence of *C. concisus* might enhance the inflammatory response in gastric epithelial cells. On the other hand, *C. concisus* did not increase IL-8 production in AGS cells incubated with *H. pylori* at MOI 100, most likely due to that the AGS cells have reached its maximum capability of producing IL-8 under the stimulation of higher numbers of *H. pylori* bacteria (**Figure 2**).

The increase in caspase 3/7 activities in AGS cells following 24 h incubation with *C. concisus* strains were significant, although *H. pylori* strain 26695 induced a significantly higher level of caspase 3/7 activity than *C. concisus* (**Figure 3**). This suggests that *H. pylori* has caused more damage to gastric epithelial cells than *C. concisus* under the same MOI, which apoptotic activity in gastric epithelial cells was known to increase in *H. pylori*-induced gastritis (Dang et al., 2020). The co-infection of *C. concisus* and *H. pylori* further increased the level of caspase 3/7 activity in AGS cells, suggesting a potential synergistic effect on apoptosis (**Figure 3**). Our findings suggest that induction of apoptosis is a potential mechanism by which *C. concisus* may contribute to gastric diseases, especially when coexisting with *H. pylori*.

C. concisus induced F-actin aggregation in AGS cells. The actin cytoskeleton regulates various cellular processes in eukaryotic cells, providing structural integrity at cell-cell junctions and promote membrane extensions (Hartsock and Nelson, 2008; Svitkina, 2018). Actin filaments are frequently targeted by bacterial pathogens, including *H. pylori*. *H. pylori* adheres to gastric epithelial cells via adhesins BabA and SabA and delivers CagA and other bacterial factors into the host epithelial cytosol. This process results in the phosphorylation and dephosphorylation of proteins in different pathways, rearrangement of actin and ZO-1, and disruption of the gastric epithelial barrier. Previous studies have reported that *H. pylori* CagA can induce a "hummingbird" phenotype change in gastric epithelial cells, which was also observed in our experiment (**Figure 4**). Interestingly, we found that *C. concisus* caused a different type of actin rearrangement, specifically actin aggregations (**Figure 4**). The virulence factors of *C. concisus* that affect the epithelial actin arrangement and their mechanisms are not clear, warranting further investigation in future studies.

C. concisus bacteria transported from the oral cavity to the stomach through swallowed saliva may not establish long-term gastric colonization. To investigate potential changes in gene expression after short-term contact with gastric epithelial cells, we investigated the global gastric epithelial gene responses to *C. concisus* using transcriptomic analysis following a 4-h incubation at a lower dose (MOI 50). Global gene response in AGS cells incubated with *C. concisus* strain P2CDO4 for 4 h was altered when compared to the untreated AGS cells (**Supplementary Figure 1**), of which a total of 30 genes and 10 genes were significantly upregulated and downregulated, respectively, which were predicted to affect several cellular functional pathways (**Figure 5** and **Supplementary Table 3**). These findings suggests that *C. concisus* bacteria passing through the stomach from the oral cavity may exert regulatory effects on gastric epithelial cell gene expression. We further confirmed the upregulation of expression of the gene coding CYP1A1 through qRT-PCR. CYP1A1, a cytochrome P450 enzyme involved in metabolism of xenobiotics (Androutsopoulos et al., 2009), has been associated with gastric cancer and precancerous gastric cancer as well as lung cancer (Kouri et al., 1982; Zhang et al., 2004; Hidaka et al., 2016; Huang et al., 2021; Sadeghi-Amiri et al., 2021). Previous research by Cui et al. (2019) linked the abundance of *C. concisus* in tongue coating microbiome to gastric precancerous cascade, which aligns with our finding of *C. concisus* upregulating CYP1A1 expression. This provides additional evidence that oral *C. concisus* may play a role in facilitating gastric cancer development or progression. This is further supported by the survival analysis of CYP1A1 in gastric cancer patients (**Figure 6**).

In summary, our study reveals that incubation of *C. concisus* with human gastric epithelial cells (AGS cells) induces the production of IL-8, apoptosis, and upregulation of CYP1A1 gene expression in gastric epithelial cells. These findings suggest that *C. concisus* may play a role in gastric inflammation and the progression of gastric cancer. Further investigation in clinical studies is warranted.

Data availability statement

The datasets presented in this study can be found in online repositories. The names of the repository/repositories and accession number(s) can be found in this article/**Supplementary material**.

Ethics statement

Ethical approval was not required for the studies on humans in accordance with the local legislation and institutional requirements because only commercially available established cell lines were used.

Author contributions

CL: Formal analysis, Writing – original draft, Investigation. SL: Methodology, Writing – review and editing. NN: Writing – review and editing, Investigation. FL: Methodology, Writing – review and editing. AT: Funding acquisition, Writing – review and editing. LW: Writing – review and editing, Conceptualization, Funding acquisition. SR: Writing – review and editing, Conceptualization. LZ: Writing – review and editing, Conceptualization, Funding acquisition, Supervision.

Funding

The author(s) declare financial support was received for the research, authorship, and/or publication of this article. This project was supported by the Xuzhou Medical University Open Research Grant (XYKF202102) and the Faculty Research

Grant (Grant no. PS46772) of the University of New South Wales awarded to Associate Professor LZ.

Conflict of interest

The authors declare that the research was conducted in the absence of any commercial or financial relationships that could be construed as a potential conflict of interest.

The author(s) declared that they were an editorial board member of Frontiers, at the time of submission. This had no impact on the peer review process and the final decision.

Publisher's note

All claims expressed in this article are solely those of the authors and do not necessarily represent those of their affiliated organizations, or those of the publisher, the editors and the reviewers. Any product that may be evaluated in this article, or claim that may be made by its manufacturer, is not guaranteed or endorsed by the publisher.

Supplementary material

The Supplementary Material for this article can be found online at: https://www.frontiersin.org/articles/10.3389/fmicb.2023.1289549/full#supplementary-material

SUPPLEMENTARY FIGURE 1
Principal component analysis (PCA) plot of RNA-seq data. A total of 6 samples were included in the analysis, red dots for treatment with *C. concisus* strain P2CDO4 and blue dots for untreated control. The plot indicates separation between control and treatment groups, suggesting significant changes in overall gene response in AGS cells upon *C. concisus* infection. Gene counts were normalized using log2 transformation. PCA plot generated using the ggplot2 package on the R platform.

References

Aagaard, M. E. Y., Kirk, K. F., Nielsen, H., and Nielsen, H. L. (2021). High genetic diversity in *Campylobacter concisus* isolates from patients with microscopic colitis. *Gut Pathog.* 13, 1–5. doi: 10.1186/s13099-020-00397-y

Androutsopoulos, V. P., Tsatsakis, A. M., and Spandidos, D. A. (2009). Cytochrome P450 CYP1A1: Wider roles in cancer progression and prevention. *BMC Cancer* 9:187. doi: 10.1186/1471-2407-9-187

Ashktorab, H., Dashwood, R. H., Dashwood, M. M., Zaidi, S. I., Hewitt, S. M., Green, W. R., et al. (2008). *H. pylori*-induced apoptosis in human gastric cancer cells mediated via the release of apoptosis-inducing factor from mitochondria. *Helicobacter* 13, 506–517. doi: 10.1111/j.1523-5378.2008.00646.x

Benoit, S. L., and Maier, R. J. (2023). The *Campylobacter concisus* BisA protein plays a dual role: Oxide-dependent anaerobic respiration and periplasmic methionine sulfoxide repair. *mBio* 14:e01475-23. doi: 10.1128/mbio.01475-23

Bolger, A. M., Lohse, M., and Usadel, B. (2014). Trimmomatic: A flexible trimmer for Illumina sequence data. *Bioinformatics* 30, 2114–2120.

Bruford, E. A., Braschi, B., Denny, P., Jones, T. E., Seal, R. L., and Tweedie, S. (2020). Guidelines for human gene nomenclature. *Nat. Genet.* 52, 754–758.

Chang, C.-C., Kuo, W.-S., Chen, Y.-C., Perng, C.-L., Lin, H.-J., and Ou, Y.-H. (2016). Fragmentation of CagA reduces hummingbird phenotype induction by *Helicobacter pylori*. *PLoS One* 11:e0150061. doi: 10.1371/journal.pone.0150061

Chung, H. K. L., Tay, A., Octavia, S., Chen, J., Liu, F., Ma, R., et al. (2016). Genome analysis of *Campylobacter concisus* strains from patients with inflammatory bowel disease and gastroenteritis provides new insights into pathogenicity. *Sci. Rep.* 6, 1–14. doi: 10.1038/srep38442

Cornelius, A. J., Huq, M., On, S. L., French, N. P., Vandenberg, O., Miller, W. G., et al. (2021). Genetic characterisation of *Campylobacter concisus*: Strategies for improved genomospecies discrimination. *Syst. Appl. Microbiol.* 44:126187. doi: 10.1016/j.syapm.2021.126187

Cui, J., Cui, H., Yang, M., Du, S., Li, J., Li, Y., et al. (2019). Tongue coating microbiome as a potential biomarker for gastritis including precancerous cascade. *Protein Cell* 10, 496–509. doi: 10.1007/s13238-018-0596-6

Danecek, P., Bonfield, J. K., Liddle, J., Marshall, J., Ohan, V., Pollard, M. O., et al. (2021). Twelve years of SAMtools and BCFtools. *Gigascience* 10:giab008. doi: 10.1093/gigascience/giab008

Dang, Y., Zhang, Y., Xu, L., Zhou, X., Gu, Y., Yu, J., et al. (2020). PUMA-mediated epithelial cell apoptosis promotes *Helicobacter pylori* infection-mediated gastritis. *Cell Death Dis.* 11:139. doi: 10.1038/s41419-020-2339-x

Fazeli, Z., Alebouyeh, M., Tavirani, M. R., Azimirad, M., and Yadegar, A. (2016). *Helicobacter pylori* CagA induced interleukin-8 secretion in gastric epithelial cells. *Gastroenterol. Hepatol. Bed Bench* 9(Suppl.1), S42–S46.

Ferreira, E. O., Lagacé-Wiens, P., and Klein, J. (2022). *Campylobacter concisus* gastritis masquerading as *Helicobacter pylori* on gastric biopsy. *Helicobacter* 27:e12864. doi: 10.1111/hel.12864

Gemmell, M. R., Berry, S., Mukhopadhya, I., Hansen, R., Nielsen, H. L., Bajaj-Elliott, M., et al. (2018). Comparative genomics of *Campylobacter concisus*: Analysis of clinical strains reveals genome diversity and pathogenic potential. *Emerg. Microbes Infect.* 7, 1–17. doi: 10.1038/s41426-018-0118-x

Harada, A., Sekido, N., Akahoshi, T., Wada, T., Mukaida, N., and Matsushima, K. (1994). Essential involvement of interleukin-8 (IL-8) in acute inflammation. *J. Leukoc. Biol.* 56, 559–564.

Hartsock, A., and Nelson, W. J. (2008). Adherens and tight junctions: Structure, function and connections to the actin cytoskeleton. *Biochim. Biophys. Acta Biomembr.* 1778, 660–669. doi: 10.1016/j.bbamem.2007.07.012

Hidaka, A., Sasazuki, S., Matsuo, K., Ito, H., Charvat, H., Sawada, N., et al. (2016). CYP1A1, GSTM1 and GSTT1 genetic polymorphisms and gastric cancer risk among Japanese: A nested case–control study within a large-scale population-based prospective study. *Int. J. Cancer* 139, 759–768. doi: 10.1002/ijc.30130

Huang, L., He, R., Zhang, Y., Yan, Q., and Veronica, C. (2021). "The role of the aryl hydrocarbon receptor (AhR) in the immune response against microbial infections," in *Antimicrobial Immune Response*, ed. O. Maria del Mar (London: IntechOpen).

Huq, M., Van, T. T. H., Gurtler, V., Elshagmani, E., Allemailem, K. S., Smooker, P. M., et al. (2017). The ribosomal RNA operon (rrn) of *Campylobacter concisus* supports molecular typing to genomospecies level. *Gene Rep.* 6, 8–14.

Ismail, Y., Mahendran, V., Octavia, S., Day, A. S., Riordan, S. M., Grimm, M. C., et al. (2012). Investigation of the enteric pathogenic potential of oral *Campylobacter concisus* strains isolated from patients with inflammatory bowel disease. *PLoS One* 7:e38217. doi: 10.1371/journal.pone.0038217

Istivan, T. S., Coloe, P. J., Fry, B. N., Ward, P., and Smith, S. C. (2004). Characterization of a haemolytic phospholipase A2 activity in clinical isolates of *Campylobacter concisus*. *J. Med. Microbiol.* 53, 483–493. doi: 10.1099/jmm.0.45554-0

Kalischuk, L. D., and Inglis, G. D. (2011). Comparative genotypic and pathogenic examination of *Campylobacter concisus* isolates from diarrheic and non-diarrheic humans. *BMC Microbiol.* 11:53. doi: 10.1186/1471-2180-11-53

Kim, D., Paggi, J. M., Park, C., Bennett, C., and Salzberg, S. L. (2019). Graph-based genome alignment and genotyping with HISAT2 and HISAT-genotype. *Nat. Biotechnol.* 37, 907–915. doi: 10.1038/s41587-019-0201-4

Kirk, K. F., Méric, G., Nielsen, H. L., Pascoe, B., Sheppard, S. K., Thorlacius-Ussing, O., et al. (2018). Molecular epidemiology and comparative genomics of *Campylobacter concisus* strains from saliva, faeces and gut mucosal biopsies in inflammatory bowel disease. *Sci. Rep.* 8, 1–8. doi: 10.1038/s41598-018-20135-4

Kouri, R., McKinney, C., Slomiany, D., Snodgrass, D., Wray, N., and McLemore, T. (1982). Positive correlation between high aryl hydrocarbon hydroxylase activity and primary lung cancer as analyzed in cryopreserved lymphocytes. *Cancer Res.* 42, 5030–5037.

Lánczky, A., and Győrffy, B. (2021). Web-based survival analysis tool tailored for medical research (KMplot): Development and implementation. *J. Med. Internet Res.* 23:e27633. doi: 10.2196/27633

Lee, H., Ma, R., Grimm, M. C., Riordan, S. M., Lan, R., Zhong, L., et al. (2014). Examination of the anaerobic growth of *Campylobacter concisus* strains. *Int. J. Microbiol* 2014, 476047. doi: 10.1155/2014/476047

Lee, S. A., Liu, F., Yun, D. Y., Riordan, S. M., Tay, A. C. Y., Liu, L., et al. (2021). *Campylobacter concisus* upregulates PD-L1 mRNA expression in IFN-γ sensitized intestinal epithelial cells and induces cell death in esophageal epithelial cells. *J. Oral Microbiol.* 13:1978732.

Lee, S. A., Liu, F., Yuwono, C., Phan, M., Chong, S., Biazik, J., et al. (2023). Emerging *Aeromonas* enteric infections: Their association with inflammatory bowel disease and novel pathogenic mechanisms. *Microbiol. Spectr.* 11:e01088-23 doi: 10.1128/spectrum.01088-23

Liao, Y., Smyth, G. K., and Shi, W. (2014). featureCounts: An efficient general purpose program for assigning sequence reads to genomic features. *Bioinformatics* 30, 923–930. doi: 10.1093/bioinformatics/btt656

Liu, F., Chen, S., Luu, L. D. W., Lee, S. A., Tay, A. C. Y., Wu, R., et al. (2020). Analysis of complete *Campylobacter concisus* genomes identifies genomospecies features, secretion systems and novel plasmids and their association with severe ulcerative colitis. *Microb. Genom* 6:mgen000457. doi: 10.1099/mgen.0.000457

Liu, F., Ma, R., Tay, C. Y. A., Octavia, S., Lan, R., Chung, H. K. L., et al. (2018). Genomic analysis of oral *Campylobacter concisus* strains identified a potential bacterial molecular marker associated with active Crohn's disease. *Emerg. Microbes Infect.* 7, 1–14. doi: 10.1038/s41426-018-0065-6

Livak, K. J., and Schmittgen, T. D. (2001). Analysis of relative gene expression data using real-time quantitative PCR and the 2- ΔΔCT method. *Methods* 25, 402–408.

Love, M. I., Huber, W., and Anders, S. (2014). Moderated estimation of fold change and dispersion for RNA-seq data with DESeq2. *Genome Biol.* 15, 1–21. doi: 10.1186/s13059-014-0550-8

Ma, R., Sapwell, N., Chung, H. K. L., Lee, H., Mahendran, V., Leong, R. W., et al. (2015). Investigation of the effects of pH and bile on the growth of oral *Campylobacter concisus* strains isolated from patients with inflammatory bowel disease and controls. *J. Med. Microbiol.* 64, 438–445. doi: 10.1099/jmm.0.000013

Macfarlane, S., Furrie, E., Macfarlane, G. T., and Dillon, J. F. (2007). Microbial colonization of the upper gastrointestinal tract in patients with Barrett's esophagus. *Clin. Infect. Dis.* 45, 29–38.

Mahendran, V., Liu, F., Riordan, S. M., Grimm, M. C., Tanaka, M. M., and Zhang, L. (2016). Examination of the effects of *Campylobacter concisus* zonula occludens toxin on intestinal epithelial cells and macrophages. *Gut Pathog.* 8, 1–10. doi: 10.1186/s13099-016-0101-9

Mahendran, V., Octavia, S., Demirbas, O. F., Sabrina, S., Ma, R., Lan, R., et al. (2015). Delineation of genetic relatedness and population structure of oral and enteric *Campylobacter concisus* strains by analysis of housekeeping genes. *Microbiol.* 161, 1600–1612. doi: 10.1099/mic.0.000112

Man, S. M., Zhang, L., Day, A. S., Leach, S. T., Lemberg, D. A., and Mitchell, H. (2010). *Campylobacter concisus* and other *Campylobacter* species in children with newly diagnosed Crohn's disease. *Inflamm. Bowel Dis.* 16, 1008–1016. doi: 10.1002/ibd.21157

Miller, W. G., Chapman, M. H., Yee, E., On, S. L., McNulty, D. K., Lastovica, A. J., et al. (2012). Multilocus sequence typing methods for the emerging *Campylobacter* species *C. hyointestinalis*, *C. lanienae*, *C. sputorum*, *C. concisus*, and *C. curvus*. *Front. Cell. Infect. Microbiol.* 2:45. doi: 10.3389/fcimb.2012.00045

Moese, S., Selbach, M., Kwok, T., Brinkmann, V., König, W., Meyer, T. F., et al. (2004). *Helicobacter pylori* induces AGS cell motility and elongation via independent signaling pathways. *Infect. Immun.* 72, 3646–3649. doi: 10.1128/IAI.72.6.3646-3649.2004

Mukhopadhya, I., Thomson, J. M., Hansen, R., Berry, S. H., El-Omar, E. M., and Hold, G. L. (2011). Detection of *Campylobacter concisus* and other *Campylobacter* species in colonic biopsies from adults with ulcerative colitis. *PLoS One* 6:e21490. doi: 10.1371/journal.pone.0021490

Nielsen, H. L., Dalager-Pedersen, M., and Nielsen, H. (2020). High risk of microscopic colitis after *Campylobacter concisus* infection: Population-based cohort study. *Gut* 69, 1952–1958. doi: 10.1136/gutjnl-2019-319771

O'Hara, A. M., Bhattacharyya, A., Mifflin, R. C., Smith, M. F., Ryan, K. A., Scott, K. G.-E., et al. (2006). Interleukin-8 induction by *Helicobacter pylori* in gastric epithelial cells is dependent on apurinic/apyrimidinic endonuclease-1/redox factor-1. *J. Immunol.* 177, 7990–7999. doi: 10.4049/jimmunol.177.11.7990

Sadeghi-Amiri, L., Barzegar, A., Nikbakhsh-Zati, N., and Mehraban, P. (2021). Hypomethylation of the XRE- 1383 site is associated with the upregulation of CYP1A1 in gastric adenocarcinoma. *Gene* 769:145216. doi: 10.1016/j.gene.2020.145216

Svitkina, T. (2018). The actin cytoskeleton and actin-based motility. *Cold Spring Harb. Perspect. Biol.* 10:a018267.

Wang, Y., Liu, F., Zhang, X., Chung, H. K. L., Riordan, S. M., Grimm, M. C., et al. (2017). *Campylobacter concisus* genomospecies 2 is better adapted to the human gastrointestinal tract as compared with *Campylobacter concisus* genomospecies 1. *Front. Physiol.* 8:543. doi: 10.3389/fphys.2017.00543

Yang, L., Lu, X., Nossa, C. W., Francois, F., Peek, R. M., and Pei, Z. (2009). Inflammation and intestinal metaplasia of the distal esophagus are associated with alterations in the microbiome. *Gastroenterology* 137, 588–597. doi: 10.1053/j.gastro.2009.04.046

Zhang, K.-L., Ma, J.-X., Chen, X.-Y., Sun, Y., Kong, Q.-Y., Liu, J., et al. (2004). Frequent CYP1A1 expression in gastric cancers and their related lesions. *Oncol. Rep.* 12, 1335–1340.

Zhang, L., Budiman, V., Day, A. S., Mitchell, H., Lemberg, D. A., Riordan, S. M., et al. (2010). Isolation and detection of *Campylobacter concisus* from saliva of healthy individuals and patients with inflammatory bowel disease. *J. Clin. Microbiol.* 48, 2965–2967. doi: 10.1128/JCM.02391-09

Zhang, L., Man, S. M., Day, A. S., Leach, S. T., Lemberg, D. A., Dutt, S., et al. (2009). Detection and isolation of *Campylobacter* species other than *C. jejuni* from children with Crohn's disease. *J. Clin. Microbiol.* 47, 453–455.

Zhang, Y., Takeuchi, H., Nishioka, M., Morimoto, N., Kamioka, M., Kumon, Y., et al. (2009). Relationship of IL-8 production and the CagA status in AGS cells infected with *Helicobacter pylori* exposed to low pH and activating transcription factor 3 (ATF3). *Microbiol. Res.* 164, 180–190. doi: 10.1016/j.micres.2006.10.010

Zhou, Y., Zhou, B., Pache, L., Chang, M., Khodabakhshi, A. H., Tanaseichuk, O., et al. (2019). Metascape provides a biologist-oriented resource for the analysis of systems-level datasets. *Nat. Commun.* 10:1523. doi: 10.1038/s41467-019-09234-6

frontiers | Frontiers in Microbiology

TYPE Original Research
PUBLISHED 25 January 2024
DOI 10.3389/fmicb.2024.1290490

OPEN ACCESS

EDITED BY
Ozan Gundogdu,
University of London, United Kingdom

REVIEWED BY
Abhinav Upadhyay,
University of Connecticut, United States
Pei Shang,
Mayo Clinic, United States
Ulrich Steinhoff,
University of Marburg, Germany
Igori Balta,
University of Life Sciences "King Mihai I", Romania

*CORRESPONDENCE
Markus M. Heimesaat
markus.heimesaat@charite.de

†These authors have contributed equally to this work and share last authorship

RECEIVED 07 September 2023
ACCEPTED 12 January 2024
PUBLISHED 25 January 2024

CITATION
Mousavi S, Foote MS, Du K, Bandick R, Bereswill S and Heimesaat MM (2024) Oral treatment of human gut microbiota associated IL-10$^{-/-}$ mice suffering from acute campylobacteriosis with carvacrol, deferoxamine, deoxycholic acid, and 2-fucosyl-lactose.
Front. Microbiol. 15:1290490.
doi: 10.3389/fmicb.2024.1290490

Oral treatment of human gut microbiota associated IL-10$^{-/-}$ mice suffering from acute campylobacteriosis with carvacrol, deferoxamine, deoxycholic acid, and 2-fucosyl-lactose

Soraya Mousavi, Minnja S. Foote, Ke Du, Rasmus Bandick, Stefan Bereswill† and Markus M. Heimesaat*†

Gastrointestinal Microbiology Research Group, Institute of Microbiology, Infectious Diseases and Immunology, Charité – Universitätsmedizin Berlin, Corporate Member of Freie Universität Berlin, Humboldt-Universität zu Berlin, and Berlin Institute of Health, Berlin, Germany

Food-borne *Campylobacter jejuni* infections constitute serious threats to human health worldwide. Since antibiotic treatment is usually not indicated in infected immune-competent patients, antibiotic-independent treatment approaches are needed to tackle campylobacteriosis. To address this, we orally applied carvacrol, deferoxamine, deoxycholate, and 2-fucosyl-lactose either alone or all in combination to human microbiota-associated IL-10$^{-/-}$ mice from day 2 until day 6 following oral *C. jejuni* infection. Neither treatment regimen affected *C. jejuni* loads in the colon, whereas carvacrol lowered the pathogen numbers in the ileum on day 6 post-infection (p.i.). The carvacrol and combination treatment regimens resulted in alleviated diarrheal symptoms, less distinct histopathological and apoptotic epithelial cell responses in the colon, as well as diminished numbers of colonic neutrophils and T lymphocytes on day 6 p.i., whereas the latter cells were also decreased upon deferoxamine, deoxycholate, or 2-fucosyl-lactose application. Remarkably, the carvacrol, deferoxamine, and combination treatment regimens dampened *ex-vivo* IFN-γ secretion in the colon, the kidneys, and even in the serum to basal concentrations on day 6 p.i. In conclusion, carvacrol alone and its combination with deferoxamine, deoxycholate, and 2-fucosyl-lactose constitute promising antibiotics-independent treatment options to fight acute campylobacteriosis.

KEYWORDS

natural compounds, *Campylobacter jejuni*, immune-modulatory effects, secondary abiotic IL-10$^{-/-}$ mice, human gut microbiota associated mice, campylobacteriosis model, host-pathogen interaction, placebo-controlled preclinical intervention study

1 Introduction

Campylobacteriosis is an acute infectious enteritis, primarily caused by foodborne *Campylobacter* species transmitted through contaminated chicken and turkey products, with *Campylobacter jejuni* being the most common pathogen (Price et al., 1979; Walker et al., 1986; Moore et al., 2005; Young et al., 2007; Kaakoush et al., 2015; Wagenaar et al., 2023). Given that the intestinal tract of poultry represents the major pathogen reservoir, the global surge in consumption of poultry products has contributed significantly to the continuous rise of human *C. jejuni* infections. As a result, campylobacteriosis has emerged as a critical global health problem with a high socioeconomic burden (Kaakoush et al., 2015; WHO, 2020; European Food Safety Authority, European Centre for Disease Prevention and Control, 2022). The asymptomatic colonization of avian intestinal tracts by the highly virulent enteropathogen has far-reaching implications for their transmission to humans. The commensal lifestyle in birds is the major reason for the tolerance of *C. jejuni* contaminations in poultry production chains and favors its adaptation to the intestines (Moore et al., 2005; Young et al., 2007; Kaakoush et al., 2015). The lack of disease symptoms in birds can be attributed to the avian innate immune system's non-responsiveness to the pathogen. Additionally, birds display a resistance to lipopolysaccharide (LPS), a cell wall structure of Gram-negative bacteria, including *Campylobacter* species. *C. jejuni* produces a truncated version of LPS known as lipo-oligosaccharide (LOS), which further complicates pathogen recognition. Previous studies suggest that these variations in pathogen recognition may arise from species-specific differences in how *Campylobacter* LOS interacts with the specific Toll-like receptor (TLR)-4 (de Zoete et al., 2010).

In contrast to the avian hosts, humans exhibit heightened sensitivity to TLR-4 ligands such as LPS and LOS of Gram-negative bacteria. Consequently, when *C. jejuni* infects the human intestinal tract, LOS triggers host immune responses and induces hyperactivation of the innate and adaptive immune system via TLR-4 and mammalian target of rapamycin (mTOR) signaling (Sun et al., 2012; Callahan et al., 2021). This cascade results in damage to intestinal cells such as apoptosis and dissolution of the tight junctions (Lobo de Sá et al., 2021). Subsequently, patients experience acute enterocolitis characterized by bloody diarrhea, intestinal cellular apoptosis, compromised barrier function, malabsorption, and ultimately, severe tissue destruction (Sun et al., 2013; Lobo de Sá et al., 2021).

Although the majority of human campylobacteriosis cases resolve without residues within 1 to 2 weeks post-infection (p.i.), the potential to develop post-infectious autoimmune diseases, including Guillain-Barré syndrome, reactive arthritis, and intestinal diseases, including chronic inflammatory bowel diseases and irritable bowel syndrome remains (Nachamkin et al., 1998; Mortensen et al., 2009; Omarova et al., 2023). Importantly, the risk for these secondary complications correlates with the severity of the initial enteritis (Mortensen et al., 2009). Therefore, severe and invasive *C. jejuni* induced enterocolitis presenting with bloody diarrhea may require antibiotic therapy, particularly in immunocompromised and multimorbid individuals (Manfredi et al., 1999; Acheson and Allos, 2001). However, the increasing prevalence of antibiotic resistance in *Campylobacter* strains, including resistance to commonly used quinolones and macrolides, restricts the efficacy of antimicrobial therapy for human campylobacteriosis (Mouftah et al., 2021). Hence, there is an urgent need to develop novel antibiotic-independent strategies to combat and/or prevent *C. jejuni* infections, aligning with the One-Health approach (Zhang et al., 2023).

To promote global health and address pressing issues like antibiotic resistance and foodborne infections, the One Health concept seeks to balance and improve the health of humans, animals, and ecosystems (Anholt and Barkema, 2021). According to the One Health approach, multi-sectoral (i.e., humans, animals, and the associated environments) and inter-disciplinary strategies (involving farming, human and veterinary medicine for instance) are crucial to combat antibiotic resistance and their collateral damages (Robinson et al., 2016). Therefore, it is important to develop pharmaceutical intervention strategies to treat human campylobacteriosis with antibiotic-independent compounds. Additionally, it is important to identify alternative measures to control antibiotic resistance in both human hosts and animal reservoirs. These actions would enhance safety aspects along the food chains and reduce morbidities in humans caused by transmitted pathogens.

In fact, current research efforts have shifted towards identifying natural compounds with both anti-microbial and anti-inflammatory properties that do not trigger resistance. These compounds hold promise for future therapeutic and preventive applications in the context of enteropathogenic infections, including those caused by Campylobacter species (Kreling et al., 2020).

Carvacrol, a phenolic monoterpenoid and main component in essential oils derived from oregano (*Origanum vulgare*) and thyme (*Thymus vulgaris*) (Gholami-Ahangaran et al., 2022), is commonly used for flavoring and food-preservation within the food industry. Furthermore, it is known for its anti-microbial, −oxidant, −diabetic, −inflammatory, and anti-carcinogenic properties, making this compound a promising candidate in the treatment of several human morbidities (Sharifi-Rad et al., 2018; Mączka et al., 2023). The anti-bacterial effects of carvacrol against food-borne pathogens, such as Gram-positive *Bacillus cereus* or Gram-negative bacteria like *Escherichia coli*, *Salmonella* species, and *C. jejuni* have already been reported in the past (Ultee et al., 2002; Obaidat and Frank, 2009; van Alphen et al., 2012; Mączka et al., 2023). Additionally, our previous pre-clinical intervention studies assessed the anti-inflammatory and immune-modulatory properties of singular carvacrol application during murine campylobacteriosis (Mousavi et al., 2020; Foote et al., 2023).

Deferoxamine B (deferoxamine, trade name Desferal®) is an iron chelator and natural siderophore produced by microorganisms such as *Streptomyces pilosus*. This compound exhibits anti-microbial, anti-inflammatory, and cell-protective properties (Jurado, 1997; Bellotti and Remelli, 2021). Given that iron is essential for the survival of most pathogens, iron binding by deferoxamine can reduce the risk of infections (Jurado, 1997). Additionally, several studies revealed synergistic effects between deferoxamine and anti-microbial agents such as gentamicin, metronidazole, and hydrogen peroxide (Van Asbeck et al., 1983; van Asbeck et al., 1983; Moon et al., 2011). Previously we reported that the oral application of deferoxamine significantly improved the clinical outcome of *C. jejuni* infected mice, which was accompanied by dampened inflammatory responses such as less pronounced colonic epithelial cell apoptosis as compared to placebo-treated infected mice (Bereswill et al., 2022).

The secondary bile acid deoxycholic acid has been shown to exhibit bactericidal effects against several bacteria, including *Staphylococcus aureus* (Zhao et al., 2023) and *Helicobacter pylori* (Itoh et al., 1999). Previous studies revealed that *C. jejuni* alter the global gene transcription in response to the bile salt deoxycholate (Gourley et al., 2017; Negretti et al., 2017). Remarkably, deoxycholic acid effectively reduced *C. jejuni* growth *in vitro* (Negretti et al., 2017) and its colonization capacity in the intestinal tract of broiler chickens (Alrubaye et al., 2019). Furthermore, deoxycholic acid possesses immune-modulatory activities such as suppressing LPS-induced expression of pro-inflammatory cytokines such as interleukin (IL)-1, IL-6, and tumor necrosis factor-alpha (TNF-α) in murine bone marrow-derived dendritic cells (Hu et al., 2021; Su et al., 2023).

Human breast milk is the main source of energy in the early stage of life. However, the lack of enzymes responsible for the release of monosaccharides makes the human milk oligosaccharides (HMOs) indigestible by the newborn (Engfer et al., 2000; Sela and Mills, 2010). Interestingly, distinct bacteria such as *Bifidobacterium* and *Lactobacillus* species use HMOs as nutrients, which indicates the prebiotic properties of HMOs by promoting intestinal colonization by a "healthy" gut microbiota (Davis et al., 2016; Garrido et al., 2016). Additionally, 2-fucosyl-lactose, one of the most abundant oligosaccharides in human breast milk is known for its immune-modulatory effects and has been shown to prevent the binding of pathogens such as *Pseudomonas aeruginosa, E. coli,* and *C. jejuni* to the host epithelial cells (Newburg, 2005; Facinelli et al., 2019).

So far, research on *C. jejuni*-host interactions has been limited by standardized *in vivo* models. The commensal gut microbiome of conventional laboratory mice exerts a strong physiological colonization resistance, which prevents infections with enteropathogens like *C. jejuni* (Mullineaux-Sanders et al., 2018; Herzog et al., 2023). Therefore, an antibiotic-pretreatment regimen of mice has been established to generate proper enteropathogenic infection models. After depleting the murine microbiome, a stable colonization of *C. jejuni* through oral gavage can be assured (Bereswill et al., 2011). However, even though *C. jejuni* colonizes in secondary abiotic wildtype mice, characteristic clinical symptoms of acute human campylobacteriosis remain absent (Bereswill et al., 2011). This is due to the resistance against TLR-4 ligands like LPS and LOS, which is 10,000 times stronger in rodents as compared to humans (Mortensen et al., 2009). To overcome this challenge, the murine *il10* gene has been knocked out to make the animals more susceptible to *C. jejuni* LOS (Mansfield et al., 2007). In consequence, secondary abiotic IL-10$^{-/-}$ mice can be colonized by the enteropathogen and also display *C. jejuni*-induced acute enterocolitis within a week post infection (p.i.) mimicking key features of severe and invasive human campylobacteriosis (Bereswill et al., 2011; Haag et al., 2012). Our previous preclinical placebo-controlled intervention studies using this acute *C. jejuni* infection and inflammation model provided evidence for anti-pathogenic and immune-modulatory properties of several natural compounds such as carvacrol (Mousavi et al., 2020), deferoxamine (Bereswill et al., 2022), and 2-fucosyl-lactose (Mousavi et al., 2023).

Previous studies also revealed that the host-specific intestinal microbiota impacts the host's susceptibility to and resistance against distinct enteropathogens including *C. jejuni* (Bereswill et al., 2011), *Campylobacter coli* (Heimesaat et al., 2020), and *Salmonella enterica* (Chung et al., 2012). In order to elucidate the triangular relationship between enteropathogens on one side and the murine immunity and human gut microbiota on the other, the host side, we generated a human gut microbiota associated (hma) mouse model for *C. jejuni* induced inflammation. Therefore, secondary abiotic IL-10$^{-/-}$ mice were subjected to oral transplantation of a fecal microbiota from healthy human donors (Foote et al., 2023; Shayya et al., 2023). Following oral *C. jejuni* infection, human gut microbiota associated IL-10$^{-/-}$ mice were shown not only to carry the pathogen in their intestines at high loads but also to present with key symptoms of acute campylobacteriosis like secondary abiotic mice do (Shayya et al., 2023).

This preclinical placebo-controlled intervention study assesses carvacrol, deferoxamine, deoxycholic acid, and 2′-fucosyl-lactose alone and as a combination in hma IL-10$^{-/-}$ mice with acute *C. jejuni* induced enterocolitis. The following parameters will be addressed: (i) human gut microbiota compositions in recipient mice following engraftment; (ii) gastrointestinal pathogens burdens; (iii) clinical outcome; (iv) intestinal, (v) extra-intestinal, and also (vi) the systemic inflammatory immune responses upon oral infection.

2 Methods

2.1 Ethics

All animal procedures were performed in accordance with protocols approved by the local commission for animal experiments ("Landesamt für Gesundheit und Soziales," LaGeSo, Berlin; registration number G0104/19). Clinical conditions of the mice were assessed daily following the European animal welfare guidelines (2010/63/EU).

2.2 Secondary abiotic IL-10$^{-/-}$ mice

IL-10$^{-/-}$ C57BL/6j mice were obtained from the Forschungsinstitute für Experimentelle Medizin of the Charité – Universitätsmedizin Berlin, Germany. Animals were bred and kept under a specified pathogen-free environment, housed in autoclaved cages with filter tops within an experimental semi-barrier, and given free access to standard chow (food pellets: ssniff R/M-H, V1534-300, Sniff, Soest, Germany) as well as autoclaved tap water. In all experiments, age- and sex-matched littermates were used. Mice were 3-week-old when subjected to an 8-week antibiotic treatment consisting of ampicillin plus sulbactam (2 g/L plus 1 g/L, respectively; Dr. Friedrich Eberth Arzneimittel, Ursensollen, Germany) *ad libitum*. To avoid cross-contamination, secondary abiotic mice were handled under aseptic conditions throughout the experiment. After eradication of the murine microbiome as described previously (Heimesaat et al., 2022), and 2 days prior to human fecal microbiota transplantation (FMT), the antibiotic treatment was substituted with autoclaved tap water to ensure proper washout.

2.3 Human fecal microbiota transplantation

Human fecal samples were collected from five healthy donors free of viruses, parasites, as well as enteropathogenic bacteria and stored

at −80°C. After thawing and resuspending in sterile phosphate buffered saline (PBS, Thermo Fisher Scientific, Waltham, MA, United States), the samples were pooled to ensure at least 0.3 mL gavage volume per mouse. The microbiota composition of the pooled FMT sample can be found in Supplementary Figure S1. One week before the first *C. jejuni* infection (respectively on days 0 and 1), secondary abiotic mice were introduced to the complex human FMT on 3 days (respectively on days −7, −6 and −5) (Figure 1) as described previously (Shayya et al., 2023).

2.4 *Campylobacter jejuni* cultures and infections

Viable cells of *C. jejuni* strain 81–176 were thawed from −80°C and grown on *Campylobacter*-selective Karmali agar plates (Oxoid, Wesel, Germany) under microaerophilic conditions (CampyGen gas packs, Oxoid, Wesel, Germany) at 37°C (Bereswill et al., 2011). After 48 h, plates were harvested and bacterial cells were resuspended in sterile PBS to achieve an inoculum of 10^9 colony forming units (CFU). Then, 0.3 mL per mouse were gavaged on days 0 and 1 as shown previously (Bereswill et al., 2011).

2.5 Course of treatment

Treatment through oral administration via drinking water of carvacrol, deferoxamine, deoxycholic acid (all from Sigma-Aldrich, Munich, Germany), 2′-fucosyl-lactose (Chr. Hansen HMO GmbH, Rheinbreitbach, Germany), and the quadruple combination commenced 2 days following the onset of *C. jejuni* infection. Dosages were calculated considering an average body weight of approximately 25 g per mouse and an estimated drinking volume of 5 mL per day. All compounds were dissolved in autoclaved tap water. The daily doses and their previously determined minimal inhibitory concentrations (MICs) are illustrated in Table 1. To enhance the water solubility of carvacrol, 50 mg of the compound were dissolved in 250 µL Tween® 80 (Sigma-Aldrich, Munich, Germany). The placebo group received vehicle dissolved in autoclaved tap water.

2.6 *Campylobacter jejuni* loads in the gastrointestinal tract

Intraluminal samples from defined parts of the gastrointestinal tract (stomach, duodenum, ileum, and colon) were taken upon necropsy of the mice. The samples were homogenized in PBS, serial diluted and streaked on Karmali agar plates (Oxoid, Wesel, Germany). After 48 h of incubation at 37°C under microaerophilic conditions, *C. jejuni* was quantified by counting CFU (Bereswill et al., 2011). The detection limit of viable bacterial cells was 100 CFU per g intestinal sample.

2.7 Microbiota analysis

Fecal samples of hma mice were collected before (i.e., day 0) and 6 days after *C. jejuni* infection for microbiota composition analysis in comparison to the original fecal donor suspensions (Heimesaat et al., 2006). Samples were homogenized in sterile PBS, diluted in series and incubated on solid media under aerobic, microaerobic, and anaerobic conditions for 48 h. Total bacterial loads and bacterial species were identified according to their colony morphology, Gram-staining, and biochemical analysis. In addition, genomic DNA extraction and real-time polymerase chain reaction (PCR) of the fecal samples have been performed culture-independently; this is to assess the abundance of fastidious and non-cultivable bacteria from the human microbiome quantitatively. 16S variable regions were targeted using species-, genera- or group-specific 16S rRNA primers (Tib MolBiol, Berlin, Germany) (Heimesaat et al., 2006). Results are illustrated as 16S rRNA gene copies per ng DNA.

2.8 Clinical outcomes

Health outcome of mice was monitored before and for 6 days after *C. jejuni* infection. Total clinical score (maximum 12 points) constituted of clinical aspect (i.e., wasting symptoms; 0: normal; 1: ruffled fur; 2: less locomotion; 3: isolation; 4: severely compromised locomotion, pre-final aspect), fecal blood (0: none; 2: microscopic detection using the Guajac method (Haemoccult, Beckman Coulter/PCD, Germany); 4: visible

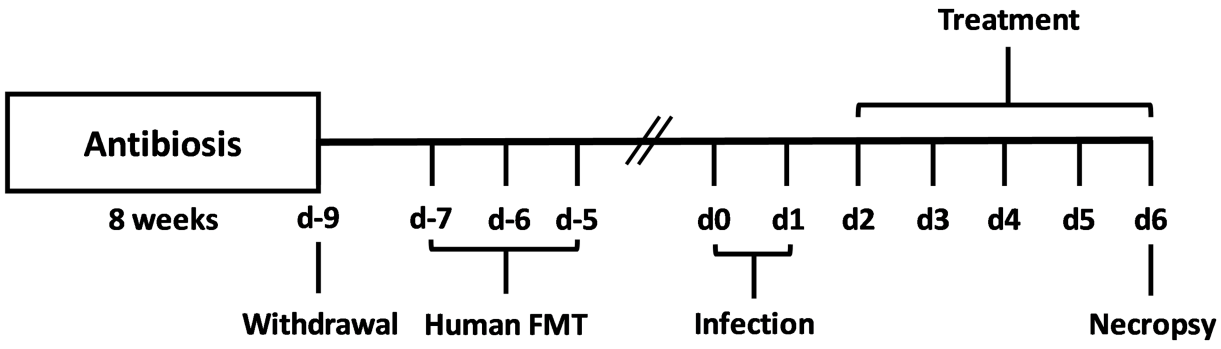

FIGURE 1
Experimental set-up. For gut microbiota depletion, conventionally raised IL-$10^{-/-}$ mice were subjected to an 8-week pretreatment with ampicillin plus sulbactam. Two days before oral human fecal microbiota transplantation (FMT) of secondary abiotic IL-$10^{-/-}$ mice on day (d)-7, d-6, and d-5, the antibiotic compounds were replaced by sterile tap water. On d0 and d1, human microbiota associated (hma) mice were perorally infected with *C. jejuni* strain 81–176, and treated with synthetic carvacrol, deferoxamine, deoxycholic acid, and 2-fucosyl-lactose alone, with a combination of all four compounds or with placebo (via the drinking water) from d2 until necropsy on d6 post-infection.

TABLE 1 Treatment regimens and concentrations of applied substances.

Treatment	Daily Dose (mg/kg)	Drinking Solution (mg/L)	MIC[a] (mg/L)
Placebo	–	–	–
Carvacrol	100	500	150
Deferoxamine	100	500	8
Deoxycholic acid	50	250	>256
2-Fucosyl-lactose	480	2,400	>32,768
Combination	730	3,650	114

[a]MIC: minimal inhibitory concentration.

blood spots), and stool appearance (0: normal/firm; 2: pasty; 4: liquid), as stated previously (Heimesaat et al., 2014).

2.9 Dissection and sampling

Six days p.i., mice were sacrificed by carbon dioxide asphyxiation and dissected in an aseptic environment. *Ex vivo* tissue samples from liver, kidneys, mesenteric lymph nodes (MLN), colon, in addition to luminal samples (from stomach, duodenum, ileum, and colon) were collected for microbiological, immunological, and immunohistopathological analyses. Heart blood was used for cytokine measurements.

2.10 Histopathological changes

Colonic tissue samples were fixed in 5% formalin and embedded in paraffin. 5-µm-sections were then stained with hematoxylin and eosin (H&E) to evaluate histopathological changes. The colonic mucosa was assessed under light microscopy (100 × magnification) using the following scoring scheme (Erben et al., 2014): Score 0, normal/no inflammatory cell infiltrates in epithelium. Score 1, minimal inflammatory cell infiltrates in mucosa but still intact epithelium. Score 2, mild inflammatory cell infiltrates in mucosa and submucosa with mild hyperplasia and mild goblet cell loss. Score 3, moderate inflammatory cell infiltrates in mucosa with moderate goblet cell loss. Score 4, extensive inflammatory cell infiltration into mucosa and submucosa with marked goblet cell loss, multiple crypt abscesses, and crypt loss.

2.11 *In situ* immunohistochemistry

5-µm-sections of colonic tissue samples were fixed in 5% formalin and embedded in paraffin as previously described (Heimesaat et al., 2018; Foote et al., 2023). Primary antibodies against cleaved caspase-3 (Asp175, Cell Signaling, Beverly, MA, United States, 1:200), MPO7 (No. A0398, Dako, Glostrup, Denmark, 1:500), CD3 (no. N1580, Dako, 1:10), and FOXP3 (clone FJK-165, no. 14-5773, eBioscience, 1:100) were used to count apoptotic epithelial cells, neutrophils, T lymphocytes, and regulatory T cells under light microscopy. The mean number of detected cells in each blinded sample was determined within at least six high power fields (HPF, 0.287 mm^2, 400 × magnification).

2.12 Mouse inflammation cytometric bead assay

Ex vivo tissue samples from colon, liver (both approximately 1 cm^3), kidney (one half after the longitudinal cut) were collected and washed in sterile PBS. Samples were incubated at 37°C for 18 h in 24-flat-bottom well culture plates (Thermo Fisher Scientific, Waltham, MA, United States) containing 500 µL serum-free RPMI 1640 medium (Thermo Fisher Scientific, Waltham, MA, United States), penicillin (100 µg/mL; Biochrom, Berlin, Germany) and streptomycin (100 µg/mL; Biochrom, Berlin, Germany). The culture supernatants and serum samples were then tested for interferon-gamma (IFN-γ) and IL-6 by applying the Mouse Inflammation Cytometric Bead Assay (BD Biosciences, Germany) in a BD FACS Canto II flow cytometer (BD Biosciences).

2.13 Statistical analysis and reproducibility

Results from animal experiments are representative of three independent repetitions. Statistical analysis was performed using GraphPad Prism (version 9; San Diego, CA, United States). The Anderson-Darling test was used to normalize data sets. The Student's *t*-test and Mann–Whitney test were applied for pairwise comparisons of normally and not normally distributed data. Multiple comparisons were performed using the one-way ANOVA with Tukey post-correction (for normally distributed data) and Kruskal-Wallis test with Dunn's post-correction (for not normally distributed data). *p* values of less than 0.05 were considered significant. Outliers were identified by the Grubb's test.

3 Results

3.1 Fecal microbiota composition in hma IL-$10^{-/-}$ mice immediately before *Campylobacter jejuni* infection

We first assessed whether the human fecal microbiota transplants had comparably engrafted in the intestinal tract of secondary abiotic mice within 1-week after triple human FMTs. To address this, we performed quantitative gut microbiota analyses immediately before *C. jejuni* infection. Both, cultural and culture-independent (i.e., molecular) analyses proved that the fecal loads of the tested intestinal bacterial groups, genera, and species were comparably high in the six prospective treatment cohorts of the hma IL-$10^{-/-}$ mice pointing towards similar engraftment of the human fecal transplants in the murine hosts (Supplementary Figure S2; Figure 2).

3.2 Gastrointestinal *Campylobacter jejuni* loads following oral infection and treatment of hma IL-$10^{-/-}$ mice with carvacrol, deferoxamine, deoxycholic acid, and 2-fucosyl-lactose alone or in combination

Following the start of oral treatment in *C. jejuni* infected hma IL-$10^{-/-}$ mice with carvacrol, deferoxamine, deoxycholic acid, and

10.3389/fmicb.2024.1290490

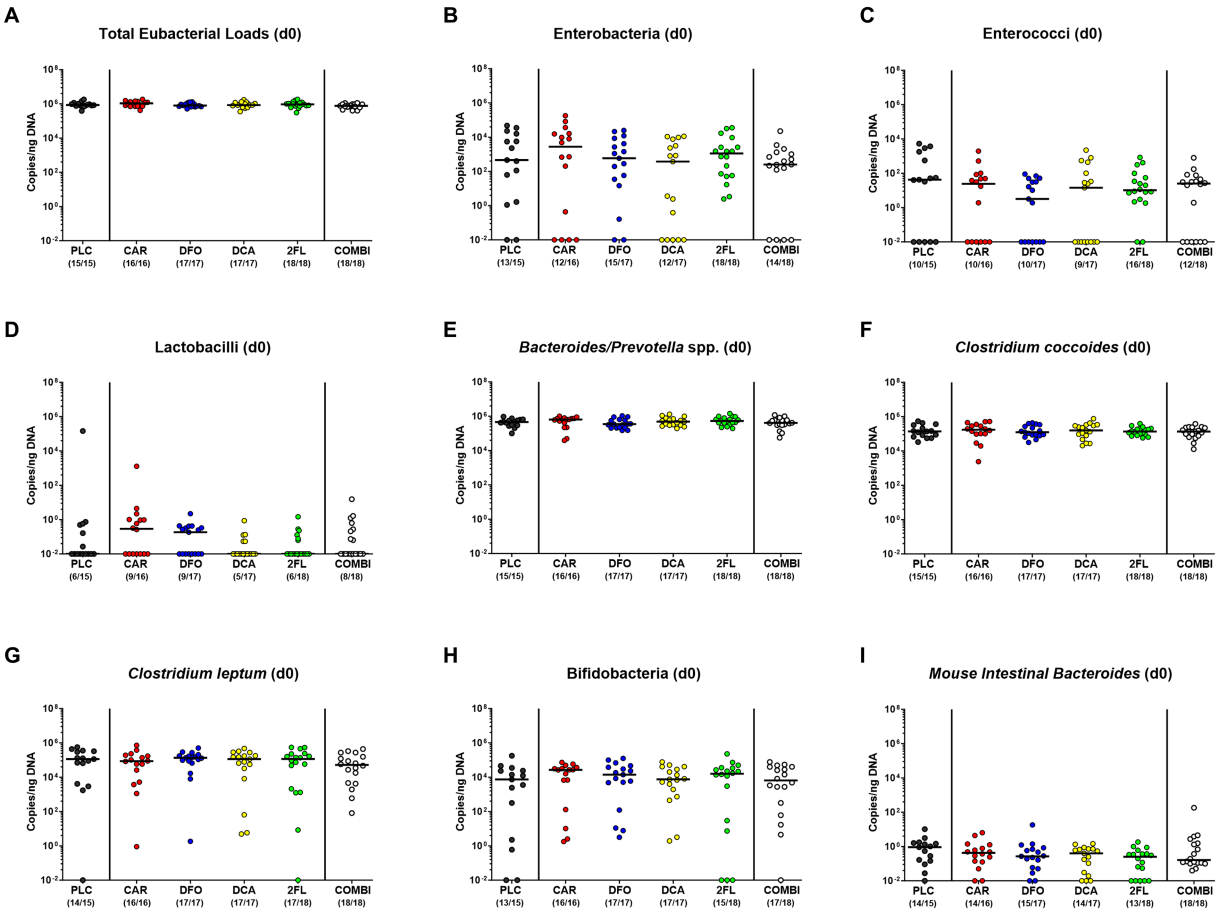

FIGURE 2
Culture-independent analysis of fecal microbiota composition in human microbiota associated IL-10$^{-/-}$ mice immediately before *C. jejuni* infection. A week before *C. jejuni* infection, secondary abiotic IL-10$^{-/-}$ mice (that had been generated by antibiotic pretreatment) were subjected to human fecal microbiota transplantation on three consecutive days by oral gavage [i.e., on day (d)-7, d-6, and d-5]. Immediately before *C. jejuni* infection on d0, the fecal microbiota composition was surveyed in mice from the prospective treatment cohorts (PLC, placebo; CAR, carvacrol; DFO, deferoxamine; DCA, deoxycholic acid; 2FL, 2-fucosyl-lactose; COMBI, a combination of all four compounds) by culture-independent, 16S rRNA real-time PCR (see methods) assessing the **(A)** total eubacterial loads, **(B)** enterobacteria, **(C)** enterococci, **(D)** lactobacilli, **(E)** *Bacteroides/Prevotella* species (spp.), **(F)** *Clostridium coccoides* group, **(G)** *Clostridium leptum* group, **(H)** bifidobacteria, and **(I)** *Mouse Intestinal Bacteroides* (expressed as copies per ng DNA). Medians (black bars) and numbers of mice with bacteria-positive detection out of the total number of analyzed animals (in parentheses) are indicated.

2-fucosyl-lactose alone or all four in combination on day 2 p.i., we surveyed the *C. jejuni* pathogen loads in fecal samples over time. Analyses by culture revealed median fecal *C. jejuni* counts of approximately 10^9 viable bacteria per gram that did not differ between the six treatment cohorts on days 2, 3, 4, and 5 p.i. [not significant (n.s.); Supplementary Figure S3]. Furthermore, we enumerated viable *C. jejuni* bacteria in luminal samples taken from defined gastrointestinal parts upon necropsy. Whereas the pathogen counts in the stomach and colon did not differ between the respective groups (n.s.; Figures 3A,D), approximately two orders of magnitude lower pathogen numbers could be cultured from the ileum lumen of carvacrol as compared to placebo treated mice on day 6 p.i. ($p < 0.05$; Figure 3C). Furthermore, the carvacrol and combination groups exhibited lower *C. jejuni* burdens in their duodenum as compared to 2-fucosyl-lactose treated mice ($p < 0.01$; Figure 3B). Therefore, all treatment regimens, whether applied individually or in combination did not affect *C. jejuni* loads in the colon. It is notable that only the carvacrol treatment lowered pathogen loads in the ileal tracts of infected hma IL-10$^{-/-}$ mice.

3.3 Clinical outcomes of hma IL-10$^{-/-}$ mice following *Campylobacter jejuni* infection and treatment with carvacrol, deferoxamine, deoxycholic acid, and 2-fucosyl-lactose alone or in combination

We further surveyed the effect of the applied treatment regimens on *C. jejuni* induced disease with campylobacteriosis scores (assessing wasting symptoms plus diarrhea plus fecal blood) over time p.i. As early as 24 h after initiation of the treatments (i.e., on day 3 p.i.), increased clinical scores were determined in the deferoxamine, deoxycholic acid, 2-fucosyl-lactose, and placebo treated groups ($p < 0.01$–0.001 versus naive; Supplementary Figure S4A), whereas carvacrol and combination treated hma mice displayed basal values

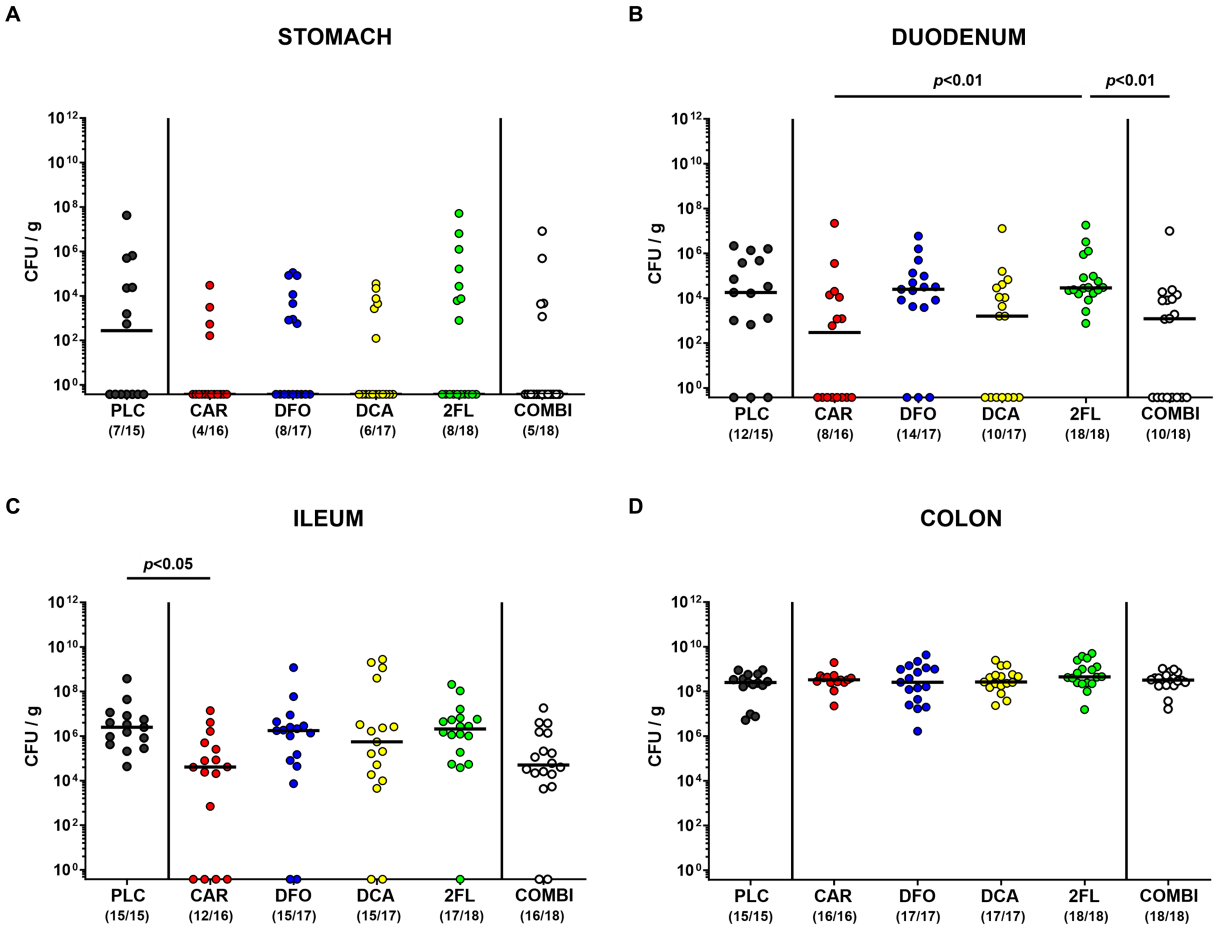

FIGURE 3
Establishment of *C. jejuni* in the gastrointestinal tract of infected hma IL-10$^{-/-}$ mice. Hma IL-10$^{-/-}$ mice were orally infected with *C. jejuni* strain 81–176 on days 0 and 1. From day 2 until day 6 post-infection, mice were treated with synthetic carvacrol (CAR), deferoxamine (DFO), deoxycholic acid (DCA), 2-fucosyl-lactose (2FL), a combination of all four compounds (COMBI) or placebo (PLC) via the drinking water. Upon sacrifice on d6 post-infection, *C. jejuni* were quantitated in luminal samples taken from the **(A)** stomach, **(B)** duodenum, **(C)** ileum, and **(D)** colon by culture and expressed as colony-forming units per gram (CFU/g). Individual data pooled from three experiments, medians (black bars), the numbers of culture-positive mice out of the total number of analyzed animals (in parentheses), and the significance levels (*p* values) determined by the Kruskal-Wallis test and Dunn's post-correction are shown.

(n.s. versus naive; Supplementary Figure S4A). This also held true for basal scores in mice from the combination group on days 4 and 5 p.i. (n.s. versus naive; Supplementary Figures S4B,C). Immediately before necropsy on day 6 p.i., mice from all infected cohorts exhibited similarly increased overall campylobacteriosis scores ($p < 0.05$–0.001 versus naive; Figure 4A), but with a trend towards lower median scores in carvacrol and combination treated mice versus placebo counterparts (n.s. due to relatively high standard deviations; Figure 4A). When specifically quantitating wasting symptoms on day 6 p.i., no differences in wasting scores could be observed between treated mice ($p < 0.05$–0.001 versus naive; Figure 4B), whereas the scores for fecal blood were increased in all cohorts except the carvacrol treatment group (n.s. versus naive; Figure 4C). Remarkably, carvacrol and combination treated mice suffered from less severe diarrheal symptoms as indicated by lower diarrhea scores if compared to placebo control mice on day 6 p.i. ($p < 0.05$; Figure 4D). Of note, mice from the carvacrol, deoxycholic acid, 2-fucosyl-lactose, and combination cohorts exhibited basal diarrheal scores at the end of the experiment (n.s. versus naive; Figure 4D). Hence, carvacrol and combination treatment alleviated diarrheal symptoms in *C. jejuni* infected hma mice.

3.4 Macroscopic and microscopic inflammatory changes in hma IL-10$^{-/-}$ mice following *Campylobacter jejuni* infection and treatment with carvacrol, deferoxamine, deoxycholic acid, and 2-fucosyl-lactose alone or in combination

Next, we assessed changes in colonic lengths, as enterocolitis is known to result in significantly shorter intestines due to inflammation (Heimesaat et al., 2006; Bereswill et al., 2011). Irrespective of the treatment, infected mice displayed shorter colons as compared to uninfected control animals ($p < 0.05$–0.001; Figure 5A). Furthermore, we quantitated the *C. jejuni* induced histopathological changes in the colon and determined lower histopathological scores in carvacrol and combination treated mice as compared to placebo counterparts on day

10.3389/fmicb.2024.1290490

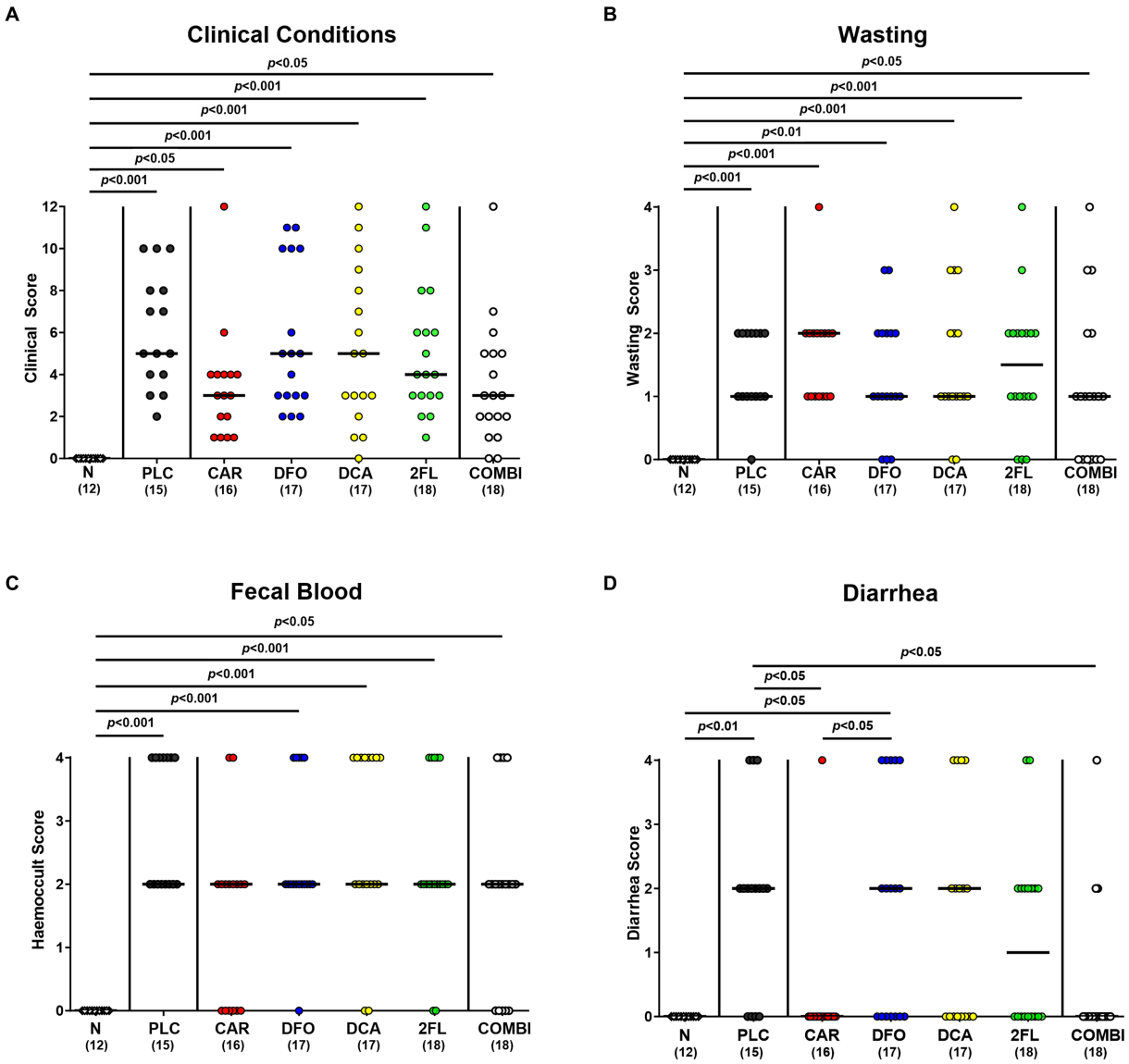

FIGURE 4
Clinical outcomes in hma IL-10$^{-/-}$ mice following *C. jejuni* infection and treatment with carvacrol, deferoxamine, deoxycholic acid, and 2-fucosyl-lactose alone or all in combination. *C. jejuni* infected hma IL-10$^{-/-}$ mice were perorally treated with synthetic carvacrol (CAR), deferoxamine (DFO), deoxycholic acid (DCA), 2-fucosyl-lactose (2FL), a combination of all four compounds (COMBI) or placebo (PLC) from day 2 until day 6 post-infection. At the end of the treatment (i.e., day 6 post-infection), the clinical outcomes were quantitated with clinical scores assessing the **(A)** overall clinical conditions and specifically, **(B)** wasting symptoms, **(C)** diarrhea, and **(D)** fecal blood. Naive (N) hma IL-10$^{-/-}$ mice served as non-infected and untreated controls. Individual data pooled from three experiments, the medians (black bars), the numbers of included mice (in parentheses), and the significance levels (*p* values) determined by the Kruskal-Wallis test and Dunn's post-correction are shown.

6 p.i., indicative for less severe pathogen-induced microscopic disease ($p < 0.01$ and $p < 0.001$, respectively; Figure 5B). In addition, the numbers of apoptotic colonic epithelial cells were lower in infected mice from the carvacrol, deferoxamine, 2-fucosyl-lactose, and combination cohorts versus placebo ($p < 0.05$–0.001; Figure 5C). The combination treatment dampened both, histopathological and apoptotic cell responses in the colon of *C. jejuni* infected mice to basal levels (n.s. versus naive; Figures 5B,C). Hence, carvacrol and combination treatment of hma IL-10$^{-/-}$ mice resulted in diminished microscopic (i.e., histopathological and apoptotic) sequelae of *C. jejuni* infection.

3.5 Immune cell subsets in the colon of hma IL-10$^{-/-}$ mice following *Campylobacter jejuni* infection and treatment with carvacrol, deferoxamine, deoxycholic acid, and 2-fucosyl-lactose alone or in combination

To test treatment impact on *C. jejuni* induced immune responses, we stained colonic paraffin sections with antibodies against surface markers of distinct innate and adaptive immune cells. On day 6 p.i., MPO7^{+} neutrophilic granulocytes were lower in

10.3389/fmicb.2024.1290490

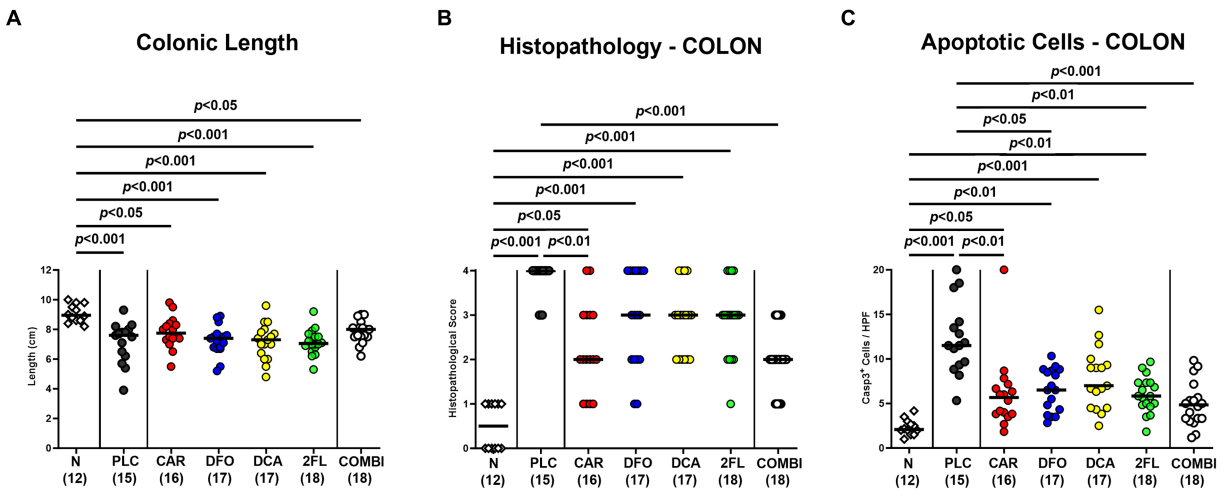

FIGURE 5
Macroscopic and microscopic inflammatory changes in hma IL-10$^{-/-}$ mice following *C. jejuni* infection and treatment with carvacrol, deferoxamine, deoxycholic acid, and 2-fucosyl-lactose alone or all in combination. *C. jejuni* infected hma IL-10$^{-/-}$ mice were perorally treated with synthetic carvacrol (CAR), deferoxamine (DFO), deoxycholic acid (DCA), 2-fucosyl-lactose (2FL), a combination of the four compounds (COMBI) or placebo (PLC) via the drinking water from day 2 until day 6 post-infection. On day 6, the **(A)** colonic lengths were measured, the **(B)** histopathological changes scored in hematoxylin and eosin-stained colonic paraffin sections, and the **(C)** numbers of apoptotic colonic epithelial cells determined in colonic paraffin sections stained with an antibody against cleaved caspase-3 (average numbers out of six representative high-power fields (HPF, 400 × magnification) per mouse). Naive (N) hma IL-10$^{-/-}$ mice served as non-infected and untreated controls. Individual data pooled from three experiments, the medians (black bars), the numbers of included mice (in parentheses), and the significance levels (*p* values) determined by the one-way ANOVA test with Tukey post-correction **(A)** and by the Kruskal-Wallis test and Dunn's post-correction **(B,C)** are shown.

the colonic mucosa and lamina propria of carvacrol and combination treated mice when compared to placebo counterparts ($p < 0.001$; Figure 6A). Remarkably, they did not even differ from uninfected controls (n.s. versus naive; Figure 6A). Irrespective of the treatment, *C. jejuni* infection resulted in colonic increases in adaptive CD3$^+$ T lymphocytes and FOXP3$^+$ regulatory T cells ($p < 0.05$–0.001 versus naive; Figures 6B,C). T cell numbers were, however, approximately 50% lower in the colon of all verum as compared to the control group on day 6 p.i. ($p < 0.001$; Figure 6B). Moreover, the combination of all four compounds did not further alleviate colonic T cell responses upon *C. jejuni* infection. Hence, oral carvacrol and combination treatment could diminish *C. jejuni* triggered immune responses.

3.6 Intestinal and extra-intestinal IFN-γ secretion in hma IL-10$^{-/-}$ mice following *Campylobacter jejuni* infection and treatment with carvacrol, deferoxamine, deoxycholic acid, and 2-fucosyl-lactose alone or in combination

C. jejuni infection resulted in enhanced IFN-γ secretion in colon and kidneys of placebo, deoxycholic acid and 2-fucosyl-lactose treated mice ($p < 0.05$–0.001; Figures 7A,B). In comparison, basal colonic and renal IFN-γ concentrations were measured in the carvacrol, deferoxamine, and combination treatment cohorts on day 6 p.i. (n.s. versus naive Figures 7A,B). This was also the case when determining IFN-γ levels in the liver of infected mice following carvacrol and combination treatment (n.s. versus naive Figure 7C). Hence, carvacrol and the combination treatment of hma IL-10$^{-/-}$ mice dampens *C. jejuni* induced IFN-γ responses in colon and extra-intestinal compartments, as observed in kidneys and liver.

3.7 Pro-inflammatory cytokine secretion in the serum of hma IL-10$^{-/-}$ mice following *Campylobacter jejuni* infection and treatment with carvacrol, deferoxamine, deoxycholic acid, and 2-fucosyl-lactose alone or in combination

Further, we addressed whether the treatment regimens could even affect systemic *C. jejuni* induced cytokine responses. As for the kidneys, basal IFN-γ levels were measured in the serum of infected mice from the carvacrol, deferoxamine, and combination cohorts (n.s. versus naive: Figure 8A), which also held true for basal serum IL-6 concentrations determined in carvacrol and combination treated mice on day 6 p.i. (n.s. versus naive; Figure 8B). Hence, carvacrol and combination treatment of hma IL-10$^{-/-}$ mice could alleviate systemic pro-inflammatory immune responses upon *C. jejuni* infection.

4 Discussion

For our current preclinical placebo-controlled intervention trial, we used (with respect to the gut microbiota) "humanized" IL-10$^{-/-}$ mice that have been generated through triple oral human FMTs of secondary abiotic IL-10$^{-/-}$ mice. Like all experimental systems, the hma IL-10$^{-/-}$ mouse model has its own limitations, which need to be critically taken into consideration. For instance, distinct human bacterial phyla might have been affected by freezing and thawing of

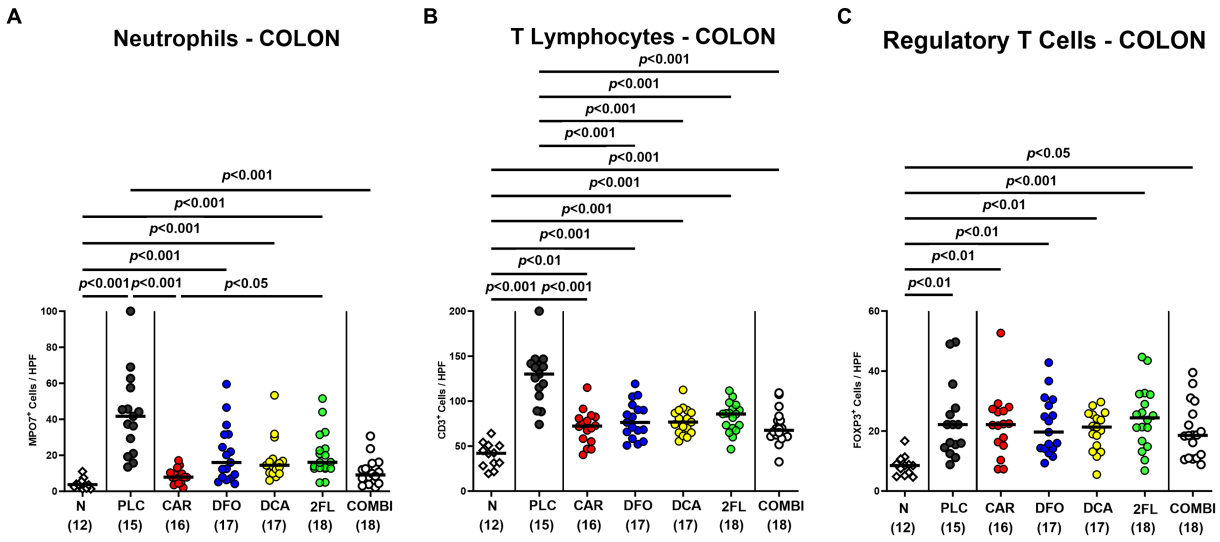

FIGURE 6
Immune cell subsets in the colon of hma IL-10$^{-/-}$ mice following *C. jejuni* infection and treatment with carvacrol, deferoxamine, deoxycholic acid, and 2-fucosyl-lactose alone or all in combination. *C. jejuni* infected hma IL-10$^{-/-}$ mice were perorally treated with synthetic carvacrol (CAR), deferoxamine (DFO), deoxycholic acid (DCA), 2-fucosyl-lactose (2FL), a combination of the four compounds (COMBI) or placebo (PLC) via the drinking water from day 2 until day 6 post-infection. **(A)** Neutrophils (MPO7^{+}), **(B)** T lymphocytes (CD3^{+}), and **(C)** regulatory T cells (FOXP3^{+}) were enumerated in immunohistochemically stained colonic paraffin sections derived on day 6 post-infection (average numbers out of six representative high-power fields (HPF, 400 × magnification) per mouse). Naive (N) hma IL-10$^{-/-}$ mice served as non-infected and untreated controls. Individual data pooled from three experiments, the medians (black bars), the numbers of included mice (in parentheses), and the significance levels (*p* values) determined by the Kruskal-Wallis test and Dunn's post-correction **(A,C)** and the one-way ANOVA test with Tukey post-correction **(B)** are shown.

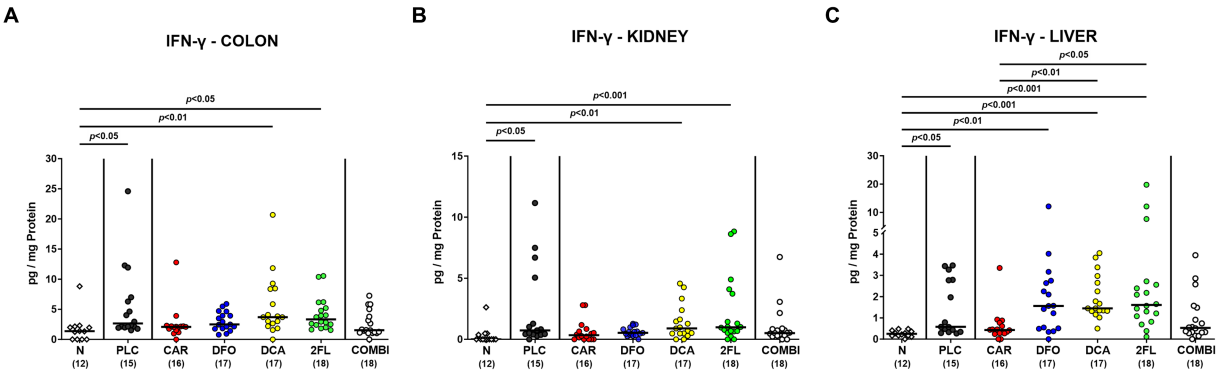

FIGURE 7
Intestinal and extra-intestinal IFN-γ concentrations in hma IL-10$^{-/-}$ mice following *C. jejuni* infection and treatment with carvacrol, deferoxamine, deoxycholic acid, and 2-fucosyl-lactose alone or all in combination. *C. jejuni* infected hma IL-10$^{-/-}$ mice were perorally treated with synthetic carvacrol (CAR), deferoxamine (DFO), deoxycholic acid (DCA), 2-fucosyl-lactose (2FL), a combination of the four compounds (COMBI) or placebo (PLC) via the drinking water from day 2 until day 6 post-infection. IFN-γ concentrations were determined in *ex vivo* biopsies taken from the **(A)** colon, **(B)** kidneys, and **(C)** liver on day 6 post-infection. Naive (N) hma IL-10$^{-/-}$ mice served as non-infected and untreated controls. Individual data pooled from three experiments, the medians (black bars), the numbers of included mice (in parentheses), and the significance levels (*p* values) determined by the Kruskal-Wallis test and Dunn's post-correction are shown.

the human fecal donor suspensions. Furthermore, differences in engraftment of the human fecal transplants in the murine intestinal tract could affect the clinical and immunopathological course of infection (Shayya et al., 2023). Both, our cultural and molecular analyses of fecal samples taken 1-week following the human FMTs and hence, immediately before *C. jejuni* infection on day 0 revealed comparable fecal loads of the main intestinal commensal bacterial phyla in all six prospective treatment cohorts indicating similar intestinal bacterial conditions upon induction of campylobacteriosis.

At the end of the observation period, no treatment regimens have affected *C. jejuni* loads in the colon, whereas on day 6 p.i. carvacrol treated hma IL-10$^{-/-}$ mice displayed approximately two orders of magnitude lower pathogen loads in the ileum, but not the colon when compared to placebo counterparts. One can speculate that most of the administered carvacrol might have already been absorbed by enterocytes before reaching the colon and exerting a direct pathogen-lowering effect in the colonic lumen. Previous *in vitro* and *in vivo* studies have proven anti-*Campylobacter* directed effects of carvacrol,

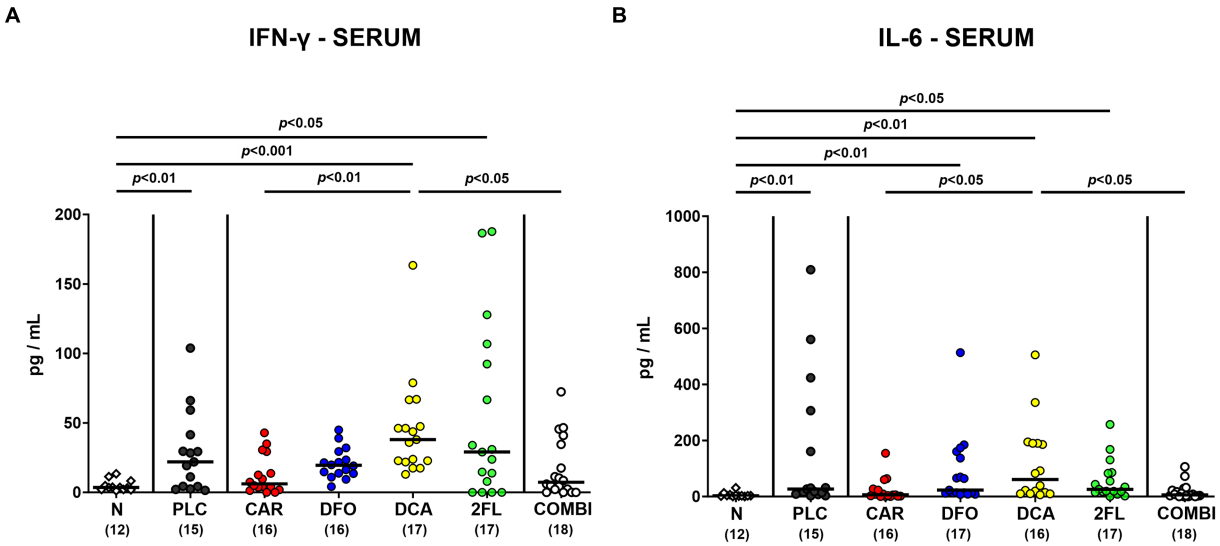

FIGURE 8
Systemic pro-inflammatory cytokine secretion in hma IL-10$^{-/-}$ mice following *C. jejuni* infection and treatment with carvacrol, deferoxamine, deoxycholic acid, and 2-fucosyl-lactose alone or all in combination. *C. jejuni* infected hma IL-10$^{-/-}$ mice were perorally treated with synthetic carvacrol (CAR), deferoxamine (DFO), deoxycholic acid (DCA), 2-fucosyl-lactose (2FL), a combination of the four compounds (COMBI) or placebo (PLC) via the drinking water from day 2 until day 6 post-infection. To assess systemic pro-inflammatory cytokine responses, **(A)** IFN-γ and **(B)** IL-6 concentrations were measured in serum samples taken on day 6 post-infection. Naive (N) hma IL-10$^{-/-}$ mice served as non-infected and untreated controls. Individual data pooled from three experiments, the medians (black bars), the numbers of included mice (in parentheses), and the significance levels (*p* values) determined by the Kruskal-Wallis test and Dunn's post-correction are shown. Outliers were excluded following identification by the Grubb's test.

but with varying efficacies depending on the experimental model, the applied carvacrol doses, and the duration of treatment (Johny et al., 2010; van Alphen et al., 2012; Kelly et al., 2017; Szott et al., 2020). Nevertheless, one could argue that the 2-log reduction in the ileal pathogen loads alone was not sufficient to explain the observed clinical effects upon oral carvacrol application. An *in vitro* study by Upadhyay et al. revealed that carvacrol treatment resulted in reduced adhesion invasion, and translocation of *C. jejuni* (Upadhyay et al., 2017). These results might explain the disease alleviating effect of oral carvacrol without pronounced antibacterial effects directed against *C. jejuni* infection *in vivo*. Nevertheless, other aspects such as the metabolization of carvacrol by members of the intestinal microbiota or direct immune-modulatory effects of the compound may have contributed to the better outcome of *C. jejuni* induced disease in treated mice.

In line with our results, even prophylactic application of deferoxamine in infected IL10$^{-/-}$ mice did not lower intestinal *C. jejuni* loads (Bereswill et al., 2022). Unexpectedly, deoxycholic acid and 2′-fucosyl-lactose did not exert antibacterial effects against *C. jejuni*, although numerous *in vitro* and *in vivo* studies have reported antimicrobial effects against various Gram-negative bacteria such as *Pseudomonas aeruginosa*, *E. coli*, *Salmonella* spp., and especially *Campylobacter*, for both substances (Yu et al., 2016; Gourley et al., 2017; Negretti et al., 2017; Alrubaye et al., 2019; Facinelli et al., 2019).

The lack of anti-*Campylobacter* effects of exogenous deoxycholic acid and 2′-fucosyl-lactose in our preclinical trial might be explained by concentrations in the drinking solutions that were below the measured MICs. Even though the concentrations of carvacrol, deferoxamine and all four combined compounds in the drinking solutions were exceeding the MIC of respective compounds measured *in vitro*, the treated mice harbored the enteropathogen at numbers that did not differ from those determined in placebo counterparts. This unexpected result might be explained due to mixing and dilution effects of the applied substances with secretory intestinal fluids, which have potentially resulted in a rather subtle or even absent antibacterial effect. This is further supported by the fact that mice do not exhibit continuous drinking behaviors during day and night.

Despite the high gastrointestinal pathogen burdens, carvacrol and the quadruple combination treatment did not only result in less severe diarrheal symptoms in *C. jejuni* infected hma mice, but also prevented diarrhea in over 80% of infected mice that did not present any changes in stool consistency on day 6 p.i. This could be confirmed by our previous study showing potent anti-diarrheal effects of prophylactic oral carvacrol in *C. jejuni* infected secondary abiotic IL10$^{-/-}$ mice (Mousavi et al., 2020). Furthermore, carvacrol was shown to inhibit the diarrheal toxin production by *Bacillus cereus in vitro* (Ultee et al., 2002) and to alleviate *Clostridioides difficile* associated diarrheal symptoms in mice (Mooyottu et al., 2017).

The marked improvement in diarrheal symptoms following carvacrol and combination treatment of hma IL-10$^{-/-}$ mice was accompanied by less pronounced microscopic inflammatory sequelae of *C. jejuni* infection like histopathological changes and apoptotic epithelial cell responses in the large intestine. In line with these findings, carvacrol strongly inhibited caspase-dependent apoptosis and down-regulated the mTOR-Signaling *in vitro* (Banik et al., 2019), whereas prophylactic carvacrol application attenuated *C. jejuni*-induced apoptosis in colonic epithelia of infected secondary abiotic IL-10$^{-/-}$ mice (Mousavi et al., 2020). Besides carvacrol, also oral deferoxamine and 2′-fucosyl-lactose alone diminished apoptotic colonic cell responses upon *C. jejuni* infection. In line with our findings, a study in adult rats showed that iron overload increased caspase-3 reactivity whereas, conversely, deferoxamine treatment

ameliorated iron-induced intestinal apoptosis and inflammation (El-Sheikh et al., 2018). Furthermore, 2-fucosyl-lactose was shown to protect small intestinal epithelial cells against 5-fluorouracil-induced apoptosis (Zhao et al., 2022).

In addition to alleviated diarrheal symptoms and colonic epithelial cell apoptosis, oral carvacrol and quadruple combination treatment dampened pro-inflammatory immune cell responses in *C. jejuni* infected hma mice as indicated by attenuated accumulation of neutrophils and T lymphocytes in the colonic mucosa and lamina propria. Moreover, *C. jejuni* induced colonic T cell responses were decreased upon deferoxamine, deoxycholic acid, and 2-fucosyl-lactose application alone. In support, our previous studies revealed that *C. jejuni* infected IL-10$^{-/-}$ mice pre-treated with carvacrol or deferoxamine exhibited lower numbers of T lymphocytes in the large intestines, as compared to placebo controls (Mousavi et al., 2020; Bereswill et al., 2022). Additionally, 2′-fucosyl-lactose pretreatment was shown to reduce CD3^{+} T cell infiltration of the colon in *C. jejuni* infected wildtype mice (Yu et al., 2016). When assessing pro-inflammatory cytokine secretion in the infected large intestines, mice from the carvacrol, the deferoxamine, and the combination cohorts exhibited colonic IFN-γ concentrations that did not differ from those determined in naive mice. The anti-inflammatory effects of the applied compounds could also be observed beyond the intestinal tract given only basal IFN-γ concentrations measured in the kidneys, the liver, and even in the serum of infected mice from the carvacrol, the deferoxamine, and the combination treatment cohorts. In support, carvacrol treatment was shown to down-regulate IFN-γ expression in splenocytes of asthmatic mice (Kianmehr et al., 2016) and to decrease IFN-γ and IL-6 secretion in mice suffering from multiple sclerosis (Mahmoodi et al., 2019). A very recent study revealed that oral treatment with the iron chelating compound deferasirox alleviated acute dextran sulfate sodium (DSS) induced colitis that was accompanied by decreased IFN-γ serum concentrations (Wu et al., 2023), further underscoring the immune-modulatory effects of iron deprivation in acute intestinal inflammation including campylobacteriosis as shown for deferoxamine in our present and earlier studies (Bereswill et al., 2022).

Although previous reports have highlighted that both deoxycholic acid and 2-fucosyl-lactose attenuated alleviated intestinal inflammation including *C. jejuni* induced colitis in mice (Yu et al., 2016; Sun et al., 2018), no overt immune-modulatory effects of both substances were observed in our present trial. These discrepancies might be due to differences in experimental settings including dosage and duration of treatment, gut microbiota composition, genetic background, and animal husbandry, for instance.

Furthermore, given the here applied 4-day therapeutic treatment regimens, the disease-alleviating effects of respective compounds alone or in combination might have been more prominent after longer application periods starting before infection (i.e., prophylactic regimen). This might be addressed in future investigations.

Finally, the here applied "humanized" IL-10$^{-/-}$ mouse model provides a useful experimental tool (i) to dissect the interactions between *C. jejuni* on the pathogen side and the immune system as well as the commensal (murine or human) gut microbiota on the host side and (ii) to test defined molecules and compounds for their potential disease-alleviating including anti-pathogenic and immune-modulatory properties (Shayya et al., 2023).

5 Conclusion

Our placebo-controlled preclinical intervention study provides evidence that oral treatment with carvacrol, deferoxamine, deoxycholate, and 2-fucosyl-lactose exerts disease-alleviating effects in acute campylobacteriosis. All substances are approved by the U.S. Food and Drug Administration (Food and Drug Administration, 2023) and have proven to exert disease-alleviating effects in acute campylobacteriosis. In particular, the highly potent intestinal, extra-intestinal, and systemic anti-inflammatory properties of the non-toxic natural compounds might point towards a promising alternative in the fight of acute campylobacteriosis with antibiotics-independent treatment options.

Data availability statement

The original contributions presented in the study are included in the article/Supplementary material, further inquiries can be directed to the corresponding author.

Ethics statement

The animal study was approved by "Landesamt für Gesundheit und Soziales", LaGeSo, Berlin. The study was conducted in accordance with the local legislation and institutional requirements.

Author contributions

SM: Formal analysis, Investigation, Visualization, Writing – original draft. MF: Formal analysis, Investigation. KD: Investigation, Writing – review & editing. RB: Investigation. SB: Conceptualization, Funding acquisition, Supervision, Writing – review & editing. MMH: Conceptualization, Funding acquisition, Investigation, Supervision, Validation, Writing – original draft.

Funding

The author(s) declare financial support was received for the research, authorship, and/or publication of this article. The project received funding from by the German Federal Ministries of Education and Research (BMBF) in frame of the Zoonoses Research Consortium PAC-Campylobacter to MMH and SB (IP7/01KI2007D) and from the Federal Ministry for Economic Affairs and Energy following a resolution of the German National Parliament, Deutscher Bundestag to MMH and SB (ZIM, ZF4117908 AJ8).

Acknowledgments

We are very grateful for the excellent contribution to this project of Alexandra Bittroff-Leben, Ines Puschendorf, Ulrike Fiebiger, Sumaya Abdul-Rahman, Gernot Reifenberger, Nizar W. Shayya, and the animal technicians at FEM of Charité – University Medicine

Berlin. We acknowledge the financial support from the Open Access Publication Fund of Charité – Universitätsmedizin Berlin and the German Research Foundation (DFG).

Conflict of interest

The authors declare that the research was conducted in the absence of any commercial or financial relationships that could be construed as a potential conflict of interest.

The author(s) declared that they were an editorial board member of Frontiers, at the time of submission. This had no impact on the peer review process and the final decision.

Publisher's note

Supplementary material

The Supplementary material for this article can be found online at: https://www.frontiersin.org/articles/10.3389/fmicb.2024.1290490/full#supplementary-material

References

Acheson, D., and Allos, B. M. (2001). *Campylobacter jejuni* infections: update on emerging issues and trends. *Clin. Infect. Dis.* 32, 1201–1206. doi: 10.1086/319760

Alrubaye, B., Abraha, M., Almansour, A., Bansal, M., Wang, H., Kwon, Y. M., et al. (2019). Microbial metabolite deoxycholic acid shapes microbiota against *Campylobacter jejuni* chicken colonization. *PLoS One* 14:e0214705. doi: 10.1371/journal.pone.0214705

Anholt, M., and Barkema, H. (2021). What is one health? *Can. Vet. J.* 62, 641–644.

Banik, S., Akter, M., Corpus Bondad, S. E., Saito, T., Hosokawa, T., and Kurasaki, M. (2019). Carvacrol inhibits cadmium toxicity through combating against caspase dependent/independent apoptosis in PC12 cells. *Food Chem. Toxicol.* 134:110835. doi: 10.1016/j.fct.2019.110835

Bellotti, D., and Remelli, M. (2021). Deferoxamine B: a natural, excellent and versatile metal chelator. *Molecules* 26:3255. doi: 10.3390/molecules26113255

Bereswill, S., Fischer, A., Plickert, R., Haag, L. M., Otto, B., Kuhl, A. A., et al. (2011). Novel murine infection models provide deep insights into the "menage a trois" of *Campylobacter jejuni*, microbiota and host innate immunity. *PLoS One* 6:e20953. doi: 10.1371/journal.pone.0020953

Bereswill, S., Mousavi, S., Weschka, D., Buczkowski, A., Schmidt, S., and Heimesaat, M. M. (2022). Iron deprivation by Oral Deferoxamine application alleviates acute Campylobacteriosis in a clinical murine *Campylobacter jejuni* infection model. *Biomol. Ther.* 13:71. doi: 10.3390/biom13010071

Bereswill, S., Plickert, R., Fischer, A., Kühl, A. A., Loddenkemper, C., Batra, A., et al. (2011). What you eat is what you get: novel *Campylobacter* models in the quadrangle relationship between nutrition, obesity, microbiota and susceptibility to infection. *Eur. J. Microbiol. Immunol. (Bp).* 1, 237–248. doi: 10.1556/EuJMI.1.2011.3.8

Callahan, S. M., Dolislager, C. G., and Johnson, J. G. (2021). The host cellular immune response to infection by *Campylobacter* spp. and its role in disease. *Infect. Immun.* 89, e00116–e00121. doi: 10.1128/IAI.00116-21

Chung, H., Pamp, S. J., Hill, J. A., Surana, N. K., Edelman, S. M., Troy, E. B., et al. (2012). Gut immune maturation depends on colonization with a host-specific microbiota. *Cell* 149, 1578–1593. doi: 10.1016/j.cell.2012.04.037

Davis, J. C., Totten, S. M., Huang, J. O., Nagshbandi, S., Kirmiz, N., Garrido, D. A., et al. (2016). Identification of oligosaccharides in feces of breast-fed infants and their correlation with the gut microbial community. *Mol. Cell. Proteomics* 15, 2987–3002. doi: 10.1074/mcp.M116.060665

de Zoete, M. R., Keestra, A. M., Roszczenko, P., and van Putten, J. P. (2010). Activation of human and chicken toll-like receptors by *Campylobacter* spp. *Infect. Immun.* 78, 1229–1238. doi: 10.1128/IAI.00897-09

El-Sheikh, A. A., Ameen, S. H., and Abd El-Fatah, S. S. (2018). Ameliorating iron overload in intestinal tissue of adult male rats: quercetin vs deferoxamine. *J. Toxicol.* 2018, 1–13. doi: 10.1155/2018/8023840

Engfer, M. B., Stahl, B., Finke, B., Sawatzki, G., and Daniel, H. (2000). Human milk oligosaccharides are resistant to enzymatic hydrolysis in the upper gastrointestinal tract. *Am. J. Clin. Nutr.* 71, 1589–1596. doi: 10.1093/ajcn/71.6.1589

Erben, U., Loddenkemper, C., Doerfel, K., Spieckermann, S., Haller, D., Heimesaat, M. M., et al. (2014). A guide to histomorphological evaluation of intestinal inflammation in mouse models. *Int. J. Clin. Exp. Pathol.* 7, 4557–4576.

European Food Safety Authority, European Centre for Disease Prevention and Control (2022). The European Union summary report on antimicrobial resistance in zoonotic and indicator bacteria from humans, animals and food in 2019–2020. *EFSA J.* 20:e07209. doi: 10.2903/j.efsa.2022.7209

Facinelli, B., Marini, E., Magi, G., Zampini, L., Santoro, L., Catassi, C., et al. (2019). Breast milk oligosaccharides: effects of 2′-fucosyllactose and 6′-sialyllactose on the adhesion of *Escherichia coli and Salmonella fyris* to Caco-2 cells. *J. Matern. Fetal Neonatal Med.* 32, 2950–2952. doi: 10.1080/14767058.2018.1450864

Food and Drug Administration F. *Food and Drug Administration-dietary supplement ingredient directory*. (2023). Available at: https://www.fda.gov/food/dietary-supplements/dietary-supplement-ingredient-directory.

Foote, M. S., Du, K., Mousavi, S., Bereswill, S., and Heimesaat, M. M. (2023). Therapeutic Oral application of Carvacrol alleviates acute Campylobacteriosis in mice harboring a human gut microbiota. *Biomol. Ther.* 13:320. doi: 10.3390/biom13020320

Garrido, D., Ruiz-Moyano, S., Kirmiz, N., Davis, J. C., Totten, S. M., Lemay, D. G., et al. (2016). A novel gene cluster allows preferential utilization of fucosylated milk oligosaccharides in *Bifidobacterium longum* subsp. longum SC596. *Sci. Rep.* 6:35045. doi: 10.1038/srep35045

Gholami-Ahangaran, M., Ahmadi-Dastgerdi, A., Azizi, S., Basiratpour, A., Zokaei, M., and Derakhshan, M. (2022). Thymol and carvacrol supplementation in poultry health and performance. *Vet. Med. Sci.* 8, 267–288. doi: 10.1002/vms3.663

Gourley, C. R., Negretti, N. M., and Konkel, M. E. (2017). The food-borne pathogen *Campylobacter jejuni* depends on the AddAB DNA repair system to defend against bile in the intestinal environment. *Sci. Rep.* 7:14777. doi: 10.1038/s41598-017-14646-9

Haag, L. M., Fischer, A., Otto, B., Plickert, R., Kuhl, A. A., Gobel, U. B., et al. (2012). *Campylobacter jejuni* induces acute enterocolitis in gnotobiotic IL-10$^{-/-}$ mice via toll-like-receptor-2 and -4 signaling. *PLoS One* 7:e40761. doi: 10.1371/journal.pone.0040761

Heimesaat, M. M., Alutis, M., Grundmann, U., Fischer, A., Tegtmeyer, N., Böhm, M., et al. (2014). The role of serine protease HtrA in acute ulcerative enterocolitis and extra-intestinal immune responses during *Campylobacter jejuni* infection of gnotobiotic IL-10 deficient mice. *Front. Cell. Infect. Microbiol.* 4:77. doi: 10.3389/fcimb.2014.00077

Heimesaat, M. M., Bereswill, S., Fischer, A., Fuchs, D., Struck, D., Niebergall, J., et al. (2006). Gram-negative bacteria aggravate murine small intestinal Th1-type immunopathology following oral infection with toxoplasma gondii. *J. Immunol.* 177, 8785–8795. doi: 10.4049/jimmunol.177.12.8785

Heimesaat, M. M., Genger, C., Klove, S., Weschka, D., Mousavi, S., and Bereswill, S. (2020). The host-specific intestinal microbiota composition impacts *Campylobacter coli* infection in a clinical mouse model of Campylobacteriosis. *Pathogens* 9:804. doi: 10.3390/pathogens9100804

Heimesaat, M. M., Giladi, E., Kühl, A. A., Bereswill, S., and Gozes, I. (2018). The octapetide NAP alleviates intestinal and extra-intestinal anti-inflammatory sequelae of acute experimental colitis. *Peptides* 101, 1–9. doi: 10.1016/j.peptides.2017.12.023

Heimesaat, M. M., Mousavi, S., Bandick, R., and Bereswill, S. (2022). *Campylobacter jejuni* infection induces acute enterocolitis in IL-10$^{-/-}$ mice pretreated with ampicillin plus sulbactam. *Eur. J. Microbiol. Immunol. (Bp).* 12, 73–83. doi: 10.1556/1886.2022.00014

Herzog, M. K.-M., Cazzaniga, M., Peters, A., Shayya, N., Beldi, L., Hapfelmeier, S., et al. (2023). Mouse models for bacterial enteropathogen infections: insights into the role of colonization resistance. *Gut Microbes* 15:2172667. doi: 10.1080/19490976.2023.2172667

Hu, J., Wang, C., Huang, X., Yi, S., Pan, S., Zhang, Y., et al. (2021). Gut microbiota-mediated secondary bile acids regulate dendritic cells to attenuate autoimmune uveitis through TGR5 signaling. *Cell Rep.* 36:109726. doi: 10.1016/j.celrep.2021.109726

Itoh, M., Wada, K., Tan, S., Kitano, Y., Kai, J., and Makino, I. (1999). Antibacterial action of bile acids against *helicobacter pylori* and changes in its ultrastructural morphology: effect of unconjugated dihydroxy bile acid. *J. Gastroenterol.* 34, 571–576. doi: 10.1007/s005350050374

Johny, A. K., Darre, M., Donoghue, A., Donoghue, D., and Venkitanarayanan, K. (2010). Antibacterial effect of trans-cinnamaldehyde, eugenol, carvacrol, and thymol on Salmonella Enteritidis and *Campylobacter jejuni* in chicken cecal contents in vitro. *J. Appl. Poult. Res.* 19, 237–244. doi: 10.3382/japr.2010-00181

Jurado, R. L. (1997). Iron, infections, and anemia of inflammation. *Clin. Infect. Dis.* 25, 888–895. doi: 10.1086/515549

Kaakoush, N. O., Castano-Rodriguez, N., Mitchell, H. M., and Man, S. M. (2015). Global epidemiology of *Campylobacter* infection. *Clin. Microbiol. Rev.* 28, 687–720. doi: 10.1128/CMR.00006-15

Kelly, C., Gundogdu, O., Pircalabioru, G., Cean, A., Scates, P., Linton, M., et al. (2017). The in vitro and in vivo effect of Carvacrol in preventing *Campylobacter* infection, colonization and in improving productivity of chicken broilers. *Foodborne Pathog. Dis.* 14, 341–349. doi: 10.1089/fpd.2016.2265

Kianmehr, M., Rezaei, A., and Boskabady, M. H. (2016). Effect of carvacrol on various cytokines genes expression in splenocytes of asthmatic mice. *Iran. J. Basic Med. Sci.* 19, 402–410.

Kreling, V., Falcone, F. H., Kehrenberg, C., and Hensel, A. (2020). *Campylobacter* sp.: pathogenicity factors and prevention methods—new molecular targets for innovative antivirulence drugs? *Appl. Microbiol. Biotechnol.* 104, 10409–10436. doi: 10.1007/s00253-020-10974-5

Lobo de Sá, F., Schulzke, J.-D., and Bücker, R. (2021). Diarrheal mechanisms and the role of intestinal barrier dysfunction in *Campylobacter* infections. *Curr. Top. Microbiol. Immunol.* 431, 203–231. doi: 10.1007/978-3-030-65481-8_8

Mączka, W., Twardawska, M., Grabarczyk, M., and Wińska, K. (2023). Carvacrol; a natural phenolic compound with antimicrobial properties. *Antibiotics* 12:824. doi: 10.3390/antibiotics12050824

Mahmoodi, M., Amiri, H., Ayoobi, F., Rahmani, M., Taghipour, Z., Ghavamabadi, R. T., et al. (2019). Carvacrol ameliorates experimental autoimmune encephalomyelitis through modulating pro-and anti-inflammatory cytokines. *Life Sci.* 219, 257–263. doi: 10.1016/j.lfs.2018.11.051

Manfredi, R., Nanetti, A., Ferri, M., and Chiodo, F. (1999). Fatal *Campylobacter jejuni* bacteraemia in patients with AIDS. *J. Med. Microbiol.* 48, 601–603. doi: 10.1099/00222615-48-6-601

Mansfield, L. S., Bell, J. A., Wilson, D. L., Murphy, A. J., Elsheikha, H. M., Rathinam, V. A., et al. (2007). C57BL/6 and congenic interleukin-10-deficient mice can serve as models of *Campylobacter jejuni* colonization and enteritis. *Infect. Immun.* 75, 1099–1115. doi: 10.1128/IAI.00833-06

Moon, J.-H., Herr, Y., Kim, S.-W., and Lee, J.-Y. (2011). In vitro activity of deferoxamine against *Porphyromonas gingivalis*. *FEMS Microbiol. Lett.* 323, 61–67. doi: 10.1111/j.1574-6968.2011.02357.x

Moore, J. E., Corcoran, D., Dooley, J. S., Fanning, S., Lucey, B., Matsuda, M., et al. (2005). *Campylobacter*. *Vet. Res.* 36, 351–382. doi: 10.1051/vetres:2005012

Mooyottu, S., Flock, G., Upadhyay, A., Upadhyaya, I., Maas, K., and Venkitanarayanan, K. (2017). Protective effect of carvacrol against gut dysbiosis and *Clostridium difficile* associated disease in a mouse model. *Front. Microbiol.* 8:625. doi: 10.3389/fmicb.2017.00625

Mortensen, N. P., Kuijf, M. L., Ang, C. W., Schiellerup, P., Krogfelt, K. A., Jacobs, B. C., et al. (2009). Sialylation of *Campylobacter jejuni* lipo-oligosaccharides is associated with severe gastro-enteritis and reactive arthritis. *Microbes Infect.* 11, 988–994. doi: 10.1016/j.micinf.2009.07.004

Mouftah, S. F., Cobo-Díaz, J. F., Álvarez-Ordóñez, A., Elserafy, M., Saif, N. A., Sadat, A., et al. (2021). High-throughput sequencing reveals genetic determinants associated with antibiotic resistance in *Campylobacter* spp. from farm-to-fork. *PLoS One* 16:e0253797. doi: 10.1371/journal.pone.0253797

Mousavi, S., Busmann, L. V., Bandick, R., Shayya, N. W., Bereswill, S., and Heimesaat, M. M. (2023). Oral application of carvacrol, butyrate, ellagic acid, and 2′-fucosyl-lactose to mice suffering from acute campylobacteriosis – results from a preclinical placebo-controlled intervention study. *Eur. J. Microbiol. Immunol. (Bp).* 13, 88–105. doi: 10.1556/1886.2023.00037

Mousavi, S., Schmidt, A.-M., Escher, U., Kittler, S., Kehrenberg, C., Thunhorst, E., et al. (2020). Carvacrol ameliorates acute campylobacteriosis in a clinical murine infection model. *Gut Pathog.* 12:2. doi: 10.1186/s13099-019-0343-4

Mullineaux-Sanders, C., Suez, J., Elinav, E., and Frankel, G. (2018). Sieving through gut models of colonization resistance. *Nat. Microbiol.* 3, 132–140. doi: 10.1038/s41564-017-0095-1

Nachamkin, I., Allos, B. M., and Ho, T. (1998). *Campylobacter* species and Guillain-Barre syndrome. *Clin. Microbiol. Rev.* 11, 555–567. doi: 10.1128/CMR.11.3.555

Negretti, N. M., Gourley, C. R., Clair, G., Adkins, J. N., and Konkel, M. E. (2017). The food-borne pathogen *Campylobacter jejuni* responds to the bile salt deoxycholate with countermeasures to reactive oxygen species. *Sci. Rep.* 7:15455. doi: 10.1038/s41598-017-15379-5

Newburg, D. S. (2005). Innate immunity and human milk. *J. Nutr.* 135, 1308–1312. doi: 10.1093/jn/135.5.1308

Obaidat, M. M., and Frank, J. F. (2009). Inactivation of Salmonella and *Escherichia coli* O157: H7 on sliced and whole tomatoes by allyl isothiocyanate, carvacrol, and cinnamaldehyde in vapor phase. *J. Food Prot.* 72, 315–324. doi: 10.4315/0362-028X-72.2.315

Omarova, S., Awad, K., Moos, V., Püning, C., Gölz, G., Schulzke, J.-D., et al. (2023). Intestinal barrier in post-*Campylobacter jejuni* irritable bowel syndrome. *Biomol. Ther.* 13:449. doi: 10.3390/biom13030449

Price, A., Jewkes, J., and Sanderson, P. (1979). Acute diarrhoea: *Campylobacter* colitis and the role of rectal biopsy. *J. Clin. Pathol.* 32, 990–997. doi: 10.1136/jcp.32.10.990

Robinson, T. P., Bu, D. P., Carrique-Mas, J., Fevre, E. M., Gilbert, M., Grace, D., et al. (2016). Antibiotic resistance is the quintessential one health issue. *Trans. R. Soc. Trop. Med. Hyg.* 110, 377–380. doi: 10.1093/trstmh/trw048

Sela, D. A., and Mills, D. A. (2010). Nursing our microbiota: molecular linkages between bifidobacteria and milk oligosaccharides. *Trends Microbiol.* 18, 298–307. doi: 10.1016/j.tim.2010.03.008

Sharifi-Rad, M., Varoni, E. M., Iriti, M., Martorell, M., Setzer, W. N., del Mar, C. M., et al. (2018). Carvacrol and human health: a comprehensive review. *Phytother. Res.* 32, 1675–1687. doi: 10.1002/ptr.6103

Shayya, N. W., Foote, M. S., Langfeld, L. Q., Du, K., Bandick, R., Mousavi, S., et al. (2023). Human microbiota associated IL-10$^{-/-}$ mice: a valuable enterocolitis model to dissect the interactions of *Campylobacter jejuni* with host immunity and gut microbiota. *Eur. J. Microbiol. Immunol. (Bp).* 12, 107–122. doi: 10.1556/1886.2022.00024

Su, X., Gao, Y., and Yang, R. (2023). Gut microbiota derived bile acid metabolites maintain the homeostasis of gut and systemic immunity. *Front. Immunol.* 14:1127743. doi: 10.3389/fimmu.2023.1127743

Sun, X., Liu, B., Sartor, R. B., and Jobin, C. (2013). Phosphatidylinositol 3-kinase-gamma signaling promotes *Campylobacter jejuni*-induced colitis through neutrophil recruitment in mice. *J. Immunol.* 190, 357–365. doi: 10.4049/jimmunol.1201825

Sun, X., Threadgill, D., and Jobin, C. (2012). *Campylobacter jejuni* induces colitis through activation of mammalian target of rapamycin signaling. *Gastroenterology* 142, 86–95.e5. doi: 10.1053/j.gastro.2011.09.042

Sun, X., Winglee, K., Gharaibeh, R. Z., Gauthier, J., He, Z., Tripathi, P., et al. (2018). Microbiota-derived metabolic factors reduce campylobacteriosis in mice. *Gastroenterology* 154, 1751–1763.e2. e2. doi: 10.1053/j.gastro.2018.01.042

Szott, V., Reichelt, B., Alter, T., Friese, A., and Roesler, U. (2020). In vivo efficacy of carvacrol on *Campylobacter jejuni* prevalence in broiler chickens during an entire fattening period. *Eur. J. Microbiol. Immunol. (Bp).* 10, 131–138. doi: 10.1556/1886.2020.00011

Ultee, A., Bennik, M. H. J., and Moezelaar, R. (2002). The phenolic hydroxyl Group of Carvacrol is Essential for action against the food-borne pathogen *Bacillus cereus*. *Appl. Environ. Microbiol.* 68, 1561–1568. doi: 10.1128/AEM.68.4.1561-1568.2002

Upadhyay, A., Arsi, K., Wagle, B. R., Upadhyaya, I., Shrestha, S., Donoghue, A. M., et al. (2017). Trans-cinnamaldehyde, carvacrol, and eugenol reduce *Campylobacter jejuni* colonization factors and expression of virulence genes in vitro. *Front. Microbiol.* 8:713. doi: 10.3389/fmicb.2017.00713

van Alphen, L. B., Burt, S. A., Veenendaal, A. K., Bleumink-Pluym, N. M., and van Putten, J. P. (2012). The natural antimicrobial carvacrol inhibits *Campylobacter jejuni* motility and infection of epithelial cells. *PLoS One* 7:e45343. doi: 10.1371/journal.pone.0045343

van Asbeck, B. S., Marcelis, J. H., Marx, J. J., Struyvenberg, A., van Kats, J. H., and Verhoef, J. (1983). Inhibition of bacterial multiplication by the iron chelator deferoxamine: potentiating effect of ascorbic acid. *Eur. J. Clin. Microbiol.* 2, 426–431. doi: 10.1007/BF02013899

Van Asbeck, B., Marcelis, J., Van Kats, J., Jaarsma, E., and Verhoef, J. (1983). Synergy between the iron chelator deferoxamine and the antimicrobial agents gentamicin, chloramphenicol, cefalothin, cefotiam and cefsulodin. *Eur. J. Clin. Microbiol.* 2, 432–438. doi: 10.1007/BF02013900

Wagenaar, J. A., Newell, D. G., Kalupahana, R. S., and Mughini-Gras, L. (2023). "*Campylobacter*: animal reservoirs, human infections, and options for control" in *Zoonoses: infections affecting humans and animals*, ed. A. Sing (Cham: Springer), 267–293.

Walker, R. I., Caldwell, M. B., Lee, E. C., Guerry, P., Trust, T. J., and Ruiz-Palacios, G. (1986). Pathophysiology of Campylobacter enteritis. *Microbiol. Rev.* 50, 81–94. doi: 10.1128/mr.50.1.81-94.1986

WHO. World Health Organisation. *Campylobacter*. (2020). Available at: https://www.who.int/news-room/fact-sheets/detail/campylobacter.

Wu, Y., Ran, L., Yang, Y., Gao, X., Peng, M., Liu, S., et al. (2023). Deferasirox alleviates DSS-induced ulcerative colitis in mice by inhibiting ferroptosis and improving intestinal microbiota. *Life Sci.* 314:121312. doi: 10.1016/j.lfs.2022.121312

Young, K. T., Davis, L. M., and Dirita, V. J. (2007). *Campylobacter jejuni*: molecular biology and pathogenesis. *Nat. Rev. Microbiol.* 5, 665–679. doi: 10.1038/nrmicro1718

Yu, Z.-T., Nanthakumar, N. N., and Newburg, D. S. (2016). The human milk oligosaccharide 2′-fucosyllactose quenches *Campylobacter jejuni*–induced inflammation in human epithelial cells HEp-2 and HT-29 and in mouse intestinal mucosa. *J. Nutr.* 146, 1980–1990. doi: 10.3945/jn.116.230706

Zhang, Q., Beyi, A. F., and Yin, Y. (2023). Zoonotic and antibiotic-resistant *Campylobacter*: a view through the one health lens. *One Health Adv.* 1:4. doi: 10.1186/s44280-023-00003-1

Zhao, G., Williams, J., Washington, M. K., Yang, Y., Long, J., Townsend, S. D., et al. (2022). 2'-Fucosyllactose ameliorates chemotherapy-induced intestinal mucositis by protecting intestinal epithelial cells against apoptosis. *Cell. Mol. Gastroenterol. Hepatol.* 13, 441–457. doi: 10.1016/j.jcmgh.2021.09.015

Zhao, C., Wu, K., Hao, H., Zhao, Y., Bao, L., Qiu, M., et al. (2023). Gut microbiota-mediated secondary bile acid alleviates *Staphylococcus aureus*-induced mastitis through the TGR5-cAMP-PKA-NF-κB/NLRP3 pathways in mice. *NPJ Biofilms Microbiomes* 9:8. doi: 10.1038/s41522-023-00374-8

frontiers | Frontiers in Microbiology

TYPE Original Research
PUBLISHED 17 April 2024
DOI 10.3389/fmicb.2024.1342573

OPEN ACCESS

EDITED BY
Stuart A. Thompson,
Augusta University, United States

REVIEWED BY
Fang Liu,
University of New South Wales, Australia
Marja-Liisa Hänninen,
University of Helsinki, Finland

*CORRESPONDENCE
Gireesh Rajashekara
✉ rajashekara.2@osu.edu

†These authors have contributed equally to this work

RECEIVED 22 November 2023
ACCEPTED 08 March 2024
PUBLISHED 17 April 2024

CITATION
Deblais L, Drozd M, Kumar A, Antwi J, Fuchs J, Khupse R, Helmy YA and Rajashekara G (2024) Identification of novel small molecule inhibitors of twin arginine translocation (Tat) pathway and their effect on the control of *Campylobacter jejuni* in chickens. *Front. Microbiol.* 15:1342573. doi: 10.3389/fmicb.2024.1342573

Identification of novel small molecule inhibitors of twin arginine translocation (Tat) pathway and their effect on the control of *Campylobacter jejuni* in chickens

Loïc Deblais[1†], Mary Drozd[2†], Anand Kumar[3†], Janet Antwi[4], James Fuchs[4], Rahul Khupse[5], Yosra A. Helmy[1] and Gireesh Rajashekara[1*]

[1]Department of Animal Sciences, The Ohio State University, OARDC, Wooster, OH, United States, [2]School of Veterinary Medicine and Biomedical Sciences, University of Nebraska-Lincoln, Lincoln, NE, United States, [3]Los Alamos National Laboratory, Bioscience Division, Group B-10: Biosecurity and Public Health, Los Alamos, NM, United States, [4]Division of Medicinal Chemistry and Pharmacognosy, College of Pharmacy, The Ohio State University, Columbus, OH, United States, [5]College of Pharmacy, University of Findlay, OH, United States

Introduction: Control of *Campylobacter* from farm to fork is challenging due to the frequent emergence of antimicrobial-resistant isolates. Furthermore, poultry production systems are known reservoirs of *Campylobacter*. The twin-arginine translocation (Tat) pathway is a crucial bacterial secretion system that allows *Campylobacter* to colonize the host intestinal tract by using formate as the main source of energy. However, Tat pathway is also a major contributing factor for resistance to copper sulfate ($CuSO_4$).

Methods: Since mammals and chickens do not have proteins or receptors that are homologous to bacterial Tat proteins, identification of small molecule (SM) inhibitors targeting the Tat system would allow the development of safe and effective control methods to mitigate *Campylobacter* in infected or colonized hosts in both pre-harvest and post-harvest. In this study, we screened 11 commercial libraries (n = 50,917 SM) for increased susceptibility to $CuSO_4$ (1 mM) in *C. jejuni* 81–176, a human isolate which is widely studied.

Results: Furthermore, we evaluated 177 SM hits (2.5μg/mL and above) that increased the susceptibility to $CuSO_4$ for the inhibition of formate dehydrogenase (Fdh) activity, a Tat-dependent substrate. Eight Tat-dependent inhibitors (T1–T8) were selected for further studies. These selected eight Tat inhibitors cleared all tested *Campylobacter* strains (n=12) at >10ng/mL in the presence of 0.5mM $CuSO_4$ *in vitro*. These selected SMs were non-toxic to colon epithelial (Caco-2) cells when treated with 50μg/mL for 24h and completely cleared intracellular *C. jejuni* cells when treated with 0.63μg/mL of SM for 24h in the presence of 0.5mM of $CuSO_4$. Furthermore, 3 and 5-week-old chicks treated with SM candidates for 5days had significantly decreased cecal colonization (up to 1.2 log; p<0.01) with minimal disruption of microbiota. *In silico* analyses predicted that T7 has better drug-like properties than T2 inhibitor and might target a key amino acid residue (glutamine 165), which is located in the hydrophobic core of TatC protein.

Discussion: Thus, we have identified novel SM inhibitors of the Tat pathway, which represent a potential strategy to control *C. jejuni* spread on farms.

KEYWORDS

Campylobacter jejuni, poultry production system, twin arginine translocase, small molecule inhibitor, microbiome

Introduction

Campylobacter is a leading cause of bacterial foodborne gastroenteritis worldwide (Igwaran and Okoh, 2019) and a major public health problem. A recent estimate by the CDC indicates that *Campylobacter* is not only among the most common causes of domestically acquired foodborne illnesses in humans (over 845,024 cases per year) but also is among the leading causes of hospitalization (over 8,463 annually) in the United States (USDA ERS–Cost Estimates of Foodborne Illnesses, 2017; Igwaran and Okoh, 2019).

Poultry products represent a key source of human *Campylobacter* infections (Kittl et al., 2013; Skarp et al., 2016). *C. jejuni* and *C. coli* densely colonize the intestine of poultry (up to 10^9 bacteria per gram of ceca in chicken) and are the most common species encountered in human infections (Allos, 2001; Newell and Fearnley, 2003; Lee and Newell, 2006; Young et al., 2007; Facciolà et al., 2017; Connerton et al., 2018). Despite extensive intestinal colonization, *Campylobacter* infection produces little or no clinical diseases in poultry (Johnson et al., 2017). Prevalence studies conducted in Europe and United States have reported *Campylobacter*-positive flocks ranging up to 100% (Newell and Fearnley, 2003; Luangtongkum et al., 2006; Jorgensen et al., 2011; Sibanda et al., 2018; Koutsoumanis et al., 2020; Kuhn et al., 2020). Colonized chickens shed *Campylobacter* in their feces until slaughter (up to 10^9 CFU/g of cecum) (Newell and Fearnley, 2003; Luangtongkum et al., 2006; Jorgensen et al., 2011; Sibanda et al., 2018; Koutsoumanis et al., 2020; Kuhn et al., 2020), increasing the risk of horizontal transmission of *Campylobacter* to the whole flock and post-harvest contaminations of the meat products (over 50% in average and up to 100%) (Logue et al., 2003; Berrang et al., 2007; Young et al., 2007; Guerin et al., 2010; Hue et al., 2010; Kaakoush et al., 2015). The high prevalence of *Campylobacter* in poultry and detection of identical genotypes in both poultry and human isolates support poultry contamination as the predominant route of human infection (Allos, 2001; Newell and Fearnley, 2003; Lee and Newell, 2006; Young et al., 2007; Facciolà et al., 2017; Connerton et al., 2018).

On-farm *Campylobacter* control efforts have not been successful in mitigating human *Campylobacter* infections as evidenced by the continuous increase in human infections (Kittl et al., 2013; Skarp et al., 2016). Although improving biosecurity has beneficial effects on lowering the overall flock prevalence (Kaakoush et al., 2015), these measures have not resulted in consistent and predictable outcomes in controlling *Campylobacter* (Wagenaar et al., 2013; Kaakoush et al., 2015). In addition, stringent biosecurity measures are cost-prohibitive and hard to maintain and their effectiveness seems to vary with production systems and they do not apply to small farm poultry operations (e.g., backyard chickens) and pet chickens (Koutsoumanis et al., 2020). Currently, there are no effective competitive exclusion products, vaccines, bacteriocins, bacteriophages, or feed/water additives to exclude *Campylobacter* from chickens under production conditions (Lin, 2009; Richards et al., 2019; Vandeputte et al., 2019; Quintel et al., 2020; Hakeem and Lu, 2021). Furthermore, the widespread use of antibiotics in poultry production has been implicated in the emergence of highly resistant *Campylobacter* strains (Young et al., 2007; Agyare et al., 2018; Yang et al., 2019; Andrew Selaledi et al., 2020). Therefore, there is a critical need for novel anti-*Campylobacter* control strategies that can amend and/or replace on-going efforts and specifically target pathways and novel mechanisms to combat both *Campylobacter* spread and antibiotic resistance.

The transport of proteins from cytoplasm to extra-cytoplasmic locations is critical for bacterial survival, virulence, and stress resistance (Berks, 2015). Extra-cytoplasmic protein transport in bacteria most commonly occurs via two major export systems, namely, the general secretory (Sec) pathway and the twin-arginine translocation (Tat) pathway (Frain et al., 2019a,b). The *Campylobacter* Tat pathway is highly conserved between strains, and the inactivation of the Tat pathway induces a multitude of functional defects in *Campylobacter* including motility, outer membrane permeability, biofilm formation, antibiotic resistance, growth under oxygen-limiting conditions, iron acquisition, and copper homeostasis (Drozd et al., 2011; Kassem et al., 2011). Copper is crucial for the survival of pathogenic bacteria in the host and external environment; however, it also exhibits antimicrobial properties at high concentration (Hall et al., 2008; Stolle et al., 2016). As a defense mechanism, *C. jejuni* expresses two important proteins for copper homeostasis as follows: (1) CopA a copper transporting P-type ATPase responsible for transporting toxic Cu (I) from cytoplasm to periplasm, (2) CueO, a multicopper oxidase that converts toxic Cu (I) into the less toxic Cu (II) in periplasm and is dependent on the Tat system. Both of these copper homeostasis proteins are essential for copper resistance and avian host colonization (Hall et al., 2008; Stolle et al., 2016; Kassem et al., 2017; Gardner and Olson, 2018). In addition, the deletion of the *tatC* gene significantly reduced *C. jejuni* persistence in the intestinal tract of chickens and decreased fecal shedding (Rajashekara et al., 2009). Previous studies have demonstrated that Tat inhibitors are an effective control method to mitigate *Pseudomonas aeruginosa* (Vasil et al., 2012; Massai et al., 2019) and *Escherichia coli* (Panahandeh et al., 2008; Bageshwar et al., 2016; Blümmel et al., 2017). Furthermore, the use of SM has been shown to be effective strategy against multi-drug resistant pathogens (i.e., *Salmonella*, *Escherichia coli*, *Campylobacter*, *Staphylococcus*, *Burkholderia*, *Pseudomonas*, and *Candida*), where conventional antibiotics failed (Hong-Geller and Micheva-Viteva, 2013; Abouelhassan et al., 2014; Selin et al., 2015; Guo et al., 2016; Deblais et al., 2018, 2019; Helmy et al., 2018, 2020; Kathayat et al., 2018). Since chickens and mammals do not have Tat protein homologs, the inactivation of the Tat pathway using small molecule (SM) inhibitors is a promising approach to discover new antimicrobial agents with no toxicity to eukaryotes as an alternative to conventional *Campylobacter* control methods.

In this study, we used commercially available SM libraries (n = 50,917) to identify several, lead SM inhibitors that targeted the

Tat-system and had anti-*C. jejuni* activity. Tat-dependent inhibitors were identified by (1) increased *C. jejuni* susceptibility to copper sulfate and (2) reduced *C. jejuni* Fdh activity. Eight potential Tat-dependent inhibitors (T1-T8) exhibited *in vitro* antimicrobial activity against *C. jejuni*. Two inhibitors (T2 and T7) were identified as promising lead compounds with good antimicrobial efficacy against *C. jejuni* in chickens and with minimal impact on the host microbiota. Furthermore, an *in silico* docking study identified that the most promising Tat inhibitor (T7) targets key amino acids in TatC.

Materials and methods

Bacterial strains

Campylobacter jejuni 81–176 was the primary model strain used for the selection of the potential Tat-dependent inhibitors by high-throughput screening. *C. jejuni* 81–176 is resistant to 0.5 and 1 mM $CuSO_4$ (Supplementary Figure S1). *C. jejuni* 81–176 *tatC* knockout mutant (*C. jejuni Δ tatC*) was used to confirm the Tat-dependent inhibitory effect of the selected SM. *C. jejuni Δ tatC* is susceptible to 0.5 mM and higher of $CuSO_4$ (Rajashekara et al., 2009). The specificity of the Tat-dependent inhibitors was also tested on 11 additional *Campylobacter* strains (*C. coli* ATCC33559 and 10 other *C. jejuni* strains isolated from chickens) and 7 commensal/beneficial bacteria (Supplementary Table S1). The 1 *C. jejuni* strains (Au-13, Au-20, Au-38, Au-39, Au-47, Au-50, Au-24, Au-32, Au-44, and Au-45) were selected based on their single nucleotide polymorphism (SNP)-type and percent of prevalence in chickens (Merchant-Patel et al., 2008; Kumar et al., 2016). Additional details about the bacterial strains are shown in Supplementary Table S1.

Eukaryotic models

Colonic epithelial cells (Caco-2) were used to evaluate the cytotoxicity and the ability of the selected eight SMs to clear intracellular *C. jejuni*. The Caco-2 cells were obtained from the American Type Culture Collection (ATCC HTB-37; Rockville, MD, United States). For *in-vivo* testing, 3 and 5-week-old White Cronish broiler chickens, obtained from Meyer's hatchery (Polk, OH, USA), were used to validate the anti-*C. jejuni* efficacy (log reduction in cecal content) of the selected four SMs (T1, T2, T7, and T8) in poultry and their impact on the cecal microbiota. Broiler chickens were grown in accordance with The Ohio State University Animal Care and Use Program (accredited by the Association for Assessment and Accreditation of Laboratory Animal Care International) and performed following the Institutional Animal Care and Use Committee. Chickens were fed a standard broiler diet (i.e., broiler starter phase from day 0 to 10; broiler growth phase from day 11 to 25; and broiler finisher phase from day 26 to 42; PNW extension #658) which was obtained from local feed mill at the Ohio Agricultural Research and Development Center (OARDC). Chickens and associated rooms were observed at least twice daily to assure that no shortage in feed or side effects occur due to the bacterial inoculation or treatments provided during the experiments.

SM libraries

A total of 50,917 SMs obtained from 11 libraries were screened in this study. SMs were suspended in 100% DMSO at concentration ranging from 2.5 μg/mL to 12.5 μg/mL between libraries and stored at −80°C (Supplementary Table S2). These libraries originated from The National Screening Laboratory for the Regional Center of Excellence in Biodefense and Emerging Infectious Disease (NSRB, United States)—The New England Regional Center of Excellence for Biodefense and Emerging Infectious Diseases (NERC, USA) collection. The NSRB and NERC libraries included FDA-approved bio-active SM, SM used by NIH in recent clinical trials, bio-active screens, and diversified SM synthesized for favorable physico-chemical properties (e.g., solubility, low/no toxicity and increased stability). Details about the origin and concentration of the libraries are shown in Supplementary Table S2.

High-throughput copper sulfate sensitivity assay

Our *in silico* study highlighted that the unique assembly and disassembly feature of Tat system is required for the translocation of several relatively large folded proteins, such as formate dehydrogenase (Fdh) and multi-copper oxidase (CueO) (Rajashekara et al., 2009). Since CueO function requires the transport of the Tat system, increased susceptibility to copper was used as an indicator during our *in vitro* screen for Tat-specific SM inhibitors. The identification of SM increasing sensitivity of *C. jejuni* 81–176 to copper sulfate (1 mM $CuSO_4$, non-lethal dose) was performed using a high-throughput screening in 384 plate formats at NSRB facilities (Harvard Medical School, Cambridge, MA, USA). Columns 1 to 24 of assay plates were filled with 40 μL of MH broth +1 mM $CuSO_4$ using a Matrix WellMate (Thermo Fisher, United States) automatic plate filler (Drozd, 2012). In total, 100 nL of SM were transferred to each well using The Institute of Chemistry and Cell Biology (ICCB, USA) Longwood Screen Facility Seiko D-TRAN XM3106-31 PN 4-axis cartesian robot (V&P Scientific), which was controlled by SRC-310A Controller/SPEL. Columns 1–23 of the assay plates were inoculated with 40 μL of *C. jejuni* 81–176 normalized at optical density (OD_{600}) of 0.16 in fresh MH broth supplemented with 1 mM $CuSO_4$. Wells in column 24 were filled with 40 μL of *C. jejuni Δ tatC* (susceptible to 1 mM $CuSO_4$) normalized at 0.16 OD_{600} in the same conditions. The *Δ tatC* mutant is susceptible to 0.5 mM $CuSO_4$; however, for screening purpose, we used the stringent 1 mM $CuSO_4$. Plates were incubated at 42°C for 36 h under microaerophilic conditions (85% N_2, 10% CO_2, and 5% O_2). Turbidimetric measurements (OD_{600}) were recorded before and after incubation using a Biotek Synergy HT spectrophotometer. The positive and negative controls on each assay plate were used to calculate a Z' value for that plate. If the Z' value was >0, the threshold for defining a compound as positive was set at three standard deviations above the average positive control value. Z' is calculated as described in the study mentioned in the reference (Zhang et al., 1999): $Z' = 1 - (3\sigma neg + 3\sigma pos)/(\mu neg - \mu pos)$, where μ is the mean and σ is the standard deviation. The Δ*tatC* mutant is the positive control mimic, and wild type without drug is the negative control.

Furthermore, validation of the primary assay was performed in a 96-well plate format for the selected 177 SMs with high drug-like

properties that significantly increased susceptibility of *C. jejuni* to $CuSO_4$. In total, 100 µL of *C. jejuni* suspension normalized at 0.08 OD_{600} in fresh MH broth supplemented with 1 mM $CuSO_4$ were transferred to each well of a 96-well plate and treated with 6.25 µg of SM. A parallel 96-well plate was prepared as described above but without $CuSO_4$, to identify SM that did not inhibit the growth of *C. jejuni* in a Tat-specific manner. Plates were incubated at 42°C under microaerophilic conditions for 24 h. Turbidimetric measurements were recorded before and after incubation, to remove a potential increase in OD_{600} caused by the SM. Only SM inhibiting *C. jejuni* WT growth in the presence of $CuSO_4$ without inhibiting *C. jejuni* WT growth in the absence of $CuSO_4$ was selected for further analyses.

Counter screens using the screensaver SM database

Based on previous publicly available bioassay data, the ICCB-longwood/NSRB Screensaver database version v2010.10.29 and v2012.01.26 was used to eliminate SMs that were less likely to target the Tat pathway (Tolopko et al., 2010). Commercial and pharmaceutical based libraries with known antibacterial applications were cross-referenced with the selected SM. In addition, SMs that had positive effects on eukaryote-based screens were deprioritized because of the absence of eukaryotic homolog Tat system.

Counter-screen using medicinal chemistry software

A series of filters were established to select SM with the optimized drug-like properties. The criteria were based on physicochemical descriptors, potential liabilities (i.e., predicted toxicity), chemical structural diversity, and novelty. ChemDraw suite (CambridgeSoft, PerkinElmer, United States) was used to calculate molecular weight from the simplified molecular-input line-entry system (SMILES) notation. Molecular weights less than 200 Daltons (Da) and more than 550 Da were deprioritized due to the golden triangle measurements for drug-like characteristics (Johnson et al., 2009). ChemBioFinder (CambridgeSoft, PerkinElmer, United States) was used to identify structural redundancy between the SM and remove highly similar candidates. SciFinder® (Chemical Abstracts Service) was used to deprioritize SM, showing more than 90% similarity with previously investigated drugs.

Formate dehydrogenase inhibition activity assay

Formate is an essential source of energy for *Campylobacter* and plays a role in optimizing the adaptation of *C. jejuni* to the oxygen-limited gastrointestinal tract of the host (Kassem et al., 2017). Fdh is translocated by the Tat system in the periplasm, and thus, the inactivation of Tat system results in a reduction of the Fdh activity. Hence, this activity was used as an indicator during our *in vitro* screening procedures, to validate Tat-dependent SM inhibitors of *C. jejuni*. The Fdh inhibition activity assay was performed with the 177 SM with drug-like properties that increased the susceptibility of *C. jejuni* to $CuSO_4$ (1 mM). *C. jejuni* 81–176 suspension normalized to 0.08 OD_{600} in fresh MH broth was incubated for 24 h in microaerophilic condition with 6.25 µg of SM. Subsequently, the treated cultures were suspended in an oxygen-restricted solution containing 25 mM sodium phosphate buffer (pH 7) with 1 mM benzyl-viologen and 10 mM sodium formate. The increase of OD_{578} was measured using a SpectraMax Plus 384 absorbance plate reader (Molecular Devices, USA), to monitor the reduction in benzyl viologen, an indicator of Fdh activity. N = three replicates per SM. *C. jejuni* 81–176 treated with 1% DMSO and *C. jejuni* Δ*tat*Cmutant were used as controls. SMs that inhibited at least 30% Fdh activity (which is equivalent to the inhibitory effect of 1 mM of azide on FDH activity (Davies, 2017)) compared with the DMSO control were further down selected for analysis.

Activity spectrum of the selected 19 SMs against several *Campylobacter jejuni*, *Campylobacter coli*, and commensal/beneficial gut bacteria

In total, 19 SMs were selected using $CuSO_4$ sensitivity and Fdh inhibition assay and further tested on 11 *Campylobacter* strains grown in MH broth supplemented with 0.5 mM CuSO4 and treated with 6.25 µg/mL of SM, as described above. A similar experiment was performed with seven commensal/beneficial gut bacteria to determine species specificity of these SMs. In brief, an overnight suspension was normalized at 0.05 OD_{600} using the appropriate medium and challenged with 6.25 µg/mL of SM. Details about the strains and their growing conditions are shown in Supplementary Table S1. Medium alone and 1% DMSO were used as controls (N = 3 replicates per SM).

Copper sulfate sensitivity dose–response assay *in vitro* using the selected 19 SM

A $CuSO_4$ sensitivity dose–response assay was performed to determine the minimal concentration of SM that completely inhibited (MIC) or killed (MBC) *C. jejuni* 81–176 in the presence of $CuSO_4$ (0.5 mM). In total, 19 SMs were two-fold serially diluted to obtain a final SM concentration ranging from 6.25 to 0.012 µg/mL. *C. jejuni* 81–176 was then treated with a determined concentration of SM, as described in the copper sensitivity assay. The lowest SM concentration that completely inhibited the growth without killing *C. jejuni* in the presence of 0.5 mM $CuSO_4$ was considered the MIC (no increase in OD_{600} over time, but viable cells were recovered on agar plate after challenge). The lowest bactericidal SM concentration was considered the MBC (no increase in OD_{600} over time and no viable cells were recovered on agar plate after challenge) (N = 3 replicates per SM). A similar copper sulfate sensitivity dose–response assay was performed with the eight most potent SMs (T1-T8) against other *Campylobacter* strains (n = 11; Supplementary Table S1) using methodology described above. However, these SMs were two-fold serially diluted to obtain a final SM concentration ranging from 5 µg to 0.0625 µg for testing (N = two independent experiments with four technical replicate for each SM).

Cytotoxicity of the selected eight SM on Caco-2 colon epithelial cells

Cytotoxicity of the eight SMs (T1-T8) was tested on Caco-2 cells at 5, 25, and 50 μg/mL, as previously described (Kumar et al., 2016; Deblais et al., 2019). In brief, a 96-well plate seeded with approximately 1.4×10^5 Caco-2 cells/well in MEM medium was challenged with a final SM concentration of 5, 25, and 50 μg/mL. After 24 h of incubation at 37°C in a humidified 5% CO_2 incubator, cytotoxic effects were determined using the PierceTM Lactate Dehydrogenase Cytotoxicity Assay Kit (Thermo Fisher Scientific). Cell death was measured based on the production of formazan (chromogenic dye), which can be read at OD_{570}. Equal concentrations (5, 25, and 50 μg/mL) of kanamycin or chloramphenicol, 1% DMSO, and 10X lysis buffer were used as control. The cytotoxicity level was calculated according to the manufacturer's instructions (N = two independent experiments with three technical replicate for each SM).

Copper sulfate sensitivity dose–response assay in infected Caco-2 colon epithelial cells

The intracellular reduction in *C. jejuni* in the presence of a given SM (T1-T8) and 0.5 mM $CuSO_4$ were evaluated using Caco-2 cells, as previously described (Kumar et al., 2016; Deblais et al., 2019). In brief, cells were infected for 2 h using a multiplicity of infection (MOI) of 100. Infected cells were treated with SM at a final concentration ranging between 5 and 0.315 μg/mL and incubated at 37°C for 24 h in a humidified 5% CO_2 incubator. Following incubation, cells were washed once with 1X PBS, lysed with 0.1% Triton-100X, serially 10-fold diluted in 1X PBS, and plated on MH agar plate. Plates were incubated in microaerophilic conditions at 42°C for 24 h, to determine the intracellular survival. Cells not infected and not treated and cells infected and treated with 1% DMSO were used as controls (N = two independent experiments with four technical replicate for each SM).

Effect of selected four SMs on *Campylobacter jejuni* persistence in chicken ceca

Four SMs (T1, T2, T7, and T8) were selected from the initial list of eight SMs based on their low MBC in Caco2 cells (<5 μg SM/ml), low cytotoxicity indexes (<20% toxicity at 5 μg SM /ml), and their minimal effect on commensal bacterial species (less than two species inhibited by the SM out of the seven strains tested; Table 1). The antimicrobial efficacy of our SM was tested on 5-week-old chickens, to assess the clearance of *C. jejuni* load right before slaughter age. Overall, 5-week-old *Campylobacter*-free, i.e., specific pathogen-free [SPF] chickens were inoculated orally with a mixture of five *C. jejuni* strains (10^5 CFU/chicken, Supplementary Table S3). Rectal swabs were collected 1 day post-inoculation (DPI) to confirm *C. jejuni* colonization (CFU/g of feces) in birds. From 2 DPI to 7 DPI, groups of 4–5 chickens were treated orally twice a day with one of the four SMs (T1, T2, T7, or T8; approximately 0.225 mg of SM per kg body weight). Details of the treatment groups and the inoculum are shown in Supplementary Table S3.

The antimicrobial efficacy of T1, T7, and T8 was also tested on 3-week-old chickens to assess the clearance of *C. jejuni* load in chicken right after inoculation. Overall, 3-week-old *Campylobacter*-free chickens were inoculated orally with a mixture of five *C. jejuni* strains (10^5 CFU/chicken, Supplementary Table S3). Rectal swabs were collected 1 DPI to confirm the intestinal colonization of the birds by *C. jejuni* (CFU/g of feces). From 2 DPI, chickens were treated orally twice a day for 5 days (from 2 DPI to 7 DPI) with one of the SMs (T1, T7, or T8; approximately 0.127 mg of SM per kg body weight; n = 5–6 chicken per group). Details of the treatment groups and the inoculum are shown in Supplementary Table S3.

For both experiments, *C. jejuni* colonized-chickens treated with 0.0001% DMSO and colonized chickens without additional carrier treatment (non-treated) were used as controls (n = 3–6 chicken per group). Details of the treatment groups and the inoculum are shown in Supplementary Table S3. Both 3 and 5-week-old chickens were euthanized at 7 DPI using carbon dioxide gas and ceca (cecal content and the pouch) and were aseptically collected. One of the ceca pairs was immediately stored at −80°C for microbiota studies. The other ceca were suspended in 1X PBS, homogenized, serially diluted, plated on MH media supplemented with *Campylobacter* Selective Supplement (CSS) agar plate, and incubated for 48 h at 42°C in microaerophilic conditions to determine *C. jejuni* load in the ceca (CFU/g of ceca).

DNA extraction and 16S MiSeq sequencing

All the samples collected during the chicken experiments (n = 58) were selected for microbiota analysis. Genomic DNA was extracted from 150 to 200 mg of cecal contents using the PureLink Microbiome DNA Purification Kit (Life Technologies, Invitrogen Corp.) and combined with RNAse treatment (10 units/h). After quality control with nanodrop, the 16S rRNA V4-V5 variable region was amplified, purified, and sequenced. Amplicon libraries were prepared by using Phusion® High-Fidelity PCR Kit (New England Biolabs Inc., Ipswich, MA, United States), as previously described (Kumar, 2015; Deblais et al., 2018, 2019; Kumar et al., 2018; Srivastava et al., 2020). PCR products were cleaned using AMPure XP PCR (Beckman Coulter Inc., Beverly MA, USA) and were sequenced using Illumina MiSeq 300-base paired-end kit at the Molecular and Cellular Imaging Center.[1] Sequencing raw data files are publicly available at NCBI Bioproject #PRJNA1023035.

Bioinformatics analysis

Quality control of the raw reads was performed using FastQC (Babraham Bioinformatics, Cambridge, United States). Trimmomatic was used for trimming and removal of NexteraPE-PE adapter sequences (Bolger et al., 2014). Trimmed reads were processed using QIIME2 v. 2020.11 (Bolyen et al., 2019). The DADA2 plugin was used to process and check the quality of the reads (Callahan et al., 2016). A sequencing depth of 6,600 reads was

1 https://mcic.osu.edu/

TABLE 1 Antimicrobial properties of the eight most potent Tat-dependent inhibitors.

SM	*C. jejuni* 81–176 *in vitro*		Growth inhibition at 6.25 μg/mL		*C. jejuni* 81–176 MBC in Caco2 cells (μg /ml)
	MIC (μg/ml)	MBC (μg/ml)	*Campylobacter* spp.	Commensal/beneficial gut bacteria	
T1	0.19	0.62	12/12	0/7	0.63
T2	0.01	0.62	12/12	2/7 (Lb and Ef)	1.25
T3	0.04	>5	12/12	2/7 (LGG and Ef)	5
T4	0.01	>5	12/12	1/7 (Ef)	10
T5	0.01	0.04	12/12	1/7 (Ef)	10
T6	1.25	2.5	12/12	0/7	10
T7	0.02	0.16	12/12	1/7 (LGG)	2.5
T8	0.08	0.12	12/12	2/7 (Lb and Ef)	5

MIC: minimal bacteriostatic concentration (μg/ml) in presence of 0.5 mM $CuSO_4$; MBC: minimal bactericidal concentration (μg/ml) in presence of 0.5 mM $CuSO_4$; >5: the MBC was higher than 5 μg/mL. Ef, *Enterococcus faecalis*; Lb, *Levilactobacillus brevis*; LGG, *Lacticaseibacillus rhamnosus* GG. Details about the *Campylobacter* and commensal/beneficial strains are displayed in Supplementary Table S1.

used for the rarefaction. Taxonomic assignment was performed using QIIME2 and the latest SILVA reference database (version 138.1; 99% homology cut off) (Quast et al., 2013). The obtained reads were further filtered for eukaryotic, mitochondrial, and chloroplastic genetic signatures.

In silico docking study of the interactions between the selected compounds and the Tat system

Autodock 4.0 (BIOVIA discovery studio visualizer) (Morris et al., 2009) was used for docking with a homology model, which was generated using an online platform Phyere 2 (Kelley et al., 2015). Due to the unavailability of the 3D crystal structure of *C. jejuni* TatC, we turned to *Aquifex aeolicus* VF5, which possessed a TatC homolog. The sequence alignment and secondary structure of *A. aeolicus* VF5 closely resemble those of *C. jejuni* TatC (Ramasamy et al., 2013). Of particular significance, the 3D crystal structure of *A. aeolicus* VF5 is readily accessible in the Protein Data Bank (PDB ID: 4HTS). Consequently, we opted to utilize this structure for the generation of a homology model and Discovery Studio Visualizer along with Chimera to visualize protein–ligand (SM) interaction. Graphical User Interface: AutoDock Tool (ADT) was used for the preparation of pdbqt files for protein and ligand and grid box creation. AutoGrid was employed for the preparation of the grid map, and the grid size was set to 60X60X60 xyz points with grid spacing at 0.375 A. During docking, both protein and ligand were considered as rigid, and the outcomes of docking with 1.0 A in positional root-mean-square deviation (RMSD) were clustered together. The docking pose with most favorable parameters (i.e., lowest energy or binding affinity) was aligned with protein structure and was further analyzed using BIOVIA discovery studio visualizer.

Data analysis

A one-way ANOVA combined with a Tukey's test was used to analyze the difference in the abundance of *C. jejuni* in ceca between treatments. A p-value ≤0.05 was considered statistically significant. Alpha diversity was analyzed using Shannon (richness and evenness) and Faith's PD (phylodiversity) indices. The Kruskal–Wallis test was used to identify difference in alpha diversity. Based on Bray–Curtis distance matrices, permutational multivariate analysis of variances (PERMANOVA) was used to identify difference in beta diversity (unweighted and weighted uniFrac). An analysis of composition of microbes (ANCOM) was used to identify differences in the relative abundance between phylum and species levels (Mandal et al., 2015). A p-value ≤0.01 was considered statistically significant. A multivariate analysis was performed to identify potential correlations between the spectrum of activity and antimicrobial efficacy (MIC/MBC) of the selected SM and the microbiota data and the *C. jejuni* load in the chicken ceca. Table 2 shows summary of the cutoff selection criteria used in this study, to select the best Tat-dependent SM inhibitors (Ramasamy et al., 2013).

Results

The growth of *Campylobacter jejuni* 81–176 affected by 177 SMs only in the presence of copper sulfate

A total of 50,917 SMs divided into 11 libraries were screened against *C. jejuni* 81–176, to identify potential inhibitors of the Tat system (Supplementary Table S2). The hits were identified by screening in the presence of 1 mM $CuSO_4$. Since CueO contributed to $CuSO_4$ resistance and its function requires Tat system transport, increased susceptibility to copper was used as an indicator during high-throughput sequencing for Tat-specific SM inhibitors. The growth profile obtained for each SM tested was compared with the growth of the Δ*tatC* mutant (susceptible to 1 mM $CuSO_4$; no OD_{600} increase over time) and *C. jejuni* 81–176 (resistant to 1 mM $CuSO_4$; Supplementary Figure S1) in the presence of 1 mM $CuSO_4$. Out of them, 679 SMs completely inhibited the growth of *C. jejuni* in the presence of 1 mM copper sulfate after comparison of the turbidimetric values obtained with the *C. jejuni* Δ*tatC* mutant. The number of SM identified per library was not proportional to the

TABLE 2 Selection criteria used in this study to identify the most potent Tat-dependent SM inhibitors.

Experiment	Selection criteria	SM concentration tested	Tool used	Measuring method	Number of SM tested	Number of SM selected
Primary screening – $CuSO_4$ sensitivity assay	Select SM that inhibited *C. jejuni* 81–176 growth only in the presence of sub-lethal dose of $CuSO_4$ (1 mM)	2.5 to 12.5 µg	384-well plate + *C. jejuni* 81–176	Turbidimetry (cell growth at 600 nm)	50,917	679
Validation of primary screening	Select SM that inhibited *C. jejuni* 81–176 growth only in the presence of sub-lethal dose of $CuSO_4$ (1 mM)	2.5 to 12.5 µg	96-well plate + *C. jejuni* 81–176	Turbidimetry (cell growth at 600 nm)	679	679
Counter *in silico* screening	Eliminate less likely to target the Tat pathway	NA	ICCB-longwood/ NSRB Screensaver database version	No known activity against eukaryote hosts	679	177
	Select SM with the optimized drug-like properties (MW between 200 and 500 Da)	NA	ChemDraw + Golden triangle measurements	Lipinski rule of 5 MW (Da)		
	Eliminate SM with structural similarities higher than 90%	NA	ChemBioFinder + SciFinder	Structural similarity		
FDH activity inhibition assay	Select SM that inhibited at least 30% of *C. jejuni* 81–176 FDH activity	6.25 µg	384-well plate + *C. jejuni* 81–176	Turbidimetry (reduction of benzyl viologen at 578 nm)	177	21
$CuSO_4$ sensitivity dose–response assay *in vitro*	Identify MIC and MBC against *C. jejuni* 81–176 in the presence of sub-lethal dose of $CuSO_4$ (0.5 mM)	0.012 to 6.25 µg	96-well plate + *C. jejuni* 81–176	Turbidimetry (cell growth at 600 nm) + cell viability	19	8
Antimicrobial activity of SM on *Campylobacter* strains and commensal / beneficial bacteria	Select SM that had completely inhibited the growth of the 11 other *Campylobacter* strains in the presence of sub-lethal dose of $CuSO_4$ (0.5 mM)	6.25 µg	96-well plate + *Campylobacter* isolates ($n = 11$) or commensal/beneficial bacteria ($n = 7$)	Turbidimetry (cell growth at 600 nm) + cell viability		
	Select SM that affected the growth of less than 2/7 commensal/beneficial bacteria in the presence of sub-lethal dose of $CuSO_4$ (0.5 mM)					
Cytoxicity of SM on colon epithelial cells	Select SM that displayed less than 20% cytotoxicity on Caco2 colon epithelial cells treated with 5 µg	5 to 50 µg	96-well plate + Caco2 colon epithelial cells	Turbidimetry (production of formazan at 570 nm)	8	4
$CuSO_4$ sensitivity dose–response assay in infected colon epithelial cells	Select SM that have MBC below 5 µg against intracellular *C. jejuni* 81–176	0.315 to 5 µg	96-well plate + infected Caco2 colon epithelial cells	cell viability		
Antimicrobial efficacy of the SM on colonized chickens	Select SM that significantly reduce *C. jejuni* load in ceca, while having no impact on cecal microbiota and body weight	0.127 and 0.225 mg of SM per kg body weight for 3- and 5-week-old chickens, respectively	Colonized 3- and 5-week-old broiler chickens	Body weight, *C. jejuni* load in ceca, and cecal microbiota	4	2
Docking study	Identify storng binding affinity of our SM on Tat proteins	NA	Autodock 4.0	Binding affinity	2	2

*All microbiology experiment presented above were conducted by growing *C. jejuni* and *C. coli* in MH broth for 24 h in microaerophilic condition at 42°C. $CuSO_4$: copper sulfate; FDH, Formate dehydrogenase; NA, not applicable; SM, small molecule; MW, molecular weight.

concentration of the libraries (ranging between 2.5 and 12.5 µg/mL). However, known bioactive collection (Biomol 4, MSDiscovery 1, Microsource 1, and MIH Clinical Collection 1 and 2) displayed higher hit rate (approximately 3.54%) than commercial libraries (Asinex, Chembridge 3, Chemdiv 4, Enamine 2, Lifechemicals 1, and Maybridge 5; approximately 1.20%), suggesting that each library might be composed of SM with distinct chemical structures (Supplementary Table S2). The average hit rate across all libraries was 1.33%, which is significantly higher than the optimal hit rate proposed by the NSRB screening guidelines (0.3% or approximately 1 hit/plate) (Drozd, 2012). Out of the 679 SMs identified, 177 SMs had no predicted bioactivity in eukaryotic cells (i.e., selected SM had no predicted interactions with known eukaryotic targets based on *in silico* counter screens) and followed the Lipinski rule of five based on *in silica* analyses (Lipinski et al., 2001; Lipinski, 2004). Among the 177 SMs, 66 SMs had a thiourea group, 46 SM had a benzimidazole group, 38 SM had an acylhydrazone group, and 11 SM had an oxadiazole group. These 177 SMs (107 SM from Asinex, 28 SM from Chembridge, 17 SM from Life chemicals, and 25 SM from Maybridge) were selected for the secondary screen upon resynthesis.

21 SMs increased the susceptibility of *Campylobacter jejuni* to $CuSO_4$ and reduced FDH activity *in vitro*

Of the selected 177 SMs tested, only 33.3% of the SM ($n = 59/177$) reduced at least 30% growth of *C. jejuni* in the presence of 0.5 mM $CuSO_4$ compared with the DMSO control (Figure 1A). Twenty-one SM completely inhibited C. jejuni growth, 19 SM reduced the growth of *C. jejuni* by 75 to 99%, and 19 SM reduced the growth of *C. jejuni* between 30 and 75% in the presence of 0.5 mM $CuSO_4$ compared to the DMSO control. The Fdh inhibition activity assay showed that 56.5% of the SMs ($n = 100/177$) reduced *C. jejuni* Fdh activity by 30 to 100% compared with the DMSO control (Figure 1B). Overall, 21 SMs that sensitized *C. jejuni* to copper sulfate also displayed a significant reduction in FDH activity (>30%), suggesting that these SMs affect the growth of *C. jejuni* in a Tat-dependent manner. These 21 SMs were selected for further testing.

The inhibitory activity of the 19/21 SM (2 SM could not be resynthesized) was also tested on other *Campylobacter* strains ($n = 11$; Supplementary Table S1) and commensal/beneficial gut bacteria ($n = 7$) using a copper sensitivity assay at 0.5 mM $CuSO_4$ with 6.25 µg of SM, as mentioned above. Overall, 19 SMs completely inhibited the growth of 12 *Campylobacter* strains in the presence of copper sulfate while having minimal impact on the growth of two commensal/beneficial gut bacteria in a similar growth condition (growth inhibition in the presence of copper sulfate lower than 50% compared with the DMSO control). The selected 19 SMs displayed a very similar spectrum of activity profiles. They completely inhibited the growth of all *Campylobacter* strains tested at 6.25 µg. Furthermore, the 19 SMs had no growth effect on *Escherichia coli* Nissle 1917, *Streptococcus bovis, Bifidobacterium adolescentis, Bifidobacterium longum,* and *Bacteroides thetaiotaomicron* at 6.25 µg in the presence of 0.5 mM $CuSO_4$; however, they affected the growth of *Lacticaseibacillus rhamnosus* GG ($n = 13$ SM), *Enterococcus faecalis* ($n = 16$ SM), and *Levilactobcillus brevis* ($n = 2$ SM; Table 1).

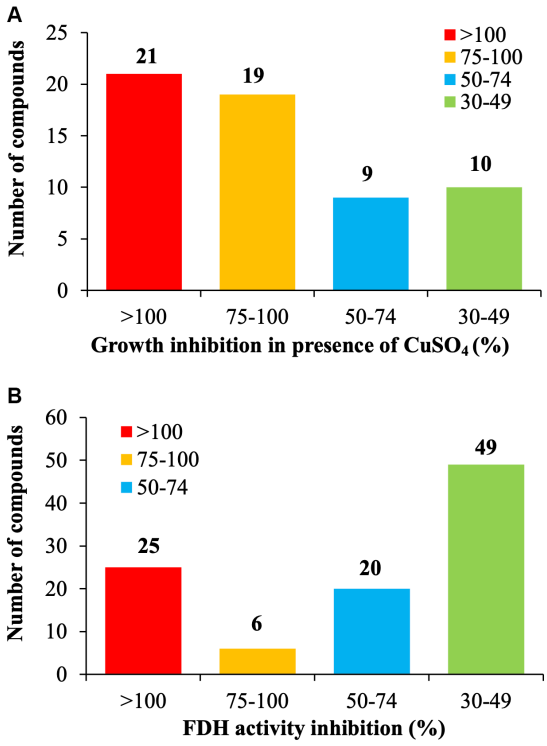

FIGURE 1
Identification of Tat dependent inhibitors in *C. jejuni* 81–176. **(A)** Copper sulfate sensitivity assay. *C. jejuni* 81–176 was challenged for 24 h with 6.25 µg/mL of SM plus 0.5 mM $CuSO_4$ in microaerophilic condition. The growth inhibition was determined by measuring the optical density and being compared to the DMSO control. **(B)** Formate Dehydrogenase (FDH) inhibition activity assay. *C. jejuni* 81–176 was challenged for 24 h with 6.25 µg/mL of SM in microaerophilic condition. The FDH activity was determined by measuring the optical density and being compared to the DMSO control. $N = 3$ replicates per group.

Selection of eight most potent Tat-dependent inhibitors

A copper sulfate sensitivity dose–response assay was performed *in vitro* on *C. jejuni* 81–176 using the selected 19 Tat-dependent inhibitors (Figure 2). One SM had an MIC of 3.13 µg/mL; two SMs had MIC at 1.56 µg/mL; three SMs had MIC at 0.78 µg/mL; one SM had MIC at 0.39 µg/mL; two SMs had MIC at 0.19 µg/mL; two SMs had MIC at 0.098 µg/mL; two SMs had MIC at 0.049 µg/mL; three SMs had MIC at 0.024 µg/mL; and one SM had MIC at 0.012 µg/mL in the presence of 0.5 mM $CuSO_4$. Interestingly, the number of strains affected by the compounds (i.e., spectrum of activity) was not correlated with their antimicrobial efficacy (e.g., MIC and MBC).

Based on the antimicrobial activity (i.e., efficacy and spectrum of activity) and *in silica* data obtained, we selected eight SMs with high drug-like properties, little or no growth effect on commensal/beneficial gut bacteria, and high efficacy against several *Campylobacter* strains (Table 1; Supplementary Table S1). Overall, the antimicrobial efficacy of the selected eight SMs was similar across the 12 *Campylobacter* strains tested with MIC values of 0.01 µg/mL and higher, and MBC values of 0.04 µg/mL and higher (Supplementary Tables S4, S5, respectively). In addition, the three-dimensional analysis of the

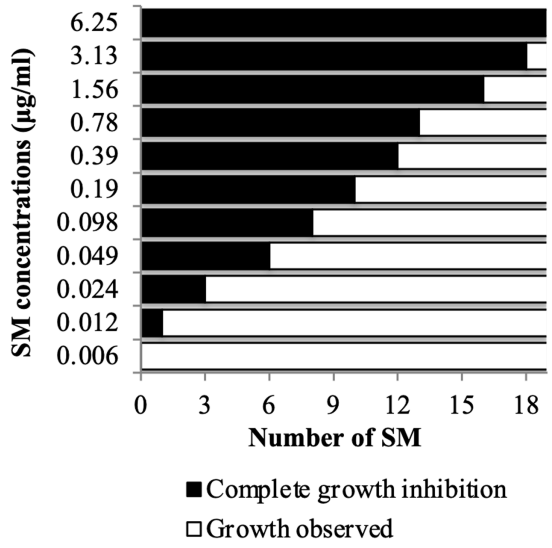

FIGURE 2
Copper sulfate sensitivity dose–response assay *in vitro*. *C. jejuni* 81–176 was challenged for 24h with SM concentration ranging between 0.006 and 6.25µg/mL in presence of 0.5mM $CuSO_4$. A total of 19 compounds were tested. *N*=four replicates per group.

chemical structure of the eight selected SMs showed that T8 and T2, T6 and T1, and T7 and T3 displayed high structural similarities, while T4 and T5 had unique chemical structures (Figure 3). Furthermore, most of the SMs have sulfur and/or nitrogen-based functional groups (thiourea, imidazole uracil, sulfonamide, thiomorpholine dioxide, phenylurea, pyridine, piperidine, oxadiazole, and quinoline). However, no association was detected between the chemical structure of the SM and their antimicrobial properties.

The eight Tat-dependent inhibitors reduced *Campylobacter jejuni* intracellular population In infected colon epithelial cells with low cytotoxicity level

All SMs completely cleared internalized *C. jejuni* 81–176 in Caco-2 cells after 24h of treatments with a concentration of SM ranging from 0.63µg/mL to 10µg/mL (Table 1). Most of the SMs displayed low toxicity (at most 10%) to Caco-2 cells when treated with 50µg/mL for 24h (Figure 4). The toxicity values were comparable to the kanamycin and chloramphenicol-treated cells. Only T1 and T8 displayed toxicity level (36 and 33%, respectively) when treated with 25µg/mL or 50µg/mL of SM for 24h; however, T1 and T8 cleared intracellular *C. jejuni* 81–176 at

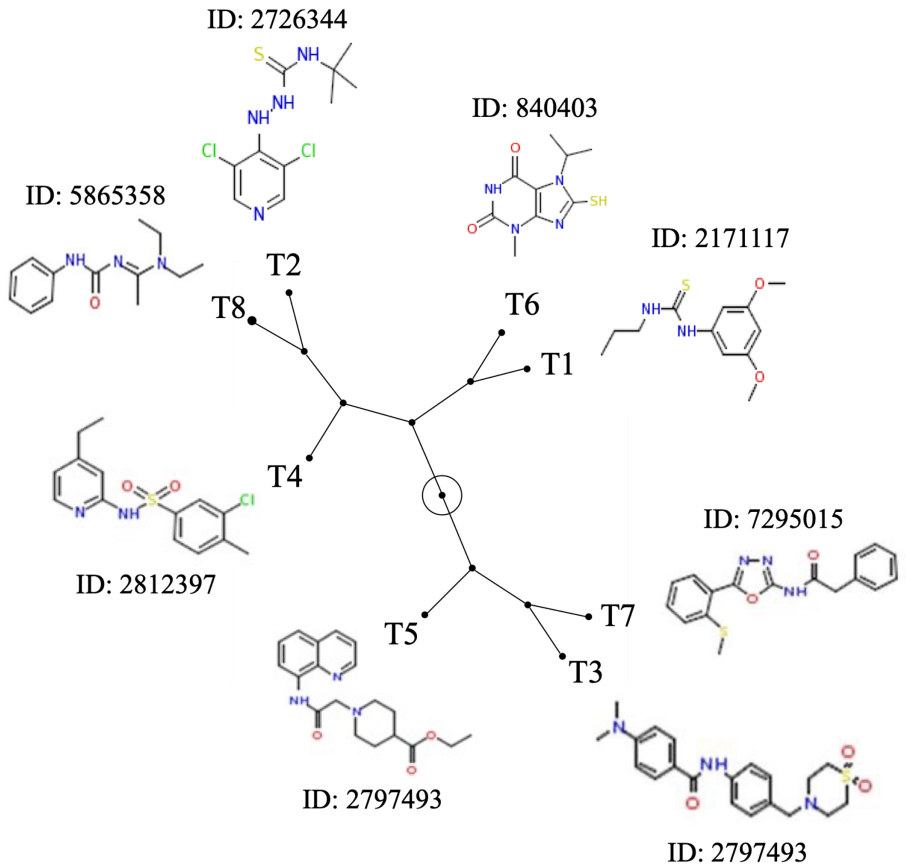

FIGURE 3
Chemical structure diversity of the eight most potent Tat-dependent inhibitors. The constellation tree was built based on the structure similarity score generated based on 3D Tanimoto scoring method in PubChem (https://pubchem.ncbi.nlm.nih.gov/assay/assay.cgi?p=clustering). The circled node represents the root of the tree. Each SM is associated with its chemical structure and its PubChem ID.

0.63 μg/mL and 5 μg/mL, respectively, which represent concentrations up to 80-fold lower compared with ones used for the toxicity assay. Overall, T1, T2, T7, and T8 displayed the most promising antimicrobial properties *in vitro* were selected for further analyses.

T2 and T7 treatments reduced *Campylobacter jejuni* load in colonized chicken ceca

As a proof of concept, the selected SMs (T1, T2, T7, and T8) were tested on 5-week-old chickens inoculated with a mixture of *C. jejuni* strains (Supplementary Table S1), to assess the clearance of *C. jejuni* in chicken right before the slaughter. Following 5 days of SM treatment (twice a day, approximately 0.225 mg of SM per kg body weight per treatment), colonized chickens treated with T2 displayed a significant reduction (1.2-log) in *C. jejuni* population per gram of cecum compared with the DMSO control group, which harbored approximately 5×10^7 CFU per gram of cecum ($p<0.01$; Figure 5A). Colonized chickens treated with the T7 and T8 groups displayed a 0.5-log reduction in *C. jejuni* population in ceca compared with the DMSO control group ($p>0.05$), while the T1 treatment did not reduce the abundance of *C. jejuni* in ceca compared with the DMSO group. No significant difference in body weight was recorded between treatment groups before or after 5 days of treatment ($p>0.05$; Supplementary Figure S2A).

The antimicrobial activity of T1, T7, and T8 was also tested on 3-week-old chickens inoculated with a cocktail of *C. jejuni* strain

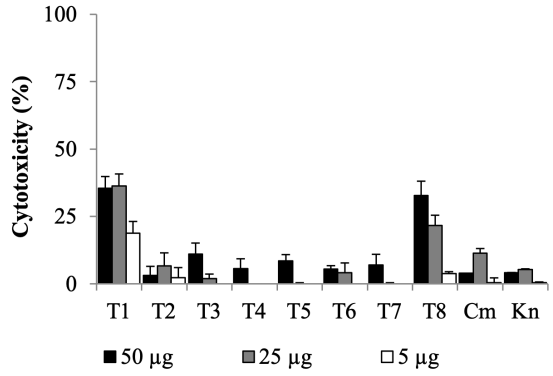

FIGURE 4
Dose-dependent cytotoxicity assay of the eight Tat-dependent inhibitors using colon epithelial (Caco-2) cells. Bar: standard deviation; Cm, chloramphenicol; Kn, kanamycin; LDH, lactate dehydrogenase; *N* = four replicates per group.

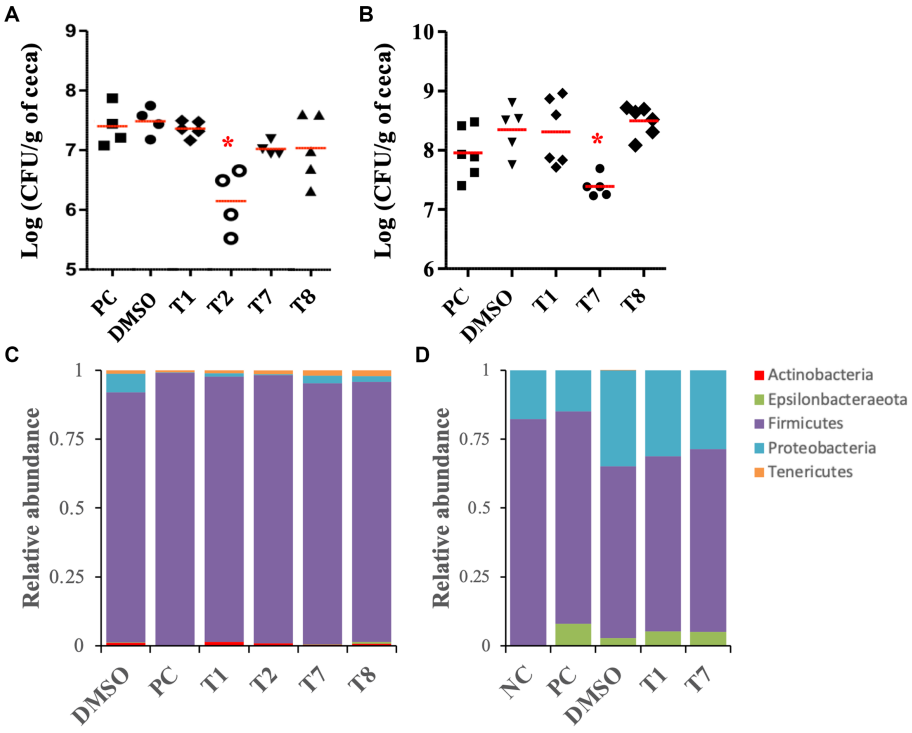

FIGURE 5
Effect of the four most potent Tat-dependent inhibitors on the persistence of *C. jejuni* in three- and five-week-old chicken ceca and its microbiota. **(A)** *C. jejuni* abundance in five-week-old chicken ceca after SM treatment ($n = 5–4$ chickens per group). The *C. jejuni* population in ceca was determined after 5 days of treatment with 0.127 mg/mL of SM. Each dot represents a chicken. Red bar represents the mean. *: significant reduction of the *C. jejuni* population in ceca compared to the DMSO control group ($p<0.01$). **(B)** *C. jejuni* abundance in three-week-old chicken ceca after SM treatment. The *C. jejuni* population in ceca was determined after 5 days of treatment with 0.255 mg/mL of SM (n = six to five chickens per group). **(C)** Relative abundance at the phylum level in five-week-old chicken ceca after treatment. **(D)** Relative abundance at the phylum level in three-week-old chicken ceca after treatment. NC: not inoculated not treated chickens; PC: colonized not treated chickens; DMSO, T1, T2, T7, T8: colonized chickens treated with DMSO or one of the selected SM.

(Supplementary Table S1), to assess the clearance of *C. jejuni* in young chicken right after inoculation. T2 could not be resynthesized in sufficient quantities and, thus, was not tested on this 3-week-old experiment. Following 5 days of SM treatment (approximately 0.127 mg of SM per kg body weight per treatment), 3-week-old chickens treated with T7 displayed a significant reduction (0.9-log) in *C. jejuni* population per gram of cecal contents compared with the DMSO-treated group, which harbored approximately 4×10^8 CFU per gram of cecal contents ($p < 0.01$; Figure 5B). Chickens treated with T1 and T8 harbored similar *C. jejuni* abundance in ceca compared with the DMSO control group. No significant difference in body weight was recorded between treatment groups before or after 5 days of treatment ($p > 0.05$; Supplementary Figure S2B).

The SM treatments had minimal impact on the chicken cecal microbiota

The impact of the SM treatments on the cecal microbiota of the 3 and 5-week-old chickens was studied using 16S sequencing. After processing and taxonomic assignment with the SILVA reference database, 682,777 sequences were obtained from the 58 samples studied. Sequencing depth varied between 6,648 and 15,749 reads per sample (mean = 9,753 reads per sample). Cecal samples were normalized to 6,600 sequences per sample for the data presented below.

For the 3-week-old chicken experiment, the analysis of the cecal alpha diversity, using Faith's PD and Shannon diversity index, indicated no significant differences between the treatment groups. On the other hand, the DMSO treatment (DMSO, T1, T2, T7, and T8 groups) significantly increased the Shannon index value (approx. 6.3) compared with the colonized, non-treated groups (PC; approx. 5.5; $p < 0.04$). The beta diversity analysis demonstrated that the SM treatments (T1, T2, T7, and T8 groups) had minimal impact on the global microbiome composition compared with the DMSO group (Supplementary Figure S3A). Most of the variations were detected between the colonized chickens treated with DMSO (DMSO, T1 and T7 groups) and the chickens that were not treated with DMSO (NC and PC groups; $p < 0.01$). Additional details concerning the impact of the DMSO and *C. jejuni* colonization on the cecal microbiome at the genus and species levels are shown in Supplementary Figures S3A–C. Overall, the cecal microbiome was composed of Firmicutes (90–99%), followed by Proteobacteria (0.1–6.7%), Tenericutes (0.6–2.1%), Actinobacteria (0.06–1.4%), and Epsilonbacteraeota (0.02–0.1%, Figure 5C). No significant differences were detected at the phylum level between the SM-treated groups (T1, T2, T7, and T8) and the associated control group (DMSO). At the species level, T8 treatment significantly increased GCA-900066225 (11.6-fold), and T7 treatment significantly increased Ruminococcaceae UCG-014 (2.2-fold) compared with the DMSO group ($p < 0.01$).

For the 3-week-old chicken experiment, the analysis of the cecal alpha diversity, using Faith's PD and Shannon diversity index, indicated no significant differences between the treatment groups of (Supplementary Figures S3D,E). Similarly, beta diversity analysis, using the weighted uniFrac, confirmed that the SM treatments (T1 and T7 groups; T8 was not included for microbiota study since it did not have positive impact on *C. jejuni* load in the cecum) had minimal impact on the global microbiome composition compared with the DMSO group (Supplementary Figure S3F). Most of the variations were detected between the colonized chickens treated with DMSO (DMSO, T1 and T7 groups) and the chickens not treated with DMSO (NC and PC groups; $p < 0.01$). Additional details concerning the impact of DMSO and inoculation of *C. jejuni* on the cecal microbiome at the genus and species levels are shown in Supplementary Figures S3D–F. Overall, the cecal microbiome was composed of Firmicutes (62–82%), followed by Proteobacteria (15–35%) and Epsilonbacteraeota (0–8%, Figure 5D). No significant differences were detected at the phylum level between the SM-treated groups (T1 and T7) and the associated control group (DMSO). At the species level, *Caproiciproducens* (6.5-fold and 4.4-fold, respectively) and *Flavonifractor* (1.7-fold) were significantly higher in T1 and T7 groups compared with the DMSO group. *Eubacterium coprostanoligenes* group (8-fold) and *Neglecta timonensis* (only detected in the T7 group at 0.8%) were significantly higher in the T7 group compared with the DMSO group ($p < 0.01$).

Docking studies predicted that T2 and T7 interact with the TatC protein of the Tat system

TatC subunit is the largest and most important part of Tat system, while Tat A and Tat B are much smaller units. The docking studies were conducted with all Tat subunits; however, TatA and B protein folding could not be predicted with high certainty due to smaller protein size. Therefore, we focused on TatC, which was modeled with a high degree of predictability and well-defined binding pockets, giving repeatable docking results. The *in silico* docking study demonstrated that both active compounds T2 and T7 bind in the same hydrophobic binding pocket associated with the key active residue Glu 165 (Figure 6). The calculated binding energy for T2 is −6.26Kcal/mol, while T7 has a higher binding energy of −8.0 Kcal/mol. The T2 thiourea nitrogen forms a hydrogen bond with Ile80, while the phenyl ring forms Pi-Pi stacking interaction with Phe87. Trp85 and Phe87 form Pi-sigma interaction with the T2 pyridine ring and tert-butyl group, respectively (Figures 6A,C). In addition, there are several hydrophobic interactions within carbon chains of T2 and Ile80, Ser 77, Ile162, Phe111, Ser107, Ile168, Met166, Gln83, and Ser17. The T7 functional groups (i.e., oxadiazole and phenyl groups) bind to several amino acids that are located inside the hydrophobic core of TatC (Figure 6B). More precisely, all aromatic rings of T7 have π-anion interactions with the key Glu165 (Figures 6B,D); the phenylacetamide group has π-alkyl interactions with Val169, π-π interactions with Phe84 and Trp85, and van der Waals interactions with Ile168 and Ser107; the methylthio-phenyl group has π-alkyl interactions with Ile80, Ile162, and Leu81, and van der Waals interactions with Phe111, Ser77, and Phe73. π- Σ interactions are also detected on the amide and methanethiol groups. Thus, anti-*C. jejuni* activity of both T2 and T7 may be attributed to their binding to hydrophobic pocket in TatC and the interaction with key residues Glu165 and Trp85 (Figure 6).

Discussion

The emergence of antibiotic-resistant isolates significantly reduces the antimicrobial efficacy of current control methods which are used

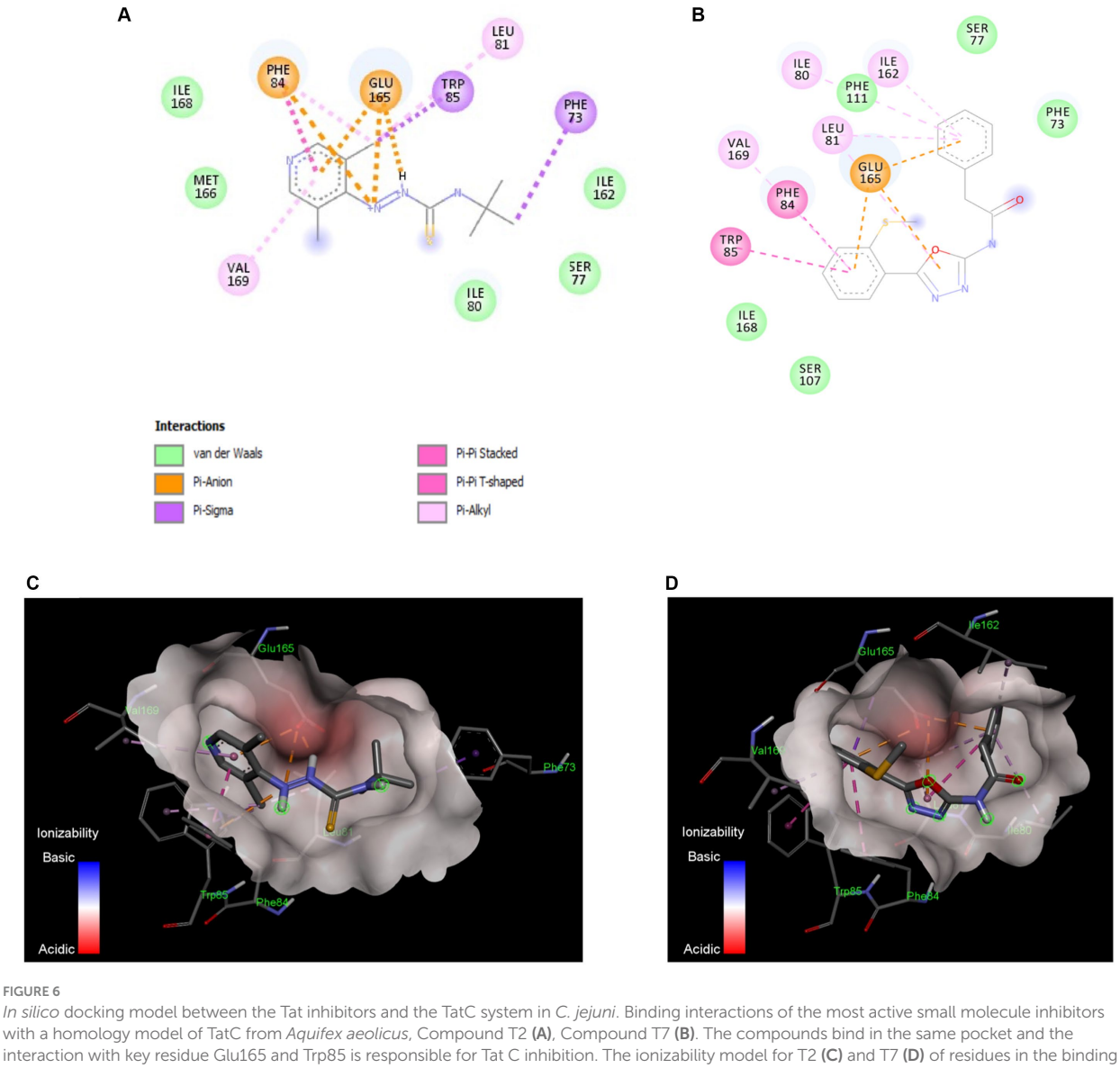

FIGURE 6
In silico docking model between the Tat inhibitors and the TatC system in *C. jejuni*. Binding interactions of the most active small molecule inhibitors with a homology model of TatC from *Aquifex aeolicus*, Compound T2 **(A)**, Compound T7 **(B)**. The compounds bind in the same pocket and the interaction with key residue Glu165 and Trp85 is responsible for Tat C inhibition. The ionizability model for T2 **(C)** and T7 **(D)** of residues in the binding pocket indicates the Pi-anion interactions with Glu165 and Pi-Pi interaction with Trp85. These docking models indicate that TatC inhibition may be responsible for the anti-*C. jejuni* activity of T2 and T7.

to mitigate human campylobacteriosis (Kaakoush et al., 2015; Subbiah et al., 2016; Yang et al., 2019). Previous studies showed that the Tat system is highly conserved in *Campylobacter* spp. and is critical for the persistence of *Campylobacter* in the intestinal tract of poultry, a recurrent reservoir for *Campylobacter* (Rajashekara et al., 2009; Hitchcock et al., 2010; Hermans et al., 2011). Additionally, the absence of homologous proteins in chickens and mammals increases the likelihood that the Tat system-based control strategies would avoid damage or unwanted interaction with host cells (Kassem and Rajashekara, 2014). Previous studies demonstrated increased copper sulfate sensitivity and reduced Fdh activity in *Campylobacter* when the Tat system was non-functional; therefore, these two indicators were used to select the compounds that are likely to specifically inhibit the Tat system (hit compounds). A total of 50,917 SMs distributed among 11 "commercial" or "known bioactive" libraries provided by ICCB-Longwood version v2010.10.29 and v2012.01.26 were screened. A total of, eight SMs (T1-T8; 10 ng/mL and higher) sensitized several *C. jejuni* and *C. coli* isolated from human and poultry to sublethal dose of copper sulfate (0.5 mM) *in vitro*, and had minimal to absent toxicity in Caco-2 colon epithelial cells. These initial findings support our hypothesis that the Tat system is a promising target for the development of the anti-*C. jejuni* control method with minimal impact on eukaryotes. Further efforts will validate the molecular target of T2 and T7 to facilitate their uses against *C. jejuni* infections in humans. Distinct chemical backbones were observed among the eight SMs, suggesting that multiple chemical scaffolds can target the Tat system in *C. jejuni* or interact with chaperoning proteins. Most of the SMs were characterized by sulfur and/or nitrogen-containing functional groups (thiourea, imidazole uracil, sulfonamide, thiomorpholine dioxide, phenylurea, pyridine, piperidine, oxadiazole, and quinoline). Furthermore, SM with low molecular weights (< 400 Da) completely cleared intracellular *C. jejuni* between 0.63 μg/mL and 2.5 μg/mL, while SM with high molecular weights (> 400 Da) completely cleared intracellular *C. jejuni* at 5.0 μg/mL and higher.

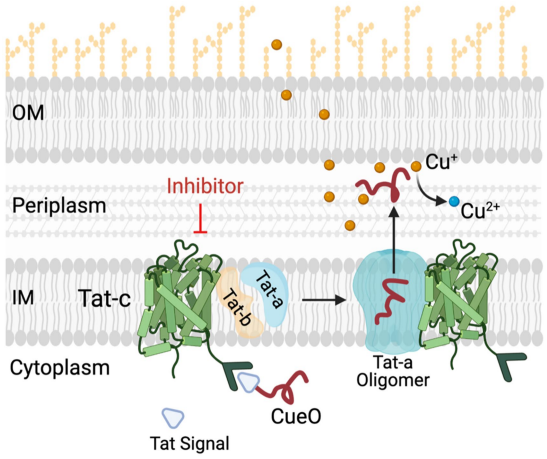

FIGURE 7
Role of Tat system in copper (Cu) homeostasis in *C Jejuni*. *C jejuni* employs a Tat complex (Tat-A, B, C) for the transport of proteins from cytoplasm to periplasm. TatC is the core transmembrane component of this complex located in inner membrane (IM), responsible for translocation of folded proteins such as multi-copper oxidase (CueO) and formate dehydrogenase (Fdh) from cytoplasm to periplasm. CueO is critical for oxidation of Cu^{+} which are highly toxic as compared to relatively non-toxic Cu^{2+} form. Thus, in the presence of TatC inhibitors the transportation of important cytoplasmic proteins such as CueO and Fdh is hampered. This results in increased sensitivity of *C jejuni* to copper. OM and IM, outer and inner membrane, respectively; CueO, copper oxidase; Cu, copper.

Therefore, the molecular weights could serve as a selection criterion of SM for testing them in a cell culture setting (Schuffenhauer et al., 2006).

This study identified two potential Tat inhibitors (T2 and T7) that significantly reduced the cecal *C. jejuni* load (up to 1.2-log) in colonized chickens after a 5-day treatment twice a day with 0.225 mg or 0.127 mg of SM per kg body weight per treatment, respectively. Furthermore, the SM treatments did not affect the chicken body weight gain or disturb the cecal microbiota. This preliminary *in vivo* data validated that the Tat system could represent a good target for the development of novel and safe control methods against *C. jejuni*. Future studies will focus on the development of T2 and T7 derivatives with improved antimicrobial efficacy, dosage titration, and testing these compounds in farm-like settings. Similarly, the addition of our SM to the feed will be tested, which is the preferred delivery method in commercial poultry operations. Since the solvent used to deliver the SM to the chickens had a significant impact on the cecal microbiota, future studies will focus on the development of water-soluble T2 and T7 derivatives, optimizing the dosage and bioavailability for these molecules in chicken tissues after treatment.

Differences in antimicrobial efficacy were observed with T7 and T8 between the 3 and 5-week-old chicken experiments. These differences might be due to SM dosage used and/or the microbial composition in chicken ceca. Interestingly, the abundance of the *Eubacterium coprostanoligenes* group was significantly increased in 3-week-old chickens treated with T7 compared with the DMSO-treated chickens. *Eubacterium coprostanoligenes* is an anaerobe genus involved in the reduction of cholesterol (Wei et al., 2020). However, it was also showed that depletion in the membrane cholesterol was associated with a reduction in *C. jejuni* cytolethal distending toxin-induced pathogenesis and, thus, attenuated the intoxication of host cells (Lin et al., 2011; Lai et al., 2013, 2015). Future studies will assess whether this bacterium has anti-*C. jejuni* properties. If true, the combination of our Tat inhibitor T7 with *Eubacterium coprostanoligenes* will also be investigated to mitigate *C. jejuni* in poultry. It was also observed that treating chickens with DMSO, using oral gavage, significantly affected the composition of the chicken ceca microbiota (*Lactobacillus*, *Romboutsia*, *and Enterobacteriaceae*). *Enterobacteriaceae* and *Lactobacillaceae* bacteria are major components of the initial intestinal microbiota and are essential for the installation and proliferation of aerobic sensitive bacteria over time (Lin and Zhang, 2017). Furthermore, certain *Lactobacillus* isolates have been shown to harbor potential antagonistic properties against *Campylobacter* in chicken (Dec et al., 2018). Therefore, the microbiome alterations caused by the DMSO treatment might have enhanced the antimicrobial efficacy of our selected compounds.

The *in silico* docking study demonstrated that our Tat inhibitors T2 and T7 bind with a key amino acid residue, Glu 165, are located in the hydrophobic core of TatC. Glu 165 is conserved as polar glutamine or glutamate across species of bacteria and plays an important role in TatC functioning. Glu 165 forms a hydrogen bonding network with Ser107 and Trp 85, which is important for generating electrochemical gradient for Tat energy function (Rollauer et al., 2012). Trp 85 forms an important interaction between Tat signal and W85G and suppresses Tat signaling and transportation (Ramasamy et al., 2013). It is also shown that TatC forms a glove- like shape, and Glu 165 sits in the concave surface, where it can interact with TatA (Figure 7). The ionized Glu 165 present in hydrophobic core of concave TatC is important for interactions with TatA. The mutation E165A severely compromises TatC functioning. Thus, our *in silico* data suggest that the binding of T2 and T7 in Glu-165 hydrophobic pocket of TatC might perturb the transport of CueO and Fdh. It is important to mention that the model displayed in this study to assess the binding affinity of our SM to TatC was conducted using the TatC crystal structure from *Aquifex aeolicus*. No crystal structure of other TatC proteins is available to date. Thereby, no predictive docking modeling of our SM with other TatC protein could have been conducted in this study to assess the specific binding of our SM to *C. jejuni* TatC. However, TatC is the most conserved protein of the Tat system across bacteria (i.e., *E. coli*, *Aquiflex aeolicus*, *C. jejuni*, *Thermus thermophilus*, and *Staphylococcus aureus*) (Lee et al., 2006; Ramasamy et al., 2013; Patel et al., 2014). Based on a NCBI Blastp analysis conducted on 01/10/2024, it was found that *C. jejuni* TatC displays at least 98.37 and 93.88% sequence similarity with other *C. jejuni* TatC sequences and *C. coli* TatC sequences ($n = 100$ sequenced tested per species), respectively. These observations support the antimicrobial efficacy of our SM against the *C. jejuni* and *C. coli* strains tested in this study. On the other hand, low sequence similarity was observed between *C. jejuni* TatC and the few TatC obtained from other non-thermophilic *Campylobacter* strains; *Campylobacter fetus* (similarity of 59.43% and above; $n = 14$), candidatus *Campylobacter infans* (similarity of 55.95%; $n = 2$), *Campylobacter hyointestinalis* (similarity of 61.76% and above; $n = 12$) and *Campylobacter upsaliensis* (similarity of 72.02% and above; $n = 48$). Future studies will investigate whether our best candidates could be also used against non-thermophilic *Campylobacter in vivo* or if better candidates can be identified from the initial libraries tested in this study. Furthermore, a similarity of 34.55 and 26.73% were observed between TatC obtained from *C. jejuni* and *Escherichia coli* Nissle 1917 and *Bifidobacterium longum*, respectively. To date, no

TatC proteins were identified in *L. brevis* and *rhamnosus L.*, *Bifidobacterium adolescentis* and *lactis*, and *Enterococcus faecalis*. These *in silico* results concord with the limited impact of our SM on commensal/beneficial bacteria.

In conclusion, data presented in this study represent a proof of concept that the Tat system represents a good target for the development of novel and safe control methods against *C. jejuni*. We have identified two Tat-dependent inhibitors (T2 and T7) with the potential to become effective control method to mitigate *C. jejuni* in poultry production systems. However, additional efforts are required to improve the antimicrobial efficacy of the Tat compounds before being used to control *C. jejuni* in large-scale poultry production systems.

Data availability statement

The datasets presented in this study can be found in the NCBI repository, accession number PRJNA1023035.

Ethics statement

The animal study was approved by Institutional Animal Care and Use Committee (IUACUC) protocol n° 2010A00000149-R2-AM1. The study was conducted in accordance with the local legislation and institutional requirements.

Author contributions

LD: Data curation, Formal analysis, Investigation, Methodology, Validation, Visualization, Writing – original draft, Writing – review & editing. MD: Conceptualization, Methodology, Validation, Writing – review & editing. AK: Conceptualization, Methodology, Validation, Writing – review & editing. JA: Methodology, Writing – review & editing. JF: Conceptualization, Investigation, Methodology, Supervision, Writing – review & editing. RK: Formal analysis, Methodology, Validation, Visualization, Writing – review & editing. GR: Conceptualization, Funding acquisition, Investigation, Methodology, Project administration, Resources, Supervision, Validation, Writing – review & editing. YH: Investigation, Methodology, Writing – review & editing.

Funding

The author(s) declare that financial support was received for the research, authorship, and/or publication of this article. The research in GR laboratory is supported by National Institute for Food and Agriculture (NIFA) Grant # 2013–67018-21240, United States Department of Agriculture; the Poultry CRC, established and supported under the Australian Government's Cooperative Research Centers Program; and the Ohio Agricultural Research and Development Center (OARDC).

Acknowledgments

The authors thank ICCB-L for assistance with high throughput screening. The authors also thank Rosario A. Candelero for the technical support. The authors thank Saranga Wijeratne, Molecular and Cellular Imaging Center, Ohio Agricultural Research and Development Center (http://oardc.osu.edu/mcic/), The Ohio State University for providing assistance with bioinformatics.

Conflict of interest

The authors declare that the research was conducted in the absence of any commercial or financial relationships that could be construed as a potential conflict of interest.

Publisher's note

Supplementary material

The Supplementary material for this article can be found online at: https://www.frontiersin.org/articles/10.3389/fmicb.2024.1342573/full#supplementary-material

References

Abouelhassan, Y., Garrison, A. T., Burch, G. M., Wong, W., Norwood, V. M., and Huigens, R. W. (2014). Discovery of quinoline small molecules with potent dispersal activity against methicillin-resistant *Staphylococcus aureus* and *Staphylococcus epidermidis* biofilms using a scaffold hopping strategy. *Bioorg. Med. Chem. Lett.* 24, 5076–5080. doi: 10.1016/j.bmcl.2014.09.009

Agyare, C., Boamah, V. E., Zumbi, C. N., and Osei, F. B. (2018). "Antibiotic use in poultry production and its effects on bacterial resistance" in *Antimicrobial resistance–a global threat*. ed. Y. Kumar (London: IntechOpen)

Allos, B. M. (2001). *Campylobacter jejuni* infections: update on emerging issues and trends. *Clin. Infect. Dis. Off. Publ. Infect. Dis. Soc. Am.* 32, 1201–1206. doi: 10.1086/319760

Andrew Selaledi, L., Mohammed Hassan, Z., Manyelo, T. G., and Mabelebele, M. (2020). The current status of the alternative use to antibiotics in poultry production: an African perspective. *Antibiot. Basel Switz.* 9:594. doi: 10.3390/antibiotics9090594

Bageshwar, U. K., VerPlank, L., Baker, D., Dong, W., Hamsanathan, S., Whitaker, N., et al. (2016). High throughput screen for *Escherichia coli* twin arginine translocation (tat) inhibitors. *PLoS One* 11:e0149659. doi: 10.1371/journal.pone.0149659

Berks, B. C. (2015). The twin-arginine protein translocation pathway. *Annu. Rev. Biochem.* 84, 843–864. doi: 10.1146/annurev-biochem-060614-034251

Berrang, M. E., Bailey, J. S., Altekruse, S. F., Patel, B., Shaw, W. K., Meinersmann, R. J., et al. (2007). Prevalence and numbers of campylobacter on broiler carcasses collected at rehang and postchill in 20 U.S. processing plants. *J. Food Prot.* 70, 1556–1560. doi: 10.4315/0362-028x-70.7.1556

Blümmel, A.-S., Drepper, F., Knapp, B., Eimer, E., Warscheid, B., Müller, M., et al. (2017). Structural features of the TatC membrane protein that determine docking and insertion of a twin-arginine signal peptide. *J. Biol. Chem.* 292, 21320–21329. doi: 10.1074/jbc.M117.812560

Bolger, A. M., Lohse, M., and Usadel, B. (2014). Trimmomatic: a flexible trimmer for Illumina sequence data. *Bioinforma. Oxf. Engl.* 30, 2114–2120. doi: 10.1093/bioinformatics/btu170

Bolyen, E., Rideout, J. R., Dillon, M. R., Bokulich, N. A., Abnet, C. C., Al-Ghalith, G. A., et al. (2019). Reproducible, interactive, scalable and extensible microbiome data science using QIIME 2. *Nat. Biotechnol.* 37, 852–857. doi: 10.1038/s41587-019-0209-9

Callahan, B. J., McMurdie, P. J., Rosen, M. J., Han, A. W., Johnson, A. J. A., and Holmes, S. P. (2016). DADA2: high-resolution sample inference from Illumina amplicon data. *Nat. Methods* 13, 581–583. doi: 10.1038/nmeth.3869

Connerton, P. L., Richards, P. J., Lafontaine, G. M., O'Kane, P. M., Ghaffar, N., Cummings, N. J., et al. (2018). The effect of the timing of exposure to *Campylobacter jejuni* on the gut microbiome and inflammatory responses of broiler chickens. *Microbiome* 6:88. doi: 10.1186/s40168-018-0477-5

Davies, J. A. (2017). *Characterisation of the reversible formate dehydrogenases of Shewanella*. University of East Anglia. School of Biological Sciences. Available at: https://ueaeprints.uea.ac.uk/id/eprint/66856/ (Accessed September 28, 2023).

Deblais, L., Helmy, Y. A., Kathayat, D., Huang, H., Miller, S. A., and Rajashekara, G. (2018). Novel imidazole and Methoxybenzylamine growth inhibitors affecting salmonella cell envelope integrity and its persistence in chickens. *Sci. Rep.* 8:13381. doi: 10.1038/s41598-018-31249-0

Deblais, L., Helmy, Y. A., Kumar, A., Antwi, J., Kathayat, D., Acuna, U. M., et al. (2019). Novel narrow spectrum benzyl thiophene sulfonamide derivatives to control campylobacter. *J. Antibiot. (Tokyo)* 72, 555–565. doi: 10.1038/s41429-019-0168-x

Dec, M., Nowaczek, A., Urban-Chmiel, R., Stępień-Pyśniak, D., and Wernicki, A. (2018). Probiotic potential of lactobacillus isolates of chicken origin with anti-campylobacter activity. *J. Vet. Med. Sci.* 80, 1195–1203. doi: 10.1292/jvms.18-0092

Drozd, M. R. (2012). *Campylobacter jejuni survival strategies and counter-attack: an investigation of campylobacter phosphate mediated biofilms and the design of a high-throughput small-molecule screen for TAT inhibition*. The Ohio State University. Available at: https://etd.ohiolink.edu/pg_10?0::NO:10:P10_ETD_SUBID:76976 (Accessed April 30, 2018).

Drozd, M., Gangaiah, D., Liu, Z., and Rajashekara, G. (2011). Contribution of TAT system translocated PhoX to *Campylobacter jejuni* phosphate metabolism and resilience to environmental stresses. *PLoS One* 6:e26336. doi: 10.1371/journal.pone.0026336

Facciolà, A., Riso, R., Avventuroso, E., Visalli, G., Delia, S. A., and Laganà, P. (2017). Campylobacter: from microbiology to prevention. *J. Prev. Med. Hyg.* 58, E79–E92.

Frain, K. M., Robinson, C., and van Dijl, J. M. (2019a). Transport of folded proteins by the tat system. *Protein J.* 38, 377–388. doi: 10.1007/s10930-019-09859-y

Frain, K. M., van Dijl, J. M., and Robinson, C. (2019b). The twin-arginine pathway for protein secretion. *EcoSal Plus* 8:2018. doi: 10.1128/ecosalplus.ESP-0040-2018

Gardner, S. P., and Olson, J. W. (2018). Interaction of copper toxicity and oxidative stress in *Campylobacter jejuni*. *J. Bacteriol.* 200, e00208–e00218. doi: 10.1128/JB.00208-18

Guerin, M. T., Sir, C., Sargeant, J. M., Waddell, L., O'Connor, A. M., Wills, R. W., et al. (2010). The change in prevalence of campylobacter on chicken carcasses during processing: a systematic review. *Poult. Sci.* 89, 1070–1084. doi: 10.3382/ps.2009-00213

Guo, Q., Wei, Y., Xia, B., Jin, Y., Liu, C., Pan, X., et al. (2016). Identification of a small molecule that simultaneously suppresses virulence and antibiotic resistance of *Pseudomonas aeruginosa*. *Sci. Rep.* 6:srep19141. doi: 10.1038/srep19141

Hakeem, M. J., and Lu, X. (2021). Survival and control of campylobacter in poultry production environment. *Front. Cell. Infect. Microbiol.* 10:5049. doi: 10.3389/fcimb.2020.615049

Hall, S. J., Hitchcock, A., Butler, C. S., and Kelly, D. J. (2008). A multicopper oxidase (Cj1516) and a CopA homologue (Cj1161) are major components of the copper homeostasis system of *Campylobacter jejuni*. *J. Bacteriol.* 190, 8075–8085. doi: 10.1128/JB.00821-08

Helmy, Y. A., Deblais, L., Kassem, I. I., Kathayat, D., and Rajashekara, G. (2018). Novel small molecule modulators of quorum sensing in avian pathogenic *Escherichia coli* (APEC). *Virulence* 9, 1640–1657. doi: 10.1080/21505594.2018.1528844

Helmy, Y. A., Kathayat, D., Ghanem, M., Jung, K., Closs, G., Deblais, L., et al. (2020). Identification and characterization of novel small molecule inhibitors to control *Mycoplasma gallisepticum* infection in chickens. *Vet. Microbiol.* 247:108799. doi: 10.1016/j.vetmic.2020.108799

Hermans, D., Van Deun, K., Martel, A., Van Immerseel, F., Messens, W., Heyndrickx, M., et al. (2011). Colonization factors of *Campylobacter jejuni* in the chicken gut. *Vet. Res.* 42:82. doi: 10.1186/1297-9716-42-82

Hitchcock, A., Hall, S. J., Myers, J. D., Mulholland, F., Jones, M. A., and Kelly, D. J. (2010). Roles of the twin-arginine translocase and associated chaperones in the biogenesis of the electron transport chains of the human pathogen *Campylobacter jejuni*. *Microbiol. Read. Engl.* 156, 2994–3010. doi: 10.1099/mic.0.042788-0

Hong-Geller, E., and Micheva-Viteva, S. (2013). *Small Molecule Screens to Identify Inhibitors of Infectious Disease*.

Hue, O., Le Bouquin, S., Laisney, M.-J., Allain, V., Lalande, F., Petetin, I., et al. (2010). Prevalence of and risk factors for campylobacter spp. contamination of broiler chicken carcasses at the slaughterhouse. *Food Microbiol.* 27, 992–999. doi: 10.1016/j.fm.2010.06.004

Igwaran, A., and Okoh, A. I. (2019). Human campylobacteriosis: A public health concern of global importance. *Heliyon* 5:e02814. doi: 10.1016/j.heliyon.2019.e02814

Johnson, T. W., Dress, K. R., and Edwards, M. (2009). Using the Golden triangle to optimize clearance and oral absorption. *Bioorg. Med. Chem. Lett.* 19, 5560–5564. doi: 10.1016/j.bmcl.2009.08.045

Johnson, T. J., Shank, J. M., and Johnson, J. G. (2017). Current and potential treatments for reducing campylobacter colonization in animal hosts and disease in humans. *Front. Microbiol.* 8:487. doi: 10.3389/fmicb.2017.00487

Jorgensen, F., Ellis-Iversen, J., Rushton, S., Bull, S. A., Harris, S. A., Bryan, S. J., et al. (2011). Influence of season and geography on *Campylobacter jejuni* and *C. coli* subtypes in housed broiler flocks reared in Great Britain. *Appl. Environ. Microbiol.* 77, 3741–3748. doi: 10.1128/AEM.02444-10

Kaakoush, N. O., Castaño-Rodríguez, N., Mitchell, H. M., and Man, S. M. (2015). Global epidemiology of campylobacter infection. *Clin. Microbiol. Rev.* 28, 687–720. doi: 10.1128/CMR.00006-15

Kassem, I. I., Candelero-Rueda, R. A., Esseili, K. A., and Rajashekara, G. (2017). Formate simultaneously reduces oxidase activity and enhances respiration in *Campylobacter jejuni*. *Sci. Rep.* 7:40117. doi: 10.1038/srep40117

Kassem, I. I., and Rajashekara, G. (2014). Formate dehydrogenase localization and activity are dependent on an intact twin arginine translocation system (tat) in *Campylobacter jejuni* 81-176. *Foodborne Pathog. Dis.* 11, 917–919. doi: 10.1089/fpd.2014.1797

Kassem, I. I., Zhang, Q., and Rajashekara, G. (2011). The twin-arginine translocation system: contributions to the pathobiology of *Campylobacter jejuni*. *Future Microbiol.* 6, 1315–1327. doi: 10.2217/fmb.11.107

Kathayat, D., Helmy, Y. A., Deblais, L., and Rajashekara, G. (2018). Novel small molecules affecting cell membrane as potential therapeutics for avian pathogenic *Escherichia coli*. *Sci. Rep.* 8:15329. doi: 10.1038/s41598-018-33587-5

Kelley, L. A., Mezulis, S., Yates, C. M., Wass, M. N., and Sternberg, M. J. E. (2015). The Phyre2 web portal for protein modeling, prediction and analysis. *Nat. Protoc.* 10, 845–858. doi: 10.1038/nprot.2015.053

Kittl, S., Korczak, B. M., Niederer, L., Baumgartner, A., Buettner, S., Overesch, G., et al. (2013). Comparison of genotypes and antibiotic resistances of *Campylobacter jejuni* and *Campylobacter coli* on chicken retail meat and at slaughter. *Appl. Environ. Microbiol.* 79, 3875–3878. doi: 10.1128/AEM.00493-13

Koutsoumanis, K., Allende, A., Alvarez-Ordóñez, A., Bolton, D., Bover-Cid, S., Davies, R., et al. (2020). Update and review of control options for campylobacter in broilers at primary production. *EFSA J.* 18:e06090. doi: 10.2903/j.efsa.2020.6090

Kuhn, K. G., Nygård, K. M., Guzman-Herrador, B., Sunde, L. S., Rimhanen-Finne, R., Trönnberg, L., et al. (2020). Campylobacter infections expected to increase due to climate change in northern Europe. *Sci. Rep.* 10:13874. doi: 10.1038/s41598-020-70593-y

Kumar, A. (2015). *Understanding the gut transcriptome responses to lactobacillus probiotics and investigating the impact of nutrition and rotavirus infection on the infant gut microbiome*. The Ohio State University. Available at: https://etd.ohiolink.edu/pg_10?0::NO:10:P10_ETD_SUBID:109268 (Accessed December 26, 2017).

Kumar, A., Drozd, M., Pina-Mimbela, R., Xu, X., Helmy, Y. A., Antwi, J., et al. (2016). Novel anti-campylobacter compounds identified using high throughput screening of a pre-selected enriched small molecules library. *Front. Microbiol.* 7:405. doi: 10.3389/fmicb.2016.00405

Kumar, A., Vlasova, A. N., Deblais, L., Huang, H.-C., Wijeratne, A., Kandasamy, S., et al. (2018). Impact of nutrition and rotavirus infection on the infant gut microbiota in a humanized pig model. *BMC Gastroenterol.* 18:93. doi: 10.1186/s12876-018-0810-2

Lai, C.-H., Lai, C.-K., Lin, Y.-J., Hung, C.-L., Chu, C.-H., Feng, C.-L., et al. (2013). Characterization of putative cholesterol recognition/interaction amino acid consensus-like motif of *Campylobacter jejuni* Cytolethal distending toxin C. *PLoS One* 8:e66202. doi: 10.1371/journal.pone.0066202

Lai, C.-K., Su, J.-C., Lin, Y.-H., Chang, C.-S., Feng, C.-L., Lin, H.-J., et al. (2015). Involvement of cholesterol in *Campylobacter jejuni* cytolethal distending toxin-induced pathogenesis. *Future Microbiol.* 10, 489–501. doi: 10.2217/fmb.14.119

Lee, M. D., and Newell, D. G. (2006). Campylobacter in poultry: filling an ecological niche. *Avian Dis.* 50, 1–9. doi: 10.1637/7474-111605R.1

Lee, P. A., Tullman-Ercek, D., and Georgiou, G. (2006). The bacterial twin-arginine translocation pathway. *Ann. Rev. Microbiol.* 60, 373–395. doi: 10.1146/annurev.micro.60.080805.142212

Lin, J. (2009). Novel approaches for campylobacter control in poultry. *Foodborne Pathog. Dis.* 6, 755–765. doi: 10.1089/fpd.2008.0247

Lin, C.-D., Lai, C.-K., Lin, Y.-H., Hsieh, J.-T., Sing, Y.-T., Chang, Y.-C., et al. (2011). Cholesterol depletion reduces entry of *Campylobacter jejuni* Cytolethal distending toxin and attenuates intoxication of host cells. *Infect. Immun.* 79, 3563–3575. doi: 10.1128/IAI.05175-11

Lin, L., and Zhang, J. (2017). Role of intestinal microbiota and metabolites on gut homeostasis and human diseases. *BMC Immunol.* 18:2. doi: 10.1186/s12865-016-0187-3

Lipinski, C. A. (2004). Lead- and drug-like compounds: the rule-of-five revolution. *Drug Discov. Today Technol.* 1, 337–341. doi: 10.1016/j.ddtec.2004.11.007

Lipinski, C. A., Lombardo, F., Dominy, B. W., and Feeney, P. J. (2001). Experimental and computational approaches to estimate solubility and permeability in drug discovery and development settings. *Adv. Drug Deliv. Rev.* 46, 3–26. doi: 10.1016/S0169-409X(00)00129-0

Logue, C. M., Sherwood, J. S., Elijah, L. M., Olah, P. A., and Dockter, M. R. (2003). The incidence of campylobacter spp. on processed Turkey from processing plants in the midwestern United States*. *J. Appl. Microbiol.* 95, 234–241. doi: 10.1046/j.1365-2672.2003.01969.x

Luangtongkum, T., Morishita, T. Y., Ison, A. J., Huang, S., McDermott, P. F., and Zhang, Q. (2006). Effect of conventional and organic production practices on the prevalence and antimicrobial resistance of campylobacter spp. in poultry. *Appl. Environ. Microbiol.* 72, 3600–3607. doi: 10.1128/AEM.72.5.3600-3607.2006

Mandal, S., Treuren, W. V., White, R. A., Eggesbø, M., Knight, R., and Peddada, S. D. (2015). Analysis of composition of microbiomes: a novel method for studying microbial composition. *Microb. Ecol. Health Dis.* 26:27663. doi: 10.3402/mehd.v26.27663

Massai, F., Saleeb, M., Doruk, T., Elofsson, M., and Forsberg, Å. (2019). Development, optimization, and validation of a high throughput screening assay for identification of tat and type II secretion inhibitors of *Pseudomonas aeruginosa*. *Front. Cell. Infect. Microbiol.* 9:250. doi: 10.3389/fcimb.2019.00250

Merchant-Patel, S., Blackall, P. J., Templeton, J., Price, E. P., Miflin, J. K., Huygens, F., et al. (2008). Characterisation of chicken *Campylobacter jejuni* isolates using resolution optimised single nucleotide polymorphisms and binary gene markers. *Int. J. Food Microbiol.* 128, 304–308. doi: 10.1016/j.ijfoodmicro.2008.09.002

Morris, G. M., Huey, R., Lindstrom, W., Sanner, M. F., Belew, R. K., Goodsell, D. S., et al. (2009). AutoDock4 and AutoDockTools4: automated docking with selective receptor flexibility. *J. Comput. Chem.* 30, 2785–2791. doi: 10.1002/jcc.21256

Newell, D. G., and Fearnley, C. (2003). Sources of campylobacter colonization in broiler chickens. *Appl. Environ. Microbiol.* 69, 4343–4351. doi: 10.1128/AEM.69.8.4343-4351.2003

Panahandeh, S., Maurer, C., Moser, M., DeLisa, M. P., and Müller, M. (2008). Following the path of a twin-arginine precursor along the TatABC translocase of *Escherichia coli*. *J. Biol. Chem.* 283, 33267–33275. doi: 10.1074/jbc.M804225200

Patel, R., Smith, S. M., and Robinson, C. (2014). Protein transport by the bacterial tat pathway. *Biochim. Biophys. Acta* 1843, 1620–1628. doi: 10.1016/j.bbamcr.2014.02.013

Quast, C., Pruesse, E., Yilmaz, P., Gerken, J., Schweer, T., Yarza, P., et al. (2013). The SILVA ribosomal RNA gene database project: improved data processing and web-based tools. *Nucleic Acids Res.* 41, D590–D596. doi: 10.1093/nar/gks1219

Quintel, B. K., Prongay, K., Lewis, A. D., Raué, H.-P., Hendrickson, S., Rhoades, N. S., et al. (2020). Vaccine-mediated protection against campylobacter-associated enteric disease. *Sci. Adv.* 6:eaba4511. doi: 10.1126/sciadv.aba4511

Rajashekara, G., Drozd, M., Gangaiah, D., Jeon, B., Liu, Z., and Zhang, Q. (2009). Functional characterization of the twin-arginine translocation system in *Campylobacter jejuni*. *Foodborne Pathog. Dis.* 6, 935–945. doi: 10.1089/fpd.2009.0298

Ramasamy, S., Abrol, R., Suloway, C. J. M., and Clemons, W. M. (2013). The glove-like structure of the conserved membrane protein TatC provides insight into signal sequence recognition in twin-arginine translocation. *Structure* 21, 777–788. doi: 10.1016/j.str.2013.03.004

Richards, P. J., Connerton, P. L., and Connerton, I. F. (2019). Phage biocontrol of *Campylobacter jejuni* in chickens does not produce collateral effects on the gut microbiota. *Front. Microbiol.* 10:476. doi: 10.3389/fmicb.2019.00476

Rollauer, S. E., Tarry, M. J., Graham, J. E., Jääskeläinen, M., Jäger, F., Johnson, S., et al. (2012). Structure of the TatC core of the twin-arginine protein transport system. *Nature* 492, 210–214. doi: 10.1038/nature11683

Schuffenhauer, A., Brown, N., Selzer, P., Ertl, P., and Jacoby, E. (2006). Relationships between molecular complexity, biological activity, and structural diversity. *J. Chem. Inf. Model.* 46, 525–535. doi: 10.1021/ci0503558

Selin, C., Stietz, M. S., Blanchard, J. E., Gehrke, S. S., Bernard, S., Hall, D. G., et al. (2015). A pipeline for screening small molecules with growth inhibitory activity against *Burkholderia cenocepacia*. *PLoS One* 10:e0128587. doi: 10.1371/journal.pone.0128587

Sibanda, N., McKenna, A., Richmond, A., Ricke, S. C., Callaway, T., Stratakos, A. C., et al. (2018). A review of the effect of management practices on campylobacter prevalence in poultry farms. *Front. Microbiol.* 9:2002. doi: 10.3389/fmicb.2018.02002

Skarp, C. P. A., Hänninen, M.-L., and Rautelin, H. I. K. (2016). Campylobacteriosis: the role of poultry meat. *Clin. Microbiol. Infect.* 22, 103–109. doi: 10.1016/j.cmi.2015.11.019

Srivastava, V., Deblais, L., Huang, H.-C., Miyazaki, A., Kandasamy, S., Langel, S. N., et al. (2020). Reduced rotavirus vaccine efficacy in protein malnourished human-faecal-microbiota-transplanted gnotobiotic pig model is in part attributed to the gut microbiota. *Benef. Microbes* 11, 733–751. doi: 10.3920/BM2019.0139

Stolle, P., Hou, B., and Brüser, T. (2016). The tat substrate CueO is transported in an incomplete folding state*. *J. Biol. Chem.* 291, 13520–13528. doi: 10.1074/jbc.M116.729103

Subbiah, M., Mitchell, S. M., and Call, D. R. (2016). Not all antibiotic use practices in food-animal agriculture afford the same risk. *J. Environ. Qual.* 45, 618–629. doi: 10.2134/jeq2015.06.0297

Tolopko, A. N., Sullivan, J. P., Erickson, S. D., Wrobel, D., Chiang, S. L., Rudnicki, K., et al. (2010). Screensaver: an open source lab information management system (LIMS) for high throughput screening facilities. *BMC Bioinformatics* 11:260. doi: 10.1186/1471-2105-11-260

USDA ERS–Cost Estimates of Foodborne Illnesses. (2017). Available at: https://www.ers.usda.gov/data-products/cost-estimates-of-foodborne-illnesses.aspx#.VDW27r4mUfy (Accessed September 28, 2017).

Vandeputte, J., Martel, A., Canessa, S., Van Rysselberghe, N., De Zutter, L., Heyndrickx, M., et al. (2019). Reducing *Campylobacter jejuni* colonization in broiler chickens by in-feed supplementation with hyperimmune egg yolk antibodies. *Sci. Rep.* 9:8931. doi: 10.1038/s41598-019-45380-z

Vasil, M. L., Tomaras, A. P., and Pritchard, A. E. (2012). Identification and evaluation of twin-arginine translocase inhibitors. *Antimicrob. Agents Chemother.* 56, 6223–6234. doi: 10.1128/AAC.01575-12

Wagenaar, J. A., French, N. P., and Havelaar, A. H. (2013). Preventing campylobacter at the source: why is it so difficult? *Clin. Infect. Dis.* 57, 1600–1606. doi: 10.1093/cid/cit555

Wei, Z.-Y., Rao, J.-H., Tang, M.-T., Zhao, G.-A., Li, Q.-C., Wu, L.-M., et al. (2020). Characterization of dynamic age-dependent changes and driver microbes in primate gut microbiota during host's development and healthy aging via captive crab-eating macaque model. *bioRxiv* 2020:015305. doi: 10.1101/2020.03.30.015305

Yang, Y., Feye, K. M., Shi, Z., Pavlidis, H. O., Kogut, M., Ashworth, A, J., et al. (2019). A historical review on antibiotic resistance of foodborne campylobacter. *Front. Microbiol.* 10:1509. doi: 10.3389/fmicb.2019.01509

Young, K. T., Davis, L. M., and Dirita, V. J. (2007). *Campylobacter jejuni*: molecular biology and pathogenesis. *Nat. Rev. Microbiol.* 5, 665–679. doi: 10.1038/nrmicro1718

Zhang, J. H., Chung, T. D., and Oldenburg, K. R. (1999). A simple statistical parameter for use in evaluation and validation of high throughput screening assays. *J. Biomol. Screen.* 4, 67–73. doi: 10.1177/108705719900400206

frontiers | Frontiers in Microbiology

TYPE Original Research
PUBLISHED 12 September 2024
DOI 10.3389/fmicb.2024.1452564

OPEN ACCESS

EDITED BY
Ozan Gundogdu,
University of London, United Kingdom

REVIEWED BY
Maria Jorge Campos,
Polytechnic Institute of Leiria, Portugal
Birgitta Duim,
Utrecht University, Netherlands

*CORRESPONDENCE
Ala E. Tabor
✉ a.tabor@uq.edu.au

RECEIVED 21 June 2024
ACCEPTED 27 August 2024
PUBLISHED 12 September 2024

CITATION
Ong CT, Blackall PJ, Boe-Hansen GB, deWet S, Hayes BJ, Indjein L, Korolik V, Minchin C, Nguyen LT, Nordin Y, Siddle H, Turni C, Venus B, Westman ME, Zhang Z and Tabor AE (2024) Whole-genome comparison using complete genomes from *Campylobacter fetus* strains revealed single nucleotide polymorphisms on non-genomic islands for subspecies differentiation. *Front. Microbiol.* 15:1452564. doi: 10.3389/fmicb.2024.1452564

Whole-genome comparison using complete genomes from *Campylobacter fetus* strains revealed single nucleotide polymorphisms on non-genomic islands for subspecies differentiation

Chian Teng Ong[1], Patrick. J. Blackall[2], Gry B. Boe-Hansen[3], Sharon deWet[4], Ben J. Hayes[1], Lea Indjein[3], Victoria Korolik[5], Catherine Minchin[6], Loan To Nguyen[1], Yusralimuna Nordin[1], Hannah Siddle[1], Conny Turni[2], Bronwyn Venus[1], Mark E. Westman[7], Zhetao Zhang[1] and Ala E. Tabor[1,8]*

[1]Queensland Alliance for Agriculture and Food Innovation, Centre for Animal Science, The University of Queensland, St Lucia, QLD, Australia, [2]Queensland Alliance for Agriculture and Food Innovation, Centre for Animal Science, The University of Queensland, Dutton Park, QLD, Australia, [3]School of Veterinary Science, The University of Queensland, Gatton, QLD, Australia, [4]Department of Agriculture and Fisheries, Biosecurity Sciences Laboratory, Coopers Plains, QLD, Australia, [5]Institute for Glycomics, Griffith University, Nathan, QLD, Australia, [6]Department of Agriculture and Fisheries, Agri-Science Queensland, Animal Science, Dutton Park, QLD, Australia, [7]Department of Primary Industries, Elizabeth Macarthur Agricultural Institute, Menangle, NSW, Australia, [8]School of Chemistry and Molecular Biosciences, The University of Queensland, St Lucia, QLD, Australia

Introduction: Bovine Genital Campylobacteriosis (BGC), caused by *Campylobacter fetus* subsp. venerealis, is a sexually transmitted bacterium that significantly impacts cattle reproductive performance. However, current detection methods lack consistency and reliability due to the close genetic similarity between *C. fetus* subsp. venerealis and *C. fetus* subsp. fetus. Therefore, this study aimed to utilize complete genome analysis to distinguish genetic features between *C. fetus* subsp. venerealis and other subspecies, thereby enhancing BGC detection for routine screening and epidemiological studies.

Methods and results: This study reported the complete genomes of four *C. fetus* subsp. fetus and five *C. fetus* subsp. venerealis, sequenced using long-read sequencing technologies. Comparative whole-genome analyses ($n = 25$) were conducted, incorporating an additional 16 complete *C. fetus* genomes from the NCBI database, to investigate the genomic differences between these two closely related *C. fetus* subspecies. Pan-genomic analyses revealed a core genome consisting of 1,561 genes and an accessory pangenome of 1,064 genes between the two *C. fetus* subspecies. However, no unique predicted genes were identified in either subspecies. Nonetheless, whole-genome single nucleotide polymorphisms (SNPs) analysis identified 289 SNPs unique to one or the *C. fetus* subspecies. After the removal of SNPs located on putative genomic islands, recombination sites, and those causing synonymous amino acid changes, the remaining 184 SNPs were functionally annotated. Candidate SNPs that were annotated with the KEGG "Peptidoglycan Biosynthesis" pathway were recruited for further analysis due to their potential association with the

glycine intolerance characteristic of *C. fetus* subsp. venerealis and its biovar variant. Verification with 58 annotated *C. fetus* genomes, both complete and incomplete, from RefSeq, successfully classified these seven SNPs into two groups, aligning with their phenotypic identification as CFF (*Campylobacter fetus* subsp. fetus) or CFV/CFVi (*Campylobacter fetus* subsp. venerealis and its biovar variant). Furthermore, we demonstrated the application of mraY SNPs for detecting *C. fetus* subspecies using a quantitative PCR assay.

Discussion: Our results highlighted the high genetic stability of *C. fetus* subspecies. Nevertheless, *Campylobacter fetus* subsp. venerealis and its biovar variants encoded common SNPs in genes related to glycine intolerance, which differentiates them from *C. fetus* subsp. fetus. This discovery highlights the potential of employing a multiple-SNP assay for the precise differentiation of *C. fetus* subspecies.

KEYWORDS

***Campylobacter fetus*, complete genomes, subspecies, SNPs, genome comparison, glycine, veterinary science**

Introduction

Campylobacter spp. are Gram-negative, microaerophilic bacteria that are generally curved-shaped rods (Sebald and Veron, 1963; Smibert, 1981). *Campylobacter fetus* was first described as *Vibrio fetus* in 1919 (Smith and Taylor, 1919), and it was identified as a pathogenic species that can cause disease in humans and a number of other hosts (Smibert, 1981). There are three subspecies of *C. fetus*—*C. fetus* subsp. *fetus*, *C. fetus* subsp. *testudinum*, and *C. fetus* subsp. *venerealis* (Tu et al., 2004; Smibert, 1978). These *C. fetus* subspecies form a distinct host dichotomy (Gilbert et al., 2016; Tu et al., 2001). Specifically, the host for *C. fetus* subsp. *testudinum* is primarily reptiles (Fitzgerald et al., 2014), while *C. fetus* subsp. *fetus* and *C. fetus* subsp. *venerealis* are primarily associated with mammals (Marsh and Firehammer, 1953).

Campylobacter fetus subsp. *fetus* has been isolated from a broader range of hosts than *C. fetus* subsp. *venerealis*, including cattle, sheep, and humans, mainly from the gastrointestinal tract and occasionally from aborted fetuses (Smibert, 1978). The epidemiology of *C. fetus* subsp. *fetus* infection features persistent but mild infection and sporadic abortion only. In contrast, the colonization of *C. fetus* subsp. *venerealis* is highly host- and niche-specific, as this organism is confined to the bovine genital tract (Penner, 1988; Hoffer, 1981; Hum, 1996; OIE, 2019). *Campylobacter fetus* subsp. *venerealis* is recognized as the etiologic agent of Bovine Genital Campylobacteriosis (BGC), which is a venereal disease associated with low herd fertility and high economic loss across multiple geographical locations (Sprenger et al., 2012). Transmission of *C. fetus* subsp. *venerealis* is through natural mating with asymptomatic bulls or insemination with contaminated semen or equipment. The persistent infection of this subspecies in the female reproductive tract results in BGC, which is often manifested as infertility, embryonic loss, and abortions in the first part of pregnancy (Mshelia et al., 2010).

The expression of Surface Array Proteins (SAP) correlates with serovars of the *C. fetus* subsp. *fetus* (serovars A, B, and AB), *C. fetus* subsp. *venerealis* (serovar A), and *C. fetus* subsp. *testudinum* (serovars A, B and AB). However, it is not distinctive at the subspecies level (Moran et al., 1994; Perez-Perez et al., 1986; Dworkin et al., 1995). Nonetheless, *C. fetus* subsp. *testudinum* has been demonstrated to be genetically distinct from its two closely related subspecies (Fitzgerald et al., 2014; Dingle et al., 2010). A phylogenetic reconstruction, which involved 61 *C. fetus* genomes, revealed a barrier to lateral gene transfer between *C. fetus* subsp. *testudinum* and the other *C. fetus* subspecies (Gilbert et al., 2016). Additionally, several genetic features segregating the reptile-associated *C. fetus* subsp. *testudinum* from mammal-associated *C. fetus* were reported, including the exclusive presence of a putative locus encoding for tricarballylate catabolism pathway in *C. fetus* subsp. *testudinum* (Gilbert et al., 2016). Biomarkers based on proteotyping have also been identified for the differentiation of *C. fetus* subsp. *testudinum* from the other two *C. fetus* subspecies (Emele et al., 2019).

In comparison, despite their differences in niche specificity, biochemical properties, and pathogenicity, there is no universally recognized method for the differentiation between *C. fetus* subsp. *fetus* and *C. fetus* subsp. *venerealis* (Nadin-Davis et al., 2021; van der Graaf-van Bloois et al., 2014). The two biochemical tests described in the OIE Terrestrial Manual (OIE, 2019) for differentiating the *C. fetus* subspecies are the 1% glycine tolerance test and H_2S production from cysteine-rich medium, with *C. fetus* subsp. The *fetus* was positive for both tests, while *C. fetus* subsp. *venerealis* is negative in both tests. Genome analysis has also confirmed

Abbreviations: SNP, Single Nucleotide Polymorphisms; BGC, Bovine Genital Campylobacteriosis; SAP, Surface Array Proteins; MLST, Multiple Locus Sequence Typing; ST, Sequence Type; PCR, Polymerase Chain Reaction; AFLP, Amplified Fragment Length Polymorphism; PFGE, Pulsed-Field Gel Electrophoresis; ONT, Oxford Nanopore Technologies; PGAP, Prokaryotic Genome Annotation Pipeline; ANI, Average Nucleotide Identity; CDS, Coding Sequences; NTC, No Template Control; Cq, Quantification Cycle; RFU, Relative Fluorescence Units; CFF, *Campylobacter fetus* subsp. *fetus;* CFV, *Campylobacter fetus* subsp. *venerealis;* CFVi, *Campylobacter fetus* subsp. *venerealis* biovar intermedius.

the partial deletion of a putative cysteine transporter in *C. fetus* subsp. *venerealis* strains (van der Graaf-van Bloois et al., 2016a). However, the reliability of the biochemical tests for subspecies differentiation is complicated by the presence of the biovar *C. fetus* subsp. *venerealis* bv. intermedius, which possesses phenotypic characteristics from both *C. fetus* subsp. *fetus* and *C. fetus* subsp. *venerealis* (Sprenger et al., 2012; Iraola et al., 2013). *Campylobacter fetus* subsp. *venerealis* bv. intermedius has been isolated from both bovine intestinal and genital tracts and is glycine intolerant, which is typical of *C. fetus* subsp. *venerealis* but H_2S positive as is typical of *C. fetus* subsp. *fetus* (OIE, 2019).

Amplified fragment length polymorphism (AFLP) and pulsed-field gel electrophoresis (PFGE) were shown to be effective in correlating the phenotypic and genotypic characteristics of *C. fetus* subsp. *fetus* and *C. fetus* subsp. *venerealis*; the high labor costs and the difficulty in isolating pure cultures of *C. fetus* from clinical samples required for these methods render them not ideal for routine testing by diagnostic laboratories (On and Harrington, 2001; van Bergen et al., 2005a; Wagenaar et al., 2001). Other discriminatory methods, for example, serotyping (Moran et al., 1994; Perez-Perez et al., 1986), DNA hybridization tests (Harvey and Greenwood, 1983; Basden et al., 1968), and protein banding patterns (Vandamme et al., 1990) were not able to accurately distinguish *C. fetus* subsp. *fetus* from *C. fetus* subsp. *venerealis*. Genomic studies suggested that these two *C. fetus* subspecies share a high level of genome synteny, with *C. fetus* subsp. *venerealis* possessing increased genome length and plasticity compared to *C. fetus* subsp. *fetus* (van der Graaf-van Bloois et al., 2014; Ali et al., 2012; Kienesberger et al., 2014). The *C. fetus* subsp. *venerealis* adaptation was attributed to the presence of hypervariable regions, pathogenicity islands and the acquisition of transposable elements, including prophages, transposons, and plasmids encoding for virulence factors (Nordin, 2013). Subspecies discrimination between *C. fetus* subsp. *fetus* and *C. fetus* subsp. *venerealis* using molecular methods has been attempted. For example, a multiple locus sequence typing (MLST) scheme based on the seven housekeeping genes categorized sequence type 4 (ST-4) exclusively with *C. fetus* subsp. *venerealis* (van Bergen et al., 2005b). However, ST-4 was later found to also be present in *C. fetus* subsp. *fetus* strain H1-UY (Iraola et al., 2015).

Several polymerase chain reaction (PCR) targets, including the plasmid partition protein A (*par*A; Hum et al., 1997) and the putative VirB6 protein truncated by the insertion element (*ISCfe1*; Abril et al., 2007), have been developed for the subspecies identification after investigating the different pathogenicity of *C. fetus* subspecies. The early research proposed that *C. fetus* subsp. *venerealis* displays a higher level of pathogenicity because of the genomic island in its genome (Iraola et al., 2012; Moolhuijzen et al., 2009). Several molecular targets were developed to target the genomic island, which encodes a type IV secretion system (T4SS). However, these assays with transfer-associated genes lacked specificity later when they were tested against multiple strains from both subspecies and related *Campylobacter* strains (Hum et al., 1997; Abril et al., 2007). For instance, the *par*A gene was not detected in 10 *C. fetus* subsp. *venerealis* in the previous study (Silva et al., 2021). Moreover, the previous PCR tests using various molecular targets on T4SS, including VirB6, also did not consistently align the *C. fetus* strains with their phenotypic identification (Nadin-Davis et al., 2021; Abril et al., 2007; van der Graaf-van Bloois et al., 2016b). There was no strong evidence of subspecies misidentification with *ISCfe1*, except its absence in *C. fetus* subsp. *venerealis* CCUG 34111 (Abril et al., 2007). Since T4SS-encoding regions are not exclusive to *C. fetus* subsp. *venerealis* and were found present in *C. fetus* subsp. *fetus* (Kienesberger et al., 2014; van der Graaf-van Bloois et al., 2016b) as well as other related *Campylobacter* bacteria, including *C. jejuni*, *C. lari*, and *C. coli* (Moolhuijzen et al., 2009), the reliability of *ISCfe1*, which is the insertion element truncated the T4SS VirB6 protein, for *C. fetus* subsp. *venerealis*, detection should be tested with a large number of *Campylobacter* strains from multiple continents. Another successful diagnostic test was developed using the L-Cys transporter-deletion polymorphism as the potential marker for H_2S-positive *C. fetus* strains (van der Graaf-van Bloois et al., 2016a; Farace et al., 2019). However, this PCR assay was not able to capture the intermedius biovar variant, which is positive for H_2S production (Farace et al., 2019, 2021).

The results from the previous study have suggested that the full genome sequence of the *C. fetus* subsp. *venerealis* and its biovars from different geographical continents will benefit the *C. fetus* subsp. *venerealis* detection research (Moolhuijzen et al., 2009). The genome completeness was demonstrated to be beneficial for whole-genome comparisons, particularly genomic regions with low coverage, high GC content, and/or high repetitiveness (Malmberg et al., 2019; Goldstein et al., 2019). Using complete genomes can therefore prevent the identification of false positives that arise from analyzing incomplete genomes, as missing data can lead to incorrect conclusions (Ribeiro et al., 2015; Ceres et al., 2022).

Therefore, in this study, we aimed to generate closed and complete genomes for nine *C. fetus* strains, including four *C. fetus* subsp. *fetus*, three *C. fetus* subsp. *venerealis*, and two *C. fetus* subsp. *venerealis* bv. intermedius, using Oxford Nanopore Technologies (ONT) long-read sequencing. Using these closed genomes in addition to the complete *C. fetus* genomes available on NCBI RefSeq, we conducted a whole-genome comparison to investigate the phylogenetic relationship between *C. fetus* subsp. *fetus* and *C. fetus* subsp. *venerealis* by examining their genome identity, differentially expressed gene orthologs, and single nucleotide polymorphisms (SNPs).

Materials and methods

Campylobacter fetus strains and genomes

The bacterial strains sequenced in this study were from three different culture collections, the details of which are summarized in Table 1. Briefly, M20-08756/1A and M20-04752/1B were kindly gifted by the Department of Primary Industries in New South Wales, Australia, while isolates BT268/06 and BT376/03 were kindly gifted by the Institute for Glycomics at Griffith University in Queensland, Australia. The other isolates, including A8, 957, 76223, 924, and 926, were in-house isolates at the Queensland Alliance for Agriculture and Food Innovation at the University of Queensland, Australia, which were previously isolated from

a local abattoir (Indjein, 2013). In total, four *C. fetus* subsp. *fetus* (M20-08756/1A, M20-04752/1B, BT268/06, and BT376/03), three *C. fetus* subsp. *venerealis* (A8, 957, and 76223), and two *C. fetus* subsp. *venerealis* bv. intermedius (924 and 926) strains were used in this study (Table 1). These strains were previously phenotyped using the standard OIE biochemical assays, and their subspecies identity was confirmed by cpn60 gene sequencing (Nordin, 2013; Indjein, 2013; Koya, 2016). The type strains for *C. fetus* subsp. *fetus* (ATCC 27374^T) and *C. fetus* subsp. *venerealis* (ATCC 19438^T), which had their complete genome published on the National Center for Biotechnology Information (NCBI) database, were also sequenced in this study to serve as internal controls. The cultures were stored at −80°C and were revived by culturing on the tryptone soya agar supplemented with 5% defibrinated sheep blood (Thermo Scientific, Delaware, USA) under micro-aerophilic conditions at 37°C for 48 h. Colonies of each bacterial strain were resuspended in sterile phosphate-buffered saline to reach an optical density measured at a wavelength of 600 nm (OD_{600}) to yield ~1 x 10^9 colony-forming units per mL (cfu/mL). Genomic DNA extraction of the pure bacterial culture was conducted using the Genomic-tip extraction kit (QIAGEN, Hilden, Germany). The quantity and quality of extracted gDNA were assessed using a Qubit™ 4 fluorometer (Thermo Scientific, Delaware, USA) and pulsed-field gel electrophoresis (Pippin Pulse, Sage Science, Massachusetts, USA).

Oxford Nanopore long-read sequencing

The Ligation Sequencing Kit SQK-LSK-109 (Oxford Nanopore Technologies, Cambridge, UK) was used to prepare sequencing libraries from the double-stranded high molecular weight genomic DNA. The sequencing libraries were loaded onto MinION (Oxford Nanopore Technologies, Cambridge, UK) for long-read sequencing with MinKNOW software (Oxford Nanopore Technologies, Cambridge, UK). Approximately 1 Gbp of data were generated for each isolate, and modified base-calling from raw signal data with minimum quality score filtering of 8 was performed using Guppy 5.0.7.

Illumina short-read sequencing

Extracted DNA was sent to the Ramaciotti Center for Genomics (University of New South Wales, Sydney, Australia) for short-read sequencing to generate 4 million read pairs or 1 Gbp of data. The libraries were prepared using the Nextera DNA Flex library prep kit (Illumina, California, USA), and the paired-end sequencing was executed on an iSeq 100 i1 sequencer with >80% bases higher than Q30 at 2 × 150 bp. The quality of the reads was assessed using FastQC 0.11.4 (Andrew, 2010) and was trimmed with Trimmomatic 0.39.1 using the paired-end mode (Bolger et al., 2014).

Oxford Nanopore sequencing reads quality control and filtering

Porechop 0.2.4 (Wick et al., 2017a) was utilized to first remove the adapters, while NanoFilt 2.7.0 (De Coster et al., 2018) was implemented to select for reads that were >8,000 bp in length and >10 in quality score. The quality of the Nanopore long-read sequencing data was assessed and visualized using FastQC 0.11.4 (Andrew, 2010) and NanoPlot 1.3.0 (De Coster et al., 2018).

Long-read assembly, assembly polish, assembly evaluation, and assembly annotation

Quality long reads were assembled into contigs using Trycycler 0.5.0 (Wick et al., 2017b). Briefly, the read files were divided into 12 subsets, with three subsets of each assembled using Flye 2.9 (Kolmogorov et al., 2019), Miniasm+Minipolish v0.1.3 (Vaser et al., 2017), Raven v1.5.1 (Vaser and Šikić, 2021), and Redbean v2.5 (Ruan and Li, 2020). The resulting long-read assemblies were grouped into per-replicon clusters. The cluster containing contigs with a genome size closest to the reference genome was manually selected for the reconciliation step, aiming to circularize the replicons.

Trycycler then conducted multiple sequence alignments of the contigs within each cluster and generated a consensus sequence for the final assembly. The expected genome size for each bacterial strain was determined based on their respective published reference genome available in the NCBI database (NCBI Resource Coordinators, 2018).

To polish the complete genomes derived from Nanopore long reads, Medaka 1.4.2 with model r941_min_high_g303 and Nanopolish 0.13.2 (Loman et al., 2015) were used. Genome polishing was accelerated using GNU Parallel (Tange, 2011). The draft assemblies were further refined by polishing with their corresponding Illumina short-read data using Pilon 1.24 (Walker et al., 2014).

The quality of the complete genomes was evaluated with Samtools 1.10 (Li et al., 2009) and QUAST 5.0.2 (Gurevich et al., 2013) using both long and short reads. The quality assessments generated for each polished assembly were combined and presented using MultiQC 1.10.1 (Ewels et al., 2016). The polished genomes were then visualized and validated using Artemis (Carver et al., 2011). The identities of the complete genomes were confirmed using BLAST (Altschul et al., 1990). Finally, the polished assemblies were submitted to the NCBI and annotated using the Prokaryotic Genome Annotation Pipeline (PGAP; Tatusova et al., 2016).

Whole-genome comparison of *Campylobacter fetus* complete genomes

For a more comprehensive whole-genome comparison, other complete genomes of *C. fetus* subsp. *fetus* ($n = 7$) and *C. fetus* subsp. *venerealis* ($n = 9$) were downloaded from the NCBI Genome database (NCBI Resource Coordinators, 2018) (Table 1).

TABLE 1 List of *Campylobacter fetus* strains sequenced and analyzed in this study.

(A) Strains analyzed in this study						
Strain	Accession	Organism	Country of origin	Year of isolation	Isolation source	Collection
M20-08756/1A	GCF_032594895.1	*Campylobacter fetus* subsp. *fetus*	New Zealand	1986	Ovine (fetal stomach contents)	1
BT376/03	GCA_030544625.1	*Campylobacter fetus* subsp. *fetus*	United Kingdom	2003	Bovine	2
BT268/06	GCA_030544645.1	*Campylobacter fetus* subsp. *fetus*	United Kingdom	2006	Ovine	2
M20-04752/1B	GCF_032594815.1	*Campylobacter fetus* subsp. *fetus*	Australia	2020	Ovine (fetal liver)	1
A8	CP075536-CP075537	*Campylobacter fetus* subsp. *venerealis*	Australia	2011	Bovine	3
957	GCF_030544565.1	*Campylobacter fetus* subsp. *venerealis*	Australia	2011	Bovine (bull prepuce)	3
76223	GCF_030544545.1	*Campylobacter fetus* subsp. *venerealis*	Australia	2012	Bovine (aborted fetus)	3
924	GCF_030544605.1	*Campylobacter fetus* subsp. *venerealis* bv. intermedius	Australia	2011	Bovine (bull prepuce)	3
926	GCF_030544585.1	*Campylobacter fetus* subsp. *venerealis* bv. intermedius	Australia	2011	Bovine (bull prepuce)	3
(B) Strains sequenced in previous studies						
Strain	Accession	Organism	Country of origin	Year of isolation	Isolation source	
ATCC 27374^T	GCA_900475935.1	*Campylobacter fetus* subsp. *fetus*	France	1952	Ovine (fetus)	
82-40	GCA_000015085.1	*Campylobacter fetus* subsp. *fetus*	USA	1982	Human	
00A031	GCA_011600945.2	*Campylobacter fetus* subsp. *fetus*	Canada	2000	Bovine (bull prepuce)	
02A725-35A	GCA_011600855.2	*Campylobacter fetus* subsp. *fetus*	Canada	2002	Bovine (bull prepuce)	
04-554	GCA_000759485.1	*Campylobacter fetus* subsp. *fetus*	Argentina	2004	Bovine (aborted fetus)	
09A980	GCA_011600995.2	*Campylobacter fetus* subsp. *fetus*	Canada	2009	Bovine (bull prepuce)	
INIA/17144	GCA_007723545.1	*Campylobacter fetus* subsp. *fetus*	Uruguay	2017	Ovine (placenta)	
ATCC 19438^T	GCA_008271385.1	*Campylobacter fetus* subsp. *venerealis*	United Kingdom	1962	Bovine (vaginal mucus)	
84-112	GCA_000967135.1	*Campylobacter fetus* subsp. *venerealis*	USA	1984	Bovine	
97-608	GCA_000759515.1	*Campylobacter fetus* subsp. *venerealis*	Argentina	1987	Bovine	
08A948-2A	GCA_011601005.2	*Campylobacter fetus* subsp. *venerealis*	Canada	2008	Bovine (bull prepuce)	
08A1102-42A	GCA_011600845.2	*Campylobacter fetus* subsp. *venerealis*	Canada	2008	Bovine (bull prepuce)	
ADRI545	GCA_011601375.2	*Campylobacter fetus* subsp. *venerealis* bv. intermedius	Australia	1984	Bovine (reproductive tract)	
ADRI1362	GCA_011600955.2	*Campylobacter fetus* subsp. *venerealis* bv. intermedius	Argentina	1989	Bovine (vaginal mucus)	
01/165	GCA_001686885.1	*Campylobacter fetus* subsp. *venerealis* bv. intermedius	Argentina	2001	Bovine (vaginal mucus)	
03-293	GCA_000512745.2	*Campylobacter fetus* subsp. *venerealis* bv. intermedius	Argentina	2003	Bovine (fetus lung)	

1. Culture collection from the Department of Primary Industries in New South Wales, Australia. 2. Culture collection from the Institute for Glycomics at Griffith University in Queensland, Australia. 3. Culture collection from the Queensland Alliance for Agriculture and Food Innovation at the University of Queensland in Queensland, Australia.

The inconsistencies of different annotation tools employed in previous studies were taken into consideration. Therefore, the complete genome sequence fasta files of the 16 *C. fetus* strains sequenced in previous studies were reannotated using the same parameters as the nine *C. fetus* strains sequenced in this study. The whole-genome average nucleotide identity (ANI) of the 25 *C. fetus* subspecies genomes was computed using FastANI 1.33 using the all-against-all mode (Jain et al., 2018). The correlation of the 25 *C. fetus* subspecies' complete whole genomes based on their ANI was computed in R (R Core Team, 2018) using the "corrplot" package (Wei, 2021).

Prokka 1.14.6 (Seemann, 2014) was utilized to annotate the complete genome sequences (n = 25). Briefly, Prokka 1.14.6 (Seemann, 2014) identified the protein-coding regions

using Prodigal 2.6.3 (Hyatt et al., 2010), followed by the functional annotation of the encoded protein by similarity search against protein databases. *Campylobacter fetus* subsp. *fetus* 04/554 (GCA_000759485.1) and *C. fetus* subsp. *venerealis* ATCC 19438^T (GCA_008271385.1) were provided as reference genomes for Prokka annotations to minimize the biases in annotation files for downstream analysis. The putative genomic islands (GIs) were predicted using IslandViewer 4 (Bertelli et al., 2017). The annotated assemblies were submitted to Roary 3.13.0 (Page et al., 2015) for pan-genome calculation. A heatmap was computed in R (R Core Team, 2018) using the "pheatmap" package (Kolde, 2019) to visualize the relationship of the 25 *C. fetus* subspecies based on the Roary results. The gene content and differences between the two closely related subspecies were also computed with GenAPI 1.0 (Gabrielaite and Marvig, 2019). The virulence factors known to be associated with *Campylobacter* were downloaded from the Virulence Factor Database (VFDB; Chen et al., 2005) for building a *Campylobacter*-specific VFDB database using ABRicate 1.0.1 (Seemann, 2016). The virulence factor encoding regions in each of the *C. fetus* subspecies were identified using the ABRicate 1.0.1 (Seemann, 2016) program.

SNPs were identified using Parsnp 1.5.6 (Treangen et al., 2014) from the whole-genome alignment generated with the complete genomes of the 25 *C. fetus* subspecies. A phylogenetic tree based on the SNPs identified in the whole-genome alignment of the 25 *C. fetus* strains was generated in R (R Core Team, 2018) using the "ape" package (Paradis and Schliep, 2018). The putative recombination regions with high SNP density were detected using Gubbins 3.0.0 (Croucher et al., 2014). The recombination-filtered SNPs were analyzed and annotated with SnpEff 4.3t (Cingolani et al., 2012) to filter out SNPs that potentially induce synonymous amino acid changes. The amino acid change was verified by examining the translated protein sequences of the SNP-coding coding sequences (CDS). The recombination-filtered synonymous SNPs that were different between *C. fetus* subsp. *fetus* and *C. fetus* subsp. *venerealis,* which are not present in putative GIs, were labeled as "candidate SNPs." Additionally, SNPs that were different between *C. fetus* subsp. *venerealis* and its biovar intermedius variant were labeled as "biovar SNPs." Any CDS that encoded for candidate SNPs were functionally annotated using eggNOG-mapper 2.1.6 (Cantalapiedra et al., 2021).

The annotated proteins of the SNP-coding CDS were retrieved from Prokka 1.14.6 (Seemann, 2014), and the interactions between the proteins were computed using STRING v11 (Szklarczyk et al., 2019) with *C. fetus* subsp. *venerealis* set as the organism of interest. The CDS, which were annotated with the "Peptidoglycan Biosynthesis" KEGG pathway, and their neighboring CDS with ≥8-degree functional association were taken for further investigation due to their potential association to the differential glycine tolerance among the subspecies. These SNPs were labeled as "Peptidoglycan SNPs." To further verify the potential of the peptidoglycan SNPs for differentiation assay, an additional 33 curated and contamination-free RefSeq assemblies (13 *C. fetus* subsp. *fetus* and 20 *C. fetus* subsp. *venerealis* and its biovar) were downloaded from the NCBI Genome database (https://www.ncbi.nlm.nih.gov/datasets/genome) on 24th May 2024. The search terms "*Campylobacter fetus* subsp. *fetus*" and "*Campylobacter fetus* subsp. *venerealis*" were used, with the filter "Annotated by NCBI RefSeq" applied. The base change and amino acid change resulting from the peptidoglycan SNPs were verified across 58 *C. fetus* assemblies. The subspecies identification of each strain was compared with the phenotypic and molecular tests reported in previous studies.

Whole-genome alignment of the 25 *C. fetus* complete genomes was computed and visualized using the Blast Ring Image Generator (BRIG) 0.95 (Alikhan et al., 2011), which incorporated BLAST+ 2.10.1 (Camacho et al., 2009) for genome alignment. Additionally, the genes that were used in the published *C. fetus* subspecies identification PCR assays, including sodium/hydrogen exchanger family protein (*nahE*; Abril et al., 2007), *ISCfe1* (Abril et al., 2007), peptide transporter carbon starvation (*cstA*; Hum et al., 1997) and *parA* (Hum et al., 1997; McMillen et al., 2006) are downloaded from the NCBI nucleotide database (NCBI Resource Coordinators, 2018). The location of putative GIs, candidate SNPs, and existing PCR targets for *C. fetus* subspecies identification was identified and labeled on the alignment image generated using BRIG (Alikhan et al., 2011).

Confirmation of *C. fetus* subspecies differentiation by TaqMan SNP quantitative PCR

One of the above-identified *C. fetus* subspecies SNPs (*mraY* gene SNP) was further exploited as a subspecies differentiating qPCR assay due to its potential association with the different glycine tolerance among *C.fetus* subspecies. Custom TaqMan MGB probes were designed using the Thermo Fisher Scientific online tool (Custom TaqMan™ SNP Genotyping Assay) targeting the *C. fetus* subsp. *venerealis* and *C. fetus* subsp. *fetus mraY* genes and labeled with VIC™ and FAM™ reporter dyes, respectively. *mraY* Forward primer: 5′ AAAATGATGATGAATTGGCGCCATT 3′; *mraY* Reverse primer: 5′ TGTGATGGAAACCTTATCTGTTATATTGCA 3′; *C. fetus* subsp. *fetus mraY* Probe: 5′FAM- CGTTTTTTGCGTATTTT-3′MGBNFQ; *C. fetus* subsp. *venerealis mraY* Probe: 5′VIC-CCGTTTTTTGTGTATTTT 3′MGBNFQ. The two probes and the forward and reverse primers were pre-mixed by Applied Biosystems and provided as a 20x mix for use in custom assays (Thermo Fisher Scientific, Australia). A 10 μL qPCR reaction was set up in duplicate using the AgPath-ID™ One-Step RT-PCR Reagent (Thermo Fisher Scientific) without the reverse transcriptase step consisting of 1x buffer, 900 nM of forward and reverse primers, 200 nM of the *C. fetus* subsp. *fetus* FAM probe, 200 nM of the *C. fetus* subsp. *venerealis* VIC probe, and 0.4 μl of the 25X RT-PCR Enzyme Mix (AmpliTaq Gold™ DNA Polymerase at 0.025 units per reaction). For positive controls, 2 ng of *C. fetus* subsp. *fetus* DNA (ATCC 27374) or 2 ng of *C. fetus* subsp. *venerealis* DNA (ATCC 19438) was added. A No Template Control (NTC, negative control) was included in every run. The assays were cycled in the Bio-Rad CFX96 Touch™ Real-Time PCR Detection System under the following conditions: activation at 95°C 10 min, followed by 45 cycles of 95°C 15 s, 69°C 1 min, and a final extension at 69°C for 7 min. Raw amplification data

[quantification cycle (Cq) values and Relative Fluorescence Units (RFU)] were exported for analysis in Excel and R Studio (R Core Team, 2018) using the ggplot2 package (Wickham, 2016). The assay was screened against the following isolates: *C. fetus* subsp. *venerealis* ATCC19438 (positive control), A8, 957, 76223, 924, and 926; *C. fetus* subsp. *fetus* ATCC27374 (positive control) and BT376/03 (Supplementary Table 1). Other closely related bacterial species were also included as further controls: *Campylobacter hyointestinalis* strain 337, *Arcobacter cryaerophilus* strain 312, *Campylobacter ureolyticus* strain 412, and *Campylobacter sputorum* strain 530, which were isolated in a previous study screening abattoir bull penises and have been shown to cross-react in previous *C. fetus venerealis* molecular assays (McMillen et al., 2006; Spence et al., 2011).

Results

Whole-genome sequencing data, assembly, and annotations

The average read length, average N50, and average read quality of the nine strains sequenced with ONT were 33.52 kb, 38.43 kb, and 12.61, respectively (Supplementary Table 2). Illumina short-read sequencing yielded a total mean of 416,870 paired-end raw reads for each sample, which provided a mean coverage of 64X for each bacterial isolate (Supplementary Table 3).

All *C. fetus* strains were assembled into complete circular genomes. The average assembly size of *C. fetus. fetus* and *C. fetus* subsp. *venerealis* were 1,818,690 and 2,136,077 bp, respectively (Table 2). The QUAST quality assessment of each assembly showed that the long reads and short reads provided an average of 745.73X and 64.56X, respectively, to the assemblies (Supplementary Tables 4, 5). The average percentage of mapped long reads and mapped short reads were 98.56 and 97.50%, respectively. The complete genomes generated in this study and published genomes of *C. fetus* subsp. *fetus* and *C. fetus* subsp. *venerealis* were annotated with an average of 1,901 and 2,177 genes, respectively (Supplementary Table 6).

Whole-genome comparison between 25 *Campylobacter fetus* strains

Pangenome analysis revealed that 1,561 core genes and 1,064 accessory genes were shared among the 25 *C. fetus* strains. The *C. fetus* subsp. *fetus* and *C. fetus* subsp. *venerealis* strains were separated in the hierarchical tree generated based on the presence and absence of gene orthologs (Figure 1). The pangenome analysis demonstrated the gene ortholog, which encoded for a peptidase S24 LexA-like protein, was exclusively encoded in all the *C. fetus* subsp. *venerealis* genomes but not in any of the *C. fetus* subsp. *fetus* genomes. However, three paralogs also encoded for peptidase S24 LexA-like proteins and were predicted in some of the *C. fetus* subsp. *fetus* and *C. fetus* subsp. *venerealis* strains (Supplementary Table 7).

In contrast, *C. fetus* subsp. *venerealis* and the bv. intermedius variant did not fall into distinct branches because none of the gene orthologs was able to differentiate *C. fetus* subsp. *venerealis* and *C. fetus* subsp. *venerealis* bv. intermedius. Interestingly, the six Australian *C. fetus* subsp. *venerealis* strains (GCA_011601375, A8, 924, 926, 957, and 76223) formed a separated clade from the other non-Australian *C. fetus* subsp. *venerealis*. A total of 14 gene orthologs were identified in the Australian *C. fetus* subsp. *venerealis* strains but not in the non-Australian strains, of which one was present in all *C. fetus* subsp. *fetus,* and nine were absent in all the *C. fetus* subsp. *fetus* strains. On the other hand, 37 gene orthologs were present in the non-Australian *C. fetus* subsp. *venerealis* and not the Australian strains, none of which were identified in all *C. fetus* subsp. *fetus,* and 34 were absent in all the *C. fetus* subsp. *fetus* strains.

A closer look at the genomic regions encoding the *Campylobacter*-specific virulence factors demonstrated that the 25 *C. fetus* subspecies commonly expressed genomic regions encoding 88 virulence factors (Figure 2). Nine virulence factors were not expressed in some of the *C. fetus* subspecies but not explicitly in either *C. fetus* subsp. *fetus* or *C. fetus* subsp. *venerealis*. The highest variation was observed within the S-layer proteins, which are categorized under the class of "colonization and immune evasion" in VFDB. Nonetheless, the variations among the predicted proteins were not consistent within either of the subspecies or the biovar.

The average nucleotide identity between 25 *C. fetus* strains was more than 95%. The correlation tree based on the ANI showed that eight of the *C. fetus* subsp. *fetus* strains, including GCA_011600855, BT268/06, M20-04752/1B, M20-08756/1A, GCA_900475935^{T}, GCA_007723545, BT376/03, and GCA_00759485, formed a separate branch from the *C. fetus* subsp. *venerealis* strains (Figure 3). The other three *C. fetus* subsp. *fetus* strains (GCA_000015085, GCA_011600995, and GCA_011600945) shared the same ancestor with three *C. fetus* subsp. *venerealis* bv. intermedius strains (GCA_011600955, GCA_001686885, and GCA_000512745) from Argentina. The remaining *C. fetus* subsp. *venerealis* strains ($n = 11$) formed a separate clade, in which the *C. fetus* subsp. *venerealis,* including both biovars from Australia (GCA_011601375, A8, 924, 926, 957, and 76223) clustered separately to all other *C. fetus* subsp. *venerealis* from around the world.

Comparative genome alignment of the *C. fetus* strains ($n = 25$) illustrated the high level of genome synteny between the *C. fetus* subspecies (Figure 4). Missing genomic regions were inconsistently observed among the 25 *C. fetus* strains where putative GIs were predicted. PCR target genes, including *sapB2* and *par*A, were located on putative GIs.

The phylogenetic tree that resulted from the whole-genome alignment clustered *C. fetus* subsp. *venerealis* into a separate branch from the *C. fetus* subsp. *fetus* (Figure 5). Moreover, the phylogenetic tree also clustered the Australian *C. fetus* subsp. *venerealis* in a separate branch from the *C. fetus* subsp. *venerealis* identified in the United Kingdom, United States, Canada, and Argentina (Figure 5). Both within the Australian and non-Australian *C. fetus* subsp. *venerealis* clades, the *C. fetus* subsp. *venerealis* bv. intermedius were clustered separately from the normal *venerealis* variant.

Nine thousand and 44 SNPs were identified from the core genome, of which only 269 SNPs were different between all *C. fetus* subsp. *fetus* and all *C. fetus* subsp. *venerealis* strains

10.3389/fmicb.2024.1452564

TABLE 2 Details of *Campylobacter fetus* complete genomes assembled in this study.

Sample ID	Species	Assembly size (bp)	GC content (%)
76223	*Campylobacter fetus* subsp. *venerealis*	2,105,546	33.47
924	*Campylobacter fetus* subsp. *venerealis* bv. intermedius	2,250,778	33.48
926	*Campylobacter fetus* subsp. *venerealis* bv. intermedius	2,123,600	33.48
957	*Campylobacter fetus* subsp. *venerealis*	2,088,026	33.41
A8	*Campylobacter fetus* subsp. *venerealis*	2,112,436	33.42
BT268/06	*Campylobacter fetus* subsp. *fetus*	1,909,714	33.26
BT376/03	*Campylobacter fetus* subsp. *fetus*	1,800,589	33.22
M20-08756/1A	*Campylobacter fetus* subsp. *fetus*	1,782,221	33.10
M20-04752/1B	*Campylobacter fetus* subsp. *fetus*	1,782,237	33.10

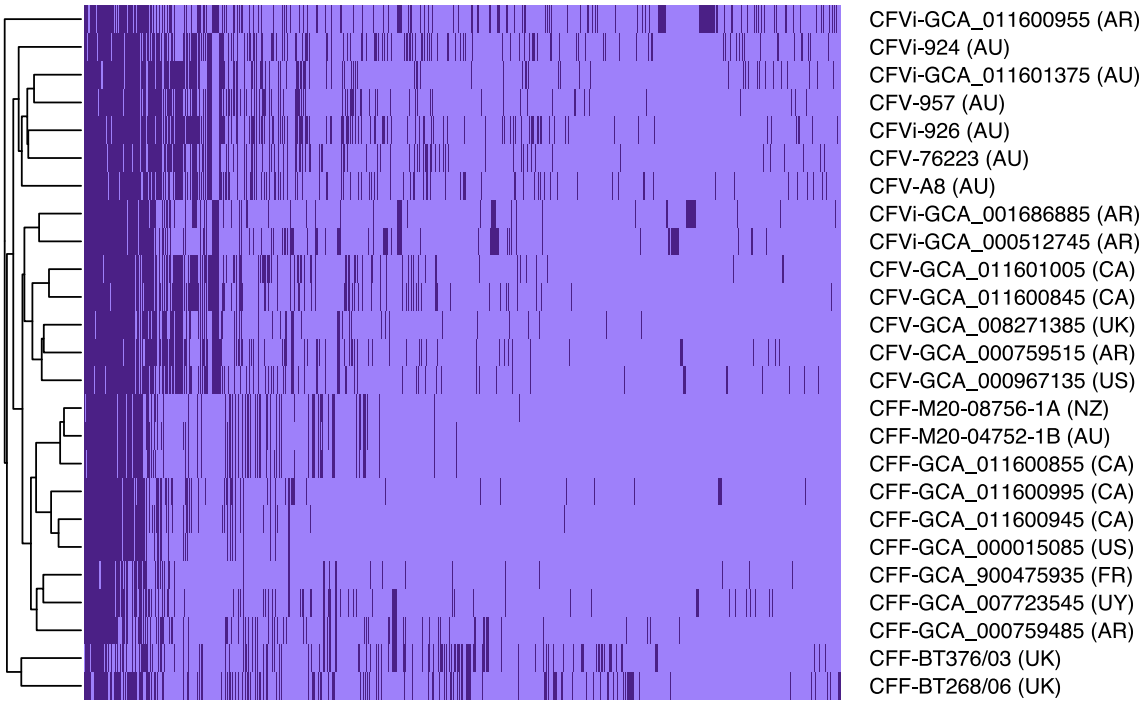

FIGURE 1
The pangenome of the 25 *Campylobacter fetus* strains. Dark purple indicates the presence of the gene ortholog, while light purple represents the absence of the gene ortholog. International Organization for Standardization (ISO) country code: Canada (CA), United States (US), France (FR), Uruguay (UY), Argentina (AR), United Kingdom (UK), Australia (AU), and New Zealand (NZ).

(Figure 6A). The SNPs that contributed to putative synonymous amino acid change, located on putative GIs, and involved in recombination events were filtered out from downstream analysis. The remaining 184 SNPs were labeled as "candidate SNPs," of which 17 were located in non-coding regions, and 167 were located in CDS (Supplementary Table 8). A total of 16 of the CDSs were encoded for two candidate SNPs, with one CDS encoded for three candidate SNPs and the other CDS encoded for five candidate SNPs. In total, the 167 candidate SNPs were located on 145 CDS, of which 15 of the CDS were encoding for hypothetical proteins. The majority of the SNPs-encoding CDS were responsible for "cellular processes and signaling" (n = 45), followed by "metabolism" (n = 44) and "information storage and processing" (n = 21; Figure 6B, Supplementary Table 9).

The potential functional association between the SNP-coding CDS was determined, and 41 candidate SNPs were identified on the SNP-coding CDS, which posed more than eight degrees of association. A subset of the 41 SNPs that were annotated with the KEGG pathway "Peptidoglycan biosynthesis" (Supplementary Figure 1) was chosen for further analysis due to their potential association with the differential glycine production in the *C. fetus* subspecies. The subset included *murC*, *ftsI*, *uppP*, and *mraY*, and their first neighbors (Figure 7). Among them, the SNP-coding CDS encoded for the candidate SNPs associated with significant amino acid change, including *rpoC*, *cysS*, *rpoB*, *flgG*, *mfd*,

10.3389/fmicb.2024.1452564

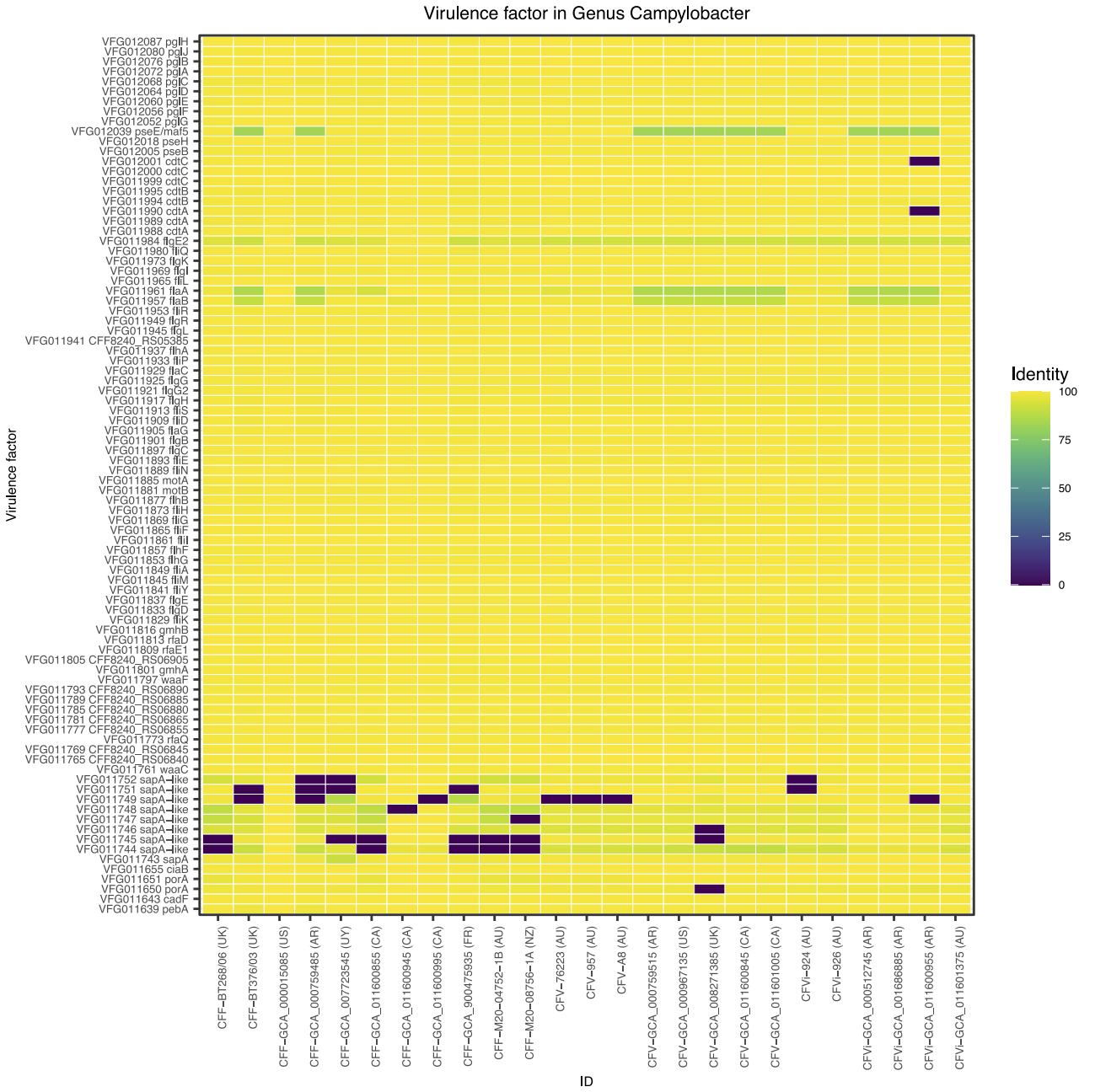

FIGURE 2
The *Campylobacter*-specific virulence factors among the 25 *Campylobacter fetus* strains. The color key indicates the percentage of identity between the genomic regions identified in each isolate and the *Campylobacter*-specific virulence factors, in which yellow represents 100% identity and purple represents 0% identity. International Organization for Standardization (ISO) country code: Canada (CA), United States (US), France (FR), Uruguay (UY), Argentina (AR), United Kingdom (UK), Australia (AU), and New Zealand (NZ).

mraY, and *mutS2*, were manually verified (Table 3). The candidate SNPs in these SNP-coding CDS were referred to as peptidoglycan SNPs (Figure 6A).

Interestingly, there were no common SNPs that could absolutely separate all the *C. fetus* subsp. *venerealis* and its biovar intermedius variant regardless of the country of origin. Therefore, this study only tested the potential of the seven peptidoglycan SNPs in differentiating the *C. fetus* subsp. *fetus* (CFF) from *C. fetus* subsp. *venerealis* and its biovar (CFV/CFVi). On top of the 25 complete genomes, an additional 33 curated RefSeq assemblies (13 *C. fetus* subsp. *fetus* and 20 *C. fetus* subsp. *venerealis* and its biovar) were recruited in the evaluation (Table 4). All seven peptidoglycan SNPs performed consistently and reliably divided the assemblies into two groups (Supplementary Table 10). The 24 *C. fetus* subsp. *fetus* assemblies, except NWU_ED24 (GCF_013406925.1), 13/344 (GCF_008527615.1), and 08/421 (GCF_008526335.1), posed SNP pattern conformed to the CFF subset. Interestingly, the three assemblies (NWU_ED24, 13/344, and 08/421) posed an SNP

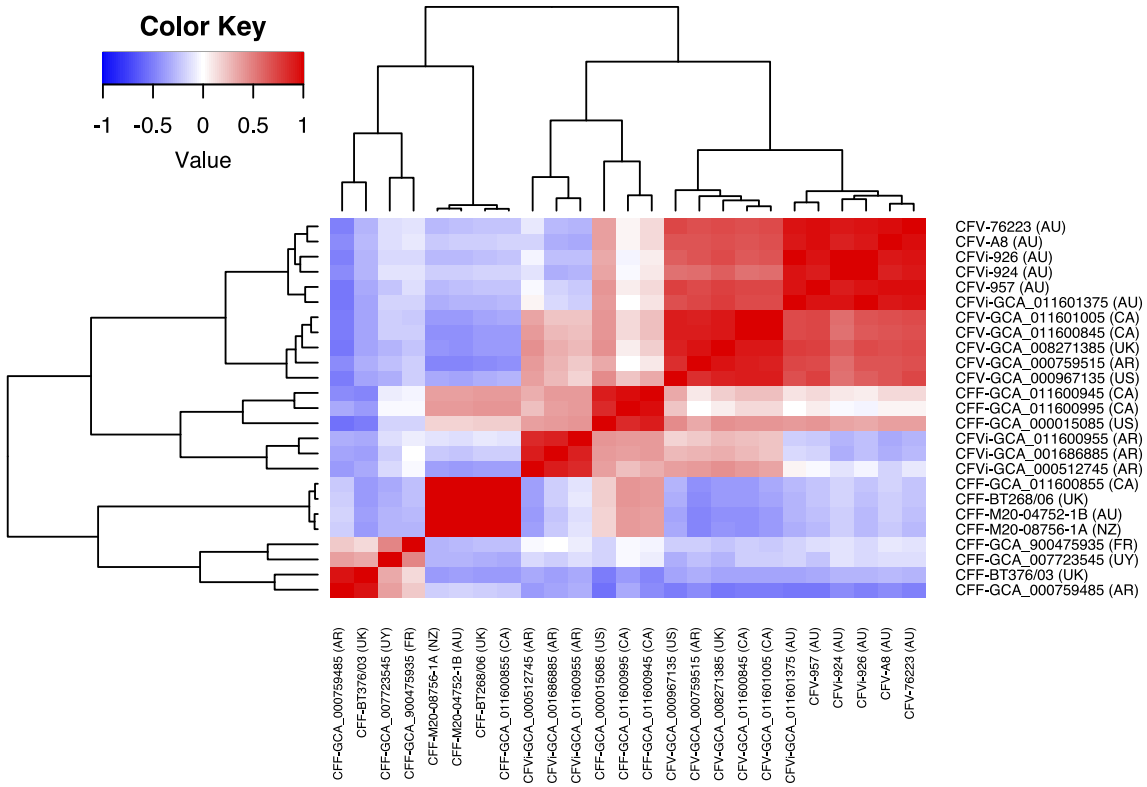

FIGURE 3
Correlation between the 25 *Campylobacter fetus* strains based on their average nucleotide identity. The color key indicates the degree of correlation between the strains, in which red represents the highest correlation while blue represents the lowest correlation. The dendrogram demonstrates the hierarchical relationship between the 25 *Campylobacter fetus* strains based on their average nucleotide identity. International Organization for Standardization (ISO) country code: Canada (CA), United States (US), France (FR), Uruguay (UY), Argentina (AR), United Kingdom (UK), Australia (AU), and New Zealand (NZ).

pattern that conformed to the CFV/CFVi subset. On the other hand, the 34 *C. fetus* subsp. *venerealis* assemblies, except P4531 (GCF_016406645.1), posed an SNP pattern conformed to the CFV/CFVi subset. The P4531 strain posed SNP pattern conformed to the CFF subset instead. Therefore, in this study, NWU_ED24, 13/344, and 08/421 were classified as *C. fetus* subsp. *venerealis* and its biovar, while the P4531 strain was classified as *C. fetus* subsp. *fetus*.

Confirmation of *C. fetus* subspecies differentiation by TaqMan SNP quantitative PCR

One of the SNPs differentiating the *C. fetus* subspecies located in the *mraY* gene (Table 3) was further exploited in a TaqMan SNP qPCR assay where the FAM channel detected the *C. fetus* subsp. *fetus* and the VIC channel *C. fetus* subsp. *venerealis*. The sensitivity of the assay was 1 pg when using pure bacterial DNA, and following testing of mixed *Campylobacter*-like species, a positive cut-off was determined at Cq 33 cycles (Figure 8A). The mraY assay was able to distinguish between *C. fetus* subsp. *venerealis* and *C. fetus* subsp. *fetus* controls, as well as other *C. fetus* isolates listed in Table 1 and other closely related *Campylobacter* species (*C. sputorum*, *C. ureolyticus*, *C. hyointestinalis,* and *A. cryoaerophilus*; Figure 8B).

Discussion

Differentiating C. fetus subspecies is crucial for the routine screening of ruminants for import and export and epidemiological investigation. Subspecies differentiation has been investigated using multiple methods, including biochemical analysis (OIE, 2019), AFLP (Wagenaar et al., 2001), PFGE (On and Harrington, 2001), MLST (van Bergen et al., 2005b; Iraola et al., 2015), PCR (Hum et al., 1997; Abril et al., 2007; Wang et al., 2002), and genome comparison methods (van der Graaf-van Bloois et al., 2014; Kienesberger et al., 2014). The results of this study demonstrated an improved and less laborious genome analysis method that successfully separated *C. fetus* subsp. *fetus* and *C. fetus* subsp. *venerealis* into two distinct clusters. According to their phenotypes, similar to previous AFLP (Wagenaar et al., 2001) and PFGE analyses (On and Harrington, 2001), but with a more efficient procedure.

In this study, the Australian *C. fetus* subsp. *venerealis* were separated from the non-Australian *C. fetus* subsp. *venerealis*, which was different from the indistinguishable geographical genotypes described in the previous core genome analysis (van der Graaf-van

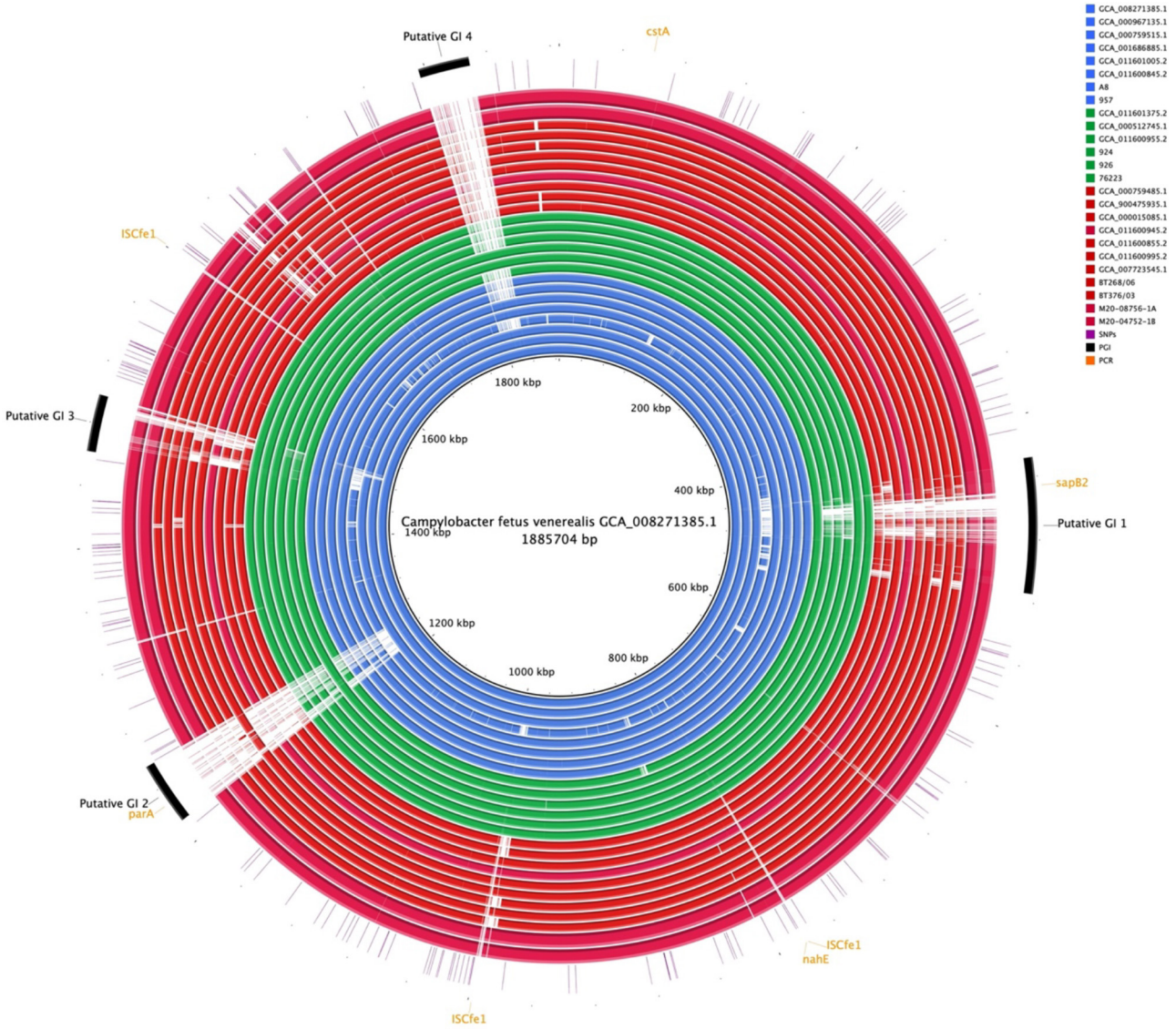

FIGURE 4
Whole-genome alignment of 25 *Campylobacter fetus* subspecies. Reference: published *C. fetus* subsp. *venerealis* ATCC 19438^T [GCA_008271385.1]. Query were complete genome sequences of *C. fetus* subsp. *Fetus* ($n = 11$) and *C. fetus* subsp. *venerealis* ($n = 14$) subspecies. Strains labeled in red are *C. fetus* subsp. *fetus*, isolated and labeled in blue, are *C. fetus* subsp. *venerealis* and strains labeled in green are *C. fetus* subsp. *venerealis* bv. intermedius. Black arcs represent the putative genomic islands. Orange arcs represent the genes that were used in PCR *C. fetus* subspecies identification. Purple lines represent candidate SNPs identified in the 25 *C. fetus* subspecies.

Bloois et al., 2014) and PFGE analysis (On and Harrington, 2001). Unique microbial lineages due to geographical separation are not novel. For example, most Australian *Glaesserella* (*Haemophilus*) *parasuis* strains were found to belong to unique sequence types not previously recorded in the relevant MLST database (Turni et al., 2018). In the phylogenetic tree generated using whole-genome alignment, the *C. fetus* subsp. *venerealis* clade shared the same ancestor with eight other *C. fetus* subsp. *fetus* strains, potentially indicating that *C. fetus* subsp. *venerealis* was derived from *C. fetus* subsp. *fetus*. The identification of a small number of SNPs ($n = 184$), which are differentially expressed in the *C. fetus* subsp. *fetus* and *C. fetus* subsp. *venerealis* strains, which were supported by the observations from the MLST analyses, indicating a limited genetic variation between *C. fetus* subspecies was driven mainly by the slow accumulation of point mutations (van Bergen et al., 2005b). Additionally, this study did not identify any SNPs that are unique to the *C. fetus* subsp. *venerealis* bv. intermedius regardless of geographical origins, suggesting that clonal evolution occurred separately within the geographically different *C. fetus* subsp. *venerealis* clades. It appears that *C. fetus* subsp. *venerealis* and its biovar-acquired point mutations, which have been vertically transmitted and enabled the development of their highly niche-specific and pathogenicity-specific characteristics.

For the comparative whole-genome analysis, only complete *C. fetus* genomes were used. This approach ensured a comprehensive comparison and prevented false positives that could result from

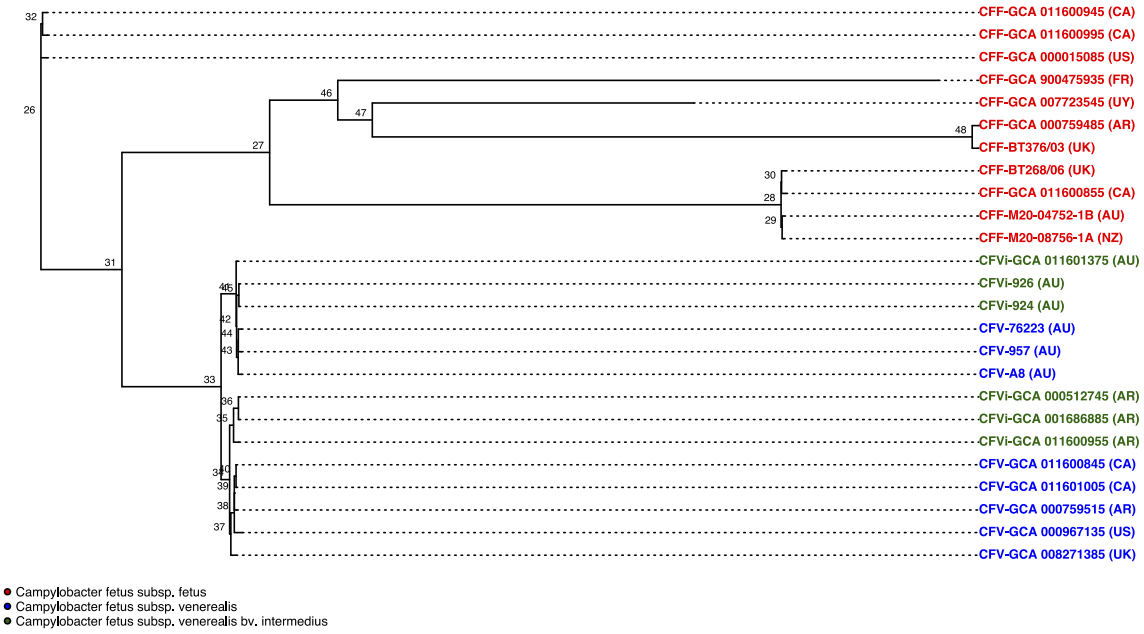

FIGURE 5
Phylogenetic tree based on single nucleotide polymorphisms (SNPs) between the 25 *Campylobacter fetus* strains. Strains labeled in red are *C. fetus* subsp. *fetus*, strains labeled in blue are *C. fetus* subsp. *venerealis*, and strains labeled in green are *C. fetus* subsp. *venerealis* bv. intermedius. All *C. fetus* subsp. *fetus* isolates clustered into a separate branch from all *C. fetus* subsp. *venerealis* and *C. fetus* subsp. *venerealis* bv. intermedius isolates, indicating that there were distinctive SNPs. *C. fetus* subsp. *venerealis* and *C. fetus* subsp. *venerealis* bv. intermedius isolates from Australia clustered separately from non-Australian isolates. International Organization for Standardization (ISO) country code: Canada (CA), United States (US), France (FR), Uruguay (UY), Argentina (AR), United Kingdom (UK), Australia (AU), and New Zealand (NZ).

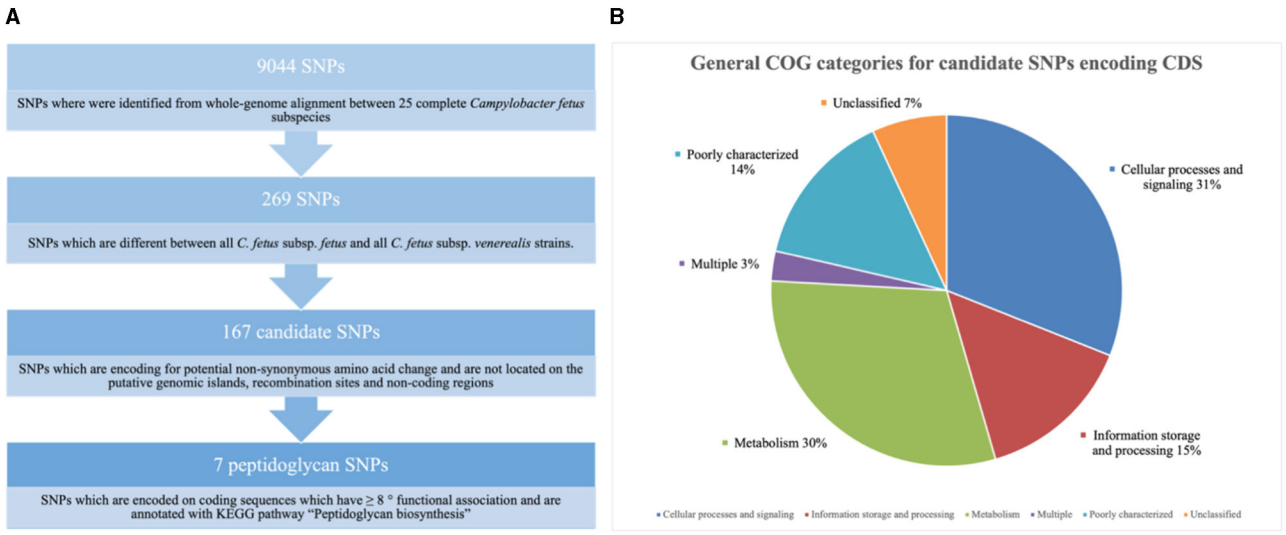

FIGURE 6
(A) Screening for single nucleotide polymorphisms (SNPs) suitable for reliable differentiation between *Campylobacter fetus* subsp. *fetus* and *Campylobacter fetus* subsp. *venerealis*. **(B)** Candidate single nucleotide polymorphisms (SNPs) are categorized into Clusters of Orthologous Groups (COGs). The blue section represents coding sequences (CDS) responsible for "cellular processes and signaling" ($n = 45$). The orange section represents the CDS responsible for "information storage and processing" ($n = 21$). The gray section represents CDS responsible for "metabolism" ($n = 44$). The yellow section represents CDS belonging to multiple groups of COGs ($n = 4$). The light blue section represents CDS, which was poorly categorized ($n = 21$). The green section represents CDS with no match return from querying the COG database ($n = 10$).

aligning the complete genome against the gaps of an incomplete genome. The previous investigation, compared one complete genome of *C. fetus* subsp. *fetus* (GCA_000015085) against one incomplete genome of *C. fetus* subsp. *venerealis* (GCA_000222425) reported that 88 and 428 gene families were unique to *C. fetus* subsp. *fetus* and *C. fetus* subsp. *venerealis*, respectively (Ali et al.,

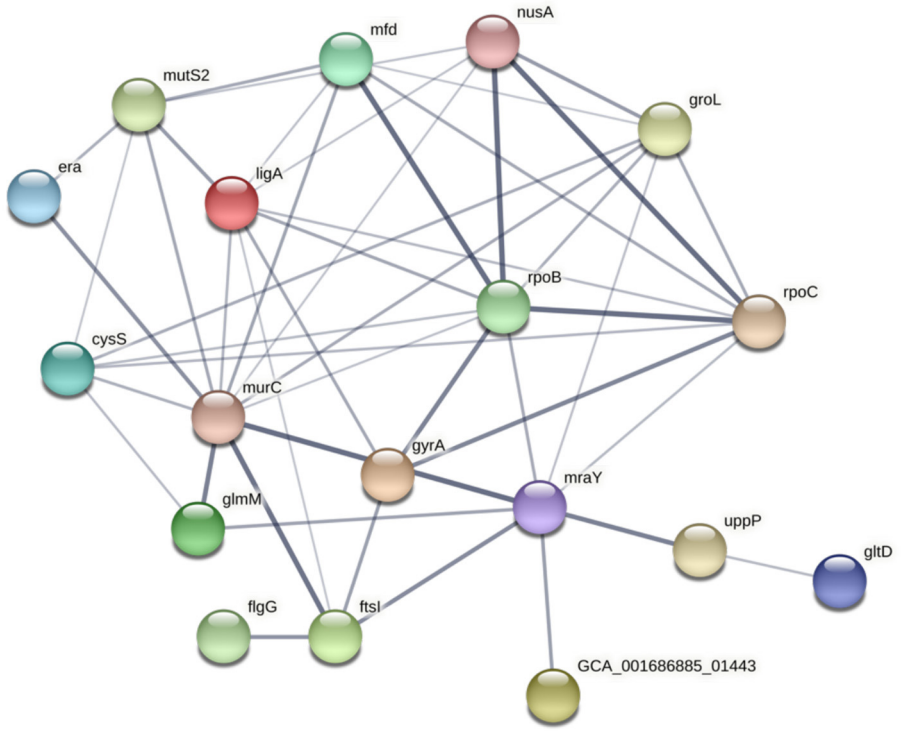

FIGURE 7
STRING network of SNP-coding CDS, which had more than eight degrees of association. The thickness of the network edges indicates the confidence level of the functional interactions.

TABLE 3 Amino acid and DNA base changes on the candidate SNP-coding CDS encoded on *C. fetus* subsp. *fetus* and *C. fetus* subsp. *venerealis*.

Gene	Product	Position on GCA_008271385.1	Locus tag on GCA_008271385.1	Type	*Campylobacter fetus* subsp. *fetus*		*Campylobacter fetus* subsp. *venerealis*	
					Amino acid	DNA base	Amino acid	DNA base
cysS	cysteinyl-tRNA	799900	CFVT_0790	Missense	Cys	C	Tyr	T
flgG	flagellar	549585	CFVT_0554	Missense	Asn	A	Ser	G
mfd	transcription-repair	744016	CFVT_0740	Missense	Thr	C	Ile	T
mraY	phospho-N-acetylmuramoyl-pentapeptide transferase	1384375	CFVT_1392	Upstream variant	Arg	C	His	T
mutS2	Endonuclease	653990	CFVT_0655	Missense	Ala	C	Val	T
rpoB	DNA-dependent RNA polymerase	1351503	CFVT_1350	Missense	Asp	C	Asn	T
rpoC	DNA-dependent RNA polymerase	1349348	CFVT_1349	Missense	Leu	G	Phe	A

2012). The current study only identified one gene ortholog, which was different between the two complete genomes of the *C. fetus* subspecies. Our results aligned with the previous suggestion, based on methods other than genome sequencing, that there is a lack of genetic diversity between the *C. fetus* subspecies because the *C. fetus* strains are at an early evolutionary stage (van Bergen et al., 2005a; Wagenaar et al., 2001). The only unique gene ortholog encoded for a peptidase S24 LexA-like protein was only identified in *C. fetus* subsp. *venerealis* and not in the *C. fetus* subsp. *fetus* strains. However, three other paralogs coding for peptidase S24 LexA-like protein were identified in both *C. fetus* subspecies in this study. While LexA is a global transcription factor responsible for regulating host SOS response, several studies have also suggested that mobile genetic elements utilize the LexA activity of the hosts

TABLE 4 Characterization of 58 *Campylobacter fetus* subspecies according to previous studies and the current study.

Assembly accession	Strain	Assembly level	NCBI annotation	*Identification #1	*Identification #2	*Identification #3	*Identification #4	Identification in this study
CP075536-CP075537	A8	Complete	CFV					CFV/CFVi
GCF_030544605.1	CFV924	Complete	CFVi					CFV/CFVi
GCF_030544585.1	CFV926	Complete	CFVi					CFV/CFVi
GCF_030544565.1	CFV957	Complete	CFV					CFV/CFVi
GCF_030544545.1	CFV76223	Complete	CFV					CFV/CFVi
GCF_016612985.1	SA21-221439	Contig	CFV	CFV (Silva et al., 2021)				CFV/CFVi
GCF_016612955.1	SA21-217832	Contig	CFV	CFV (Silva et al., 2021)				CFV/CFVi
GCF_016612945.1	SA21-217833	Contig	CFV	CFV (Silva et al., 2021)				CFV/CFVi
GCF_016612925.1	IS16-01257	Contig	CFV	CFV (Silva et al., 2021)				CFV/CFVi
GCF_016612875.1	IS26-07793	Contig	CFV	CFV (Silva et al., 2021)				CFV/CFVi
GCF_016406645.1	P4531	Complete	CFV	CFV (Kim et al., 2021)				CFF
GCF_013406955.1	NWU_ED23	Contig	CFV	CFV (Tshipamba et al., 2020a)	CFVi (Silva et al., 2021)	CFF/CFVi (Farace et al., 2021)		CFV/CFVi
GCF_012274465.1	NW_ME2	Contig	CFV	CFV (Tshipamba et al., 2020b)	CFVi (Silva et al., 2021)			CFV/CFVi
GCF_008526355.1	06/341	Contig	CFV	CFV (Hum et al., 1997)	CFVi (Farace et al., 2021, 2022)	CFF/CFVi (Farace et al., 2019)		CFV/CFVi
GCF_008271385.1	NCTC 10354	Complete	CFV	CFV (van Bergen et al., 2005a; Farace et al., 2019)				CFV/CFVi
GCF_002592365.1	66Y	Contig	CFV	CFV (Farace et al., 2019; Iraola et al., 2017)				CFV/CFVi
GCF_002592335.1	TD	Contig	CFV	CFV (Farace et al., 2019; Iraola et al., 2017)				CFV/CFVi
GCF_001699745.1	ADRI513	Contig	CFVi	CFVi (van der Graaf-van Bloois et al., 2016a)	CFV/CFVi (van der Graaf-van Bloois et al., 2014)	CFF/CFVi (Farace et al., 2019)		CFV/CFVi
GCF_001699735.1	zaf3	Contig	CFVi	CFVi (van der Graaf-van Bloois et al., 2014)	CFF/CFVi (Farace et al., 2019)			CFV/CFVi
GCF_001699685.1	cfvi9825	Contig	CFVi	CFVi (van der Graaf-van Bloois et al., 2014; van Bergen et al., 2005b)	CFV (Farace et al., 2019)			CFV/CFVi
GCF_001699645.1	CCUG 33872	Contig	CFV	CFV (Willoughby et al., 2005)	CFVi (van der Graaf-van Bloois et al., 2016a)	CFF/CFVi (Farace et al., 2019)	CFV/CFVi (van der Graaf-van Bloois et al., 2014)	CFV/CFVi
GCF_001699615.1	cfvi03/596	Contig	CFVi	CFVi (van der Graaf-van Bloois et al., 2014, 2016a; Farace et al., 2021)	CFF (Hum et al., 1997; Iraola et al., 2017)	CFF/CFVi (Farace et al., 2019)		CFV/CFVi

(Continued)

TABLE 4 (Continued)

Assembly accession	Strain	Assembly level	NCBI annotation	*Identification #1	*Identification #2	*Identification #3	*Identification #4	Identification in this study
GCF_001699565.1	cfvi92/203	Contig	CFVi	CFVi (van der Graaf-van Bloois et al., 2014, 2016a)	CFV (Hum et al., 1997)	CFF/CFVi (Farace et al., 2019)		CFV/CFVi
GCF_001686885.1	01/165	Complete	CFV	CFVi (van der Graaf-van Bloois et al., 2014, 2016a; Farace et al., 2021; Iraola et al., 2017)	CFF (Hum et al., 1997)	CFF/CFVi (Farace et al., 2019)		CFV/CFVi
GCF_000967135.1	84-112	Complete	CFV	CFV (van der Graaf-van Bloois et al., 2014, 2016a; van Bergen et al., 2005a; Hum et al., 1997; Farace et al., 2019; Iraola et al., 2017)				CFV/CFVi
GCF_000759515.1	97/608	Complete	CFV	CFV (van der Graaf-van Bloois et al., 2014, 2016a; Hum et al., 1997; Farace et al., 2019, 2021; Iraola et al., 2017)				CFV/CFVi
GCF_000744035.1	B6	Scaffold	CFV	CFV (van der Graaf-van Bloois et al., 2016a; Farace et al., 2019; Iraola et al., 2017; Barrero et al., 2014)				CFV/CFVi
GCF_000744025.1	642-21	Scaffold	CFVi	CFVi (van der Graaf-van Bloois et al., 2016a; Barrero et al., 2014)	CFF/CFVi (Farace et al., 2019)			CFV/CFVi
GCF_000512745.2	cfvi03/293	Complete	CFVi	CFVi (Iraola et al., 2017)	CFV (Hum et al., 1997)	CFF/CFVi (van der Graaf-van Bloois et al., 2014, 2016a; Farace et al., 2019)		CFV/CFVi
GCF_000414135.1	99541	Contig	CFVi	CFVi (van der Graaf-van Bloois et al., 2016a; Iraola et al., 2013; Farace et al., 2021; Iraola et al., 2017)	CFF (Hum et al., 1997)	CFF/CFVi (Farace et al., 2019)		CFV/CFVi
GCA_011600845.2	08A1102-42A	Complete	CFV	CFV (Nadin-Davis et al., 2021; Farace et al., 2021; Mukhtar, 2013)				CFV/CFVi
GCA_011600955.2	ADRI1362	Complete	CFVi	CFVi (Nadin-Davis et al., 2021)	Cff/CFVi (van der Graaf-van Bloois et al., 2014, 2016a; Farace et al., 2019)			CFV/CFVi
GCA_011601005.2	08A948-2A	Complete	CFV	CFV (Nadin-Davis et al., 2021; Farace et al., 2021; Mukhtar, 2013)				CFV/CFVi
GCA_011601375.2	ADRI545	Complete	CFVi	CFVi (Nadin-Davis et al., 2021)				CFV/CFVi

(Continued)

TABLE 4 (Continued)

Assembly accession	Strain	Assembly level	NCBI annotation	*Identification #1	*Identification #2	*Identification #3	*Identification #4	Identification in this study
GCF_000015085.1	82-40	Complete	CFF	CFF (van der Graaf-van Bloois et al., 2014, 2016a; van Bergen et al., 2005a; Iraola et al., 2017)	CFF/CFVi (Farace et al., 2019)			CFF
GCF_000759485.1	04/554	Complete	CFF	CFF (van der Graaf-van Bloois et al., 2014, 2016a; Hum et al., 1997; Farace et al., 2021; Iraola et al., 2017)	CFF/CFVi (Farace et al., 2019)			CFF
GCF_001399955.1	H1-UY	Contig	CFF	CFF (van der Graaf-van Bloois et al., 2016a; Iraola et al., 2015, 2017)	CFF/CFVi (Farace et al., 2019)			CFF
GCF_001699505.1	98/v445	Contig	CFF	CFF (van der Graaf-van Bloois et al., 2014, 2016a; van Bergen et al., 2005a)	CFV (Hum et al., 1997)	CFF/CFVi (Farace et al., 2019)		CFF
GCF_001699575.1	BT 10/98	Contig	CFF	CFF (van der Graaf-van Bloois et al., 2014, 2016a)	CFF/CFVi (Farace et al., 2019)			CFF
GCF_003426005.1	HC1	Contig	CFF	CFF (Iraola et al., 2017)	CFF/CFVi (Farace et al., 2019)			CFF
GCF_003426015.1	HC2	Contig	CFF	CFF (Iraola et al., 2017)	CFF/CFVi (Farace et al., 2019)			CFF
GCF_007723545.1	INIA/17144	Complete	CFF	CFF/CFVi (Farace et al., 2021)				CFF
GCF_008014295.1	D0052	Contig	CFF	CFF/CFVi (Farace et al., 2021)				CFF
GCF_008526335.1	08/421	Contig	CFF	CFF (Farace et al., 2021, 2022)	CFV (Hum et al., 1997)	CFF/CFVi (Farace et al., 2019)		CFV/CFVi
GCF_008527615.1	13/344	Contig	CFF	CFF (Hum et al., 1997; Farace et al., 2021, 2022)	CFF/CFVi (Farace et al., 2019)			CFV/CFVi
GCF_008693125.1	CCUG 6823 AT	Contig	CFF	CFF	CFF/CFVi (Farace et al., 2021)			CFF
GCF_013406925.1	NWU_ED24	Contig	CFF	CFF	CFF/CFVi (Farace et al., 2021)			CFV/CFVi
GCF_017896385.1	CITCf01	Complete	CFF	CFF (Lynch et al., 2021)				CFF
GCF_017896405.1	CITCf02	Complete	CFF	CFF (Lynch et al., 2021)				CFF
GCF_020828935.1	YZU0709	Contig	CFF	CFF (Li et al., 2022)				CFF
GCF_900475935.1	NCTC10842	Complete	CFF	CFF (van Bergen et al., 2005a; Farace et al., 2019; Willoughby et al., 2005)	CFF/CFVi (Farace et al., 2019)			CFF
GCA_011600855.2	02A725-35A	Complete	CFF	CFF (Nadin-Davis et al., 2021)				CFF
GCA_011600945.2	00A031	Complete	CFF	CFF (Nadin-Davis et al., 2021)				CFF

(Continued)

TABLE 4 (Continued)

Assembly accession	Strain	Assembly level	NCBI annotation	*Identification #1	*Identification #2	*Identification #3	*Identification #4	Identification in this study
GCA_011600995.2	09A980	Complete	CFF	CFF (Nadin-Davis et al., 2021)				CFF
GCF_032594895.1	M20-08756/1A	Complete	CFF	CFF				CFF
GCA_030544625.1	BT376/03	Complete	CFF	CFF				CFF
GCA_030544645.1	BT268/06	Complete	CFF	CFF				CFF
GCF_032594815.1	M20-04752/1B	Complete	CFF	CFF				CFF

*The identification of the Campylobacter strain in the previous studies.

for their induction (Fornelos et al., 2016; Quinones et al., 2005; Kimsey and Waldor, 2009). The previous comparison of 14 *C. fetus* strains observed that the *lexA* gene, which served as a prophage regulator, was mostly identified at the boundary of a prophage element (Nadin-Davis et al., 2021).

Additionally, we found no gene ortholog that was unique to either *C. fetus* subsp. *venerealis* or the *C. fetus* subsp. *venerealis* biovar variant. This is in contrast to the previous pangenome analysis of 31 *C. fetus* subsp. *venerealis* strains using a mixture of complete and incomplete genomes, which identified inconsistent expressions of *parA* and T4SS encoding genes (*virB2-virB11* and *virD4*) in the *C. fetus* strains (Silva et al., 2021). Additionally, the virulence gene investigation in this study demonstrated variations in the *sap* genes among the 25 *C. fetus* strains. This result corresponded to the previous studies, which categorized *C. fetus* subspecies to serovars based on the variable expression of genes in the *sap* locus that encode for surface layer protein (SLP; Tu et al., 2001; Dworkin et al., 1995). Our results reinforced that the serovar classification is not unique at the *C. fetus* subspecies level.

The biochemical tests that are currently recommended by OIE (2019) for identifying *C. fetus* subspecies include glycine tolerance test and H_2S production. *C. fetus* subsp. *fetus* is positive for both tests, while *C. fetus* subsp. *venerealis* is negative for both. Previous studies have suggested the ATP-binding cassette-type L-cysteine transporter as a potential marker for H_2S-positive *C. fetus* strains, leading to the development of an accurate diagnostic test based on the L-Cys transporter-deletion polymorphism (van der Graaf-van Bloois et al., 2016a; Farace et al., 2019).

However, unlike *C. fetus* subsp. *venerealis*, the intermedius biovar variant is positive for H_2S production. As a result, previous tests using molecular techniques to detect the L-Cys transporter-deletion polymorphism were unable to distinguish *C. fetus* subsp. *venerealis* biovar intermedius strains from *C. fetus* (Farace et al., 2019, 2021). This study provided 167 SNPs as new candidates for *C. fetus* subspecies genotyping, which may be valuable for precise and efficient routine screening on farms, international trade, and for epidemiological investigations and diagnostics.

In this study, SNP-coding CDS was investigated for a correlation with the differential tolerance to glycine among the *C. fetus* subspecies, which separates the *C. fetus* subsp. *fetus* from the *C. fetus* subsp. *venerealis* and its biovar intermedius. Glycine has been suggested to inhibit bacterial cell wall biosynthesis, particularly the peptidoglycan component, and thus can show an antibacterial effect (Hishinuma et al., 1969). Therefore, candidate CDS annotated with the "peptidoglycan biosynthesis" KEGG pathway and posed potential functional association with one another, including *cysS*, *flgG*, *mfd*, *mraY*, *mutS2*, *rpoB,* and *rpoC*, were recruited for further analysis. Gene *mraY* was part of the gene set found in peptidoglycan-intermediate obligate intracellular bacteria (Otten et al., 2018). Phospho-N-acetylmuramoyl-pentapeptide-transferase (*mraY*) is a catalytic enzyme that initiates the lipid cycle reactions during bacterial peptidoglycan synthesis (Struve et al., 1966). Under normal circumstances, *mraY* has high specificity to L-alanine and D-alanine (Hammes and Neuhaus, 1974). However, the non-synonymous amino acid change introduced by the peptidoglycan SNP identified in our study potentially modified *mraY* and thus allowed glycine substitution. As a result, bacteriolysis or morphological aberrations of the bacterial cells could be induced and lead to differential glycine tolerance between the *C. fetus* subspecies. The presence of this SNP was further exploited in a novel *C. fetus* subspecies TaqMan SNP qPCR, which demonstrated specific detection of each subspecies using different fluorophores and no detection of other closely related species such as *C. hyointestinalis* as reported for other diagnostic targets present on mobile elements (Spence et al., 2011).

Other peptidoglycan SNPs were previously reported to be associated with variations in niche adaption and virulence between closely related bacterial strains. The *rpoB* and *rpoC* genes code for the β- and β'-like subunits of the DNA-dependent RNA polymerase, which regulates gene expression in bacteria and archaea (Zakharova et al., 1998). Mutations in *rpoB* and *rpoC* genes were reported to be responsible for the different degrees of antibiotic resistance observed in *Staphylococcus aureus* (Matsuo et al., 2015), *Mycobacterium tuberculosis* (Ma et al., 2021) and

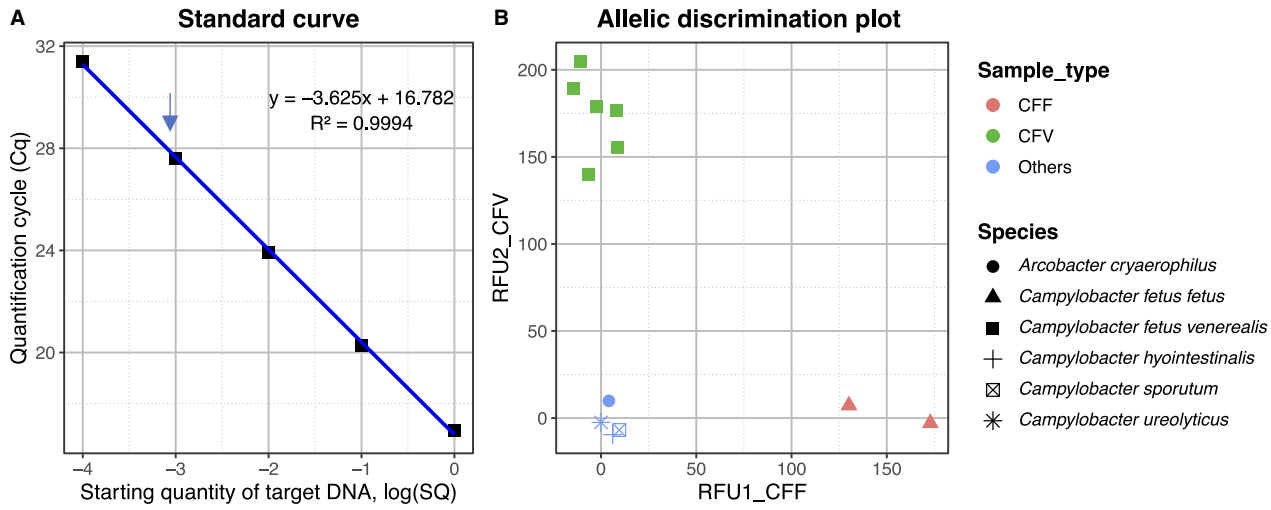

FIGURE 8
(A) Standard curve for the *mraY* SNP assay plotting the quantification cycle (Cq) value against the starting quantity of *C. fetus venerealis* DNA. Data points are from 1 ng to 0.1 pg, with 1 pg indicated by an arrow. The R^2 of the standard curve is 0.994. **(B)** Allelic discrimination plot for *mraY* Taqman SNP assay using Relative Fluorescent Units (RFU) for VIC and FAM. Red—CFF control (ATCC 27374), brown—CFF isolate (strain BT376/03), green—CFV control (ATCC 19438), blue—CFV isolates (strains A8, 957, 76223, 924, and 926), and light blue—other *Campylobacter* species (*C. sputorum*, *C. ureolyticus*, *C. hyointestinalis*, and *A. cryoaerophilus*).

Clostridium difficile (Kuehne et al., 2018). Similar observations on the impact of these mutations have been demonstrated for the virulence of *C. difficile* strains (Kuehne et al., 2018), as well as the differences in the ability of *E. coli* (Conrad et al., 2010) and *Helicobacter pylori* (Zakharova et al., 1998) to colonize different niches. SNPs in both *rpoB* and *cysS* were suggested to contribute to the niche adaptation of the multi-host pathogen *S. aureus* (Bacigalupe et al., 2019). The interaction between the "mutation frequency decline" (*mfd*) gene and RNA polymerase, for example, *rpoB*, plays a role in the development of antimicrobial resistance in highly divergent bacterial species (Ragheb et al., 2019). Additionally, *mfd* is recognized as the "pro-evolutionary factor," as studies suggested that *mfd* plays a significant role in prokaryotic virulence and survival (Lindsey-Boltz and Sancar, 2021; Strick and Portman, 2019). Mutations on the outer membrane proteins, including *flgG* (Palau et al., 2021) and genes of the *hop* family (Linz et al., 2013), facilitated the niche adaptations of different strains *of Helicobacter pylori* and allowed the colonization of the new host. Non-synonymous mutations in the *mutS2*, a gene coding for endonuclease responsible for suppressing homologous recombination, were linked to increased mutation rates during niche adaptation in *Streptococcus pneumoniae* (Green et al., 2021) and species-specific variation among the *Aquilegia* species (Wang et al., 2022).

Each of the seven peptidoglycan SNPs consistently divided the 58 *C. fetus* strains into two distinct groups, CFF and CFV/CFVi, suggesting the potential of developing a reliable assay for the subspecies differentiation. The CFF or CFV/CFVi identification in this study is consistent with the reported identity of the *C. fetus* strains, except for P4531 (GCF_016406645.1). P4531 was announced as a *C. fetus* subsp. *venerealis* but was typed as a *C. fetus* subsp. *fetus* using the seven peptidoglycan SNPs in this study. Nonetheless, P4531 was previously identified as a *C. fetus* subsp. *venerealis* using a microbial identification system and 16S rRNA sequence analysis (Kim et al., 2021), which are not sufficient to accurately differentiate between the subspecies (van der Graaf-van Bloois et al., 2016a). In some cases where there was inconsistency between the reported phenotypic and genomic identification of the *C. fetus* subspecies, including cfvi03/596, 01/165, 99541, 98/v445, and 08/421, the identification using the seven peptidoglycan SNPs in this study demonstrated consistent alignment with the reported phenotypic identification, which was typed with the biochemical tests, glycine tolerance and H_2S production, recommended by OIE.

Moreover, the identification of subspecies reported in this study was consistent with biochemical and other molecular tests. For example, the *C. fetus* subsp. *fetus* reference strain NCTC10842 (GCF_900475935.1) was reported as a CFF/CFVi (Farace et al., 2019) by the L-Cys transporter PCR assay. However, several phenotypic and genomic tests have confirmed the identity of NCTC10842 as a *C. fetus* subsp. *fetus*. A similar observation was observed at multiple strains, including NWU_ED23, 06/341, ADRI513, zaf3, 82-40, 04/554, H1-UY, and so on. A reliable and accurate identification of *C. fetus* subsp. *venerealis* biovars, which are commonly identified in the bovine genital tract, has been an objective goal in BGC diagnostics research. Hence, we propose the seven peptidoglycan SNPs described in this study could be potential tools for BGC diagnostics and differentiation from *C. fetus* subsp. *fetus*.

One limitation of this study was the number of *C. fetus* strains ($n = 25$) recruited for SNP calling. However, we carefully conducted the whole-genome comparison with only the complete genomes to avoid the potential of false positive results arising from incomplete genomes. Additionally, the peptidoglycan SNPs were further verified using all the annotated and contamination-free *C.*

fetus genomes ($n = 58$) available on the NCBI RefSeq database, which is a curated database with a non-redundant, high-quality set of sequences with detailed annotations. Ideally, more *C. fetus* strains from multiple geographical regions and sources should be included in the whole-genome comparison to provide a more comprehensive view of the evolutionary events of *C. fetus* subspecies as well as the branching of *C. fetus* subsp. *venerealis* bv. intermedius at different geographical regions. To obtain a detailed evolutionary history of the genus *Campylobacter*, future investigations should also include the complete genomes of the other subspecies, such as *Campylobacter fetus* subsp. *testudinum*, as well as other closely related *Campylobacter* species. Additionally, the impacts of amino acid change on SNP-coding CDSs should be further investigated and validated with phenotypic assays to examine the effect on glycine tolerance.

Conclusion

Our results have reinforced the high genetic stability of *C. fetus* subspecies, suggesting that they are at the early stage of their evolutionary history and their genomic diversity is at the nucleotide base level. Clonal evolution was found to have occurred separately within the non-Australian and Australian strains. Regardless of geographical regions, *C. fetus* subsp. *venerealis* and the biovar variants have potentially acquired common point mutations from the vertical transmission that have enabled their niche-specificity and pathogenicity that separates them from *C. fetus* subsp. *fetus*. The *C. fetus* subsp. *venerealis* and the biovar intermedius variant also acquired different SNPs. The peptidoglycan SNPs identified and verified in this study are key candidates for the development of more accurate multi-SNP genotyping assays because of their association with the differential glycine tolerance between *C. fetus* subsp. *fetus* and *C. fetus* subsp. *venerealis*.

Data availability statement

The datasets presented in this study can be found in online repositories. The names of the repository/repositories and accession number(s) can be found at: https://www.ncbi.nlm.nih.gov/, PRJNA675960.

Ethics statement

The manuscript presents research on animals that do not require ethical approval for their study.

Author contributions

CO: Conceptualization, Data curation, Formal analysis, Investigation, Methodology, Visualization, Writing – original draft, Writing – review & editing. PB: Supervision, Writing – review & editing. GB-H: Supervision, Writing – review & editing. Sd: Investigation, Methodology, Writing – review & editing. BH: Supervision, Writing – review & editing. LI: Formal analysis, Methodology, Writing – review & editing. VK: Resources, Writing – review & editing. CM: Formal analysis, Methodology, Writing – review & editing. LN: Methodology, Supervision, Writing – review & editing. YN: Formal analysis, Methodology, Writing – review & editing. HS: Formal analysis, Investigation, Methodology, Writing – review & editing. CT: Methodology, Supervision, Validation, Writing – review & editing. BV: Methodology, Writing – review & editing. MW: Resources, Validation, Writing – review & editing. ZZ: Formal analysis, Investigation, Methodology, Writing – review & editing. AT: Conceptualization, Funding acquisition, Project administration, Resources, Supervision, Validation, Writing – review & editing.

Funding

The author(s) declare financial support was received for the research, authorship, and/or publication of this article. This work was supported by the Meat and Livestock Australia Donor Company (grant number: P.PSH.0799) and the Queensland Department of Agriculture and Fisheries.

Acknowledgments

The authors thank Meat and Livestock Australia Donor Company Project P.PSH.0799 for funding this research. The authors thank Diane Newell for sharing the bacterial strains BT268/06 and BT376/03 and Ingrid Flemming of IFM Quality Services for sharing the bacterial isolate M20-08756/1A.

Conflict of interest

The authors declare that the research was conducted in the absence of any commercial or financial relationships that could be construed as a potential conflict of interest.

The author(s) declared that they were an editorial board member of Frontiers, at the time of submission. This had no impact on the peer review process and the final decision.

Publisher's note

Supplementary material

The Supplementary Material for this article can be found online at: https://www.frontiersin.org/articles/10.3389/fmicb.2024.1452564/full#supplementary-material

References

Abril, C., Vilei, E. M., Brodard, I., Burnens, A., Frey, J., Miserez, R., et al. (2007). Discovery of insertion element ISCfe 1: a new tool for *Campylobacter fetus* subspecies differentiation. *Clin. Microbiol. Infect*. 13, 993–1000. doi: 10.1111/j.1469-0691.2007.01787.x

Ali, A., Soares, S. C., Santos, A. R., Guimarães, L. C., Barbosa, E., Almeida, S. S., et al. (2012). *Campylobacter fetus* subspecies: comparative genomics and prediction of potential virulence targets. *Gene* 508, 145–156. doi: 10.1016/j.gene.2012.07.070

Alikhan, N. F., Petty, N. K., Ben Zakour, N. L., and Beatson, S. A. (2011). BLAST Ring Image Generator (BRIG): simple prokaryote genome comparisons. *BMC Genom*. 12:402. doi: 10.1186/1471-2164-12-402

Altschul, S. F., Gish, W., Miller, W., Myers, E. W., and Lipman, D. J. (1990). Basic local alignment search tool. *J. Mol. Biol*. 215, 403–410. doi: 10.1016/S0022-2836(05)80360-2

Andrew, S. (2010). *FastQC: a Quality Control Tool for High Throughput Sequence Data*. Available at: http://www.bioinformatics.babraham.ac.uk/projects/fastqc (accessed January 15, 2020).

Bacigalupe, R., Tormo-Mas, M. Á., Penadés, J. R., and Fitzgerald, J. R. (2019). A multihost bacterial pathogen overcomes continuous population bottlenecks to adapt to new host species. *Sci. Adv*. 5:eaax0063. doi: 10.1126/sciadv.aax0063

Barrero, R. A., Moolhuijzen, P., Indjein, L., Venus, B., Keeble-Gagnère, G., Power, J., et al. (2014). Draft genome sequences of *Campylobacter fetus* subsp. venerealis bv. venerealis Strain B6 and bv. intermedius Strain 642-21. *Genome Announc*. 2:e00943–14. doi: 10.1128/genomeA.00943-14

Basden, E. H. 2nd., Tourtellotte, M. E., Plastridge, W. N., and Tucker, J. S. (1968). Genetic relationship among bacteria classified as Vibrios. *J. Bacteriol*. 95, 439–443. doi: 10.1128/jb.95.2.439-443.1968

Bertelli, C., Laird, M. R., Williams, K. P., Lau, B. Y., and Hoad, G. (2017). IslandViewer 4: expanded prediction of genomic islands for larger-scale datasets. *Nucl. Acids Res*. 45, W30-W35. doi: 10.1093/nar/gkx343

Bolger, A. M., Lohse, M., and Usadel, B. (2014). Trimmomatic: a flexible trimmer for Illumina sequence data. *Bioinformatics* 30, 2114–2120. doi: 10.1093/bioinformatics/btu170

Camacho, C., Coulouris, G., Avagyan, V., Ma, N., Papadopoulos, J., Bealer, K., et al. (2009). BLAST+: architecture and applications. *BMC Bioinform*. 10:421. doi: 10.1186/1471-2105-10-421

Cantalapiedra, C. P., Hernández-Plaza, A., Letunic, I., Bork, P., and Huerta-Cepas, J. (2021). eggNOG-mapper v2: functional annotation, orthology assignments, and domain prediction at the metagenomic scale. *Mol. Biol. Evol*. 2021:msab293. doi: 10.1093/molbev/msab293

Carver, T., Harris, S. R., Berriman, M., Parkhill, J., and McQuillan, J. A. (2011). Artemis: an integrated platform for visualization and analysis of high-throughput sequence-based experimental data. *Bioinformatics* 28, 464–469. doi: 10.1093/bioinformatics/btr703

Ceres, K. M., Stanhope, M. J., and Gröhn, Y. T. (2022). A critical evaluation of *Mycobacterium bovis* pangenomics, with reference to its utility in outbreak investigation. *Microb. Genom*. 8:839. doi: 10.1099/mgen.0.000839

Chen, L., Yang, J., Yu, J., Yao, Z., Sun, L., Shen, Y., et al. (2005). VFDB: a reference database for bacterial virulence factors. *Nucl. Acids Res*. 33, D325–D328. doi: 10.1093/nar/gki008

Cingolani, P., Platts, A., Wang, L. L., Coon, M., Nguyen, T., Wang, L., et al. (2012). A program for annotating and predicting the effects of single nucleotide polymorphisms, SnpEff: SNPs in the genome of *Drosophila melanogaster* strain w(1118) iso-2; iso-3. *Fly* 6, 80–92. doi: 10.4161/fly.19695

Conrad, T. M., Frazier, M., Joyce, A. R., Cho, B. K., Knight, E. M., Lewis, N. E., et al. (2010). RNA polymerase mutants found through adaptive evolution reprogram *Escherichia coli* for optimal growth in minimal media. *Proc. Natl. Acad. Sci. U. S. A*. 107, 20500–20505. doi: 10.1073/pnas.0911253107

Croucher, N. J., Page, A. J., Connor, T. R., Delaney, A. J., Keane, J. A., Bentley, S. D., et al. (2014). Rapid phylogenetic analysis of large samples of recombinant bacterial whole genome sequences using Gubbins. *Nucl. Acids Res*. 43:e15. doi: 10.1093/nar/gku1196

De Coster, W., D'Hert, S., Schultz, D. T., Cruts, M., and Van Broeckhoven, C. (2018). NanoPack: visualizing and processing long-read sequencing data. *Bioinformatics* 34, 2666–2669. doi: 10.1093/bioinformatics/bty149

Dingle, K. E., Blaser, M. J., Tu, Z. C., Pruckler, J., Fitzgerald, C., van Bergen, M. A. P., et al. (2010). Genetic relationships among reptilian and mammalian *Campylobacter fetus* strains determined by multilocus sequence typing. *J. Clin. Microbiol*. 48, 977–980. doi: 10.1128/JCM.01439-09

Dworkin, J., Tummuru, M. K. R., and Blaser, M. J. (1995). Segmental conservation of sapA sequences in type B *Campylobacter fetus* cells. *J. Biol. Chem*. 270, 15093–15101. doi: 10.1074/jbc.270.25.15093

Emele, M. F., Karg, M., Hotzel, H., Bloois, L. G. V., Groß, U., Bader, O., et al. (2019). Differentiation of *Campylobacter fetus* subspecies by proteotyping. *Eur. J. Microbiol. Immunol*. 9, 62–71. doi: 10.1556/1886.2019.00006

Ewels, P., Magnusson, M., Lundin, S., and Käller, M. (2016). MultiQC: summarize analysis results for multiple tools and samples in a single report. *Bioinformatics* 32, 3047–3048. doi: 10.1093/bioinformatics/btw354

Farace, P., Cravero, S., Taibo, C., Diodati, J., Morsella, C., Paolicchi, F., et al. (2022). *Campylobacter fetus* releases S-layered and immunoreactive outer membrane vesicles. *Rev. Argent Microbiol*. 54, 74–80. doi: 10.1016/j.ram.2021.06.001

Farace, P. D., Irazoqui, J. M., Morsella, C. G., García, J. A., Méndez, M. A., Paolicchi, F. A., et al. (2021). Phylogenomic analysis for *Campylobacter fetus* ocurring in Argentina. *Vet. World* 14, 1165–1179. doi: 10.14202/vetworld.2021.1165-1179

Farace, P. D., Morsella, C. G., Cravero, S. L., Sioya, B. A., Amadio, A. F., Paolicchi, F. A., et al. (2019). L-cysteine transporter-PCR to detect hydrogen sulfide-producing *Campylobacter fetus*. *PeerJ* 7:e7820. doi: 10.7717/peerj.7820

Fitzgerald, C., Tu, Z., Patrick, M., Stiles, T., Lawson, A. J., Santovenia, M., et al. (2014). *Campylobacter fetus* subsp. testudinum subsp. nov., isolated from humans and reptiles. *Int. J. Syst. Evol. Microbiol*. 64, 2944–2948. doi: 10.1099/ijs.0.057778-0

Fornelos, N., Browning, D. F., and Butala, M. (2016). The use and abuse of LexA by mobile genetic elements. *Trends Microbiol*. 24, 391–401. doi: 10.1016/j.tim.2016.02.009

Gabrielaite, M., and Marvig, R. L. (2019). GenAPI: a tool for gene absence-presence identification in fragmented bacterial genome sequences. *bioRxiv*. 2019:658476. doi: 10.1101/658476

Gilbert, M. J., Miller, W. G., Yee, E., Zomer, A. L., van der Graaf-van Bloois, L., Fitzgerald, C., et al. (2016). Comparative genomics of *Campylobacter fetus* from reptiles and mammals reveals divergent evolution in host-associated lineages. *Genome Biol. Evol*. 8, 2006–2019. doi: 10.1093/gbe/evw146

Goldstein, S., Beka, L., Graf, J., and Klassen, J. L. (2019). Evaluation of strategies for the assembly of diverse bacterial genomes using MinION long-read sequencing. *BMC Genom*. 20:23. doi: 10.1186/s12864-018-5381-7

Green, A. E., Howarth, D., Chaguza, C., Echlin, H., Langendonk, R. F., Munro, C., et al. (2021). Pneumococcal colonization and virulence factors identified via experimental evolution in infection models. *Mol. Biol. Evol*. 38, 2209–2226. doi: 10.1093/molbev/msab018

Gurevich, A., Saveliev, V., Vyahhi, N., and Tesler, G. (2013). QUAST quality assessment tool for genome assemblies. *Bioinformatics* 29, 1072–1075. doi: 10.1093/bioinformatics/btt086

Hammes, W. P., and Neuhaus, F. C. (1974). On the specificity of phospho-N-acetylmuramyl-pentapeptide translocase. *J. Biol. Chem*. 249, 3140–3150. doi: 10.1016/S0021-9258(19)42649-5

Harvey, S. M., and Greenwood, J. R. (1983). Relationships among catalase-positive *Campylobacters* determined by deoxyribonucleic acid-deoxyribonucleic acid hybridization. *Int. J. Syst. Evol. Microbiol*. 33, 275–284. doi: 10.1099/00207713-33-2-275

Hishinuma, F., Izaki, K., and Takahashi, H. (1969). Effects of glycine and D-amino acids on growth of various microorganisms. *Agric. Biol. Chem*. 33, 1577–1586. doi: 10.1080/00021369.1969.10859511

Hoffer, M. A. (1981). *Bovine campylobacteriosis*: a review. *Can. Vet. J*. 22, 327–330.

Hum, S. (1996). "*Bovine venereal campylobacteriosis*," in *Campylobacters, Helicobacters, and Related Organisms*, eds. D. G. Newell, J. M. Ketley, and R. A. Feldman (Boston, MA: Springer US), 355–358.

Hum, S., Quinn, K., Brunner, J., and On, S. (1997). Evaluation of a PCR assay for identification and differentiation of *Campylobacter fetus* subspecies. *Aust. Vet. J*. 75, 827–831. doi: 10.1111/j.1751-0813.1997.tb15665.x

Hyatt, D., Chen, G. L., Locascio, P. F., Land, M. L., Larimer, F. W., Hauser, L. J., et al. (2010). Prodigal: prokaryotic gene recognition and translation initiation site identification. *BMC Bioinform*. 11:119. doi: 10.1186/1471-2105-11-119

Indjein, L. (2013). *Molecular Diagnostic Protocols for Bovine genital campylobacteriosis Using Comparative Genomics and Virulence Studies* (Ph.D. Thesis). The University of Queensland, St Lucia, QLD, Australia.

Iraola, G., Betancor, L., Calleros, L., Gadea, P., Algorta, G., Galeano, S., et al. (2015). A rural worker infected with a bovine-prevalent genotype of *Campylobacter fetus* subsp. fetus supports zoonotic transmission and inconsistency of MLST and whole-genome typing. *Eur. J. Clin. Microbiol. Infect. Dis*. 34, 1593–1596. doi: 10.1007/s10096-015-2393-y

Iraola, G., Forster, S. C., Kumar, N., Lehours, P., Bekal, S., Garcia-Pena, F. J., et al. (2017). Distinct *Campylobacter fetus* lineages adapted as livestock pathogens and human pathobionts in the intestinal microbiota. *Nat. Commun*. 8:1367. doi: 10.1038/s41467-017-01449-9

Iraola, G., Hernández, M., Calleros, L., Paolicchi, F., Silveyra, S., Velilla, A., et al. (2012). Application of a multiplex PCR assay for *Campylobacter fetus* detection and

subspecies differentiation in uncultured samples of aborted bovine fetuses. *J. Vet. Sci.* 13, 371–376. doi: 10.4142/jvs.2012.13.4.371

Iraola, G., Perez, R., Naya, H., Paolicchi, F., Harris, D., Lawley, T. D., et al. (2013). Complete genome sequence of *Campylobacter fetus* subsp. venerealis biovar intermedius, isolated from the prepuce of a bull. *Genome Announc.* 1, e00526–e00513. doi: 10.1128/genomeA.00526-13

Jain, C., Rodriguez, R. L. M., Phillippy, A. M., Konstantinidis, K. T., and Aluru, S. (2018). High throughput ANI analysis of 90K prokaryotic genomes reveals clear species boundaries. *Nat. Commun.* 9:5114. doi: 10.1038/s41467-018-07641-9

Kienesberger, S., Sprenger, H., Wolfgruber, S., Halwachs, B., Thallinger, G. G., Perez-Perez, G. I., et al. (2014). Comparative genome analysis of *Campylobacter fetus* subspecies revealed horizontally acquired genetic elements important for virulence and niche specificity. *PLoS ONE* 9:e85491. doi: 10.1371/journal.pone.0085491

Kim, S. G., Summage-West, C. V., Sims, L. M., and Foley, S. L. (2021). Complete genome sequence of *Campylobacter fetus* subsp. venerealis P4531 from a Rhesus Monkey. *Microbiol. Resour. Announc.* 10:e0073921. doi: 10.1128/MRA.00739-21

Kimsey, H. H., and Waldor, M. K. (2009). *Vibrio cholerae* LexA coordinates CTX prophage gene expression. *J. Bacteriol.* 191, 6788–6795. doi: 10.1128/JB.00682-09

Kolde, R. (2019). *Pheatmap: Pretty Heatmaps.* R Package Version 1. p. 726.

Kolmogorov, M., Yuan, J., Lin, Y., and Pevzner, P. A. (2019). Assembly of long, error-prone reads using repeat graphs. *Nat. Biotechnol.* 37, 540–546. doi: 10.1038/s41587-019-0072-8

Koya, A. (2016). *Bovine genital campylobacteriosis: Isolation, Identification and Virulence Profiling of Campylobacter fetus subsp. venerealis in a small animal model* (Ph.D. Thesis). The University of Queensland, St Lucia, QLD, Australia.

Kuehne, S. A., Dempster, A. W., Collery, M. M., Joshi, N., Jowett, J., Kelly, M. L., et al. (2018). Characterization of the impact of rpoB mutations on the *in vitro* and *in vivo* competitive fitness of *Clostridium difficile* and susceptibility to fidaxomicin. *J. Antimicrob. Chemother.* 73, 973–980. doi: 10.1093/jac/dkx486

Li, H., Handsaker, B., Wysoker, A., Fennell, T., Ruan, J., Homer, N., et al. (2009). The sequence alignment/map format and SAMtools. *Bioinformatics* 25, 2078–2079. doi: 10.1093/bioinformatics/btp352

Li, X., Tang, H., Xu, Z., Tang, H., Fan, Z., Jiao, X., et al. (2022). Prevalence and characteristics of *Campylobacter* from the genital tract of primates and ruminants in Eastern China. *Transbound. Emerg. Dis.* 69, e1892–e8. doi: 10.1111/tbed.14524

Lindsey-Boltz, L. A., and Sancar, A. (2021). The transcription-repair coupling factor Mfd prevents and promotes mutagenesis in a context-dependent manner. *Front. Mol. Biosci.* 8:668290. doi: 10.3389/fmolb.2021.668290

Linz, B., Windsor, H. M., Gajewski, J. P., Hake, C. M., Drautz, D. I., Schuster, S. C., et al. (2013). *Helicobacter pylori* genomic microevolution during naturally occurring transmission between adults. *PLoS ONE* 8:e82187. doi: 10.1371/journal.pone.0082187

Loman, N. J., Quick, J., and Simpson, J. T. (2015). A complete bacterial genome assembled *de novo* using only nanopore sequencing data. *Nat. Methods* 12, 733–735. doi: 10.1038/nmeth.3444

Lynch, C. T., Buttimer, C., Epping, L., O'Connor, J., Walsh, N., McCarthy, C., et al. (2021). Phenotypic and genetic analyses of two *Campylobacter fetus* isolates from a patient with relapsed prosthetic valve endocarditis. *Pathog Dis.* 79:ftab055. doi: 10.1093/femspd/ftab055

Ma, P., Luo, T., Ge, L., Chen, Z., Wang, X., Zhao, R., et al. (2021). Compensatory effects of *M. tuberculosis* rpoB mutations outside the rifampicin resistance-determining region. *Emerg. Microbes Infect.* 10, 743–752. doi: 10.1080/22221751.2021.1908096

Malmberg, M. M., Spangenberg, G. C., Daetwyler, H. D., and Cogan, N. O. I. (2019). Assessment of low-coverage nanopore long read sequencing for SNP genotyping in doubled haploid canola (*Brassica napus* L.). *Sci. Rep.* 9:8688. doi: 10.1038/s41598-019-45131-0

Marsh, H., and Firehammer, B. D. (1953). Serological relationships of twenty three ovine and three bovine strains of *Vibrio fetus*. *Am. J. Vet. Res.* 14, 396–398.

Matsuo, M., Hishinuma, T., Katayama, Y., and Hiramatsu, K. (2015). A mutation of RNA polymerase β' subunit (RpoC) converts heterogeneously vancomycin-intermediate *Staphylococcus aureus* (hVISA) into "slow VISA". *Antimicrob. Agents Chemother.* 59, 4215–4225. doi: 10.1128/AAC.00135-15

McMillen, L., Fordyce, G., Doogan, V. J., and Lew, A. E. (2006). Comparison of culture and a novel 5′ Taq nuclease assay for direct detection of *Campylobacter fetus* subsp. venerealis in clinical specimens from cattle. *J. Clin. Microbiol.* 44, 938–945. doi: 10.1128/JCM.44.3.938-945.2006

Moolhuijzen, P. M., Lew-Tabor, A. E., Wlodek, B. M., Aguero, F. G., Comerci, D. J., Ugalde, R. A., et al. (2009). Genomic analysis of *Campylobacter fetus* subspecies: identification of candidate virulence determinants and diagnostic assay targets. *BMC Microbiol.* 9:86. doi: 10.1186/1471-2180-9-86

Moran, A. P., O'Malley, D. T., Kosunen, T. U., and Helander, I. M. (1994). Biochemical characterization of *Campylobacter fetus* lipopolysaccharides. *Infect. Immun.* 62, 3922–3929. doi: 10.1128/iai.62.9.3922-3929.1994

Mshelia, G. D., Amin, J. D., Woldehiwet, Z., Murray, R. D., and Egwu, G. O. (2010). Epidemiology of *Bovine venereal campylobacteriosis*: geographic distribution and recent advances in molecular diagnostic techniques. *Reprod. Domest. Anim.* 45, e221–e230. doi: 10.1111/j.1439-0531.2009.01546.x

Mukhtar, L. (2013). *Evaluation of the Genetic Differences Between Two Subtypes of Campylobacter fetus (fetus and venerealis) in Canada* (Ph.D. Thesis). University of Ottawa, Ottawa, ON, Canada.

Nadin-Davis, S. A., Chmara, J., Carrillo, C. D., Amoako, K., Goji, N., Duceppe, M., et al. (2021). A comparison of fourteen fully characterized mammalian-associated *Campylobacter fetus* isolates suggests that loss of defense mechanisms contribute to high genomic plasticity and subspecies evolution. *PeerJ.* 9:e10586. doi: 10.7717/peerj.10586

NCBI Resource Coordinators (2018). Database resources of the National Center for Biotechnology Information. *Nucl. Acids Res.* 46, D8–D13. doi: 10.1093/nar/gkx1095

Nordin, Y. (2013). *Campylobacter fetus subspecies Molecular Typing, Polymerase Chain Reaction (PCR) and High- Resolution Melt (HRM) Analyses for Bovine campylobacteriosis diagnosis* (Honours Thesis). Univerisity of Queensland, St Lucia, QLD, Australia.

OIE (2019). "*Bovine genital campylobacteriosis*," in *Manual of Diagnostic Tests and Vaccines for Terrestrial Animals 2019.* World Organisation For Animal Health OIE, 1031–1044. Available at: https://www.oie.int/en/what-we-do/standards/codes-and-manuals/terrestrial-manual-online-access/ (accessed December 19, 2019).

On, S. L. W., and Harrington, C. S. (2001). Evaluation of numerical analysis of PFGE-DNA profiles for differentiating *Campylobacter fetus* subspecies by comparison with phenotypic, PCR and 16S rDNA sequencing methods. *J. Appl. Microbiol.* 90, 285–293. doi: 10.1046/j.1365-2672.2001.01247.x

Otten, C., Brilli, M., Vollmer, W., Viollier, P. H., and Salje, J. (2018). Peptidoglycan in obligate intracellular bacteria. *Mol. Microbiol.* 107, 142–163. doi: 10.1111/mmi.13880

Page, A. J., Cummins, C. A., Hunt, M., Wong, V. K., Reuter, S., Holden, M. T., et al. (2015). Roary: rapid large-scale prokaryote pan genome analysis. *Bioinformatics* 31, 3691–3693. doi: 10.1093/bioinformatics/btv421

Palau, M., Piqué, N., Ramírez-Lázaro, M. J., Lario, S., Calvet, X., Miñana-Galbis, D., et al. (2021). Whole-genome sequencing and comparative genomics of three *Helicobacter pylori* strains isolated from the stomach of a patient with Adenocarcinoma. *Pathogens* 10:331. doi: 10.3390/pathogens10030331

Paradis, E., and Schliep, K. (2018). ape 5.0: an environment for modern phylogenetics and evolutionary analyses in R. *Bioinformatics* 35, 526–528. doi: 10.1093/bioinformatics/bty633

Penner, J. L. (1988). The genus *Campylobacter*: a decade of progress. *Clin. Microbiol. Rev.* 1, 157–172. doi: 10.1128/CMR.1.2.157

Perez-Perez, G. I., Blaser, M. J., and Bryner, J. H. (1986). Lipopolysaccharide structures of *Campylobacter fetus* are related to heat-stable serogroups. *Infect. Immun.* 51, 209–212. doi: 10.1128/iai.51.1.209-212.1986

Quinones, M., Kimsey, H. H., and Waldor, M. K. (2005). LexA cleavage is required for CTX prophage induction. *Mol. Cell* 17, 291–300. doi: 10.1016/j.molcel.2004.11.046

R Core Team (2018). *R: a Language and Environment for Statistical Computing.* Available at: https://www.R-project.org/ (accessed June 7, 2020).

Ragheb, M. N., Thomason, M. K., Hsu, C., Nugent, P., Gage, J., Samadpour, A. N., et al. (2019). Inhibiting the evolution of antibiotic resistance. *Mol. Cell* 73, 157–165.e5. doi: 10.1016/j.molcel.2018.10.015

Ribeiro, A., Golicz, A., Hackett, C. A., Milne, I., Stephen, G., Marshall, D., et al. (2015). An investigation of causes of false positive single nucleotide polymorphisms using simulated reads from a small eukaryote genome. *BMC Bioinform.* 16:382. doi: 10.1186/s12859-015-0801-z

Ruan, J., and Li, H. (2020). Fast and accurate long-read assembly with wtdbg2. *Nat. Methods* 17, 155–158. doi: 10.1038/s41592-019-0669-3

Sebald, M., and Veron, M. (1963). Base DNA content and classification of *Vibrios*. *Ann. Inst. Pasteur.* 105, 897–910.

Seemann, T. (2014). Prokka: rapid prokaryotic genome annotation. *Bioinformatics* 30, 2068–2069. doi: 10.1093/bioinformatics/btu153

Seemann, T. (2016). *ABRicate: Mass Screening of Contigs for Antibiotic Resistance Genes.* Available at: https://github.com/tseemann/abricate (accessed August 31, 2020).

Silva, M. F., Pereira, A. L., Fraqueza, M. J., Pereira, G., Mateus, L., Lopes-da-Costa, L., et al. (2021). Genomic and phenotypic characterization of *Campylobacter fetus* subsp. venerealis strains. *Microorganisms* 9:340. doi: 10.3390/microorganisms9020340

Smibert, R. M. (1978). The genus *Campylobacter*. *Annu. Rev. Microbiol.* 32, 673–709. doi: 10.1146/annurev.mi.32.100178.003325

Smibert, R. M. (1981). "The genus *Campylobacter*," in *The Prokaryotes: A Handbook on Habitats, Isolation, and Identification of Bacteria*, eds. M. P. Starr, H. Stolp, H. G. Trüper, A. Balows, and H. G. Schlegel (Berlin; Heidelberg: Springer Berlin Heidelberg), 609–617.

Smith, T., and Taylor, M. S. (1919). Some morphological and biological characters of the spirilla (*Vibrio fetus*, n. sp.) associated with disease of the fetal membranes in cattle. *J. Exp. Med.* 30, 299–311. doi: 10.1084/jem.30.4.299

Spence, R. P., Bruce, I. R., McFadden, A. M. J., Hill, F. I., Tisdall, D., Humphrey, S., et al. (2011). Cross-reaction of a *Campylobacter fetus* subspecies venerealis real-time PCR. *Vet. Rec.* 168:131. doi: 10.1136/vr.c5264

Sprenger, H., Zechner, E. L., and Gorkiewicz, G. (2012). So close and yet so far—molecular microbiology of *Campylobacter fetus* subspecies. *Eur. J. Microbiol. Immunol.* 2, 66–75. doi: 10.1556/EuJMI.2.2012.1.10

Strick, T. R., and Portman, J. R. (2019). Transcription-coupled repair: from cells to single molecules and back again. *J. Mol. Biol.* 431, 4093–4102. doi: 10.1016/j.jmb.2019.05.040

Struve, W. G., Sinha, R. K., Neuhaus, F. C., and Prime, M. S. (1966). On the initial stage in peptidoglycan synthesis. Phospho-N-acetylmuramyl-pentapeptide translocase (*Uridine monophosphate*). *Biochemistry* 5, 82–93. doi: 10.1021/bi00865a012

Szklarczyk, D., Gable, A. L., Lyon, D., Junge, A., Wyder, S., Huerta-Cepas, J., et al. (2019). STRING v11: protein-protein association networks with increased coverage, supporting functional discovery in genome-wide experimental datasets. *Nucl. Acids Res.* 47, D607–D613. doi: 10.1093/nar/gky1131

Tange, O. (2011). GNU parallel—the command-line power tool. *USENIX Mag.* 36, 42–47. Available at: https://www.usenix.org/publications/login/february-2011-volume-36-number-1/gnu-parallel-command-line-power-tool

Tatusova, T., DiCuccio, M., Badretdin, A., Chetvernin, V., Nawrocki, E. P., Zaslavsky, L., et al. (2016). NCBI prokaryotic genome annotation pipeline. *Nucl. Acids Res.* 44, 6614–6624. doi: 10.1093/nar/gkw569

Treangen, T. J., Ondov, B. D., Koren, S., and Phillippy, A. M. (2014). The Harvest Suite for rapid core-genome alignment and visualization of thousands of intraspecific microbial genomes. *Genome Biol.* 15:524. doi: 10.1186/s13059-014-0524-x

Tshipamba, M. E., Akinola, S. A., Ngoma, L., and Mwanza, M. (2020a). Genome sequence of *Campylobacter fetus* subsp. venerealis NW_ED23, isolated from bovine sheath wash. *Microbiol. Resour. Announc.* 9:20. doi: 10.1128/MRA.00854-20

Tshipamba, M. E., Lubanza, N., and Mwanza, M. (2020b). Genome analysis of antimicrobial resistance genes and virulence factors in multidrug-resistant *Campylobacter fetus* subspecies isolated from sheath wash. *World's Vet. J.* 10, 465–480. doi: 10.54203/scil.2020.wvj57

Tu, Z. C., Dewhirst, F. E., and Blaser, M. J. (2001). Evidence that the *Campylobacter fetus* sap locus is an ancient genomic constituent with origins before mammals and reptiles diverged. *Infect. Immun.* 69, 2237–2244. doi: 10.1128/IAI.69.4.2237-2244.2001

Tu, Z. C., Zeitlin, G., Gagner, J. P., Keo, T., Hanna, B. A., Blaser, M. J., et al. (2004). *Campylobacter fetus* of reptile origin as a human pathogen. *J. Clin. Microbiol.* 42, 4405–4407. doi: 10.1128/JCM.42.9.4405-4407.2004

Turni, C., Singh, R., and Blackall, P. J. (2018). Virulence-associated gene profiling, DNA fingerprinting and multilocus sequence typing of *Haemophilus parasuis* isolates in Australia. *Aust. Vet. J.* 96, 196–202. doi: 10.1111/avj.12705

van Bergen, M. A., Dingle, K. E., Maiden, M. C., Newell, D. G., van der Graaf-Van Bloois, L., van Putten, J. P., et al. (2005b). Clonal nature of *Campylobacter fetus* as defined by multilocus sequence typing. *J. Clin. Microbiol.* 43, 5888–5898. doi: 10.1128/JCM.43.12.5888-5898.2005

van Bergen, M. A., Simons, G., Graaf-van Bloois, L., van Putten, J. P., Rombout, J., Wesley, I., et al. (2005a). Amplified fragment length polymorphism based identification of genetic markers and novel PCR assay for differentiation of *Campylobacter fetus* subspecies. *J. Med. Microbiol.* 54, 1217–1224. doi: 10.1099/jmm.0.46186-0

van der Graaf-van Bloois, L., Duim, B., Miller, W. G., Forbes, K. J., Wagenaar, J. A., and Zomer, A. (2016a). Whole genome sequence analysis indicates recent diversification of mammal-associated *Campylobacter fetus* and implicates a genetic factor associated with H2S production. *BMC Genom.* 17:713. doi: 10.1186/s12864-016-3058-7

van der Graaf-van Bloois, L., Miller, W. G., Yee, E., Gorkiewicz, G., Forbes, K. J., Zomer, A. L., et al. (2016b). *Campylobacter fetus* subspecies contain conserved type IV secretion systems on multiple genomic islands and plasmids. *PLoS ONE* 11:e0152832. doi: 10.1371/journal.pone.0152832

van der Graaf-van Bloois, L., Miller, W. G., Yee, E., Rijnsburger, M., Wagenaar, J. A., and Duim, B. (2014). Inconsistency of phenotypic and genomic characteristics of *Campylobacter fetus* subspecies requires reevaluation of current diagnostics. *J. Clin. Microbiol.* 52, 4183–4188. doi: 10.1128/JCM.01837-14

Vandamme, P., Pot, B., Falsen, E., Kersters, K., and De Ley, J. (1990). Intra- and interspecific relationships of veterinary *Campylobacters* revealed by numerical analysis of electrophoretic protein profiles and DNA:DNA hybridizations. *Syst. Appl. Microbiol.* 13, 295–303. doi: 10.1016/S0723-2020(11)80201-8

Vaser, R., and Šikić, M. (2021). Raven: a *de novo* genome assembler for long reads. *bioRxiv*. 2021:242461. doi: 10.1101/2020.08.07.242461

Vaser, R., Sović, I., Nagarajan, N., and Šikić, M. (2017). Fast and accurate *de novo* genome assembly from long uncorrected reads. *Genome Res.* 27, 737–746. doi: 10.1101/gr.214270.116

Wagenaar, J. A., van Bergen, M. A. P., Newell, D. G., Grogono-Thomas, R., and Duim, B. (2001). Comparative study using amplified fragment length polymorphism fingerprinting, PCR genotyping, and phenotyping to differentiate *Campylobacter fetus* strains isolated from animals. *J. Clin. Microbiol.* 39:2283. doi: 10.1128/JCM.39.6.2283-2286.2001

Walker, B. J., Abeel, T., Shea, T., Priest, M., Abouelliel, A., Sakthikumar, S., et al. (2014). Pilon: an integrated tool for comprehensive microbial variant detection and genome assembly improvement. *PLoS ONE* 9:e112963. doi: 10.1371/journal.pone.0112963

Wang, G., Clark, C. G., Taylor, T. M., Pucknell, C., Barton, C., Price, L., et al. (2002). Colony multiplex PCR assay for identification and differentiation of *Campylobacter jejuni*, *C. coli*, *C. lari*, *C. upsaliensis*, and *C. fetus* subsp. fetus. *J. Clin. Microbiol.* 40, 4744–4747. doi: 10.1128/JCM.40.12.4744-4747.2002

Wang, Z., Lu, T., Li, M., Ding, N., Lan, L., Gao, X., et al. (2022). Genetic and epigenetic signatures associated with the divergence of *Aquilegia* species. *Genes* 13:793. doi: 10.3390/genes13050793

Wei, T. V. S. (2021). *R Package "corrplot": Visualization of a Correlation Matrix.0.91*. Available at: https://github.com/taiyun/corrplot (accessed July 22, 2022).

Wick, R. R., Judd, L. M., Gorrie, C. L., and Holt, K. E. (2017a). Completing bacterial genome assemblies with multiplex MinION sequencing. *Microb. Genom.* 3:e000132. doi: 10.1099/mgen.0.000132

Wick, R. R., Judd, L. M., Gorrie, C. L., and Holt, K. E. (2017b). Unicycler: resolving bacterial genome assemblies from short and long sequencing reads. *PLoS Comput. Biol.* 13:e1005595. doi: 10.1371/journal.pcbi.1005595

Wickham, H. (2016). *ggplot2: Elegant Graphics for Data Analysis*. Available at: https://ggplot2.tidyverse.org (accessed June 30, 2020).

Willoughby, K., Nettleton, P. F., Quirie, M., Maley, M. A., Foster, G., Toszeghy, M., et al. (2005). A multiplex polymerase chain reaction to detect and differentiate *Campylobacter fetus* subspecies fetus and *Campylobacter fetus* subspecies venerealis: use on UK isolates of *C. fetus* and other *Campylobacter* spp. *J. Appl. Microbiol.* 99, 758–766. doi: 10.1111/j.1365-2672.2005.02680.x

Zakharova, N., Hoffman, P. S., Berg, D. E., and Severinov, K. (1998). The largest subunits of RNA polymerase from gastric helicobacters are tethered. *J. Biol. Chem.* 273, 19371–19374. doi: 10.1074/jbc.273.31.19371

frontiers | Frontiers in Microbiology

TYPE Original Research
PUBLISHED 25 October 2024
DOI 10.3389/fmicb.2024.1488114

OPEN ACCESS

EDITED BY
Ozan Gundogdu,
University of London, United Kingdom

REVIEWED BY
Andreas Erich Zautner,
University Hospital Magdeburg, Germany
Bassam A. Elgamoudi,
Griffith University, Australia

*CORRESPONDENCE
Anja Klančnik
✉ anja.klancnik@bf.uni-lj.si

RECEIVED 29 August 2024
ACCEPTED 07 October 2024
PUBLISHED 25 October 2024

CITATION
Pavlinjek N, Klančnik A and Sabotič J (2024) Evaluation of physical and chemical isolation methods to extract and purify *Campylobacter jejuni* extracellular polymeric substances. *Front. Microbiol.* 15:1488114. doi: 10.3389/fmicb.2024.1488114

Evaluation of physical and chemical isolation methods to extract and purify *Campylobacter jejuni* extracellular polymeric substances

Natalija Pavlinjek[1,2], Anja Klančnik[1]* and Jerica Sabotič[2]

[1]Department of Food Science and Technology, Biotechnical Faculty, University of Ljubljana, Ljubljana, Slovenia, [2]Department of Biotechnology, Jožef Stefan Institute, Ljubljana, Slovenia

The pathogenic bacterium *Campylobacter jejuni* is a major food safety concern as it can form biofilms that increase its survival and infective potential. Biofilms consist of microbial cells and extracellular matrix (ECM), which is made of water and extracellular polymeric substances (EPS), which are critical for structural integrity and pathogenicity. The aim of this study was to optimize a protocol for the isolation of *C. jejuni* ECM. We employed eight physical and chemical isolation methods to extract and purify ECM, followed by different qualitative and quantitative analyses using gel electrophoresis and spectroscopy. This comprehensive approach enabled the evaluation of ECM composition in terms of polysaccharides, proteins, and extracellular DNA. The isolation methods resulted in different yields and purities of the extracted ECM components. Centrifugation in combination with chemical treatments proved to be most effective, isolating higher concentrations of polysaccharides and proteins. Additionally, extraction with ether solution facilitated the recovery of high-molecular-weight extracellular DNA. Overall, we provide a refined methodology for ECM extraction from *C. jejuni*. As polysaccharides and proteins participate in biofilm stability and microbial communication, and extracellular DNA participates in genetic exchange and virulence, our study contributes towards a better understanding of the persistence of this pathogen in the food industry.

KEYWORDS

***Campylobacter jejuni*, biofilm, extracellular polymeric substances, isolation methods, extraction and purification**

1 Introduction

The Gram-negative bacterium *Campylobacter jejuni* is found in the intestines of many wild and domestic animals, making them potential asymptomatic carriers or zoonotic transmission (Blaser, 1997; Snelling et al., 2005; Burnham and Hendrixson, 2018). It is one of the main causes of bacterial foodborne gastroenteritis worldwide and the most common cause of foodborne zoonotic infections (EFSA and ECDC, 2023). Infections in humans usually occur through the ingestion of contaminated food of animal origin or untreated water or direct contact with infected animals, particularly pets. However, most human cases are associated with the consumption of contaminated poultry (Blaser, 1997; Sheppard and Maiden, 2015). *C. jejuni* has an optimal growth temperature of around 42°C, which facilitates its colonization in chicken intestine and makes poultry an important vector for its transmission into the human food chain (Snelling et al., 2005; Levin, 2007; Sheppard and Maiden, 2015; Burnham and Hendrixson, 2018).

Contrary to previous assumptions that *C. jejuni* cannot survive outside hosts in aerobic natural environments or in the food chain (Solomon and Hoover, 1999; Klančnik et al., 2013, 2014; Giaouris et al., 2015), it now shows a wide distribution in the environment and has been detected in food, water, and microbial biofilms on microplastics from seawater (Good et al., 2019; Tram et al., 2020; Kolenc et al., 2024). Recent studies have further elucidated its pathogenesis, persistence, and resilience and have linked these properties to genomic polymorphism, limited catabolic capacity, abnormalities in gene regulation, and a protective biofilm matrix that shields it from environmental stressors (Klančnik et al., 2021; Sabotič et al., 2023).

The formation of biofilms is an important survival strategy for *C. jejuni*, providing protection against environmental stress and increasing its infectivity. These biofilms comprise dynamic microbial communities that form on both abiotic and biotic surfaces and are driven by multiple cellular interactions and complex adhesion mechanisms. Biofilms can rapidly (within 48 h) develop into dense structures with strong adhesion and structural complexity and are thus difficult to treat (Sabotič et al., 2023; Joshua et al., 2006; Teh et al., 2010; Reuter et al., 2010; Püning et al., 2021; Ramić et al., 2023; Ma et al., 2022; Carpentier and Cerf, 1993; Sulaeman et al., 2012; Kemper and Hensel, 2023).

Biofilms are complex assemblies of microorganisms embedded in an extracellular matrix (ECM) of water and extracellular polymeric substances (EPS; Aguilera et al., 2008). EPS are crucial for the formation, architecture, and functionality of biofilms and account for 50–90% of biofilm mass. They include polysaccharides, proteins, lipids, and extracellular DNA (eDNA) at different concentrations, depending on environmental conditions and nutrient availability (Donlan, 2002; Vu et al., 2009; Flemming et al., 2016; Karygianni et al., 2020; Flemming et al., 2023).

ECM plays a crucial role in improving the resistance of *C. jejuni* biofilms to environmental stress. It forms a protective barrier around cells that not only protects against physical disturbances, antimicrobial agents, bacteriophages, and biocides but also contributes to the mechanical strength and stability of the biofilm. This barrier increases the antimicrobial resistance of the biofilm by hindering the diffusion of antibiotics and complicating the treatment of associated infections by promoting the intercellular exchange of resistance genes (Donlan, 2002; Karygianni et al., 2020; Flemming et al., 2016). The bacterial ECM also significantly affects the heterogeneity of biofilms by influencing porosity, density, and water content, thereby improving the adaptability of biofilms to different environmental conditions. In addition, bacterial ECM promotes unique microenvironments by enriching biofilms with nutrients and supporting vital functions, such as resource acquisition, hydration, and external digestion, all of which are important for cell survival, metabolic activity, and intercellular interactions. The bacterial ECM contains environmental materials, such as dissolved nutrients, humic substances, and exopolymer particles, which are crucial for cellular metabolism and the structural integrity of the biofilm. Furthermore, most bacterial ECM consist of neutral or polyanionic polysaccharides, which are crucial for the attraction of divalent cations such as calcium and magnesium. These cations bind to bacterial ECM polymers and form hydrogen bonds that stabilize biofilm structure, provide structural cohesion, and protect the biofilm from desiccation (Donlan, 2002). Environmental factors, such as temperature, pH, nutrient availability, and stress, influence bacterial regulatory pathways and lead to increased bacterial ECM production and modifications (Moorhead and Griffiths, 2011; Lu et al., 2012; Feng et al., 2016). Components of ECM, such as eDNA, can be degraded by enzymes or external factors, leading to the dissolution of biofilms and potential bacterial proliferation (Brown et al., 2015; Flemming et al., 2016; Karygianni et al., 2020). This degradation underlines the dynamic nature of biofilms and their susceptibility to environmental influences.

ECM is also central to the formation and maintenance of *C. jejuni* biofilms, thereby increasing biofilm resistance and facilitating *C. jejuni* spread. In *C. jejuni*, ECM plays a complex role in biofilms and are thus important for microbial ecology, pathogenesis, and treatment resistance (Table 1). Different methods have been used to study ECM characteristics, composition and function (Table 2). Crystal violet staining was usually used to quantify biofilms, which is essential for the estimation of ECM content (Feng et al., 2016; Oh et al., 2018). Fluorescence microscopy was used for ECM visualization, with methods such as high-content screening with TAMRA and SytoX fluorescent markers providing quantitative insights into the integrity and composition of ECM (Oh et al., 2018; Whelan et al., 2021).

The techniques used to characterize ECM components range from microscopic methods such as confocal microscopy and scanning electron microscopy to spectroscopic methods such as Raman spectroscopy and Fourier transform infrared spectroscopy, which help determine the biochemical composition of ECM in detail (Moorhead and Griffiths, 2011; Feng et al., 2016; Melo et al., 2017). In addition, high-performance anion exchange chromatography and nuclear magnetic resonance provide more precise details about the molecular structure of ECM components (Jowiya et al., 2015). Moreover, molecular techniques and genetic analyses link ECM components to their functional roles (Melo et al., 2017; Yu et al., 2020). Quantitative PCR with SYBR Green I and specific primers is used to investigate specific components (e.g., eDNA), also in combination with confocal microscopy (Feng et al., 2018). DNase-I is used to investigate the roles of flagella-mediated adhesion and eDNA in biofilm formation and maturation (Svensson et al., 2014; Feng et al., 2018; Brown et al., 2015). Fluorescence lectin binding analysis is used to characterize glycoconjugates in ECM, providing insights into the complex interactions within biofilms (Turonova et al., 2016).

The aim of this study was to optimize a protocol that isolates the ECM of *C. jejuni* and to evaluate its composition. We investigated different physical and chemical methods for isolating essential ECM components, such as polysaccharides, proteins, and eDNA, to determine the most effective techniques to extract these molecules at high concentrations.

2 Materials and methods

2.1 Growth conditions

Cultures of *C. jejuni* ATCC 11168 were stored at −80°Cin 20% glycerol (Kemika, Croatia) and 80% Mueller Hinton broth (MHB, Oxoid, UK). *C. jejuni* was incubated on Karmali agar (Oxoid, UK) supplemented with *Campylobacter*-selective Karmali supplement (Oxoid, UK) for 24 h under microaerobic conditions (5% O_2, 10%

TABLE 1 The roles of extracellular polymeric substances (EPS) in *Campylobacter jejuni* biofilms. eDNA: extracellular DNA.

Role of EPS	Key findings	Bacteria studied	Study
EPS is crucial for the integrity and protection of biofilms. The EPS matrix mediates cell-to-cell communication and protects microorganisms against environmental stress.	Diallyl sulphide exerts strong antimicrobial activity against sessile *C. jejuni* cells by disrupting the EPS structure of biofilms.	*C. jejuni*	Lu et al. (2012)
EPS provides structural support and protection against aerobic stress.	Dual-species *C. jejuni* biofilms show enhanced survival under aerobic stress, attributed to higher amounts of and more diverse chemical compositions of EPS compared to mono-species biofilms. EPS contributes to the structural integrity, water retention, and resistance to desiccation of biofilms, thereby protecting *C. jejuni*.	*C. jejuni*, *Staphylococcus aureus*, *Salmonella enterica*, and *Pseudomonas aeruginosa*	Feng et al. (2016)
Iron supplementation increased biofilm formation by stimulating the production of eDNA and EPS.	EPS production was stimulated by iron, which contributed to the formation of biofilm matrices encasing *C. jejuni* and possibly helped decrease exposure to oxygen and other stress conditions.	*C. jejuni*	Oh et al. (2018)
EPS support the structural stability and improve substrate exchange and nutrient circulation in biofilms.	Cinnamaldehyde was effective in inhibiting and degrading *Campylobacter* biofilms, influencing auto-aggregation, motility, and EPS production.	*C. jejuni* and *C. coli*	Yu et al. (2020)
Exposure to pancreatic amylase results in secretion of α-dextran, a component of biofilm EPS, enhancing biofilm formation.	Exposure to pancreatic amylase results in secretion of α-dextran, a component of biofilm exopolymeric matrix, enhancing biofilm formation.	*C. jejuni*	Jowiya et al. (2015)
EPS provide a protective matrix for biofilms but is penetrable by ZnO nanoparticles.	ZnO nanoparticles penetrate EPS and cause cell death without damaging EPS structure. The inactivation mechanism involves alterations in quinone structures and DNA damage likely due to reactive oxygen species generated by the ZnO nanoparticles.	*C. jejuni*	Lu et al. (2012)
Autoinducer-2 might influence EPS composition, as it affects biofilm density and viability.	Autoinducer-2 affected the expression of virulence genes, which could be related to changes in EPS composition and function.	*C. jejuni*	Moorhead and Griffiths (2011)
eDNA is a major component of *C. jejuni* biofilms. eDNA facilitates the initial attachment, establishment, and maintenance of biofilms and bacterial allocation.	Environmental stress induces bacterial lysis, which leads to the release of eDNA and formation of *C. jejuni* biofilms.	*C. jejuni*	Feng et al. (2018)
eDNA is required for the maturation and three-dimensional development of biofilms. It is not involved in initial adhesion but is released following flagella-mediated bacterial attachment.	DNase treatment degrades eDNA and thereby disrupts biofilms, which highlights the role of eDNA in biofilm integrity and stress tolerance.	*C. jejuni*	Svensson et al. (2014)
eDNA is an essential component of *C. jejuni* biofilms when attached to stainless steel surfaces. It provides hydration, traps nutrients, and reduces access to antimicrobials. Biofilms allow genetic transfer of antibiotic resistance, which might occur through natural transformation facilitated by eDNA within the biofilm.	eDNA is present in *C. jejuni* biofilms under both aerobic and microaerobic conditions and contributes to biofilm formation and structure.	*C. jejuni*	Brown et al. (2015)

CO_2, and 85% N_2; Thermo Scientific Oxoid CampyGen atmosphere, USA) in anaerobic jar (3.5 L, Oxoid, UK) in incubator (Kambič, Slovenia) at 42°C. The pure culture was transferred to Mueller Hinton agar (MHA, Oxoid, UK) and incubated under the same conditions overnight.

2.2 ECM isolation

Eight different methods were used to isolate the ECM, all of which were preceded by the same step. *C. jejuni* biomass was scraped off four plates using a sterile disposable cotton swab and added to

TABLE 2 The methods used in studies of *Campylobacter jejuni* extracellular polymeric substances (EPS).

Method category	Techniques	Purpose	Common applications	Study
Extraction and purification	Centrifugation and ethanol precipitation	To isolate EPS and purify it from other biofilm components.	Purification of cells and other biofilm components from biofilm.	Yu et al. (2020)
Extraction and purification	Cold acetone precipitation	To isolate and purify EPS from biofilms.	Isolation of EPS from bacterial cultures.	Jowiya et al. (2015)
Biofilm quantification	Crystal violet staining	To quantify biofilm biomass, indicating the potential quantity of EPS within biofilms.	Standard method for biofilm biomass determination.	Feng et al. (2016), Oh et al. (2018)
EPS analysis	High-content screening with TAMRA and SytoX fluorescent markers	To quantitatively assess the integrity and composition of EPS in adherent *C. jejuni* biofilms under aerobic conditions.	Analysis of homogeneity and consistency of biofilm formation.	Whelan et al. (2021)
EPS analysis	Confocal microscopy and staining	To study the production and effects of cell-signaling compounds on EPS characteristics and biofilm formation.	Determination of the molecular composition of biofilms.	Moorhead and Griffiths (2011)
Component characterization	Raman spectroscopy in combination with confocal laser scanning microscopy	To determine the chemical composition of EPS.	Imaging and molecular analysis of biofilm structure and EPS matrices.	Feng et al. (2016)
Component characterization	Scanning electron microscopy	To visualize biofilm architecture and provide insights into the EPS matrix within the biofilm.	Morphological analysis of biofilms and their EPS matrix.	Melo et al. (2017)
Component characterization	Phenol-sulfuric acid assay	To quantify total carbohydrates in EPS.	Quantification of polysaccharide content in EPS.	Jowiya et al. (2015)
Component characterization	Fourier transform infrared spectroscopy, Raman spectroscopy, scanning electron microscopy	To characterize the biochemical composition and structural integrity of EPS after ZnO nanoparticle treatment and observe interactions between nanoparticles, EPS, and cells in biofilm.	Studying the impact of nanoparticles on biofilms, bacterial cells, and EPS.	Lu et al. (2012)
Component characterization and structure determination	Fluorescence lectin-binding analysis	To characterize glycoconjugates in the EPS matrix.	Visualization and analysis of EPS components in *C. jejuni* biofilms.	Turonova et al. (2016)
Detailed characterization of components	Nuclear magnetic resonance	To characterize the molecular structure of EPS.	Characterization of the molecular structure of EPS.	Jowiya et al. (2015)
Biofilm matrix composition	Fluorescence microscopy	To analyze the presence of eDNA and EPS within the biofilm matrix.	Visualization of biofilm structure and EPS components.	Oh et al. (2018)
Biofilm matrix composition	Stability test with proteinase K and sodium metaperiodate and crystal violet staining	To assess the structural roles of proteins and carbohydrates in the biofilm EPS matrix and to quantify the remaining biofilm biomass after stability tests.	Evaluation of biofilm resistance to enzymatic degradation of EPS. Measurements of biofilm mass and the presence of EPS.	Melo et al. (2017)
Monosaccharide composition analysis	High-performance anion-exchange chromatography	Monosaccharide analysis of EPS.	Glycan composition analysis of EPS.	Jowiya et al. (2015)
Molecular techniques	SDS-PAGE	To analyze the protein profile of EPS components.	Analysis of the protein profile of EPS components.	Yu et al. (2020)
Genetic analysis	Pulsed-field gel electrophoresis	To understand genetic diversity that affects EPS composition and biofilm formation.	Genetic typing of bacterial strains in biofilm studies.	Melo et al. (2017)

1.5 ml microcentrifuge tubes containing 1 ml of phosphate-buffered saline (PBS; 10 mM Na_2HPO_4, 1.8 mM KH_2PO_4, 137 mM NaCl, and 2.7 mM KCl, pH 7.4). Suspension was centrifuged at 12,000 × *g* for 3 min at 4°C. The supernatant with weakly bound ECM components (named as method SV) was then removed using an automated pipette, filtered through a 0.2 µm pore size membrane (Whatman, UK), and stored at −20°C until further use. The obtained biomass pellet was used for the eight isolation methods (named A–H) described below. The isolated ECM was stored at −20°C until further use.

2.2.1 Isolation with weakly bound ECM (named as method SV)

The supernatant containing weakly bound ECM components was obtained after centrifugation of the resuspended *C. jeuni* biomass at 12,000 × *g* for 3 min at 4°C. It was removed using an automated pipette, filtered through a 0.2 µm pore size membrane (Whatman, UK), and stored at −20°C until further use.

2.2.2 Isolation with NaCl (named as method A)

The pellet was resuspended in 1 ml of 1.5 M NaCl (KEFO 7647-14-5) solution by vortexing. This suspension was centrifuged at 5,000 × *g* for 10 min at 25°C, and the supernatant, containing the isolated ECM, was filtered through a 0.2 µm pore size membrane (Whatman, UK; Chiba et al., 2015).

2.2.3 Isolation by centrifugation (named as method B)

The pellet was resuspended in 1 ml of PBS (10 mM Na_2HPO_4, 1.8 mM KH_2PO_4, 137 mM NaCl, and 2.7 mM KCl, pH 7.4) by vortexing. This suspension was centrifuged at 20,000 × *g* for 20 min at 4°C, and the supernatant, containing the isolated ECM, was filtered through a 0.2 µm pore size membrane (Whatman, UK; Liu and Fang, 2002).

2.2.4 Isolation by heating in Na_2CO_3 (named as method C)

The pellet was resuspended in 1 ml of PBS by vortexing, and this suspension was transferred into a new 1.5 ml microcentrifuge tube with 5 mg of Na_2CO_3 (Honeywell Fluka 31432). The solution was then incubated for 35 min in a ThermoShaker thermoblock at 80°C with simultaneous stirring at 400 rpm and then cooled at room temperature and centrifuged at 12,000 × *g* for 20 min at 4°C (Felz et al., 2016). The supernatant, containing the isolated ECM, was filtered through a 0.2 µm pore size membrane (Whatman, UK).

2.2.5 Isolation with ethylenediaminetetraacetic acid (EDTA; named as method D)

The pellet was resuspended in 1 ml of PBS by vortexing, and the suspension was divided into two 2 ml microcentrifuge tubes for further steps, to each of which 500 µl of 2% EDTA (Serva 11280.02) was added to give a final EDTA concentration of 1%. This was followed by incubation with agitation on an orbital shaker for 3 h at 4°C and then centrifugation at 12,000 × *g* for 20 min at 4°C (Jachlewski et al., 2015). The supernatant, containing the isolated ECM, was filtered through a 0.2 µm pore size membrane (Whatman, UK).

2.2.6 Isolation with NaOH (named as method E)

The pellet was resuspended in 1 ml of PBS by vortexing, and 0.4 g of NaOH (Fisher 1310-73-2) was added. This was followed by incubation with agitation on an orbital shaker for 3 h at 4°C and centrifugation at 20,000 × *g* for 20 min at 4°C (Jachlewski et al., 2015). The supernatant, containing the isolated ECM, was filtered through a 0.2 µm pore size membrane (Whatman, UK).

2.2.7 Isolation with formaldehyde and NaOH (named as method F)

The pellet was resuspended in 1 ml of PBS by vortexing, and 6 µl of 37% formaldehyde (Sigma-Aldrich 1.04003.1000, Merck, Germany) was added. This was followed by incubation with agitation on an orbital shaker for 1 h at 4°C. Next, 0.4 ml of 1 M NaOH was added, followed by incubation with agitation on an orbital shaker for 3 h at 4°C and centrifugation at 20,000 × *g* for 20 min at 4°C (Liu and Fang, 2002). The supernatant, containing the isolated ECM, was filtered through a 0.2 µm pore size membrane (Whatman, UK).

2.2.8 Isolation with a Dowex cation exchange resin (named as method G)

First, the extraction buffer and Dowex cation exchange resin were prepared. The extraction buffer contained 17.8 mg of $Na_2HPO_4 \cdot 2H_2O$ (Serva 30200.01), 27.5 mg of $NaH_2PO_4 \cdot H_2O$ (Serva 30186), 26 mg of NaCl (KEFO 7647-14-5), 3.7 mg of KCl (Serva 26868.02), and 50 ml of distilled water. The Dowex cation exchanger was prepared by adding 1 g of Dowex cation exchange resin (Supelco 44514, Merck, Germany) to 10 ml of extraction buffer, mixing well with an automatic pipette, and incubating for 15 min. The extraction buffer was then removed using an automated pipette, and the washing procedure repeated. The extraction buffer was then removed again using an automated pipette, and 10 ml of extraction buffer was added. The prepared cation exchanger was stored at 4°C until use.

The pellet was resuspended in 1 ml of PBS by vortexing, and the suspension was divided into two 2 ml microcentrifuge tubes, to each of which 1 ml of Dowex cation exchanger was added. This was followed by incubation with agitation on an orbital shaker for 3 h at 4°C and centrifugation at 12,000 × *g* for 10 min at 4°C (Frølund et al., 1996). The supernatant, containing the isolated ECM, was filtered through a 0.2 µm pore size membrane (Whatman, UK).

2.2.9 Isolation with ether solution (named as method H)

First, 10 ml of 30 mM ether solution was prepared from 112 mg of dicyclohexano-18-crown-6 (Sigma-Aldrich 158402, Merck, Germany) and 50 mM Tris–HCl, pH 8 (Tris, Serva 37180.04; HCl, VWR Chemicals BDH 20252.290).

The pellet was resuspended in 1 ml of PBS by vortexing, and the suspension was divided into two 2 ml microcentrifuge tubes, to each of which 500 µl of 30 mM ether solution was added. This was followed by incubation with agitation on an orbital shaker for 3 h at 4°C and then centrifugation at 16,000 × *g* for 20 min at 4°C (Jachlewski et al., 2015). The supernatant, containing the isolated ECM, was filtered through a 0.2 µm pore size membrane.

2.3 Preparation of total cell lysate (named as method CL)

Before cell lysate preparation, empty 15 ml centrifuge tubes were weighed. Next, *C. jejuni* biomass was scraped off eight plates with a sterile disposable cotton swab and added to tubes containing 4 ml of cell lysate buffer (2 mM EDTA and 1% Triton X-100 (9036-19-5, Merck) in PBS). This was followed by centrifugation at 4,400 × *g* for 20 min at 4°C. The supernatant was then removed, and the remaining pellet was weighed to calculate the amount of biomass scraped from the plates. The pellet was then resuspended in 4 ml of cell lysate buffer. This was followed by sonication with the Hielscher UP200St (Ultrasound Technology, Germany) sonicator (cycle, 90%; amplitude, 90; power 200 W) for four rounds of 5 min each. This was followed by centrifugation at 18,000 × *g* for 5 min at 4°C. Cell lysates were filtered through a 0.2 µm pore size membrane and stored at −20°C until further use.

2.4 Analysis of isolated ECM

The isolated ECM samples were analyzed for polysaccharides, proteins and eDNA. The polysaccharides were analyzed using the phenol-sulfuric acid method. In addition, SDS-PAGE and periodic acid-Schiff staining were used to detect glycoproteins and polysaccharides and SDS-PAGE and Alcian blue staining were used to detect acidic polysaccharides and polysaccharides with sulfate groups. The total protein content of the samples was determined using the commercial colorimetric DC protein assay (Bio-Rad, USA). The proteins in the sample were also analyzed by SDS-PAGE and Coomassie staining. The eDNA content was determined by agarose gel electrophoresis.

2.4.1 Phenol-sulfuric acid method

The phenol-sulphuric acid method is a quantitative spectrophotometric method for determining the concentration of carbohydrates in a sample. A calibration curve was established with glucose standard solutions prepared from a stock concentration of 1 mg/ml. A glucose solution of the indicated concentration was prepared in sterile glass tubes to a final volume of 100 µl in two technical replicates of each concentration. Samples were prepared in two technical replicates by adding 50 µl of dH_2O to 50 µl of the sample. 50 µl of 80% phenol (Sigma-Aldrich P9346) was then added to all tubes and the contents shaken. Then 2 ml of sulfuric acid (Carlo Erba Reagents 410301, Italy) was added to each tube and incubated for 10 min at room temperature. After 10 min, 1 ml of each solution was transferred to cuvettes and the absorbance was measured at 490 nm using a Lambda-25 spectrophotometer (PerkinElmer, USA). The concentrations of polysaccharides in each ECM sample were then determined using the calibration curve. For the statistical analysis of the results, an ordinary one-way ANOVA with Dunnett's comparison tests was performed in GraphPad Prism (GraphPad Software, San Diego, United States).

2.4.2 DC protein assay kit analysis

The commercial DC Protein Assay Kit (Bio-Rad, USA) was used to determine the protein concentration in ECM samples. A calibration curve for bovine serum albumin was established to determine the protein concentration. The calibration curve for bovine serum albumin (Sigma-Aldrich 9048-46-8) was generated with a stock concentration of 10 mg/ml. 5 µl of the standard solution of bovine serum albumin or 5 µl of each ECM sample was applied to a microtiter plate. To ensure comparability with the calibration curve, 2- and 5-fold dilutions were also prepared for the samples. Subsequently, 25 µl of reagent A' (Bio-Rad, USA) and 200 µl of reagent B (Bio-Rad, USA) were added to all wells of the microtiter plate and incubated on an orbital shaker for 5 s while shaking. This was followed by a 15-min incubation at room temperature. After 15 min, the absorbance was measured at 750 nm using a Tecan Infinite M1000 spectrophotometer (Tecan, Switzerland). The protein concentration of each sample was determined using the calibration curve. For the statistical analysis of the results, an ordinary one-way ANOVA with Dunnett's comparison tests was performed in GraphPad Prism (GraphPad Software, San Diego, United States).

2.4.3 SDS-PAGE and different staining methods

The protein content of the ECM samples was analyzed by SDS-PAGE. 30 µl of ECM was mixed with 5 µl of 6× loading buffer and loaded onto a 1.5 mm 10% polyacrylamide geL. The Amersham Low Molecular Weight Calibration Kit for SDS electrophoresis (Cytiva 17-0446-01, GE HealthCare, USA) was used as a size marker. Electrophoresis was performed in 1X SDS buffer in a SDS-PAGE device (Mini Protean II, Bio-Rad, USA). A constant current of 35 mA/gel was used for protein separation.

2.4.3.1 Glycoprotein and polysaccharide detection

Periodic acid staining and Schiff's reagent (Sigma-Aldrich, USA) were used to detect glycoproteins and polysaccharides following manufacturer's instructions. The SDS-PAGE gel was first fixed in 50% methanol (Carlo Erba Reagents 412721) for 30 min. The gel was then washed twice with 3% glacial acetic acid (J.T.Baker 64–19-7) solution, each wash lasting 20 min. This was followed by incubation with oxidation reagent (to prepare 100 ml of oxidation reagent, 1 g of periodic acid (Sigma-Aldrich P7875) was weighed, 3 ml of 100% glacial acetic acid and up to 100 ml of dH_2O were added) for 15 min with constant stirring. The gel was then washed three times with 3% glacial acetic acid solution, each wash lasting 15 min. The gel was then incubated with Schiff's reagent (Sigma-Aldrich S5133) for 35 min and then with reducing reagent (0.5 g $Na_2S_2O_5$ (Sigma-Aldrich 71932, Merck) was used to prepare 100 ml reducing reagent and added up to 100 ml dH_2O) for 5 min. It was washed with 3% glacial acetic acid solution for 5 min and finally with ultrapure water for 5 min. The gel was photographed with the camera of a cell phone.

2.4.3.2 Polysaccharide detection

To detect acidic polysaccharides and polysaccharides with sulphate groups, staining with the dye Alcian blue was performed. The SDS-PAGE gel was first fixed in EAW (Ethanol, Acetic acid and distilled Water) solution for 4 h (to prepare 100 ml of EAW, 40 ml of absolute ethanol, 5 ml of 100% glacial acetic acid and up to 100 ml of dH_2O were added). The gel was then incubated in Alcian blue solution for 30 min (to prepare 100 ml of Alcian blue solution, 0.5 g of Alcian blue dye (Merck 1.05234.0010) was weighed out, 2 ml of 100% glacial acetic acid and up to 100 ml of dH_2O were added). After incubation, the gel was washed twice with 2% glacial acetic acid solution, each wash lasting 15 min, and

then incubated overnight. The gel was photographed the next day using a ChemiDoc gel documenter (Bio-Rad, USA) and a cell phone camera.

2.4.3.3 Protein detection

The proteins on the SDS-PAGE gels were detected using Coomassie Brilliant Blue staining. After electrophoresis, the gel was transferred to a Petri dish containing Coomassie dye (ThermoScientific, USA). The gel was incubated in the solution for 1 h on an orbital shaker at room temperature. After 1 h of incubation, destaining was performed with 30% destaining solution (300 ml ethanol (Carlo Erba Reagents 4146072), 100 ml glacial acetic acid, and 600 ml dH_2O were used to prepare 1 L solution), which was changed three times every 15 min. A 10% destaining solution (140 ml ethanol, 50 ml glacial acetic acid and 810 ml dH_2O) was then added and the gel was incubated overnight. The gel was photographed the next day using a ChemiDoc gel documentation device (Bio-Rad, USA).

2.4.4 Agarose gel electrophoresis

Agarose gel electrophoresis was used to analyze the DNA content of the ECM. A 1% agarose gel was prepared. The gel was prepared by weighing 0.5 g of agarose (Sigma-Aldrich A9539) into a flask and dissolving it in 50 ml of TAE (40 mM Tris-acetate, pH 8, 1 mM EDTA) electrophoresis buffer. The melted agarose was cooled to 60°C and 5 µl of the intercalating dye SYBR Safe (Invitrogen S33102) was added. The solution was poured into an electrophoresis beaker (Bio-Rad, USA). After the gel had set, 1X TAE buffer was added and 20 µl of the sample was applied to the pockets to which 4 µl of 6-fold loading buffer had already been added. The DNA size marker 1 kb GeneRuler (Thermo Scientific, USA) for the determination of fragment size above 1 kbp (6 µl) was also applied to the gel to which 1 µl of 6-fold loading buffer had been added. Agarose gel electrophoresis was performed at a constant voltage of 80 V for approximately 40 min. After completion of electrophoresis, the gel was transferred from the beaker to a UV beam gel imager (UVItec, UK) or an Image Lab Touch gel imager (Bio-Rad, USA).

3 Results and discussion

After extraction, we determined the eDNA content in each sample, the protein content and the polysaccharide content to evaluate the yield of these macromolecules for each protocol. We used eight different protocols that utilized NaCl, centrifugation, heating in Na_2CO_3, EDTA, NaOH, formaldehyde and NaOH, the cation exchanger Dowex, and an ether solution. Different protocols for isolating the ECM of *C. jejuni* yielded variable amounts of polysaccharides, proteins, and eDNA. Interestingly, Flemming and Wingender (2010) and Aguilera et al. (2008) came to similar conclusions for ECM of other types of microbial biofilms. Numerous studies have endeavoured to develop a protocol for the optimal isolation of ECM components (Liang et al., 1992; Tabouret et al., 1992; Tapia et al., 2009; Wu and Xi, 2009), however, a universal method for ECM isolation remains elusive and challenging in terms of cost-effectiveness, simplicity, and applicability to different types of components and bacteria (Aguilera et al., 2008; Chiba et al., 2015).

To evaluate the isolated ECM samples, we assessed which isolation methods are most suitable for (1) isolating the ECM of *C. jejuni*, (2) isolating individual major components of the ECM, and (3) yielding the highest concentrations of individual ECM components. Table 3 summarizes the main components of the ECM in samples prepared by different isolation methods in our study.

3.1 Polysaccharides

The polysaccharide content in samples obtained according to different extraction protocols was analyzed using the phenol-sulfuric acid method and SDS-PAGE followed by periodic acid-Schiff or Alcian blue staining. First, polysaccharide concentrations were determined using the phenol-sulfuric acid method (Figure 1A). The highest polysaccharide concentrations were found in isolates obtained with both centrifugation methods (B and SV) and with NaOH (E). In other ECM isolates and in the cell lysate (CL), lower but comparable polysaccharide concentrations were found. The lowest polysaccharide concentrations were found in isolates obtained with NaCl (A), EDTA (D), and by heating in Na_2CO_3 (C). Despite these differences, all the methods yielded polysaccharide concentrations of less than 0.5 mg/ml. Our results indicate that the methods that most effectively isolate high polysaccharide concentrations from the ECM of *C. jejuni* employ either NaOH (E) or centrifugation only (B and SV).

SDS-PAGE and periodic acid-Schiff staining (Figure 1B) showed that many individual bands were present in the isolates obtained by centrifugation (B and SV), heating in Na_2CO_3 (C), and the cation exchanger Dowex (G), and in the cell lysate. The patterns of these bands resemble those of SDS-PAGE and Coomassie blue staining (Figure 2B), suggestive of glycoproteins. In other isolates, no glycoproteins or polysaccharides were isolated, or the stains were less distinct.

SDS-PAGE and Alcian blue staining (Figure 1C) revealed similar patterns of acidic polysaccharides or polysaccharides with sulfate groups as SDS-PAGE and Coomassie blue staining (Figure 2B), indicating the presence of glycoproteins. No or very few glycoproteins were isolated with NaCl (A), EDTA (D), and ether solution (H). The presence of high-molecular-weight acidic polysaccharides or polysaccharides with sulfate groups was also detected by the methods using centrifugation (B and SV), heating in Na_2CO_3 (C), formaldehyde and NaOH (F), and the cation exchanger (G).

3.2 Proteins

The protein concentration was measured with the DC Protein Assay kit (Figure 2A). No protein was found in the isolates obtained with NaCl (A) and EDTA (D). The highest protein concentration was detected in the isolate obtained with NaOH (E), which is probably due to protein precipitation by denaturation with NaOH. Lower and comparable protein concentrations were detected in all other isolates and the cell lysate (CL). Protein concentrations were below 10 mg/ml in all samples except the sample obtained with NaOH, in which the protein concentration was 19 mg/ml ± 1.5 mg/ml. As such, this method is the most effective for isolating the highest protein concentrations from the ECM of *C. jejuni*, however, these proteins are most likely denatured and have lost their functionality.

SDS-PAGE and Coomassie staining (Figure 2B) detected proteins in all the isolates. Based on the intensity of the stains, a significant amount of proteins was detected in the cell lysates and all isolates, except isolates obtained with NaCl (A) and ether solution (H), in which fewer proteins were present. The same protein patterns were

TABLE 3 Analysis results for determining the presence of major extracellular matrix components in samples prepared using different methods for isolating the extracellular matrix of *C. jejuni*, including the estimation of total isolation time and assessment of isolation performance.

Method	Label	Agarose gel electrophoresis	Protein concentration	Coomassie staining	Polysaccharide concentration	PAS staining	Alcian blue staining	Estimation of total isolation time	Assessment of isolation performance
Isolation with sodium chloride	A	+	-	+	+	+	+	35 min	+++
Isolation by centrifugation	B	++	+	++	++	+++	++	45 min	+++
Supernatant	SV	++	+	++	+	+++	++	18 min	+++
Isolation by heating in sodium carbonate	C	++	+	+++	+	+++	+++	85 min	++
Isolation with EDTA	D	+	-	++	+	+	-	225 min	++
Isolation with sodium hydroxide	E	++	++	++	++	+	+	225 min	++
Isolation with formaldehyde and sodium hydroxide	F	+	+	+	+	+	+	285 min	++
Isolation with cationic Dowex exchanger	G	+	+	+++	+	+++	+	215 min	+
Isolation with ether solution	H	+++	-	+	+	+	+	225 min	++
Cell lysate	CL	++	+	++	+	+++	++	80 min	+

Protein content is indicated as very high (+++; > 20 mg/ml), high (++; 10–20 mg/ml), low (+; 0.1–10 mg/ml), and very low (–; < 0.1 mg/ml). Polysaccharide content is indicated as very high (+++; > 0.5 mg/ml), high (++; 0.25–0.5 mg/ml), low (+; 0.1–0.25 mg/ml), and very low (–; < 0.1 mg/ml). The table also includes an estimate of the time required for isolation without reagent preparation and an evaluation of the performance of each isolation method. The ease of the methods is labelled as follows: easy to perform (+++), moderately difficult (++), and difficult (+).

10.3389/fmicb.2024.1488114

FIGURE 1
Polysaccharides in the ECM isolates of *Campylobacter jejuni*. **(A)** Polysaccharide content as revealed by the phenol-sulphuric acid method. The mean values and standard deviations of two measurements are shown. Dunnett's multiple comparisons with the control cell lysate tested at significance levels of * $p < 0.05$, ** $p < 0.01$, *** $p < 0.001$, and **** $p < 0.0001$. The ANOVA results were significant [F (9, 3) = 60.98, $p < 0.0001$]. **(B)** SDS-PAGE analysis with periodic acid-Schiff staining. **(C)** SDS-PAGE analysis with Alcian blue staining. Samples were obtained by sodium chloride isolation (A), centrifugation (B), a procedure that yielded a supernatant of weakly bound extracellular matrix components (SV), heating in sodium carbonate (C), EDTA (D), sodium hydroxide (E), formaldehyde and sodium hydroxide (F), Dowex cation exchanger (G) and ether solution (H). Total cell lysate (CL) was also tested.

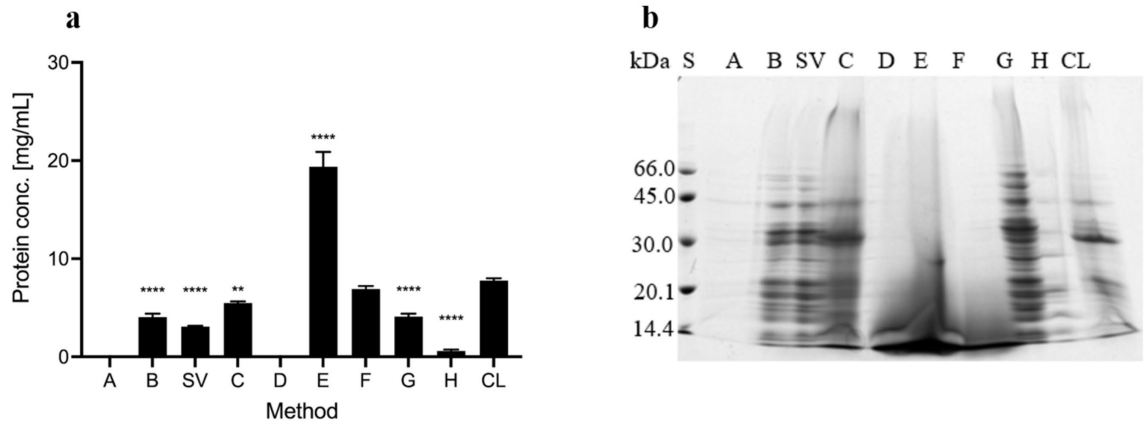

FIGURE 2
Proteins in the ECM isolates of *Campylobacter jejuni*. **(A)** Protein content as revealed by the DC Protein Assay. The mean values and standard deviations of three measurements are shown. Dunnett's multiple comparisons with the control cell lysate tested at significance levels of $p^{**} < 0.01$ and $^{****}p < 0.0001$. The ANOVA results were significant [F (7, 16) = 286.1, $p < 0.0001$]. **(B)** SDS-PAGE analysis with Coomassie Brilliant Blue staining. Samples were obtained by sodium chloride isolation (A), centrifugation (B), a procedure that yielded a supernatant of weakly bound extracellular matrix components (SV), heating in sodium carbonate (C), EDTA (D), sodium hydroxide (E), formaldehyde and sodium hydroxide (F), Dowex cation exchanger (G) and ether solution (H). Total cell lysate (CL) was also tested.

determined in isolates obtained with both centrifugation methods (B and SV), the cation exchanger Dowex (G), NaCl (A), and ether solution (H). The protein patterns of these samples differed from those of the cell lysate (CL). The protein pattern of the isolate obtained by heating in Na_2CO_3 (C) was similar to the protein pattern of the cell lysate. In other isolates (D, E, and F), predominantly low-molecular-weight, possibly denatured proteins (< 30 kDa) were detected (Figure 2B).

3.3 eDNA

Agarose gel analysis (Figure 3) revealed the presence of high-molecular-weight eDNA in isolates obtained with NaCl (A), both centrifugation methods (B and SV), EDTA (D), and ether solution (H), the latter showing the strongest signal. The isolate obtained by heating in Na_2CO_3 (C) contained fragments of >10 kbp and < 2 kbp. The isolate obtained with NaOH (E) contained fragments of 1–10 kbp. The isolate obtained with formaldehyde and NaOH (F) contained fragments of 0.5–2 kbp. The isolate obtained with the cation exchanger Dowex (G) contained a weak band of a fragment of >6 kbp. Cell lysates contained fragments of <1 kbp.

Mostly high-molecular-weight eDNA was present in the ECM of *C. jejuni*, and only cell lysates contained low-molecular-weight eDNA. This is expected because the cell lysates were sonicated during preparation, which fragmented the DNA. Our findings indicate that the most suitable method for isolating high concentrations of high-molecular-weight DNA is extraction with ether solution (H; Figure 3).

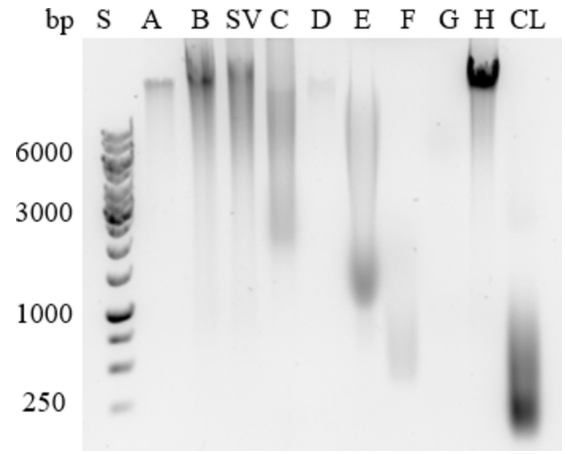

FIGURE 3
Extracellular DNA in the ECM isolates of *Campylobacter jejuni*. A representative example of agarose gel electrophoresis. Samples were obtained by sodium chloride isolation (A), centrifugation (B), a procedure that yielded a supernatant of weakly bound extracellular matrix components (SV), heating in sodium carbonate (C), EDTA (D), sodium hydroxide (E), formaldehyde and sodium hydroxide (F), Dowex cation exchanger (G) and ether solution (H). Total cell lysate (CL) was also tested.

3.4 ECM

An overview of the methods previously used for investigating ECM, divided into extraction and purification techniques, biofilm quantification and ECM analysis (Table 2) shows the variety of methods used for ECM studies. For accurate analysis of the ECM in *C. jejuni* biofilms, the ECM must first be extracted and purified, which was usually achieved by ethanol or acetone precipitation in combination with centrifugation (Jowiya et al., 2015; Yu et al., 2020), which favours the isolation of polysaccharides and proteins. Each method can illuminate a part of the ECM mosaic from a different angle, so that one can only interpret the results correctly if one knows the method well. In *ex situ* research, sample isolation and extraction is the first step, and it is extremely important to know and understand which part of the mosaic we can investigate with it. Here we have provided an overview of how the different isolation or extraction protocols can lead to different ratios and qualities of ECM components. The selection of the extraction method is an important step that can influence the outcome of the study. However, when selecting the method, not only the quantity of isolated macromolecules should be considered, but also their quality, as some extraction methods that yield the largest quantity are also destructive (e.g., NaOH for proteins). Therefore, when selecting the method for ECM extraction, the intended downstream analysis should be considered, e.g., preference of proteins for proteomics and polysaccharides for glycomics, but also the impact of the chemicals used in the purification as they may affect the quality of samples. Finally, it is recommended to use more than one method for ECM isolation in a study to compensate for any bias in ECM composition due to the isolation method.

4 Conclusion

Different isolation and extraction protocols for the extracellular matrix enriched different molecular components, resulting in very different ECM samples. For the isolation of *C. jejuni* ECM and its major components, the centrifugation method, the method in which the supernatant is obtained from weakly bound components, and heating in Na_2CO_3 were found to be the most suitable methods. These methods isolated all biopolymers and are simple, reliable and fast. The isolation methods using NaCl and EDTA were less suitable because they isolated lower amounts of eDNA and polysaccharides and failed to isolate proteins. All other isolation methods were considered suitable. The isolation method using NaOH isolated proteins and polysaccharides at the highest concentrations most effectively, but they were degraded. The ether dissolution method was best suited for the isolation of eDNA because it isolates high-molecular-weight DNA. Depending on the intended subsequent use or analytical method for the ECM sample, the isolation protocol should be carefully selected, ideally using more than one protocol to obtain more meaningful conclusions, as different protocols result in different compositions of the main ECM components.

Data availability statement

The raw data supporting the conclusions of this article will be made available by the authors, without undue reservation.

Author contributions

NP: Writing – original draft, Writing – review & editing, Formal analysis, Investigation. AK: Writing – original draft, Writing – review & editing, Conceptualization, Funding acquisition, Project administration. JS: Conceptualization, Funding acquisition, Project administration, Writing – review & editing.

Funding

The author(s) declare that financial support was received for the research, authorship, and/or publication of this article. This research was funded by the Slovenian Research and Innovation Agency by projects numbers J4-4555, J4-4550, J7-4420, J4-3088, J4-4548, J2-50064, P4-0432, and P4-0116.

Acknowledgments

We thank Eva Lasic for editing and reviewing a draft of this manuscript.

Conflict of interest

The authors declare that the research was conducted in the absence of any commercial or financial relationships that could be construed as a potential conflict of interest.

Publisher's note

References

Aguilera, A., Souza-Egipsy, V., San Martín-Úriz, P., and Amils, R. (2008). Extraction of extracellular polymeric substances from extreme acidic microbial biofilms. *Appl. Microbiol. Biotechnol.* 78, 1079–1088. doi: 10.1007/s00253-008-1390-9

Blaser, M. J. (1997). Epidemiologic and clinical features Ofcampylobacter jejuniinfections. *J. Infect. Dis.* 176, S103–S105. doi: 10.1086/513780

Brown, H. L., Hanman, K., Reuter, M., Betts, R. P., and van Vliet, A. H. M. (2015). *Campylobacter jejuni* biofilms contain extracellular DNA and are sensitive to DNase I treatment. *Front. Microbiol.* 6:699. doi: 10.3389/fmicb.2015.00699

Burnham, P. M., and Hendrixson, D. R. (2018). *Campylobacter jejuni*: collective components promoting a successful enteric lifestyle. *Nat. Rev. Microbiol.* 16, 551–565. doi: 10.1038/s41579-018-0037-9

Carpentier, B., and Cerf, O. (1993). Biofilms and their consequences, with particular reference to hygiene in the food industry. *J. Appl. Bacteriol.* 75, 499–511. doi: 10.1111/j.1365-2672.1993.tb01587.x

Chiba, A., Sugimoto, S., Sato, F., Hori, S., and Mizunoe, Y. (2015). A refined technique for extraction of extracellular matrices from bacterial biofilms and its applicability. *Microb. Biotechnol.* 8, 392–403. doi: 10.1111/1751-7915.12155

Donlan, R. M. (2002). Biofilms: microbial life on surfaces. *Emerg. Infect. Dis.* 8, 881–890. doi: 10.3201/eid0809.020063

EFSA and ECDC (2023). The European Union one health 2022 Zoonoses report. *EFSA J.* 21:e8442. doi: 10.2903/j.efsa.2023.8442

Felz, S., Al-Zuhairy, S., Aarstad, O. A., van Loosdrecht, M. C., and Lin, Y. M. (2016). Extraction of Structural Extracellular Polymeric Substances from Aerobic Granular Sludge. *J. Vis. Exp.* e54534. doi: 10.3791/54534

Feng, J., Lamour, G., Xue, R., Mirvakliki, M. N., Hatzikiriakos, S. G., Xu, J., et al. (2016). Chemical, physical and morphological properties of bacterial biofilms affect survival of encased *Campylobacter jejuni* F38011 under aerobic stress. *Int. J. Food Microbiol.* 238, 172–182. doi: 10.1016/j.ijfoodmicro.2016.09.008

Feng, J., Ma, L., Nie, J., Konkel, M. E., and Lu, X. (2018). Environmental stress-induced bacterial lysis and extracellular DNA release contribute to *Campylobacter jejuni* biofilm formation. *Appl. Environ. Microbiol.* 84, e02068–e02017. doi: 10.1128/aem.02068-17

Flemming, H.-C., van Hullebusch, E. D., Neu, T. R., Nielsen, P. H., Seviour, T., Stoodley, P., et al. (2023). The biofilm matrix: multitasking in a shared space. *Nat. Rev. Microbiol.* 21, 70–86. doi: 10.1038/s41579-022-00791-0

Flemming, H.-C., and Wingender, J. (2010). The biofilm matrix. *Nat. Rev. Microbiol.* 8, 623–633. doi: 10.1038/nrmicro2415

Flemming, H.-C., Wingender, J., Szewzyk, U., Steinberg, P., Rice, S. A., and Kjelleberg, S. (2016). Biofilms: an emergent form of bacterial life. *Nat. Rev. Microbiol.* 14, 563–575. doi: 10.1038/nrmicro.2016.94

Frølund, B., Palmgren, R., Keiding, K., and Nielsen, P. H. (1996). Extraction of extracellular polymers from activated sludge using a cation exchange resin. *Water Res.* 30, 1749–1758. doi: 10.1016/0043-1354(95)00323-1

Giaouris, E., Heir, E., Desvaux, M., Hébraud, M., Møretrø, T., Langsrud, S., et al. (2015). Intra- and inter-species interactions within biofilms of important foodborne bacterial pathogens. *Front. Microbiol.* 6:841. doi: 10.3389/fmicb.2015.00841

Good, L., Miller, W. G., Niedermeyer, J., Osborne, J., Siletzky, R. M., Carver, D., et al. (2019). Strain-specific differences in survival ofCampylobacterspp. In naturally contaminated Turkey feces and water. *Appl. Environ. Microbiol.* 85, e01579–e01519. doi: 10.1128/aem.01579-19

Jachlewski, S., Jachlewski, W. D., Linne, U., Bräsen, C., Wingender, J., and Siebers, B. (2015). Isolation of extracellular polymeric substances from biofilms of the thermoacidophilic archaeon *Sulfolobus acidocaldarius*. *Front. Bioeng. Biotechnol.* 3:123. doi: 10.3389/fbioe.2015.00123

Joshua, G. W. P., Guthrie-Irons, C., Karlyshev, A. V., and Wren, B. W. (2006). Biofilm formation in *Campylobacter jejuni*. *Microbiology* 152, 387–396. doi: 10.1099/mic.0.28358-0

Jowiya, W., Brunner, K. T., Abouelhadid, S., Hussain, H., Nair, S. P., Sadiq, S., et al. (2015). Pancreatic amylase is an environmental signal for regulation of biofilm formation and host interaction in *Campylobacter jejuni*. *Infect. Immun.* 83, 4884–4895. doi: 10.1128/iai.01064-15

Karygianni, L., Ren, Z., Koo, H., and Thurnheer, T. (2020). Biofilm matrixome: extracellular components in structured microbial communities. *Trends Microbiol.* 28, 668–681. doi: 10.1016/j.tim.2020.03.016

Kemper, L., and Hensel, A. (2023). *Campylobacter jejuni*: targeting host cells, adhesion, invasion, and survival. *Appl. Microbiol. Biotechnol.* 107, 2725–2754. doi: 10.1007/s00253-023-12456-w

Klančnik, A., Šimunović, K., Sterniša, M., Ramić, D., Smole Možina, S., and Bucar, F. (2021). Anti-adhesion activity of phytochemicals to prevent *Campylobacter jejuni* biofilm formation on abiotic surfaces. *Phytochem. Rev.* 20, 55–84. doi: 10.1007/s11101-020-09669-6

Klančnik, A., Vučković, D., Jamnik, P., Abram, M., and Smole Možina, S. (2014). Stress response and virulence of heat-stressed *Campylobacter jejuni*. *Microbes Environ.* 29, 338–345. doi: 10.1264/jsme2.me14020

Klančnik, A., Vučković, D., Plankl, M., Abram, M., and Smole Možina, S. (2013). In vivo modulation of *Campylobacter jejuni* virulence in response to environmental stress. *Foodborne Pathog. Dis.* 10, 566–572. doi: 10.1089/fpd.2012.1298

Kolenc, Ž., Kovač Viršek, M., Klančnik, A., and Janecko, N. (2024). Microbial communities on microplastics from seawater and mussels: insights from the northern Adriatic Sea. *Sci. Total Environ.* 949:175130. doi: 10.1016/j.scitotenv.2024.175130

Levin, R. E. (2007). *Campylobacter jejuni*: a review of its characteristics, pathogenicity, ecology, distribution, subspecies characterization and molecular methods of detection. *Food Biotechnol.* 21, 271–347. doi: 10.1080/08905430701536565

Liang, O. D., Ascencio, F., Fransson, L. A., and Wadström, T. (1992). Binding of heparan sulfate to *Staphylococcus aureus*. *Infect. Immun.* 60, 899–906. doi: 10.1128/iai.60.3.899-906.1992

Liu, H., and Fang, H. H. P. (2002). Extraction of extracellular polymeric substances (EPS) of sludges. *J. Biotechnol.* 95, 249–256. doi: 10.1016/s0168-1656(02)00025-1

Lu, X., Weakley, A. T., Aston, D. E., Rasco, B., Wang, S., and Konkel, M. E. (2012). Examination of nanoparticle inactivation of *Campylobacter jejuni* biofilms using infrared and Raman spectroscopies. *J. Appl. Microbiol.* 113, 952–963. doi: 10.1111/j.1365-2672.2012.05373.x

Ma, L., Feng, J., Zhang, J., and Lu, X. (2022). *Campylobacter* biofilms. *Microbiol. Res.* 264:127149. doi: 10.1016/j.micres.2022.127149

Melo, R. T., Mendonça, E. P., Monteiro, G. P., Siqueira, M. N., Pereira, C., Peres, P. A. B. M., et al. (2017). Intrinsic and extrinsic aspects on *Campylobacter jejuni* biofilms. *Front. Microbiol.* 8:1332. doi: 10.3389/fmicb.2017.01332

Moorhead, S. M., and Griffiths, M. W. (2011). Expression and characterization of cell-signalling molecules in *Campylobacter jejuni*. *J. Appl. Microbiol.* 110, 786–800. doi: 10.1111/j.1365-2672.2010.04934.x

Oh, E., Andrews, K. J., and Jeon, B. (2018). Enhanced biofilm formation by ferrous and ferric iron through oxidative stress in *Campylobacter jejuni*. *Front. Microbiol.* 9:1204. doi: 10.3389/fmicb.2018.01204

Püning, C., Su, Y., Lu, X., and Gölz, G. (2021). Molecular mechanisms of *Campylobacter* biofilm formation and quorum sensing. *Curr. Top. Microbiol. Immunol.* 431, 293–319. doi: 10.1007/978-3-030-65481-8_11

Ramić, D., Jug, B., Šimunović, K., Tušek Žnidarič, M., Kunej, U., Toplak, N., et al. (2023). The role ofluxSin *Campylobacter jejuni* beyond intercellular signaling. *Microbiol. Spectrum* 11:e0257222. doi: 10.1128/spectrum.02572-22

Reuter, M., Mallett, A., Pearson, B. M., and van Vliet, A. H. M. (2010). Biofilm formation by *Campylobacter jejuni* is increased under aerobic conditions. *Appl. Environ. Microbiol.* 76, 2122–2128. doi: 10.1128/aem.01878-09

Sabotič, J., Janež, N., Volk, M., and Klančnik, A. (2023). Molecular structures mediating adhesion of *Campylobacter jejuni* to abiotic and biotic surfaces. *Vet. Microbiol.* 287:109918. doi: 10.1016/j.vetmic.2023.109918

Sheppard, S. K., and Maiden, M. C. J. (2015). The evolution of *Campylobacter jejuni* and *Campylobacter coli*. *Cold Spring Harb. Perspect. Biol.* 7:a018119. doi: 10.1101/cshperspect.a018119

Snelling, W. J., Matsuda, M., Moore, J. E., and Dooley, J. S. G. (2005). Campylobacter jejuni. *Lett. Appl. Microbiol.* 41, 297–302. doi: 10.1111/j.1472-765x.2005.01788.x

Solomon, E. B., and Hoover, D. G. (1999). *Campylobacter jejuni*: a bacterial paradox. *J. Food Saf.* 19, 121–136. doi: 10.1111/j.1745-4565.1999.tb00239.x

Sulaeman, S., Hernould, M., Schaumann, A., Coquet, L., Bolla, J.-M., Dé, E., et al. (2012). Enhanced adhesion of *Campylobacter jejuni* to abiotic surfaces is mediated by membrane proteins in oxygen-enriched conditions. *PLoS One* 7:e46402. doi: 10.1371/journal.pone.0046402

Svensson, S. L., Pryjma, M., and Gaynor, E. C. (2014). Flagella-mediated adhesion and extracellular DNA release contribute to biofilm formation and stress tolerance of *Campylobacter jejuni*. *PLoS One* 9:e106063. doi: 10.1371/journal.pone.0106063

Tabouret, M., De Rycke, J., and Dubray, G. (1992). Analysis of surface proteins of *Listeria* in relation to species, serovar and pathogenicity. *J. Gen. Microbiol.* 138, 743–753. doi: 10.1099/00221287-138-4-743

Tapia, J., Muñoz, J. A., González, F., Blázquez, M. L., Malki, M., and Ballester, A. (2009). Extraction of extracellular polymeric substances from the acidophilic bacterium *Acidiphilium* 3.2Sup(5). *Water Sci. Technol.* 59, 1959–1967. doi: 10.2166/wst.2009.192

Teh, K. H., Flint, S., and French, N. (2010). Biofilm formation by *Campylobacter jejuni* in controlled mixed-microbial populations. *Int. J. Food Microbiol.* 143, 118–124. doi: 10.1016/j.ijfoodmicro.2010.07.037

Tram, G., Day, C. J., and Korolik, V. (2020). Bridging the gap: a role for *Campylobacter jejuni* biofilms. *Microorganisms* 8:452. doi: 10.3390/microorganisms8030452

Turonova, H., Neu, T. R., Ulbrich, P., Pazlarova, J., and Tresse, O. (2016). The biofilm matrix of *Campylobacter jejuni* determined by fluorescence lectin-binding analysis. *Biofouling* 32, 597–608. doi: 10.1080/08927014.2016.1169402

Vu, B., Chen, M., Crawford, R., and Ivanova, E. (2009). Bacterial extracellular polysaccharides involved in biofilm formation. *Molecules* 14, 2535–2554. doi: 10.3390/molecules14072535

Whelan, M. V. X., Simpson, J. C., and Ó Cróinín, T. (2021). A novel high-content screening approach for the elucidation of *C. jejuni* biofilm composition and integrity. *BMC Microbiol.* 21:2. doi: 10.1186/s12866-020-02062-5

Wu, J., and Xi, C. (2009). Evaluation of different methods for extracting extracellular DNA from the biofilm matrix. *Appl. Environ. Microbiol.* 75, 5390–5395. doi: 10.1128/aem.00400-09

Yu, H. H., Song, Y. J., Yu, H., Lee, N., and Paik, H. (2020). Investigating the antimicrobial and antibiofilm effects of cinnamaldehyde against *Campylobacter* spp. using cell surface characteristics. *J. Food Sci.* 85, 157–164. doi: 10.1111/1750-3841.14989

frontiers | Frontiers in Microbiology

TYPE Original Research
PUBLISHED 22 November 2024
DOI 10.3389/fmicb.2024.1493849

OPEN ACCESS

EDITED BY
Nicolae Corcionivoschi,
Agri-Food and Biosciences Institute,
United Kingdom

REVIEWED BY
Catherine Couzens,
AFBI Northern Ireland, United Kingdom
Michael Harvey,
Agri-Food and Biosciences Institute,
United Kingdom

*CORRESPONDENCE
Sangryeol Ryu
✉ sangryu@snu.ac.kr
Byeonghwa Jeon
✉ bjeon@umn.edu

†These authors have contributed equally to this work and share first authorship

‡PRESENT ADDRESSES
Jinshil Kim,
Gene Expression and Regulation Section, Laboratory of Biochemistry and Genetics, National Institute of Diabetes and Digestive and Kidney Diseases, National Institutes of Health, Bethesda, MD, United States
Jeong In Hur,
Department of Microbial Pathogenesis, Yale University School of Medicine, New Haven, CT, United States

RECEIVED 09 September 2024
ACCEPTED 06 November 2024
PUBLISHED 22 November 2024

CITATION
Cho E, Kim J, Hur JI, Ryu S and Jeon B (2024) Pleiotropic cellular responses underlying antibiotic tolerance in *Campylobacter jejuni*. *Front. Microbiol.* 15:1493849. doi: 10.3389/fmicb.2024.1493849

Pleiotropic cellular responses underlying antibiotic tolerance in *Campylobacter jejuni*

Eunshin Cho[1,2†], Jinshil Kim[1,2,3,4†‡], Jeong In Hur[1,2‡], Sangryeol Ryu[1,2,3*] and Byeonghwa Jeon[5*]

[1]Department of Food and Animal Biotechnology, Research Institute of Agriculture and Life Sciences, Seoul National University, Seoul, Republic of Korea, [2]Department of Agricultural Biotechnology, Seoul National University, Seoul, Republic of Korea, [3]Center for Food and Bioconvergence, Seoul National University, Seoul, Republic of Korea, [4]Department of Food Science and Biotechnology, Carbohydrate Bioproduct Research Center, Sejong University, Seoul, Republic of Korea, [5]Division of Environmental Health Sciences, School of Public Health, University of Minnesota, St. Paul, MN, United States

Antibiotic tolerance enables antibiotic-susceptible bacteria to withstand prolonged exposure to high concentrations of antibiotics. Although antibiotic tolerance presents a major challenge for public health, its underlying molecular mechanisms remain unclear. Previously, we have demonstrated that *Campylobacter jejuni* develops tolerance to clinically important antibiotics, including ciprofloxacin and tetracycline. To identify cellular responses associated with antibiotic tolerance, RNA-sequencing was conducted on *C. jejuni* after inducing antibiotic tolerance through exposure to ciprofloxacin or tetracycline. Additionally, knockout mutants were constructed for genes exhibiting significant changes in expression levels during antibiotic tolerance. The genes involved in protein chaperones, bacterial motility, DNA repair system, drug efflux pump, and iron homeostasis were significantly upregulated during antibiotic tolerance. These mutants displayed markedly reduced viability compared to the wild-type strain, indicating the critical role of these cellular responses in sustaining antibiotic tolerance. Notably, the protein chaperone mutants exhibited increased protein aggregation under antibiotic treatment, suggesting that protein chaperones play a critical role in managing protein disaggregation and facilitating survival during antibiotic tolerance. Our findings demonstrate that various cellular defense mechanisms collectively contribute to sustaining antibiotic tolerance in *C. jejuni*, providing novel insights into the molecular mechanisms underlying antibiotic tolerance.

KEYWORDS

***Campylobacter jejuni*, antibiotic tolerance, RNA-sequencing, protein chaperones, gene expression**

1 Introduction

Antibiotic tolerance enables antibiotic-susceptible bacteria to survive antibiotic treatments without acquiring resistance, significantly compromising the effectiveness of antibiotic treatment (Levin-Reisman et al., 2017; Liu et al., 2020). Unlike antibiotic resistance, antibiotic tolerance is a transient state in which bacteria can survive antibiotic exposure without undergoing genetic alterations or acquiring resistance genes (Brauner et al., 2016; Levin-Reisman et al., 2019). Both antibiotic tolerance and persistence are common bacterial strategies to survive under antibiotic treatment, and they are often referred to interchangeably (Brauner et al., 2016; Balaban et al., 2019). However, it is important to note that they represent distinct characteristics (Balaban et al., 2019; Ronneau et al., 2021). Antibiotic persistence occurs in a small subpopulation of persister cells that are transiently tolerant to antibiotics and can resume

growth upon removal of antibiotic treatment (Balaban et al., 2019; Ronneau et al., 2021). In contrast, antibiotic tolerance refers to a population-wide temporary state where bacteria can withstand and survive the toxic effects of antibiotics (Brauner et al., 2016; Balaban et al., 2019; Westblade et al., 2020). Additionally, persistence is characterized by physiological dormancy as the lethal effects of antibiotics can be evaded in dormant bacteria with extremely slow metabolic and proliferation rates in response to antibiotics, whereas tolerance does not necessarily involve physiological dormancy (Brauner et al., 2016; Balaban et al., 2019). The distinction between antibiotic persistence and tolerance results in distinct time-kill curve patterns. Antibiotic persistence leads to a unique biphasic pattern, characterized by the survival of a tolerant subpopulation followed by the killing of the majority of non-tolerant bacterial populations. In contrast, tolerance produces a monophasic pattern, demonstrating low levels of bacterial killing over time (Brauner et al., 2016; Balaban et al., 2019). Upon the removal of antibiotic stress, bacteria can be resuscitated to their normal physiological state. Recovery from antibiotic persistence from dormancy requires a relatively long time compared to that from tolerance (Meredith et al., 2015; Levin-Reisman et al., 2019).

To investigate tolerance mechanisms using persister cells, specific procedures are required to selectively isolate and enrich a tolerant subpopulation (Balaban et al., 2004; Gefen and Balaban, 2009; Cañas-Duarte et al., 2014; Sulaiman and Lam, 2020). However, the transient nature and scarcity of persister cells present considerable challenges in researching antibiotic tolerance (Huemer et al., 2020). Furthermore, most studies on tolerance have been constrained to a few hours of antibiotic treatment due to the rapid onset of bacterial death (Santi et al., 2021; Shin et al., 2021), which may not accurately reflect clinical scenarios where pathogens are typically exposed to antibiotics over extended periods, ranging from days to weeks (Aliberti et al., 2010; Wilson et al., 2019). It is also critical to note that tolerance and persistence likely involve different cellular pathways, as they are distinct phenomena (Brauner et al., 2016; Westblade et al., 2020). Persister cells survive antibiotics by entering a physiological state of dormancy and slowing metabolic processes, which may enable them to evade the lethal effects of antibiotics (Bollen et al., 2021).

Furthermore, antibiotic tolerance can facilitate the development of antibiotic resistance as extended survival through tolerance can provide antibiotic-susceptible bacteria with the opportunity to acquire antibiotic resistance under antibiotic treatment (Levin-Reisman et al., 2017; Windels et al., 2019; Liu et al., 2020). In a previous study, we discovered that *Campylobacter jejuni* (C. jejuni) develops tolerance when exposed to high concentrations of clinically important antibiotics, including ciprofloxacin (CIP) and tetracycline (TET) (Park et al., 2022). *C. jejuni* is a leading bacterial cause of gastroenteritis, causing 92 million to 300 million infection cases worldwide per year (Kirk et al., 2015). *Campylobacter* infections are generally self-limiting; however, antimicrobial therapies are required for severe infection cases, especially for the elderly and individuals with compromised immune systems (Balaban et al., 2004; Cañas-Duarte et al., 2014; Sulaiman and Lam, 2020). However, *C. jejuni* is increasingly resistant to clinically important antibiotics, particularly fluoroquinolones (FQs), the most commonly prescribed class of antibiotics for oral treatment of various bacterial infections, including gastroenteritis (Andersson and MacGowan, 2003; Schierenberg et al., 2019).

In our previous study, we demonstrated that high antibiotic concentrations promote the generation of reactive oxygen species (ROS) in *C. jejuni* during antibiotic tolerance, leading to DNA mutations resulting in antibiotic resistance, particularly FQ resistance (Park et al., 2022). Moreover, we have found that antioxidation processes play a critical role in maintaining antibiotic tolerance in *C. jejuni*. Our current understanding of the molecular mechanisms of antibiotic tolerance is highly limited (Meredith et al., 2015). Especially, there is a lack of information on how bacteria can address cellular damage resulting from antibiotic treatment. *C. jejuni* offers a unique and feasible model for studying antibiotic tolerance due to its relatively faster growth compared to other tolerance-developing bacteria, such as *Mycobacterium tuberculosis* (Goossens et al., 2020). Utilizing *C. jejuni*, in this study, we reveal the complex interplay of molecular processes that enable bacterial survival under high antibiotic concentrations through tolerance.

2 Materials and methods

2.1 Bacterial strains and growth conditions

C. jejuni NCTC 11168 was used as wild type (WT) in this study. *C. jejuni* strains were grown microaerobically (5% O_2, 10% CO_2, and 85% N_2) at 42°C on Mueller-Hinton (MH) media (Oxoid, Hampshire, UK). *Escherichia coli* MG1655 (ATCC 700926) was grown at 37°C on Luria-Bertani (LB) media (Difco, MI, United States). For the growth of mutants harboring an antibiotic resistance cassette, the culture media were supplemented with antibiotics, including carbenicillin (100 μg/mL), kanamycin (50 μg/mL), or chloramphenicol (12.5 μg/mL).

2.2 Time-kill assay

Overnight cultures of *C. jejuni* grown on MH agar were resuspended in 5 mL of MH broth in a 14-mL round-bottom tube (BD Falcon, MA, United States) to an optical density at 600 nm (OD_{600}) of 0.08. The bacterial suspension was then incubated with shaking under microaerobic conditions. After 7 h incubation, antibiotic exposure was initiated by adding 100× minimum inhibitory concentrations (MICs) of CIP (6.3 μg/mL) or TET (3.1 μg/mL) (Supplementary Table S1). TET and CIP were used for testing because they are clinically important antibiotics that *C. jejuni* is known to develop tolerance (Luangtongkum et al., 2009; Schierenberg et al., 2019). Moreover, these antibiotics are commonly used in both human and veterinary medicine, making them relevant choices for studying antibiotic tolerance in this pathogen (European Medicines Agency, 2022; US Food and Drug Administration, 2023). Our previous studies show that *C. jejuni* develops antibiotic tolerance when exposed to concentrations greater than 10× MICs, including 100× MICs (Park et al., 2022). To more effectively differentiate non-tolerant populations in our experiment, we opted to use 100× MICs. Moreover, employing high antibiotic concentrations is a commonly accepted experimental method for inducing antibiotic tolerance (Fridman et al., 2014; Mechler et al., 2015). The concentrations were determined based on the MICs of WT. After 24, 48, and 72 h incubation, 100 μL of *C. jejuni* cultures were harvested

and washed with ice-cold phosphate-buffered saline (PBS) three times. After washing, bacterial cells were resuspended in 1 mL of PBS and diluted with MH broth. Five microliters of bacterial cells were spotted onto MH agar and incubated for 2 days to assess viability. To examine the effect of an efflux pump inhibitor on antibiotic tolerance, *C. jejuni* was incubated with phenylalanine-arginine β-naphthylamide (PAβN) (10 or 20 μg/mL) for 7 h in the presence of antibiotics as described above. The assay was also conducted with *E. coli*. *E. coli* MG1655 was incubated in LB broth with shaking under aerobic conditions. At the exponential growth phase, the bacterial population was adjusted to a concentration of 10^8 CFU/mL. Subsequently, the cultures were treated with 100× MICs of CIP (1.6 μg/mL) or TET (50 μg/mL). The samples were harvested after incubation for 2, 4, 8, 12, 24, and 48 h. After washing with ice-cold PBS three times, the bacterial cells were resuspended in PBS, diluted, and spotted onto the LB agar plates. After 12 h of incubation, bacterial viability was assessed.

2.3 Total RNA extraction, RNA-Seq, and analysis

Overnight cultures of *C. jejuni* NCTC 11168 grown on MH agar were harvested and suspended in MH broth to an OD_{600} of 0.08. A 3 mL bacterial suspension in a 19 mL glass culture tube was incubated for 7 h with shaking under microaerobic conditions. After 7 h, cultures were treated with 100× MICs of either CIP (6.3 μg/mL) or TET (3.1 μg/mL) for 24 h. Bacterial cultures (2.5 mL) were treated with 5% ice-cold phenol-ethanol solution, and total bacterial RNAs were isolated using the RNeasy Minikit (Qiagen, Hilden, Germany) according to the manufacturer's instructions. The quantity and quality of total RNA samples were assessed using a NanoPhotometer N60 (Implen, Munich, Germany), and three biological replicate RNA samples were sent to Macrogen (Seoul, Republic of Korea) for RNA sequencing.

The quality and quantity of total RNA were further evaluated using an Agilent Technologies 2100 Bioanalyzer, ensuring an RNA integrity number (RIN) value greater than 7. A library was prepared independently with 1 μg of total RNA for each sample by Illumina TruSeq Stranded mRNA Sample Prep Kit (Illumina, Inc., CA, United States). Initially, bacterial rRNA-depleted samples were prepared by using the NEBNext rRNA Depletion kit (NEB, NA, United States). After rRNA depletion, the remaining RNA was fragmented into small pieces using divalent cations under elevated temperature. The RNA fragments were converted into first-strand cDNA using SuperScript II reverse transcriptase (Invitrogen, MA, United States) and random primers. This is followed by second-strand cDNA synthesis using DNA Polymerase I, RNase H, and dUTP. These cDNA fragments underwent an end repair process, the addition of a single 'A' base, and ligation of the adapters. The products were then purified, enriched with PCR, and processed to create the final cDNA library. Library quantification was carried out using KAPA Library Quantification kits for Illumina Sequencing platforms, and qualification was performed using the TapeStation D1000 ScreenTape (Agilent, CA, United States). Indexed libraries were then submitted to an Illumina NovaSeq 6000 (Illumina, Inc., CA, United States), employing paired-end (2 × 100 bp) sequencing by Macrogen (Seoul, Republic of Korea).

The expression level of each gene was normalized by calculating reads per kilobase per million mapped reads (RPKM) using CLC Workbench. Fold change was determined in comparison to the untreated control (No antibiotics). Differentially expressed genes (DEGs; fold change ≥ 2 or ≤ -2; $p < 0.05$) were filtered and visualized using the Gitools.

2.4 Quantitative real-time PCR

Total RNA was extracted as described above, and cDNA was synthesized using cDNA EcoDry premix (Takara Bio Inc., Kusatsu, Japan). qRT-PCR was performed in a 20 μL reaction volume containing cDNA, iQ SYBR Green supermix (Bio-Rad, CA, United States), and each primer, using the CFX Connect real-time PCR detection system (Bio-Rad, CA, United States). The primer sets used in qRT-PCR are described in Supplementary Table S2. The cycling conditions were as follows: 95°C for 5 min; 40 cycles at 95°C for 15 s, 55°C for 15 s, and 72°C for 30 s; followed by 72°C for 7 min. The transcriptional levels of each gene were normalized to the 16S rRNA gene.

2.5 Construction of *Campylobacter jejuni* mutants and complemented strains

The *dnaK*, *clpB*, *groESL*, *cheY*, *ruvC*, *cmeC*, and *cmeF* knockout mutants were constructed as described previously (Kim et al., 2023). The *aphA3* (kanamycin resistance) cassette and *cat* (chloramphenicol resistance) cassette were amplified with PCR from pMW10 and pRY112 plasmids, respectively, using primers described in Supplementary Table S2. Flanking regions of the target genes were also amplified by PCR (Supplementary Table S2). Subsequently, the PCR products and pUC19 were digested using BamHI and SalI enzymes, followed by ligation. The resulting plasmids were amplified by inverse PCR and ligated with *aphA3* for constructing *dnaK*, *clpB*, *groESL*, *cheY*, *ruvC*, and *cmeC* mutants or *cat* for the *cmeF* mutant (Supplementary Table S2). The constructed suicide plasmid was electroporated into *C. jejuni*, and the mutations were confirmed with PCR and sequencing. For the construction of *flaA* and *flaB* mutants, natural transformation was performed as previously described (Wang and Taylor, 1990). Briefly, the genomic DNAs were extracted from *C. jejuni* 81-176 Δ*flaA*::*cat* (Hwang et al., 2011) and *C. jejuni* 81-176 Δ*flaB*::*cat* mutants in the laboratory collection, digested by SphI and NdeI for Δ*flaA*, and SphI and SalI for Δ*flaB*, respectively. The DNA was spotted directly on the *C. jejuni* cultures grown overnight on MH agar plates and further incubated for 5 h under microaerobic conditions. The bacterial culture was collected and spread on the MH agar plate containing chloramphenicol (12.5 μg/mL). After incubation for 48 h, the chloramphenicol-resistant colonies were selected, and the mutations were confirmed by PCR and sequencing using specific primer sets (Supplementary Table S2). In addition, complemented strains were constructed using the chromosomal integration method (Kim et al., 2023). The genes (*dnaK*, *clpB*, *groESL*, *ruvC*, *flaA*, *cmeC*, and *cmeF*) were amplified with PCR using primers listed in Supplementary Table S2, and digested by XbaI or NotI and ligated with the pFMBcomCM plasmid (Hwang et al., 2012) (for *dnaK*, *clpB*, *groESL*, *ruvC*, and *cmeC*), or pFMBcomC (Hwang et al., 2011) (for

flaA, *cmeF*, and *fur*). The complementation plasmids were introduced to the corresponding mutant strains by electroporation. The complementation into the bacterial chromosome was confirmed with PCR and sequencing. The Δ*fur* mutant strain was previously constructed (Kim et al., 2011).

2.6 Cross-section transmission electron microscopy

C. jejuni cells were treated with antibiotics for 24 h, as described above. After harvest, *C. jejuni* cells were washed with ice-cold PBS three times and fixed with Karnovsky's fixative solution overnight at 4°C. The pellets were washed with 0.05 M sodium cacodylate buffer three times, following post-fixation with 1% osmium tetroxide in the same buffer at room temperature for 1 h. After washing with distilled water three times, en bloc staining was performed with 0.5% uranyl acetate overnight at 4°C. The next day, the samples were washed with distilled water three times, and dehydrated in a series of ethanol gradients (30, 50, 70, 80, 90, and 100%) for 20 min in each step while slowly rotating. The final 100% ethanol step was repeated three times. Finally, cells were incubated in a 1:1 mixture of Spurr's resin (Wallis and Griffin, 1973) and ethanol for 90 min at room temperature while slowly rotating and subsequently left in a mixture of 2:1 Spurr's resin and ethanol at room temperature for 90 min while slowly rotating. The cells were placed in 100% Spurr's resin and incubated overnight while slowly rotating. The next day, samples were embedded in fresh 100% epoxy resin for 3 h and replaced with fresh 100% epoxy resin. The resin was polymerized for 2 days in an oven at 70°C. The samples cut with an ultramicrotome UC7 (Leica, Wetzlar, Germany) were placed on copper grids and double-stained with 2% uranyl acetate and 3% lead citrate. The sections were observed on a JEM-1010 TEM (JEOL, Tokyo, Japan) operated at 80 kV.

2.7 Confocal fluorescence microscopy

C. jejuni cells were treated with antibiotics for 24 h, as described above. *C. jejuni* cells were then washed with ice-cold PBS three times. The pellets were resuspended in 1:500 diluted Proteostat dye (Enzo Life Sciences, NY, United States) and incubated for 20 min in the dark at RT. The cells were simultaneously incubated with SYTO9 (Invitrogen, MA, United States) for 15 min. Then, the sample was washed with PBS. The cells were fixed with 4% paraformaldehyde for 30 min at RT. After washing with PBS, the pellets were resuspended with PBS. 5 μL of each sample was placed on the slides. Confocal images of *C. jejuni* cells were captured using a laser scanning confocal microscope SP8X (Leica, Wetzlar, Germany) using a 488 nm argon laser and a 580 nm emission filter. Images were digitally captured and analyzed with LAS X Software (Leica, Wetzlar, Germany).

2.8 Measurement of intracellular iron levels

The intracellular iron levels were measured as previously described (Hur et al., 2022). Briefly, *C. jejuni* cells were treated with antibiotics for 24 h, as described above. *C. jejuni* cells were then washed with ice-cold PBS three times. After resuspending the pellet with PBS, the cells were disrupted by sonication. Samples were mixed with an iron detection reagent (6.5 mM ferrozine, 6.5 mM neocuproine, 2.5 M ammonium acetate, and 1 M ascorbic acid) and incubated at RT for 30 min. The intracellular iron level was calculated by comparing it to a standard curve obtained from a 1 mM $FeCl_3$ (Sigma-Aldrich, MO, United States) solution. The absorbance was measured at 550 nm using a SpectraMax i3 platform (Molecular Devices, CA, United States). The intracellular iron levels were normalized to total protein concentrations, which were determined by the Bradford assay (Bio-Rad, CA, United States).

2.9 Statistical analysis

All assays were conducted using three independent biological replicates. The figures indicate the mean value and error bars represent the standard deviations of each experiment. Student's *t* test was used to determine significance using GraphPad Prism software v8.0.1. The *p*-value threshold was set at $^{*}p<0.05$; $^{**}p<0.01$; $^{***}p<0.001$; $^{****}p<0.0001$.

3 Results

3.1 Transcriptome changes during antibiotic tolerance in *Campylobacter jejuni*

In order to understand transcriptome changes underlying antibiotic tolerance, we performed RNA-Seq after exposing *C. jejuni* to high concentrations of CIP or TET. These two antibiotics were chosen based on our previous findings that *C. jejuni* can survive in the presence of high concentrations of these antibiotics through tolerance for an extended period (Park et al., 2022). Notably, CIP and TET have different modes of action, with CIP disrupting bacterial DNA synthesis by targeting DNA gyrase (Appelbaum and Hunter, 2000) and TET inhibiting protein synthesis by targeting the 30S subunit of ribosomes (Grossman, 2016). Upon exposure to 100× MICs of CIP, *C. jejuni* underwent viability reduction for 2 days, followed by the emergence of CIP-resistant populations (Figure 1A). The survival pattern of *C. jejuni* in the presence of these antibiotics differs from that of *E. coli*. In *E. coli*, CIP significantly reduces viability within a few hours, followed by the survival of persister cells at extremely low levels (Figure 1B). Moreover, high TET concentrations led to the killing of *C. jejuni* (Figure 1A), whereas TET exhibited only bacteriostatic activity in *E. coli* (Figure 1B).

The results of the RNA-Seq analysis have revealed that significant transcriptome changes occur during antibiotic tolerance. Compared to the untreated sample, CIP was found to induce differential expression in a total of 1,026 genes, including 475 upregulated genes and 551 downregulated genes (Figures 1C,D), whereas TET exhibited differential expression in a total of 602 genes, with 281 upregulated genes and 321 downregulated genes (Figures 1C,D). Additionally, a total of 477 genes were differentially expressed in both CIP and TET (Figure 1D). Notably, CIP upregulated genes involved in various cellular functions, such as cell cycle control, cell division, chromosome partitioning, and cell motility, while downregulating

10.3389/fmicb.2024.1493849

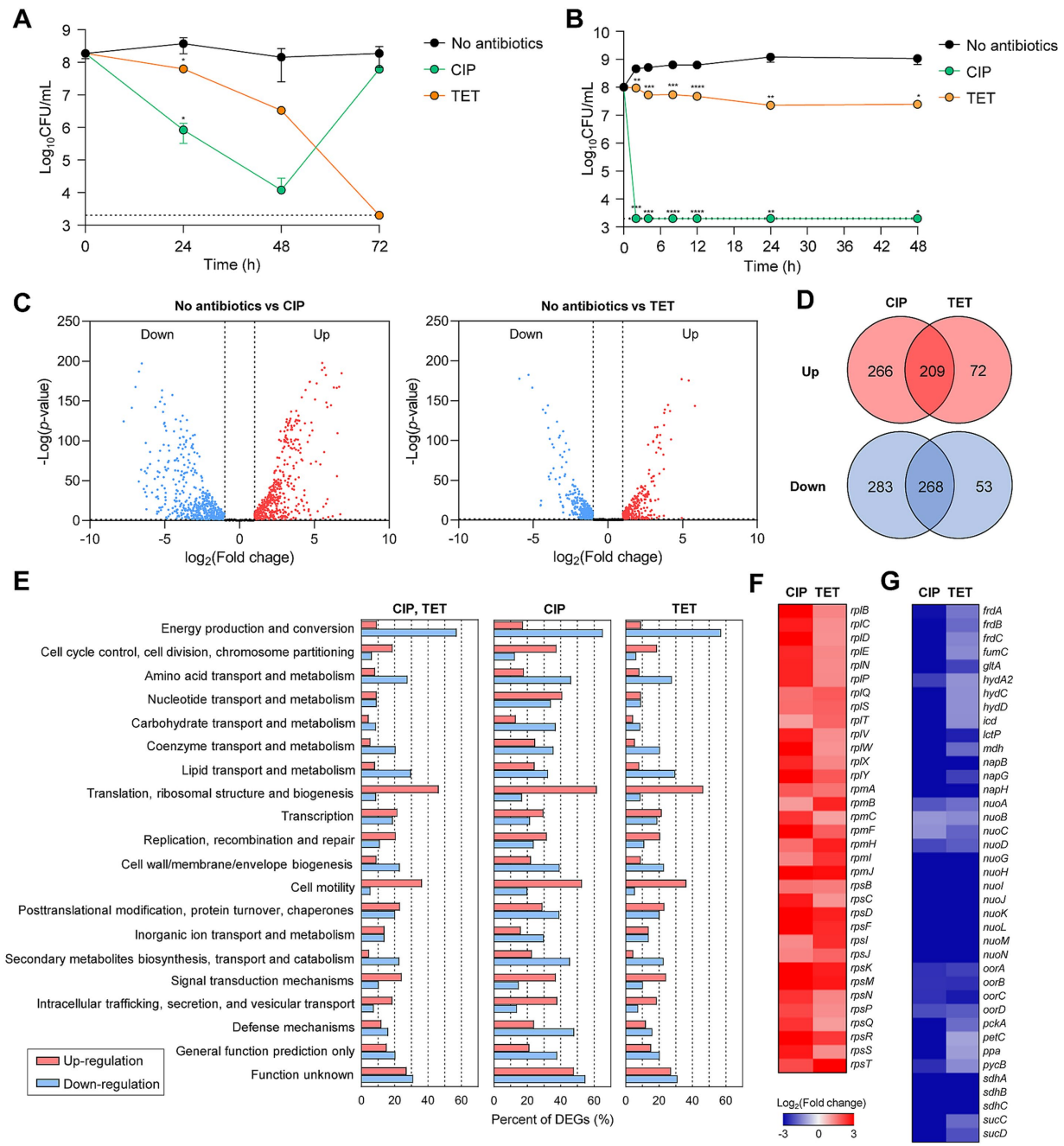

FIGURE 1
Antibiotic tolerance and transcriptomic changes in *C. jejuni* in the presence of high concentrations of ciprofloxacin (CIP) or tetracycline (TET). **(A,B)** Induction of antibiotic tolerance in *C. jejuni* **(A)** and *E. coli* **(B)** by exposure to 100× minimum inhibitory concentrations (MICs) of CIP (6.3 μg/mL and 1.6 μg/mL, respectively) or TET (3.1 μg/mL and 50 μg/mL, respectively). Dashed line shows detection threshold. Error bars represent the standard deviations of three biological replications. The data were statistically analyzed by the Student's *t* test in comparison with the untreated control (No antibiotics); $*p < 0.05$; $**p < 0.01$; $***p < 0.001$; $****p < 0.0001$. **(C–G)** The transcriptomic changes in *C. jejuni* after exposure to 100× MICs of ciprofloxacin (CIP; 6.3 μg/mL) or tetracycline (TET; 3.1 μg/mL) based on RNA-Seq. Fold change was defined compared to the untreated control. Volcano plots **(C)** and Venn diagrams **(D)** depicting differentially expressed genes (DEGs) in *C. jejuni* after exposure to 100× MICs of CIP or TET. The percentages of DEGs **(E)** in *C. jejuni* during antibiotic tolerance. Heat maps of the genes associated with translation, ribosomal structure, and biogenesis **(F)** or energy production and conversion **(G)** after exposure to 100× MICs of CIP or TET. The heat maps were constructed with Gitools.

genes associated with amino acid transport and metabolism, secondary metabolites biosynthesis, and defense mechanisms (Figure 1E). On the other hand, both CIP and TET commonly increased the transcription of genes associated with translation and ribosomal structure, while downregulating those related to energy production and conversion (Figures 1E,G). Notably, genes involved in protein translation and tRNA genes were upregulated (Figure 1F), indicating that *C. jejuni* is not dormant during antibiotic tolerance and actively synthesizes proteins to respond to antibiotic stress.

3.2 Protein chaperones contribute to sustaining antibiotic tolerance

Protein chaperones are critical for assisting in proper protein folding and disaggregation, particularly under stress conditions (Mayer, 2021). The three major bacterial chaperone complexes are the trigger factor, the DnaK-DnaJ, and the GroEL-GroES complexes (Sabate et al., 2010). RNA-Seq analysis has revealed that genes encoding these chaperone complexes, specifically *clpB*, *dnaK*, *groES*, *groEL*, and *tig*, are significantly upregulated during antibiotic tolerance (Figure 2A), suggesting that these chaperones play an important role in bacterial survival under antibiotic treatment. The Δ*dnaK*, Δ*clpB*, and Δ*groESL* mutant strains were constructed to further examine the role of protein chaperones in conferring antibiotic tolerance. The deletion mutants exhibited no substantial growth impairments compared to WT in the absence of antibiotic exposure (Supplementary Figure S1A). Notably, Δ*dnaK*, Δ*clpB*, and Δ*groESL* mutations have been shown to compromise antibiotic tolerance, resulting in significant viability reductions after 48 h of antibiotic exposure (Figure 2B). This was particularly evident under treatment with TET, where Δ*clpB* and Δ*groESL* mutations facilitated bacterial cell death (Figure 2B).

Environmental stress can disrupt protein homeostasis, leading to the formation of insoluble protein aggregates within bacterial cells (Vaubourgeix et al., 2015; Schramm et al., 2019). TEM has been employed to investigate whether antibiotic exposure induces protein

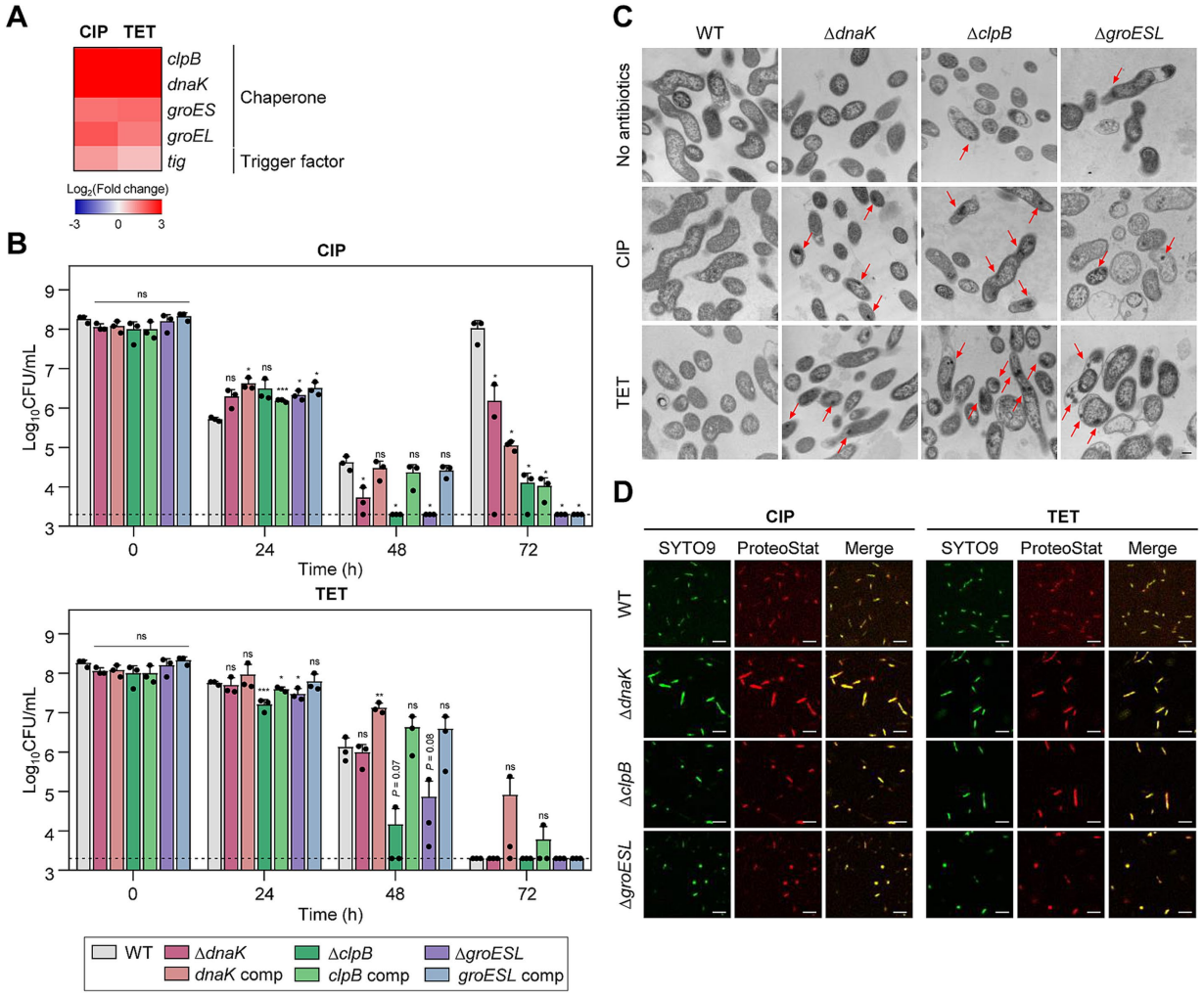

FIGURE 2
Effects of chaperones on antibiotic tolerance in *C. jejuni* in the presence of high concentrations of ciprofloxacin (CIP) or tetracycline (TET). **(A)** Heat maps of the genes associated with chaperones after exposure to 100× minimum inhibitory concentrations (MICs) of CIP (6.3 μg/mL) or TET (3.1 μg/mL). The heat maps were constructed with Gitools. **(B)** Induction of antibiotic tolerance by exposure to 100× MICs of CIP (6.3 μg/mL) or TET (3.1 μg/mL). The concentrations were determined based on the MICs of WT. Dashed line shows detection threshold. Error bars represent the standard deviations of three biological replications. The data were statistically analyzed by the Student's *t* test in comparison with WT. $*p < 0.05$; $**p < 0.01$; $***p < 0.001$; ns, not significant; WT, wild type; Δ*dnaK*, *dnaK* mutant; *dnaK* comp, *dnaK*-complemented strain; Δ*clpB*, *clpB* mutant; *clpB* comp, *clpB*-complemented strain; Δ*groESL*, *groESL* mutant; *groESL* comp, *groESL*-complemented strain. **(C)** Formation of protein aggregates induced after exposure to 100× MICs of CIP or TET. The concentrations were determined based on the MICs of WT. Red arrows indicated protein aggregates observed by cross-section transmission electron microscopy (TEM). The formation of protein aggregates was compared to the untreated control (No antibiotics). The scale bar represents 0.2 μm. **(D)** Protein aggregates were visualized with fluorescent probes. Live cells were stained with SYTO9 (green) and protein aggregates with Proteostat (red). The merged images are shown in yellow. The scale bar represents 5 μm.

aggregation during antibiotic tolerance. Compared to WT, more protein aggregates were detected in Δ*dnaK*, Δ*clpB*, and Δ*groESL* mutants (Figure 2C). Additionally, the use of Proteostat, a fluorescent dye that selectively binds to misfolded and aggregated proteins (Bagnoli et al., 2023), has corroborated these observations. Consistently, enhanced protein aggregation was observed in the chaperone mutants compared to WT (Figure 2D). In contrast, there was no discernible difference in the negative controls without antibiotic treatment (Supplementary Figure S2). These findings indicate the critical function of chaperone proteins in bacterial survival during antibiotic tolerance.

3.3 Association of bacterial motility with antibiotic tolerance

The motility of *C. jejuni* is facilitated by polar flagella that consist of flagellins encoded by *flaA* and *flaB*, which are regulated by the sigma factors FliA and RpoN, respectively (Guerry et al., 1991; Alm et al., 1993). Among these flagellin genes, *flaA* is the major flagellin as its inactivation leads to a loss of motility and a decrease in virulence, whereas an inactivation of *flaB* results in the formation of truncated flagella but does not reduce motility (Alm et al., 1993). Genes related to motility were significantly upregulated during tolerance (Figure 3A), suggesting that bacterial motility is critical for antibiotic tolerance. Additionally, the *cheY* gene, which is integral to bacterial chemotaxis (Yao et al., 1997), was also upregulated during antibiotic tolerance (Figure 3A).

To better understand the contributions of motility and chemotaxis to antibiotic tolerance, we constructed Δ*flaA*, Δ*flaB*, and Δ*cheY* mutants. These mutant strains did not display any significant growth defects compared to WT without antibiotics treatment (Supplementary Figure S1B). When treated with CIP, the Δ*flaA* mutant demonstrated a significant reduction in viability compared to WT, suggesting that *flaA*-mediated motility is crucial for CIP tolerance (Figure 3B). Under TET treatment, there was no observable difference in viability reduction between the mutants and WT (Figure 3B), indicating that the role of motility and chemotaxis in antibiotic tolerance may vary depending on the antibiotic.

3.4 DNA repair is critical for antibiotic tolerance

A number of genes involved in DNA repair were significantly upregulated during antibiotic tolerance (Figure 4A). Specifically, the *ssb* gene, which encodes the single-stranded DNA-binding protein crucial for DNA replication, recombination, and repair (Xu et al., 2023), was upregulated by exposure to high concentrations of antibiotics. Additionally, antibiotic treatment also upregulated *dprA* encoding DNA processing protein A (DprA), which assists in the integration of single-stranded DNA into the genome and is involved in natural transformation in *C. jejuni* (Takata et al., 2005). Interestingly, antibiotic treatment did not upregulate *recA* (Figure 4A), presumably due to the absence of SOS response systems in *C. jejuni* (Parkhill et al., 2000).

To evaluate the impact of DNA repair systems on antibiotic tolerance, we constructed a Δ*ruvC* mutant and measured its viability in the presence of 100× MICs of CIP or TET. In the absence of antibiotic exposure, the deletion of the *ruvC* gene did not lead to a significant growth defect compared to WT (Supplementary Figure S1C). RuvC plays an important role in DNA repair and recombination by cleaving Holliday junctions (Iwasaki et al., 1991). The *ruvC* was selected for testing because its transcriptional level was significantly enhanced by both CIP and TET (Figure 4A). Moreover, the Δ*ruvC* mutation severely impaired antibiotic tolerance in *C. jejuni* (Figure 4B). Additionally, the Δ*ruvC* mutation sensitized *C. jejuni* to antibiotics, displaying a decrease in the MICs of CIP and TET by 4-fold and 2-fold, respectively (Supplementary Table S1).

It is noteworthy that the upregulation of DNA repair genes was also observed during tolerance induced by TET, a broad-spectrum antibiotic that works by inhibiting protein synthesis in bacteria (Figure 4A). Potentially, TET exposure triggers a general stress response, which could include the activation of various protective mechanisms, including DNA repair systems. Alternatively, while TET does not directly target DNA, its effects on protein synthesis might indirectly lead to DNA stress or damage. Furthermore, the inactivation of *ruvC* markedly diminished bacterial viability in the presence of TET (Figure 4B). These findings indicate the importance of DNA repair processes in maintaining antibiotic tolerance, regardless of the mode of action of an antibiotic used for tolerance induction.

3.5 Drug efflux pumps contribute to maintaining antibiotic tolerance

Drug efflux pumps play a critical role in antibiotic resistance by reducing the intracellular concentration of antibiotics (Du et al., 2018; Colclough et al., 2020; Kumawat et al., 2023). In *C. jejuni*, CmeABC is the primary efflux system that confers resistance across various antibiotic classes (Lin et al., 2002; Wieczorek and Osek, 2013; Sharifi et al., 2021). CmeDEF is another drug efflux pump that operates alongside CmeABC to maintain cell viability under antibiotic treatment (Akiba et al., 2006). Transcriptomic analysis showed that the expression of these efflux pump genes is modulated in response to antibiotic exposure (Supplementary Figure S3). To further elucidate the role of these pumps during antibiotic tolerance, we constructed Δ*cmeC* and Δ*cmeF* mutants. CmeABC and CmeDEF are the resistance-nodulation-cell division (RND)-type efflux pumps, which are composed of three proteins spanning the cytoplasmic space and both cell membranes; thus, the absence of any one component renders the entire pump nonfunctional. Without antibiotic treatment, the mutants showed comparable growth to WT (Supplementary Figure S1D). Under CIP treatment, the viability reductions in these efflux pump mutants were slightly more substantial compared to WT after 48 h (Figure 5A). In contrast to WT, notably, the emergence of FQ-resistant strains was not observed in the Δ*cmeC* mutant after 72 h (Figure 5A). In the presence of 100× MICs of TET, tolerance was significantly compromised in both Δ*cmeC* and Δ*cmeF* mutants (Figure 5A).

The role of efflux pumps in antibiotic tolerance was also assessed using the efflux pump inhibitor PAβN. Similarly, PAβN did not affect bacterial viability during CIP-induced tolerance, whereas PAβN significantly reduced viability in the presence of 100× MICs of TET (Figure 5B; Supplementary Figure S1E). These results suggest that drug efflux pumps may contribute to antibiotic tolerance depending on the antibiotic.

10.3389/fmicb.2024.1493849

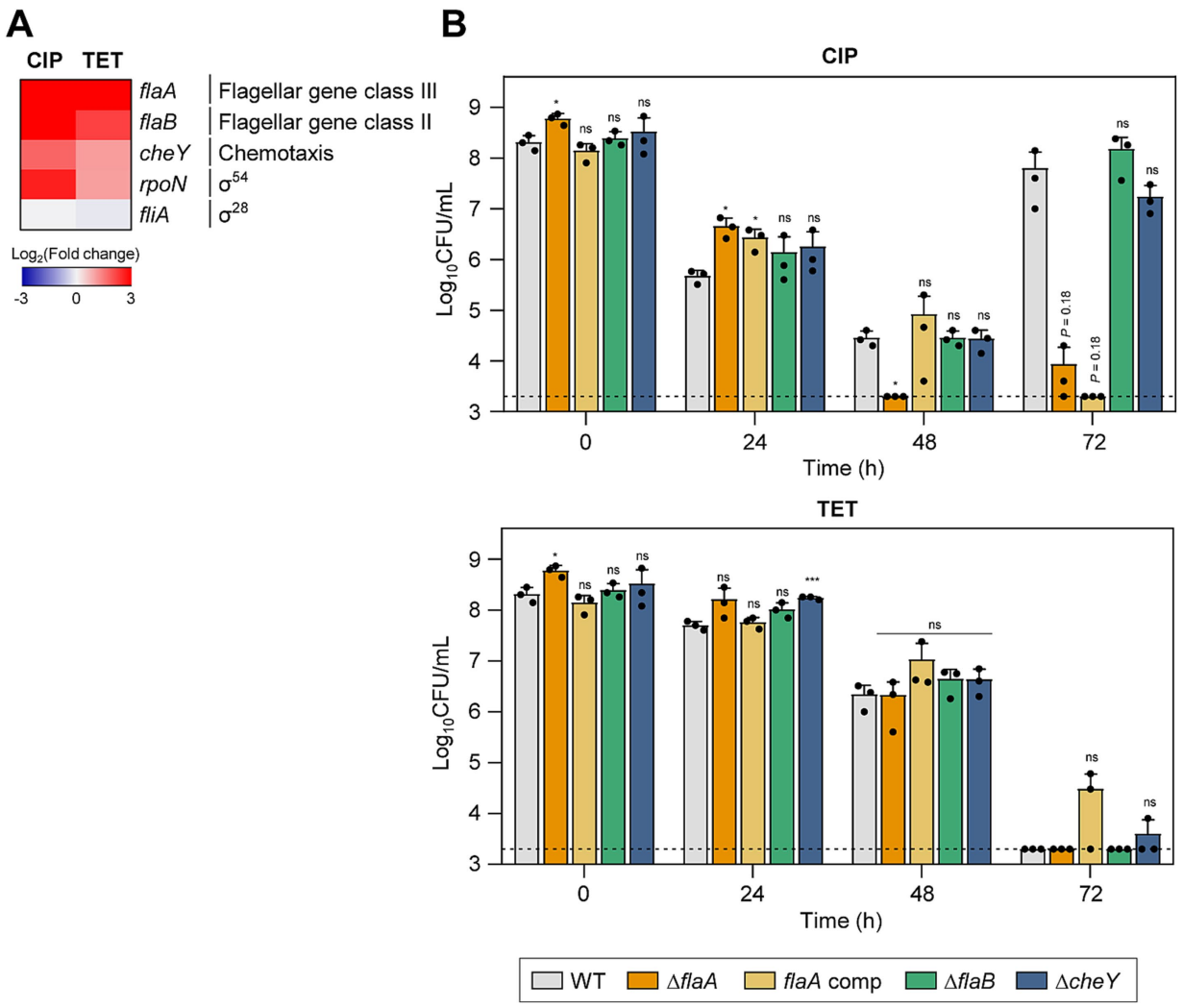

FIGURE 3
Effects of motility-related genes on antibiotic tolerance in *C. jejuni* in the presence of high concentrations of ciprofloxacin (CIP) or tetracycline (TET). **(A)** Heat maps of the genes associated with motility after exposure to 100× minimum inhibitory concentrations (MICs) of CIP (6.3 μg/mL) or TET (3.1 μg/mL). The heat maps were constructed with Gitools. **(B)** Induction of antibiotic tolerance by exposure to 100× MICs of CIP (6.3 μg/mL) or TET (3.1 μg/mL). The concentrations were determined based on the MICs of WT. Dashed line shows detection threshold. Error bars represent the standard deviations of three biological replications. The data were statistically analyzed by the Student's *t* test in comparison with WT; $*p < 0.05$; $***p < 0.001$; ns, not significant; WT, wild type; Δ*flaA*, *flaA* mutant; *flaA* comp, *flaA*-complemented strain; Δ*flaB*, *flaB* mutant; Δ*cheY*, *cheY* mutant.

3.6 Increased iron accumulation during antibiotic tolerance

RNA-Seq analysis has also revealed a notable upregulation of *fur* transcription during antibiotic tolerance, particularly when tolerance was induced by CIP (Figure 6A). A Δ*fur* mutation significantly compromised the viability in the presence of 100× MICs of TET and reduced the emergence of FQ resistance under the treatment with 100× MICs of CIP (Figure 6B; Supplementary Figure S1F). Interestingly, the level of intracellular iron is significantly increased during antibiotic tolerance (Figure 6C). Iron is a cofactor of a range of proteins essential for fundamental physiological processes (Andrews et al., 2003; Frawley and Fang, 2014). Most Gram-negative bacteria, including *C. jejuni*, maintain cytoplasmic iron levels using Fur, a transcriptional repressor (Lee and Helmann, 2007; Butcher et al., 2012). Iron exists in either the reduced ferrous form (Fe^{2+}) or the oxidized ferric form (Fe^{3+}). Fe^{2+} can passively diffuse through the outer-membrane porins and is imported by FeoB, which is the only Fe^{2+} transport system that has been identified in *C. jejuni* (Naikare et al., 2006). Fe^{3+} is imported through specific ligand-gated outer-membrane receptor proteins using siderophores, including Fe^{3+}-enterochelin (CeuBCDE, CfrA) and Fe^{3+}-rhodotorulic acid (P19, Cj1658-63) (Palyada et al., 2004; Miller et al., 2008), During antibiotic tolerance, genes for Fe^{3+}-uptake systems involving rhodotorulic acid and hemin, and the Fe^{2+}-uptake FeoB were also down-regulated (Figure 6A). Presumably, *fur* transcription was increased so that Fur can prevent further iron uptake to maintain iron homeostasis and reduce cellular toxicity. After the acquisition, iron can be stored in the form of ferritin or incorporated into iron–sulfur complexes

10.3389/fmicb.2024.1493849

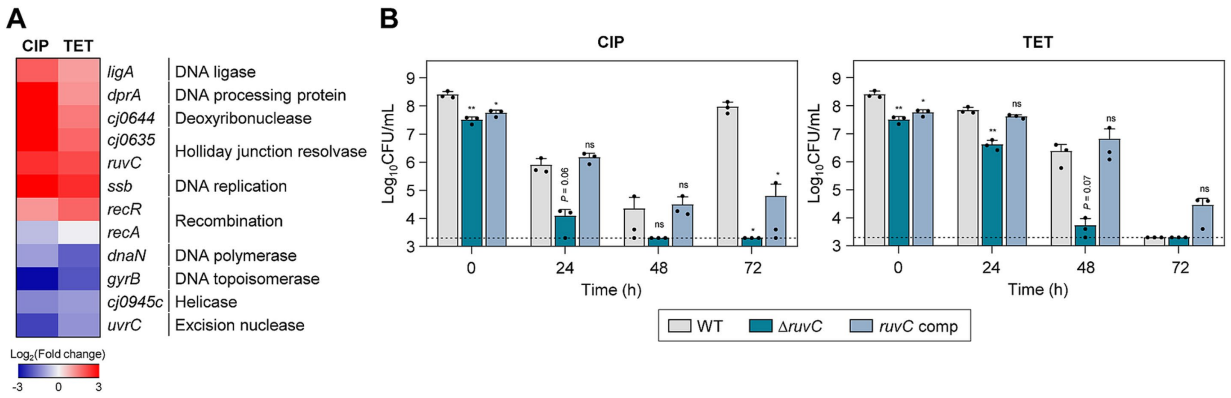

FIGURE 4
Effects of DNA repair genes on antibiotic tolerance in *C. jejuni* in the presence of high concentrations of ciprofloxacin (CIP) or tetracycline (TET). **(A)** Heat maps of the genes associated with DNA repair after exposure to 100× minimum inhibitory concentrations (MICs) of CIP (6.3 μg/mL) or TET (3.1 μg/mL). The heat maps were constructed with Gitools. **(B)** Induction of antibiotic tolerance by exposure to 100× MICs of CIP (6.3 μg/mL) or TET (3.1 μg/mL). The concentrations were determined based on the MICs of WT. Dashed line shows detection threshold. Error bars represent the standard deviations of three biological replications. The data were statistically analyzed by the Student's *t* test in comparison with WT; $*p < 0.05$; $**p < 0.01$; ns, not significant; WT, wild type; Δ*ruvC*, *ruvC* mutant; *ruvC* comp, *ruvC*-complemented strain.

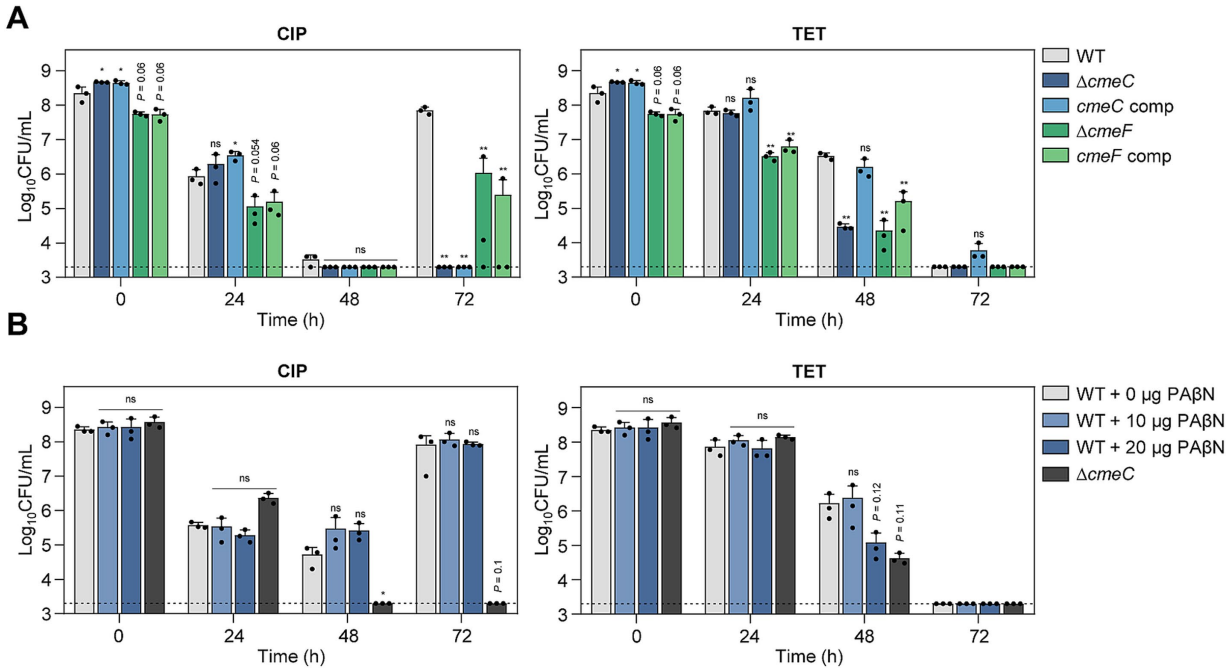

FIGURE 5
Effects of drug efflux pumps on antibiotic tolerance in *C. jejuni* in the presence of high concentrations of ciprofloxacin (CIP) or tetracycline (TET). **(A,B)** Induction of antibiotic tolerance in efflux pump knockout mutants **(A)** by exposure to 100× minimum inhibitory concentrations (MICs) of CIP (6.3 μg/mL) or TET (3.1 μg/mL). The concentrations were determined based on the MICs of WT. Induction of antibiotic tolerance in WT in the presence of phenylalanine-arginine β-naphthylamide (PAβN), an efflux pump inhibitor **(B)** after exposure to 100× MICs of CIP (6.3 μg/mL) or TET (3.1 μg/mL). Dashed line shows detection threshold. Error bars represent the standard deviations of three biological replications. The data were statistically analyzed by the Student's *t* test in comparison with WT; $*p < 0.05$; $**p < 0.01$; ns, not significant; WT, wild type; Δ*cmeC*, *cmeC* mutant; *cmeC* comp, *cmeC*-complemented strain; Δ*cmeF*, *cmeF* mutant; *cmeF* comp, *cmeF*-complemented strain.

(Carrondo, 2003; Krewulak and Vogel, 2008). Moreover, the transcription of *dps*, involved in the sequestration of intracellular free iron (Ishikawa et al., 2003), is significantly increased during tolerance, which is aligned with cellular changes to mitigate cellular toxicity caused by increases in iron levels. These findings suggest that during antibiotic tolerance, *C. jejuni* actively modulates its iron acquisition and storage systems to mitigate the deleterious effects of iron overload. The coordinated regulation of iron uptake and storage genes reflects *C. jejuni*'s adaptive response to maintain iron homeostasis during antibiotic tolerance.

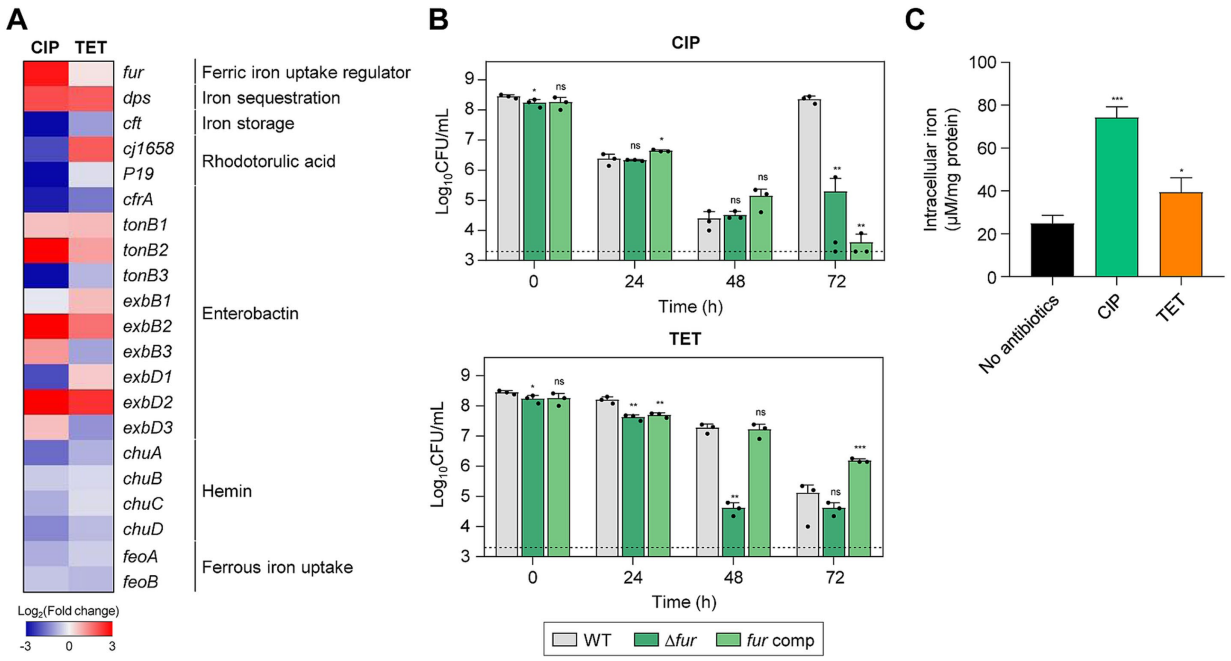

FIGURE 6
Effects of iron accumulation in *C. jejuni* in the presence of high concentrations of ciprofloxacin (CIP) or tetracycline (TET). **(A)** Heat maps of the genes associated with iron metabolism after exposure to 100× minimum inhibitory concentrations (MICs) of CIP (6.3 μg/mL) or TET (3.1 μg/mL). The heat maps were constructed with Gitools. **(B)** Induction of antibiotic tolerance by exposure to 100× MICs of CIP (6.3 μg/mL) or TET (3.1 μg/mL). The concentrations were determined based on the MICs of WT. Dashed line shows detection threshold. Error bars represent the standard deviations of three biological replications. The data were statistically analyzed by the Student's *t* test in comparison with WT; $*p < 0.05$; $**p < 0.01$; $***p < 0.001$; ns, not significant; WT, wild type; Δ*fur*, *fur* mutant; *fur* comp, *fur*-complemented strain. **(C)** The intracellular iron content in *C. jejuni* after exposure to 100× MICs of CIP (6.3 μg/mL) or TET (3.1 μg/mL). Error bars represent the standard deviations of three biological replications. The data were statistically analyzed by the Student's *t* test in comparison with the untreated control (No antibiotics); $*p < 0.05$; $***p < 0.001$.

4 Discussion

The extensive transcriptomic analysis presented in this study provides new insights into the multifaceted cellular responses during antibiotic tolerance in *C. jejuni*, a leading cause of bacterial gastroenteritis worldwide. The research reveals that *C. jejuni* employs diverse cellular defense mechanisms to withstand high concentrations of clinically important antibiotics. Notably, we discovered that the function of protein chaperones is critical for antibiotic tolerance. In the presence of environmental stress, bacteria may encounter protein aggregation, disrupting protein homeostasis and resulting in the formation of insoluble protein aggregates (Vaubourgeix et al., 2015; Schramm et al., 2019). While protein aggregation is typically linked to adverse cellular effects, such as impaired functions and cell death, it is also considered a survival strategy against antibiotic treatment by inducing bacterial dormancy in persister cells (Bollen et al., 2021). During antibiotic persistence, DnaK and ClpB play a role in maintaining a dormant state, enabling persister cells to survive antibiotic challenges and subsequently return to active growth upon removal of antibiotic stress (Pu et al., 2019). DnaK is a chaperone protein that recognizes and binds to exposed hydrophobic regions on partially misfolded proteins (Calloni et al., 2012; Anglès et al., 2017). It then transfers these partially folded proteins to ClpB, an AAA+ ATPase chaperone, which disaggregates and solubilizes aggregated proteins (Alam et al., 2021). ClpB and DnaK interplay to address protein misfolding and aggregation issues, preventing the formation of toxic protein aggregates in response to stress conditions, including antibiotic treatment (Acebrón et al., 2009; Mogk et al., 2015). While the function of chaperone proteins in bacterial dormancy has been documented in persister cells (Pu et al., 2019), our findings suggest that chaperone proteins facilitate protein disaggregation to maintain bacterial viability during antibiotic tolerance, as antibiotic tolerance does not necessarily involve dormancy (Brauner et al., 2016; Balaban et al., 2019). Although the precise role of molecular chaperones during antibiotic tolerance remains unexplained, our data suggest that protein chaperones contribute to bacterial survival under antibiotic treatment by contributing to protein disaggregation.

We conducted transcriptome analysis after antibiotic exposure for 24 h to capture the effects of extended antibiotic exposure on gene expression. Notably, the transcriptional levels of chaperon genes were increased over the duration of antibiotic exposure from 2 h to 24 h (Supplementary Figure S4), confirming the critical function of chaperons in antibiotic tolerance. Moreover, chaperone mutations did not reduce viability at 24 h but rendered the mutants significantly vulnerable to antibiotics after 48 h. The observed delay in viability reduction of the chaperone mutants may be attributed to the gradual accumulation of cellular damage and stress over time. The absence of chaperones may not immediately result in cell death; instead, misfolded proteins and cellular damage gradually accumulate over time. This cumulative effect may reach a critical threshold after 48 h, leading to a significant decrease in viability. Nevertheless, these findings underscore the significance of protein chaperones in antibiotic tolerance and bacterial survival during prolonged antibiotic exposure.

Our results also further demonstrate the pivotal role of DNA repair in sustaining antibiotic tolerance. This finding strongly

suggests that *C. jejuni* is not dormant during tolerance but rather actively engaged in cellular processes to ensure survival. By increasing the expression of DNA repair mechanisms, *C. jejuni* actively works to preserve its genetic integrity, which is essential for maintaining vital physiological functions. This active state in antibiotic tolerance contrasts with the concept of antibiotic persistence, where bacteria often enter a dormant state to evade antibiotic effects (Brauner et al., 2016; Balaban et al., 2019). Additionally, it is noteworthy that *C. jejuni* does not have the SOS response system which is critical for addressing DNA damage in various bacteria (Parkhill et al., 2000). While other bacteria primarily rely on the SOS response-mediated DNA repair system for antibiotic tolerance, *C. jejuni* appears to utilize alternative DNA repair systems that operate independently of the SOS response (Theodore et al., 2013; Podlesek and Žgur Bertok, 2020; Kamat and Badrinarayanan, 2023). During antibiotic tolerance, high antibiotic concentrations lead to the generation of toxic ROS, particularly hydroxyl radicals, which can damage DNA (Park et al., 2022). Presumably, DNA repair during tolerance may contribute to addressing DNA damage and mutations, especially those that interrupt the function of essential genes, thereby ensuring the maintenance of bacterial survival.

Notably, this study has revealed an increase in intracellular iron concentration during antibiotic tolerance (Figure 6C). Although the exact mechanisms are not fully elucidated, potentially, it is known that intracellular free iron can interact with hydrogen peroxide to generate DNA-damaging hydroxyl radicals through the Fenton reaction (Imlay, 2008). Our previous research has indicated a significant elevation of oxidative stress in *C. jejuni* during tolerance, with antioxidant enzymes, such as alkyl hydroperoxide reductase (AhpC), playing a crucial role in maintaining antibiotic tolerance (Park et al., 2022). To mitigate oxidative stress associated with increased intracellular iron levels during antibiotic tolerance, *C. jejuni* should inhibit further iron uptake and sequester intracellular free iron. This is supported by the observed substantial increase in the transcriptional levels of *fur* (a Fe^{3+} uptake repressor) and *dps* (an intracellular iron sequestration protein), along with the down-regulation of *feoB*, which encodes a ferrous iron transporter (Figure 6A). Given the pivotal role of iron in the generation of hydroxyl radicals, maintaining iron homeostasis is crucial for sustaining antibiotic tolerance, likely through the control of oxidative stress.

In conclusion, this study has uncovered the diverse cellular responses that contribute to *C. jejuni*'s tolerance to antibiotics. Our findings demonstrate that *C. jejuni* extensively utilizes various cellular defense mechanisms, including antioxidation, protein chaperoning, DNA repair, drug efflux, and iron homeostasis, to survive antibiotic treatment (Figure 7). Particularly, the regulation of intracellular iron levels through iron homeostasis appears to be linked to antibiotic tolerance. These findings have the potential to inform the development

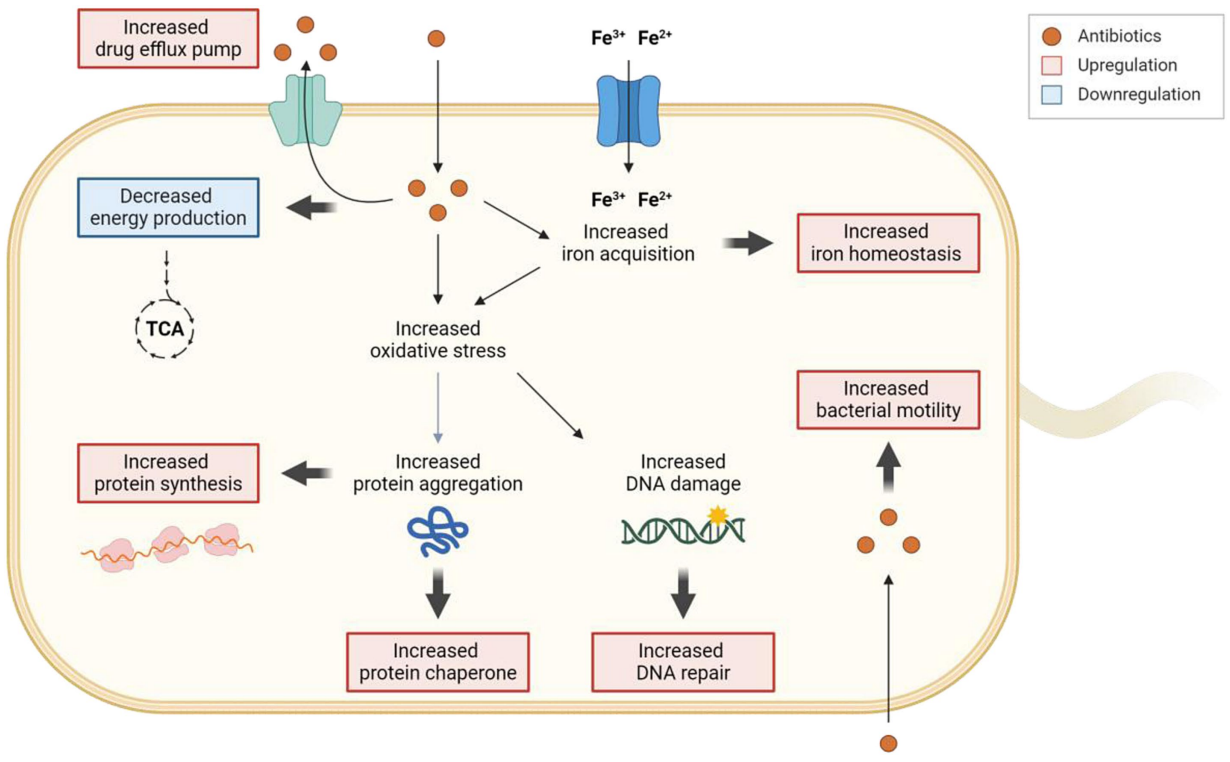

FIGURE 7
Schematic representation of the cellular responses involved in the development of antibiotic tolerance in *C. jejuni*. When exposed to high levels of antibiotics, drug efflux pumps actively work to decrease the intracellular concentrations of antibiotics. Exposure to high concentrations of antibiotics leads to an accumulation of iron within the cell, subsequently influencing the gene expression of iron acquisition and storage systems to maintain iron homeostasis. The increased oxidative stress caused by antibiotics induces DNA damage, prompting the upregulation of the DNA repair system. Furthermore, oxidative stress may also trigger protein aggregation, resulting in the upregulation of protein synthesis and protein chaperones to disaggregate protein aggregates. Intriguingly, intracellular antibiotics may also stimulate bacterial motility. Additionally, exposure to high concentrations of antibiotics leads to the downregulation of genes associated with energy production. The transcriptional changes are visually represented with bold arrows, with upregulation highlighted in red and downregulation in blue. The figure was created with Biorender.com.

of novel strategies to combat antibiotic tolerance and resistance, thereby assisting in tackling this significant issue in global public health.

Data availability statement

The datasets presented in this study can be found in online repositories. The names of the repository/repositories and accession number(s) can be found in the article/Supplementary material.

Author contributions

EC: Methodology, Validation, Formal analysis, Investigation, Writing – original draft, Writing – review & editing, Visualization. JK: Methodology, Validation, Formal analysis, Investigation, Writing – original draft, Writing – review & editing, Visualization, Funding acquisition. JH: Investigation, Writing – review & editing. SR: Resources, Writing – review & editing, Supervision, Project administration, Funding acquisition. BJ: Conceptualization, Formal analysis, Writing – original draft, Writing – review & editing, Supervision, Project administration, Funding acquisition.

Funding

The author(s) declare that financial support was received for the research, authorship, and/or publication of this article. This study was supported by funding from MnDRIVE (Minnesota's Discovery, Research, and InnoVation Economy) to BJ and the Ministry of Education of the Republic of Korea and the National Research Foundation of Korea (NRF-2023R1A2C1006359) to SR; the Basic Science Research Program through the National Research Foundation of Korea, funded by the Ministry of Education (2022R1A6A1A03055869) to JK; EC and JIH were supported by the BK21 Plus Program of the Department of Agricultural Biotechnology, Seoul National University, Seoul, Korea.

Conflict of interest

The authors declare that the research was conducted in the absence of any commercial or financial relationships that could be construed as a potential conflict of interest.

Publisher's note

All claims expressed in this article are solely those of the authors and do not necessarily represent those of their affiliated organizations, or those of the publisher, the editors and the reviewers. Any product that may be evaluated in this article, or claim that may be made by its manufacturer, is not guaranteed or endorsed by the publisher.

Supplementary material

The Supplementary material for this article can be found online at: https://www.frontiersin.org/articles/10.3389/fmicb.2024.1493849/full#supplementary-material

References

Acebrón, S. P., Martín, I., del Castillo, U., Moro, F., and Muga, A. (2009). DnaK-mediated association of ClpB to protein aggregates. A bichaperone network at the aggregate surface. *FEBS Lett.* 583, 2991–2996. doi: 10.1016/j.febslet.2009.08.020

Akiba, M., Lin, J., Barton, Y. W., and Zhang, Q. (2006). Interaction of CmeABC and CmeDEF in conferring antimicrobial resistance and maintaining cell viability in *Campylobacter jejuni*. *J. Antimicrob. Chemother.* 57, 52–60. doi: 10.1093/jac/dki419

Alam, A., Bröms, J. E., Kumar, R., and Sjöstedt, A. (2021). The role of ClpB in bacterial stress responses and virulence. *Front. Mol. Biosci.* 8:668910. doi: 10.3389/fmolb.2021.668910

Aliberti, S., Blasi, F., Zanaboni, A. M., Peyrani, P., Tarsia, P., Gaito, S., et al. (2010). Duration of antibiotic therapy in hospitalised patients with community-acquired pneumonia. *Eur. Respir. J.* 36, 128–134. doi: 10.1183/09031936.00130909

Alm, R. A., Guerry, P., and Trust, T. J. (1993). The *Campylobacter* sigma 54 *flaB* flagellin promoter is subject to environmental regulation. *J. Bacteriol.* 175, 4448–4455. doi: 10.1128/jb.175.14.4448-4455.1993

Andersson, M. I., and MacGowan, A. P. (2003). Development of the quinolones. *J. Antimicrob. Chemother.* 51, 1–11. doi: 10.1093/jac/dkg212

Andrews, S. C., Robinson, A. K., and Rodríguez-Quiñones, F. (2003). Bacterial iron homeostasis. *FEMS Microbiol. Rev.* 27, 215–237. doi: 10.1016/s0168-6445(03)00055-x

Anglès, F., Castanié-Cornet, M. P., Slama, N., Dinclaux, M., Cirinesi, A. M., Portais, J. C., et al. (2017). Multilevel interaction of the DnaK/DnaJ(HSP70/HSP40) stress-responsive chaperone machine with the central metabolism. *Sci. Rep.* 7:41341. doi: 10.1038/srep41341

Appelbaum, P. C., and Hunter, P. A. (2000). The fluoroquinolone antibacterials: past, present and future perspectives. *Int. J. Antimicrob. Agents* 16, 5–15. doi: 10.1016/s0924-8579(00)00192-8

Bagnoli, S., Terzibasi Tozzini, E., and Cellerino, A. (2023). Immunofluorescence and aggresome staining of *Nothobranchius furzeri* cryosections. *Cold Spring Harb. Protoc.* 2023, 693–697. doi: 10.1101/pdb.prot107791

Balaban, N. Q., Helaine, S., Lewis, K., Ackermann, M., Aldridge, B., Andersson, D. I., et al. (2019). Definitions and guidelines for research on antibiotic persistence. *Nat. Rev. Microbiol.* 17, 441–448. doi: 10.1038/s41579-019-0196-3

Balaban, N. Q., Merrin, J., Chait, R., Kowalik, L., and Leibler, S. (2004). Bacterial persistence as a phenotypic switch. *Science* 305, 1622–1625. doi: 10.1126/science.1099390

Bollen, C., Dewachter, L., and Michiels, J. (2021). Protein aggregation as a bacterial strategy to survive antibiotic treatment. *Front. Mol. Biosci.* 8:669664. doi: 10.3389/fmolb.2021.669664

Brauner, A., Fridman, O., Gefen, O., and Balaban, N. Q. (2016). Distinguishing between resistance, tolerance and persistence to antibiotic treatment. *Nat. Rev. Microbiol.* 14, 320–330. doi: 10.1038/nrmicro.2016.34

Butcher, J., Sarvan, S., Brunzelle, J. S., Couture, J. F., and Stintzi, A. (2012). Structure and regulon of *Campylobacter jejuni* ferric uptake regulator Fur define apo-Fur regulation. *Proc. Natl. Acad. Sci. USA* 109, 10047–10052. doi: 10.1073/pnas.1118321109

Calloni, G., Chen, T., Schermann, S. M., Chang, H. C., Genevaux, P., Agostini, F., et al. (2012). DnaK functions as a central hub in the *E. coli* chaperone network. *Cell Rep.* 1, 251–264. doi: 10.1016/j.celrep.2011.12.007

Cañas-Duarte, S. J., Restrepo, S., and Pedraza, J. M. (2014). Novel protocol for persister cells isolation. *PLoS One* 9, –e88660. doi: 10.1371/journal.pone.0088660

Carrondo, M. A. (2003). Ferritins, iron uptake and storage from the bacterioferritin viewpoint. *EMBO J.* 22, 1959–1968. doi: 10.1093/emboj/cdg215

Colclough, A. L., Alav, I., Whittle, E. E., Pugh, H. L., Darby, E. M., Legood, S. W., et al. (2020). RND efflux pumps in gram-negative bacteria; regulation, structure and role in antibiotic resistance. *Future Microbiol.* 15, 143–157. doi: 10.2217/fmb-2019-0235

Du, D., Wang-Kan, X., Neuberger, A., van Veen, H. W., Pos, K. M., Piddock, L. J. V., et al. (2018). Multidrug efflux pumps: structure, function and regulation. *Nat. Rev. Microbiol.* 16, 523–539. doi: 10.1038/s41579-018-0048-6

European Medicines Agency (2022). Sales of veterinary antimicrobial agents in 31 European countries in 2021 – Trends from 2010 to 2021 – Twelfth ESVAC report:

Publications Office of the European Union. Available at: https://op.europa.eu/en/publication-detail/-/publication/d07e60db-ab50-11ed-b508-01aa75ed71a1/language-en

Frawley, E. R., and Fang, F. C. (2014). The ins and outs of bacterial iron metabolism. *Mol. Microbiol.* 93, 609–616. doi: 10.1111/mmi.12709

Fridman, O., Goldberg, A., Ronin, I., Shoresh, N., and Balaban, N. Q. (2014). Optimization of lag time underlies antibiotic tolerance in evolved bacterial populations. *Nature* 513, 418–421. doi: 10.1038/nature13469

Gefen, O., and Balaban, N. Q. (2009). The importance of being persistent: heterogeneity of bacterial populations under antibiotic stress. *FEMS Microbiol. Rev.* 33, 704–717. doi: 10.1111/j.1574-6976.2008.00156.x

Goossens, S. N., Sampson, S. L., and Van Rie, A. (2020). Mechanisms of drug-induced tolerance in *Mycobacterium tuberculosis*. *Clin. Microbiol. Rev.* 34:e00141-20. doi: 10.1128/cmr.00141-20

Grossman, T. H. (2016). Tetracycline antibiotics and resistance. *Cold Spring Harb. Perspect. Med.* 6:a025387. doi: 10.1101/cshperspect.a025387

Guerry, P., Alm, R. A., Power, M. E., Logan, S. M., and Trust, T. J. (1991). Role of two flagellin genes in *Campylobacter* motility. *J. Bacteriol.* 173, 4757–4764. doi: 10.1128/jb.173.15.4757-4764.1991

Huemer, M., Mairpady Shambat, S., Brugger, S. D., and Zinkernagel, A. S. (2020). Antibiotic resistance and persistence-implications for human health and treatment perspectives. *EMBO Rep.* 21:e51034. doi: 10.15252/embr.202051034

Hur, J. I., Kim, J., Ryu, S., and Jeon, B. (2022). Phylogenetic association and genetic factors in cold stress tolerance in *Campylobacter jejuni*. *Microbiol. Spectr.* 10, e02681–e02622. doi: 10.1128/spectrum.02681-22

Hwang, S., Jeon, B., Yun, J., and Ryu, S. (2011). Roles of RpoN in the resistance of *Campylobacter jejuni* under various stress conditions. *BMC Microbiol.* 11, 1–8. doi: 10.1186/1471-2180-11-207

Hwang, S., Zhang, Q., Ryu, S., and Jeon, B. (2012). Transcriptional regulation of the CmeABC multidrug efflux pump and the KatA catalase by CosR in *Campylobacter jejuni*. *J. Bacteriol.* 194, 6883–6891. doi: 10.1128/JB.01636-12

Imlay, J. A. (2008). Cellular defenses against superoxide and hydrogen peroxide. *Annu. Rev. Biochem.* 77, 755–776. doi: 10.1146/annurev.biochem.77.061606.161055

Ishikawa, T., Mizunoe, Y., Kawabata, S., Takade, A., Harada, M., Wai, S. N., et al. (2003). The iron-binding protein Dps confers hydrogen peroxide stress resistance to *Campylobacter jejuni*. *J. Bacteriol.* 185, 1010–1017. doi: 10.1128/jb.185.3.1010-1017.2003

Iwasaki, H., Takahagi, M., Shiba, T., Nakata, A., and Shinagawa, H. (1991). *Escherichia coli* RuvC protein is an endonuclease that resolves the Holliday structure. *EMBO J.* 10, 4381–4389. doi: 10.1002/j.1460-2075.1991.tb05016.x

Kamat, A., and Badrinarayanan, A. (2023). SOS-independent bacterial DNA damage responses: diverse mechanisms, unifying function. *Curr. Opin. Microbiol.* 73:102323. doi: 10.1016/j.mib.2023.102323

Kim, M., Hwang, S., Ryu, S., and Jeon, B. (2011). Regulation of *perR* expression by iron and PerR in *Campylobacter jejuni*. *J. Bacteriol.* 193, 6171–6178. doi: 10.1128/JB.05493-11

Kim, J., Park, M., Ahn, E., Mao, Q., Chen, C., Ryu, S., et al. (2023). Stimulation of surface polysaccharide production under aerobic conditions confers aerotolerance in *Campylobacter jejuni*. *Microbiol. Spectr.* 11, e03761–e03722. doi: 10.1128/spectrum.03761-22

Kirk, M. D., Pires, S. M., Black, R. E., Caipo, M., Crump, J. A., Devleesschauwer, B., et al. (2015). World Health Organization estimates of the global and regional disease burden of 22 foodborne bacterial, protozoal, and viral diseases, 2010: a data synthesis. *PLoS Med.* 12:e1001921. doi: 10.1371/journal.pmed.1001921

Krewulak, K. D., and Vogel, H. J. (2008). Structural biology of bacterial iron uptake. *Biochim. Biophys. Acta Biomembr.* 1778, 1781–1804. doi: 10.1016/j.bbamem.2007.07.026

Kumawat, M., Nabi, B., Daswani, M., Viquar, I., Pal, N., Sharma, P., et al. (2023). Role of bacterial efflux pump proteins in antibiotic resistance across microbial species. *Microb. Pathog.* 181:106182. doi: 10.1016/j.micpath.2023.106182

Lee, J. W., and Helmann, J. D. (2007). Functional specialization within the Fur family of metalloregulators. *Biometals* 20, 485–499. doi: 10.1007/s10534-006-9070-7

Levin-Reisman, I., Brauner, A., Ronin, I., and Balaban, N. Q. (2019). Epistasis between antibiotic tolerance, persistence, and resistance mutations. *Proc. Natl. Acad. Sci. USA* 116, 14734–14739. doi: 10.1073/pnas.1906169116

Levin-Reisman, I., Ronin, I., Gefen, O., Braniss, I., Shoresh, N., and Balaban, N. Q. (2017). Antibiotic tolerance facilitates the evolution of resistance. *Science* 355, 826–830. doi: 10.1126/science.aaj2191

Lin, J., Michel, L. O., and Zhang, Q. (2002). CmeABC functions as a multidrug efflux system in *Campylobacter jejuni*. *Antimicrob. Agents Chemother.* 46, 2124–2131. doi: 10.1128/aac.46.7.2124-2131.2002

Liu, J., Gefen, O., Ronin, I., Bar-Meir, M., and Balaban, N. Q. (2020). Effect of tolerance on the evolution of antibiotic resistance under drug combinations. *Science* 367, 200–204. doi: 10.1126/science.aay3041

Luangtongkum, T., Jeon, B., Han, J., Plummer, P., Logue, C. M., and Zhang, Q. (2009). Antibiotic resistance in *Campylobacter*: emergence, transmission and persistence. *Future Microbiol.* 4, 189–200. doi: 10.2217/17460913.4.2.189

Mayer, M. P. (2021). The Hsp70-chaperone machines in bacteria. *Front. Mol. Biosci.* 8:694012. doi: 10.3389/fmolb.2021.694012

Mechler, L., Herbig, A., Paprotka, K., Fraunholz, M., Nieselt, K., and Bertram, R. (2015). A novel point mutation promotes growth phase-dependent daptomycin tolerance in *Staphylococcus aureus*. *Antimicrob. Agents Chemother.* 59, 5366–5376. doi: 10.1128/aac.00643-15

Meredith, H. R., Srimani, J. K., Lee, A. J., Lopatkin, A. J., and You, L. (2015). Collective antibiotic tolerance: mechanisms, dynamics and intervention. *Nat. Chem. Biol.* 11, 182–188. doi: 10.1038/nchembio.1754

Miller, C. E., Rock, J. D., Ridley, K. A., Williams, P. H., and Ketley, J. M. (2008). Utilization of lactoferrin-bound and transferrin-bound iron by *Campylobacter jejuni*. *J. Bacteriol.* 190, 1900–1911. doi: 10.1128/jb.01761-07

Mogk, A., Kummer, E., and Bukau, B. (2015). Cooperation of Hsp70 and Hsp100 chaperone machines in protein disaggregation. *Front. Mol. Biosci.* 2:22. doi: 10.3389/fmolb.2015.00022

Naikare, H., Palyada, K., Panciera, R., Marlow, D., and Stintzi, A. (2006). Major role for FeoB in *Campylobacter jejuni* ferrous iron acquisition, gut colonization, and intracellular survival. *Infect. Immun.* 74, 5433–5444. doi: 10.1128/iai.00052-06

Palyada, K., Threadgill, D., and Stintzi, A. (2004). Iron acquisition and regulation in *Campylobacter jejuni*. *J. Bacteriol.* 186, 4714–4729. doi: 10.1128/jb.186.14.4714-4729.2004

Park, M., Kim, J., Feinstein, J., Lang, K. S., Ryu, S., and Jeon, B. (2022). Development of fluoroquinolone resistance through antibiotic tolerance in *Campylobacter jejuni*. *Microbiol. Spectr.* 10:e0166722. doi: 10.1128/spectrum.01667-22

Parkhill, J., Wren, B. W., Mungall, K., Ketley, J. M., Churcher, C., Basham, D., et al. (2000). The genome sequence of the food-borne pathogen *Campylobacter jejuni* reveals hypervariable sequences. *Nature* 403, 665–668. doi: 10.1038/35001088

Podlesek, Z., and Žgur Bertok, D. (2020). The DNA damage inducible SOS response is a key player in the generation of bacterial persister cells and population wide tolerance. *Front. Microbiol.* 11:1785. doi: 10.3389/fmicb.2020.01785

Pu, Y., Li, Y., Jin, X., Tian, T., Ma, Q., Zhao, Z., et al. (2019). ATP-dependent dynamic protein aggregation regulates bacterial dormancy depth critical for antibiotic tolerance. *Mol. Cell* 73, 143–156.e4. doi: 10.1016/j.molcel.2018.10.022

Ronneau, S., Hill, P. W., and Helaine, S. (2021). Antibiotic persistence and tolerance: not just one and the same. *Curr. Opin. Microbiol.* 64, 76–81. doi: 10.1016/j.mib.2021.09.017

Sabate, R., de Groot, N. S., and Ventura, S. (2010). Protein folding and aggregation in bacteria. *Cell. Mol. Life Sci.* 67, 2695–2715. doi: 10.1007/s00018-010-0344-4

Santi, I., Manfredi, P., Maffei, E., Egli, A., Jenal, U., and Buchrieser, C. (2021). Evolution of antibiotic tolerance shapes resistance development in chronic *Pseudomonas aeruginosa* infections. *MBio* 12, e03482–e03420. doi: 10.1128/mBio.03482-20

Schierenberg, A., Bruijning-Verhagen, P. C. J., van Delft, S., Bonten, M. J. M., and de Wit, N. J. (2019). Antibiotic treatment of gastroenteritis in primary care. *J. Antimicrob. Chemother.* 74, 207–213. doi: 10.1093/jac/dky385

Schramm, F. D., Schroeder, K., and Jonas, K. (2019). Protein aggregation in bacteria. *FEMS Microbiol. Rev.* 44, 54–72. doi: 10.1093/femsre/fuz026

Sharifi, S., Bakhshi, B., and Najar-Peerayeh, S. (2021). Significant contribution of the CmeABC efflux pump in high-level resistance to ciprofloxacin and tetracycline in *Campylobacter jejuni* and *Campylobacter coli* clinical isolates. *Ann. Clin. Microbiol. Antimicrob.* 20:36. doi: 10.1186/s12941-021-00439-6

Shin, J. H., Choe, D., Ransegnola, B., Hong, H. R., Onyekwere, I., Cross, T., et al. (2021). A multifaceted cellular damage repair and prevention pathway promotes high-level tolerance to β-lactam antibiotics. *EMBO Rep.* 22:e51790. doi: 10.15252/embr.202051790

Sulaiman, J. E., and Lam, H. (2020). Proteomic investigation of tolerant *Escherichia coli* populations from cyclic antibiotic treatment. *J. Proteome Res.* 19, 900–913. doi: 10.1021/acs.jproteome.9b00687

Takata, T., Ando, T., Israel, D. A., Wassenaar, T. M., and Blaser, M. J. (2005). Role of *dprA* in transformation of *Campylobacter jejuni*. *FEMS Microbiol. Lett.* 252, 161–168. doi: 10.1016/j.femsle.2005.08.052

Theodore, A., Lewis, K., and Vulić, M. (2013). Tolerance of *Escherichia coli* to fluoroquinolone antibiotics depends on specific components of the SOS response pathway. *Genetics* 195, 1265–1276. doi: 10.1534/genetics.113.152306

US Food and Drug Administration (2023). 2022 summary report on antimicrobials sold or distributed for use in food-producing animals [Online]. Available at: https://www.fda.gov/animal-veterinary/antimicrobial-resistance/2022-summary-report-antimicrobials-sold-or-distributed-use-food-producing-animals (Accessed October, 1 2024).

Vaubourgeix, J., Lin, G., Dhar, N., Chenouard, N., Jiang, X., Botella, H., et al. (2015). Stressed mycobacteria use the chaperone ClpB to sequester irreversibly oxidized

proteins asymmetrically within and between cells. *Cell Host Microbe* 17, 178–190. doi: 10.1016/j.chom.2014.12.008

Wallis, M., and Griffin, R. (1973). A routine method for embedding animal tissues in Spurr resin for electron microscopy. *J. Clin. Pathol.* 26, 77–78. doi: 10.1136/jcp.26.1.77

Wang, Y., and Taylor, D. (1990). Natural transformation in *Campylobacter* species. *J. Bacteriol.* 172, 949–955. doi: 10.1128/jb.172.2.949-955.1990

Westblade, L. F., Errington, J., and Dörr, T. (2020). Antibiotic tolerance. *PLoS Pathog.* 16:e1008892. doi: 10.1371/journal.ppat.1008892

Wieczorek, K., and Osek, J. (2013). Antimicrobial resistance mechanisms among *Campylobacter*. *Biomed. Res. Int.* 2013:340605. doi: 10.1155/2013/340605

Wilson, H. L., Daveson, K., and Del Mar, C. B. (2019). Optimal antimicrobial duration for common bacterial infections. *Aust. Prescr.* 42, 5–9. doi: 10.18773/austprescr.2019.001

Windels, E. M., Michiels, J. E., Fauvart, M., Wenseleers, T., Van den Bergh, B., and Michiels, J. (2019). Bacterial persistence promotes the evolution of antibiotic resistance by increasing survival and mutation rates. *ISME J.* 13, 1239–1251. doi: 10.1038/s41396-019-0344-9

Xu, L., Halma, M. T. J., and Wuite, G. J. L. (2023). Unravelling how single-stranded DNA binding protein coordinates DNA metabolism using single-molecule approaches. *Int. J. Mol. Sci.* 24:2806. doi: 10.3390/ijms24032806

Yao, R., Burr, D. H., and Guerry, P. (1997). CheY-mediated modulation of *Campylobacter jejuni* virulence. *Mol. Microbiol.* 23, 1021–1031. doi: 10.1046/j.1365-2958.1997.2861650.x

Frontiers in Microbiology

Explores the habitable world and the potential of microbial life

The largest and most cited microbiology journal which advances our understanding of the role microbes play in addressing global challenges such as healthcare, food security, and climate change.

Discover the latest Research Topics

See more →

Frontiers

Avenue du Tribunal-Fédéral 34
1005 Lausanne, Switzerland
frontiersin.org

Contact us

+41 (0)21 510 17 00
frontiersin.org/about/contact